



irc 2023  
XVII. international research conference  
proceedings

open science index 17 2023

june 22-23, 2023 paris france  
international scholarly and scientific research & innovation



## **Open Science**

### **Open Science Philosophy**

Open science encompasses unrestricted access to scientific research articles, access to data from public research, and collaborative research enabled by information and communication technology tools, models, and incentives. Broadening access to scientific research publications and data is at the heart of open science. The objective of open science is to make research outputs and its potential benefits available to the entire world and in the hands of as many as possible:

- Open science promotes a more accurate verification of scientific research results. Scientific inquiry and discovery can be sped up by combining the tools of science and information technologies. Open science will benefit society and researchers by providing faster, easier, and more efficient availability of research outputs.
- Open science reduces duplication in collecting, creating, transferring, and re-using scientific material.
- Open science increases productivity in an era of tight budgets.
- Open science results in great innovation potential and increased consumer choice from public research.
- Open science promotes public trust in science. Greater citizen engagement leads to active participation in scientific experiments and data collection.

### **Open Science Index**

The Open Science Index (OSI) currently provides access to over thirty thousand full-text journal articles and is working with member and non-member organizations to review policies to promote and assess open science. As part of the open science philosophy, and by making open science a reality; OSI is conducting an assessment of the impact of open science principles and restructuring the guidelines for access to scientific research. As digitalization continues to accelerate science, Open science and big data hold enormous promise and present new challenges for policymakers, scientific institutions, and individual researchers.

OSI is helping the global scientific research community discover, evaluate, and access high-quality research output. Renowned for its editorially curated and refereed collection of the highest-quality publications, OSI has always been and will remain free-of-charge.

OSI provides an efficient and thorough discovery process to the open science research database and provides links and free access to full-text articles. There are 50 open access journal categories that are curated and refereed by international scientific committees, the in-house editorial team, and trusted partners. Since its inception in 2007, OSI has made more than thirty thousand peer-reviewed open access full-text journal articles (PDF versions) freely available online without cost, barriers, or restrictions.

### **Open Science Access**

With the Open Science Index, researchers can discover and access trusted peer-reviewed open access full-text scientific research articles with confidence. OSI helps researchers find appropriate non-profit open access journals to publish their work.

OSI gives one-click access to online full-text PDFs and expands the reach to global society by giving users free access from anywhere around the globe. Through cutting-edge open science collaboration, in an innovative public partnership, the non-profit OSI is devoted to making science open and reusable.

To learn more, visit online at [waset.org](http://waset.org)

## **Open Science**

### **Open Society**

An open society allows individuals to change their roles and to benefit from corresponding changes in status. Open science depends to a greater or lesser extent on digital technologies and innovations in structural processes by an open society. When realized, open science research and innovation can create investment opportunities for new and better products and services and therefore increase competitiveness and employment. Open science research and innovation is a key component of thematic open science priorities. Central to the open science digital infrastructure is enabling industry to benefit from digital technology and to underpin scientific advances through the development of an open society. Open science research and innovation can also contribute to society as a global actor because scientific relations can flourish even where global relations are strained. Open science has a critical role across many areas of decision making in providing evidence that helps understand the risks and benefits of different open science choices. Digital technology is making the conduct of open science and innovation more collaborative, more global, and more open to global citizens. Open society must embrace these changes and reinforce its position as the leading power for science, for new ideas, and for investing sustainably in the future.

It is apparent in open society that the way science works is fundamentally changing, and an equally significant transformation is taking place in how organizations and societies innovate. The advent of digital technology is making research and innovation more open, collaborative, and global. These exchanges are leading open society to develop open science and to set goals for research and innovation priority. Open science goals are materializing in the development of scientific research and innovation platforms and greater acceptance of scientific data generated by open science research. Open science research and innovation do not need help from open society to come up with great ideas, but the level of success ideas ultimately reach is undoubtedly influenced by regulation, financing, public support, and market access. Open society is playing a crucial role in improving all these success factors.

### **Open Science**

Open science represents a new approach to the scientific process based on cooperative work and new ways of diffusing knowledge by using digital technologies and collaborative tools. These innovations capture a systemic change to the way science and research have been carried out for the last fifty years. Science is shifting from the standard practice of publishing research results in scientific publications after the research and reviews are completed. The shift is towards sharing and using all available knowledge at an earlier stage in the research process. Open science is to science what digital technology is to social and economic transactions: allowing end users to be producers of ideas, relations, and services and in doing so, enabling new working models, new social relationships and leading to a new *modus operandi* for science. Open science is as important and disruptive as e-commerce has been for the retail industry. Just like e-commerce, the open science research paradigm shift affects the whole business cycle of doing science and research. From the selection of research subjects to the carrying out of research, to its use and re-use, to the role of universities, and that of publishers are all dramatically changed. Just as the internet and globalization have profoundly changed the way we do business, interact socially, consume culture, and buy goods, these changes are now profoundly impacting how one does research and science.

The discussion on broadening the footprint of science and on novel ways to produce and spread knowledge gradually evolved from two global trends: Open Access and Open Source. The former refers to online, peer-reviewed scholarly outputs, which are free to read, with limited or no copyright and licensing restrictions, while open source refers to software created without any proprietary restriction and which can be accessed and freely used. Although open access became primarily associated with a particular publishing

## Open Science

or scientific dissemination practice, open access already sought to induce a broader practice that includes the general re-use of all kinds of research products, not just publications or data. It is only more recently that open science has coalesced into the concept of a transformed scientific practice, shifting the focus of researchers' activity from publishing as fast as possible to sharing knowledge as early as possible. Open science is defined as the idea that scientific knowledge of all kinds should be openly shared as early as is practical in the discovery process. As a result, the way science is done in the future will look significantly different from the way it is done now. Open science is the ongoing evolution in the modus operandi of doing research and organizing science. This evolution is enabled by digital technology and is driven by both the globalization of the scientific community and increasing public demand to address the societal challenges of our times. Open science entails the ongoing transitions in the way research is performed, researchers collaborate, knowledge is shared, and science is organized.

Open science impacts the entire research cycle, from the inception of research to its publication, and on how this cycle is organized. The outer circle reflects the new interconnected nature of open science, while the inner circle shows the entire scientific process, from the conceptualization of research ideas to publishing. Each step in the scientific process is linked to ongoing changes brought about by open science, including the emergence of alternative systems to establish a scientific reputation; changes in the way quality and impact of research are evaluated; the growing use of scientific blogs; open annotation; and open access to data and publications. All institutions involved in science are affected, including research organizations, research councils, and funding bodies. The trends are irreversible, and they have already grown well beyond individual projects. These changes predominantly result from a bottom-up process driven by a growing number of researchers who increasingly employ social media in their research and initiate globally coordinated research projects while sharing results at an early stage in the research process.

Open science is encompassed in five schools of thought:

- the infrastructure school, concerned with technological architecture
- the public school, concerned with the accessibility of knowledge creation
- the measurement school, concerned with alternative impact assessment
- the democratic school, concerned with access to knowledge
- the pragmatic school, concerned with collaborative research

According to the measurement school, the reputation and evaluation of individual researchers are still mainly based on citation-based metrics. The h-index is an author-level metric that attempts to measure both the productivity and citation impact of the publications of a scientist or scholar. The impact factor is a measure reflecting the average number of citations to articles published in an academic journal and is used as a proxy for the relative importance of a journal.

Numerous criticisms have been made of citation-based metrics, primarily when used, and often misused, to assess the performance of individual researchers. These metrics:

- are often not applicable at the individual level
- do not take into account the broader social and economic function of scientific research
- are not adapted to the increased scale of research
- cannot recognize new types of work that researchers are performing

Web-based metrics for measuring research output, popularized as altmetrics, have recently received much attention: some measure the impact at the article level, others make it possible to assess the many outcomes of research in addition to the number of scientific articles and references. The current reputation and evaluation system has to adapt to the new dynamics of open science and acknowledge and incentivize



## **Open Science**

engagement in open science. Researchers engaging in open science have growing expectations that their work, including intermediate products such as research data, will be better rewarded or taken into account in their career development. Vice-versa, the use, and reuse of open data will require appropriate codes of conduct requiring, for example, the proper acknowledgment of the original creator of the data.

These ongoing changes are progressively transforming scientific practices with innovative tools to facilitate communication, collaboration, and data analysis. Researchers that increasingly work together to create knowledge can employ online tools and create a shared space where creative conversation and collaboration can occur. As a result, the problem-solving process can be faster, and the range of problems that can be solved can be expanded. The ecosystem underpinning open science is evolving very rapidly. Social network platforms for researchers already attract millions of users and are being used to begin and validate more research projects.

Furthermore, the trends towards open access are redefining the framework conditions for science and thus have an impact on how open innovation is produced by encouraging a more dynamic circulation of knowledge. It can enable more science-based startups to emerge thanks to the exploitation of openly accessible research results. Open science, however, does not mean free science. It is essential to ensure that intellectual property is protected before making knowledge publicly available in order to subsequently attract investments that can help translate research results into innovation. If this is taken into account, fuller and broader access to scientific publications and research data can help to accelerate innovation. Investments that boost research and innovation in open science would benefit society with fewer barriers to knowledge transfer, open access to scientific research, and greater mobility of researchers. In this context, open access can help overcome the barriers that innovative organizations face in accessing the results of research funded by the public.

## **Open innovation**

An open society is the largest producer of knowledge, but the phenomenon of open science is changing every aspect of the scientific method by becoming more open, inclusive, and interdisciplinary. Ensuring open society is at the forefront of open science means promoting open access to scientific data and publications alongside the highest standards of research integrity. There are few forces in this globe as engaging and unifying as science. The universal language of science maintains open channels of communication globally. Open society can maximize its gains through maintaining its presence at the highest level of scientific endeavor, and by promoting a competitive edge in the knowledge society of the information age. The ideas and initiatives described in this publication can stimulate anyone interested in open science research and innovation. It is designed to encourage debate and lead to new ideas on what and open society should do, should not do, or do differently.

An open society can lead to a research powerhouse; however, open society rarely succeeds in turning research into innovation and in getting research results to the global market. Open society must improve at making the most of its innovation talent, and that is where open innovation comes into play. The basic premise of open innovation is to open up the innovation process to all active players so that knowledge can circulate more freely and be transformed into products and services that create new markets while fostering a stronger culture of entrepreneurship. Open innovation is defined as the use of purposive inflows and outflows of knowledge to accelerate internal innovation. This original notion of open innovation was primarily based on transferring knowledge, expertise, and even resources from one company or research institution to another. This notion assumes that firms can and should use external ideas as well as internal ideas, and internal and external paths to market, as they seek to improve their performance. The concept of open innovation is continually evolving and is moving from linear, bilateral transactions and collaborations

## Open Science

towards dynamic, networked, multi-collaborative innovation ecosystems. This means that a specific innovation can no longer be seen as the result of predefined and isolated innovation activities but rather as the outcome of a complex co-creation process involving knowledge flows across the entire economic and social environment. This co-creation takes place in different parts of the innovation ecosystem and requires knowledge exchange and absorptive capacities from all the actors involved, whether businesses, academia, financial institutions, public authorities, or citizens.

Open innovation is a broad term, which encompasses several different nuances and approaches. Two main elements underpin the most recent conceptions of open innovation: the users are in the spotlight and invention becomes an innovation only if users become a part of the value creation process. Notions such as user innovation emphasize the role of citizens and users in the innovation processes as distributed sources of knowledge. This kind of public engagement is one of the aims of open science research and innovation. The term 'open' in these contexts has also been used as a synonym for 'user-centric'; creating a well-functioning ecosystem that allows co-creation and becomes essential for open innovation. In this ecosystem, relevant stakeholders are collaborating along and across industry and sector-specific value chains to co-create solutions for socio-economic and business challenges. One important element to keep in mind when discussing open innovation is that it cannot be defined in absolutely precise terms. It may be better to think of it as a point on a continuum where there is a range of context-dependent innovation activities at different stages, from research to development through to commercialization, and where some activities are more open than others. Open innovation is gaining momentum thanks to new large-scale trends such as digitalization and the mass participation and collaboration in innovation that it enables. The speed and scale of digitalization are accelerating and transforming the way one designs, develops, and manufactures products, the way one delivers services, and the products and services themselves. It is enabling innovative processes and new ways of doing business, introducing new cross-sector value chains and infrastructures.

Open society must ensure that it capitalizes on the benefits that these developments promise for citizens in terms of tackling societal challenges and boosting business and industry. Drawing on these trends, and with the aim of helping build an open innovation ecosystem in open society, the open society's concept of open innovation is characterized by:

- combining the power of ideas and knowledge from different actors to co-create new products and find solutions to societal needs
- creating shared economic and social value, including a citizen and user-centric approach
- capitalizing on the implications of trends such as digitalization, mass participation, and collaboration

In order to encourage the transition from linear knowledge transfer towards more dynamic knowledge circulation, experts agree that it is essential to create and support an open innovation ecosystem that facilitates the translation of knowledge into socio-economic value. In addition to the formal supply-side elements such as research skills, excellent science, funding and intellectual property management, there is also a need to concentrate on the demand side aspects of knowledge circulation, making sure that scientific work corresponds to the needs of the users and that knowledge is findable, accessible, interpretable and reusable. Open access to research results aims to make science more reliable, efficient, and responsive and is the springboard for increased innovation opportunities, e.g. by enabling more science-based startups to emerge. Prioritizing open science does not, however, automatically ensure that research results and scientific knowledge are commercialized or transformed into socio-economic value. In order for this to happen, open innovation must help to connect and exploit the results of open science and facilitate the faster translation of discoveries into societal use and economic value.

## **Open Science**

Collaborations with global partners represent important sources of knowledge circulation. The globalization of research and innovation is not a new phenomenon, but it has intensified in the last decade, particularly in terms of collaborative research, international technology production, and worldwide mobility of researchers and innovative entrepreneurs. Global collaboration plays a significant role both in improving the competitiveness of open innovation ecosystems and in fostering new knowledge production worldwide. It ensures access to a broader set of competencies, resources, and skills wherever they are located, and it yields positive impacts in terms of scientific quality and research results. Collaboration enables global standard-setting, allows global challenges to be tackled more effectively, and facilitates participation in global value chains and new and emerging markets.

To learn more, visit online at [waset.org](http://waset.org)

## Open Science

### Scholarly Research Review

The scholarly research review is a multidimensional evaluation procedure in which standard peer review models can be adapted in line with the ethos of scientific research, including accessible identities between reviewer and author, publishing review reports and enabling greater participation in the peer review process. Scholarly research review methods are employed to maintain standards of quality, improve performance, provide credibility, and determine suitability for publication. *Responsible Peer Review Procedure:* Responsible peer review ensures that scholarly research meets accepted disciplinary standards and ensures the dissemination of only relevant findings, free from bias, unwarranted claims, and unacceptable interpretations. Principles of responsible peer review:

- Honesty in all aspects of research
- Accountability in the conduct of research
- Professional courtesy and fairness in working with others
- Good stewardship of research on behalf of others

The responsibilities of peer review apply to scholarly researchers at all stages of peer review: Fairness, Transparency, Independence, Appropriateness and Balance, Participation, Confidentiality, Impartiality, Timeliness, Quality and Excellence, Professionalism, and Duty to Report.

#### *Scholarly Research Review Traits:*

- Scholarly Research Review Identities: Authors and reviewers are aware of each other's identity
- Scholarly Research Review Reports: Review reports are published alongside the relevant article
- Scholarly Research Review Participation: The wider academic community is able to contribute to the review process
- Scholarly Research Review Interaction: Direct reciprocal discussion between author(s) and reviewers, and/or between reviewers, is allowed and encouraged
- Scholarly Research Pre-review Manuscripts: Manuscripts are made immediately available in advance of any formal peer review procedures
- Scholarly Research Review Final-version Reviewing: Editorial revision of the language and format is conducted on the final version of the manuscript for publication
- Scholarly Research Review Platforms: The scholarly research review process is independent of the final publication of the manuscript and it is facilitated by a different organizational entity than the venue of publication

All submitted manuscripts are subject to the scholarly research review process, in which there are three stages of evaluation for consideration: pre-review manuscripts, chair-review presentation, and final-review manuscripts. All submitted full text papers, that may still be withstand the editorial review process, are presented in the conference proceedings. Manuscripts are tracked and all actions are logged by internal and external reviewers according to publication policy. External reviewers' editorial analysis consists of the evaluation reports of the conference session chairs and participants in addition to online internal and external reviewers' reports. Based on completion of the scholarly research review process, those manuscripts meeting the publication standards are published 10 days after the event date.

To learn more, visit online at [waset.org](http://waset.org)

## TABLE OF CONTENTS

1	Review and Comparison of Iran`s Sixteenth Topic of the Building with the Ranking System of the Water Sector Lead to Improve the Criteria of the Sixteenth Topic <i>O. Fatemi</i>	1
2	Technological Measures to Reduce the Environmental Impact of Swimming Pools <i>Fátima Farinha, Miguel J. Oliveira, Gina Matias, Armando Inverno, Jânio Monteiro, Cristiano Cabrita</i>	2
3	Characterization of a Three-Electrodes Bioelectrochemical System from Mangrove Water and Sediments for the Reduction of Chlordecone in Martinique <i>Malory Jonata</i>	6
4	Unsaturated Sites Constructed Grafted Polymer Nanoparticles to Promote CO <sub>2</sub> Separation in Mixed-Matrix Membranes <i>Boyu Li</i>	7
5	Ultimate Buckling Load Comparison With Eurocode 3 and Finite Element for Different Slenderness Ratio <i>Lahlou Dahmani, Warda Mekiri, Ahmed Boudjemia</i>	8
6	Operator Optimization Based on Hardware Architecture Alignment Requirements <i>Qingqing Gai, Junxing Shen, Yu Luo</i>	19
7	Performance Analysis and Optimization for Diagonal Sparse Matrix-Vector Multiplication on Machine Learning Unit <i>Qiuyu Dai, Haochong Zhang, Xiangrong Liu</i>	26
8	A Framework for Blockchain Vulnerability Detection and Cybersecurity Education <i>Hongmei Chi</i>	38
9	Molecular Dynamics Studies of Main Factors Affecting Mass Transport Phenomena on Cathode of Polymer Electrolyte Membrane Fuel Cell <i>Jingjing Huang, Nengwei Li, Guanghua Wei, Jiabin You, Chao Wang, Junliang Zhang</i>	39
10	Reuse of Wastewater After Pretreatment Under Teril and Sand in Bechar City <i>Sara Seddiki, Maazouzi Abdelhak</i>	48
11	Etude et investigation sur la pollution les macro déchets et les micro déchets de pastique dans le nord est Algérien (golfe d'Annaba). <i>HADJOU Mohamed Cherif</i>	54
12	Planning Quality and Maintenance Activities in a Closed-Loop Serial Multi-Stage Manufacturing System under Constant Degradation <i>Amauri Josafat Gomez Aguilar, Jean Pierre Kenné</i>	55
13	Stakeholder Mapping and Requirements Identification for Improving Traceability in the Halal Food Supply Chain <i>Laila A. H. F. Dashti, Tom Jackson, Andrew West, Lisa Jackson</i>	56
14	Sustainable Supply Chain Management Practices, Challenges, and Opportunities – A Case Study of Small and Medium-Sized Enterprises Within the Oil and Gas Sector <i>Igho Ekiugbo, Christos Papanagnou</i>	68
15	Simultaenous improved Performance in the Time Domain and in the Frequency Domain <i>Bensoussan David, Azeddine Ghodbane, Hammami Maher</i>	69
16	Improved Simultaneous Performance in the Time Domain and in the Frequency Domain <i>Azeddine Ghodbane, David Bensoussan, Maher Hammami</i>	70

17	Determination of Rotational and Vibrational Temperatures of a Non-Equilibrium Nitrogen Atmospheric Pressure Plasma Torch dedicated for Surface Treatment by Optical Emission Spectroscopy and Diatomic Molecular Spectra Simulation <i>V.E.Solofondrakotroka, Y.Cressault, M.Masquère, R.Rakotosaona, V.Ramarozatovo, R.Ramanantsoa</i>	76
18	LTE Modelling of a DC Arc Ignition on Cold Electrodes <i>O. Ojeda Mena, Y. Cressault, P. Teulet, J. P. Gonnet, D. F. N. Santos, MD. Cunha, M. S. Benilov</i>	77
19	Thermal and Dielectric Breakdown Criterium for Low Voltage Switching Devices <i>Thomas Merciris, Mathieu Masquere, Yann Cressault, Pascale Petit</i>	78
20	A new lemma of the Optical Equivalence Theorem: Analytical statement, applications and comparisons <i>Orchidea Maria Lecian</i>	79
21	Assessing the Physical Conditions of Motorcycle Taxi Stands and Comfort Conditions of the Drivers in the Central Business District of Bangkok <i>Nissa Phloimontri</i>	80
22	OPTICAL DRESSING OF N ATOMS BY A COHERENT EM FIELD <i>REUBEN SHUKER</i>	95
23	Understanding the Impact of Climate-Induced Rural-Urban Migration on the Technical Efficiency of Maize Production in Malawi <i>Innocent Pangapanga-Phiri, Eric Dada Mungatana</i>	96
24	The Optimal Production of Long-Beans in the Swamp Land by Application of Rhizobium and Rice Husk Ash <i>Hasan Basri Jumin</i>	97
25	Tenure Security, Agricultural Diversity and Food Security <i>Amanuel Hadera Gebreyesus</i>	101
26	Comparative Genomic Scan Reveals Milk Quality Traits in Ethiopian Begait Goat Breeds <i>Haile Berihulay, Yuehui Ma, Jiang lin, Jianlin Han</i>	102
27	Autopoiesis: Case Study New Perspectives for Online Art Therapy <i>Nárima Alemsan, Francisco Fialho</i>	103
28	Creating Inclusive Workplace Practices to Support Individuals with Dyslexia across the Employment Lifecycle; Perspectives from Employers, Managers and Employees with Dyslexia <i>Shae Wissell, Leila Karimi, Tanya Serry, Lisa Furlong, Judith Hudson</i>	108
29	The Reception of Caspar David Friedrich: A Case Study in the Contested Cultural Legacy of the German 19th Century <i>Zhaoyu Cheng</i>	110
30	Antibacterial Evaluation of Zn(II)-Porphyrin-Based Nanostructure: Bactericidal Effect From the Point of View of Nanoparticles Formation <i>Sajedeh Tehrani Nejad, Rahmatollah Rahimi, Sadegh Rostamnia, Mahboubeh Rabbani</i>	111
31	Conspiracy Theories Affecting Radicalization Trajectories: Anti-government Conspiracy Theories and Great Replacement Narratives on Telegram <i>Julius Brejohn Calvert</i>	112
32	The Effectiveness of Congressional Redistricting Commissions: A Comparative Approach Investigating the Ability of Commissions to Reduce Gerrymandering with the Wilcoxon Signed-Rank Test <i>Arvind Salem</i>	118
33	An Auxiliary Technique for Coronary Heart Disease Prediction by Analyzing Electrocardiogram Based on ResNet and Bi-Long Short-Term Memory <i>Yang Zhang, Jian He</i>	119
34	Assisted Prediction of Hypertension Based on Heart Rate Variability and Improved Residual Networks <i>Yong Zhao, Jian He, Cheng Zhang</i>	126



35	Twitter Ego Networks and the Capital Markets: A Social Network Analysis Perspective of Market Reactions to Earnings Announcement Events <i>Gregory D. Saxton</i>	132
36	Circular Economy Maturity Models: A Systematic Literature Review <i>Dennis Kreutzer, Sarah Müller-Abdelrazeq, Ingrid Isenhardt</i>	139
37	Design a circular business framework for the construction companies in the developing economies <i>Shreya Kanther</i>	155
38	Circular Economy: An Overview of Principles, Strategies, and Case Studies <i>Dina Mohamed Ahmed Mahmoud Bakr</i>	156
39	See No Evil: Corporate Environmental, Social and Governance Profile and EPS-Motivated Repurchases <i>Feng Zhao</i>	157
40	Circular Tool and Dynamic Approach to Grow the Entrepreneurship of Macroeconomic Metabolism <i>Maria Areias, Diogo Simões, Ana Figueiredo, Anishur Rahman, Filipa Figueiredo, João Nunes</i>	158
41	Business Intelligent to a Decision Support Tool for Green Entrepreneurship: Meso and Macro Regions <i>Anishur Rahman, Maria Areias, Diogo Simões, Ana Figueiredo, Filipa Figueiredo, João Nunes</i>	159
42	PLA Production from Multi Supply Lignocellulosic Biomass Residues: A Pathway for Agrifood Sector <i>Sónia Ribeiro, Diana Farinha, Hélia Sales, Rita Pontes, João Nunes</i>	160
43	Portuguese Pine Resin: The Economic and Activity Decline to a New Forestry and Biotechnology Approach <i>Carolina Nunes, Sónia Ribeiro, Hélio Faustinho, Hélia Sales, Rita Pontes, João Nunes</i>	161
44	Ecodesign of Bioplastic Films for Food Packaging and Shelf-life Extension <i>Sónia Ribeiro, Diana Farinha, Elsa Pereira, Hélia Sales, Filipa Figueiredo, Rita Pontes, João Nunes</i>	162
45	Policies for Circular Bioeconomy in Portugal: Barriers and Constraints <i>Ana Fonseca, Ana Gouveia, Edgar Ramalho, Rita Henriques, Filipa Figueiredo, João Nunes</i>	163
46	Agricultural Organized Areas Approach for Resilience to Droughts, Nutrient Cycle and Rural and Wild Fires <i>Diogo Pereira, Maria Moura, Joana Campos, João Nunes</i>	164
47	Designing a Model to Increase the Flow of Circular Economy Startups Using a Systemic and Multi-Generational Approach <i>Luís Marques, João Rocha, Andreia Fernandes, Maria Moura, Cláudia Caseiro, Filipa Figueiredo, João Nunes</i>	165
48	Teacher-Child Interactions within Learning Contexts in Prekindergarten <i>Angélique Laurent, Marie-Josée Letarte, Jean-Pascal Lemelin, Marie-France Morin</i>	166
49	Creating an Enabling Learning Environment for Learners with Visual Impairments Inlesotho Rural Schools by Using Asset-Based Approaches <i>Mamochana, A. Ramatea, Fumane, P. Khanare</i>	167
50	Exploring the Use of Universal Design for Learning to Support The Deaf Learners in Lesotho Secondary Schools: English Teachers Voice <i>Ntloyalefu Justinah, Fumane Khanare</i>	168
51	Teaching and Learning with Picturebooks: Developing Multimodal Literacy with a Community of Primary School Teachers in China <i>Fuling Deng</i>	169
52	The New World Kirkpatrick Model as an Evaluation Tool for a Publication Writing Programme <i>Eleanor Nel</i>	170
53	Threat Analysis: A Technical Review on Risk Assessment and Management of National Testing Service (NTS) <i>Beenish Urooj, Ubaid Ullah, Sidra Riasat</i>	171
54	Open Access in the Economic Sphere: A Framework Interpreting the Rise of the UK, US and China Different Historical Times <i>Guanghua Yu</i>	177

55	Place Attachment and Human Ethos: A Narrative-Integrative Review and an Attempt to Apply It to the Case of Residents of Jardim Pantanal <i>Adriano Francisco de Oliveira, Sandra Maria Patricio Ribeiro</i>	178
56	Evaluating Language Loss Effect on Autobiographical Memory by Examining Memory Phenomenology in Bilingual Speakers <i>Anastasia Sorokina</i>	179
57	Expanding Behavioral Crisis Care: Expansion of Psychiatric and Addiction-Care Services through a 23/7 Behavioral Crisis Center <i>Garima Singh</i>	180
58	Role of Tele-health in Expansion of Medical Care <i>Garima Singh, Kunal Malhotra</i>	181
59	Monitoring Public Attitudes Towards Tourism Valorisation of the Dinara Nature Park's Dry Grasslands <i>Sven Ratković</i>	182
60	Enhancing Archaeological Sites: Interconnecting Physically and Digitally <i>Eleni Maistrou, D. Kosmopoulos, Carolina Moretti, Amalia Konidi, Katerina Boulougoura</i>	183
61	Experimental Investigation of Air-Water Two-Phase Flow Pattern in T-Junction Microchannel <i>N. Rassoul-ibrahim, E. Siahmed, L. Tadrist</i>	184
62	A Case Report on the Multidisciplinary Approach on Rectal Adenocarcinoma in Pregnancy <i>Maria Cristina B. Cabanag, Elijinese Marie S. Culangen</i>	185
63	Microbiological Analysis of Polluted Water with Pesticides in Ben Mhidi (Northeastern of Algeria) <i>Aimeumadjet, Hammoudi Abd Erahmen, Bordjibaouahiba</i>	196
64	Collision Tumor of Plasmacytoma with Hematological and Non-Hematological Malignancies <i>Arati Inamdar, Siddharth Bhattacharyya, Kester Haye</i>	197
65	Size and Content of the Doped Silver Affected the Pulmonary Toxicity of Silver-Doped Nano-Titanium Dioxide Photocatalysts and the Optimization of These Two Parameters <i>Xiaoquan Huang, Congcong Li, Tingting Wei, Changcun Bai, Na Liu, Meng Tang</i>	198
66	USING FETPs TO SUPPORT nOPV CAMPAIGNS IN UGANDA <i>NICHOLAS AYEBAZIBWE</i>	199
67	The Effects of Whitening Toothpastes Containing Blue Covarine on the Discoloration of Resin Composites and Teeth <i>Elham Zajkani, Paria Faraji Dizaji, Saeideh Asdag</i>	200
68	Tracking of Intramuscular Stem Cells by Magnetic Resonance Diffusion Weighted Imaging <i>Balakrishna Shetty</i>	208
69	Burnout Prevalence and Contributing Factors among Healthcare Workers during the COVID19 Pandemic: Across-Sectional Survey Study in an Urban Community in Thailand <i>Jadsada Kunno, Busaba Supawattanabodee, Chavanant Sumanasrethakul, Budsaba Wiriyasirivaj, Pataraporn Yubonpunt</i>	209
70	Comparison the Effectiveness of Pain Cognitive- Behavioral Therapy and Its Computerized Version on Reduction of Pain Intensity, Depression, Anger and Anxiety in Children with Cancer: A Randomized Controlled Trial <i>Najmeh Hamid, Vajiheh Hamedy, Zahra Rostamianasl</i>	210
71	The Impact of Diseases and Epidemics in the Field of Medicine and Health in General <i>Bousseka Asma</i>	212
72	Improving Functionality of Radiotherapy Department Through: Systemic Periodic Clinical Audits <i>Kamal Kaushik, Trisha, Dandapni, Sambit Nanda, A. Mukherjee, S. Pradhan</i>	213
73	Bacterial Interactions of Upper Respiratory Tract Microbiota <i>Sarah Almuhayya, Andrew Mcbain, Gavin Humphreys</i>	214

74	Characterization of Soil Microbial Communities from Vineyard under a Spectrum of Drought Pressures in Sensitive Area of Mediterranean Region <i>Gianmaria Califano, Júlio Augusto Lucena Maciel, Olfa Zarrouk, Miguel Damasio, Jose Silvestre, Ana Margarida Fortes</i>	215
75	The Effect of Six Weeks Aerobic Training and Taxol Consumption on Interleukin 8 and Plasminogen Activator Inhibitor-1 on Mice with Cervical Cancer <i>Alireza Barari, Maryam Firoozi, Maryam Ebrahimzadeh, Romina Roohan Ardeshiri, Maryam Kamarloeei</i>	216

# Review and Comparison of Iran's Sixteenth Topic of the Building with the Ranking System of the Water Sector Lead to Improve the Criteria of the Sixteenth Topic

O. Fatemi

**Abstract**— Considering growing building construction industry in developing countries and sustainable development concept, as well as the importance of taking care of the future generations, codifying buildings scoring system based on environmental criteria, has always been a subject for discussion. The existing systems cannot be used for all the regions due to several reasons, including but not limited to variety in regional variables. In this article, the most important common LEED (Leadership in Energy and Environmental Design) and BREEAM (Building Research Establishment Environmental Assessment Method) common and Global environmental scoring systems, used in UK, USA, and Japan, respectively, have been discussed and compared with a special focus on CASBEE (Comprehensive Assessment System for Built Environment Efficiency), to credit assigning field (weighing and scores systems) as well as sustainable development criteria in each system. Then, converging and distinct fields of the foregoing systems are examined considering National Iranian Building Code. Furthermore, the common credits in the said systems not mentioned in National Iranian Building Code have been identified. These credits, which are generally included in well-known fundamental principles in sustainable development, may be considered as offered options for the Iranian building environmental scoring system. It is suggested that one of the globally and commonly accepted systems is chosen considering national priorities in order to offer an effective method for buildings environmental scoring, and then, a part of credits is added and/or removed, or a certain credit score is changed, and eventually, a new scoring system with a new title is developed for the country. Evidently, building construction industry highly affects the environment, economy, efficiency, and health of the relevant occupants. Considering the growing trend of cities and construction, achieving building scoring systems based on environmental criteria has always been a matter of discussion. The existing systems cannot be used for all the regions due to several reasons, including but not limited to variety in regional variables.

**Keywords**— scoring system, sustainability assessment, water efficiency, national Iranian building code.

# Technological Measures to Reduce the Environmental Impact of Swimming Pools

Fátima Farinha, Miguel J. Oliveira, Gina Matias, Armando Inverno,  
Jânio Monteiro, Cristiano Cabrita

**Abstract**—In the last decades, the construction of swimming pools for recreational activities has grown exponentially in southern Europe. Swimming pools are used both for private use in villas and for collective use in hotels or condominiums. However, they have a high environmental impact, mainly in terms of water and energy consumption, being used for a short period of time, depending significantly on favorable atmospheric conditions. Contrary to what would be expected, not enough research has been conducted to reduce the negative impact of this equipment. In this context, this work proposes and analyses technological measures to reduce the environmental impacts of swimming pools, such as thermal insulation of the tank, water balance in order to detect leaks and optimize the backwash process, integration of renewable energy generation, and a smart control system that meets the requirements of the user. The work was developed within the scope of the Ecopool+++ project, which aims to create innovative heated pools with reduced thermal losses and integration of SMART energy plus water management systems. The project is in the final phase of its development, with very encouraging results.

**Keywords**—Swimming Pools, Sustainability, Thermal Losses, Water Management System.

## I. INTRODUCTION

OUTDOOR swimming pools are attractive equipment, that are very common in villas, condominiums and touristic facilities, in southern European countries, like Portugal, Spain, Italy, Cyprus and Malta. In summer months the high temperatures and solar radiation stimulates outdoor activities and in contact with water. These pools are normally used for short periods of the year, dependent from good weather conditions in the summer period (4-5 months). Beyond these months, in order to increase the periods of utilization, the water is commonly heated, with high costs and environmental impact.

In terms of water losses and energy consumption, these are mainly caused by: 1) evaporation of water into the surrounding air, 2) radiation to the sky; 3) convection near the surface of the water and 4) conduction through the walls and floor to the ground.

In this context, the objectives of the Ecopool+++ project - *Innovative heated pools with reduced thermal losses and*

*integration of SMART energy plus water management systems* [1] are to find solutions to: (i) mitigate water leakage, (ii) minimize energy losses, (iii) integrate renewable energy generation & thermal storage systems and (iv) develop and test predictive and intelligent control systems for energy and water management, contributing to the sustainability of these equipment and the maximization of their utilization throughout the year.

The rest of this paper has the following structure. Section II presents the state of the art in terms of solutions that allow water and energy conservation. Section III describes the proposed technological measures that allow reducing the environmental impact of swimming pools and section IV concludes the paper.

## II. STATE OF THE ART SOLUTIONS FOR WATER AND ENERGY CONSERVATION

The Architecture, Engineering and Construction (AEC) sector has seen very significant developments over the last years. The project and construction of swimming pools require a high level of expertise [2]. The negative environmental impacts of the sector are recognized, which in turn require an increase for technological solutions to improve the environmental performance and to ensure attaining to the Sustainable Development Goals (SDGs) of the United Nations [3].

In swimming pools, water and energy consumption have a high environmental impact. The control of energy losses, avoiding water temperature reduction and the control of water consumption are the biggest challenges.

In swimming pools, energy losses are mainly due to walls and floor's conduction and evaporation process. In buildings, the envelope is, nowadays, thermally insulated with materials, such as, XPS - extruded polystyrene plates, EPS - expanded polystyrene insulation or ICB - Expanded cork agglomerate.

At this level, Rose [4] proposes, thermal insulation of the interior walls and floor of the tank, using rigid phenolic panels (high pressure laminates) or cellular glass (FOAMGLAS), together with a rigid waterproof mortar and PVC coating. Unfortunately, it was not possible to find detailed information regarding its effective thermal performance, mechanical strength, and durability/longevity.

The evaporation process causes both heat and water losses. To minimize these losses, a surface coverage of the water is a relevant measure whose performance is dependent on the solution chosen and the number of hours of coverage (this is very dependent on the simplicity of its utilization). Using a

F. F., is with Universidade do Algarve and C-Made, Campus da Penha 8005-139 Faro Portugal (corresponding author, phone:+351-919364990; e-mail: mfarinha@ualg.pt).

M. O., A. I., J. M., C. C., are with Universidade do Algarve, Campus da Penha 8005-139 Faro Portugal (e-mail: mjoliv@ualg.pt; ainverno@ualg.pt; jmmonte@ualg.pt; ccabrita@ualg.pt).

G. M., is with Universidade de Coimbra, CERIS/Itecons, Rua Pedro Hispano, 3030-289 Coimbra, Portugal (e-mail: ginamatias@itecons.uc.pt).

cover that is transparent to solar radiation allows heat gains in the water, even during the periods that it is covered.

Security is another important function of a surface cover of the water. For that it needs to be resistant to support a children's weight.

The evaporation process is also very dependent on the intensity of the wind - since the wind is the motor for convection and evaporation heat losses. To minimize them a water surface cover and tree barriers or walls can be used.

Water and energy losses also result from filter backwashing, since the water required for it is normally lost. Part of the heat, and thus energy [5], [6], [7], [8], can still be recovered if a wastewater's heat recovery device is used. A tank to store the wastewater can also be used to allow using this water for a garden's irrigation or outdoor washing [9].

Electricity generation from renewable energy sources, such as, solar, wind, geothermal, have a great potential for heating swimming pools directly or through heat pumps. At this level, Ribeiro et al. [10] focuses on the use of intelligent control systems to perform demand control on indoor pools. In it, the integration of renewable energy systems combined with a Building Energy Management Systems (BEMS) have shown to support a great potential to reduce electricity and thermal costs.

### III. TECHNOLOGICAL MEASURES TO REDUCE THE ENVIRONMENTAL IMPACT

In the scope of the Ecopool+++ project, several technological measures are being studied to reduce the environmental impact of outdoor swimming pools.

One of the measures includes the adoption of a thermal insulation system, inside the pool, with the analysis of different thermal insulation materials, such as: XPS (Extruded polystyrene insulation), EPS (Expanded polystyrene insulation) or ICB (Expanded cork agglomerate), their thicknesses and connection between layers (Fig. 1).

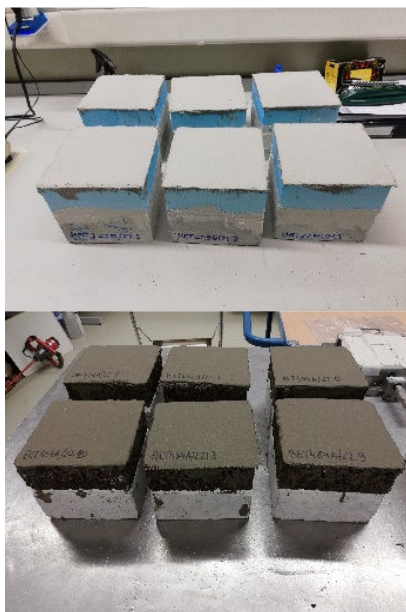


Fig. 1 Thermal insulation systems. Lab tests: (a) XPS (b) ICB  
A simulation model of the water balance is also considered, to allow a leak detection system. An optimizing system for the backwash process (as shown in Figs. 2 and 3). The reutilization

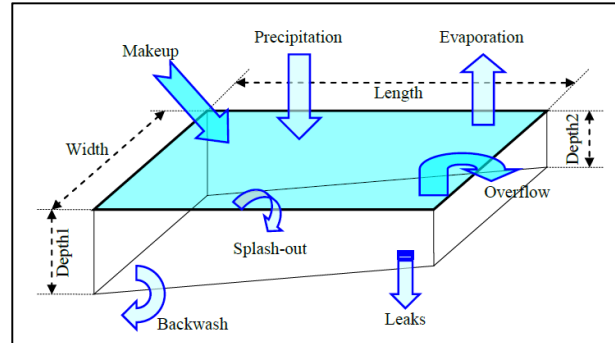


Fig. 2 Water balance (adapted [9])

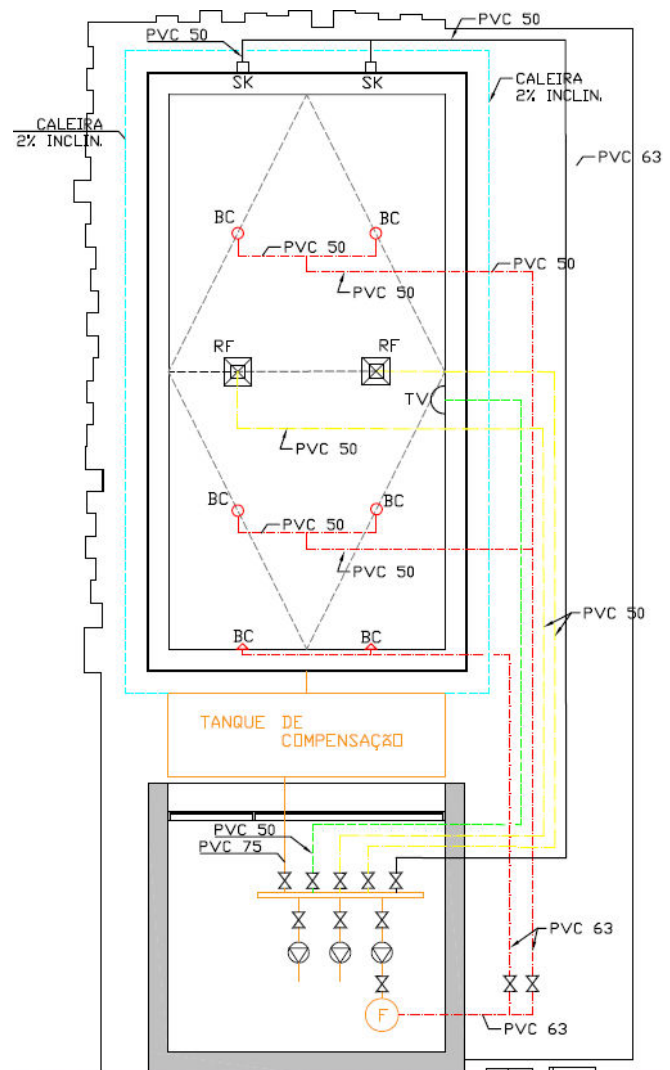


Fig. 3 Hydraulic circuit



of water for the washing and/or irrigation of the surroundings spaces.

The project also includes a study and design of renewable energy systems including solar collectors, Phase-change material (PCM), and PC-Ground. The application of these solutions depend on the location of the outdoor swimming pool (Fig. 4).

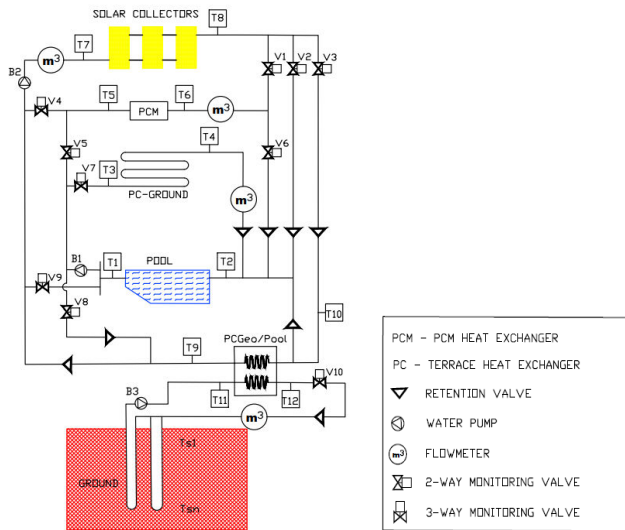


Fig. 4 Renewable energy system

All the equipment, including the thermal insulation system, water surface coverage, renewable energy systems, among others, were numerical modelled, allowing their simulation in terms of thermal and mechanical performance. It also allows the optimization of the final solutions to be considered.

The control procedure is summarized by Fig. 5. The control principle is identical to the ON/OFF control with hysteresis, which is to establish a  $\Delta T$  around a reference or desired value,  $T_{setpoint}$ . When the observed water temperature (decreasing) reaches a value below the  $T_{setpoint} - \Delta T/2$ , the control signal turns to the ON state, which translates to switching on the solenoid valves. If the observed temperature (ascending) reaches a value above  $T_{setpoint} + \Delta T/2$ , the control signal switches to OFF state meaning the solenoid valves are turned off. When the observed temperature reaches the value of  $(T_{setpoint} + \Delta T/2)$  and the temperature of the water at the outlet of the solar collectors is higher than the water in the tank, the water is circulated through the geothermal subsystem, so that it retains the excess energy.

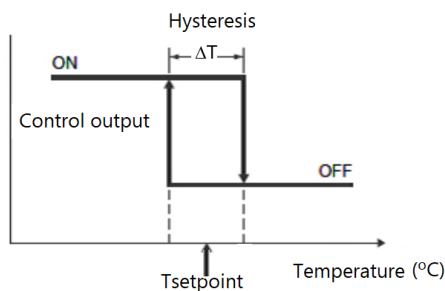


Fig. 5 Control scheme applied

Fig. 6, shows the results of a simulation of the SMART control system, considering a setpoint temperature of 25°C, a  $\Delta T=2^\circ\text{C}$  and solar collectors with an area of 50 m<sup>2</sup>. Two simulations are shown for different sets of months.

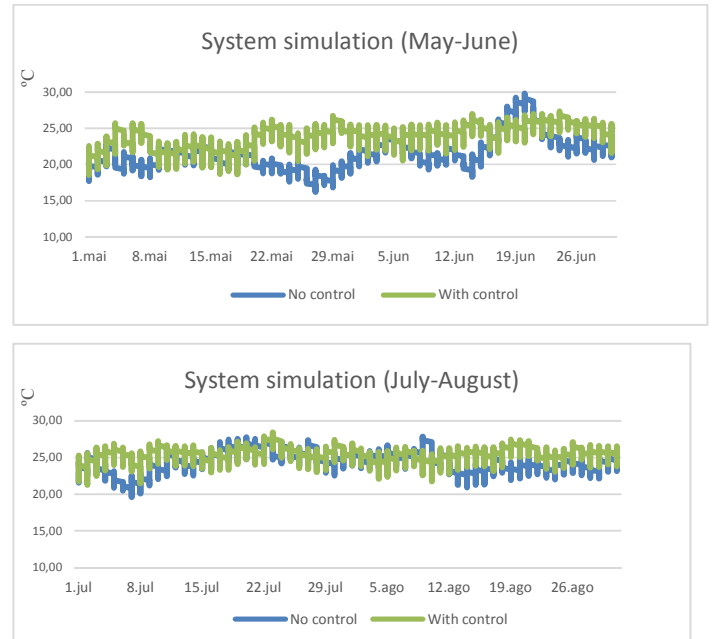


Fig. 6 Numerical modelling control for a setpoint of 25°C,  $\Delta T=2^\circ\text{C}$  and solar collectors with an area of 50m<sup>2</sup>. Top plot: simulation for the months of May and June. Bottom plot: simulation for the months of July and August

The project also integrates a SMART monitor and control system for the integrated management of the various systems (Fig. 7).

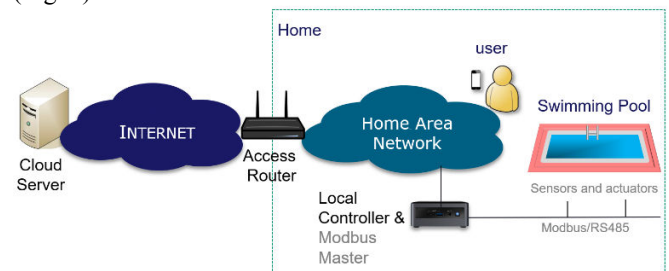


Fig. 7 SMART platform

#### IV. CONCLUSION

Oliveira et al [11], in a study carried out in the Algarve region, reported that 72% of swimming pools have no water surface coverage and 65% of pools have no water heating system. The coverage not only guarantees the safety of users, in particular children, but also limits water losses through evaporation, while minimizing heat losses. The non-existence of a water heating system means that the use of the pool is restricted to the period when the water temperature is satisfactory, which depends on the existence of very good climatic conditions, which in southern Europe is normally

limited to the summer period.

Nowadays there are a significant set of technological measures, used in other sectors, which properly operationalized can decisively contribute to reducing the negative environmental impact of swimming pools. Laboratory testing and construction of sustainable swimming pools is the way forward. The use of thermal isolating materials inside the tank, water coverage systems, automatic control of filtering system and water leakage, integration of renewable energy sources and intelligent control of the whole system, reflecting user preferences, are some of the technological measures that are being developed and tested by Ecopool+++ project.

#### ACKNOWLEDGMENT

The project ECOPOOL+++ is funded by FEDER, PROJETOS DE I&DT EMPRESAS EM COPROMOÇÃO, Programa Operacional Regional do Algarve, contact n. ALG-01-0247-FEDER-047231. The professional expertise and valuable cooperation of all the partners are gratefully acknowledged.

#### REFERENCES

- [1] "ECOPOOL+++ - Piscinas aquecidas inovadoras com redução de perdas térmicas e integração de sistemas de gestão energética e hídrica SMART". <https://www.itecons.uc.pt/services/projects/103?locale=en> (accessed January 17 2023).
- [2] Oliveira, M.J., Farinha, F., Inverno, A., Monteiro, J., Cabrita, C., Venturinha, A. (2022). Sustainability Challenges in Outdoor Swimming Pools. In: Bienvenido-Huertas, D., Moyano-Campos, J. (eds) *New Technologies in Building and Construction. Lecture Notes in Civil Engineering*, vol 258. Springer, Singapore. [https://doi.org/10.1007/978-981-19-1894-0\\_18](https://doi.org/10.1007/978-981-19-1894-0_18).
- [3] The 17 Goals. United Nations. Sustainable Development <https://sdgs.un.org/goals> (accessed January 17, 2023).
- [4] N. P. Rose, Method of thermal insulation of a pool, US patent 2007/0180603 A1, 2007. Available: <https://patents.google.com/patent/US20070180603>.
- [5] Culha, O.; Gunerhan, H.; Biyik, E.; Ekren, O.; Hepbasli, A. Heat exchanger applications in wastewater source heat pumps for buildings: A key review. *Energy Build.* 2015, 104, 215–232.
- [6] Shen, C.; Lei, Z.; Wang, Y.; Zhang, C.; Yao, Y. A review on the current research and application of wastewater source heat pumps in China. *Therm. Sci. Eng. Prog.* 2018, 6, 140–156.
- [7] Ferreira, A.; Ribeiro, B.; Marques, P.; Ferreira, A.; Dias, A.; Pinheiro, H.; Reis, A.; Gouveia, L. *Scenedesmus obliquus* mediated brewery wastewater remediation and CO<sub>2</sub> bio fixation for green energy purposes. *J. Clean. Prod.* 2017, 165, 1316–1327.
- [8] Piwowar, A.; Dzikuć, M. Development of renewable energy sources in the context of threats resulting from low-altitude emissions in rural areas in Poland: A Review. *Energies* 2019, 12, 3558.
- [9] J. G. Lee and J. P. Heaney, "Measure 4: Swimming Pool Water Use Analysis by Observed Data and Long-Term Continuous Simulation". Conserve Florida Water Clearinghouse Department of Environmental Engineering Sciences, University of Florida: Gainesville, FL, USA. 2008, 25pp. <https://www.academia.edu/49408183> (accessed January 17 2023).
- [10] Ribeiro, Eliseu Manuel Artilheiro, Humberto Manuel Matos Jorge, and Divo Augusto Alegria Quintela. "Control of Indoor Swimming Pools with Potential for Demand Response." *Journal of Energy and Power Engineering* 8.1 (2014): 20.
- [11] Oliveira M.J. et al. (2020) Common Typology, Durability and Pathologies of the Swimming Pools in the Algarve Region - Implications in the Sustainability. In: Monteiro J. et al. (eds) *INCREaSE 2019. INCREaSE 2019*. Springer, Cham. [https://doi.org/10.1007/978-3-030-30938-1\\_70](https://doi.org/10.1007/978-3-030-30938-1_70).

# Characterization of a Three-Electrodes Bioelectrochemical System from Mangrove Water and Sediments for the Reduction of Chlordecone in Martinique

M. Jonata, F. Robert, P. Salvin

**Abstract**— Chlordecone (CLD) is an organochlorine pesticide used between 1971 and 1993 in both Guadeloupe and Martinique for the control of banana black weevil. The bishomocubane structure which characterizes this chemical compound led to high stability in organic matter and high persistence in the environment. Recently, researchers found that CLD can be degraded by isolated bacteria consortium and, particularly, by bacteria such as *Citrobacter* sp 86 and *Delsulfovibrio* sp 86. Actually, six transformation products families of CLD are known. Moreover, latest discover showed that CLD was disappearing faster than firstly predicted in high contaminated soil in Guadeloupe. However, toxicity of transformation products is still unknown, and knowledge has to be deepen on degradation ways and chemical characteristics of chlordecone and its transformation products.

Microbial fuel cells (MFC) are electrochemical systems that can convert organic matters into electricity thanks to electroactive bacteria. These bacteria can exchange electrons through their membranes to solid surfaces or molecules. MFC had proven their efficiency as bioremediation systems in water and soils. They are already used for bioremediation of several organochlorine compounds such as perchlorate, trichlorophenol or hexachlorobenzene. In this study, a three-electrodes system, inspired of MFC, is used to try to degrade chlordecone using bacteria from mangrove swamp in Martinique. As we know, some mangrove bacteria are electroactives. Furthermore, CLD rate seems to decline in mangrove swamp sediments. This study aims to prove that electroactive bacteria from mangrove swamp in Martinique can degrade CLD thanks to a three-electrodes bioelectrochemical system.

To achieve this goal, the tree-electrodes assembly have been connected to a potentiostat. The substrate used is mangrove water and sediments, sampled in mangrove swamp of La Trinité, a coastal city in Martinique, where CLD contamination have already been study. Electroactive biofilms are formed by imposing a potential relative to Saturated Calomel Electrode using chronoamperometry. Moreover, their comportment has been studied by using cyclic voltametry. Biofilms have been studied under different imposed potential, several condition of substrate and with or without CLD.

In order to quantify the evolution of CLD rates in the substrate's system, gas chromatography coupled with mass spectrometry (GC-MS) was performed on pre-treated samples of water and sediments, after a short, medium and long term contact with the electroactive biofilms.

Results showed that between -0,8V and -0,2V the three-electrodes system was able to reduce chemical in substrate solution. The first GC-MS analysis result of samples spiked with CLD seem to reveal decreased CLD concentration over time.

In conclusion, the designed bioelectrochemical system can provide the necessary conditions to chlordecone degradation. Though it is necessary to improve three-electrodes control settings in order to increase degradation rates. The biological pathways are yet to enlighten by biologicals analysis of electroactive biofilms formed in this system. Moreover, the electrochemical study of mangrove substrate gives new informations on the potential use of this substrate for bioremediation. But further studies are needed to a better understanding of the electrochemical potential of this environment.

**Keywords**— Bioelectrochemistry, Bioremediation, Chlordecone, Mangrove swamp.

M. Jonata, Phd student in the Science and Environmental Technology department, French West Indies University, Schoelcher, 97233, Martinique (phone: +33 650 036 011; e-mail: Malory.Beaujolais@etu.univ-antilles.fr).

F. Robert, is with the Science and Environmental Technology department, French West Indies University, Schoelcher, 97233, Martinique (e-mail: florent.robert@univ-antilles.fr).

P. Salvin is with the Science and Environmental Technology department, French West Indies University, Schoelcher 97233, Martinique (email: paule.salvin@martinique.univ-ag.fr)

# Unsaturated Sites-prepared Polymer Nanoparticles Embedded Mixed Matrix Membranes for Highly Efficient CO<sub>2</sub> Separation

<sup>a</sup> State Key Laboratory of Pollution Control and Resource Reuse, College of Environmental Science and Engineering, Tongji University, 1239 Siping Road, Shanghai, 200092, China

<sup>b</sup> Shanghai Institute of Pollution Control and Ecological Security, Shanghai, 200092, China

## Abstract

Mixed matrix membranes (MMMs), as a separation technology, can improve CO<sub>2</sub> recycling efficiency and reduce the environmental impacts associated with huge emissions. Nevertheless, many challenges must be overcome to design excellent selectivity and permeability performance MMMs. Herein, this work demonstrates the design of nano-scale GNPs (Cu-BDC@PEG) with strong compatibility, and high free friction volume (FFV) is an effective way to construct non-interfacial voids MMMs with a desirable combination of selectivity and permeability. Notably, the FFV boosted thanks to the chain length and shape of the GNPs. With this, the permeability and selectivity of Cu-BDC@PEG/PVDF MMMs had also been significantly improved. As such, compatible Cu-BDC@PEG proves very efficient for resolving challenges of MMMs with poor compatibility on the basis of the interfacial defect. Poly (Ethylene Glycol) (PEG) with oxygen groups can be finely coordinated with Cu-MOFs to disperse Cu-BDC@PEG homogeneously and form hydrogen bonds with matrix to achieve continuous phase. The resultant MMMs exhibited a simultaneous enhancement of gas permeability (853.1 Barrer) and ideal CO<sub>2</sub>/N<sub>2</sub> selectivity (41.7), which has surpassed Robeson's upper bound. Moreover, Cu-BDC@PEG/PVDF has a high-temperature resistance and a long time sustainably. This attractive separation performance of Cu-BDC@PEG/PVDF offered an exciting platform for the development of composite membranes for sustainable CO<sub>2</sub> separations.

**Keywords:** CO<sub>2</sub> separation; Metal organic frameworks; Polymer; Mixed matrix membrane.

# Comparative Study Between Numerical and Analytical Buckling Analysis of a Steel Column with Various Slenderness Ratio

W. Mekiri, A. Boudjemia, L. Dahmani

*Common hot rolled and built-up steel members used for carrying axial compression, usually fail by flexural buckling. The buckling strength of these members is affected by residual stresses, initial bow and accidental eccentricities of load. In this paper the ultimate buckling load of a steel column is calculated by the use of eurocode design buckling curves with a different slenderness ratio. The obtained results are then compared to those obtained by a finite element simulation by means of a geometrical and material non-linear analysis on a column including imperfections.*

**Keywords:** Ansys , Linear buckling, Eigen value, Nonlinear buckling, Eurocode 3, Slenderness ratio, Steel column.

**Introduction.** The key parameter in structural steel column design is the buckling phenomenon [1]–[4]. Steel columns subjected to compression load about their minor axis may develop buckling of the element. In slender columns, buckling can govern their ultimate limit state.

A short column with a compact cross section can reach its full plastic capacity without any buckling. However, if the column is slender, a different phenomenon occurs. As the column is loaded in compression about its weak axis, it deforms in the direction of loading, but after buckling it demonstrates an angular deformation (Fig. 1).

The buckling capacity depends upon a number of material and geometric properties, support conditions and slenderness ratio.

In order to calculate the buckling resistance of a laminated cross section shown in a figure 1, different approaches were used:

- 1- Linear buckling analysis (Euler approach);
- 2- Numerical Eigen-value theory with ANSYS[5] ;
- 3- Eurocode design buckling curves [6];
- 4- Nonlinear buckling analysis, using ANSYS.

**1. Finite element analysis of buckling.** The structural steel column become unstable according to the critical buckling load. The buckled mode shape associated with each load is the shape that the structure assumes in a buckled condition. There are three primary means to perform a buckling analysis:

**1.1. Eigenvalue.** Linear-buckling analysis is also called eigenvalue buckling or Euler buckling analysis because it predicts the theoretical buckling strength of an elastic structure. Eigenvalues are values of load at which buckling takes place. Eigenvectors are buckling shapes associated with the corresponding eigenvalues.

However, in real-life, structural imperfections, residual stresses and nonlinearities prevent most real-world structures from reaching their eigenvalue predicted buckling strength; i.e. the prediction of the expected buckling load is over estimated. Nonlinear buckling analysis is the best and realistic way to predict the buckling load.

**Notation:** The force value is only a magnitude of 1 because eigenvalues are calculated by a factor of the load applied, so having a force of 1 will make the eigenvalue answer equal to the critical load.

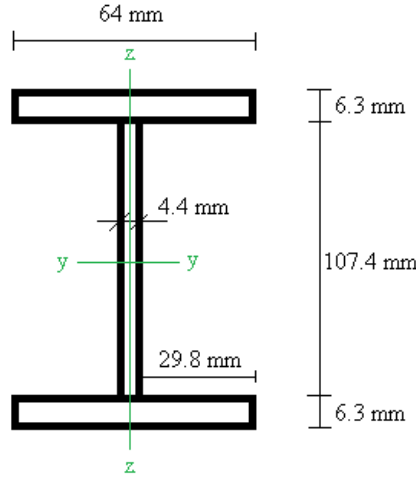


**Fig.1:** Geometrical properties of the cross section.

$$I_{yy} = 306.32 \text{ cm}^4 ; \quad I_{zz} = 27.60 \text{ cm}^4 ; \quad I_{\min} = I_{zz} = 27.60 \text{ cm}^4$$

$$I_{zz} = 2 \times \frac{0.63 \times 6.4^3}{12} + \frac{10.74 \times 0.44^3}{12} = 27.60 \text{ cm}^4$$

$$i_{\min} = \sqrt{\frac{I_{\min}}{A}} = \sqrt{\frac{27.60}{12.7896}} = 1.47 ; \quad \lambda = \frac{l}{i} ; \quad l = 2l_0 \text{ (buckling length)}$$

$$\lambda_1 = \pi \sqrt{\frac{E}{f_y}} = 93.9 \varepsilon = 93.9 \quad \text{avec : } \varepsilon = \sqrt{\frac{235}{f_y}} = 1.0 \text{ (S235)}$$

$$N_{cr} = \frac{\pi^2 EI_{zz}}{(kl_0)^2} = \frac{\pi^2 \times 2.1 \times 10^7 \times 27.60}{(2 \times 150)^2} = 63560.2 \text{ N}$$

**1.2. Linear buckling analysis with ANSYS.** The theoretical buckling strength of an ideal elastic structure predicted by the Eigen-value buckling analysis is computed by the use of Ansys software for the different slenderness ratio. For this numerical approach, we used a finite BEAM 188 element. BEAM 188 is a linear elastic finite element, with three degrees of freedom (axial and transversal displacement and also nodal rotation). The material behavior is considered elastic, which means that the elastic modulus should be considered equal to 200.000 Mpa (N/mm<sup>2</sup>) and the Poisson coefficient equal to 0.3. The Eigen-value solver uses a unit force to determine the necessary buckling load. Applying a load other than 1 will scale the result by a factor dependent on load level. Buckling is inherently nonlinear, but we linearize the problem through the Eigen-value method. The absence of imperfections and nonlinearities led to the overestimate of theoretical values. We model the beam with 2D elements.



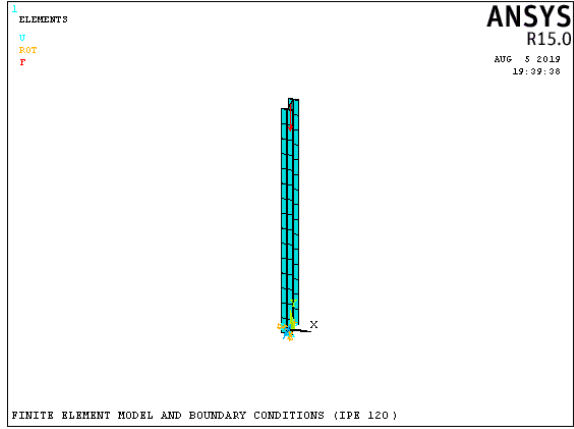
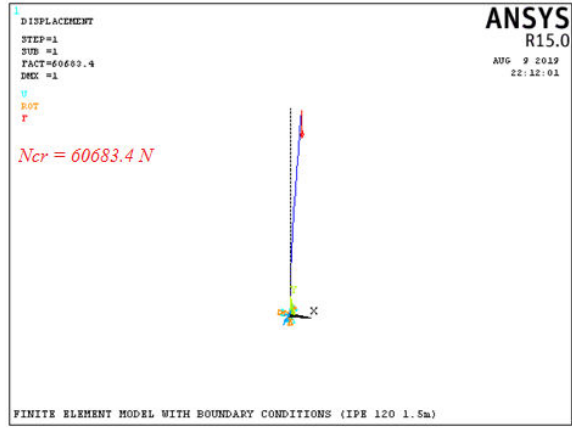
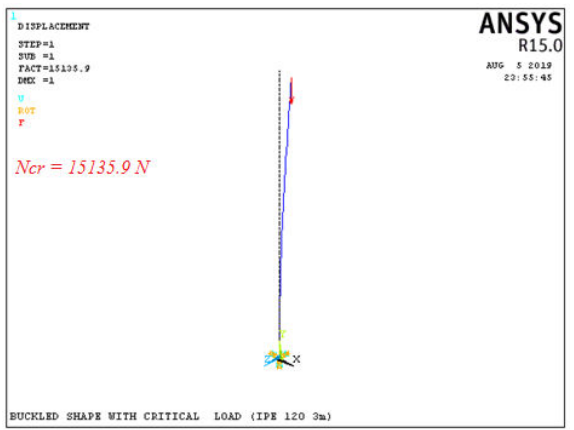
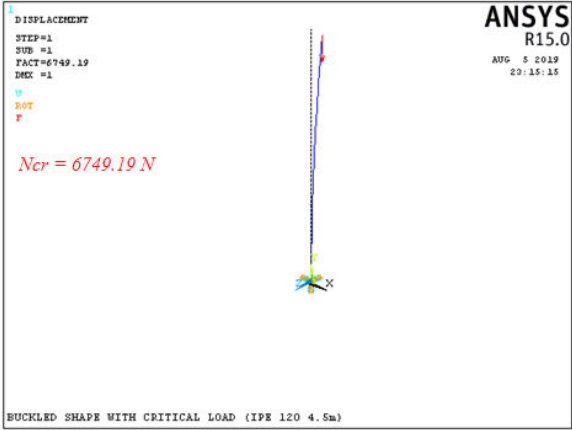
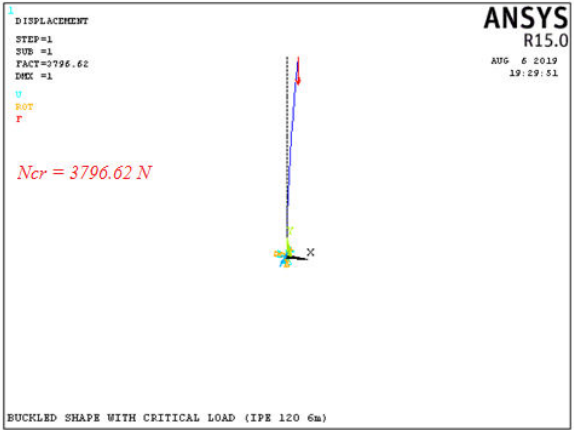
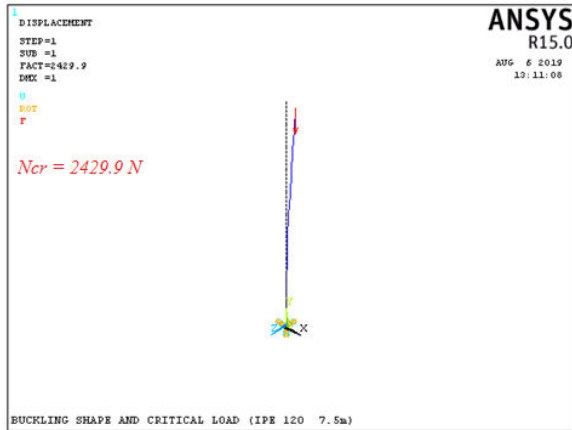


Fig.2: Finite element model

Fig.3: Eigenvalue buckling load ( $l = 1.5m$ )Figure 4. Eigenvalue buckling load ( $l = 3.0m$ )Figure 5. Eigenvalue buckling load ( $l = 4.5m$ )Fig.6: Eigenvalue buckling load ( $l = 6.0m$ )Fig.7: Eigenvalue buckling load ( $l = 7.5m$ )

**2. Theoretical aspect of buckling.** Euler was the first in the eighteenth century to formalize the buckling problem and to determine the limit value of compressive force that separates the two structural behaviors of the column. This theoretical limit value of the compressive force is called the Euler critical load.

The general critical Euler load  $N_{cr}$  for a compressed component, (figure 1) is given by the expression:

$$N_{cr} = \frac{\pi^2 EI}{(kl_0)^2} \quad (1)$$

Where :

$E$  : Young modulus.

$I$  : Moment of inertia of the column section with respect to the buckling plan.

$l_0$  : Element length.

$k$  : is a coefficient allowing to define an equivalent buckling length to that of a simply supported column .

Tests on actual sections show that buckling always occurs at loads below Euler's critical load. This result is explained by the presence of geometric imperfections and residual stresses resulting from the manufacturing and assembly process. However, Euler's theory has the merit of highlighting the essential geometrical parameter of the phenomenon: slenderness parameter  $\lambda$  . Indeed, the critical Euler stress deduced from the relation above makes the slenderness parameter  $\lambda$  to appear.

If  $A$  define the section area of the column, The Euler critical stress will be:

$$\sigma_{cr} = \frac{N_{cr}}{A} = \frac{\pi^2 E I}{l^2 A} = \frac{\pi^2 E}{l^2} i^2 = \frac{\pi^2 E}{\lambda^2} \quad (2)$$

with  $i = \sqrt{\frac{I}{A}}$  radius of gyration of the column section in the buckling plan.

$\lambda = \frac{l}{i}$  element slenderness.

**3.1- Approximate results using eurocode design buckling curves (Fig.10), [6].** In order to compare the results of the various tests, the relation (2) is rendered dimensionless by introducing a particular value of  $\lambda$  ,  $\lambda_1$  which gives a critical Euler stress equal to the elastic limit (Figures 8 and 9):

$$f_y = \frac{\pi^2 E}{\lambda_1^2} \quad (3)$$

By dividing equation (2) by equation (3) member to member, we obtain:

$$\chi = \frac{\sigma_{cr}}{f_y} = \frac{\frac{\pi^2 E}{\lambda^2}}{\frac{\pi^2 E}{\lambda_1^2}} = \frac{1}{\bar{\lambda}^2} \text{ or } \bar{\lambda} = \lambda / \lambda_1 \quad (4)$$

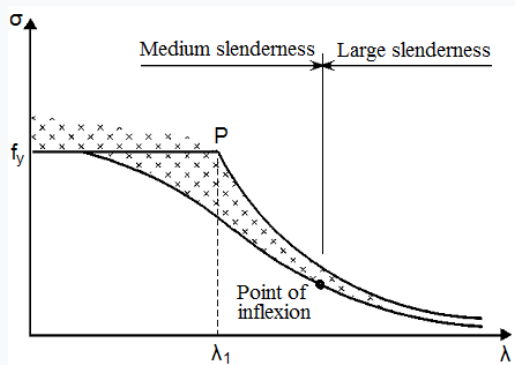


**Fig.8:** Real column test results and buckling curves.

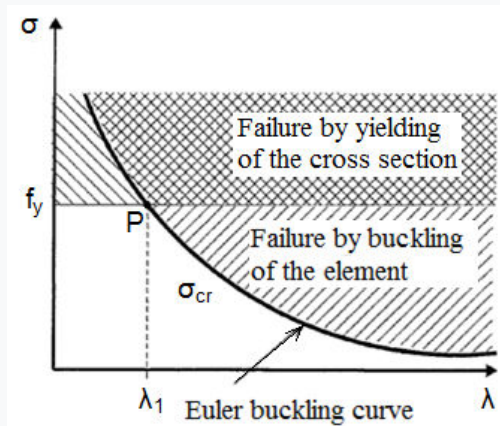


**Fig.9:** Euler buckling curve and modes of failure

Eurocode 3 [6], is required for the design of steel structures or elements of steel structures. The stability of the compression member will be checked against buckling phenomena with the following inequality formula.

$$\frac{N_{E.d}}{N_{b.Rd}} \leq 1.0 \quad (5)$$

$N_{E.d}$  is the compression force and  $N_{b.Rd}$  is the buckling resistance of the compression member.

The design resistance to normal forces of the cross-section for uniform compression  $N_{c.Rd}$  is then computed with equation 6 in order to be normalized with the buckling resistance value  $N_{b.Rd}$ .

$$N_{c.Rd} = \frac{A \cdot f_y}{\gamma_{M0}} \quad (6)$$

The design buckling resistance of the compression member,  $N_{b.Rd}$ , may be calculated according to next equation.

$$N_{b.Rd} = \chi \frac{A f_y}{\gamma_{M1}} \quad (7)$$

Where  $\chi$  is the reduction factor for the relevant buckling mode, and should be determined as function of the appropriate non-dimensional slenderness  $\bar{\lambda}$ .

$$\chi = \frac{1}{\phi + [\phi^2 - \bar{\lambda}^2]^{0.5}} \quad (8)$$

The intermediate factor  $\phi$  should be determined according to:

$$\phi = 0.5 \left[ 1 + \alpha(\bar{\lambda} - 0.2) + \bar{\lambda}^2 \right] \quad (9)$$

Where the non dimensional slenderness for class 1, 2 and 3 cross sections is calculated by:

$$\bar{\lambda} = \sqrt{\frac{A f_y}{N_{cr}}} \quad (10)$$

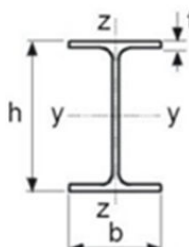
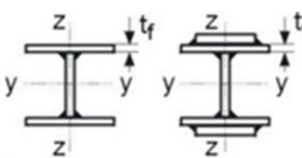
The imperfection factor  $\alpha$  corresponding to the appropriate buckling curve should be obtained from the Tables 1 and 2.

Imperfection factor  $\alpha$  :

Buckling axis zz:  $\frac{h}{b} = \frac{120}{64} = 1.875 > 1.2 \rightarrow$  buckling curve (b) **(Table 1)**

$\alpha_z = 0.34$  **(Table 2)**

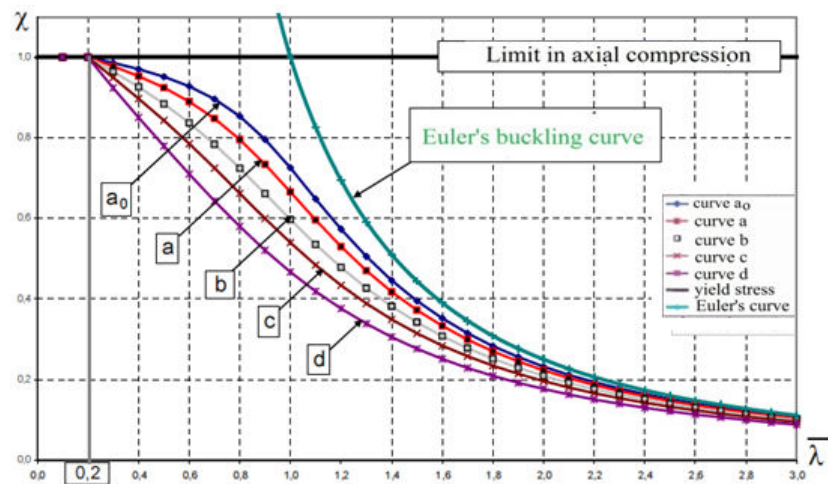
**Table 1.** Selection of appropriate buckling curve for a cross-section. [1]

Cross section	Limits	Buckling about axis	Buckling curve
Rolled I section 	$h/b > 1.2$ $t_f \leq 40 \text{ mm}$	y – y z – z	a b
	$40 \text{ mm} < t_f \leq 100 \text{ mm}$	y – y z – z	b c
	$h/b \leq 1.2$ $t_f \leq 100 \text{ mm}$	y – y z – z	b c
	$t_f > 100 \text{ mm}$	y – y z – z	d d
Welded I section 	$t_f \leq 40 \text{ mm}$	y – y z – z	b C
	$t_f > 40 \text{ mm}$	y – y z – z	c d

For other cases: see Table 6.2 of the Eurocode 3.

**Table 2.** Imperfection factor  $\alpha$  for each buckling curve.[6]

Buckling curve	a <sub>0</sub>	a	b	c	d
Imperfection factor	0.13	0.21	0.34	0.49	0.76

**Fig.10:** European buckling curves [6]

The force value is only a magnitude of 1 because eigenvalues are calculated by a factor of the load applied, so having a force of 1 will make the eigenvalue answer equal to the critical load.

**3. Geometry and material non-linear analysis, using ANSYS.[5]** Buckling, or the loss of stability when the load reaches a certain critical value, is caused by geometrically nonlinear effects. In order to predict accurately the buckling load it's more realistic to use a nonlinear buckling analysis which gives a better result than the linear one. Most physical structures will contain imperfections that will cause buckling well below theoretical buckling limits. Eigenvalue buckling analysis was performed to provide a starting point for this analysis. A small off-axis loads are applied in order to initiate the desired buckling mode.

The element type used in nonlinear analysis is 3 BEAM 189. With 3 degrees of freedom (translation along the X and Y axis's, and rotation about the Z axis) the elements can only be used in 2D analysis.

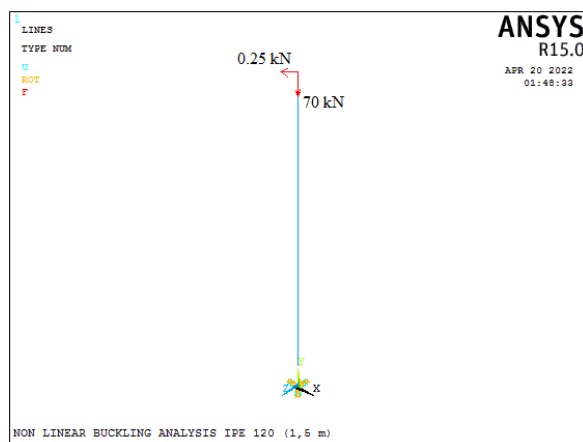


**Fig.11:** Boundary conditions

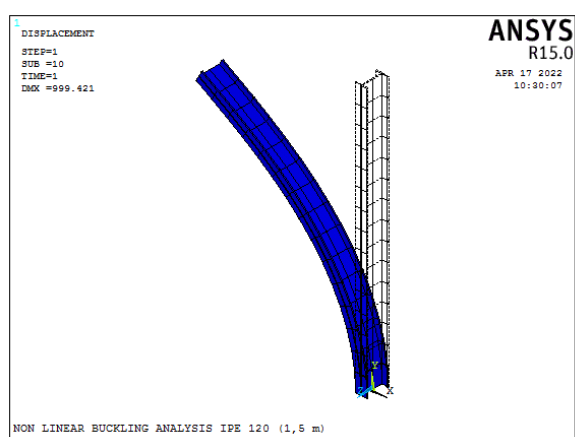


**Fig.12:** Non linear buckling mode

The ANSYS Eigen results obtained in this study were the key to the continuity of the nonlinear Analysis. We apply on the top of the beam (Figure 11) a load of -70,000 N in the FY direction and a load of -250N in the FX direction. This horizontal load will persuade the beam to buckle at the minimum buckling load. (Figure 12)

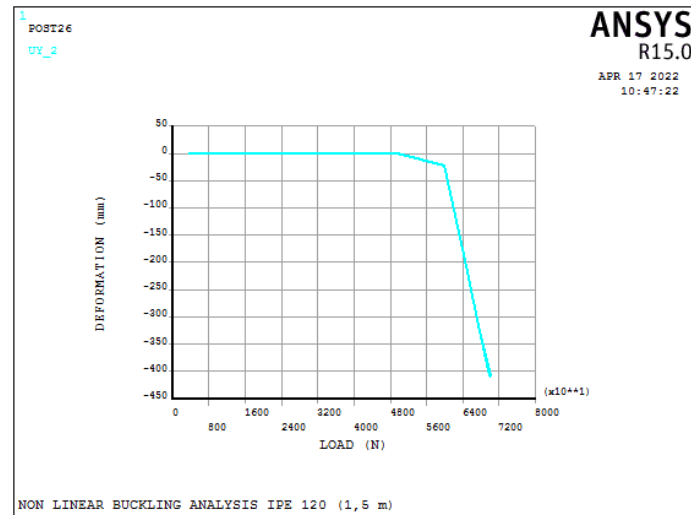


**Fig.13:** Load history analysis of IPE 120

The figure 13 shows how the beam became unstable and buckled with a load of approximately 60,000 N, the point where a large deflection occurred due to a small increase in force. This is slightly less than the Eigen-value solution of 60683.4N shown in figure 3, which was expected due to non-linear geometry issues discussed above.

**3.1. Solver convergence.** The figure 14 shows the cumulative iteration number and solution convergence. ANSYS determine appropriate size to break the load steps by the mean of automatic time stepping. In order to ensure better accuracy it is always recommended to decrease the step size. In a case of convergence failure an allowed recovery is obtained by means of Ansys bisection feature. The Newton Raphson solver will converge easily when the Line Search feature in Ansys was activated.

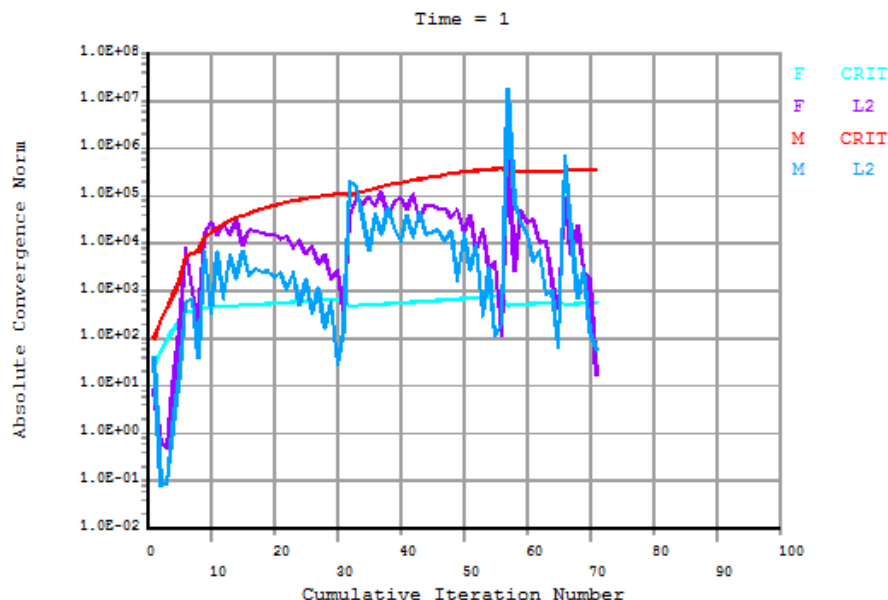


**Fig.14:** Cumulative iteration number and solution convergence



Table 3 presents the predicted critical buckling load ( $N_{cr}$ ) for the Eigen and Non linear analysis compared against those determined from Euler and Eurocode 3 formulas.

**Table 3.** Critical buckling loads (Theoretical versus numerical)

	$l_0 = 1.5\text{m}$		$l_0=3\text{m}$	$l_0=4.5\text{m}$	$l_0=6\text{m}$	$l_0=7.5\text{m}$
$N_{cr}$ [N] THEORY	63560.0		15890.0	6900.5	3972.3	2524.4
$N_{cr}$ [N] ANSYS LINEAR	60683.4		15135.9	6749.19	3966.62	2510.9
$N_{cr}$ [N] ANSYS NONLINEAR	60000		15100	6700	3900	2500
%E	5.6%		4.9%	2.9%	1.8%	0.9%
Slenderness ratio $\lambda = 2l_0 / i_{zz}$	205.48		410.9	616.44	821.92	1027.4
$\bar{\lambda} = \sqrt{\frac{Af_y}{N_{cr}}} = \sqrt{\frac{300.56}{N_{cr}}}$	Ec3	2.17	4.35	6.52	8.70	10.91
	Ansyp	2.22	4.45	6.67	8.90	10.91
$\phi = 0.5 \left[ 1 + \alpha(\bar{\lambda} - 0.2) + \bar{\lambda}^2 \right]$	Ec3	3.19	10.67	22.83	39.79	61.84
	Ansyp	3.31	11.12	23.84	41.58	61.84
$\chi = \frac{1}{\phi + [\phi^2 - \bar{\lambda}^2]^{0.5}}$	Ec3	0.18	0.049	0.022	0.012	0.008
	Ansyp	0.17	0.047	0.021	0.012	0.008
$N_{c.Rd} = \frac{A.f_y}{\gamma_{M0}}$ [kN]	273.23		273.23	273.23	273.23	273.23
$N_{b.Rd} = \frac{\chi A f_y}{\gamma_{M1}}$ [kN]	Ec3	49.18	13.38	6.01	3.28	2.18
	Ansyp	46.44	12.84	5.73	3.28	2.18
$\frac{N_{b.Rd}}{N_{c.Rd}}$	Ec3	0.18	0.05	0.02	0.01	0.007
	Ansyp	0.17	0.04	0.02	0.01	0.007
$\frac{N_{cr}}{N_{c.Rd}}$	Ec3	0.23	0.058	0.025	0.014	0.009
	Ansyp	0.22	0.058	0.025	0.014	0.009

The percent error (%E) in our model can be defined as:

$$\%E = \text{abs} \left( \frac{\text{Theory} - \text{Anys}}{\text{Theory}} \right) \times 100$$

$$N_{cr} = \frac{\pi^2 EI_{zz}}{(kl_0)^2} = \frac{\pi^2 \times 2.1 \times 10^4 \times 27.6}{(2 \times 150)^2} = 63.56 \text{ kN}$$

$$i_{zz} = \sqrt{\frac{I_{zz}}{A}} = \sqrt{\frac{27.6}{12.7896}} = 1.46 \text{ cm}$$

$$\lambda_z = \frac{l_z}{i_z} = \frac{2 \times 150}{1.46} = 205.49$$

$$\bar{\lambda}_z = \sqrt{\frac{A f_y}{N_{cr}}} = \sqrt{\frac{12.7896 \times 23.5}{N_{cr}}} = \sqrt{\frac{300.56}{N_{cr}}}$$

$$N_{c.Rd} = \frac{A f_y}{\gamma_{M0}} = \frac{12.7896 \times 23.5}{1.1} = 273.23 \text{ kN}$$

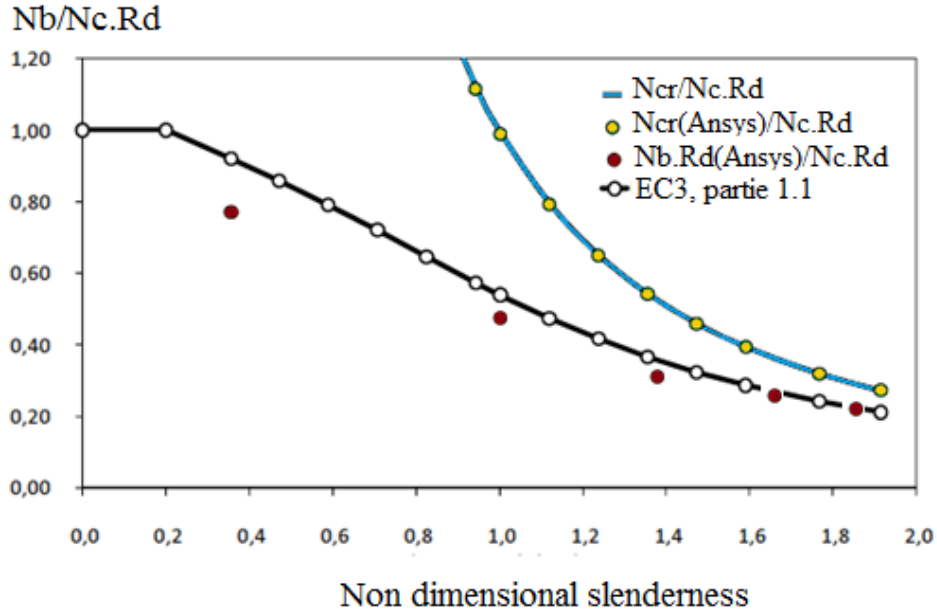


**Fig.15:** Design buckling resistance for IPE 120, for different slenderness values.

The buckling resistance of the cross section beam for linear and nonlinear buckling is checked for different column lengths ( $l = 1.5, 3.0, 4.5, 6.0$  and  $7.5$  [m]). (Figure 15)

**4. Results and discussion.** The results from ANSYS (linear and nonlinear values) are almost the same as the theoretical buckling load obtained using Euler Formula. Figures 2 to 7 show the buckled shape of the cantilever beam for the BEAM188 models.

The deformed shapes in all the cases (where the column is modeled using the beam elements), clearly agree with the mode shape that would result if a first mode Euler buckling is to occur. It is also important to note from the buckling shapes of BEAM188,[6] that the buckling occurs about the weak axis.

The results given in table 3, show very clearly that the critical Euler load gives a good account of the reality for normalized slenderness  $\bar{\lambda}$  higher than 1.6. [3]-[4] Below this value, in the field of current use of the profiles, the real critical load is much lower than that given by Euler.

Table 3 provides also the critical buckling loads and corresponding error from the Theory (Euler).

**5- Conclusion.** This paper compares the ultimate buckling loads of steel column in compression based on eurocode 3 design code to ultimate buckling loads obtained with finite element simulations. It can be concluded that the results obtained by the eurocode 3 design formulas can lead to the underestimations of even less than 4% of the ultimate buckling load of column section obtained from finite element simulations. The design method gives good results for buckling of steel column loaded in compression. For these situations, there is a quite good agreement between the values given by the eurocode 3 design code and the numerical results of the finite element methods.

## References

1. N. Boissonnade, R. Greiner, J. P. Jaspart, and J. Lindner, “Rules for Member Stability in EN1993-1-1 – Background Documentation and Design Guidelines”, ECCS TC8 – Stability, ECCS Report No. 119, ISBN 92-9147-000-84, ECCS, Brussels, Belgium **(2007)**.
2. L. Dahmani , A. Boudjemia , “Lateral torsional buckling response of steel beam with different boundary conditions and loading “, Strength of Material Journal, Ed. Springer New York, Vol.46, N°3, pp.429-432, Mai **2014**.
3. L. Dahmani , S.Drizi , “ Lateral Torsional Buckling of an Eccentrically Loaded Channel Section Beam “, Strength of Material Journal, Ed. Springer New York, Vol.47, N°6, pp.912-916, November **2015**.
4. Jean-Pierre MUZEAU, “ Construction métallique & Résistance des sections et des barres“ Université Blaise Pascal, Département de Génie Civil, Septembre **(2010)**.
5. ANSYS 15.0. The General Purpose of Finite Element Software. Documentation.**(2014)**
6. EN 1993-1-1; Eurocode 3, Design of steel structures - Part 1-1: General rules and rules for buildings, May **2006**.

# Operator Optimization Based on Hardware Architecture Alignment Requirements

Higher Computation but Faster Speed

Qingqing Gai, Junxing Shen, Yu Luo

**Abstract**—Due to the hardware architecture characteristics, some operators tend to acquire better performance if the input/output tensor dimensions are aligned to a certain minimum granularity, such as convolution and deconvolution commonly used in deep learning. Furthermore, if the requirements are not met, the general strategy is to pad with 0 to satisfy the requirements, potentially leading to the under-utilization of the hardware resources. Therefore, for the convolution and deconvolution whose input and output channels do not meet the minimum granularity alignment, we propose to transfer the  $W$ -dimensional data to the  $C$ -dimension for computation( $W2C$ ) to enable the  $C$ -dimension to meet the hardware requirements. This scheme also reduces the number of computations in the  $W$ -dimension. Although this scheme substantially increases computation, the operator’s speed can improve significantly. It achieves remarkable speedups on multiple hardware accelerators, including Nvidia Tensor cores, Qualcomm digital signal processors(DSPs), and Huawei neural processing units(NPUs). All you need to do is modify the network structure and rearrange the operator weights offline without retraining. At the same time, for some operators, such as the Reducemax, we observe that transferring the  $C$ -dimensional data to the  $W$ -dimension( $C2W$ ) and replacing the Reducemax with the Maxpool can accomplish acceleration under certain circumstances.

**Index Terms**—convolution, deconvolution,  $W2C$ ,  $C2W$ , alignment, hardware accelerator

## I. Introduction

Efficient deep convolutional neural networks (CNNs) make it ubiquitous in more and more domains such as speech recognition [1], [2], [3], computer vision [4], [5], [6], and image recognition [7], [8], driving the rapid development of technology. Usually, underlying the accuracy improvements of CNNs are substantial increases in the calculation. To bring the ultimate experience to users, balancing accuracy and speed is a hot research topic in recent years, which greatly promotes the development of network structures and artificial intelligence(AI)-based hardware accelerators.

The state-of-the-art models generally require performing a large number of matrix computations, resulting in lower speed performance. Lots of network structure optimization work has been done to improve computing

efficiency. MobileNetV1 [9] proposes to use depthwise separable convolution to mitigate the computational cost. MobileNetV2 [10] introduces a resource-efficient block with inverted residuals and linear bottlenecks to go one step further. MobileNetV3 [11] combines automated search algorithms with network structure design, achieving higher accuracy and less computation than mobilenetV2. ShuffleNet [12], [13] exploits channel shuffle and group convolution to reduce the number of operations further. Moreover, Fused-Layer [14] and DLFusion [15] recommend fusing the processing of multiple CNN layers to improve the speed. And the paper [16], Once-for-all [17], Fbnet [18], Proxylessnas [19], and Mnasnet [20] utilize automating search neural network architecture based on hardware-aware to penalize operations that are too slow.

Many hardware manufacturers have also introduced AI hardware accelerators, such as GPUs, DSPs, and NPUs. Devices equipped with any or all of these components can speed up machine learning (ML) inference. For NVIDIA, graphics processor units(GPUs) are commonly adopted for deep learning. Moreover, NVIDIA introduced Tensor Cores specialized function units for accelerating tensor operations found in Deep neural networks (DNNs) since the Volta architecture. Hexagon DSPs [21] and Huawei NPUs are aided in ML inference for Qualcomm and Huawei devices, respectively. However, due to hardware architecture characteristics, commonly used operators, such as convolution and deconvolution, tend to perform better if the input/output channel dimensions are aligned to a certain minimum granularity. This means that the convolution and deconvolution with small input/output channel dimensions that differ significantly from the alignment requirements do not fully utilize the hardware resources, which generally reduces the overall workload and ensures network depth. Consequently, we propose the  $W2C$  scheme to optimize the operators that do not satisfy the requirements to make full use of hardware resources.

This paper makes the following contributions:

- It provides an in-depth analysis of the reasons for the slow speed of operators that do not meet the alignment requirements in different hardware.
- It shows how to use the  $W2C$  scheme to tremendously reduce computation time for convolution that does not satisfy alignment requirements, especially for small input/output channel dimensions on Nvidia

Qingqing Gai is with the Department of High-Performance Computing, Agora Corporation, ShangHai, 200000 China e-mail: gaiqingqing\_gai@163.com.

Junxing Shen and Yu Luo are with the Department of High-Performance Computing, Agora Corporation, ShangHai, 200000 China e-mail: shenjunning@agora.io, luoyu@agora.io.

GPUs, Qualcomm DSPs, and Huawei NPUs.

- It reveals how to adopt the  $C2W$  scheme to speed up Reducemax performance under certain circumstances.

## II. Foundation

Many hardware vendors have introduced their own specialized DNNs hardware accelerators for superior performance and efficiency. Many hardware architectures require channel dimension alignment for convolution and deconvolution layers for better performance.

For NVIDIA GPUs, Tensor Core is a crucial technology to deliver high-performance inference, which can compute much faster than the CUDA core. Most math-bound operations will be accelerated with Tensor Cores: convolution, deconvolution, fully connected, and matrix multiply. Nonetheless, in TensorRT, Tensor Core layers earn better performance if the input/output tensor channel dimensions are aligned to a certain minimum granularity, given that it operates on the small matrix block. The input/output tensor channel dimensions of the convolution and deconvolution layers need to fulfill the alignment requirements: the suggested channel dimension alignment in elements is 4 when the operation type is TF32, and the suggested channel dimension alignment in elements is 8 for dense math when the operation type is TF16, and the suggested channel dimension alignment in elements is 32 when the operation type is INT8, as shown in Table I. When using Tensor Core implementations where these requirements are not met, TensorRT will implicitly pad the tensors to the nearest multiple of alignment rounding up the dimensions in the model definition [22].

TABLE I  
Types of Tensor Cores

Tensor Core operation Type	Suggested Tensor Dimension Alignment
TF32	4
FP16	8 for dense math ,16 for sparse math
INT8	32

Let us take the dense math operator whose operator type is FP16 as an example. Its input/output tensor channel dimensions demand to meet the alignment of 8; otherwise, TensorRT automatically pads it to the nearest multiple of 8 when taking advantage of Tensor Cores, which brings additional invalid calculations. This means that convolution layers' inference time is the same as the time after padding when its input/output channel is less than the multiple of 8. The experimental results below also demonstrate this point of view.

We build a basic model with 3 convolution layers: model\_ori, whose input tensor shape is  $1 \times 720 \times 1280 \times 1$  (NHWC), the parameters of the first convolution layer of conv\_0 are:  $in\_channel = 1$ ,  $out\_channel = 4$ , the parameters of the second convolution layer of conv\_1 are:  $in\_channel = 4$ ,

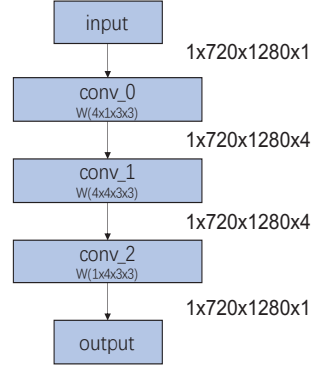


Fig. 1. model\_ori architecture

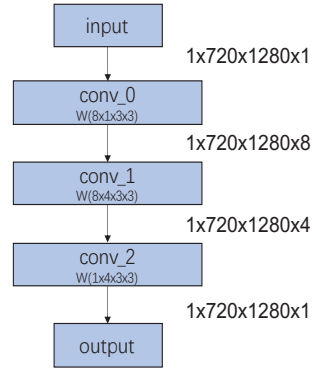


Fig. 2. model\_1 architecture

$out\_channel = 4$ , the parameters of the third convolution layer of conv\_2 are:  $in\_channel = 4$ ,  $out\_channel = 1$ . And  $kernel\_size = [3, 3]$ ,  $stride = [1, 1]$ ,  $pads = [1, 1, 1, 1]$  are all same for the three convolution layers. The architectures of model\_ori, model\_1, and model\_2 are shown in Fig. 1, Fig. 2, and Fig. 3, respectively. The difference among the three models is that the input/output tensor channel dimensions of the convolution are different.  $W$  represents the weight tensor of the convolution with

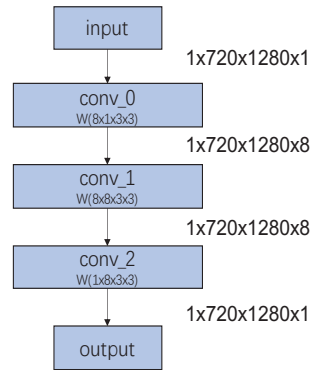


Fig. 3. model\_2 architecture

$shape = [out\_channel, in\_channel, k\_h, k\_w]$  in Fig. 1, Fig. 2 and Fig. 3,  $k\_h$  and  $k\_w$  mean kernel size. The amount of floating-point operations of the whole model is 0.39 GFLOPS, 0.72 GFLOPS, and 2.57 GFLOPS, respectively.

To measure the latency of model\_ori, model\_1, and model\_2 on Tensor Cores, we use NVIDIA GeForce RTX 3090. TensorRT version is 8.2.3 with tensor type FP16. See the “Measurement setup” section below for more details. From Table II, we can obtain that even though the computation amount of model\_2 is 6.5 times that of model\_ori, the inference time of the two models is almost the same.

TABLE II  
Model inference time on Tensor Cores

	conv_0/ms	conv_1/ms	conv_2/ms	Total inference time/ms
model_ori	0.0604	0.0616	0.0605	0.1825
model_1	0.0586	0.0592	0.0606	0.1783
model_2	0.0588	0.0610	0.0610	0.1808

For Qualcomm Hexagon DSPs, there are also alignment requirements for convolution operators to achieve faster speed. Qualcomm Hexagon DSPs are specially designed for multi-media acceleration, which can offload the compute-intensive operator from CPU to DSPs to diminish the overall power consumption offering optimum performance. Consider SM8150 chipset, which includes four separate DSPs, each dedicated to a specific application space: sensor(sDSP), compute(cDSP), modem(mDSP), and audio(aDSP) [23]. All DSPs include a scalar unit, and some DSPs also include a Qualcomm Hexagon™ Vector eXtensions (HVX) unit for extended vectorized support. The cDSP, which always includes HVX, is aimed at math-intensive tasks such as computer vision, image processing, and so on. From the V62 architecture, the default size of the Hexagon Vector is 1024bit, which is 128 bytes. DSPs currently only support 8-bit quantized execution. When using it for AI model inference, considering the convolution layer, although input and weight are both INT8, the multiply-add operation may overflow, so it will employ the INT32 accumulator to store the calculation results, and the Hexagon Vector can store 32 INT32 values. So it is recommended to align vector loads or stores to 32 for best performance.

Similar to the experiment done on the Tensor Cores, we modify the in\_channel of conv\_1 in model\_1 to 32 as the model : model\_1\_dsp, and the in\_channel and out\_channel of conv\_1 in model\_2 are modified to 32 as the model: model\_2\_dsp. We conduct the experiments on Mi10 with the 865 chip. See “Measurement setup” section for details. The experimental results are shown in Table III. And from that, we can observe that the output tensor channel for convolution needs to meet the alignment requirement of 32. Huawei NPU also require that convolution input/output tensor channel dimensions are aligned to a certain minimum granularity [24].

TABLE III  
Model inference time on DSPs(Mi 10 Snapdragon 865)

	conv_0/ms	conv_1/ms	conv_2/ms	Total inference time/ms
model_ori	3.838	5.296	5.628	25.160
model_1_dsp	3.853	15.164	5.604	33.527
model_2_dsp	3.878	15.111	15.442	41.099

It can be confirmed from Table II and Table III that when the Tensor Cores and Qualcomm DSPs convolution layer input/output tensor channel dimensions do not satisfy its relative alignment requirements, the inference time of this layer is the same as the layer after padding, deconvolution layer as well. When input/output tensor channel dimensions of the convolution differ greatly from its alignment counts, the effective utilization of hardware resources is relatively low, resulting in not saturating hardware resources.

### III. Innovations

To get the most out of hardware resources, we propose a solution to transfer data from W-dimension to C-dimension for optimal performance. As shown in Fig. 4, for the tensor with small input/output channel dimensions in NHWC format, we can transfer  $Mul$  times the W-dimensional data to the C-dimension so that the W-dimension is reduced to the original  $Mul$  times:  $\bar{W} = W/Mul$ , and the C-dimension is expanded to the original  $Mul$  times:  $\bar{C} = C * Mul$ , and since the memory layout of the tensor has not changed, this operation takes no time. To maximize the effective utilization of the hardware resources, in the case that  $W$  can be divisible by  $Mul$ , it is best that  $\bar{C}$  can meet the alignment requirements of the hardware.

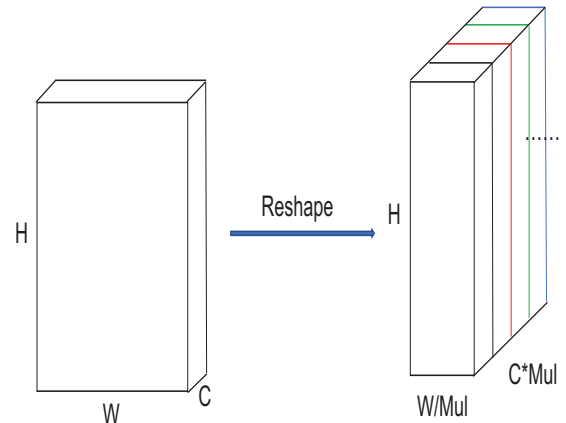


Fig. 4. W2C scheme

For the convolution layer, assuming the layer input and output tensor channel are  $C$ ,  $O$  respectively,  $input\_shape = [N, H, W, C]$  is the original input tensor shape,  $output\_shape = [N, P, Q, O]$  is the output tensor shape,  $weight\_shape = [O, K_h, K_w, C]$  is the

weight tensor shape, and  $K_h$  and  $K_w$  is kernel size,  $bias\_shape = [O]$  is the bias tensor shape,  $Flops\_ori = 2 * C * K_h * K_w * P * Q * O$  is the amount of floating-point operations. After the input tensor goes through the W2C scheme of  $Mul$  times, the input channel is converted from  $C$  to  $\bar{C} = C * Mul$ . To achieve the consistency of the output, We also need to rebuild the weight tensor of the convolution layer, increasing the input and output channel to the original  $Mul$  times.  $input\_shape\_1 = [N, H, W/Mul, C * Mul]$  is the new input tensor shape, the new output tensor shape is expected to be:  $output\_shape\_1 = [N, P, Q/Mul, O * Mul]$ ,  $weight\_shape\_1 = [O * Mul, K_h, K_w, C * Mul]$  is the new weight tensor shape,  $bias\_shape\_1 = [O * Mul]$  is the new bias tensor shape, and  $Flops\_1 = 2 * C * Mul * K_h * K_w * P * Q / Mul * O * Mul$  is the new amount of floating-point operations and  $Flops\_1 = Mul * Flops\_ori$ . The amount of calculation of the converted new layer is  $Mul$  times of the origin. Since the output tensor memory layout is the same, we can also use the Reshape operator to transfer the C-dimensional data to the W-dimension ( $C2W$ ) to get the same results for the layer if necessary, which is also not time-consuming.

Through the W2C scheme, we transfer the data that needs to be calculated in the W dimension to the C-dimension, comprehensively use the hardware resources and calculate multiple output points simultaneously, reducing the number of computations in the W-dimension. This solution can significantly improve the effective utilization of hardware and computing performance and compensate for the defects of hardware architecture in computing convolution with small input/output tensor channels. All you need is to insert the Reshape operator into the model and rearrange the weight and bias tensor in offline mode. Although the computation amount will increase by  $Mul$  times, it provides tremendous speedups in performance.

Here we briefly explain the principle of rearrangement of convolution weights when using the W2C scheme. Suppose the relevant parameters of convolution are as follows:  $kernel\_size = [3, 3]$ ,  $stride = [1, 1]$ ,  $dilation = [1, 1]$ ,  $pads = [1, 1, 1, 1]$ , input channel is 2, output channel is 1, and the W2C scheme with  $Mul = 2$  is adopted for simplicity. Assuming that the part of the input tensor in W and C dimension is shown in Fig. 5 and after the W2C scheme of  $Mul = 2$  and padding operation, the data arrangement is shown in Fig. 6. In Fig. 5, we use the columns [1, 2], [3, 4], [5, 6], [7, 8] as 4 center points, and each center point calculates an output value, to get  $a, b, c, d$  4 output values. And after the W2C scheme with  $Mul = 2$ , we require to calculate the two output values of  $a$  and  $b$  with the column [1, 2, 3, 4] as the center point, and calculate two output values of  $c$  and  $d$  with the column [5, 6, 7, 8] as the center point, and so on. We can rearrange the weights tensor accordingly. The

source code is available in [25]. For the convolution of  $kernel\_size = [3, 3]$ ,  $stride = [1, 1]$ ,  $dilation = [1, 1]$ ,  $pads = [1, 1, 1, 1]$ , the program supports W2C scheme with arbitrary  $Mul$  multiples. For the deconvolution of  $kernel\_size = [5, 5]$ ,  $strides = [3, 3]$ ,  $dilation = [1, 1]$ ,  $pads = [1, 1, 1, 1]$ , the program currently supports the W2C scheme of  $Mul=2, 4$ .



Fig. 5. Part of the input tensor



Fig. 6. Part of the input tensor after W2C scheme with  $Mul = 2$

#### A. Measurement setup

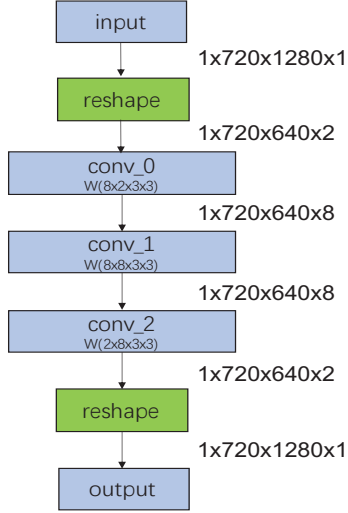
Model `model_ori` is still used as the basic model, and each layer is tested with  $Mul = 2, 4, 8, 16$ , and the models named `model_Mul2`, `model_Mul4`, `model_Mul8`, and `model_Mul16`, respectively. Fig. 7 shows the model architecture when  $Mul=2$ , similar when  $Mul = 4, 8, 16$ .

To measure inference time on Tensor Cores, we use NVIDIA GeForce RTX 3090, TensorRT version is 8.2.3, and run all networks through a command-line wrapper tool called `trtexec` which can quickly utilize TensorRT.

To measure inference time on Qualcomm DSPs, we use a benchmark tool that runs a network on a target Android/Linux Embedded device and collects performance metrics. The benchmark tool is shipped in Snapdragon Neural Processing Engine (SNPE) SDK. We use the 1.55 version of the SNPE and experiment on Mi 10, Mi 11, and Black Shark 4. For more details on using the benchmark tool, please refer to the SNPE reference guide [26].

To measure inference time on Huawei NPUs, we use the Android Neural Networks API (NNAPI), an Android C API designed for running computationally intensive operations for machine learning on Android devices [27].



Fig. 7. Model architecture when  $Mul=2$ : model\_Mul2

We could use NNAPI to perform hardware-accelerated inference using available on-device processors, including GPUs, DSPs, and NPUs. With the help of ANeuralNetworksExecution\_getDuration API, we can get the model inference time on the specific accelerator. The inference time of each layer cannot be accurately obtained through NNAPI, and we only show the inference time of the entire model here.

## B. Results

The model's inference time on NVIDIA GeForce RTX 3090 using Tensor Cores with tensor type FP16 is shown in Table IV. Compared to the speed of each layer of the original model, we can observe that  $Mul = 8$  is the best choice for conv\_0,  $Mul = 2$  is the best choice for conv\_1, and  $Mul = 8$  is the best choice for conv\_2. The architecture of the best model named model\_Mul828 is shown in Fig. 8. Table V shows the performance comparison between model\_ori and model\_Mul828. The time-consuming of the Reshape operator can be negligible. The model's overall performance through the W2C scheme has been improved by 128%, even though computation increased almost three times.

TABLE IV  
Models inference time on Tensor Core with different  $Mul$

	conv_0/ms	conv_1/ms	conv_2/ms	Total inference time/ms
model_ori	0.0604	0.0616	0.0605	0.1825
model_Mul2	0.0332	0.0333	0.0332	0.0996
model_Mul4	0.0214	0.0336	0.0293	0.0829
model_Mul8	0.0181	0.0432	0.0291	0.0904
model_Mul16	0.0276	0.0543	0.0433	0.1252

As can be discovered from Table I, when the Tensor Cores operation type is INT8, the suggested tensor dimension alignment is 32 for convolution operation. In this case, we also conduct a set of experiments similar to Table IV,

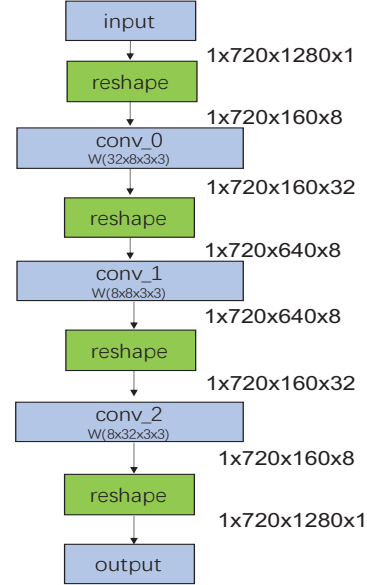


Fig. 8. model\_Mul828 architecture

TABLE V  
Model inference time on Tensor Cores with model\_ori and model\_Mul828

	conv_0	conv_1	conv_2	reshape	Total inference time/ms
model_ori	0.0604	0.0616	0.0605	0	0.1825
model_Mul828	0.0183	0.0336	0.0294	0.0017	0.0799

and the difference between the two sets of experiments is tensor type, except that there is an additional set of experiments with  $Mul=32$ . The results are shown in Table VI, which demonstrates that  $Mul = 16$  is a better choice, with the performance being improved by more than three times(311%), even if the number of computations increases by 15 times.

TABLE VI  
Model inference time on Tensor Cores with tensor type INT8

	conv_0/ms	conv_1/ms	conv_2/ms	Total inference time/ms
model_ori	0.0732	0.0732	0.0746	0.2645
model_Mul2	0.0400	0.0516	0.0526	0.1688
model_Mul4	0.0231	0.0427	0.0426	0.1228
model_Mul8	0.0246	0.0251	0.0255	0.0742
model_Mul16	0.0193	0.0249	0.0202	0.0644
model_Mul32	0.0195	0.0252	0.0204	0.0651

The W2C solution can effectively improve the performance of convolution operators that do not meet the alignment requirements not only on Tensor Cores but also on Qualcomm DSPs and Huawei NPUs. We perform experiments similar to Table IV on Mi 10 (Snapdragon 865, SM8250), and the experimental results are shown in Table VII. From Table VII, it can be verified that the W2C scheme is also available on Qualcomm DSPs. When  $Mul = 16$ , the total inference time is 8.554ms, compared to 25.16ms of the original model, which is nearly two



times faster. Notice that when  $Mul=2, 8, 16$ , the time consuming of conv\_0, conv\_1, conv\_2 is the shortest, respectively, so conv\_0, conv\_1, conv\_2 adopt the  $W2C$  scheme with  $Mul=2, 8, 16$  respectively is a faster solution. We also do experiments on Mi 11 (Snapdragon 888, SM8350) and Black Shark 4 (Snapdragon 870, SM8250) to get the model total inference time, as shown in Table VIII. The  $W2C$  scheme has significant performance improvement on Snapdragon 865, 870, and 888 for convolution with small channels due to Qualcomm DSPs requiring its output tensor channel dimension alignment in elements to be 32.

TABLE VII

Model inference time on Mi 10(Snapdragon 865) with different  $Mul$ 

	conv_0/ms	conv_1/ms	conv_2/ms	Total inference time/ms
model_ori	3.838	5.296	5.628	25.160
model_Mul2	1.510	4.030	4.386	15.341
model_Mul4	0.785	2.000	2.323	9.551
model_Mul8	1.068	1.037	1.371	8.928
model_Mul16	1.064	1.848	1.294	8.554

TABLE VIII

Model total inference time on Mi 11(Snapdragon 888) and Black Shark 4(Snapdragon 870) with different  $Mul$ 

	Mi 11/ms	Black Shark 4/ms
model_ori	9.813	7.201
model_Mul2	8.381	5.874
model_Mul4	7.422	4.773
model_Mul8	7.441	4.661
model_Mul16	7.011	4.829

Meanwhile, we notice that this solution is also reasonably practical on Huawei NPUs, so we carry out comparable experiments on Huawei P40. The experimental results are revealed in Table IX. The  $W2C$  scheme with  $Mul=32$  is the most effective, and the model inference speed increased by 82.69%, even with 31 times more computation.

TABLE IX

Model total inference time on Huawei P40(NPU) with different  $Mul$ 

	Total inference time/ms
model_ori	28.783
model_Mul8	24.135
model_Mul16	16.368
model_Mul32	14.645
model_Mul64	15.755

Furthermore, we can not only apply the  $W2C$  scheme to the convolution operators to get the most out of various hardware resources effectively, but we can also use it on other operators, such as the Reducemax operator. Assuming that the input tensor shape with NHWC format of the Reducemax operator is  $1x80x136x36$ , the output tensor shape is  $1x80x136x1$ , and the inference time on the Snapdragon 870 DSPs is 0.785ms. In contrast, the convolution of  $kernel\_size=[1,1]$  with the same input and output tensor size consumes 0.124ms, which implies the Reducemax takes a long time. We suspect

that the Reducemax operator with large C-dimensions is not well optimized, so we put forward the opinion of transferring the input tensor from the C-dimension to the W-dimension( $C2W$ ) with  $Mul$  times. Next, we use  $kernel\_size=(1, Mul)$ ,  $stride=(1, Mul)$  of the Maxpool to reduce the computation on the C dimension of the Reducemax. The original Reducemax with large C-dimensions can be replaced with the Maxpool and the Reducemax with smaller C-dimensions through  $C2W$ . The improvement schemes of Reducemax with input tensor set to  $1x80x136x36$  are as follows:

- 1) Adopt the  $C2W$  scheme with  $Mul=2$ . First, use the Reshape to convert the input tensor from  $1x80x136x36$  to  $1x80x272x18$ , and then adopt the Maxpool with  $kernel\_size=(1, 2)$ ,  $stride=(1, 2)$  and the Reducemax whose input tensor is  $1x80x136x18$ . The experimental results are shown in Table X, and the model's name is maxpool\_reducemax\_Mul2.
- 2) Adopt the  $C2W$  scheme with  $Mul=4$ . First, use the Reshape to convert the input tensor from  $1x80x136x36$  to  $1x80x544x9$ , and then adopt the Maxpool with  $kernel\_size=(1, 4)$ ,  $stride=(1, 4)$  and the Reducemax whose input tensor is  $1x80x136x9$ . The experimental results are shown in Table X, and the model's name is maxpool\_reducemax\_Mul4.

TABLE X

Reducemax on Snapdragon 870 DSP with different  $Mul$ 

	Reshape/ms	Maxpool/ms	Reducemax/ms	Total inference time/ms
reducemax			0.785	0.785
maxpool_reducemax_Mul2	0.017	0.067	0.506	0.590
maxpool_reducemax_Mul4	0.017	0.176	0.336	0.529

As can be seen from Table X, using the  $C2W$  scheme with  $Mul=4$ , we can reduce the Reducemax inference time from 0.785ms to 0.529ms when the input tensor is  $1x80x136x36$ , and the speed is increased by 48.39%. It's also worth pointing out that Maxpool takes less time and the time-consuming of Maxpool with  $kernel\_size=(1, 2)$ ,  $stride=(1, 2)$  is much shorter than Maxpool with  $kernel\_size=(1, 4)$ ,  $stride=(1, 4)$ , so finally we use 2 Maxpool with  $kernel\_size=(1, 2)$ ,  $stride=(1, 2)$  and 2 Maxpool with  $kernel\_size=(1, 3)$ ,  $stride=(1, 3)$  instead of Reducemax with input tensor  $1x80x136x36$ , consuming 0.351ms and the speed finally increased by 123%.

#### IV. Conclusions

In this paper, we introduce the  $W2C$  scheme to accelerate the convolution whose input/output tensor channel dimensions do not satisfy alignment requirements and make full and effective use of hardware resources, including Nvidia Tensor Cores, Qualcomm DSPs, and Huawei NPUs. And all you need is to rearrange the weights and adjust the network structure offline, which can

provide massive speedups for the operator. The scheme also has performance-enhancing on deconvolution, and the principle is the same as convolution. We also propose the *C2W* scheme to use Maxpool instead of Reducemax to increase speed under certain circumstances. We believe this scheme will play its role in more scenarios, and we will continue to explore it.

## References

- [1] D. S. Park, Y. Zhang, Y. Jia, W. Han, C.-C. Chiu, B. Li, Y. Wu, and Q. V. Le, "Improved noisy student training for automatic speech recognition," *Interspeech 2020*, Oct 2020.
- [2] W. Xiong, J. Droppo, X. Huang, F. Seide, M. Seltzer, A. Stolcke, D. Yu, and G. Zweig, "The microsoft 2016 conversational speech recognition system," in *IEEE International Conference on Acoustics, Speech and Signal Processing (ICASSP)*, 2017, pp. 5255–5259.
- [3] G. Hinton, L. Deng, D. Yu, G. E. Dahl, A.-r. Mohamed, N. Jaitly, A. Senior, V. Vanhoucke, P. Nguyen, T. N. Sainath et al., "Deep neural networks for acoustic modeling in speech recognition: The shared views of four research groups," *IEEE Signal processing magazine*, vol. 29, no. 6, pp. 82–97, 2012.
- [4] P. Sermanet, D. Eigen, X. Zhang, M. Mathieu, R. Fergus, and Y. LeCun, "Overfeat: Integrated recognition, localization and detection using convolutional networks," *arXiv preprint arXiv:1312.6229*, 2013.
- [5] K. Simonyan and A. Zisserman, "Very deep convolutional networks for large-scale image recognition," *arXiv preprint arXiv:1409.1556*, 2014.
- [6] M. D. Zeiler and R. Fergus, "Visualizing and understanding convolutional networks," in *European conference on computer vision*. Springer, 2014, pp. 818–833.
- [7] S. Ren, K. He, R. Girshick, and J. Sun, "Fasterrcnn: Towards real-time object detection with region proposal networks," in *Advances in Neural Information Processing Systems*, pp. 91–99, 2015.
- [8] K. Simonyan and A. Zisserman, "Very deep convolutional networks for large-scale image recognition," *CoRR*, vol. abs/1409.1556, 2014.
- [9] Andrew G. Howard, Menglong Zhu, Bo Chen, Dmitry Kalenichenko, Weijun Wang, Tobias Weyand, Marco Andreetto, and Hartwig Adam. Mobilenets: Efficient convolutional neural networks for mobile vision applications. *CoRR*, abs/1704.04861, 2017. 2
- [10] Mark Sandler, Andrew G. Howard, Menglong Zhu, Andrey Zhmoginov, and Liang-Chieh Chen. Mobilenetv2: Inverted residuals and linear bottlenecks. mobile networks for classification, detection and segmentation. *CoRR*, abs/1801.04381, 2018. 2,3,6,7,8
- [11] Andrew Howard, Mark Sandler, Grace Chu, Liang-Chieh Chen, Bo Chen, Mingxing Tan, Weijun Wang, Yukun Zhu, Ruoming Pang, Vijay Vasudevan, et al. Searching for MobileNetV3. In *Proceedings of the IEEE International Conference on Computer Vision (ICCV)*, 2019. 2, 4
- [12] Xiangyu Zhang, Xinyu Zhou, Mengxiao Lin, and Jian Sun. ShuffleNet: An extremely efficient convolutional neural network for mobile devices. In *Proceedings of the IEEE Conference on Computer Vision and Pattern Recognition (CVPR)*, pages 6848–6856, 2018. 2
- [13] Ningning Ma, Xiangyu Zhang, Hai-Tao Zheng, and Jian Sun. ShuffleNetV2: Practical guidelines for efficient cnn architecture design. In *Proceedings of the European Conference on Computer Vision (ECCV)*, pages 116–131, 2018. 2
- [14] M. Alwani, H. Chen, M. Ferdman, and P. Milder, "Fused-layer CNN accelerators," in *MICRO*, 2016.
- [15] Z. Liu, J. Leng, Q. Chen, C. Li, W. Zheng, L. Li, and M. Guo, "DLFusion: An Auto-Tuning Compiler for Layer Fusion on Deep Neural Network Accelerator," in *IEEE International Conference on Parallel & Distributed Processing with Applications (ISPA)*, pp. 118–127, IEEE, 2020.
- [16] X. Zhang, W. Jiang, Y. Shi, and J. Hu, "When neural architecture search meets hardware implementation: from hardware awareness to co-design," in *IEEE Computer Society Annual Symposium on VLSI (ISVLSI)*, 2019, pp. 25–30.
- [17] H. Cai, C. Gan, T. Wang, Z. Zhang, and S. Han, "Once-for-all: Train one network and specialize it for efficient deployment," in *8th International Conference on Learning Representations, ICLR*. OpenReview.net, 2020. [Online]. Available: <https://openreview.net/forum?id=HylxE1HKwS>
- [18] B. Wu, X. Dai, P. Zhang, Y. Wang, F. Sun, Y. Wu, Y. Tian, P. Vajda, Y. Jia, and K. Keutzer, "Fbnet: Hardware-aware efficient convnet design via differentiable neural architecture search," in *Conference on Computer Vision and Pattern Recognition, CVPR*. Computer Vision Foundation / IEEE, 2019, pp. 10 734–10 742.
- [19] H. Cai, L. Zhu, and S. Han, "Proxylessnas: Direct neural architecture search on target task and hardware," *CoRR*, vol. abs/1812.00332, 2018. [Online]. Available: <http://arxiv.org/abs/1812.00332>
- [20] M. Tan, B. Chen, R. Pang, V. Vasudevan, and Q. V. Le, "Mnasnet: Platform-aware neural architecture search for mobile," *CoRR*, vol. abs/1807.11626, 2018. [Online]. Available: <http://arxiv.org/abs/1807.11626>
- [21] Codrescu, L., Anderson, W., Venkumanhanti, S., Zeng, M., Plondke, E., Koob, C., Ingle, A., Tabony, C., Maule, R.: Hexagon dsp: An architecture optimized for mobile multimedia and communications. *IEEE Micro* (2), 34–43 (2014)
- [22] NVIDIA Corporation. TensorRT Developer Guide. 2022.
- [23] Qualcomm Corporation. Qualcomm Hexagon™ V67 Programmer's Reference Manual. 2020.
- [24] TBE Custom Operator Development Guide. [https://support.huaweicloud.com/odevg-Inference-cann/atlaste\\_10\\_0002.html](https://support.huaweicloud.com/odevg-Inference-cann/atlaste_10_0002.html). 2020.
- [25] The W2C scheme source code. <https://github.com/pianogGG/W2C>.
- [26] Qualcomm Corporation. Snapdragon Neural Processing Engine SDK Reference Guide. 2021.
- [27] Neural Networks API. <https://developer.android.com/ndk/guides/neuralnetworks>.

# Performance Analysis and Optimization for Diagonalsparse Matrix-Vector Multiplication on MLU

Qiuyu Dai, Haochong Zhang, and Xiangrong Liu\*

**Abstract**— Diagonal sparse matrix-vector multiplication is a well-studied topic in the fields of scientific computing and big data processing. However, when diagonal sparse matrices are stored in DIA format, there can be a significant number of padded zero elements and scattered points, which can lead to a degradation in performance of the current DIA kernel. This can also lead to an excessive consumption of computational and memory resources. In order to address these issues, the authors propose the DIA-Adaptive scheme and its kernel, which leverages the parallel instruction sets on MLU. The researchers analyze the effect of allocating a varying number of threads, clusters, and hardware architectures on the performance of SpMV using different formats. The experimental results indicate that the proposed DIA-Adaptive scheme performs well and offers excellent parallelism.

**Keywords**— adaptive method, DIA, diagonal sparse matrices, MLU, sparse matrix-vector multiplication

## I. INTRODUCTION

ONE of the important problems in scientific computing and deep learning is the fast evaluation of diagonal sparse matrix-vector multiplication (SpMV), and the optimization of its operational procedure has attracted the attention of numerous researchers in recent years. More and more computers provide powerful computing capacities base on a heterogeneous architecture. Nowadays, most of the SpMV algorithms are specific optimization for the hardware architecture of graphics processing unit (GPU). GPUs have attracted increasing attention from researchers as the size of data has grown. In particular, in the field of deep learning, where the recent surge in the development of artificial neural networks has led to an exponential increase in the power required to compute them, the advantage of GPU parallelism over conventional CPU terminology is enormous. However, GPUs are designed for general-purpose processing, and because of this, other specialized multicore processors are used to perform computations in place of GPUs. Specifically, the number of cores is so large that non-equilibrium load problems can easily arise when performing a specific computational task. Its performance is thus limited not by computational capabilities, but by memory bandwidth[4].

To overcome these shortcomings and performance bottlenecks, numerous researchers have taken various approaches[2], including reducing memory access times[17], designing efficient parallel algorithms[12, 14, 19], and using additional

high-performance multicore processors[7, 22] to improve the performance of SpMV. In this paper, the authors leverage a modern multicore processor and design a high-performance parallel algorithm for the hardware architecture and memory hierarchy of the processor to improve the performance of diagonal sparse matrix-vector multiplication.

SpMV for diagonal sparse matrices is defined as:

$$y = Ax \quad (1)$$

where  $A \in R^{m \times n}$  is the diagonal sparse matrix,  $x \in R^n$  is the known vector, and  $y \in R^n$  is the output vector. Unlike the alternative sparse matrix, the nonzero elements of the diagonal sparse matrix are restricted to the main diagonal and its adjacent diagonals. This property makes it possible to optimize hardware based on it.

The Cambrian MLU (Machine Learning Unit) is a domain-specific processor for artificial intelligence applications. It is tailored and optimized for operations commonly used in the field of artificial intelligence, such as convolution, pooling, and activation. Compared to general purpose computing devices such as GPU, MLU has higher performance, energy efficiency, and flexibility when processing AI applications[6, 8].

The MLU designs special data paths and computing components for accessing data streams with different characteristics in AI and implementing isolation between different data streams. At the same time, the flexible access capability of on-chip storage space is exposed to the software and the performance will be improved. The basic building block is the MLU core that is a processor core with full computing, IO, and control capabilities. It can perform computational tasks independently or in collaboration with other MLU cores. Each of the four MLU cores forms a cluster, and each cluster contains an additional memory core and a block of Shared RAM shared by memory core and four MLU cores. Memory core cannot execute vector and tensor computation instructions. It can only be used for Shared RAM and DDR (Double Data Rate, Synchronous Dynamic Random Access Memory). DDR data transfer between SDRAM and MLU cores. In this paper, the hardware this research uses is MLU270, and Fig. 1 [21] shows the hardware architecture of MLU270.

The entire abstract model is divided into five levels: server level, board level, chip level, cluster level, and MLU core level. Each level consists of an abstract control unit, a computation unit, and a storage unit.

- Level 0 is the server level and consists of a control unit consisting of multiple CPUs, a local DDR storage unit,

X. Liu is with Xiamen University, Xiamen, China, email: xrlu@xmu.edu.cn.

Q. Dai is with Xiamen University, Xiamen, China, email: qydai@stu.xmu.edu.cn

H.Zhang is with Institute of Artificial Intelligence, Hefei Comprehensive National Science Center, Hefei, China, email: solomonz@mail.ustc.edu.cn.

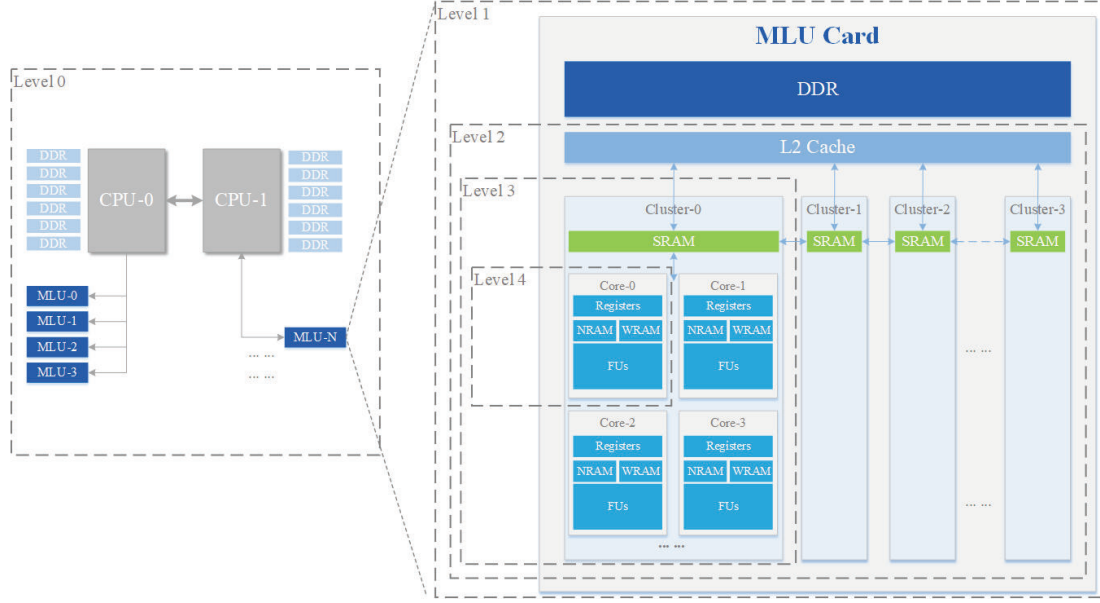


Fig. 1. A MLU architecture

and a computing unit consisting of multiple MLU board cards.

- Level 1 is the board level. Each MLU board consists of a computing unit consisting of a local control unit, a DDR memory unit, and an MLU chip.
- Level 2 is the chip level. Each chip is composed of a local control unit, a local storage unit (such as L2 Cache), and a computing unit composed of one or more clusters.
- Level 3 is the cluster level, where each cluster consists of a local control unit, shared storage, and multiple MLU core computing units.
- Level 4 is the MLU core level. Each MLU core consists of a local control unit, a private storage unit, and a computation unit. Both instruction-level and data-level parallelism are supported within the MLU core.

The rest of this paper is organized as follows. Section II introduces the related work, Section III presents the formats and MLU architecture, Section IV includes the algorithms and its implementation on MLU, the evaluation of kernel performance is in Section V, and Section VI contains conclusions and points to this research's future work.

## II. RELATED WORK

Sparse matrix-vector multiplication (SpMV) is one of the central problems in the field of scientific computing, which makes the speed-up of its operation attractive to a large number of researchers, who have proposed numerous speed-up algorithms.

In general, when large-scale sparse matrix operations are involved, they will be compressed according to a certain compression scheme, and then the corresponding operations will be executed according to a different compression scheme. For

example, the original coordinate (COO) format and the compressed column/row (CSC/CSR) format are common sparse matrix compression methods[24]. Although these storage formats can effectively reduce the space and time needed to operate and store the matrix, for some diagonal sparse matrices, a different storage format is needed, such as the diagonal format (DIA)[20], which only stores nonzero elements according to the diagonal. Moreover, the ellpack format (ELL)[13], which is suitable for sparse matrices that store non-zero elements with relatively uniform row distribution. Designing the corresponding storage structure according to the hardware architecture can considerably improve the performance of SpMV[1]. Bell and Garland[5] first proposed to accelerate SpMV on CUDA based GPUs. They designed the corresponding algorithms based on several different memory structures and GPU hardware architectures. They conclude that different types of sparse matrices can adopt the best storage format and achieve the best performance on the GPU. From then on, numerous different storage structures and their corresponding kernels have been proposed, including the hybrid ELL/COO (HYB)[5], the sliced ellpack (SELL-C-sigmoid)[18], the compressed sparse row 5 (CSR5)[16], the blocked stored format mixed CSR and ELL (BCE)[26], and many more. The above storage structures and their kernels make extensive use of the parallel characteristics of GPU and x86 CPU SIMD devices, which can be found in [10].

DIA is a suitable storage structure for storing diagonally sparse matrices because it allows elements on the same diagonal to be in the same column[5, 12, 15]. However, DIA can also lead to potential space wastage problems, such as if a diagonal has few non-zero elements, then a large number of zeros will be generated in the columns of its corresponding dense matrix. To address this problem, some DIA-based



storage structures have been proposed[3, 23]. Both of them can effectively alleviate the large space waste caused by the original DIA storage structure. Xia et al.[11] proposed DIA-adaptive, which modified the original DIA kernel function and developed two new storage structures and kernel functions for different diagonal sparse matrices and ran them on GPU.

### III. DIAGONAL SPARSE MATRIX COMPRESSION AND MLU ARCHITECTURE

In this section, the authors introduce DIA-Adaptive, which is the basis of the proposed model. Since specific optimizations are performed based on the hardware properties of the MLU.

#### A. DIA-Adaptive

To illustrate the DIA-adaptive and its kernel function, the researchers assume two diagonal sparse matrices as follows.

$$A = \begin{pmatrix} 1 & 2 & 0 & 0 & 3 & 0 \\ 0 & 4 & 5 & 0 & 0 & 6 \\ 7 & 0 & 8 & 9 & 0 & 0 \\ 0 & 10 & 0 & 11 & 12 & 0 \\ 0 & 0 & 13 & 0 & 14 & 15 \\ 0 & 0 & 0 & 16 & 0 & 17 \end{pmatrix}$$

and

$$B = \begin{pmatrix} 1 & 0 & 2 & 0 & 0 & 0 \\ 3 & 4 & 0 & 5 & 0 & 0 \\ 0 & 0 & 6 & 7 & 0 & 0 \\ 0 & 0 & 0 & 8 & 0 & 0 \\ 0 & 0 & 0 & 0 & 9 & 10 \\ 0 & 0 & 0 & 0 & 0 & 11 \end{pmatrix}$$

##### 1) DIA format

For matrix  $A$ , its DIA storage format is split into a matrix  $data$  and a vector  $offset$ . The matrix  $data$  stores the non-zero values of the original matrix according to the diagonal, and the vector  $offset$  is used to store the offset of each diagonal line in the  $data$  from the main diagonal.

$$data = \begin{pmatrix} 0 & 1 & 2 & 3 \\ 0 & 4 & 5 & 6 \\ 7 & 8 & 9 & 0 \\ 10 & 11 & 12 & 0 \\ 13 & 14 & 15 & 0 \\ 16 & 17 & 0 & 0 \end{pmatrix}, offset = (-2 \ 0 \ 1 \ 4)$$

##### 2) BRCSD format

Evidently, when the non-zero values in the matrix are far from the main diagonal, a large number of zero elements will be padded in the  $data$ . Therefore, for this class containing additional non-zero elements away from the main diagonal, an alternative approach can be used to reduce the waste of space. To alleviate this drawback of DIA, Diagonal Compressed Storage based on Row-Blocks (BRCSD) has been proposed in [25]. First, the diagonal sparse matrix is divided into blocks according to the rows, and each block is kept as small as

possible. E.g., the matrix  $A$  can be divided into two blocks. Second, the sparse matrix can be represented as follows:

$$matrix = \{offset[0], offset[1], \dots, offset[n]\}$$

where  $offset[i]$  is the offset of each diagonal from the main diagonal in the  $i$ th piece. And  $A$  can be represented as follows:

$$A = \{(0 \ 1 \ 4), (-2 \ 0 \ 1)\}$$

Finally, the sparse matrix can be represented by two arrays:

$$brcsd\_offsets = \{r_0|offsets[0], \dots, r_n|offsets[n]\}, \\ brcsd\_data = \{data[0], data[1], \dots, data[n]\}$$

where  $r_i$  is the starting row number of the  $i$ th row piece. The matrix  $A$  is represented as follows:

$$brcsd\_offsets = \{0|(0 \ 1 \ 4), 2|(-2 \ 0 \ 1)\} \\ brcsd\_data = \left\{ \begin{pmatrix} 1 & 4 & 2 & 5 & 3 & 6 \\ 7 & 10 & 13 & 16 & 8 & 11 \\ 14 & 17 & 9 & 12 & 15 & 0 \end{pmatrix} \right\}$$

##### 3) BRCSD-II format

While DIA and BRCSD have been able to efficiently store most diagonal sparse matrices, for some matrices with scattered points or countably many zero elements on the diagonal, these two storage formats will still be padded with a large number of zeros. For instance, for the diagonal sparse matrix  $B$ , using DIA and BRCSD, it is respectively stored as

$$data = \begin{pmatrix} 0 & 1 & 0 & 2 \\ 3 & 4 & 0 & 5 \\ 0 & 6 & 7 & 0 \\ 0 & 8 & 0 & 0 \\ 0 & 9 & 10 & 0 \\ 0 & 11 & 0 & 0 \end{pmatrix}, offset = (-1 \ 0 \ 1 \ 2)$$

and

$$brcsd\_offsets = \{0|(-1 \ 0 \ 1 \ 2) \ 4|(0 \ 1)\} \\ brcsd\_data = \left\{ \begin{pmatrix} 0 & 3 & 0 & 0 & 1 & 4 & 6 & 8 \\ 0 & 0 & 7 & 0 & 2 & 5 & 0 & 0 \\ 9 & 11 & 10 & 0 \end{pmatrix} \right\}$$

Apperently, regardless of whether DIA or BRCSD is used to store matrix  $B$ , a large number of zeros will be filled in, because matrix  $B$  contains numerous scatter points and lengthy zero sections.

Therefore, Xia et al. [11] proposed the extension of BRCSD, called BRCSD-II. First, according to BRCSD, the matrix is divided into  $data$  and  $offsets$ . Second, set  $nrows$  equal to the number of threads per block on the GPU. Third, divide the sparse matrix into row pieces according to the row, where  $m$  is the number of rows in the sparse matrix. Finally, accumulate the  $offset$  array. Hence, the sparse matrix can be represented by the following two arrays:

$$brcsdII\_offsets = \{p_0|offsets[0], \dots, p_s|offsets[s]\} \\ brcsdII\_data = \{data[0], data[1], \dots, data[p-1]\}$$

where  $p$  is the number of row pieces,  $s$  is the size of *offsets* after accumulating row pieces. The matrix  $B$  is represented as follows:

$$\begin{aligned} \text{brcsdII\_offsets} &= \{1|(-1 \ 0 \ 2), 2|(0 \ 1)\} \\ \text{brcsdII\_data} &= \left\{ \begin{pmatrix} 0 & 3 & 1 & 4 & 2 & 5 \end{pmatrix}, \right. \\ &\quad \left. \begin{pmatrix} 6 & 8 & 7 & 0 \end{pmatrix}, \right. \\ &\quad \left. \begin{pmatrix} 9 & 11 & 10 & 0 \end{pmatrix} \right\} \end{aligned}$$

It can be observed that the number of zeros in BRCS-D-II decreases from 13 to 3 and from 11 to 3 compared to DIA and BRCS-D, respectively.

### B. MLU architecture

A MLU device is made up of a memory subsystem, a MTP (Multi-Tensor Processor) subsystem, and a media subsystem. The MTP subsystem is the core component of the Cambrian MLU architecture, and a MLU chip typically includes one or more MTP clusters, a PCIE, a memory controller, an L2 Cache, a media processing unit, and an MLU-Link. Each MTP cluster is composed of multiple IPU(Intelligence Processing Unit) cores and a Shared RAM, which is the smallest unit of execution in the MTP architecture. When the number of TP architectures is the same as the MTP, the MTP can run programs that have been developed and compiled for binary compatibility with the TP. In this way, the MTP is similar to the GPC (GPU Processing Cluster) or SE (Shader Engine) of a GPU.

TP (Tensor Processor) is the codename for a single-core architecture that can be thought of as a hardware unit consisting of an IPU core and a memory system. A TP core includes an ALU for performing scalar operations, a VFU(Vector Function Unit)/TFU(Tensor Function Unit) functional unit for AI-related operations, and various DMA units for data movement. The TP also features on-chip NRAM(Neuron RAM) and WRAM(Weight RAM) that are directly connected to the VFU/TFU in order to fully exploit data locality and bandwidth for improved performance.

The MLU offers a range of storage levels, including GPR (General Purpose Register), NRAM, WRAM, Shared RAM, L2 Cache, LDRAM (Local DRAM), GDRAM (Global DRAM), and more. GPR, WRAM, and NRAM are private storage for a core, although memory cores do not have their own private WRAM and NRAM storage resources. The L2 Cache is an on-chip global shared memory that is currently primarily used to cache instructions, kernel parameters, and read-only data. LDRAM is the private storage of each MLU and memory core, and it has a larger capacity than WRAM and NRAM. It is typically used to address storage shortages on the chip. GDRAM, on the other hand, is a global shared storage that can be used to enable data sharing between hosts and devices, as well as between computing tasks.

The MLU allows software to directly manage the movement of data between its various storage levels. To facilitate this, the compiler provides heavy-duty address space declarations for upper-layer software, as well as a wide range of mechanisms

and programming interfaces for explicit or implicit data movement. This allows users to explicitly control the movement of data between different storage levels, allowing them to precisely control the timing and volume of data movement in order to achieve a balance between computation and IO and maximize computational efficiency.

MLU supports parallel computation at seven different levels: the server level, the board level, the chip level, the cluster level, the MLU core level, the pipeline level, and the data level. In particular, server-level and board-level parallelism are determined by the specific system, while chip-level, cluster-level, and core-level parallelism are determined by the user when configuring the task size and type on the host side. The pipeline level and data within each core are also determined by the user through programming on the device side. On the device side, the main unit of user programming is a task. Each task will only be executed on one core during a specific execution, and no task-switching will occur during this time. Multiple tasks can be executed in parallel within each cluster, and the number of clusters supported by each chip may vary. Each core is a processor core that is capable of controlling streaming, scalar, and vector operations. Scalar operation instructions and control flow instructions are mainly used for implementing control flow functions, while vector instructions are used for implementing parallel data processing. A vector operation instruction can process data of arbitrary length.

MLU cores have four instruction pipelines: the IO stream, move stream, compute stream, and scalar stream. All instructions involving reading and writing off-chip DDR memory are executed in the IO stream. The move stream handles memory access instructions that do not read and write off-chip DDR. The compute stream is responsible for tensor, vector calculation, and all scalar instructions. All operations are performed in the scalar stream. All instruction pipelines are able to run in parallel. By default, IO, move, compute, and scalar streams are executed concurrently, but the hardware guarantees register dependencies between the scalar stream and the other streams. For example, if an IO, move, or compute stream instruction modifies a universal scalar register, the hardware will ensure that the corresponding register-reading instruction in the scalar stream is executed after the specified execution of the additional streams. When an instruction in a scalar stream modifies a register, instructions in different streams that need to read the corresponding register must also wait for the scalar stream's write operation to be completed before executing.

### IV. PARALLEL ALGORITHM OF DIAGONAL SPMV AND ITS MLU IMPLEMENTATION

In this section, the authors present the proposed method for adapting sparse matrix-vector multiplication for diagonal sparse matrices on MLU. This adaptive approach allows for efficient and effective calculation of matrix-vector products when dealing with diagonal sparse matrices on MLU hardware. By utilizing the unique capabilities of MLU, this method is able to improve upon existing methods and achieve better

performance in these specific scenarios. The research will provide a detailed description of this proposed method and its advantages in the following sections.

#### A. DIA kernel

---

**Algorithm 1:** The kernel function of DIA for SpMV

---

**Data:** The known vector  $x$ , the number of rows  $num\_rows$ , cols  $num\_cols$ , and diagonals  $num\_diags$  of the matrix and the arrays in DIA  $format(data, offsets)$

**Result:** The output vector  $y$

```

1 row = taskId;
2 if row ≤ num_rows then
3   sum = 0.0;
4   NRAM int offset_n[num_diags];
5   NRAM float data_n[num_diags];
6   NRAM float x_n[num_cols];
7   memory copy from offsets to offset_n;
8   memory copy from data to data_n with stride
   num_rows;
9   memcopy copy from x to x_n;
10  for i = 0 to num_diags with i = i + 1 do
11    uint32_t col = row + offset_n[i];
12    float val = data_n[num_rows * i + row];
13    if col ≥ 0 and col ≤ num_cols then
14      sum += val * x_n[col];
15    end
16  end
17  y[row] = sum;
18 end

```

---

Parallelizing SpMV on MLU for DIA is intuitive: one task processes one row. Algorithm. 1 shows the main procedure of the DIA kernel. It seems that since this research moves  $x$ ,  $data$ , and  $offsets$  from DDR to NRAM in advance, it is faster on each memory access. Moreover, memory accesses to  $data$  and  $x$  are contiguous, which ensures higher performance of the DIA kernel.

#### B. BRCSD kernel

The parallelization of SpMV for BRCSD on MLU is intuitive, with each task processing a single row piece. However, the number of rows contained in a row piece for BRCSD varies, leading to unbalanced workloads for each task. For example, when processing the matrix  $B$ , the first row piece may be assigned to one task and the second row piece to another, but the difference in the number of rows contained in these pieces may be too large. To address this issue, it is necessary to ensure that each task processes the same number of rows as much as possible.

Specifically, the authors pre-specify a value  $n$ , which is the maximum number of rows each task needs to process. Let a row piece size be  $t$ , then when  $t$  is larger than  $n$ , and divide it into  $\lceil t/n \rceil$  row pieces again. In this way, it can be

---

**Algorithm 2:** The kernel function of BRCSD for SpMV

---

**Data:** The known vector  $x$ , the number of rows  $num\_rows$ , cols  $num\_cols$ , and diagonals  $n\_diags$  of the matrix and the arrays in BRCSD  $format(brcsd\_data, brcsd\_offsets)$

**Result:** The output vector  $y$

```

1 local_id = taskId;
2 offset_id = taskId < 1 ? 0 : 1;
3 NRAM float tmp = 0.0;
4 NRAM float data_n[n_diags];
5 NRAM float x_n[n_diags];
6 NRAM float result[n_diags];
7 switch offset_id do
8   case 0 do
9     memory copy from brcsd_data starting from
       local_id + 2 to data_n in strides of 2;
10    memory copy from x starting from local_id to
       x_n in strides of 3;
11    bang_mul(result, data_n, x_n, 3);
12    bang_reduce_sum(&tmp, result, 3);
13    y[local_id] = tmp;
14  end
15  case 1 do
16    memory copy from brcsd_data starting from
       local_id + 4 to data_n in strides of 4;
17    memory copy from x starting from local_id - 2
       to x_n in strides of 3;
18    bang_mul(result, data_n, x_n, 3);
19    bang_reduce_sum(&tmp, result, 3);
20    y[local_id + coreId] = tmp;
21  end
22 end

```

---

guaranteed that the number of rows in the final row pieces is at most  $n$ . For the matrix  $B$ , for example, Algorithm 2 shows the main procedure of BRCSD kernel. The researchers set  $n = 2$ . Apparently, the matrix was split two row pieces. And the second row piece was split two row pieces again. Therefore, as shown in Algorithm 2, one task processes three rows respectively.

In this kernel, the authors utilize the *bang\_mul* and *bang\_reduce\_sum* instructions. The *bang\_mul* instruction performs element-wise multiplication of two vectors, storing the result in the *result* vector. The final parameter specifies the number of elements participating in the multiplication. The *bang\_reduce\_sum* instruction performs a summation of the elements in a vector, storing the result in the *tmp* variable. The final parameter specifies the number of elements to be summed.

#### C. BRCSD-II kernel

Parallelizing SpMV on MLU for BRCSD-II is also intuitive. Given a matrix split into row pieces by BRCSD-II, one core

**Algorithm 3:** The kernel function of BRCSD-II for SpMV

**Data:** The known vector  $x$ , the number of rows  $num\_rows$ , cols  $num\_cols$ , and diagonals  $n\_diags$  of the matrix and the arrays in BRCSD  $format(brcsd\_data, brcsdII\_offsets)$

**Result:** The output vector  $y$

```

1   $core\_id = coreId$ ;
2   $local\_id = taskId$ ;
3   $offset\_id = taskId < 1 ? 1 : 2$ ;
4  NRAM float  $tmp = 0.0$ ;
5  NRAM float  $data\_n[n\_diags]$ ;
6  NRAM float  $x\_n[n\_diags]$ ;
7  NRAM float  $result[n\_diags]$ ;
8  SRAM float  $y\_n[n\_diags]$ ;
9  NRAM uint32_t  $offset\_n[n\_diags][n\_diags]$ ;
10 memory copy from  $brcsdII\_offsets$  to  $offset\_n$ ;
11 switch  $offset\_id$  do
12   case 1 do
13     memory copy from  $brcsdII\_data$  starting from
        $core\_id * 3 + local\_id$  to  $data\_n$  in strides of
       2;
14     memory copy from  $x$  starting from
        $offset\_n[offset\_id]$  to  $x\_n$ ;
15      $bang\_mul(result, data\_n, x\_n, 3)$ ;
16      $bang\_reduce\_sum(&tmp, result, 3)$ ;
17      $y\_n[local\_id + core\_id * 2] = tmp$ ;
18   end
19   case 2 do
20     memory copy from  $brcsdII\_data$  starting from
        $(core\_id - 1) * 2 * 2 + local\_id + 3 * 2 * 1$  to
        $data\_n$  in strides of 2;
21     memory copy from  $x$  starting from
        $offset\_n[offset\_id]$  to  $x\_n$ ;
22      $bang\_mul(result, data\_n, x\_n, 2)$ ;
23      $bang\_reduce\_sum(&tmp, result, 2)$ ;
24      $y\_n[local\_id + coreId * 2] = tmp$ ;
25   end
26 end
27 synchronize all cores;
28 memory copy from  $y\_n$  to  $y$ ;
```

processes one row piece, and within each core, one task processes one row. Algorithm 3 presents this process.

First, the authors get the absolute ID  $core\_id$  of the core, because each MLU includes 4 clusters, and each cluster has 4 cores, so  $clusterId * 4 + coreId$  needs to be used when calculating the absolute ID of the core. After determining the ID of the core, the present study gets the  $local\_id$  through  $taskId$ , where  $local\_id$  is the absolute ID of the thread inside each core. Specifically,  $core\_id$  locates the row piece number to be processed in the matrix, and  $local\_id$  locates the specific row in each row piece.

When performing an operation, the  $offset$  needs to be

moved to the NRAM first, so that subsequent SpMV can read the  $offset$  directly from the NRAM. It is then necessary to determine which part of the  $offset$  is required to extract the value of the vector  $x$  from the current  $core\_id$ . Finally, based on the read values, the results are obtained using the vector multiplication and addition operator functions provided by MLU and stored in a temporary vector. The reason it is not directly stored in the result  $y$  is the vector  $y$  is currently stored in DDR. If the result vector is stored directly in the DDR, it needs to be written to the DDR, which results in a large waste of bandwidth per thread. To alleviate this situation, the authors temporarily store the results in SRAM(Shared RAM). Since all cores share the same Shared RAM, the operation of applying to the Shared RAM space is executed only once during the actual execution. Moreover, the performance of the kernel can be substantially improved due to the considerably higher access speed of Shared RAM compared to DDR. After the operation is completed, the synchronization instruction waits for all four cores to complete the operation, and then writes the data in Shared RAM to the DDR at once. It can also be done with only one vector operation instruction.

#### D. MLU implementation

In this subsection, the researchers describe the implementation of the algorithm on MLU because its architecture and programming mode are different from those of general-purpose GPUs. The hardware platform used in the experiments is an MLU270, whose characteristics are shown in Figure 1.

When conducting experiments, the authors the default configuration of the MLU, which consists of four clusters with four cores each. The four clusters in the MLU share a single main memory, where data transferred from the CPU is typically stored. Each cluster includes one Shared RAM that is shared by the four cores, as well as private NRAM and WRAM within each core. Like the CPU, each core also has its own set of registers, but they cannot be programmed. Only memories with storage structures above the NRAM and WRAM levels can be directly programmed. When running a kernel, it is necessary to first transfer the data and the basic configuration of the MLU to the MLU and then call the startup function on the CPU side to start the MLU for operation. During operation, data that is frequently used is first moved from DDR to NRAM inside each core, and the results of the operation are first stored in the Shared RAM shared by the four cores. This speeds up data access, resulting in improved performance.

In practice, the MLU assigns default data to the stack of each thread. The advantage of a stack is that access is very fast, but the disadvantage is that each thread cannot share data with other threads and the space inside the stack is relatively small. This is not sufficient to meet the performance requirements of large-scale SpMV operations. Therefore, in the experiments, researchers store commonly used data in NRAM and store the results of the operation in the Shared RAM shared by the four cores, so that threads within each core can share data and the results of the same cluster are also stored in one place.



This allows the algorithm to avoid slowing down too much when reading and writing data. After a cluster computation is completed, the four cores need to be synchronized and then all of the results are written to the DDR at once, which also reduces the time overhead of MLU bus calls. The remaining four clusters can operate in parallel, increasing the parallelism of the kernel. The authors also use techniques such as loop unrolling when compiling and executing the kernel.

## V. EVALUATION AND ANALYSIS

The experimental evaluation has two goals: (1) to compare the performance of the algorithm to several state-of-the-art SpMV kernels running on GPU, and (2) to evaluate the performance improvement of the memory-level optimization using MLU relative to the non-optimized version.

TABLE I  
EXPERIMENT ENVIRONMENT

Processor	MLU270-S4
Architecture	MLUv02
INT16 peak/TOPS	64
Precision Support	INT16, INT8, FP32, FP16
Memory	16GB DDR4, ECC
Bandwidth	102GB/s
Interface	x16 PCIe Gen.3
Bitwidth	256-bit

Table I presents the MLU270 used in this experiment. The performance is measured by the runtime of the kernel, which is calculated from the time the program calls the MLU's side functions until the MLU hands the console back to the CPU. Due to the fact that the data is pre-written to the MLU's DDR at the time the computation is performed, there is no write-back time for the computation results here, so the runtime is equal to the computation time of the MLU. The diagonal sparse matrices used in this experiment is from the University of Florida Sparse Matrix Collection [9]. Table II summarizes information about the tested diagonal sparse matrices, including the dimension, the number of diagonals (i.e., the number of diagonals containing nonzero elements), and the number of nonzero elements.

For simplicity, in the following experiments, all data was run with single precision.

### A. Experimental analysis

In this subsection, the researchers present an implementation of the kernel on the MLU and demonstrate how they classified test matrices into three types based on their structure. They then used different kernels for each type, with the optimal kernels for each type shown in Table III. The evaluation of the performance of these kernels on both the GPU and MLU shows that, in most cases, the kernels perform better on the MLU than on the GPU, and they outperform existing state-of-the-art kernels on the GPU. Finally, the authors compare the performance of four algorithms (CRSD, HDI, DIA, and the proposed DIA-Adaptive algorithm) on the MLU and show that

TABLE II  
DESCRIPTIONS OF TEST MATRICES

Matrix	Dimension	Diagonals	nonzeros
wang3	26,064×26,064	21	177,168
wang4	26,068×26,068	23	177,196
s3dkt3m2	90,449×90,449	655	3,686,223
s3dkq4m2	90,449×90,449	661	4,427,725
kim1	38,415×38,415	25	933,195
kim2	456,976×456,976	25	11,300,020
nemeth21	9,506×9,506	169	1,173,746
nemeth22	9,506×9,506	197	1,358,832
af_1_k101	503,625×503,625	897	17,550,675
af_2_k101	503,625×503,625	897	17,550,675
crystk02	13,965×13,965	99	968,583
crystk03	24,696×24,696	99	1,751,178
pde225	225×225	5	1,065
pde900	900×900	5	4,380
pde2961	2,961×2,961	5	14,585

TABLE III  
OPTIMAL KERNELS FOR TEST MATRICES

Matrix	Optimal kernel
wang3	BRCS-D-II
wang4	BRCS-D-II
s3dkt3m2	BRCS-D-II
s3dkq4m2	BRCS-D-II
kim1	BRCS-D-II
kim2	BRCS-D-II
nemeth21	BRCS-D-II
nemeth22	BRCS-D-II
af_1_k101	BRCS-D-II
af_2_k101	BRCS-D-II
crystk02	BRCS-D-II
crystk03	BRCS-D-II
pde225	BRCS-D-I
pde900	BRCS-D-I
pde2961	BRCS-D-I

DIA-Adaptive consistently outperforms the other algorithms for the same test matrices.

In this work, this research identified three types of diagonal sparse matrices, which are depicted in Fig. 2 [25]. These matrix types can be distinguished based on their structures and the distribution of their non-zero elements. A type I matrix is a diagonal matrix with dense diagonal elements that are concentrated on the main diagonal. Type II matrices have dense diagonal elements that are located on diagonals further from the main diagonal and have shorter lengths. Type III has both type II elements and zero elements on its diagonal, in addition to additional scattered points. Type I matrices can be stored using the normal DIA format because their diagonal elements are close to the main diagonal, which reduces the number of padded zeros. Type II matrices are best stored using the BRCS-D format because DIA would produce too many padded zeros. However, BRCS-D-II may also be used for type II matrices, though it is more complex. Type III matrices must be stored using BRCS-D-II in order to minimize padded zeros.

In the experiments, the researchers selected 16384, 4096, and 1024 threads for the MLU in each of the four clusters,

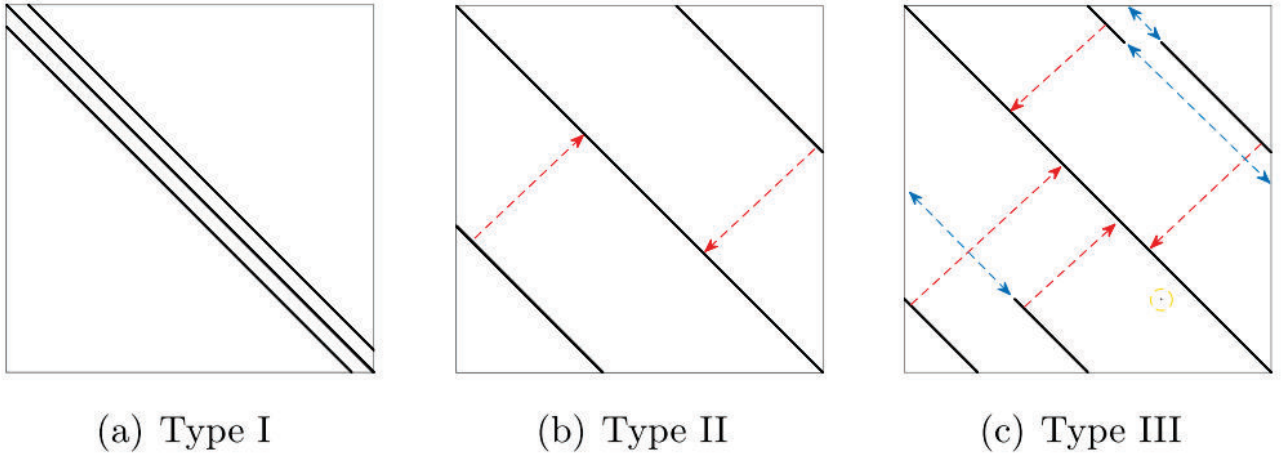


Fig. 2. Three types of diagonal sparse matrices

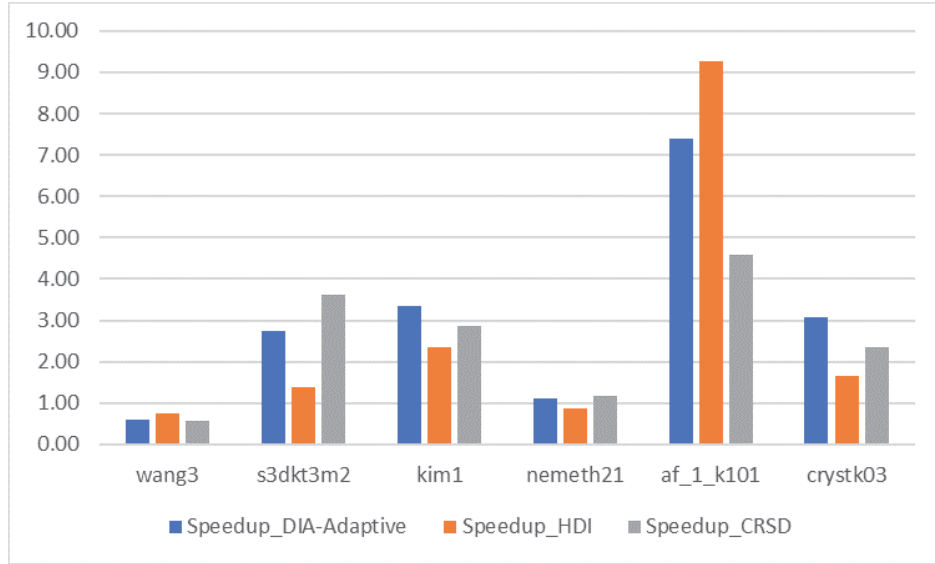


Fig. 3. Speedup of CRSD, HDI, and DIA-Adaptive on MLU versus GPU

because the number of threads on the MLU is closely linked to its running efficiency. As shown in Fig. 7, the kernel performance improves as the number of threads per core decreases, particularly when the number of threads is reduced from 16384 to 4096. However, reducing the number of threads from 4096 to 1024 does not lead to a significant improvement, which is unexpected because, in theory, the more threads there are, the better the performance should be. This is because the hardware characteristics and optimization strategies of the software stack on MLU are different from those of traditional GPUs. Therefore, kernels running on MLU should not be assigned too many threads. The reason is that MLU primarily relies on different cores to perform parallel tasks, and the role of threads on GPU is equivalent to that of cores. Furthermore, cores have stronger computational capabilities compared to

threads on GPU.

#### B. Performance evaluation

##### 1) MLU acceleration for CRSD, HDI, and DIA-Adaptive

Fig. 3 presents the performance speedup of the CRSD, HDI, and DIA-Adaptive formats on the MLU and GPU. The vertical coordinate indicates the speedup of the performance improvement. On average, the CRSD, HDI, and DIA-Adaptive formats achieve speedups of  $2.53\times$ ,  $2.71\times$  and  $3.05\times$  on the MLU, respectively.

Clearly, the immediate impact of MLU on performance improvement is evident. However, for wang3, the speedup is not very impressive. As shown in Fig. 4, the structure of wang3 is depicted, and Fig. 5 illustrates the structure of wang3 after scaling. By examining Fig. 5, it can be inferred that wang3 belongs to type III. Based on this information, the

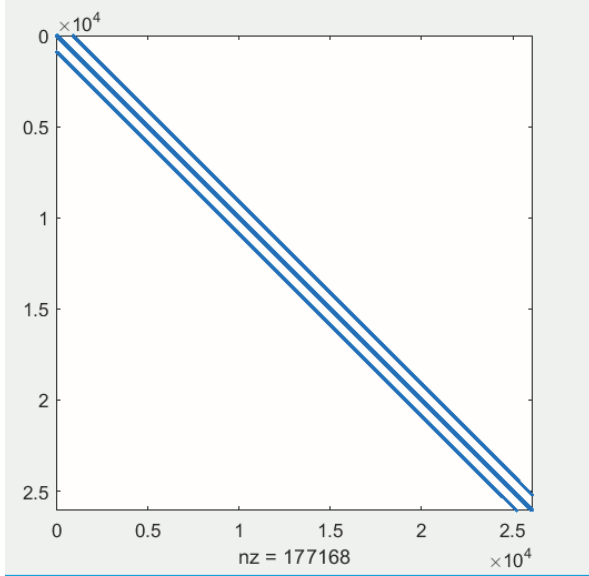


Fig. 4. Structure of wang3

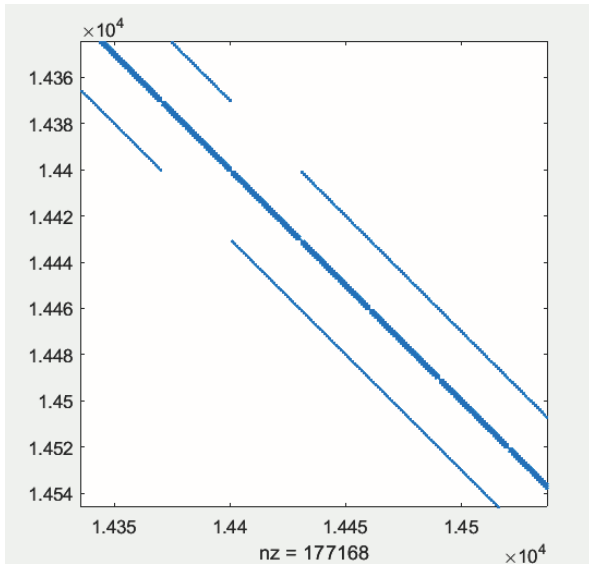


Fig. 5. Structure of wang3 after scaling

authors speculate that the poor performance of wang3 when using MLU may be attributed to the excessive offsets that result from its conversion to the BRCSD-II structure. As it closely resembles a typical type I matrix, it is divided into many smaller blocks when converted to BRCSD-II storage, which leads to the optimization of the BRCSD-II kernel by the memory hierarchy. Consequently, during actual operation, there is frequent swapping of data from DDR to NRAM, resulting in a loss of performance.

In further experiments, SpMV based on CRSD, HDI and DIA-Adaptive are all accelerated by MLU.

### 2) Performance of DIA-Adaptive

In this particular subsection of the experiment, this research compares the computation time of SpMV on MLU using CRSD, HDI, and DIA-Adaptive kernels. The authors find that DIA-Adaptive consistently performs the best among these options in most cases. As shown in Fig. 6, the performance improvement of DIA-Adaptive compared to SpMV in CRSD, HDI, and DIA on MLU is clearly evident.

In this experiment, the researchers discovered that the DIA-Adaptive format of SpMV was able to outperform the CRSD, HDI, and DIA formats in terms of performance. When compared to these three formats, DIA-Adaptive demonstrated average performance improvements of 35.21%, 37.36%, and 69.69%, respectively.

### 3) Performance of different threads

Before running a kernel, the MLU must be configured to set the number of threads that will be allocated to it, much like the GPU. By default, the MLU270 will use four clusters for parallel computation, with each cluster containing four cores that also perform parallel operations. In order to execute a task on an MLU, it is necessary to specify the number of clusters and threads that will be required for this task. With this in mind, the authors will now explore the impact that different numbers of clusters and threads can have on the performance of DIA-Adaptive in this particular subsection.

The researchers analyze the impact of the number of threads and clusters on the performance of SpMV for the DIA-Adaptive scheme through the results presented in Figs. 7 and 8.

As shown in Fig. 7, the performance of the DIA-Adaptive kernel varies based on the number of threads used in the same 4-cluster configuration. It is clear from the figure that for almost all of the sparse matrices, the kernel performance improves as the number of threads decreases. This is likely due to the fact that a smaller number of threads leads to a reduction in thread switching overhead, resulting in improved performance. Fig. 8 illustrates the performance of the DIA-Adaptive kernel when using different numbers of clusters in the same thread configuration. As with Fig. 7, the performance improvement is more significant for smaller numbers of clusters.

## VI. CONCLUSION

In this paper, the authors introduce the DIA-Adaptive scheme and its associated kernel for the MLU, which focuses on the use of vector instruction sets to optimize the parallel performance of single-precision SpMV. The researchers then evaluate the improvement of the DIA-Adaptive scheme and kernel over alternative storage schemes on both the GPU and MLU, and also investigate the impact that varying the number of threads and clusters can have on performance. In the future, the researchers plan to further study the effect of additional types of diagonal sparse matrices and multi-MLU platforms on kernel performance.

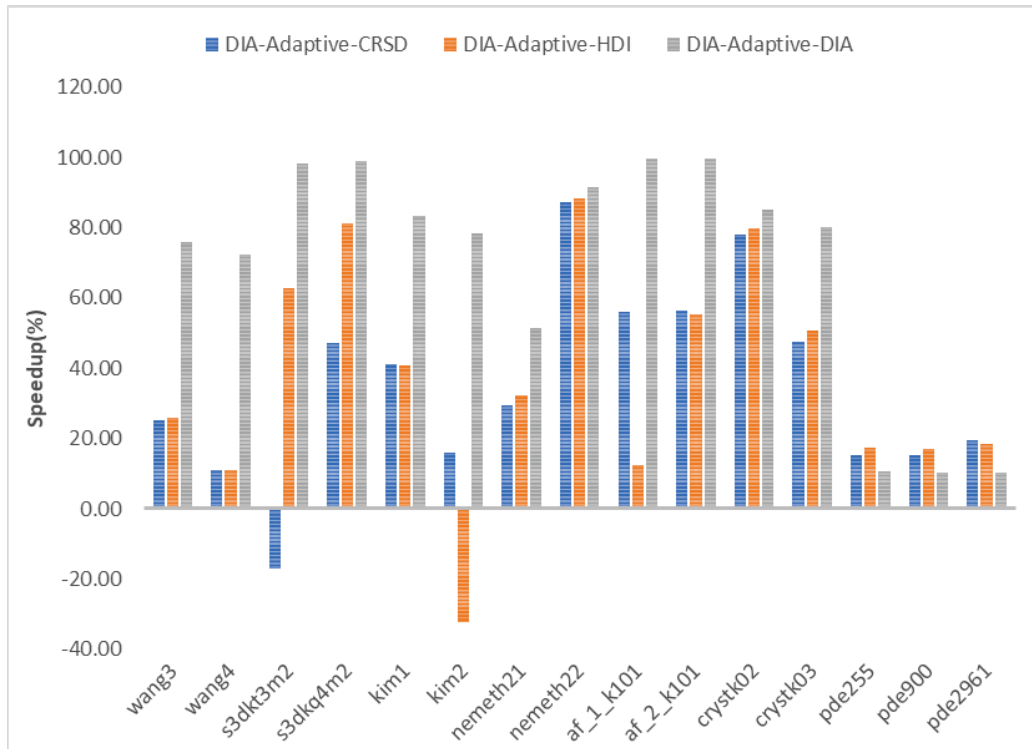


Fig. 6. The performance improvement of DIA-Adaptive

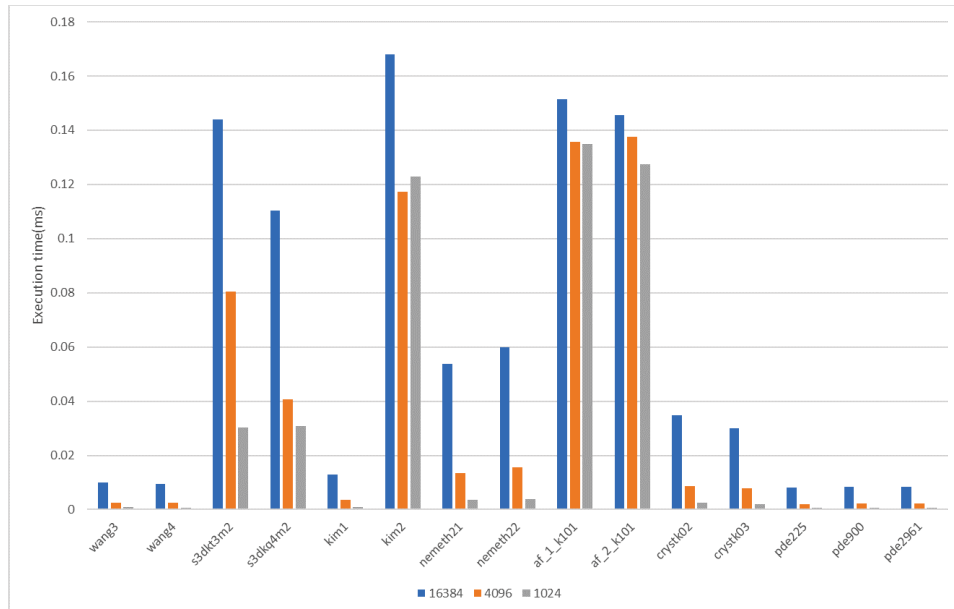


Fig. 7. The performance of SpMV with different threads

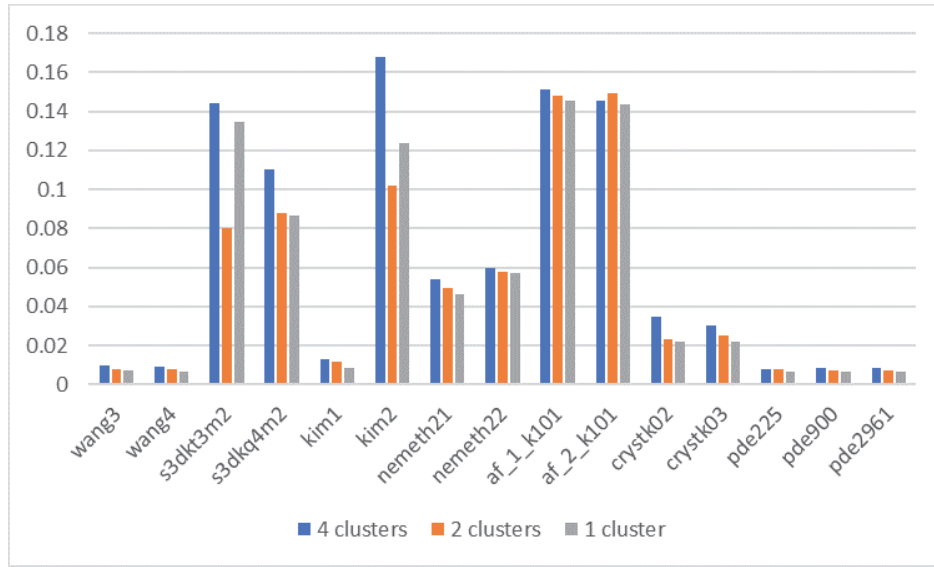


Fig. 8. The performance of SpMV with different clusters

## REFERENCES

- [1] Abubaker, N., et al. (2018). "Spatiotemporal graph and hypergraph partitioning models for sparse matrix-vector multiplication on many-core architectures." *IEEE Transactions on Parallel and Distributed Systems* 30(2): 445-458.
- [2] Aleksei, S., et al. (2022). "Comparing the performance of general matrix multiplication routine on heterogeneous computing systems." *Journal of Parallel and Distributed Computing* 160.
- [3] Barbieri, D., et al. (2015). "Three storage formats for sparse matrices on GPGPUs."
- [4] Beaumont, O., et al. (2019). "Recent Advances in Matrix Partitioning for Parallel Computing on Heterogeneous Platforms." *IEEE Transactions on Parallel and Distributed Systems* 30(1).
- [5] Bell, N. and M. Garland (2009). Implementing sparse matrix-vector multiplication on throughput-oriented processors. *Proceedings of the conference on high performance computing networking, storage and analysis*.
- [6] Chen, T., et al. (2014). "DianNao." *ACM SIGARCH Computer Architecture News* 42(1).
- [7] Chen, Y., et al. (2019). "Performance-Aware Model for Sparse Matrix-Matrix Multiplication on the Sunway TaihuLight Supercomputer." *IEEE Transactions on Parallel and Distributed Systems* 30(4).
- [8] Chen, Y., et al. (2014). "DaDianNao." *Microarchitecture*.
- [9] Davis, T. A. and Y. Hu (2011). "The University of Florida sparse matrix collection." *ACM Transactions on Mathematical Software (TOMS)* 38(1): 1-25.
- [10] Filippone, S., et al. (2017). "Sparse matrix-vector multiplication on GPGPUs." *ACM Transactions on Mathematical Software (TOMS)* 43(4): 1-49.
- [11] Gao, J., et al. (2021). "Adaptive diagonal sparse matrix-vector multiplication on GPU." *Journal of Parallel and Distributed Computing* 157: 287-302.
- [12] Gao, J., et al. (2017). "A multi-GPU parallel optimization model for the preconditioned conjugate gradient algorithm." *Parallel Computing* 63: 1-16.
- [13] Im, E.-J., et al. (2004). "Sparsity: Optimization framework for sparse matrix kernels." *The International Journal of High Performance Computing Applications* 18(1): 135-158.
- [14] Kunchum, R., et al. (2017). "On improving performance of sparse matrix-matrix multiplication on GPUs." *Supercomputing*.
- [15] Li, K., et al. (2014). "Performance analysis and optimization for SpMV on GPU using probabilistic modeling." *IEEE Transactions on Parallel and Distributed Systems* 26(1): 196-205.
- [16] Liu, W. and B. Vinter (2015). CSR5: An efficient storage format for cross-platform sparse matrix-vector multiplication. *Proceedings of the 29th ACM on International Conference on Supercomputing*.
- [17] Ma, S., et al. (2019). "Coordinated DMA: Improving the DRAM Access Efficiency for Matrix Multiplication." *IEEE Trans. Parallel Distrib. Syst.* 30(10).
- [18] Monakov, A., et al. (2010). Automatically tuning sparse matrix-vector multiplication for GPU architectures. *International Conference on High-Performance Embedded Architectures and Compilers*, Springer.
- [19] Ruoxi, W., et al. (2021). "PBBFMM3D: a parallel black-box algorithm for kernel matrix-vector multiplication." *Journal of Parallel and Distributed Computing*(prepublish).
- [20] Saad, Y. (1990). SPARSKIT: A basic tool kit for sparse matrix computations.
- [21] Cambricam[Image]. MLU Server Hierarchy.

[https://www.cambricon.com/docs/bangc/developer\\_guide\\_html/\\_images/4.1.png](https://www.cambricon.com/docs/bangc/developer_guide_html/_images/4.1.png)

- [22] Sergio, B., et al. (2022). "Efficient and portable GEMM-based convolution operators for deep neural network training on multicore processors." *Journal of Parallel and Distributed Computing* 167.
- [23] Sun, X., et al. (2011). Optimizing SpMV for diagonal sparse matrices on GPU. 2011 international conference on parallel processing, IEEE.
- [24] Williams, S., et al. (2007). Optimization of sparse matrix-vector multiplication on emerging multicore platforms. SC'07: Proceedings of the 2007 ACM/IEEE Conference on Supercomputing, IEEE.
- [25] Xia, Y., et al. (2018). A parallel solving algorithm on GPU for the time-domain linear system with diagonal sparse matrices. *Workshop on Big Scientific Data Benchmarks, Architecture, and Systems*, Springer.
- [26] Yang, W., et al. (2018). "A parallel computing method using blocked format with optimal partitioning for SpMV on GPU." *Journal of Computer and System Sciences* 92: 152-170.

# A Framework for Blockchain Vulnerability Detection and Cybersecurity Education

Hongmei Chi

Dept. of Computer & info Sciences  
Florida A&M University Tallahassee, FL, USA  
hongmei.chi@famu.edu

**Abstract**—The Blockchain has become a necessity for many different societal industries and ordinary lives including cryptocurrency technology, supply chain, health care, public safety, education, etc. Therefore, training our future blockchain developers to know blockchain programming vulnerability and I.T. students' cyber security is in high demand. In this work, we propose a framework including learning modules and hands-on labs to guide future I.T. professionals towards developing secure blockchain programming habits and mitigating source code vulnerabilities at the early stages of the software development lifecycle following the concept of Secure Software Development Life Cycle (SSDLC). In this research, our goal is to make blockchain programmers and I.T. students aware of the vulnerabilities of blockchains. In summary, we develop a framework that will (1) improve students' skills and awareness of blockchain source code vulnerabilities, detection tools, and mitigation techniques (2) integrate concepts of blockchain vulnerabilities for IT students, (3) improve future IT workers' ability to master the concepts of blockchain attacks.

**Keywords**—*software vulnerability detection; hands-on lab; static analysis tools; vulnerabilities, Blockchain; active learning.*



# Molecular Dynamics Studies of Main Factors Affecting Mass Transport Phenomena on Cathode of Polymer Electrolyte Membrane Fuel Cell

Jingjing Huang, Nengwei Li, Guanghua Wei, Jiabin You, Chao Wang, Junliang Zhang

**Abstract**— In this work, molecular dynamics (MD) simulation is applied to analyze the mass transport process in the cathode of proton exchange membrane fuel cell (PEMFC), of which all types of molecules situated in the cathode is considered., a reasonable and effective MD simulation process is provided and models are built and compared using both Materials Studio and LAMMPS. The mass transport is one of the key issues in the study of proton exchange membrane fuel cells (PEMFCs). In this report, molecular dynamics (MD) simulation is applied to analyze the influence of Nafion ionomer distribution and Pt nano-particle size on mass transport process in the cathode. It is indicated by the diffusion coefficients calculation that a larger quantity of Nafion as well as a higher equivalent weight (EW) value will hinder the transport of oxygen. In addition, medium-sized Pt nano-particles (1.5-2nm) are more advantageous in terms of proton transport compared with other particle sizes (0.94-2.55nm) when the center-to-center distance between two Pt nano-particles is around 5 nm. Then mass transport channels are found to be formed between the hydrophobic backbone and the hydrophilic side chains of Nafion ionomer according to the radial distribution function (RDF) curves. And morphology of these channels affected by the Pt size is believed to influence the transport of hydronium ions and consequently the performance of PEMFC.

**Keywords**—cathode catalytic layer, mass transport, molecular dynamics, proton exchange membrane fuel cell

## I. INTRODUCTION

NOWADAYS, low-carbon transformation has become a necessary condition for all countries to achieve long-term sustainable development goals. As a secondary energy source, hydrogen energy has much attention because of its abundant sources, cleanness, flexibility and high-efficiency, etc. It can be widely used in various fields, particularly in transportation and industry. An energy economy based on hydrogen energy may become one of the ultimate solutions of human society, which can greatly alleviate the problems of energy shortage, climate change and environmental pollution. The use of hydrogen energy is therefore an important part of the global energy strategy, which is being transforming from the efficient use of traditional fossil fuels to the vigorous development of renewable energies [1].

Hydrogen can be efficiently used by engines and fuel cells. Engines burn hydrogen in the similar way as gasoline and natural gas; while fuel cells convert the chemical energy stored in hydrogen to electricity and heat. Because the electrochemical reaction process is not limited by the Carnot cycle efficiency, its theoretical efficiency is much higher than that of the combustion process [2]. Most importantly, the single reaction product, water, is harmless to human health and the environment.

Among all different types of fuel cells, polymer electrolyte membrane fuel cell (PEMFC) is believed to have a very high performance and a great application value [3]. A PEMFC is typically composed of two bipolar plates (BP), gas diffusion layer (GDL), catalyst layer (CL) and proton exchange membrane (PEM). The last three components form a sandwich-like system which is named membrane electrode assembly (MEA) and leads to its advantages. First, since the cathode and anode are separated by solid polymer film, together with the relatively low work temperatures (typically 60 to 80°C), PEMFC is much easier to be sealed, assembled and operated, and it can start up faster than almost all the other high temperature fuel cells [4]. Second, the only liquid phase product in PEMFC is the water, for which the system is barely corrosive. No special anti-corrosion materials or processes are needed in the parts of the cell, which reduces the manufacturing cost.

Critical progress has been made in key technologies of PEMFC, however, PEMFC is still not able to provide an affordable cost to meet the needs of consumers for basic services, issues including durability, reliability and economy remain to be resolved. Therefore, the development and optimization of hydrogen fuel cells, as important measures and effective ways to realize future energy strategies, have been the focus of researches in recent decades. Compared with the traditional experimental methods, many simulation methods have been proved to be more effective in observing, understanding and predicting the complex physicochemical process in PEMFC. Under such a circumstance, molecular dynamics (MD) methods have been developed and utilized to simulate and analyze the mass transport in MEA. It can simply

Jingjing Huang, Nengwei LI and Guanghua Wei are with the SJTU-Paris Tech Elite Institute of Technology, Shanghai Jiao Tong University, Shanghai, 200240, China (e-mail: ghwei@sjtu.edu.cn; jane0730@sjtu.edu.cn).

Jiabin You and Junliang Zhang are with the Institute of Fuel Cells, School of Mechanical Engineering, Shanghai Jiao Tong University, Shanghai, 200240, China (e-mail: junliang.zhang@sjtu.edu.cn).

Chao Wang is with Shanghai Tangfeng Energy Co., LTD, [NSF 21905172] & [SNSF] (e-mail: ghwei@sjtu.edu.cn).



and intuitively present the process of a PEMFC at the molecular level, and then make a reasonable prediction for the impact of various factors on PEMFC performance. It also helps to understand the experimental mechanism and plays an important role in the optimization of PEMFC.

The Catalytic Layer (CL) is the place where the oxidation-reduction reaction of PEMFC takes place. The CL is mostly porous composites of Pt, carbon and Nafion ionomers. Pt, in the form of nano-particles, is the most employed catalyst in PEMFC, usually attached on carbonaceous substrates such as Vulcan XC-72. Nafion ionomer consists of fluorinated backbone and pendent sulfonic acid groups, and it plays a vital role in the formation of agglomerate structure of CL [5]. The properties of Nafion ionomers, Pt nano-particles and the carbon support are believed to affect the agglomerates greatly, which influences the transport of protons and oxygen, and finally determines the performance of the fuel cell [6]-[8].

One of the most important properties of Nafion ionomer is equivalent weight (EW), which signifies grams of dry Nafion containing one mole of sulfonic acid groups. The value of EW characterizes the number of fluorinated carbon as well as the length of backbone, which can affect the diameter of the agglomerates and the waters fixed by the hydrophilic sulfonic acid groups. Büchi et al. [9] measured oxygen concentrations and diffusion coefficients in various proton exchange membranes with chronoamperometry at microelectrodes. They found that increasing EW of the membranes would lead to an increase of oxygen concentrations and a decrease of its diffusion coefficient. Their model was based on the idea of separating the membranes structure into a hydrophobic phase and a hydrophilic phase, and this idea can be also applied to the structure of the agglomerate. Basura et al. [10] studied the influence of ionomer EW value on limiting current density and oxygen diffusion coefficient; they concluded that the two properties both decreased with the increasing of EW value, and that the solubility of oxygen was related to the water content in the system. Based on the X-ray measurements by Lee et al. [11], it is considered that the differences in the mass transport parameters, the cluster sizes and water uptakes are due to the growth of the clusters and the crystallinity in the electrolyte. All these related studies can reflect the significance of Nafion ionomer properties associated with fuel cell's performance.

When it comes to the Pt catalyst, its high price is the biggest limiting factor of the application and popularization of PEMFC, accounting for about 45% of total battery cost [12]. Thus, it is of great importance to maintain the similar performance of the PEMFC with the lowest possible Pt load. Yang et al. [13] utilized electrocatalyst decay protocols to accelerate cathode performance loss for Pt catalysts of different sizes. They found that the performance decay of the electrodes with the smallest Pt particle size was the highest and that of the largest Pt particle size was the lowest. Furthermore, the close contact of Pt particles and the carbon support has been studied with different methods [14]-[16]. Carbon support in the form of both carbon blacks and graphite is also a meaningful component for the agglomerate in CL.

Hence a MD model will be utilized in this study to simulate

and analyze PEMFC cathode mass transport process. It will be focused on a small scale of the triple phase boundary (TPB) of Pt, Nafion and oxygen. The effects of ionomer distribution and Pt nano-particle size will be reflected in the transport characteristics of proton and oxygen. Subsequently, analyses will be given associated with existing research results, in order to understand the PEMFC working mechanisms and to extract possible techniques for better performance. It was found that as the number of Nafion increases, the higher the EW value, the more oxygen transport is hindered. Secondly, larger size Pt particles (2 to 2.5 nm) showed better absorption, while medium size Pt particles (1.5 to 2 nm) performed better in terms of proton transport due to the formation of channels promoting mass transport within the catalytic layer between the agglomerates formed by medium Pt particles ( $\sim 10$  Å) and the main/side chains of the Nafion ionomer film. This paper explores the mass transport process of PEMFC cathode catalyst layer from the perspective of molecular dynamics simulation, providing a theoretical basis for further fuel cell optimization, such as water management and catalyst modification.

## II. MOLECULAR DYNAMICS SIMULATIONS

The MD calculation in this study contains two models, established with Large-scale Atomic / Molecular Massively Parallel Simulator (LAMMPS) and Materials Studio (MS) respectively. LAMMPS and MS are both useful tools and commonly used in the domain of MD simulations. Although the compositions of the two models are very similar, they are focused on different issues in our model. In fact, the two softwares have respective characteristics and are therefore utilized to solve specific problems. After combined the two models, the conclusions are more reasonable and reliable than results from either one. All-atom simulations are conducted, which means that the fundamental calculation unit is molecule. The basic idea of MD simulations is to analyze the microscopic structures and molecular movements in order to deduce the macroscopic properties. However, the number of molecules in each macroscopic object is tremendous, and the simulation of the molecules could be time consuming and sometimes even unachievable. The strategy to simplify the calculation is therefore one of the research focus areas over the years [17]. This is also one of the reasons why both two tools have been employed in the present study.

Six components in the CL are present in the models: Nafion ionomer, carbon support, Pt particle, water, proton and oxygen, which are the key species of CL. They form a complete PEMFC cathode microscopic structure, which is in fact one advantage of the model. Although some components can be removed to simplify the calculation towards specific research [18], the completeness contributes to a more flexible adjustment of the model as well as consistency with the reality because the components have different impacts on the whole system. A complete model is also a promising tool that can be adapted for more potential studies.

The Nafion ionomer model is exhibited in Fig. 1. Each ionomer contains 10 side chains with an EW of 1147 ( $\text{g} \cdot \text{mol}^{-1}$ ). Two extra types of Nafion ionomer with EW of 947 ( $\text{g} \cdot \text{mol}^{-1}$ ) and 747 ( $\text{g} \cdot \text{mol}^{-1}$ ) are obtained by decreasing the length of

fluorinated backbone. They are employed to study the effects of EW value and compared with the existing experiment results, which are used to validate the model.

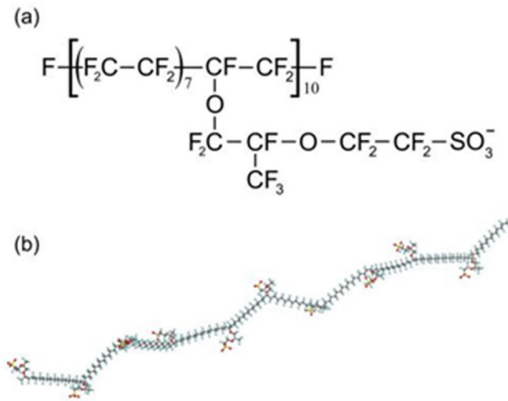


Fig. 1 Basic chemical structure of Nafion:  
(a) structural formula; (b) initial configuration constructed in MS

Each Pt nano-particle is built in MS from the repetition of fundamental crystal structure of face centered cubic. The shape of the particle is subsequently modified to an approximate truncated octahedron, which is reported to be one of the most possible equilibrium shapes for Pt nano-particle [19] and is confirmed by experimental data [20]. Six types of nano-particles are used in the simulations; their forms are exhibited in Fig. 2, with respectively 490, 314, 260, 116, 62, and 38 Pt atoms in one particle. They are employed to study the effects of Pt nano-particle size on ionomer distribution, oxygen and proton transport.

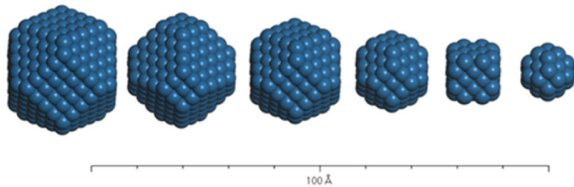


Fig. 2 Pt nano-particles of different sizes in the MD model

The water in the models is characterized by the coefficient of water content  $\lambda$ , which indicates the ratio of the number of water molecules (including the water molecules in hydronium ions) to the number of sulfonic acid groups. This value is usually 5-15, and it is set to 10 in this study. The protons exist in the form of hydronium ions, which is set to achieve the charge equilibrium of the system. The oxygen is considered as ideal gas, whose number is determined by (1):

$$N = \frac{PV}{k_B T} \quad (1)$$

where  $P$ ,  $T$  are the initial pressure and temperature of the gas, and are set to 10 MPa and 300 K;  $k_B$  is the Boltzmann constant;  $V$  is the initial volume of oxygen, which is a cuboid zone initially above the Pt nano-particle, and its value will be adjusted according to the size of the cell. Finally, the order of  $N$  will be  $10^3$ . The carbon support in the study is in the form of amorphous carbon structure which can well represent the carbon black used in experimental study.

The structure of the simulated system is firstly built in MS and the final four-layer structure is a lattice of about  $50 \text{ Å} \times 50 \text{ Å} \times 120 \text{ Å}$ . They are layers of amorphous carbon, Pt nano-particle, Nafion and oxygen respectively. Particularly, the layer of Nafion is composed of 6 Nafion ionomers, 540 water molecules and 60 hydronium ions. The initial density is set to  $1.6 \text{ (g cm}^{-3}\text{)}$ , and the lattice type is orthorhombic. Subsequently, the structure of each layer is exported to LAMMPS. The initial and final structure of the whole model is exhibited in Fig. 3. Special designed vacuum layer with thickness of  $100 \text{ Å}$  is added above the oxygen layer, which is used to eliminate the influence of periodic boundary conditions (PBC) on z-axis (vertical axis). In fact, the PBC of the system can largely simplify the calculation [21].

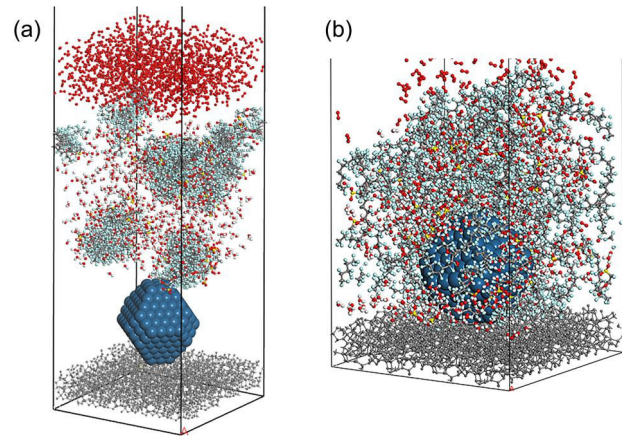


Fig. 3 Initial (a) and final (b) structure of the MD model (legend of particle colors: gray-C, blue-Pt, cyan-F, red-O, yellow-S, white-H)

In terms of energetic parameters, COMPASS force field [22] is applied to the MS model, while CVFF force field [23] is applied to the LAMMPS model. The force fields include most of the bonding parameters, such as bond stretching, angle bending and torsional potentials. The non-bonded interactions are defined as van der Waals and electrostatic potentials, treated respectively with Lennard-Jones (LJ) potential and Ewald summation method. The cut-off radii are set to  $12.5 \text{ Å}$ , which are far smaller than the thickness of the vacuum layer. The time steps are mostly set to  $1.0 \text{ fs}$ , while a few cases are set to  $0.5 \text{ fs}$  when the system easily diverges. Rather than increase the integration tolerance which is  $5 \times 10^4 \text{ (kcal mol}^{-1}\text{)}$  by default, it is preferred to reduce the time step for the improvement of accuracy. The precise MD simulation steps are as follows:

- 1) Geometry optimization is conducted with the steepest descent algorithm [24], the maximum iterations are set to 2000.
- 2) Dynamics process for an NPT ensemble is maintained for 10 ps, with  $P = 0.1 \text{ MPa}$  and  $T = 300 \text{ K}$ . The Nosé-Hoover [25] thermostat and Berendsen barostat [26] are employed, with  $Q$  ratio of 0.01 and decay constant of  $0.1 \text{ ps}$ . After the process, the temperature of the system should be stabilized around  $300 \text{ K}$ . For some cases,  $10 \text{ ps}$  is not enough to converge in the isothermal process, and a repetition of the present step will be needed.
- 3) An annealing process is conducted for an NVT ensemble.

The system is heated up and cooled down between 300 K and 700 K for 4 cycles. Each cycle contains 100 heating ramps and each ramp contains 200 dynamics steps.

- 4) After the annealing process, the system is maintained at 300 K for 10 ps (a dynamics process for the same NVT ensemble).
- 5) Finally, a dynamic process for an NVE ensemble for 50 ps is conducted, so as to obtain the data for the analysis of morphology and transport properties.

After the MD simulations finished, the system arrives at equilibrium state, which is confirmed by the stability of system potential energy. The vacuum layer as well as those overly free molecules (water or oxygen molecules that are too far away from the bulk) are considered as disturbance and therefore removed from the system. Subsequently, the morphology of Pt nano-particle and the distribution of Nafion ionomers are observed. Finally, important values including radial distribution function, mean square displacement and diffusion coefficient are obtained based on the final equilibrium state of our simulation system.

Firstly, the radial distribution function (RDF) is computed with (2):

$$g_{A-B}(r) = \frac{N_B dn_{A-B}(r)}{4\pi V dr} \quad (2)$$

where  $N_B$  is the total amount of B atoms in the system,  $n_{A-B}(r)$  is the amount of B atoms within the distance of  $r$  from A atoms, and  $V$  is the volume of the cell. The RDF represents the density probability of a species around another species. Its value shows the species' distribution and morphology. With the similar idea, the concentration profile is employed to study the distribution of a species along a given direction (z-axis in the present study).

Besides, for the sake of analysis for molecular transport, the mean square displacement (MSD) is computed with (3):

$$MSD(t) = \langle |x(t) - x(0)|^2 \rangle = \frac{1}{N} \sum_{i=1}^N |x^{(i)}(t) - x^{(i)}(0)|^2 \quad (3)$$

where  $N$  is the total amount of a certain species and  $x(t)$  is the position of a unit at time  $t$ . The MSD describes the kinestate of a species. Moreover, the diffusion coefficient  $D$  is computed in conjunction with the running diffusion constant (RDC):

$$RDC(t) = \frac{dMSD(t)}{6dt} \approx \frac{MSD(t)}{6t} \quad (4)$$

$$D = \lim_{t \rightarrow \infty} RDC(t) \approx \langle RDC(t) \rangle_t \quad (5)$$

Compared with MSD, the diffusion coefficient can more intuitively describe the dynamical behavior of a species. The diffusion coefficient of hydronium ions and oxygen are therefore computed in the study in order to characterize the performance of the PEMFC.

With this fundamental MD process, parameters can be easily modified for different cases. In addition to the EW of Nafion ionomer and the size of Pt Nano-particle, the number of Nafion ionomer is also a variable in the study: 6, 12, 18 and 24 Nafion ionomers are added in the lattice to conduct the MD simulations. Following the principle of controlling variables,

there will be only one variable changed each time, so that the effects of the specific parameter is clearer.

### III. RESULTS AND DISCUSSION

The final structure of model after the MD simulation is exhibited above in Fig. 3 (b). The initially layered structure agglomerates and becomes much denser, which is the typical microstructure in the real PEMFC cathode. Before analyzing the morphology and the transport of different molecules, it is necessary to ensure the convergence of the calculation, which means that the simulated system is relaxed enough and at equilibrium state. In fact, to complete the MD calculation in the shortest time while guaranteeing the rationality of the result is one of the major goals in this study. Fig. 4 exhibits the final state of the MD simulation process in the baseline case with 314 Pt atoms, 6 Nafion ionomers of EW of 1147 ( $\text{g} \cdot \text{mol}^{-1}$ ), 540 water molecules and 60 hydronium ions.

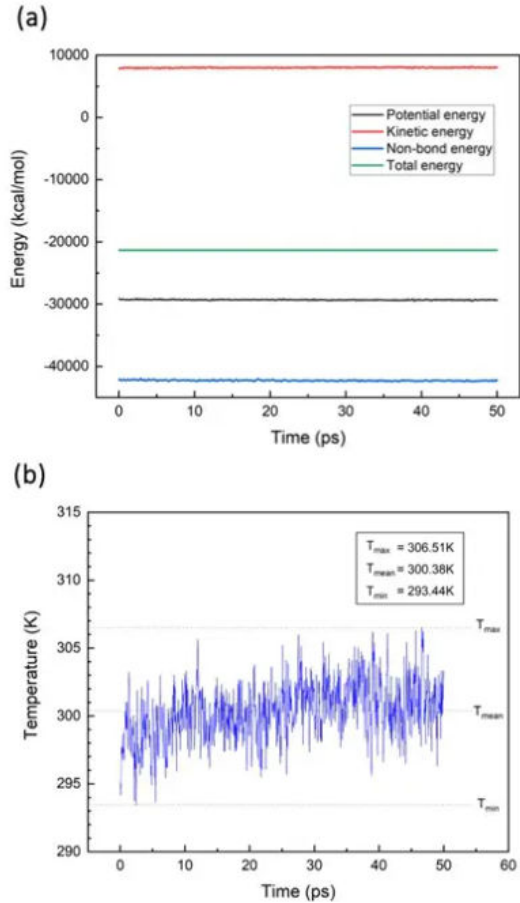


Fig. 4 Results of MD simulation process: (a)final energy; (b)final temperature

Fig. 4 (a) represents the system status in the dynamics process of NVE ensemble, where the kinetic and potential energy remain stable. Furthermore, as shown in Fig. 4 (b), the temperature varies closely around 300 K even without a thermostat, which is a significant proof of the equilibrium of the system. Similar results are observed for all MD simulations for the other cases in the study.

In the first group, different amount of Nafion ionomers is

studied and the diffusion coefficient of oxygen are compared. 6, 12, 18, and 24 Nafion ionomers of EW of 1147 ( $\text{g} \cdot \text{mol}^{-1}$ ) are added in the lattice to form 4 cases. The results of this group are exhibited in Fig. 5 (a), which shows that the diffusion coefficient of oxygen decreases rapidly with the increase of the amount of Nafion ionomers in the lattice. The initial thickness of the Nafion layer increases proportionally, while the density of the layer is fixed. It is found by Soboleva et al. [8] that the pores of the agglomerate were gradually blocked as the ionomer content increased, which might hinder the transport of oxygen.

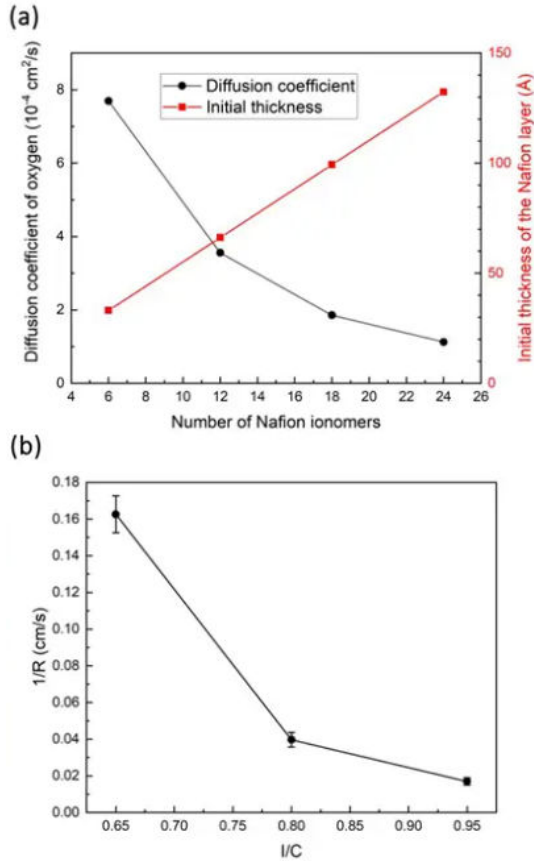


Fig. 5 (a) MD simulation results of oxygen diffusion coefficient and (b) experimentally measured variation trend of reciprocal mass transfer resistance [27]

Moreover, related experiments [27] are conducted and show that the mass ratio of ionomer and carbon support (I/C) is one of the important factors affecting the performance and microstructure of the catalytic layer. The increase of I/C value within a certain range can lead to a huge raise of transport resistance, which explains the drop of diffusion coefficient in the MD simulation. In fact, the relationship between transport resistance  $R$  and diffusion coefficient  $D$  is as (6):

$$R = \frac{h}{D} \quad (6)$$

where  $h$  is the thickness of Nafion ionomer layer. In order to compare the results of the experiment and simulation, and to ignore the influence of Nafion thickness, the value of  $1/R$  is considered. Fig. 5 (b) shows the variation of  $1/R$  with I/C value.

Compared with the oxygen diffusion coefficient in Fig. 5 (a), the variation trends with the increase of ionomer are consistent.

A similar set of different Nafion EW values is also conducted, with the results exhibited in TABLE I. For the sake of I/C value control, different numbers of Nafion ionomers are added in the lattice so that their total mass in each case remains close. According to the results, with shorter fluorinated backbone, the oxygen can be better transported into the surface of Pt. The variation trend and the order of the diffusion coefficient of oxygen are both consistent with the experiment results by Basura et al. [10] The Nafion ionomer study validates the MD model and demonstrate the credibility of the results.

TABLE I  
THE OXYGEN DIFFUSION COEFFICIENT CORRESPONDING TO DIFFERENT EW VALUES OF NAFION

EW value of Nafion ( $\text{g} \cdot \text{mol}^{-1}$ )	1147	947	747
number of Nafion ionomers	6	7	9
diffusion coefficient of oxygen ( $10^{-4} \text{ cm}^2 \text{ s}^{-1}$ )	7.70	10.32	11.87

The next group of simulation is conducted for different size of Pt nano-particle. Except the number of Pt atoms, all other parameters are the same with the baseline case of the study. The MSD of ions hydronium ions as well as their diffusion coefficient are plotted in Fig. 6 and TABLE II, where the final size of Pt nano-particle is calculated after the MD simulation.

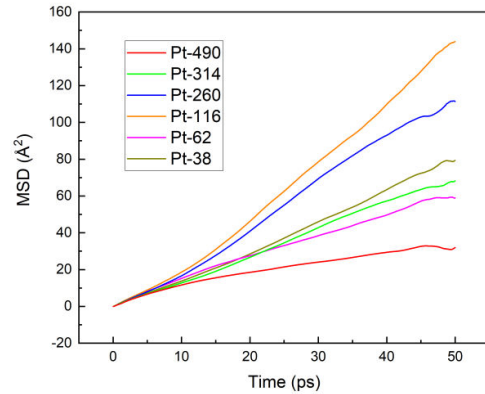


Fig. 6 MSD of hydronium ions corresponding to different Pt particle sizes

TABLE II  
DIFFUSION COEFFICIENT OF HYDRONIUM IONS CORRESPONDING TO DIFFERENT PT PARTICLE SIZE

number of Pt atoms in the Pt nano-particle	final size of Pt nano-particle (nm)	diffusion coefficient of hydronium ions ( $10^{-5} \text{ cm}^2/\text{s}$ )
490	2.55	0.882
314	2.17	2.46
260	1.98	4.18
116	1.43	5.28
62	1.10	1.92
38	0.94	2.94

In general, the hydronium ions have a lower diffusion coefficient than oxygen. These hydronium ions are generated in the Nafion layer and are initially mixed with Nafion ionomers, and due to the positive charge they carry, the distribution of side



chains can have a great impact on their transport. The results show that Pt nano-particles with medium size contribute to a better transport of hydronium ions. On one hand, when the Pt nano-particle is too small, the Nafion ionomers will be less easily to unfold themselves to form a porous agglomerate with Pt, as the effective surface area of Pt is small. On the other hand, when the Pt nano-particle is too big, the space between two adjacent Pt nano-particles in the simulation lattice will be compressed. Consequently, the Nafion ionomers suffer more resistance approaching the Pt as well as the carbon support. The Pt particle size of 1.5-2 nm will be most advantageous in terms of proton transport when the centre-to-centre distance between two Pt nano-particle is around 5 nm (the size of the lattice).

Also, the concentration profile of water molecules is computed and exhibited in Fig. 7. In fact, the water absorption towards the carbon support as well as the Pt is one of the important indicators of the MD simulation [28]-[29], which shows the degree of the formation of agglomerate. If the parameters are not well set, a number of water molecules will be free outside the agglomerate, especially when a vacuum layer is added on the cell in the present study. According to the curves in Fig. 7, where 0 of abscissa represents the upper surface of the carbon support, most of the water molecules are close to the carbon as well as the agglomerate. There is a connection between the size of Pt and the absorptive capacity. The very leftmost peak is situated under the center of Pt nano-particle, representing the water molecules absorbed by the carbon support. It can be noticed that the larger Pt nano-particles (Pt-490, Pt-314, and Pt-260) have high peaks, which reflects stronger absorption. Meanwhile, their second leftmost peaks are relatively close to carbon surface. The small Pt nano-particles (Pt-62 and Pt-38) have their highest peak farther from the carbon surface, which reflects weaker absorption.

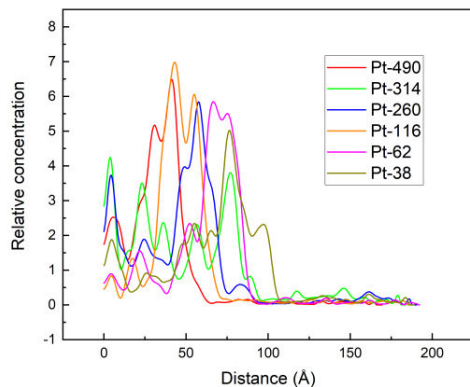


Fig. 7 Longitudinal distributions of water molecules corresponding to different Pt particle sizes

To better understand the morphology of the agglomerates, the RDF of Pt-C<sub>main</sub> (carbon atoms in the main chain/backbone of Nafion), the RDF of Pt-C<sub>side</sub> (carbon atoms in the side chains of Nafion), and the RDF of Pt-S (sulfur atoms in sulfonic acid groups) are computed and exhibited in Fig. 8, with each figure representing a certain size of Pt nano-particle. The RDF shows the probability of finding certain molecules at a given distance from the center of Pt particle. The cut-off radius is set to 100 Å where the all values of the RDF approaches 1, which means infinity. The leftmost and highest peak of the function is very

important information because it indicates where the molecules are most likely to be located. It can be noticed that the carbon atoms in side chains and the sulfur atoms, which are situated at the end of the side chain, are mostly found at the same position, as their peaks are roughly synchronized. This indicates that the side chains are more likely to be parallel to the surface of Pt nano-particle. For the two small ones (Pt-62 and Pt-38), this phenomenon is no longer observed for the same reason as before. It is that the Nafion ionomers cannot unfold themselves on a small surface area of Pt.

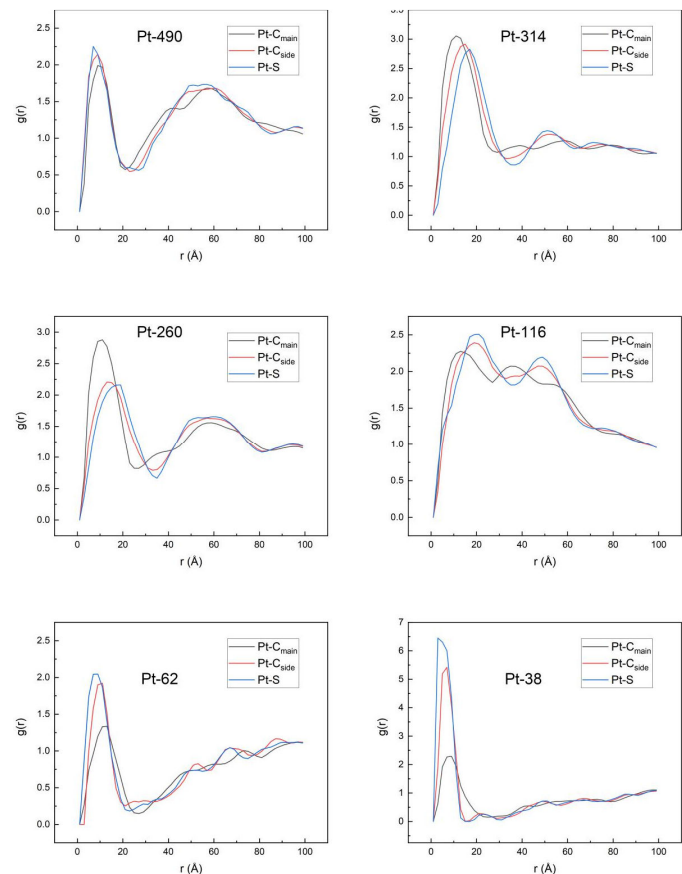


Fig. 8 RDF of various atoms in Nafion corresponding to different Pt particle sizes

It is noticed that there is a distance between the leftmost and highest peak of the main chains and that of the side chains, which is particularly distinct for the medium-sized Pt nano-particles (Pt-314, Pt-260, and Pt-116). This distance could be considered as the size of transport channel between the main chains and the side chains. It is believed [30]-[32] that the interface of the hydrophilic/hydrophobic phase plays an important role in the mass transport, including water, oxygen and proton (hydronium ion). In fact, the separation of the hydrophobic main chain and the hydrophilic side chain form a spacing that other smaller molecules can pass through. The medium size of Pt nano-particles help forming a relatively large channel of around 10 Å, which is beneficial to the transport of hydronium ions. This result is also confirmed by the diffusion coefficient, where the medium size of Pt nano-particles contributes to better transport capacity. Besides, for the two small Pt particle cases in Fig. 8 (Pt-62 and Pt-38), the Nafion

ionomers form a similar core-shell structure found by Chen et al. [32]-[33], where the side chains wrap snugly around the Pt nano-particle. This indicates that the effect of carbon support under the Pt becomes negligible when the particle is too small. In this case, the transport channel is difficult to form because the Nafion ionomers are not completely unfolded, which is reflected by the peaks in the RDF curves.

Considering Pt load control, an associated case is conducted for different size of carbon support, which determines the size of the lattice and therefore the center-to-center distance between two Pt nano-particles. The Pt nano-particles in this case contain respectively 490, 260, and 116 Pt atoms, corresponding to carbon supports of  $70 \text{ \AA} \times 70 \text{ \AA}$ ,  $50 \text{ \AA} \times 50 \text{ \AA}$  and  $38 \text{ \AA} \times 38 \text{ \AA}$  so that the Pt load on carbon support is close to 0.1 Pt atom per square angstrom. The thickness of Nafion ionomer layer and oxygen layer is also adjusted to fit in the lattice.

By MD simulation the data of diffusion coefficient are listed in TABLE III.

TABLE III  
DIFFUSION COEFFICIENT OF OXYGEN AND HYDRONIUM IONS CORRESPONDING TO DIFFERENT PT PARTICLE SIZES AND SPACING

number of Pt atoms in the Pt nano-particle	distance between adjacent Pt particles( $\text{\AA}$ )	diffusion coefficient of oxygen ( $10^{-4} \text{ cm}^2/\text{s}$ )	diffusion coefficient of hydronium ions ( $10^{-5} \text{ cm}^2/\text{s}$ )
490	70	5.04	1.73
260	50	7.62	4.18
116	33	4.32	1.61

It can be discovered that medium-sized Pt particle (Pt-260) leads to the best mass transport performance, especially reflected in its high diffusion coefficient of hydronium ions. The little Pt particle (Pt-116) has the highest diffusion coefficient of hydronium ions in the precious case, but when the distance between adjacent Pt decreases to  $33 \text{ \AA}$ , the mass transfer resistance becomes much higher. From a molecular perspective the downward diffusion of Nafion ionomer will be hindered when the platinum spacing is too small. Besides, the adsorption capacity of little Pt particle is too weak to attract the ionomers and form an agglomerate. As a result, the mass transport channel is not well formed, and a considerable amount of oxygen and hydronium ions cannot reach the surface of Pt particle. For the big Pt particle (Pt-490), the downward diffusion of Nafion ionomer is much easier due to bigger spacing and stronger absorption of Pt particle. However, the distribution of ionomer becomes uneven, which results in an irregular agglomerate. There is vacuum space among the Pt particles, which goes against the transport of hydronium ions. These analyses can be confirmed by the final structure of the three cases, showed in Fig. 9. The oxygen, water molecules and hydronium ions are removed in the plotting for the better view of the structure. As can be seen from the figure, medium-sized Pt particles (Pt-260) form an agglomerate that is relatively homogeneous, with a lower structural complexity. The transport channel can be therefore easier to form.

Similarly, the RDF of Pt-C<sub>main</sub>, Pt-C<sub>side</sub>, and Pt-S are computed and plotted in Fig. 10.

The results are close enough to the previous cases of different sizes of Pt in Fig. 8: for the big Pt particle (Pt-490), the leftmost and highest peaks of the three curves are almost in the same position; for the smaller Pt particle (Pt-116), the three leftmost peaks form the same core-shell structure as the two smallest particles do (Pt-62 and Pt-38) in the previous case. For the medium Pt particle (Pt-260), the gap between the main chains and side chains of Nafion ionomer still exists, which indicates that the mass transport channel is formed. These gaps result in the increased diffusion coefficient of both oxygen and hydronium ions for medium Pt particle case.

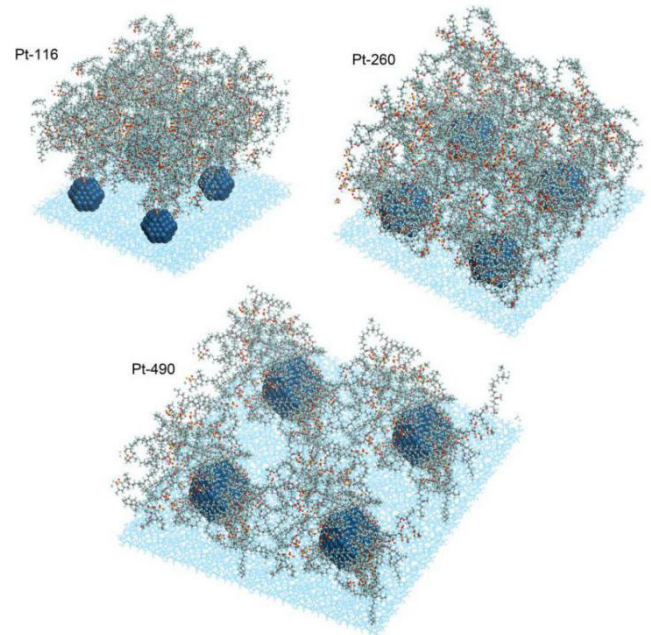


Fig. 9 Final MD structures for 3 Pt particle and carbon support sizes (legend of particle colors: gray-C, blue-Pt, cyan-F, red-O, yellow-S, light blue at the bottom-carbon support)

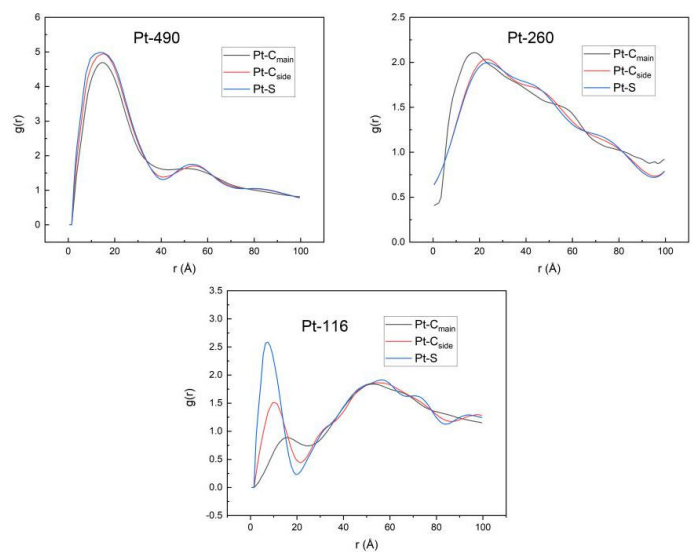


Fig. 10 RDF of various atoms in Nafion corresponding to three Pt particle and carbon support sizes

In order to achieve a reasonable and efficient Pt particle distribution on the carbon support, it is necessary to comprehensively consider the size of the Pt particles as well as the distance between adjacent Pt particles. In an ideal state, where the size of Pt particles is suitable for the very spacing (medium sizes in previous cases), the ionomers are adsorbed to the surface of the carbon carrier and form a regular and uniform agglomerate with the Pt particles. As a consequence, channels will be easier to form, which could promote the mass transport in the system. This can provide possible ideas and directions for the future design of platinum-carbon catalysts in PEMFC cathodes.

#### IV. CONCLUSIONS

In this paper, molecular dynamics modeling is conducted to analyze the mass transport in the PEMFC cathode. The model is established with MS and LAMMPS, which consists of 6 types of molecules in the cathode: Pt nano-particle, Nafion ionomer, carbon support, proton, water and oxygen. Proceeding from the baseline case, different parameters are calculated to analyze their effect on transport properties of both oxygen and proton.

Firstly, MD simulation process is built, as well as the method of equilibrium validation. This paper studied how to complete a MD calculation in the shortest time while guaranteeing the rationality of the result. Secondly, the Nafion ionomer is studied as a variate, whose quantity in the simulation cell and EW value are modified. According to the computed diffusion coefficient, the transport of oxygen is hindered more with a larger quantity of Nafion as well as a higher EW value. These results are consistent with the experiments, which validate the model. Finally, the size of Pt nano-particle is varied, and the diffusion coefficient of proton and the RDF between Pt and other molecules are computed. The results indicate that large Pt particles (2-2.5 nm) have a stronger absorptive capacity, while medium-sized Pt particles (1.5-2 nm) are more advantageous in terms of proton transport. The reason can be explained by the leftmost and highest peaks of RDF curves. It is considered that the gap between the main chains and side chains of Nafion ionomer form a channel, which is beneficial to mass transport. The channel is particularly distinct (of around 10 Å) in the agglomerates formed with medium Pt nano-particles, which explains their performance in proton transport. This morphology is supported by the theory of the interface of hydrophobic and hydrophilic phase, which is believed to play a vital role in mass transport in proton exchange membranes.

The MD model presented in this study can be employed to conduct further research on the PEMFC cathode. It is a complete model that contributes to easier modifications of variate and parameters. However, the model still has some limitations and can be improved, for instance, the embedment of Pt nano-particles into the carbon support has not been considered in this paper. The morphology of carbon support as well as the embedment depth can change the structure of the agglomerate. These issues should be taken into consideration in the future study.

#### ACKNOWLEDGMENT

This work is supported by Natural Science Foundation of Shanghai (SNSF:19ZR1426000) and National Natural Science

Youth Foundation of China (NSF 21905172).

#### REFERENCES

- [1] K. Smith Stegen, "Understanding China's global energy strategy," *International Journal of Emerging Markets*, vol. 10, pp. 194-208, 04/20, 2015.
- [2] A. Lutz, R. Larson, and J. Keller, "Thermodynamic comparison of fuel cells to the Carnot cycle," *International Journal of Hydrogen Energy - INT J HYDROGEN ENERG*, vol. 27, pp. 1103-1111, 10/01, 2002.
- [3] M. Hirscher, T. Autrey, and S.-i. Orimo, "Hydrogen Energy," *ChemPhysChem*, vol. 20, no. 10, pp. 1157-1157, 2019/05/16, 2019.
- [4] R. O'hayre, S. Cha, W. Colella, "Fuel Cell Fundamentals, 3rd Edition," *Mechanical engineering*, pp. 9.7-1-9.7-6, 2016.
- [5] A. Suzuki, U. Sen, T. Hattori et al., "Ionomer content in the catalyst layer of polymer electrolyte membrane fuel cell (PEMFC): Effects on diffusion and performance," *International Journal of Hydrogen Energy*, vol. 36, no. 3, pp. 2221-2229, 2011/02/01, 2011.
- [6] T. Suzuki, K. Kudo, and Y. Morimoto, "Model for investigation of oxygen transport limitation in a polymer electrolyte fuel cell," *Journal of Power Sources*, vol. 222, pp. 379-389, 01/15, 2013.
- [7] R. N. Bonifácio, A. O. Neto, and M. Linardi, "Comparative analysis between mass and volume of catalysts as a criterion to determine the optimal quantity of Nafion ionomer in catalyst layers," *International Journal of Hydrogen Energy*, vol. 40, no. 6, pp. 2840-2849, 2015/02/19, 2015.
- [8] T. Soboleva, X. Zhao, K. Malek et al., "On the Micro-, Meso- and Macroporous Structures of Polymer Electrolyte Membrane Fuel Cell Catalyst Layers," *ACS applied materials & interfaces*, vol. 2, pp. 375-84, 02/01, 2010.
- [9] F. N. Büchi, M. Wakizoe, and S. Srinivasan, "Microelectrode Investigation of Oxygen Permeation in Perfluorinated Proton Exchange Membranes with Different Equivalent Weights," *Journal of The Electrochemical Society*, vol. 143, no. 3, pp. 927, 1996/03/01, 1996.
- [10] V. I. Basura, C. Chuy, P. D. Beattie et al., "Effect of equivalent weight on electrochemical mass transport properties of oxygen in proton exchange membranes based on sulfonated  $\alpha,\beta$ -trifluorostyrene (BAM®) and sulfonated styrene-(ethylene-butylene)-styrene triblock (DAIS-analytical) copolymers," *Journal of Electroanalytical Chemistry*, vol. 501, no. 1, pp. 77-88, 2001/03/23, 2001.
- [11] K. Lee, A. Ishihara, S. Mitsushima et al., "Effect of Recast Temperature on Diffusion and Dissolution of Oxygen and Morphological Properties in Recast Nafion," *Journal of The Electrochemical Society*, vol. 151, no. 4, pp. A639, 2004/03/04, 2004.
- [12] A. Wilson, G. Kleen, D. Papageorgopoulos, "Fuel Cell System Cost - 2017," *DOE Hydrogen and Fuel Cells Program Record*, 2017.
- [13] Z. Yang, S. Ball, D. Condit et al., "Systematic Study on the Impact of Pt Particle Size and Operating Conditions on PEMFC Cathode Catalyst Durability," *Journal of The Electrochemical Society*, vol. 158, pp. B1439, 01/01, 2011.
- [14] X. Cheng, G. Wei, C. Wang et al., "Experimental probing of effects of carbon support on bulk and local oxygen transport resistance in ultra-low Pt PEMFCs," *International Journal of Heat and Mass Transfer*, vol. 164, pp. 120549, 2021/01/01, 2021.
- [15] Z. Liu, L. Gan, L. Hong et al., "Carbon-Supported Pt Nanoparticles as Catalysts for Proton Exchange Membrane Fuel Cells," *Journal of Power Sources*, vol. 139, pp. 73-78, 01/04, 2005.
- [16] W. S. Jung, "Study on durability of Pt supported on graphitized carbon under simulated start-up/shut-down conditions for polymer electrolyte membrane fuel cells," *Journal of Energy Chemistry*, vol. 27, no. 1, pp. 326-334, 2018/01/01, 2018.
- [17] E. Paquet, and H. Viktor, "Molecular Dynamics, Monte Carlo Simulations, and Langevin Dynamics: A Computational Review," *BioMed Research International*, vol. 2015, pp. 1-18, 02/16, 2015.
- [18] Y. Kurihara, T. Mabuchi, and T. Tokumasu, "Molecular dynamics study of oxygen transport resistance through ionomer thin film on Pt surface," *Journal of Power Sources*, vol. 414, pp. 263-271, 2019/02/28, 2019.
- [19] A. Bruix, and K. Neyman, "Modeling Ceria-Based Nanomaterials for Catalysis and Related Applications," *Catalysis Letters*, vol. 146, 10/01, 2016.
- [20] Z. L. Wang, "Structural Analysis of Self-Assembling Nanocrystal Superlattices," *Advanced Materials*, vol. 10, no. 1, pp. 13-30, 1998.

- [21] Makov, and Payne, "Periodic boundary conditions in ab initio calculations," *Physical review. B, Condensed matter*, vol. 51 7, pp. 4014-4022, 1995.
- [22] H. Sun, P. Ren, and J. R. Fried, "The COMPASS force field: parameterization and validation for phosphazenes," *Computational and Theoretical Polymer Science*, vol. 8, no. 1, pp. 229-246, 1998/01/01/, 1998.
- [23] J. L. Asensio, M. Martin-Pastor, and J. Jimenez-Barbero, "The use of CVFF and CFF91 force fields in conformational analysis of carbohydrate molecules. Comparison with AMBER molecular mechanics and dynamics calculations for methyl  $\alpha$ -lactoside," *International Journal of Biological Macromolecules*, vol. 17, no. 3, pp. 137-148, 1995/01/01/, 1995.
- [24] J. Fliege, and B. F. Svaiter, "Steepest descent methods for multicriteria optimization," *Mathematical Methods of Operations Research*, vol. 51, no. 3, pp. 479-494, 2000/08/01, 2000.
- [25] D. J. Evans, and B. L. Holian, "The Nose-Hoover thermostat," *Journal of Chemical Physics*, vol. 83, pp. 4069-4074, 1985.
- [26] H. J. C. Berendsen, J. P. M. Postma, W. F. van Gunsteren et al., "Molecular dynamics with coupling to an external bath," *The Journal of Chemical Physics*, vol. 81, no. 8, pp. 3684-3690, 1984/10/15, 1984.
- [27] C. Wang, X. Cheng, X. Yan et al., "Respective Influence of Ionomer Content on Local and Bulk Oxygen Transport Resistance in the Catalyst Layer of PEMFCs with Low Pt Loading," *Journal of The Electrochemical Society*, vol. 166, no. 4, pp. F239, 2019/02/23, 2019.
- [28] T. Mashio, K. Malek, M. Eikerling et al., "Molecular Dynamics Study of Ionomer and Water Adsorption at Carbon Support Materials," *The Journal of Physical Chemistry C*, vol. 114, 08/19, 2010.
- [29] X.-y. Zhang, and Y.-h. Ding, "Thickness-dependent structural and transport behaviors in the platinum-Nafion interface: a molecular dynamics investigation," *RSC Advances*, vol. 4, no. 83, pp. 44214-44222, 2014.
- [30] K. Sung, W.-K. Kim, K.-H. Oh et al., "Proton exchange membranes based on hydrophilic-hydrophobic multiblock copolymers using different hydrophobic oligomer," *Fuel and Energy Abstracts*, vol. 36, pp. 3956-3964, 03/01, 2011.
- [31] R. Jinnouchi, K. Kudo, N. Kitano et al., "Molecular Dynamics Simulations on O<sub>2</sub> Permeation through Nafion Ionomer on Platinum Surface," *Electrochimica Acta*, vol. 188, 12/01, 2015.
- [32] H. Mendil-Jakani, I. Lopez, V. H. Mareau et al., "Optimization of hydrophilic/hydrophobic phase separation in sPEEK membranes by hydrothermal treatments," *Phys. Chem. Chem. Phys.*, vol. 19, 05/22, 2017.
- [33] L. Chen, X. Xiang, S. Wang et al., "Effects of Pt particle on structure and protons transport of Nafion membrane," *International Journal of Heat and Mass Transfer*, vol. 148, pp. 118977, 2020/02/01/, 2020.



# Reuse of Waste Water after Pretreatment Under Teril and Sand in Bechar City

Seddiki Sara<sup>1</sup>, Maazouzi abdelhak<sup>2</sup>,

<sup>1</sup> Conference Master "B" at Tahri Mohammed Bechar University BP 417, 08000 Bechar

<sup>2</sup> Teacher Researchers at Tahri University Mohammed Bechar B.P. 417, 08000 Bechar

Email : sara82002dz@yahoo.fr

**Abstract**—The main objective of this modest work is to follow the physicochemical and bacteriological evolution of the wastewater from the town of Bechar subjected to purification by filtration according to various local supports, namely Sable and Terril by reducing nuisances that undergo the receiving environment (Oued Bechar) and therefore make this water source reusable in different areas.

The study first made it possible to characterize the urban wastewater of the Bechar wadi, which presents an environmental threat, thus allowing an estimation of the pollutant load, the chemical oxygen demand COD (145 mg / l) and the biological oxygen demand BOD5 (72 mg / l) revealed that these waters are less biodegradable (COD / BOD5 ratio = 0.62), have a fairly high conductivity (2.76 mS/cm), and high levels of mineral matter presented by chlorides and sulphates 390 and 596.1 mg / l respectively, with a pH of 8.1.

The characterization of the sand dune (Beni Abbes) shows that quartz (97%) is the most present mineral. The granular analysis allowed us to determine certain parameters like the uniformity coefficient (CU) and the equivalent diameter, and scanning electron microscope (SEM) observations and X-ray analysis were performed.

The study of filtered wastewater shows satisfactory and very encouraging treatment results, with complete elimination of total coliforms and streptococci and a good reduction of total aerobic germs in the sand and clay-sand filter. A good yield has been reported in the sand Terrill filter for the reduction of turbidity. The rates of reduction of organic matter in terms of the biological oxygen demand, in chemical oxygen demand recorded, are of the order of 60%. The elimination of sulphates is 40% for the sand filter.

**Keywords**— Urban wastewater, filtration, bacteriological and physico-chemical parameters, Sand, Terrill, Oued Bechar.

## 1. INTRODUCTION

The objective of our work is a contribution to the valorization of the dune sand of the western Great Erg used as a filter bed, for the pre-treatment of urban wastewater combined with a geo-material (Terril) available in the South-West region. Algerian and who presents an environmental threat. The surface on which the slag heaps extends from Bechar Djedid and to the town of Kenadza with a strip of width that can reach in places

the 20 Km. The valorization of the materials contained in the heaps becomes an urgency because these heaps disfigure the Our contribution is based, on the one hand, on the estimation of the polluting load of the urban waste water of wad Bechar (Ri) and on the other hand the contribution to the purification by local materials.

## II. MATERIAL AND METHOD

### 1.1. EQUIPMENT

#### 1 Wastewater

##### • Sampling site

The sampling of waste water was taken at Oued Bechar (Bechar djedid) (Fig. 01) according to WHO recommendations [1]. A volume of 20 l destined for pretreatment by local materials (filtration) is taken from polyethylene flasks. Laboratory transport of the sampling vials was carried out in a cooler at low temperature (4 ° C)

Sampling of the urban discharge was carried out on several points along Oued Bechar. The choice of sites was established in the light of a preliminary study of the physicochemical parameters, the frequency of use by local residents, and the upstream flow direction downstream of the wastewater. Of polyethylene a volume of 1.5 l for physico-chemical analyzes.

In the laboratory, the dosing methods used are as follows :

- pH, salinity and conductivity, potentiometric method (Consort 861)

Pectrophotometry was used for the determination of sulphates;

- Potassium dichromate method for determination of chemical demand of oxygen (COD) (Eco thermoreactor VELP scientific) thus a method for determining the biological oxygen demand for 5 days BOD5.

Agar incorporation methods for the search and enumeration of germs.

Figure 01 Wastewater Collection Site.



## 2-Filter beds

Two types of filter media are used, namely sand from the Beni bbes dune and Bechar Djedid's Terrill.

### • Experimental pilot

After sampling at Oued Bechar level (Bechar djedid), we went to the laboratory of the University of Bechar or we assembled our experiment equipment which is composed of two large bins equipped with valves to in submarters and a submerged pump and a piping installation for recycled water, inside the bins contains each a two layer of gravel of size 8/15 and 3/8 with a thickness of 5 cm all over the tray surface and the third layer is 10 cm of erg sand (Beni Abbes) and in the other tank a 10 cm layer of a homogeneous mixture of 95% sand and 5% Terrill; then we poured the collected wastewater, illustrated in the following figure

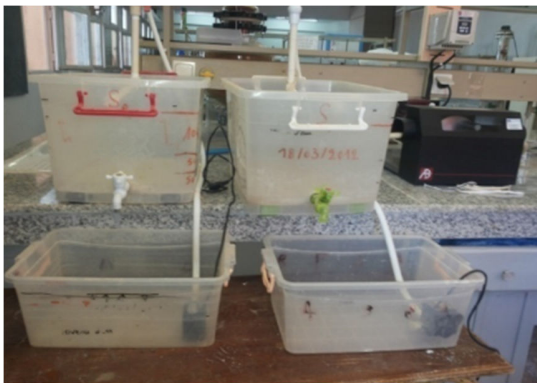


Figure 02: experimental device

## 2 Results and discussion

### 2.1. Characteristics of the media used

#### Physical characteristics

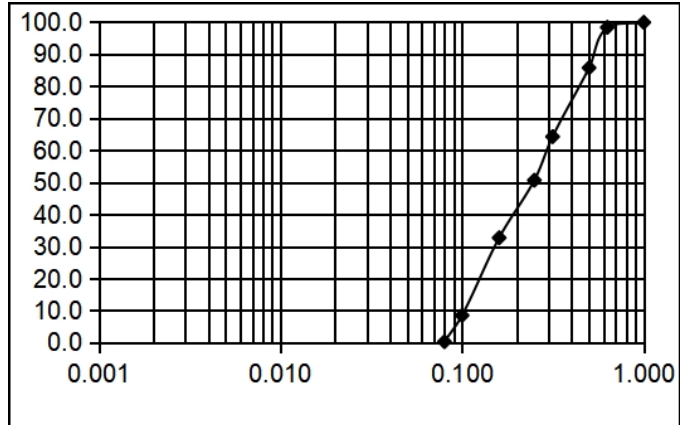


Figure 3 The granulometric curves of sand filter beds

The granulometric curves of sand filter beds (fig.03) were established by passage on sieve columns (standardized method NF ISO 565). From the granulometric data, the fineness module (MF) and the uniformity coefficient (CU) are easily accessible [2,3].

Figure 03 Granulometric curve of 95% sand and 5% terril [3]

Table 1 The physical characteristics of sand and slag

Parameter	S <sub>100</sub>	S <sub>95</sub> T <sub>5</sub>
Fineness module (MF)	2.16	1.04
Effective diameter d <sub>10</sub> mm	0.17	0.11
Coefficient of uniformity CU	1.76	2.73
Specific area of the cm-1 material	36.69	
Permeability (m / s) 10-4	7.26	
Density kg / m <sup>3</sup>	2.63	2.77
Porosity (ε)%	42.01	88.08

### 2.2 Physicochemical parameter

-Estimation of the polluting load and spatial representation of the urban wastewater of the city of Bechar

#### • Conductivity and pH

In the graph below, we find that the rejection R4 represents the highest values by contribution to the other discharges, ie 4.51mS / cm for the conductivity and 7.2 for the pH.

The conductivity of waste water from Oued Bechar ranges from the north (4.51mS / cm) to the south (2.55mS / cm). Waste water from Oued Bechar is characterized by a low alkaline pH, between 6.8 and 7.2.

#### • Sulfate and Chloride

Sulphates represent very high concentrations respectively a maximum of 638.6 mg / l recorded in R6 and a minimum of 490mg / l for R1 which exceed the maximum allowable value

to standards of 400 mg / l. These levels may very probably be due to the use of sulphite-based detergents (metastable state) which are transformed (oxidation) into sulphate, due to the nature of the discharged water, (urban water).

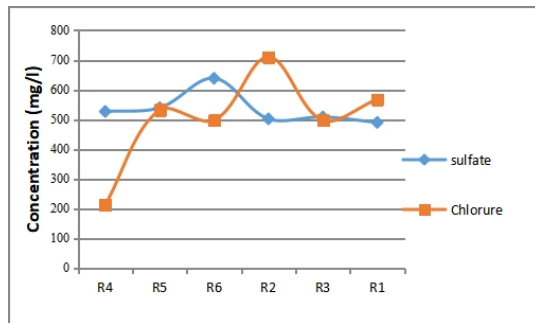


Figure4 Evolution of the concentration of chlorides and sulphates along Oued Bechar.

A much larger spatial evolution is observed for chlorides which vary between 213 mg / l upstream and 568 mg / l downstream thus causing a significant increase in chloride concentration in R2, which are higher than the maximum value allowed to Algerian standards is 500mg / l. Sulphates show less variation compared to chloride.

#### • Chemical Oxygen Demand (COD) and Biological Oxygen Demand (BOD5)

The COD is expressed in milligrams per liter (mg / l) of oxygen and corresponds effectively to the amount of oxygen necessary to oxidize under defined operating conditions. The levels of COD recorded in the waters studied are between 40 and 59 mg / l thus presenting a significant load according to the standards of the World Health Organization (WHO) which is 30 mg / l. BOD5 is the amount of dissolved oxygen consumed by microorganisms in the dark at 20 ° C for 5 days. It allows the evaluation of biodegradable organic materials.

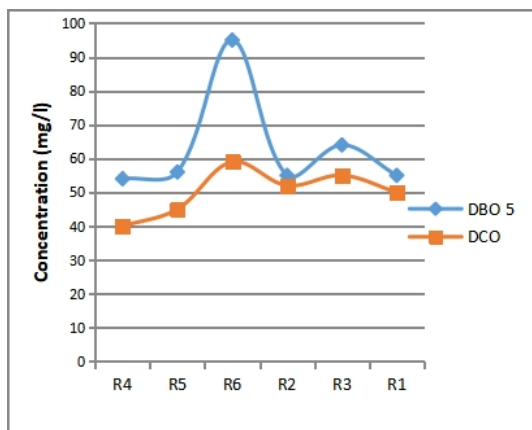


Figure 5 Evolution of BOD5 and COD along Oued Bechar.

The COD / BOD5 ratio gives a first estimate of the biodegradability of the organic matter of a given effluent; we agree in our case:

Table 2 COD / BOD5 ratio

R4	R5	R6	R2	R3	R1
0,740	0,803	0,621	0,945	0,859	0,909

For a COD / BOD5 value <2 [4] oued Bechar is easily biodegradable.

#### • Nitrates and Nitrites

##### 1. Nitrites

The nitrite concentrations in the wastewater studied show large spatial variations. These levels vary between 7 mg / l (R2) and 25 mg / l (R3) towards the north, which may be due to oxidation by oxygen present in the soil or dissolved in water.

##### 2. Nitrates.

The results of the nitrate analyzes show that their contents oscillate between 18.9 mg / l (R2) and 41.91 mg / l (R5). Figure 8 shows a south to north decrease in nitrate content. This decrease in nitrate content may be due to processing and consumption by microorganisms.

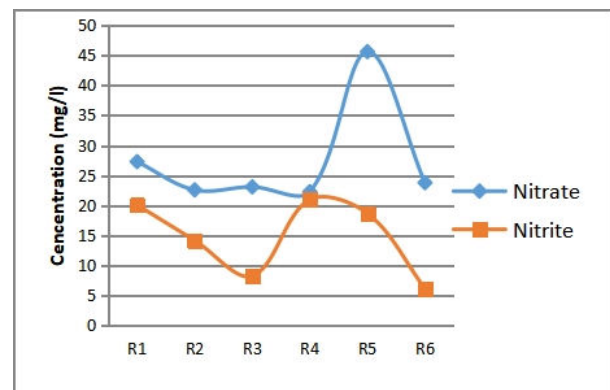


Figure 6 Evolution of Nitrate and Nitrite over the long Bechar oued

#### • Treatment of urban wastewater in the city of Bechar

The results of the analysis of urban wastewater from Oued Béchar are summarized in the following table:

Table 3: Results of analysis of wastewater from Oued Bechar

Paramètre	Unité	Valeur moyenne
pH	-	8.1
Température	°C	25
Conductivité	mS/cm	2.76
Salinité	mg/l	1.97
DCO	mg O <sub>2</sub> /l	145
DBO <sub>5</sub>	mg/l	72
Sulfate	mg/l	596.1
Chlorure	mg/l	390
Nitrate	mg/l	45.6
Nitrate	mg/l	20.1

#### Filtration contribution

At the laboratory level, daily samples were taken where the pH, conductivity, turbidity, Chloride, Sulfate, BOD and COD of the pretreated water were measured for 96 h, the results are shown here dissolved:

The results of the analysis of the pretreated wastewater are as follows:

#### • Conductivity and pH

The results show that the conductivities are respectively:

For the sand-slag mixture, a minimum of 3.92 mS / cm and a maximum of 4.21 mS / cm is recorded, and for the sand a minimum of 2.64 mS / cm and a maximum of 2.89 mS / cm.

The conductivity of the water treated with the sand is low with a reduction of 30% compared to that treated with the sand heaps during the duration of the experiment with a reduction of 70%; that is to say that the degree of impurities as well as the ionic concentration of dissolved salts are greater in the water treated in the sand Terril than in the sand.

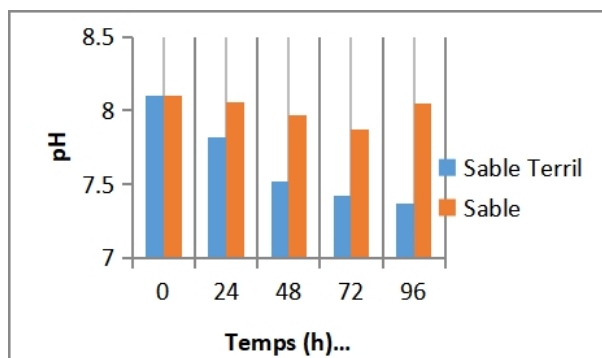


Figure.7 Evolution of the pH as a function of time.

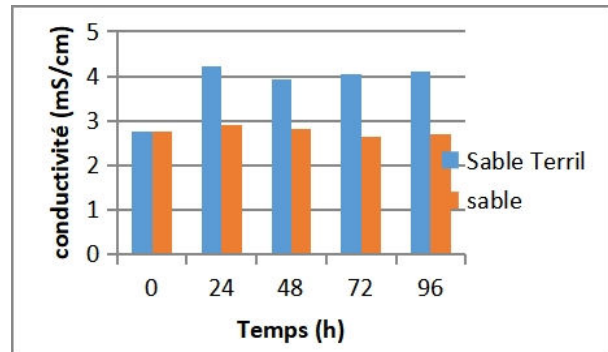


Figure 8 Evolution of conductivity as a function of time

#### • Chloride

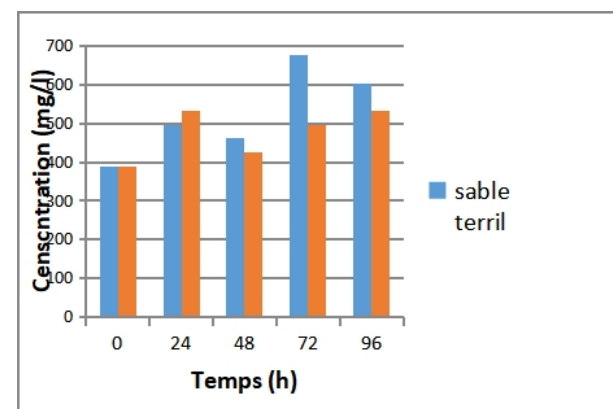


Figure 9 Evolution of chlorides as a function of time.

Based on the results of the chloride content obtained for the two samples studied sand and sand-slag during the 96h starting with the content of the raw sample are shown below.

The chloride content for the raw sewage sample is 390 mg / l. The sand filter contents are at least 426mg / l and 532.5 mg / l at most during the 96h. The chloride contents of the sand-slag filter have higher values than those of the sand.

We thus observe an increase in the chloride concentration as a function of time for the two samples compared to the rejection.

#### • Sulphate

The sulphate concentrations are shown below:

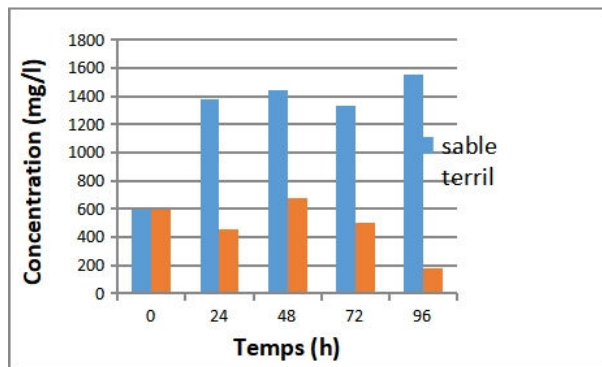


Figure 10 Evolution of sulphates as a function of time.

Note that the sulfate content for the sand is reduced by a reduction of 50% and an increase in the sulfate concentration for the sand-slag filter by 60%.

- Biochemical demand and chemical oxygen demand

The results gathered in the graph below attest that there is a decrease in the concentration of (BOD) by contribution to the discharge, which is 72 mg / l. We therefore observe a reduction of 60% for the two average values , which are 50.4 mg / l for the sand filter and 40.4 mg / l for the sand-slag filter

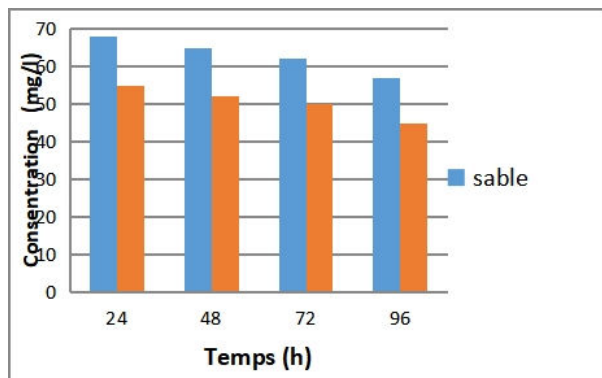


Figure 11 Evolution of BOD5 as a function of time

The reduction in chemical oxygen demand (COD) shows a significant variation between the sand filter and the sand-slag filter compared to the COD of the reject which has a value of 145 mg / l with a reduction of 70%. The results grouped together in the figure below show the influence of the water circulation on the COD concentration for the two filters during the 96h.

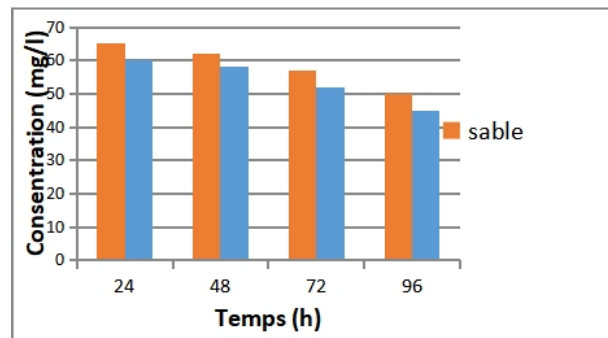


Figure 12 Evolution of the COD as a function of time.

### 2.3 Microbiological result and discussion

- The results of the coliform count

Coliforms are rods, facultative anaerobes, Gram (-), non-sporulating allowing the hydrolysis of lactose at 35 ° C (WHO, 1979). Based on the histogram of the Figure 12, and compared to the rate of CT (Total Coliforms), and CF (Fecal Coliforms) in the wastewater before filtration, a considerable decrease in the rate of coliforms of up to 100% respectively was recorded for CT and CF in the sand filter and up to 100% respectively for the CT and CF for the sand heap filter. So, according to the results obtained, the two filters used constitute an effective means of removing coliforms sufficient for the first 24 hours of filtration. These results are similar to those of [5] which were marked by an average percentage of elimination of 84% of CT and CF, by means of a slow filtration on a filter consisting of layers of fine and coarse sand [5].

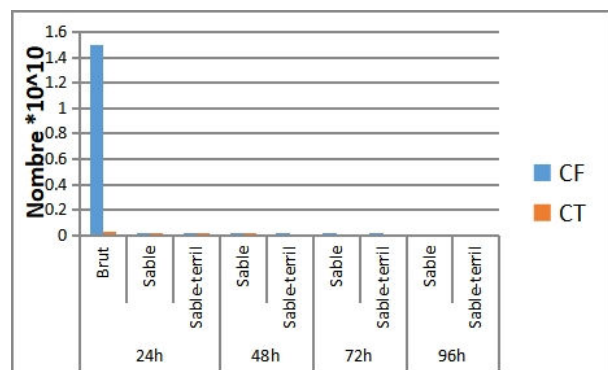


Figure 13 Graphic representation of the results of the research for Clostridium sulfito-reducing agents in wastewater before and after filtration.

- Results of the enumeration of the total mesophilic aerobic flora

It is the flora encompassing all natural or contaminating germs that live in the presence of oxygen. In all the samples of the reject analyzed, we notice the presence of total germs, these results show that the germ rate is very high ( $2 \times 10^{14}$  CFU)

at 20 ° C and 37 ° C (fig. 15), they exceed the Algerian standard which is 20 CFU / ml these concentrations are very high, they can cause health problems.

The results of the FAMT count are presented in fig. 15. It was observed from the first 24 hours of filtration that the FAMT is reduced to 100% for the GT (total germs) at 37 ° C and the GT at 20 ° C with the sand filter and in the sand heap mixture.

This efficiency can be explained by the absorption of microorganisms on the surface of the filter granules. The addition of heaps reduces the intergranular space, where the retention of microorganisms reaches its maximum.

### III-CONCLUSION

The results obtained in this study of physicochemical and microbiological analysis of urban discharge before and after filtration mostly confirm that there is a variation in the levels of the various parameters studied.

The characterization of urban wastewater from Oued Béchar has enabled us to assess and estimate the pollutant load, which turns out to be quite loaded with pollutants. The latter constitute a real threat to the region's environment, in particular to groundwater.

The results obtained from the filtration for the two filter beds used in this work show encouraging reductions for the various physicochemical parameters such as chlorides, sulphates, chemical oxygen demand (COD), biochemical oxygen demand (BOD). As for the microbiological parameters, they indicate a significant elimination of pollutants such as total mesophilic aerobic flora up to 100%.

### Reference

- [1] Kjeldsen P., Barlaz M.A., Rooker A.P., Baun A., Ledin A. & Christensen T.H. 2002.« Present and long-term composition of MSW landfill leachate»A review. Crit. Rev. Env.Sci.Tec., 32(4), 297-336.
- [2] Yves MICHEL Licence pro Traitement des eaux
- [3] Kendouci A, 2012 Contribution à la valorisation des matériaux locaux destinés au prétraitement des eaux usées.
- [4] La qualité et les analyses d'eau Action contre la Faim .
- [5] Vinay Kumar Tyagi, Abid Ali Khan, Kazmi Indu Mehrotra, Chopra 2009.Slow sand filtration of UASB reactor effluent: A promising post treatment technique. P 574

# Etude et Investigation Sur la Pollution Les Macro Déchets et Les Micro Déchets de Pastique Dans le Nord Est Algérien (Golfe d'Annaba)

Hadjou Mohamed Cherif

**Abstract**—Même si elle est largement observée dans les écosystèmes marins, ce n'est que récemment que la pollution par les macro déchets et les micro déchets de pastique a été documentée dans les écosystèmes aquatiques , et ce presque exclusivement dans les eaux de surface . Les macro déchets accumulés sur les plages constituent une nuisance et peuvent être un danger pour les usagers, ainsi que pour les espèces marines.

Nous avons identifié et quantifié ces macro déchets de plastique sur quatre stations dans le nord est Algérien ( golfe d'Annaba). Les résultats montrent qu'au total 4000 items ont été collectés, avec un poids de 610 Kg. Ce sont les emballages de plastique, principalement les bouteilles qui montrent le plus fort pourcentage avec 60% au niveau de la station Seybouse la plus polluées.

Quant à la pollution des eaux de surface par les micro plastiques (< 5 mm), Nos résultats montrent la présence de particule de plastique dans les eaux de surface des deux stations Seybouse et Sidi Salem, les concentrations les plus élevées sont relevées au niveau de la station de Sidi Salem située à proximité de l'embouchure de l'oued Seybouse. Les sources de ces particules et la quantité des apports restent à identifier et quantifier. D'autres questions restent ouvertes, notamment le devenir du micro plastique.

**Keywords**—Macro déchets, Micro déchets, Microplastique, nord est Algérien.



# Planning Quality and Maintenance Activities in a Closed-Loop Serial Multi-Stage Manufacturing System Under Constant Degradation

Amauri Josafat Gomez Aguilar. Jean Pierre Kenné

Jean Pierre Kenné is with the University of Quebec, ETS, Canada (e-mail: jean-pierre.kenne@etsmtl.ca).

## ***Abstract.***

This research presents the development of a self-sustainable manufacturing system from a circular economy perspective, structured by a multi-stage serial production system consisting of a series of machines under deterioration in charge of producing a single product and a reverse remanufacturing system constituted by the same productive systems of the first scheme and different tooling, fed by-products collected at the end of their life cycle, and non-conforming elements of the first productive scheme. Since the advanced production manufacturing system is unable to satisfy the customer's quality expectations completely, we propose the development of a mixed integer linear mathematical model focused on the optimal search and assignment of quality stations and preventive maintenance operation to the machines over a time horizon, intending to segregate the correct number of non-conforming parts for reuse in the remanufacturing system and thereby minimizing production, quality, maintenance, and customer non-conformance penalties. Numerical experiments are performed to analyze the solutions found by the model under different scenarios. The results showed that the correct implementation of a closed manufacturing system and allocation of quality inspection and preventive maintenance operations generate better levels of customer satisfaction and an efficient manufacturing system.

## ***Keywords.***

Closed loop, Mixed integer linear programming, Preventive maintenance, Quality Inspection.

# Tentative Title for Conference Paper: Stakeholder Mapping and Requirements Identification for Improving Traceability in the Halal Food Supply Chain

Laila A. H. F. Dashti<sup>1</sup>, Prof. Tom Jackson<sup>1</sup>, Prof. Andrew West<sup>1</sup>, Prof. Lisa Jackson<sup>1</sup>.

<sup>1</sup> Department of Business and Economics, University of Loughborough, UK

## Abstract

Traceability systems are important in the agri-food and halal food sectors for monitoring ingredient movements, tracking sources, and ensuring food integrity. However, designing a traceability system for the halal food supply chain is challenging due to diverse stakeholder requirements and complex needs. Existing literature on stakeholder mapping and identifying requirements for halal food supply chains is limited. To address this gap, a pilot study was conducted to identify the objectives, requirements, and recommendations of stakeholders in the Kuwaiti halal food industry. The study collected data through semi-structured interviews with an international halal food manufacturer based in Kuwait. The aim was to gain a deep understanding of stakeholders' objectives, requirements, processes, and concerns related to the design of a traceability system in the country's halal food sector. Traceability systems are being developed and tested in the agri-food and halal food sectors due to their ability to monitor ingredient movements, track sources, and detect potential issues related to food integrity. Designing a traceability system for the halal food supply chain poses significant challenges due to diverse stakeholder requirements and the complexity of their needs (including varying food ingredients, different sources, destinations, supplier processes, certifications, etc.). Achieving a halal food traceability solution tailored to stakeholders' requirements within the supply chain necessitates prior knowledge of these needs. Although attempts have been made to address design-related issues in traceability systems, literature on stakeholder mapping and identification of requirements specific to halal food supply chains is scarce. Thus, this pilot study aims to identify the objectives, requirements, and recommendations of stakeholders in the halal food industry. The paper presents insights gained from the pilot study, which utilized semi-structured interviews to collect data from a Kuwait-based international halal food manufacturer. The objective was to gain an in-depth understanding of stakeholders' objectives, requirements, processes, and concerns pertaining to the design of a traceability system in Kuwait's halal food sector. The stakeholder mapping results revealed that government entities, food manufacturers, retailers, and suppliers are key stakeholders in Kuwait's halal food supply chain. Lessons learned from this pilot study regarding requirement capture for traceability systems include the need to streamline communication, focus on communication at each level of the supply chain, leverage innovative technologies to enhance process structuring and operations and reduce halal certification costs. The findings also emphasized the limitations of existing traceability solutions, such as limited cooperation and collaboration among stakeholders, high costs of implementing traceability systems without government support,

lack of clarity regarding product routes, and disrupted communication channels between stakeholders. These findings contribute to a broader research program aimed at developing a stakeholder requirements framework that utilizes "business process modelling" to establish a unified model for traceable stakeholder requirements.

**Keywords:** *Supply chain, traceability system, halal food, stakeholders' requirements*

## Introduction

Halal food refers to food processed and manufactured in accordance with Islamic regulations governing food consumption (Al-Teinaz et al., 2020). With the global increase in the Muslim population, the demand for halal food is growing, leading to the expansion of the halal food industry. In 2022, the halal food industry captured a share of US\$2,221.3 billion in the global food market industry (Impactful Insights, 2023). Not only is halal food consumed by Muslims, but its popularity is also rising in non-Muslim countries due to its high quality and safety standards during manufacturing (Zulkifli, 2013).

However, despite the high demand for halal food in both Muslim and non-Muslim countries with Muslim minorities, there is a lack of unified standards for halal food, which poses significant challenges to the integrity of halal food in the market (Randeree, 2019). This situation creates opportunities for unethical practices, such as the fabrication of halal food ingredients during sourcing, mixing, and manufacturing processes. There have even been reports of manufacturers displaying fake halal food certificates on products in Muslim countries (Majid et al., 2015). Implementing a food traceability system provides hope for consumers and governments to regulate the halal food industry, ensuring the integrity of halal food by increasing transparency regarding processing, manufacturing, and distribution (Zailani et al., 2020; Aniqoh and Hanastiana, 2020).

Traceability plays a critical role in the halal food supply chain as it enables efficient tracking of halal food ingredients, allowing the identification of sources and verification of halal status for products marketed in halal food markets (Poniman et al., 2015). Developing and implementing halal traceability systems pose challenges for both manufacturers and governments due to the involvement of various stakeholders in the delivery, manufacturing, and distribution processes of halal food products (Samsi et al., 2012). Cooperation and coordination among stakeholders are crucial for managing relationships within the halal food supply chain, and data from each stakeholder contribute to the development of an efficient and effective traceability system (Kadir et al., 2016).

Without understanding the needs and requirements of stakeholders in the halal food supply chain, building an effective traceability system becomes jeopardized. Incorporating halal food requirements into traceability systems can ensure their adoption within halal food networks. For example, communication between suppliers and manufacturers of halal food products can contribute valuable data on the integrity of halal food, which can be traced and tracked by governments and consumers to verify the integrity of ingredients used in processing and manufacturing (Samsi et al., 2012).

Similarly, the adoption of traceability systems can be related to their mandatory status for certain food products. For instance, the European Union mandated traceability systems for beef sales in member countries, leading to wider adoption and enforcement of traceability systems among beef sellers (Charlebois et al., 2014). There are also instances of voluntary adoption of

traceability systems in the dairy and poultry sectors. However, mandatory traceability systems are generally more effective and regulated due to government involvement as a key stakeholder in monitoring and verifying the integrity of food products through enforced traceability systems (Smith et al., 2008). Successful execution and implementation of traceability systems in both Muslim and non-Muslim countries require willingness from key players such as suppliers, farmers, manufacturers, distributors, and government entities (Poniman et al., 2015).

Kuwait, situated in the Arabian Peninsula, is a Muslim country with a population of approximately 4.45 million Muslims (WorldMeter, 2023). The Kuwaiti market faces significant challenges, including the presence of fake certificates and the sale of halal food products containing non-halal ingredients. These issues arise due to the absence of a fully operational and effective traceability system mandated by the government or voluntarily adopted by halal manufacturing firms. As a result, consumer confidence in the integrity of halal food products in the market has been compromised. Without a clear understanding of stakeholder requirements, attempts to establish or develop a traceability system may prove unsuccessful (Samsi et al., 2012). This study serves as a pilot investigation designed to identify the challenges faced by stakeholders and their needs and requirements in building an effective traceability system. It lays the groundwork for future research in the Kuwaiti halal industry.

The remaining sections of this paper are divided into five main parts: a literature review, research methods, results and discussion, and conclusion.

## **Literature Review**

### **Traceability system in halal food ecosystem**

According to Poniman et al (2015), traceability system is the mechanism through which products or ingredients of the food products can be tagged for tracing the origin and nature of the products. Traceability system in the context of the halal food products is defined as the tracking and tracing of the food ingredients or the finished products with the aim to satisfy the end consumers and government with the provision of the related data on the request or online (Rashid and Bojei, 2020). Muslims follow the Islamic Sharia (Laws) which prohibits the consumption of the halal food, the food which is prepared in contact with the blood, the meat slaughtered without the name of God, and many other considerations (Najmi et al., 2023).

In the European countries traceability is regarded as an emblem of the safety and quality of the food products. The quality and safety issues of the food are dealt with tracing and tracking the sources and processing of the food items during the manufacturing process through the use of an effective traceability system (Aung and Chang, 2014). The traceability system may be based on the keeping the records of events as part of the supply chain management system using the paper-based method or the technological tools and instruments including RFID, blockchain or computer software for storing, accessing and transferring the data from one end of the supply chain to the end consumers on the other side of the supply chain (Olsen and Borit, 2018; Kesna et al., 2017).

The most common challenges faced by building a traceability system is the lack of the information at different timepoints within the supply chain about movement of the products, which arises from the limited level of participation of certain stakeholders such as famers and suppliers in supplying the required information to other stakeholders such as manufacturers and consumers (Karippacheril et al., 2017; Purwandoko and Seminar, 2018). The data about

all aspects of the products can only be ensured through the constant communication and coordination among stakeholders, and their participation in sustaining the traceability system for maintaining the food safety, integrity and quality as desired by the end users (Mohamed et al., 2016; Usman et al., 2018).

### Halal traceability and stakeholders

According to stakeholder theory, the important stakeholders governing the operations in the supply chain involve firms, employees, government, consumers, suppliers, and government agencies (Friedman and Miles, 2006; Freeman et al., 2010).

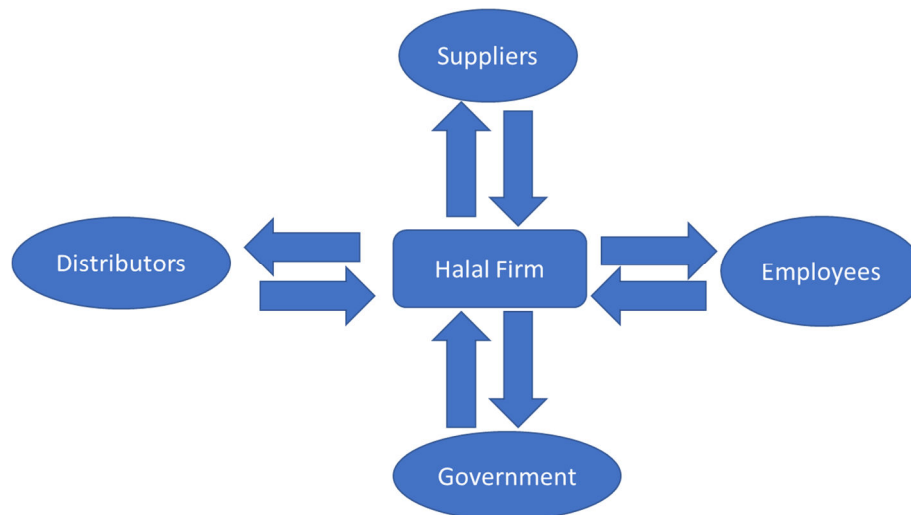


Figure 1: The key stakeholders involved in the halal food supply chain

Government plays a critical role in creating and maintaining the halal markets through the legislation in the halal food sectors. They establish the monitoring and supervision structures for verifying the integrity of the halal food products (Zulfakar et al., 2014; Adekunle and Filson, 2020). Additionally, the government is responsible for increasing the awareness among the players in halal industry and consumers about the adherence to the halal standards and its benefits to the health of consumers and productivity of the halal business (Batu and Regenstein, 2014; Supian and Rashid, 2018). As long as the halal firms are concerned, they have responsibilities of verifying the halal status of the ingredients prior to purchasing with the suppliers, keep record of all events about the ingredients in their systems, obtaining the halal certification by following the local regulations, and production of all relevant data relating to the processing, storage, packaging and distribution of the halal foods (Zailani et al., 2020; Zailani et al., 2015; Talib et al., 2017).

Employees constitute a key stakeholder, and they need to be trained by halal firms about the halal standards while processing, storing, packing and distributing the halal foods in order to maintain the integrity of the halal food products (Supian and Rashid, 2018; Zailani et al., 2020). Suppliers supply the ingredients, hold key relationships with farmers, located closer to the points where qualitative information about the production, farming, and harvesting of ingredients can easily be obtained (Supian and Rashid, 2018). Therefore, they have the responsibility to provide the adequate level of information to the production firms about the sourcing and quality of the ingredients to the firms, so that relevant data can be furnished to the traceability system (Tan et al., 2017; Samsi et al., 2011). Distributors or trade associations

form another important stakeholder, as they are supposed to market the halal logos, and provide the relevant information to retailers and consumers on demand. They serve as facilitators between the consumers and food production firms to provide the relevant information (Samsi et al., 2011)

There is common misconception that only firms carry the responsibility of implementing the food traceability system, rather than it is the shared responsibility of all stakeholders involved in carrying out various processes along the halal food supply chain (see Figure 2) to support and implement the halal food traceability along each and every phase of the halal food supply chain (Randeree, 2019; Samsi et al., 2011; Mohamed et al., 2016). Talib et al (2017) viewed the contribution of each stakeholder to the halal food traceability system, and must be prioritized within the management of the supply chain. The consumers' confidence is highly reliant on type of information and data provided by suppliers, farmers and manufacturers to the consumers, and its availability to the consumers online or on the request.

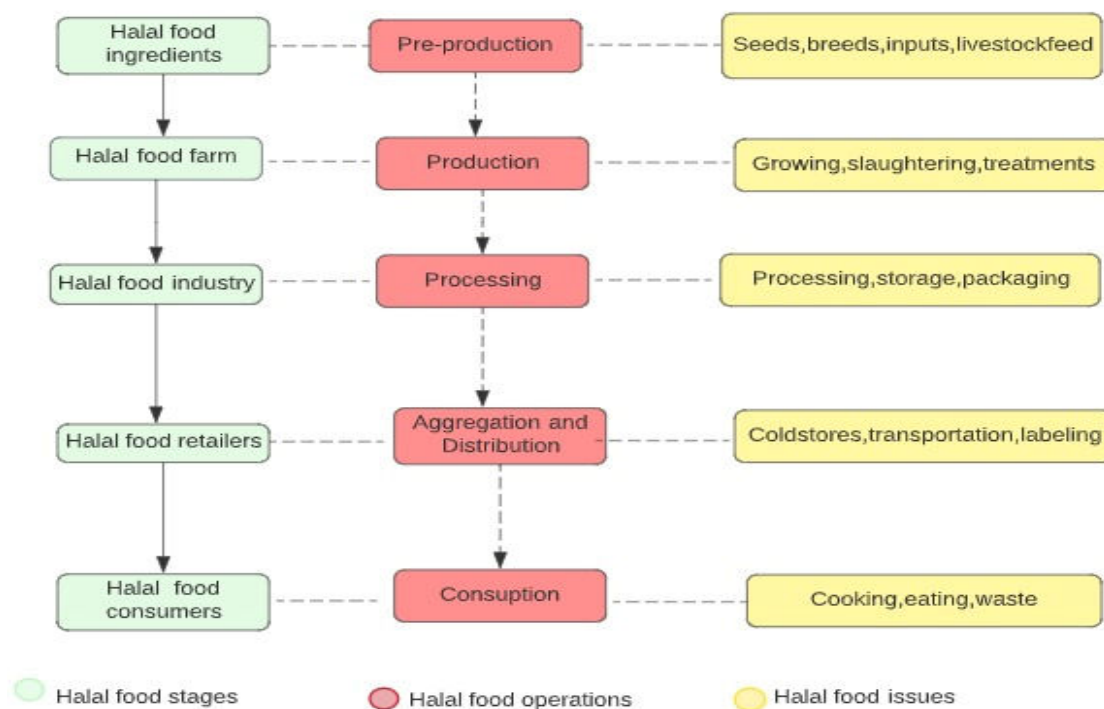


Figure 2: The different phases of the supply chain for traceability associated with stakeholders.

The presence of the food control system and generation of the food quality data with all stakeholders including farmer, suppliers, manufacturers and distributors can ensure the satisfaction of consumers and government agencies about the sourcing, processing and movement of the ingredients of food products and ready-to-be-used halal food products (Yunos et al., 2014). The current focus of the halal food manufacturers is to obtain and show the halal food certification, but it does not inform the consumers and government bodies – key stakeholders in the halal food supply chain – about the underlying processes food handling, packaging and movement of the food products in the supply chain to reach the table of consumers. Therefore, scholars and practitioners in the supply chain emphasized the

installation of an effective quality management at the production and distribution levels (Samsi et al., 2011; Kadir et al., 2016).

Tan et al (2017) argued the inclusion of the assurance system from all stakeholders in the halal food supply chain, which can be integrated into the traceability system for enabling the firms to meet the needs and requirements of the Muslim consumers and halal monitoring agencies. This boils down to the participation of all stakeholders along the supply chain to develop the assurance system along with halal certification system for fulfilling the needs of the Muslim consumers.

## **Research Methods**

This research adopted the qualitative research design. The qualitative research helps the researchers to collect an in-depth information about social phenomenon under investigation with the aim of having a deeper understanding of the experiences of the people with knowledge about the research problem (Hannink et al., 2020; Hammerberg et al., 2016). As this research work aims to understand the issues in the halal food industry, and to gain the in-depth insight into the requirements and needs of the consumers for the modelling the traceability system for halal market in Kuwait. Therefore, the qualitative research design is the most optimal approach for addressing the research questions posed in this study.

## **Qualitative interviews**

The purpose of the interview is to gather the maximum data from respondents, so that all objectives of the study are satisfied (Wilson, 2012). This was a pilot study with aim to gain preliminary data regarding the research problem under discussion, allowing the development of more refined approach and data to model the traceability system. Therefore, initially 4 interviewees were selected for this study. The interviews are conducted with a set of questions relating to the traceability, strengths and weaknesses of existing traceability systems with focus on the needs for further development. The respondents were motivated to provide information related to varied search without influencing the interviewees (Rosenthal, 2016). Respondents were clarified the questions, asked the prompt questions with the intention gather in-depth understanding of their experiences in halal industry and importance of the traceability system. The interviews were lasted for 45 minutes approximately, and list of topics recommended by the researcher and the respondent were thoroughly discussed. The strength of the semi-structure interview is that it helps researchers to devise as many prompt questions or sub-topics which are deemed to be necessary for addressing the research issue (Knox and Burkard, 2009). This helped the investigator to collect as much data as was important for answering the research questions raised in this study

## **Data analysis**

The interview data were analysed using the thematic approach which is frequently applied method for analysing the qualitative data such as interview or textual data (Braun and Clarke, 2012). It allows the researchers to identify the common themes and patterns of topics and ideas appearing repeatedly within the textual data (Clarke et al., 2015). The following procedure was adopted to conduct the thematic analysis (Peterson, 2017)



- The textual data obtained from the interviews were read and reread to gain thorough understanding of the contents
- The phrases or sentences with comprehensive meaning relating to the research problem and coming up repeatedly were classed as codes and entered in the code and theme notebook.
- The codes generated in the step 2 were compared exhaustively; similar codes were grouped, and each group was categorized as a distinct theme.
- Themes were compared exhaustively, followed by creation of the broader themes or categories which were used for describing and interpreting the results.

## **Results and discussion**

### **Integration of the farm-to-fork approach**

All the respondents unanimously acknowledged the significance of implementing a farm-to-fork approach in constructing a robust and effective traceability system. One participant emphasized that the current state of halal food traceability lacks this approach, which jeopardizes the quality, safety, and integrity of halal food products. Consequently, consumer confidence is undermined. Additionally, another participant highlighted the inadequate attention given to the movement of food products from factories to retailers.

Numerous studies align with our findings, emphasizing the indispensability of a farm-to-fork approach in establishing an efficient and trustworthy traceability system, for example, halal food traceability using the internet of things in Malaysian agro-food sector (Ahmad-Tarmizi et al., 2020), the halal food traceability implementation in the post slaughter process within the slaughterhouses (Smith et al (2008); and halal food traceability using the blockchain (Vanany et al., 2020). Tan et al. (2022) argued that integrating processes and technologies into the traceability system to enhance the halal food supply chain, from farm to fork, is of utmost importance in meeting the requirements of stakeholders. Particularly, consumers' trust heavily relies on comprehensive data spanning from farm to fork, encompassing all stages of food product delivery. Similarly, Ling et al. (2020) regarded the farm-to-fork approach as a fundamental component of halal food traceability, as it mitigates the risks of contamination throughout the movement, sourcing, production, and distribution of food products to end stakeholders, specifically consumers.

### **Cooperation and Collaboration among stakeholders**

Virtually all participants acknowledged the imperative of cooperation and collaboration among stakeholders. They observed that the existing level of cooperation is limited and insufficient in maintaining a high-quality traceability system for halal food products. This deficiency primarily arises from the absence of crucial information regarding the safety, quality, and integrity of the products, which is lacking from farmers and suppliers. One participant highlighted that while companies focus solely on halal food certification, comprehensive data regarding the sourcing, feeding, and maintenance of animals for meat production are not consistently available from all suppliers.

To corroborate the findings of this study, Samsi et al. (2011) emphasized the significance of a positive relationship among stakeholders in the Malaysian halal industry. Such a relationship facilitates the provision of relevant data on halal food ingredients and products to all pertinent stakeholders within the halal food supply chain. Furthermore, Kadir et al. (2016) suggested that

collaboration between stakeholders, including research institutions and production firms, can foster stronger relationships and enhance the visibility of food products and ingredients throughout the supply chain. This increased transparency benefits key stakeholders, such as the government and consumers, in managing halal supply chain operations.

### **Need for strong communication channels**

The participants unanimously emphasized the critical need for strong communication channels, supported by advanced technologies, to facilitate the timely dissemination of information regarding changes in the sourcing and procurement of halal ingredients used in halal food products. One participant specifically highlighted the government's role in promptly updating regulations, certification requirements, and recommended labelling specifications to the production firms operating within the Kuwaiti halal ecosystem.

Collectively, it can be argued that communication channels should be an integral part of the traceability system, enabling stakeholders to access and update the system with proposed changes in ingredient supply, halal food products, and regulations pertaining to labelling and processing requirements for halal food manufacturing. Mohamed et al. (2016) assert that the traceability system serves as a communication platform for stakeholders, which should be enhanced with state-of-the-art technologies to facilitate effective communication among the various participants in the traceability system. Technologies such as blockchain, Internet of Things (IoT), and RFID are widely employed to enhance data communication among stakeholders in food traceability (Osman et al., 2018; Najmi et al., 2023; Bux et al., 2022).

### **Innovative technologies in building traceability systems**

The data obtained from the respondents underscored the critical importance of adopting innovative technological solutions to promote and sustain traceability systems within the Kuwaiti halal market. The participants recognized the potential benefits of employing blockchain and RFID technologies to establish traceability for halal food products. By utilizing these technologies, the monitoring of halal food product movements could be conducted by government entities, suppliers, and firms without limitations of time and space.

However, the respondents also highlighted the limited utilization of innovative technologies in record-keeping practices. Currently, the use of technology is primarily restricted to basic record-keeping software. This limitation poses a risk of data fabrication, as it may enable the concealment of information regarding contaminations from governmental monitoring agencies and social organizations dedicated to upholding the integrity of halal food products. From the above data, it is evident that innovative technologies are needed by production firms, an important stakeholder in the halal food industry in Kuwait. Importance of the innovative technologies for traceability systems are acknowledged by many studies, which corroborate the findings of this study.

For instance, Bux et al (2022) pinpointed the application of blockchain for increasing the trustworthiness of traceability system due to communication of data among stakeholders with limited potential of fabrication of data on behalf of the stakeholders at different phases of the supply chain of the halal food products. Rejeb et al (2021) included the internet of things for building the traceability system with higher level of communication among stakeholders

participating in the halal food supply chain management. Rejeb et al (2021) included the internet of things for building the traceability system with higher level of communication among stakeholders participating in the halal food supply chain management. Furthermore, some other practitioners and academics in the field of traceability in halal food sector recommended the application of internet of things for enabling faster and better communication among the stakeholders in the halal food traceability (Rejeb et al., 2021; Osman et al., 2018; Najmi et al., 2023).

### **Halal Certification and Legislations**

Most of respondents argued that halal certification procedure is costly and lengthy, which causes difficulties to the firms to obtain the halal certification on regular basis, so that they market their halal food products in the Kuwaiti market. They all recommended to lower the halal certification fee, so that they can make investments in the development of halal traceability system. Furthermore, two participants also mentioned of the high cost of maintaining the halal traceability system which may discourage halal food production firms to adopt it on the long-run basis.

From the above data, the cost of halal food certification and maintenance of the halal traceability systems are major factors which may discourage wide-scale adoption of the traceability system. Therefore, government should lower the cost of the halal certification in Kuwaiti market to cater to needs of the halal food production firms. Several other studies have reported that cost of maintaining halal certification is high, but the companies are paid off by the consumers who are willing to pay higher prices due to halal certified meat products (Fuseini, 2017; Iranmanesh et al., 2020; Verbeke et al., 2013). The government may reduce the price of certification to decrease the burden of high prices of halal certified products on the consumers.

### **Conclusion and Future work**

This pilot study aimed to capture the needs and requirements of stakeholders in the Kuwaiti halal ecosystem, with the ultimate goal of developing a traceability system that aligns with their specific needs. The findings of this study highlighted several key factors, including the integration of a farm-to-fork approach, enhanced cooperation and collaboration among stakeholders, efficient communication channels, reduced costs of halal certification, and the application of innovative technologies. Incorporating these elements into the traceability system will ensure its suitability for the Kuwaiti halal food sector.

By integrating the requirements and concerns of the stakeholders into the development process, the adoption of the traceability system is expected to increase significantly. Moving forward, we will expand our participant pool to include representatives from the government and other companies operating in the halal food sector. This broader analysis will enable us to further understand their specific requirements and subsequently model the traceability system for the Kuwaiti halal food ecosystem accordingly, ensuring a tailored solution that meets stakeholders' needs.

## References

- Ahmad Tarmizi, H., Kamarulzaman, N. H., Abd Rahman, A., & Atan, R. (2020). Adoption of internet of things among Malaysian halal agro-food SMEs and its challenges. *Food Research*, 4(S1), 256-265.
- Adekunle, B., & Filson, G. (2020). Understanding halal food market: Resolving asymmetric information. *Food ethics*, 5, 1-22.
- Al-Teinaz, Y. R., Spear, S., & Abd El-Rahim, I. H. (Eds.). (2020). *The halal food handbook*. John Wiley & Sons.
- Aniqoh, N. A. F. A., & Hanastiana, M. R. (2020). Halal food industry: challenges and opportunities in Europe. *Journal of Digital Marketing and Halal Industry*, 2(1), 43-54.
- Aung, M. M., & Chang, Y. S. (2014). Traceability in a food supply chain: Safety and quality perspectives. *Food control*, 39, 172-184.
- Batu, A., & Regenstein, J. M. (2014). Halal food certification challenges and their implications for Muslim societies worldwide. *Electronic Turkish Studies*, 9(11).
- Braun, V., & Clarke, V. (2012). *Thematic analysis*. American Psychological Association.
- Bux, C., Varese, E., Amicarelli, V., & Lombardi, M. (2022). Halal food sustainability between certification and blockchain: A review. *Sustainability*, 14(4), 2152.
- Charlebois, S., Sterling, B., Haratifar, S., & Naing, S. K. (2014). Comparison of global food traceability regulations and requirements. *Comprehensive reviews in food science and food safety*, 13(5), 1104-1123.
- Clarke, V., Braun, V., & Hayfield, N. (2015). Thematic analysis. *Qualitative psychology: A practical guide to research methods*, 3, 222-248.
- Freeman, R. E., Harrison, J. S., Wicks, A. C., Parmar, B. L., & De Colle, S. (2010). Stakeholder theory: The state of the art.
- Friedman, A. L., & Miles, S. (2006). *Stakeholders: Theory and practice*. OUP oxford.
- Fuseini, A. (2017). Halal food certification in the UK and its impact on food businesses: a review in the context of the European Union. *CABI Reviews*, (2017), 1-7.
- Haleem, A., & Khan, M. I. (2017). Towards successful adoption of Halal logistics and its implications for the stakeholders. *British Food Journal*.
- Hammarberg, K., Kirkman, M., & de Lacey, S. (2016). Qualitative research methods: when to use them and how to judge them. *Human reproduction*, 31(3), 498-501.
- Hennink, M., Hutter, I., & Bailey, A. (2020). *Qualitative research methods*. Sage.
- Impactful Insights. (2023). Halal food market: Global industry, trends, share, size, growth, opportunity and forecast 2023-2028. Available at < <https://www.imarcgroup.com/halal-food-market#:~:text=The%20global%20halal%20food%20market%20was%20valued%20at%20US%24%202%2C221.3,10.8%25%20during%202023%2D2028> > [Accessed on 07 April 2023].

- Iranmanesh, M., Mirzaei, M., Parvin Hosseini, S. M., & Zailani, S. (2020). Muslims' willingness to pay for certified halal food: an extension of the theory of planned behaviour. *Journal of Islamic Marketing*, 11(1), 14-30.
- Kadir, M. H. A., Rasi, R. Z. R. M., Omar, S. S., & Manap, Z. I. A. (2016, November). Halal supply chain management streamlined practices: Issues and challenges. In *IOP Conference Series: Materials Science and Engineering* (Vol. 160, No. 1, p. 012070). IOP Publishing.
- Karippacheril, T. G., Rios, L. D., & Srivastava, L. (2017). Global markets, global challenges: Improving food safety and traceability while empowering smallholders through ICT.
- Knox, S., & Burkard, A. W. (2009). Qualitative research interviews. *Psychotherapy research*, 19(4-5), 566-575.
- Kresna, B. A., Seminar, K. B., & Marimin, M. (2017). Developing a traceability system for tuna supply chains. *International Journal of Supply Chain Management*, 6(3), 52-62.
- Mohamed, Y. H., Rahim, A. A., Ma'ram, A. B., & Hamza, M. G. (2016). Halal traceability in enhancing halal integrity for food industry in Malaysia—a review. *International Research Journal of Engineering and Technology*, 3(3), 68-74.
- Najmi, A., Ahmed, W., & Jahangir, S. (2023). Firm's readiness for halal food standard adoption: assessing the importance of traceability system. *Journal of Islamic Accounting and Business Research*.
- Olsen, P., & Borit, M. (2018). The components of a food traceability system. *Trends in Food Science & Technology*, 77, 143-149.
- Peterson, B. L. (2017). Thematic analysis/interpretive thematic analysis. *The international encyclopedia of communication research methods*, 1-9.
- Poniman, D., Purchase, S., & Sneddon, J. (2015). Traceability systems in the Western Australia halal food supply chain. *Asia Pacific Journal of Marketing and Logistics*, 27(2), 324-348.
- Purwandoko, P. B., & Seminar, K. B. (2018, May). Framework for Design of Traceability System on Organic Rice Certification. In *IOP Conference Series: Earth and Environmental Science* (Vol. 147, No. 1, p. 012044). IOP Publishing.
- Randeree, K. (2019). Challenges in halal food ecosystems: the case of the United Arab Emirates. *British Food Journal*.
- Rashid, N., & Bojei, J. (2020). The relationship between halal traceability system adoption and environmental factors on halal food supply chain integrity in Malaysia. *Journal of Islamic Marketing*, 11(1), 117-142.
- Rejeb, A., Rejeb, K., Zailani, S., Treiblmaier, H., & Hand, K. J. (2021). Integrating the Internet of Things in the halal food supply chain: A systematic literature review and research agenda. *Internet of Things*, 13, 100361.
- Rosenthal, M. (2016). Qualitative research methods: Why, when, and how to conduct interviews and focus groups in pharmacy research. *Currents in pharmacy teaching and learning*, 8(4), 509-516.

- Samsi, S. Z. M., Ibrahim, O., & Tasnim, R. (2012). Review on knowledge management as a tool for effective traceability system in halal food industry supply chain. *Journal of Research and Innovation in Information Systems*, 1(1), 78-85.
- Samsi, S. Z. M., Tasnim, R., & Ibrahim, O. (2011, March). Stakeholders' role for an efficient traceability system in halal industry supply chain. In *Annual International Conference on Enterprise Resource Planning and Supply Chain Management (ERP-SCM 2011)* (pp. 14-15).
- Smith, G. C., Pendell, D. L., Tatum, J. D., Belk, K. E., & Sofos, J. N. (2008). Post-slaughter traceability. *Meat science*, 80(1), 66-74.
- Supian, K., & Ab Rashid, N. (2018). The role of supplier, top management and government in halal practices integrity of malaysian food business. *International Journal of Asian Social Science*, 8(8), 549-559.
- Talib, M. S., Ai Chin, T., & Fischer, J. (2017). Linking Halal food certification and business performance. *British Food Journal*, 119(7), 1606-1618.
- Tan, A., Gligor, D., & Ngah, A. (2022). Applying blockchain for halal food traceability. *International Journal of Logistics Research and Applications*, 25(6), 947-964.
- Usman, Y. V., Fauzi, A. M., Irawadi, T. T., & Djatna, T. (2018, April). Augmented halal food traceability system: Analysis and design using UML. In *IOP Conference Series: Materials Science and Engineering* (Vol. 337, No. 1, p. 012050). IOP Publishing.
- Vanany, I., Rakhmawati, N. A., Sukoso, S., & Soon, J. M. (2020, November). Indonesian halal food integrity: Blockchain platform. In 2020 International Conference on Computer Engineering, Network, and Intelligent Multimedia (CENIM) (pp. 297-302). IEEE.
- Verbeke, W., Rutsaert, P., Bonne, K., & Vermeir, I. (2013). Credence quality coordination and consumers' willingness-to-pay for certified halal labelled meat. *Meat science*, 95(4), 790-797.
- Wilson, V. (2012). Research methods: interviews. *Evidence Based Library and Information Practice*, 7(2), 96-98.
- WorldMeters. (2023). Kuwait Population (Live). Available at < <https://www.worldometers.info/world-population/kuwait-population/>> [Accessed on 07 April 2023]
- Yunos, R. M., Mahmood, C. F. C., & Abd Mansor, N. H. (2014). Understanding mechanisms to promote halal industry-the stakeholders' views. *Procedia-Social and Behavioral Sciences*, 130, 160-166.
- Zailani, S., Iranmanesh, M., Jafarzadeh, S., & Foroughi, B. (2020). The influence of halal orientation strategy on financial performance of halal food firms: Halal culture as a moderator. *Journal of Islamic Marketing*, 11(1), 31-49.
- Zailani, S., Kanapathy, K., Iranmanesh, M., & Tieman, M. (2015). Drivers of halal orientation strategy among halal food firms. *British Food Journal*.
- Zulfakar, M. H., Anuar, M. M., & Ab Talib, M. S. (2014). Conceptual framework on halal food supply chain integrity enhancement. *Procedia-Social and Behavioral Sciences*, 121, 58-67.

# Sustainable Supply Chain Management Practices, Challenges, and Opportunities – A Case Study of SMEs Within the Oil & Gas Sector

Dr Igbo Ekiugbo

Lecturer in Management – Logistics and Supply Chain Management, Birmingham City Business School, Birmingham City University, Birmingham

and

Dr. Christos Papanagnou

Senior Lecturer in Logistics Engineering, School of Infrastructure and Sustainable Engineering, Aston University, Manchester

**Abstract**—The energy sector continues to face increased scrutiny due to climate change challenges emanating from the burning of fossil fuels, such as, coal, oil, and gas. These climate change challenges have motivated industry practitioners and researchers alike to gain an interest in the way businesses operate. This paper aimed to investigate and assess how small and medium-sized enterprises (SMEs) are reducing the impact of their operations, especially those within their supply chains, by assessing the sustainability practices they have adopted and implemented as well as the benefits, and challenges of adopting such practices. Data will be collected from SMEs operating across the downstream oil and gas sector in Nigeria using questionnaire surveys. To analyse the data, confirmatory factor analysis and regression analysis will be performed. This method is deemed more suitable and appropriate for testing predefined measurements of sustainable supply chain practices as contained in the extant literature. Preliminary observations indicate a consensus on the awareness of sustainability concept amongst the target participants. To the best of our knowledge, this paper is among the first to investigate the sustainability practices of SMEs operating in the Nigerian oil and gas sector and will therefore contribute to the sustainability and circular economic literature.

**Keywords**—Small and medium-sized enterprises (SMEs), sustainability practices, supply chains (SC), sustainable supply chain management (SSCM), corporate sustainability, oil and gas, business performance.



# Simultaneous improved Performance in the Time Domain and in the Frequency Domain

Bensoussan David, Azeddine Ghodbane, Hammami Maher

**Abstract**— The paper addresses the problem of controller Design taking into account frequency design parameters (gain margin, phase margin, bandwidth, maximum compensator gain, maximum input plant, sensitivity bounds and tracking.) as well as time performances (minimum overshoot, smaller settling time and static error) [1]. This can be achieved by using quasi linear control [2] where gain and poles are interrelated. The algorithm has been experimented on the control of a levitation system [3], and a drone. Simulations have also shown improved performance of a satellite dish controller, and arm of a hard disk as well on a MIMO system described by its frequency response.

**Keywords**— LTI control, High gain feedback, Time and frequency performance, sensitivity design.

# Improved Simultaneous Performance in the Time Domain and in the Frequency Domain

Azeddine Ghodbane, David Bensoussan and Maher Hammami  
École de technologie supérieure, University of Quebec, Montreal, Canada

**Abstract**— An innovative approach for controlling unstable and invertible systems has demonstrated superior performance compared to conventional controllers. It has been successfully applied to a levitation system and drone control. Simulations have yielded satisfactory performances when applied to a satellite antenna controller. This design method, based on sensitivity analysis, has also been extended to handle multivariable unstable and invertible systems that exhibit dominant diagonal characteristics at high frequencies, enabling decentralized control.

Furthermore, this control method has been expanded to the realm of adaptive control. In this study, we introduce an alternative adaptive architecture that enhances both time and frequency performance, helpfully mitigating the effects of disturbances from the input plant and external disturbances affecting the output. To facilitate superior performance in both the time and frequency domains, we have developed a user-friendly interactive design methods using the GeoGebra platform.

**Keywords**— Control theory, decentralized control, sensitivity theory, input-output stability theory, robust multivariable feedback control design.

## I. INTRODUCTION

THE principle of quasi linear control was presented in the context of sensitivity minimization [1]. In a quasi linear controller, the gain and the poles of the compensator are interrelated. The principle can be illustrated by a Nichols chart: when the gain is increased, the pole is also increased in such a way that the critical point (0 dB, 180°) is avoided. Doing so, stability with an acceptable gain margin is maintained. The advantages of high gain feedback are improved sensitivity and improved tracking.

The design of the quasi linear controller has been formalized for the case of a second order system [2] allowing arbitrarily fast and robust tracking by feedback. The result has been extended to a transfer function of any order [3]. However, implementation of a quasi linear controller has shown that it applies perfectly only when the gain is increased unboundedly.

To remedy to this problem the B control method [4,5], has been proposed. The gain to pole dependency is calibrated differently. It has been shown that for the same gain, B control offers better settling times while keeping the system stable. It has been tested for the control of the arm of a hard disk [6], the orientation of a satellite antenna [7], a levitation system [8] and the control of a drone [9,10]. Simulations have also shown that integrating a B controller to a L1 adaptive controller results in a better settling time, as well as an improved attenuation of the

effects of plant input and plant output perturbations on the feedback system output [11].

Moreover, it has been shown that B control can be extended to multivariable unstable and invertible system and ensures decentralized control [12].

## II. HEURISTIC PRESENTATION OF THE SISO B CONTROLLER

The B compensator structure [1] is represented in Fig. 1.

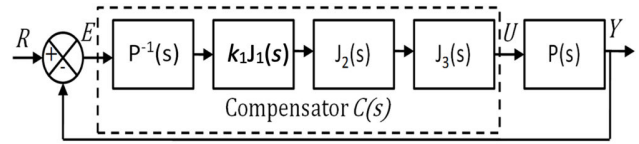


Fig. 1. Structure of the compensator  $C(s)$ .

Note that the closed loop transmission  $T(s)$  and the sensitivity  $S(s)$  are related to the output, the input and the error signal as follows:

$$Y(s) = T(s)R(s), \text{ with } T(s) = P(s)C(s)(1 + P(s)C(s))^{-1} \quad (1)$$

$$E(s) = S(s)R(s), \text{ with } S(s) = (1 + P(s)C(s))^{-1} \quad (2)$$

$$T(s) + S(s) = 1 \quad (3)$$

We will present the case where the plant  $P(s)$  is minimum phase, i.e. it is stable and invertible [13] and has the attenuation property, i.e. there exist constants  $c$  and  $q$  at a frequency high enough such that

$$|P(j\omega)| > \frac{c}{|s|^q}, \text{ for all } |s| > \omega_0 \quad (4)$$

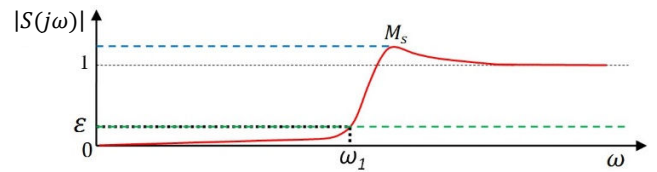


Fig. 2. Modulus of the sensitivity in the SISO case.

The design of the series compensator aims at having sensitivity on a limited frequency range  $\omega_1$  smaller than any positive constant  $\epsilon$  and the sensitivity norm is less than any constant  $M_s$  greater than unity (Fig. 2).

$$\|(1 + PC)^{-1}\|_{\infty} < M_s, \quad M_s > 1 \quad (5)$$

$$\|(1 + PC)^{-1}\|_{\omega_1} < \epsilon, \quad 0 < \epsilon < 1 \quad (6)$$

$$C(s) = P^{-1}(s)J_1(s)J_3(s) = P^{-1}(s)\left(\frac{k_1}{s+\omega_1}\right)\left(\frac{\omega_2}{s+\omega_2}\right)^k \quad (7)$$

$k, k_1, \omega_1$  and  $\omega_2$  are chosen according to the following criteria. for  $J_2(s) = 1$ , keeping in mind that the addition of phase circuits in the mid frequencies allows to better tune the time response.

$$k \geq n \quad (8)$$

$$k_1 \geq \max \left[ 2^{(k+1)/2} \omega_1 \left( \frac{1+\varepsilon}{\varepsilon} \right), \omega_1 \left( \frac{M_s-1}{M_s} \right) \right] \quad (9)$$

$$\omega_b > \omega_1 \left[ \frac{k_1^2}{\omega_1^2 \left( 1 - \frac{1}{M_s} \right)} - 1 \right]^{1/2} \quad (10)$$

$$k \tan^{-1} \left( \frac{\omega_b}{\omega_2} \right) + \tan^{-1} \left( \frac{\omega_b}{\omega_1} \right) < \frac{\pi}{2} \quad (11)$$

$$\omega_2 > \max(\omega_b, s_0) \quad (12)$$

### III. THE QUASI LINEAR CONTROLLER

Given the plant represented by rational functions of the complex variable  $s$  with the form  $P(s) = \frac{N_P(s)}{D_P(s)}$  and a compensator represented by  $C(s) = k \frac{N_C(s)}{D_C(s)}$ , the closed loop is represented by:

$$\frac{Y(s)}{R(s)} = T(s) = k \frac{N_P(s)N_C(s)}{1 + kD_P(s)D_C(s)} \quad (13)$$

Let  $d$  represent the excess of poles over zeros of  $T(s)$  and  $f$  be a real number  $(d-1)f < 1 < df$ .

For  $k > 0$  large the closed loop transfer function is:

$$T_k(s) = T_{zk}(s)T_{dk}(s) \quad (14)$$

$$T_{zk}(s) = \frac{(s+z_1)(s+z_2)\dots(s+z_m)}{(s+\bar{z}_1)(s+\bar{z}_2)\dots(s+\bar{z}_m)}, \text{Re}[z_1] \leq \dots \leq \text{Re}[z_m] \quad (15)$$

$$T_{dk}(s) = \frac{k}{(s+\bar{p}_1)\dots(s+\bar{p}_d)}, \text{Re}[\bar{p}_1] \leq \dots \leq \text{Re}[\bar{p}_d] \quad (16)$$

It has been shown [2] that when  $k$  approaches infinity, the poles  $\bar{z}_1$  are approaching the zeros  $z_i$  so that we can concentrate on  $T_{dk}(s)$ , the poles of which take negative real values, the module of which becomes bigger as the gain increases, ensuring the stability and the fast response of the feedback system.

The compensator takes the form:

$$C_k(s) = \frac{k(s+z_1)(s+z_2)\dots(s+z_{d-1})}{(s+a_1kf)(s+a_2kf)\dots(s+a_{d-1}kf)} \quad (17)$$

Where the constants  $a_1$  is given by:

$$k^{1-(d-1)f}\bar{p}_1 = \frac{1}{a_1\dots a_{d-1}}, \bar{p}_i = a_ik^f, i > 1 \quad (18)$$

As an example, for  $P(s) = \frac{1}{s^2}$ , the linear compensator

$C(s) = \frac{k(s+1)}{(s+2)}$  is modified to become gain dependent:

$$C_k(s) = \frac{k(s+1)}{(s+2k^{0.6})}, d=2, f=0.6 \in \left(\frac{1}{2}, \frac{1}{1}\right) \quad (19)$$

Fig. 3 and Fig. 4 show how the stability the stability of the feedback system is maintained after the introduction of a quasi linear controller: as the gain increases, so does the pole  $\bar{p}_1$  so that the Nichols chart keeps a secure distance from the critical point (0 dB, 180°).

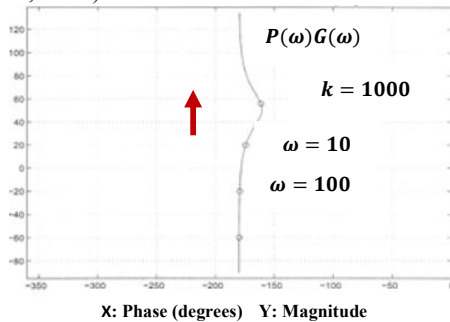


Fig. 3: Nichols chart without using the quasi linear controller [3].

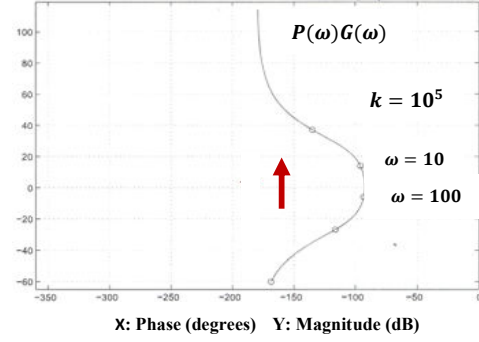


Fig. 4: Nichols chart using the quasi-linear controller [3].

### IV. THE STABLE AND INVERTIBLE CASE

We apply the B control to the design of the controller of a hard disk (Fig. 5).

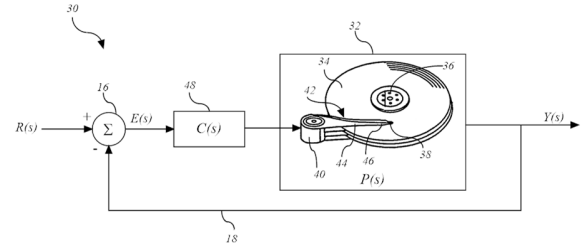


Fig. 5: B controller design of the control of the arm of a hard disk.

The arm of a hard disk model is given by [14]:

$$P(s) = \frac{6.4013 \times 10^7}{s^2} \prod_{i=1}^4 P_{r,i}(s) \quad (20)$$

with:

$$P_{r,1}(s) = \frac{0.912s^2 + 457.4s + 1.433 \times 10^8}{s^2 + 359.2s + 1.433 \times 10^8} \quad (21)$$

$$P_{r,2}(s) = \frac{0.7586s^2 + 962.2s + 2.491 \times 10^8}{s^2 + 789.1s + 2.491 \times 10^8} \quad (22)$$

$$P_{r,3}(s) = \frac{9.917 \times 10^8}{s^2 + 1575s + 9.917 \times 10^8} \quad (23)$$

$$P_{r,4}(s) = \frac{2.731 \times 10^9}{s^2 + 2613s + 2.731 \times 10^9} \quad (24)$$

$$C(s) = P^{-1}(s)J(s) \quad (25)$$

$$P(s)C(s) = J(s) = J_1(s)J_2(s)J_3(s) \quad (26)$$

$k_1J_1(s)$  is the transfer function of a high gain filter having a fast time response. For example,  $J_1(s)$  can have the following form:

$$J_1(s) = k_1 \left( \frac{\omega_1}{s + \omega_1} \right) \quad (27)$$

The  $J_2(s)$  compensator contains a set of lead/lag compensator elements operating in the intermediate frequency range. For example,  $J_2(s)$  can have the following form:

$$J_2(s) = \prod_{i=1}^n \frac{s+z_i}{s+p_i} \quad (28)$$

$J_3(s)$  is the transfer function of a low-pass filter acting at a very high frequency so as to ensure that the controller  $C(s)$  remains strictly proper. It can have the general form:

$$J_3(s) = \prod_{i=1}^k \frac{\omega_{2i}}{s + \omega_{2i}}, \quad k \geq q \quad (29)$$

Note that the choice of  $\omega_{2i}$  could be reduced in various ways to improve the implementation, such as a reduction in energy

requirements. The compensator parameters [15] are given by  $n = 2$ ,  $\omega_1 = 50$ ,  $\omega_B = 13 \times 10^4$ ,  $p_1 = p_2 = 50$ ,  $z_1 = z_2 = 33$ ,  $q = k = 6$ ,  $k_1 = 6223$ .  $\omega_{2i} = \omega_2$  is a fraction of  $\omega_b$ .

Our design leads to the following results. Fig.6 shows the temporal performances when tuning  $\omega_2$ . It allows the designer to study the effect of the increased bandwidth of the compensator.

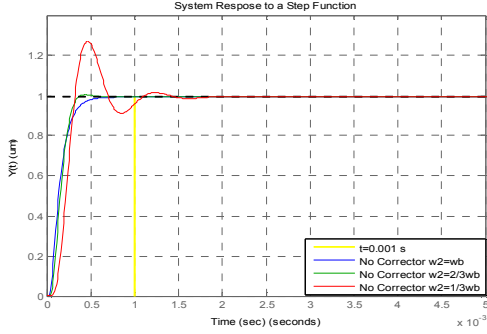


Fig. 6 Temporal response to a step input vs  $\omega_2$  [15].

Fig. 7 shows the temporal performances when tuning  $k$ .

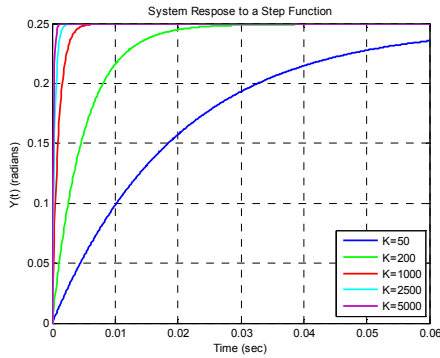


Fig. 7: Temporal response to a step input vs the exponent  $k$  [15].

Applying the quasi linear compensator to a hard disk, the settling time is greater than the one that can be obtained with B control for the same compensator gain. However, improvement of the settling time of the quasi linear compensator can be obtained with a much greater and impracticable gain.

The performances of B controller are compared to existing control methods in Table I.  $GM$  and  $PM$  represent the Gain Margin and the Phase margin,  $t_r$  and  $t_s$  are the rise time and the settling time.

TABLE I  
Control of the arm of the hard disk [6]

Type of control	$GM$ (dB)	$PM$ (°)	$t_r$ (s)	$t_s$ (s)
Proportional	11.9	12	0.0158	0.406
PID	54.1	47.8	0.0156	0.0637
State feedback	22.8	49	0.0219	0.0738
Quasi Linear	89.8	91.3	4.39	5.95
Present method	13.2	66	0.00019	0.00027

Similarly, the control for positioning satellite antennas is handled. The model of the rigid satellite antenna presented in Figure 8 and modelled by the transfer function [7]:

$$P(s) = \frac{1}{s^2 + 1.72s + 1.9} \quad (30)$$

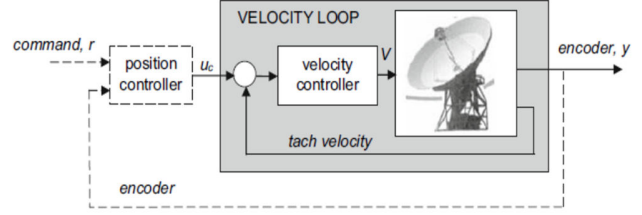


Fig. 8: Closed loop control of the orientation of a satellite [16].

To compare the B controller to the existing control methods, simulations for the velocity feedback and the position feedback are compared to those obtained by PID controllers and were published in the literature.

The PID is defined as follows [7]:

$$C_{PID}(s) = 99.6827 + 0.03 \frac{1}{s + 9.8203} - 903.9207.s \quad (31)$$

The parameters of the B controller follow:  $\omega_1 = 42$ ,  $\omega_2 = 10750$ ,  $k_1 = 37$ ,  $k = 3$ .

Fig. 9 and Fig. 10 present the improvements achieved for the step time response for the velocity feedback and the position feedback loops.

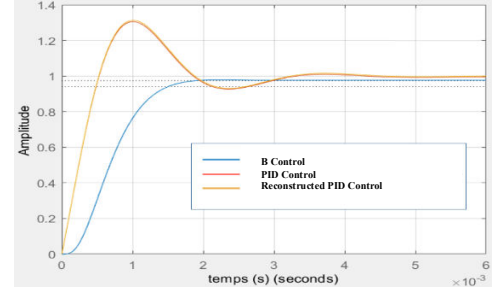


Fig. 9: PID vs B controller for closed loop velocity control [7].

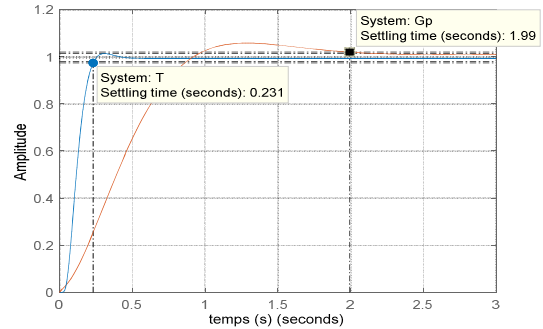


Fig. 10: PID vs B controller for closed loop position control [7].

Table II presents the time and frequency performances of these two controllers.

TABLE II  
Control of a satellite antenna [7]

Type of control	Velocity feedback		Position feedback	
	PID	B	PID	B
$PM$ (°)	46.7	70.3	147	63
$GM$ (dB)	$\infty$	14.9	$\infty$	12
$OS$ (%)	30	0.06	15.2	0.12
$t_s$ (s)	4	1.5	3.5	0.45

## V. THE UNSTABLE AND INVERTIBLE CASE

The unstable process can be decomposed into the product of its minimum-phase part  $P_1(s)$  and its unstable part  $P_2(s)$ , so that the process  $P(s)$  is represented by:

$$P(s) = P_1(s)P_2(s) \quad (32)$$

A transfer function  $H(s)$  can be defined such that, for some value  $s_0$ :

$$H(s) = \left[ \frac{c}{(s+s_0)^q} \right] P_2^{-1}(s)P(s) = \frac{c}{(s+s_0)^q} P_1(s) \quad (33)$$

So that  $H(s)$  has the same behavior as  $P(s)$  at high frequency.

$$\|P(s)H(s)^{-1} - 1\| < \alpha < 1 \quad (34)$$

Where  $\alpha$  is a value less than unity. Note that  $H(s)$  is holomorphic by its design and that its inverse is holomorphically invertible in  $\text{Re}(s) \geq 0$ . The controller  $C(s)$  is designed as follows:

$$C(s) = H^{-1}(s)J(s) = \left( \frac{1}{c} \right) (s+s_0)^q P_1^{-1}(s)J(s) \quad (35)$$

So that the loop gain is  $P(s)C(s) = P(s)H^{-1}(s)J(s)$ .

For example, we could choose:

$$J(s) = J_1(s)J_2(s)J_3(s) = \frac{k_1\omega_1}{(s+\omega_1)} \prod_{i=1}^n \frac{(s+zi)}{(s+pi)} \left[ \frac{\omega_2}{(s+\omega_2)} \right]^k \quad (36)$$

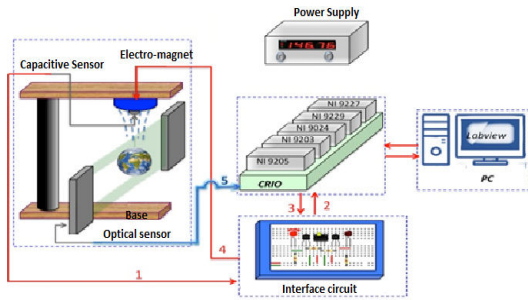


Fig. 11: Magnetic levitation system: Experimental setup.

We apply the B control design to a levitation system which is open loop unstable (Fig. 11):

$$P(s) = P_1(s)P_2(s) = \frac{-7817.5}{(s-30.51)(s+31.34)(s+184.38)} \quad (37)$$

with:

$$P_1(s) = \frac{-7817.5}{(s+31.34)(s+184.38)} \quad (38)$$

$$P_2(s) = \frac{1}{(s-30.51)} \quad (39)$$

$$P(s)C(s) = P(s)H^{-1}(s)J(s) = \frac{1}{c} (s+s_0)^q J(s)P_2(s) \quad (40)$$

which leads to

$$C(s) = \frac{-\left(5000 + 1000 \frac{(n-1)^2}{2}\right) \left(1 + \frac{s}{70}\right) \left(1 + \frac{s}{3}\right) \left(1 + \frac{s}{31.38}\right) \left(1 + \frac{s}{184.38}\right)}{\left(1 + \frac{s}{100}\right) \left(1 + \frac{s}{0.019}\right) \left(1 + \frac{s}{3000}\right)} \quad (41)$$

The index  $n$  is modified to increase the value of the gain. Fig. 12 shows the time response using B controller.

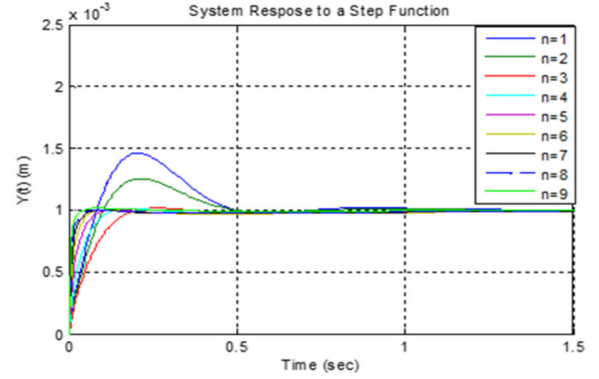


Fig. 12: Time response of B controller for different values of  $n$  [8].

Applying the proposed compensator with  $\omega_2 = 3000 \text{ rad/s}$ ,  $k = 3$ ,  $s_0 = 3$ ,  $\omega_1 = 0.019$ ,  $z_1 = 70$ ,  $p_1 = 100$  and  $K_{sc} = -6100$ :

$$C(s) = \frac{-6100 \left(1 + \frac{s}{3}\right) \left(1 + \frac{s}{70}\right) \left(1 + \frac{s}{31.3407}\right) \left(1 + \frac{s}{184.378}\right)}{\left(1 + \frac{s}{0.019}\right) \left(1 + \frac{s}{100}\right) \left(1 + \frac{s}{3000}\right)^3} \quad (42)$$

The simulation results using (42) lead to the following optimal values [8, 17]: Static gain of the compensator  $K_{sc} = 6100$ ,  $t_r = 60 \text{ ms}$ ,  $t_s = 60 \text{ ms}$ , overshoot:  $D\% = 1.25\%$ ,  $GM = 4.92 \text{ dB}$ , and  $PM = 68.6^\circ$ .

For a sampling time of  $10 \text{ ms}$ , the digital compensator  $C(z)$  is:

$$C(z) = \frac{n_4 z^4 + n_3 z^3 + n_2 z^2 + n_1 z + n_0}{z^5 + d_4 z^4 + d_3 z^3 + d_2 z^2 + d_1 z + d_0} \quad (43)$$

$$C(z) = \frac{-37.9z^4 + 46.54z^3 - 9.372z^2 - 1.159 \times 10^{-6}z - 1.25 \times 10^{-19}}{z^5 - 1.368z^4 + 0.368z^3 - 1.033 \times 10^{-13}z^2 + 9.611 \times 10^{-27}z - 3.09 \times 10^{-40}} \quad (44)$$

The performances of time response using the B controller are compared to the PID controller. These controllers have been applied to the same experimental setup. Fig. 13 and Fig. 14 illustrate this comparison.

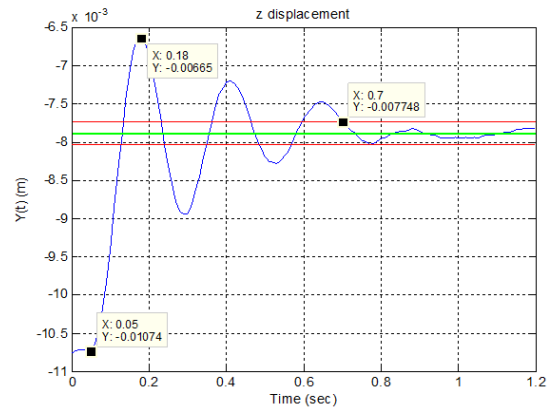


Fig. 13: PID control of a levitation system [17].

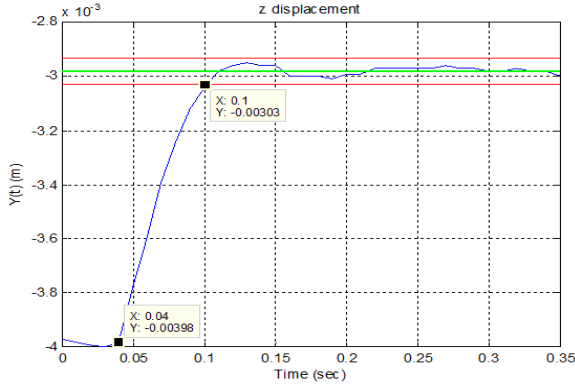
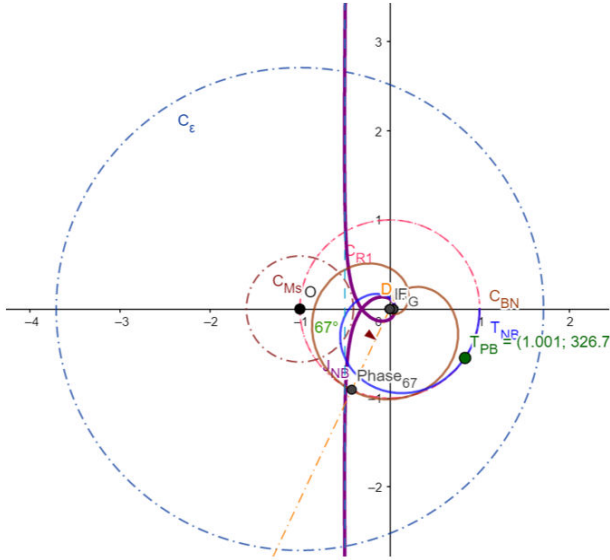


Fig. 14: B control of a levitation system [17].

Fig. 15 shows the effects of the various Nyquist diagrams plotted with GeoGebra software for:

$$J_2(s) = \frac{\left(1 + \frac{s}{z_1}\right)\left(1 + \frac{s}{z_2}\right)}{\left(1 + \frac{s}{p_1}\right)\left(1 + \frac{s}{p_2}\right)} \quad (45)$$

with:  $z_1 = 3.7, p_1 = 3.9, z_2 = 8.5, p_2 = 10.8$

Fig. 15: Nyquist diagram of  $J(s)$  [4].

In violet,  $H^{-1}(s)J(s)$ ; in blue: the normalized gain curves of the compensator  $C(s)/C_{max}$  and in brown: the modulus of the transmittance  $T(s)$ .

Similarly, B control has been successfully applied to the control of a drone.

## VI. THE L1 ADAPTIVE CONTROL CASE

The insertion of the low pass filter  $C(s)$  decouples the high frequency adaptation feedback from the feedback system loop.  $C(s)$  is usually a simple pole low pass filter. In Fig. 15,  $z$  is the output of the plant that takes into consideration the effects of input and output plant perturbation  $n$  and  $\sigma$ . The plant input  $v$  takes in consideration the plant input perturbation  $\sigma$ . The adaptation feedback gain (the MIT gain)  $\hat{\sigma} = \frac{\gamma}{s}$  amplifies the

error signal  $\tilde{x} = z - \hat{x}$ . The input of the feedback system  $r$  is multiplied by a constant gain  $k_r$ .

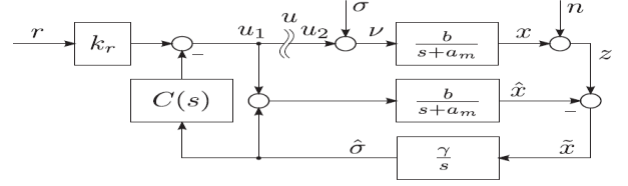


Fig. 16: Architecture L1 [18].

Application of Masson formula (Fig.16) leads to the following relations:

$$\begin{bmatrix} x \\ z \\ u \\ v \end{bmatrix} = \begin{bmatrix} H_{x\sigma}(s) & H_{x\sigma}(s) & H_{x\sigma}(s)-1 \\ H_{x\sigma}(s) & H_{x\sigma}(s) & H_{x\sigma}(s) \\ P^{-1}(s)H_{x\sigma}(s) & P^{-1}(s)H_{x\sigma}(s)-1 & P^{-1}(s)(H_{x\sigma}(s)-1) \\ P^{-1}(s)H_{x\sigma}(s) & P^{-1}(s)H_{x\sigma}(s) & P^{-1}(s)(H_{x\sigma}(s)-1) \end{bmatrix} \begin{bmatrix} r \\ \sigma \\ n \end{bmatrix} \quad (46)$$

with:

$$H_{xr}(s) = \frac{k_r(1+P_m(s)\Gamma(s))P(s)}{1+P_m(s)\Gamma(s)+C(s)\Gamma(s)(P(s)-P_m(s))} \quad (47)$$

$$H_{x\sigma}(s) = \frac{(1+\Gamma(s)P_m(s)-C(s)\Gamma(s)P_m(s))P(s)}{1+P_m(s)\Gamma(s)+C(s)\Gamma(s)(P(s)-P_m(s))} \quad (48)$$

$$H_{xn}(s) = \frac{-C(s)\Gamma(s)P(s)}{1+P_m(s)\Gamma(s)+C(s)\Gamma(s)(P(s)-P_m(s))} \quad (49)$$

For the particular case:

$$P(s) = P_m(s) = \frac{b}{s+a_m}, \quad \Gamma(s) = \frac{\gamma}{s} \quad \text{and} \quad P_1(s) = s^2 + a_ms + b\gamma,$$

we get:

$$\begin{bmatrix} x \\ z \\ u \\ v \end{bmatrix} = \begin{bmatrix} \frac{k_r b}{s+a_m} \left(1 - \frac{b\gamma C(s)}{P_1(s)}\right) P_m(s) & -\frac{b\gamma C(s)}{P_1(s)} \\ \frac{k_r b}{s+a_m} \left(1 - \frac{b\gamma C(s)}{P_1(s)}\right) P_m(s) & 1 - \frac{b\gamma C(s)}{P_1(s)} \\ k_r & -\frac{b\gamma C(s)}{P_1(s)} \\ k_r & 1 - \frac{b\gamma C(s)}{P_1(s)} \end{bmatrix} \begin{bmatrix} r \\ \sigma \\ n \end{bmatrix} \quad (50)$$

It is wise to study the stability of the loop  $L_{u_1 u_2}$  (Fig. 16).

$$L_{u_1 u_2} = \frac{u_1}{u_2} = -\frac{C(s)(1+\Gamma(s)P_m(s))^{-1}\Gamma(s)P(s)}{1-C(s)(1+\Gamma(s)P_m(s))^{-1}\Gamma(s)P_m(s)} \quad (51)$$

which leads to:

$$L_{u_1 u_2} = -\frac{\gamma b C(s)}{s(s+a_m)+b\gamma(1-C(s))} = -\frac{\gamma b C(s)}{P_1(s)-\gamma b C(s)} \quad (52)$$

One example of integration of B control and L1 adaptive control is the BL1 architecture (Fig. 17).

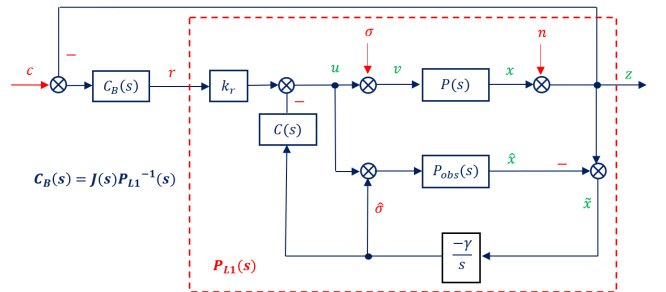


Fig. 17: BL1 architecture [11].

$C_B(s)$  is a serial B controller applied to the L1 adaptive system of Fig. 17. This scheme leads to the following relations:



$$H_{zc}(s) = \frac{P(s)C_B(s)}{1+P(s)C_B(s)+C(s)\Gamma(s)(1+\Gamma(s)P_m(s))^{-1}(P(s)-P_m(s))} \quad (53)$$

$$H_{z\sigma}(s) = \frac{1-C(s)(1+\Gamma(s)P_m(s))^{-1}\Gamma(s)P_m(s)}{1+P(s)C_B(s)+C(s)\Gamma(s)(1+\Gamma(s)P_m(s))^{-1}(P(s)-P_m(s))}P(s) \quad (54)$$

$$H_{zn}(s) = \frac{1-C(s)(1+\Gamma(s)P_m(s))^{-1}\Gamma(s)P_m(s)}{1+P(s)C_B(s)+C(s)\Gamma(s)(1+\Gamma(s)P_m(s))^{-1}(P(s)-P_m(s))} \quad (55)$$

The gang of six of the system described in Fig. 17) is:

$$\begin{bmatrix} x \\ z \\ u \\ v \end{bmatrix} = \begin{bmatrix} H_{zc}(s) & H_{z\sigma}(s) & H_{zn}(s)-1 \\ H_{zc}(s) & H_{z\sigma}(s) & H_{zn}(s) \\ P^{-1}(s)H_{zc}(s) & P^{-1}(s)H_{z\sigma}(s)-1 & P^{-1}(s)(H_{zn}(s)-1) \\ P^{-1}(s)H_{zc}(s) & P^{-1}(s)H_{z\sigma}(s) & P^{-1}(s)(H_{zn}(s)-1) \end{bmatrix} \begin{bmatrix} c \\ \sigma \\ n \end{bmatrix} \quad (56)$$

For the particular case:

$$P(s) = P_m(s) = \frac{b}{s+a_m}, \Gamma(s) = \frac{\gamma}{s} \text{ and } P_1(s) = s^2 + a_ms + b\gamma,$$

the new open loop gain is given by:

$$J(s) = H_{xr}(s)C_B(s) = \frac{k_r(1+P_m(s)\Gamma(s))P(s)}{1+P_m(s)\Gamma(s)+C(s)\Gamma(s)(P(s)-P_m(s))} = k_rP(s)C_B(s) \quad (57)$$

Simulation of the plant output versus the feedback system input  $c$ , the plant perturbation input  $\sigma$  and the plant output  $n$  respectively applied at times 0, 1 and 10 seconds. Fig. 18 shows the time response improvement of BL1 architecture over the L1 architecture.

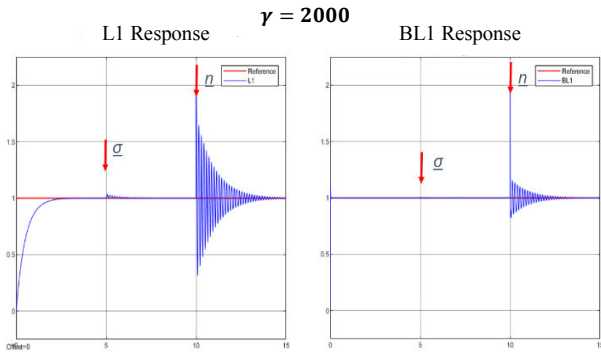


Fig. 18: The effect of plant perturbations - L1 vs BL1 [11].

## VII. CONCLUSION

B control exhibits tangible advantages for the minimum phase case such as the control of a hard disk or a satellite antenna, for the unstable and invertible SISO case exemplified by the levitation experiment, as well as the MIMO unstable (but invertible) case [12]. It can also improve the L1 adaptive control. Time response improvements were obtained while maintaining appreciable gain and phase margins.

Research on the B control method can be extended to time delay systems, internal model control, state space formulations and nonlinear systems.

## VIII. REFERENCES

- [1] Bensoussan, David. System and method for feedback control, P, US Patent 8,831,755, Deposited September 9, 2014.
- [2] Kelemen, Mattei, 2002, Arbitrarily fast and robust tracking by feedback, *International Journal of Control*, 75, 443-465
- [3] Kelemen, Bensoussan David, "On the Design, Robustness, Implementation and Use of Quasi-Linear Feedback Compensator", *International Journal of Control*, 15 avril 2004, Vol 77, No 6, pp 527-545 - 77, no. 6 (2004): 527-545

- [4] Bensoussan David, Benkhellat Lyes, Geogebra as a tool of design of ultrafast and robust controller, 2017 IEEE International Conference on Industrial Technology, Toronto, March 22-25, 2017.
- [5] Bensoussan David, Robust and Ultrafast Response Compensator for Unstable Invertible Plants, *Automatica*, Volume 60, Octobre 2015 pp. 43-47, 2015.
- [6] Bensoussan David, Sun Yulan, Hammami Maher, "Robust and ultrafast design of a control system based on optimal sensitivity and optimal complementary sensitivity", The 14th international conference on Sciences and Techniques of Automatic control & computer engineering, December 20-22, 2013, Sousse, Tunisia.
- [7] Bensoussan David, Houimdi Amine, Hammami Maher, Sun Yulan, Loo Darren, Brossard Jeremy, Demonstration of a New Control Method for Positioning Satellite Antennas, Internal Report INNOV B, École de technologie supérieure, 2020.
- [8] Sun. Yulan, Bensoussan David, Hammami M, Wang Tao., and Houimdi Amine, Robust and Ultrafast Response Compensator Applied to a Levitation System, *European Control Conference ECC15*, Linz, Austria, July 15-17, 2015.
- [9] Brossard Jeremy, Bensoussan David, Landry René, Hammami Maher, A new fast compensator design applied to a quadcopter, 2019 8th International Conference on Systems and Control, Octobre 2019, Marrakech, Maroc.
- [10] Brossard Jeremy, Bensoussan David, Landry René, Hammami Maher, Robustness Studies on Quadrotor Control, *International Conference on Unmanned Aircraft Systems, ICUAS'19*, Atlanta, GA, USA, on June 11-14 2019.
- [11] Ghodbane Azeddine, Madali Adem Soufiane, Bensoussan David, and Hammami Maher An improved L1 Adaptive controller, 2022 10th International Conference on Systems and Control (ICSC), 23-25 novembre 2022.
- [12] Bensoussan David, Brossard Jérémy, Decentralized and ultrafast control, 21st International Conference on System Theory, Control and Computing, Sinaia, Romania, October 19 – 21, 2017.
- [13] Bensoussan, D. Sensitivity reduction in single-input single-output systems, *International Journal of Control*, Vol. 39, p. 321-335, 1984. <https://doi.org/10.1080/00207178408933168>
- [14] Chen Ben M., Lee T. H., Peng K., Venkataramanan V., *Hard Disk Drive Servo Systems*, Springer, 2006.
- [15] M. Hammami, D. Bensoussan and Y. Sun, "Fine tuning the time response of a robust and ultrafast compensator," *22nd Mediterranean Conference on Control and Automation*, Palermo, Italy, 2014, pp. 1400-1405, doi: 10.1109/MED.2014.6961572.
- [16] Wodek Gawronski. "Modeling and Control of Antenna and Telescopes", Springer Science, 2008.
- [17] M.-A. Houimdi, « Ajustement d'un nouvel algorithme d'optimisation simultanée des réponses temporelles et fréquentielles », École de technologie supérieure, MSc. Thesis, 2015.
- [18] Kharisov, Evgeny et al. "Comparison of architectures and robustness of model reference adaptive controllers and L1 adaptive controllers." *International Journal of Adaptive Control and Signal Processing* 28 (2014): 633 - 663.



# Preparation of Papers - Determination of Rotational and Vibrational Temperatures of a Non-Equilibrium Nitrogen Atmospheric Pressure Plasma Torch Dedicated for Surface Treatment by Optical Emission Spectroscopy and Diatomic Molecular Spectra Simulation

V.E.Solofondrakotroka, Y.Cressault, M.Masquère, R.Rakotosaona, V.Ramarozatovo, R.Ramanantsoa

**Abstract**— Non equilibrium plasmas are widely used technologies for surface treatment. Their physical properties allow high reactivity while keeping the gas temperature low. In fact, non-equilibrium plasmas are characterized by a high electron temperature responsible for high reactivity and a low gas temperature allowing to treat temperature sensitive materials. The relatively low temperature of the gas is often not enough for dissociation reaction so molecular species from the composition of the gas prevails in the plasma. Therefore, this type of plasma can't be described by a single temperature but different translational temperatures (the electron temperature and the heavy particles temperature) and internal temperatures (electronic excitation temperature for atoms, electronic excitation temperature, vibrational temperature and rotational temperature for molecules). In order to have a better understanding of the chemical reactivity of the plasma at a molecular level, this work is interested in the determination of the vibrational temperature since the reactivity of plasma is known in the literature to be highly affected by vibrational levels and the determination of the rotational temperature which is known to be relatively close to the gas temperature. The experimental setup works at atmospheric pressure and delivers a quasi-sinusoidal discharge in the frequency range of 80 kHz to 200 kHz through a gas flow rate of 30 slm to 60 slm in order to generate a plasma plume. Optical Emission Spectroscopy is preferred as a non-intrusive method for the diagnostic of the plume. The analysis of the molecular spectra is performed using simulation

with a code developed within the research team. The code is able to simulate diatomic molecular spectra of the nitrogen compound molecules and computes the lines of each molecular band present on the experimental spectra to allow comparison by fitting one spectra on its simulation.

**Keywords**— Atmospheric plasma, non-equilibrium, optical emission spectroscopy, rotational temperature, spectra simulation, vibrational temperature.

V.E.Solofondrakotroka is with the LAPLACE Laboratory, PhD Candidate at Paul Sabatier University, Toulouse, 31400 France and the ESPA, Antananarivo University, 101 Madagascar (e-mail: eric.solofondrakotroka@laplace.univ-tlse.fr).

Y.Cressault is with the LAPLACE Laboratory and Professor lecturer at Paul Sabatier University, Toulouse, 31400 France (e-mail: yann.cressault@laplace.univ-tlse.fr).

M.Masquère is with the LAPLACE Laboratory and Senior lecturer at Paul Sabatier University, Toulouse, 31400 France (e-mail: masquere@laplace.univ-tlse.fr).

R.Rakotosaona is the Director of the ESPA and Professor at Antananarivo University, 101 Madagascar (e-mail: rijalalaina.rakoto@gmail.com).

V.Ramarozatovo is with the Department of Electrical Engineering, ESPA and Senior lecturer at Antananarivo University, 101 Madagascar (e-mail: vonjy.ramarozatovo@polytechnique.mg).

R.Ramanantsoa is with the Department of Physics and Senior lecturer at Antananarivo University, 101 Madagascar (e-mail: ramravo@yahoo.fr).

# LTE Modelling of a DC Arc Ignition on Cold Electrodes

O. Ojeda Mena, Y. Cressault, P. Teulet, JP. Gonnet, DFN. Santos, MD. Cunha, MS. Benilov.

**Abstract**— The assumption of plasma in local thermal equilibrium (LTE) is commonly used to perform electric arc simulations for industrial applications. This assumption allows to model the arc using a set of magneto-hydrromagnetic equations that can be solved with a computational fluid dynamic code. However, the LTE description is only valid in the arc column, whereas in the regions close to the electrodes the plasma deviates from the LTE state. The importance of these near-electrode regions is non-trivial since they define the energy and current transfer between the arc and the electrodes. Therefore, any accurate modelling of the arc must include a good description of the arc-electrode phenomena.

**Keywords**—Arc-electrode interaction, thermal plasmas, electric arc simulation, cold electrodes.

Due to the modelling complexity and computational cost of solving the near-electrode layers, a simplified description of the arc-electrode interaction was developed in a previous work to study a steady high-pressure arc discharge, where the near-electrode regions are introduced at the interface between arc and electrode as boundary conditions. The present work proposes a similar approach to simulate the arc ignition in a free-burning arc configuration following an LTE description of the plasma. To obtain the transient evolution of the arc characteristics, appropriate boundary conditions for both the near-cathode and the near-anode regions are used based on recent publications. The arc-cathode interaction is modeled using a non-linear surface heating approach considering the secondary electron emission. On the other hand, the interaction between the arc and the anode is taken into account by means of the heating voltage approach.

From the numerical modelling, three main stages can be identified during the arc ignition. Initially, a glow discharge is observed, where the cold non-thermionic cathode is uniformly heated at its surface and the near-cathode voltage drop is in the order of a few hundred volts. Next, a spot with high temperature is formed at the cathode tip followed by a sudden decrease of the near-cathode voltage drop, marking the glow-to-arc discharge transition. During this stage, the LTE plasma also presents an important increase of the temperature in the region adjacent to the hot spot. Finally, the near-cathode voltage drop stabilizes at a few volts and both the electrode and plasma temperatures reach the steady solution. The results after some seconds are similar to those presented for thermionic cathodes.

O. Ojeda Mena is with the LAPLACE laboratory, Toulouse, 31077 France.  
(e-mail: ojedomena@laplace.univ-tlse.fr).

Y. Cressault is the LAPLACE laboratory, Toulouse, 31077 France.

P. Teulet is with the LAPLACE laboratory, Toulouse, 31077 France.

JP. Gonnet is with Schneider Electric, Eybens 38320 France.

DFN. Santos is with the Departamento de Física, Universidade da Madeira, Largo do Município, 9000 Funchal, Portugal.

MD. Cunha is with the Departamento de Física, Universidade da Madeira, Largo do Município, 9000 Funchal, Portugal.

MS. Benilov is with the Departamento de Física, Universidade da Madeira, Largo do Município, 9000 Funchal, Portugal.

# Thermal & Dielectric Breakdown Criterium for Low Voltage Switching Devices

T.Merciris, M. Masquere, Y. Cressault, P. Petit

**Abstract**— The goal of an alternative current (AC) switching device is to allow the arc (created during the opening phase of the contacts) to extinguish at the current zero. The plasma temperature rate of cooling down, the electrical characteristic of the arc (current – voltage) and the rise rate of the Transient Recovery Voltage (TRV) are critical parameters which influence the performance of a switching device.

To simulate the thermal extinction of the arc and to obtain qualitative data on the processes responsible of this phenomenon, a 1D MHD fluid model in the air was developed and coupled to an external electric circuit.

After thermal extinction, the dielectric strength of the hot air ( $< 4\text{kK}$ ) was then estimated by the Bolsig+ software and the critical electric fields method with the temperature obtained by the MHD simulation. The influence of copper Cu and silver Ag vapors was investigated on the thermal and dielectric part of the simulation with various current form (100A to 1kA).

Finally, those values of dielectric strength have been compared to the experimental values obtained in the case of two separating silver contacts. The preliminary results seem to indicate the dielectric strength after multiples hundreds of microseconds is the same order of magnitude as experimentally found.

**Keywords**— MHD simulation, dielectric recovery, Bolsig+, silver vapors, copper vapors, breakers, electric arc

T. Merciris is with Schneider Electric, Eybens, France (e-mail: [thomas.merciris@se.com](mailto:thomas.merciris@se.com)).

M. Masquere is with the LAPLACE, University of Toulouse, Toulouse, 31000 France. (e-mail: [masquere@laplace.univ-tlse.fr](mailto:masquere@laplace.univ-tlse.fr)).

Y. Cressault is with the LAPLACE, University of Toulouse, Toulouse, 31000 France. (e-mail: [cressault@laplace.univ-tlse.fr](mailto:cressault@laplace.univ-tlse.fr)).

P. Petit is with Schneider Electric, Eybens, France (e-mail: [pascale.petit@se.com](mailto:pascale.petit@se.com)).

# A new Lemma of the Optical Equivalence Theorem: Analytical Statement, Applications and Comparisons

Orchidea Maria Lecian

**Abstract**— A new lemma of the Optical Equivalence Theorem is stated: the new definitions of operators, of density matrix and of states are provided with. Applications are calculated within the framework of opto-mechanical systems, spectroscopy, interferometry, metrology, Markov processes, jump processes between states, protein folding, metrologies, noises. Implementations are given of non-Hermitian systems, of which alternative investigation guidelines with respect to the Quantum Fisher Information (QFI) techniques follow.

**Keywords**— optics, opto-mechanical systems, spectroscopy, interferometry, metrology, non-Hermitian systems, Quantum Fisher Information.

# Assessing the Physical Conditions of Motorcycle Taxi Stands and Comfort Conditions of the Drivers in the Central Business District of Bangkok

Nissa Phloimontri

**Abstract**—This research explores the current physical conditions of motorcycle taxi stands located near the BTS stations in the central business district (CBD) and the comfort conditions of motorcycle taxi drivers. The criteria set up for physical stand survey and assessment are the integration of multimodal access design guidelines. After the survey, stands that share similar characteristics are classified into a series of typologies. Based on the environmental comfort model, questionnaires and in-depth interviews are conducted to evaluate the comfort levels of drivers including physical, functional, and psychological comfort. The results indicate that there are a number of motorcycle taxi stands that are not up to standard and are not conducive to the work-related activities of drivers. The study concludes by recommending public policy for integrated paratransit stops that support the multimodal transportation and seamless mobility concepts within the specific context of Bangkok as well as promote the quality of work life of motorcycle taxi drivers.

**Keywords**—Motorcycle taxi, paratransit stops, environmental comfort, quality of work life

## I. INTRODUCTION

IN recent years, Bangkok has developed the Bangkok Mass Transit System (BTS) covering most of area in the inner Bangkok along trunk roads. Motorcycle taxis have gained popularity among commuters, particularly in the core central business district (CBD), where there is a significant demand for feeder modes to serve the first and last-mile from the rail transit station to the workplace. This demand is evident through the presence of motorcycle taxi stands, known as "Sùm-win" in Thai, which are located and operated near BTS stations. However, unlike other transit stops, these stands are established without standardized design, regulatory control, and responsible agency causing not only spatial conflicts with other public transit passengers and pedestrians but also unsupportive working conditions to drivers who regularly wait for customers and take a rest at the stands.

Existing research on Bangkok's motorcycle taxis primarily focuses on their economic aspects and social contributions. Ratanawaraha and Chalermpong examine the market of Bangkok motorcycle taxi services, investigating economic rent, rent-seeking activities, and their influence on fares [1]. Kulpanich analyzes locational and management factors affecting fares charged by motorcycle taxis along the BTS route [2]. Sirijintana Sirijintana explores the role of motorcycle taxis

as contributors to neighborhood surveillance, referred to as "eyes on the street," with implications for crime prevention [3]. Pannoi studies the potential of motorcycle taxi drivers in being community reporters, facilitating public space improvement in Bangkok [4]. Ibrahim and Amiel describe how waiting together within the motorcycle taxi stand fosters solidarity, social bond, and collective practices among drivers which generate social security and welfare [5].

Scholars have also examined the quality of work life for motorcycle taxi drivers, considering aspects such as health and work behavior. De Conto, Gerges, and Gonçalves focus on the hearing characteristics and noise exposure risk for motorcycle taxi drivers in a Brazilian city [6]. Chuenban Chuenban, Visutsiri, and Banhansupawa explore health behavior factors among motorcycle taxi drivers in a district of Bangkok [7]. Arphorn, Ishimaru, Hara, and Mahasandana investigate the association between PM10 exposure and lung function decline among motorcycle taxi drivers in Bangkok [8]. However, no research has specifically studied motorcycle taxi stands as transit stops or workspaces for drivers, nor the effects of these stands on drivers.

This paper aims to explore the current physical conditions and characteristics of motorcycle taxi stands located near BTS stations in Bangkok's CBD, as well as the comfort conditions experienced by drivers. The study begins by presenting the concepts of multimodal transportation and seamless mobility, along with relevant standards and design guidelines for transit stops that support these concepts. The following section provides an overview of motorcycle taxi services and the establishment of motorcycle taxi stands in Bangkok. Subsequently, the methodologies employed for data collection and analysis are presented, followed by survey and assessment results linking driver comfort to stand characteristics. Finally, the paper concludes with policy recommendations based on the research findings.

## II. THE CONCEPTS OF MULTIMODAL TRANSPORTATION AND SEAMLESS MOBILITY

Multimodal transport involves using different modes of transportation within a transportation system to move people or goods. It encompasses various modal options, infrastructure, services, and coordination to enhance

Nissa Phloimontri is Graduate student at Chulalongkorn University, Department of Urban and Regional Planning, 254 Phayathai Road, Bangkok 10330, Thailand (phone: +66818289718; e-mail: nissa.phloi@gmail.com).

mobility, access, and safety for urban travelers. By providing connections and choices for all users, including motorists, pedestrians, cyclists, and transit riders, multimodal transport promotes public transportation usage, balanced transportation modes, and optimal network capacity [9].

Seamless mobility is a key characteristic of a multimodal transport system, ensuring smooth transfers and enhancing public transportation usage [10]. At the macro-scale, integration of various transport modes, multimodal transit nodes, and convenient payment and scheduling systems are crucial. At the micro-scale, physical conditions of transfer nodes and pathways, accessibility to each mode, and facilities within transit stations play a significant role.

There are four for assessing seamless mobility at the micro-scale: integration of transport modes within transit stations, ease and comfort of transfer pathways, minimized transit distance and time, and provision of convenient facilities. These factors contribute to a pleasant and efficient transit experience, promoting public transport usage and reducing reliance on private automobiles.

### III. DESIGN GUIDELINES FOR ON-STREET TRANSIT STOPS

Several public transport agencies have established transit stop standards and design guidelines that align with the principles of multimodal transportation and seamless mobility.

The American Public Transport Association (APTA) has developed guidelines for on-street transit stop design, aiming to enhance access to and from transit and improve the overall passenger experience [11]. These guidelines support transit agencies and communities in achieving access improvements within the multimodal transport system, leading to increased public transportation ridership, safety, pedestrian opportunities, development value, and balanced transportation modes.

The San Francisco Bay Area Rapid Transit District (BART) has released the Multimodal Access Design Guidelines (MADG) to support sustainable communities and enhance connections between people, places, and services [12]. By recognizing that all transportation users eventually become pedestrians, the MADG sets access standards to facilitate safe, comfortable, affordable, and efficient travel to and from transit stations. The MADG provides detailed design requirements and measurements for multimodal transit station components.

The Delaware Valley Regional Planning Commission (DVRPC), a designated metropolitan planning organization, has published transit planning principles and design guidelines to promote an equitable and sustainable region [13]. These guidelines, including the SEPTA bus stop design report, aim to increase mobility choices and integrate land use with various transport modes. The report provides collective guidelines for designing surface transit stops, offering guidance on stop placement, in-street design, curbside design, and stop elements. These components improve the connection between transit stops and neighborhoods, enhancing the waiting experience for passengers.

WeGo Public Transit (WeGo) has been serving the Nashville metropolitan area with public transportation services since 1973, offerings include fixed-route buses, paratransit services, and downtown circulators. WeGo has published a manual that provides guidelines for designing transit facilities and amenities, ensuring compliance with Americans with Disabilities Act (ADA) standards [14]. The manual aims to create consistent and well-designed transit facilities and can serve as a template for transportation planning in various locations. The following are selected guidelines for transit stop design as well as the various amenities incorporated to enhance comfort and efficiency for transit riders (see Table I).

TABLE I  
STANDARDS AND GUIDELINES FOR ON-STREET TRANSIT STOPS

Component	APTA	BART	DVRPC	WeGo
	<p><i>Frontage Zone:</i> The space in front of a building, not utilized by pedestrians or included in the clear zone.</p> <p><i>Pedestrian Clear Zone:</i> Pathway accommodating pedestrian activity and contextual considerations.</p> <p><i>Buffer Zone:</i> Transitional area between the clear zone and the street, including edge and street furniture.</p>	<p><i>Frontage Zone:</i> A section of the sidewalk extending from the building, including the building facade and adjacent space.</p> <p><i>Clear Path of Travel:</i> Unobstructed pathway for pedestrians, also known as accessible paths</p> <p><i>Furniture Zone:</i> Sidewalk area between the curb and clear path of travel, housing street furniture, plantings, and amenities</p>	<p><i>Loading Area:</i> A designated space for safe passenger loading</p> <p><i>Waiting Area:</i> An area adjacent to the loading area, sized to accommodate expected passenger volumes</p> <p><i>Accessible Pedestrian Path:</i> A clear path for pedestrian access to the stop areas.</p>	<p><i>Boarding Areas:</i> Designated areas allowing safe and convenient passenger ingress and egress at all vehicle doors.</p> <p><i>Accessible Routes:</i> Clearly defined paths connecting the accessible landing pad to pedestrian paths.</p> <p><i>Clear Space:</i> Adequate space around stop features such as shelters and seats to enable safe pedestrian movement.</p>
Stop location	<p><i>Far-side Stop:</i> Stops located immediately after passing through an intersection.</p> <p><i>Near-side Stop:</i> Stops situated immediately prior to an intersection.</p> <p><i>Midblock Stop:</i> Stops positioned within the block.</p>	N/A	<p><i>Far-side Stop:</i> Placement of stops after passing through the intersection.</p> <p><i>Near-side Stop:</i> Placement of stops before the intersection.</p> <p><i>Midblock Stop:</i> Stops located in the middle of a block.</p>	N/A
Stop shelter	Locate shelters at the end of the transit stop for visibility	Ensure a 5 ft (1.5 m) sidewalk clear zone around the shelter structure and	Constructed with durable materials for long-term use	Weather protection Provide a 5 ft (1.5 m) buffer behind shelters

	<p>Maintain a 2 ft (0.6 m) set back from the curb for shelter panels</p> <p>Ensure a minimum clearance of 7.5 ft (2.3 m) between roof and sidewalk surface</p> <p>Weather protection</p> <p>Emphasize visibility and sightlines in shelter design, using transparent or semi-transparent materials</p>	<p>parallel placement to the curbside</p> <p>Maintain a 6 ft (1.8 m) clear path of travel zone around the shelter structure</p> <p>Maximize canopy area while keeping the shelter structure compact to avoid hindering pedestrian traffic</p>	<p>Roofed and enclosed on two sides for weather protection</p> <p>Oriented towards pedestrian path but shielded from weather</p> <p>Use clear materials for visibility of approaching buses</p> <p>Preferred height of 8 ft (2.7 m)</p>	<p>Enhance visibility and vandal-resistance with transparent panels or steel mesh.</p> <p>Consider existing facilities for shelter location and passenger security.</p> <p>Use a two-pole support system for canopies to address site restrictions</p>
Signage	<p>Clearly indicate transit service presence and be identifiable from a distance</p> <p>Utilize standard symbols and lettering for identification, considering the overall aesthetic and surroundings</p>	<p>Coordinate signs with lighting by using low-glare materials and illuminate signs</p>	<p>Clearly marked stop with two-sided sign on its own pole</p> <p>Distinct signage ensures riders are at the correct location</p>	<p>Consistent color, style, visible and legible character size and spacing</p> <p>Vandalism prevention, easy maintenance, and replacement.</p>
Service information	<p>Contacts of transit agency</p> <p>Name or identification of stop</p> <p>Service routes or system map</p> <p>Destination of routes</p> <p>Fare information</p> <p>Schedule or frequency of service including first and last service time of the day</p>	N/A	<p>Stop identification</p> <p>Destination</p> <p>fare information</p> <p>Maps</p> <p>Local wayfinding</p> <p>Customer service contact</p> <p>Real-time information displays providing arrival times, weather, schedules, and ads</p>	<p>Stop identification</p> <p>Destination</p> <p>Bus numbers</p> <p>Schedules and timetables</p>
Seating	<p>Install benches for passenger comfort and visibility without obstructing clear zones</p>	N/A	<p>Made of durable, vandal-resistant material</p> <p>Minimum length of 6.5 ft (2 m) or three seats</p> <p>Alternative seating options like leaning rails or masonry walls can be considered</p>	<p>Place benches within shelters or near natural cover for comfort and protection</p> <p>Back-supported benches in shelters, not fixed back</p> <p>Use durable and comfortable materials to encourage use</p> <p>Consider ambient lighting for safety and visibility</p>
Lighting	<p>Install lights in shelters if sufficient street lighting is available</p>	N/A	<p>Illuminating stops enhances security and defines the waiting area, Recommended lighting levels range from 1.3 to 2.6 foot candles (13 to 26 lux)</p> <p>Utilize nearby streetlights for illumination</p> <p>LED lighting is recommended.</p>	<p>Consider context and existing lighting before adding new fixtures</p> <p>Orient light fixtures downward to reduce light pollution</p> <p>Ensure a smooth transition from darkness to light in sheltered areas</p>
Trash receptacle	<p>Secure the receptacle to the ground to prevent movement</p> <p>Maintain a minimum 3 ft (1.5 m) spacing from other street furniture</p> <p>Place the receptacle at least 2 ft (0.6 m) from the curb</p> <p>Use leak-proof materials to prevent fluid leakage</p>	N/A	<p>Install trash receptacles at high-ridership stops</p> <p>Avoid placing receptacles in loading areas, pedestrian pathways, and direct access routes between waiting and loading areas.</p>	<p>Place next to benches or shelters, anchored to prevent tipping</p> <p>Maintain clearance from driveways and neighboring land uses</p> <p>Include lids for security and containment</p> <p>Use durable materials like stainless steel or aluminum</p>
Integrated advertisement	N/A	N/A	N/A	<p>Adheres to state and local requirements</p> <p>Blends seamlessly with the surrounding environment</p> <p>Blends seamlessly with the surrounding environment</p>
Other amenities	<p>Landscaping</p> <p>Street furniture</p> <p>Kiosks</p>	<p>Wayfinding</p> <p>Benches</p> <p>Paratransit loading</p>	Public art	<p>Public art and placemaking</p> <p>Employee restrooms</p> <p>Wi-Fi</p>



#### IV. THE CONCEPT OF ENVIRONMENTAL COMFORT

The quality of work life (QWL) is part of the quality of life which is affected by the job itself and work-related experience. The idea of QWL has gradually evolved and encompassed broader aspects of working life since the early twentieth century. From the eight criteria of QWL suggested by Walton, Safe and healthy working conditions have been identified as a fundamental aspect of QWL, impacting employee well-being and productivity [15].

The growing awareness of safe and healthy workplaces is reflected in many studies on the effects of the physical environment of work on workers and key component of effective workspaces. To organize the growing knowledge in this area of study into a comprehensive framework, Vischer proposes the concept of environmental comfort [16]. Comfort arose from the awareness that people require more than a healthy and safe building in which to work; they require the environmental support for the activities they are there to perform. It is associated with the psychological aspect of users' environmental satisfaction and perception. Environmental comfort comprises three hierarchically related categories: physical, functional, and psychological comfort (see Fig. 1).

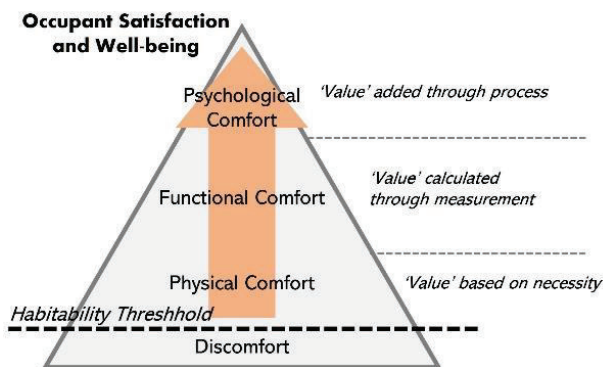


Fig. 1 Environmental comfort model

Physical comfort is at the base of environmental comfort model, establishing the habitability of a workplace. It includes safety, hygiene, and accessibility, ensuring that workers are not subjected to excessive stress caused by extreme environmental conditions. Factors such as temperature, noise, odor, and air quality are considered in creating a physically comfortable environment. If a building fails to meet physical comfort requirements, it is unlikely to be deemed acceptable in other aspects. Achieving physical comfort involves adhering to building codes, occupational safety regulations, and architectural design standards, which govern construction quality and provide essential building services such as elevators, bathrooms, parking, cleaning, and maintenance.

Functional comfort, situated at the intermediate level of the comfort model, addresses the need for workspace support to facilitate task performance. A supportive work environment allows workers to conserve energy and attention for their specific tasks, leading to improved job performance and productivity. Conversely, an unsupportive environment drains

energy and impairs concentration. Chronic environmental obstacles, such as poor lighting, uncomfortable furniture, and distracting layouts, can result in fatigue, stress, and health issues for employees. User feedback is vital in assessing functional comfort and designing more supportive workspaces, considering individual work requirements, job roles, and subjective perspectives. This feedback helps identify ergonomic elements that enhance both individual and collaborative work experiences.

Psychological comfort, situated at the summit of the comfort model, is influenced by environmental psychology and the psychosocial aspects of territoriality, privacy, and control. Territoriality involves a sense of ownership and belonging, both individually and as a group. Privacy refers to freedom from public attention or disturbance, while control relates to the ability to adjust workspace features and participate in decision-making. Increased privacy and environmental control have been associated with positive psychological effects on workers, including higher job satisfaction and creative problem-solving. Personalization of the workspace through personal objects and decorations also contributes to a sense of territoriality and belonging. Measuring psychological comfort involves assessing personalization, defining territory, satisfaction ratings, and interviews with occupants. In addition, the level of involvement in workspace design decisions can reflect one's ability to control the environment and predict the level of psychological comfort experienced.

#### V. AN OVERVIEW OF BANGKOK MOTORCYCLE TAXIS

##### A. Background of the Motorcycle Taxi Service

In the 1980s, the first Bangkok motorcycle taxi service emerged in the *Ngam Du Phli* alley. At that time, there were several high-density communities located inside the deep alleys, namely *Soi* in Thai, and lacked access to public transportation. Low-income residents helped each other by using their own motorcycles to transport neighbors. This led to the formation of a motorcycle taxi service with set fares and rules. The success of this service inspired the establishment of similar stands in other areas of Bangkok [17].

The proliferation of motorcycle taxi groups can be attributed to three factors. Firstly, Bangkok urban fabric, characterized by narrow alleys and a lack of effective urban planning, created a need for alternative transportation options. Secondly, the government's inability to provide adequate public transport services and the rise of private vehicles contributed to traffic congestion, making motorcycles a preferred mode of transport. Lastly, the growing population and demand for jobs in Bangkok led to motorcycle taxi services becoming a source of income and employment, particularly for unskilled laborers and provincial migrants. The ease of job market entry, higher wages, and self-employment opportunities were attractive factors for individuals engaging in motorcycle taxi services.

##### B. Organization of Motorcycle Taxi Services

Motorcycle taxi services in Bangkok, known as "Win," are organized and managed by members within groups. Each win operates within specific service routes and areas to avoid conflicts with other Wins.

The organizational structure typically includes Win leaders, Win committee members, and in members (operators). Win leaders are chosen by Win members and oversee various responsibilities such as obtaining permission to establish a Win, organizing the service, and representing the group in external affairs. Win committee members assist the leader in decision-making and may provide financial assistance to members. Win members are registered motorcycle taxi drivers [1].

#### *C. Establishment of Motorcycle Taxi Stands*

Motorcycle taxi stands distinguish themselves from other transit stops as drivers are required to wait at specific stands instead of picking up passengers along the service routes. Moreover, unlike other transit stops designated by government or private entities, stand locations are primarily chosen by the operators themselves. The process of establishing a motorcycle taxi stand involves several steps and interactions with government officials. To apply for certification of a new stand, representatives from the Win submit various documents to the sub-committee of the Bangkok Metropolitan Administration (BMA) district where the stand will be located. These documents include a map and photos of the stand location, consent letters from property owners, proof of land ownership, driver and vehicle information, route details, and fares. The sub-committee verifies the documents and presents them to the board for approval. Once approved, an announcement displaying the list of drivers and the detail of new stand is posted at the district office and the responsible transport office. Representatives are tasked with supervising their group, ensuring compliance with the regulations of the Department of Land Transport (DLT) and BMA. This includes the prescribed Win signage and maintaining cleanliness and orderliness at the stand [18].

## VI. METHODOLOGY

### *A. Scope of Study Area and Sampling Methods*

The scope of the study area was the core CBD of Bangkok, comprising the Ratchathewi, Pathumwan, Bang Rak, and Sathorn districts. Within this area, there were 13 BTS stations along the Silom and Sukhumvit lines, including 5 stations in Bang Rak and Sathorn districts, 5 stations in Pathumwan district, and 3 stations in Ratchathewi district.

The research targeted registered motorcycle taxi stands located within a maximum distance of 200 meters from the BTS access points (stairs, escalators, or elevators). This distance aligns with the commonly accepted walking distance for convenient pick-up points or transit stops. The number of motorcycle taxi stands varied across locations, with some stations having more than four stands nearby and others having very few. To ensure a representative sample, at least one stand was selected from each station.

Convenience sampling was employed to gather data on the comfort and opinions of motorcycle taxi drivers regarding the stands. Samples were selected based on availability and consent, without limitations on age, sex, education level, or years of experience. At least two members from each stand were chosen to represent the stand users in the survey questionnaires and in-depth interviews.

### *B. Data Collection*

Data collection for physical condition of motorcycle taxi stands involved two methods:

- 1) Spatial mapping was utilized to demonstrate the distribution of stands near each BTS station.
- 2) Observation was conducted on-site, capturing videos and photos of the characteristics and spatial relationships of each stand with its surroundings. Alongside observation, survey checklists were employed to evaluate the location, physical form, and features of the stands.

Regarding the comfort conditions of motorcycle taxi drivers, data collection encompassed three methods:

- 1) Observations were made during peak and off-peak hours to study their working behavior, space utilization, activities, and social interactions at the stands.
- 2) Surveys employed questionnaires with Likert scales, multiple-choice questions, and completion questions to gather information on stand-related details, space utilization, activities, emotions, and perspectives.
- 3) In-depth interviews were conducted, employing open-ended questions to gain insights into the establishment, improvement, current issues, opinions, suggestions, and daily experiences at the stands.

### *C. Data Processing*

The collected data on the physical conditions of motorcycle taxi stands were analyzed and categorized based on their shared characteristics and features. Subsequently, a comparison was made between the surveyed stands and the standards and guidelines for transit stops to evaluate their physical conditions.

The comfort conditions of the drivers were assessed using a descriptive approach based on the environmental comfort model. Comfort scores were calculated from a 5-point scale and subjected to analysis. T-test and Chi-square analysis were utilized to investigate significant differences among stand types and the relationship between stand characteristics and the physical and psychological comfort of the drivers.

## VII. PHYSICAL CONDITIONS OF MOTORCYCLE TAXI STANDS

### *A. General Information on Surveyed Stands*

Within the study area, there were 25 motorcycle taxi stands registered near BTS stations along the main roads. These stands consisted of 22 small groups, encompassing less than 30 drivers, and 3 medium-sized groups with 31-70 drivers. On average, each stand had 18 members. However, members of the medium-sized groups reported a lower number of regular drivers in practice than those officially registered.

Most motorcycle taxis have been operating for more than a decade, ranging from 8-10 years to 30-40 years. Newer motorcycle taxi stands strategically chose locations near BTS stations to cater to the high demand for short-distance travel.

The key tag system is widely used as the primary method for managing motorcycle taxi queues. Most stands adopt this system, while only a small number of eight stands simply implement a turnover queuing system that prioritizes riders based on their arrival order.



### B. Location

The majority of motorcycle taxi stands were strategically located in the middle of blocks near BTS stations, serving as feeder services, while far-side stands and near-side stands were least prevalent. The strategic positioning of motorcycle taxi stands on sidewalks was predominantly at the corner, which allows for convenient connections between main roads and side streets, as well as easy access for motorcycles entering and exiting. Among the stands, 64% were located at the corner of building entrances, 16% on the curbside pathway, 12% at alley entrances, and 8% at road corners.

### C. Stand Typology

All identified motorcycle taxi stands lacked fixed and permanent structures. Their form was determined by the physical surroundings, with operators utilizing the built and natural environment to define boundaries and provide shade. These stands could be categorized based on common physical characteristics, such as space utilization and the incorporation of elements that shape their form and space. The typologies include BTS-attached stands, tree-reliant stands, and canopy-based stands (see Fig. 2).

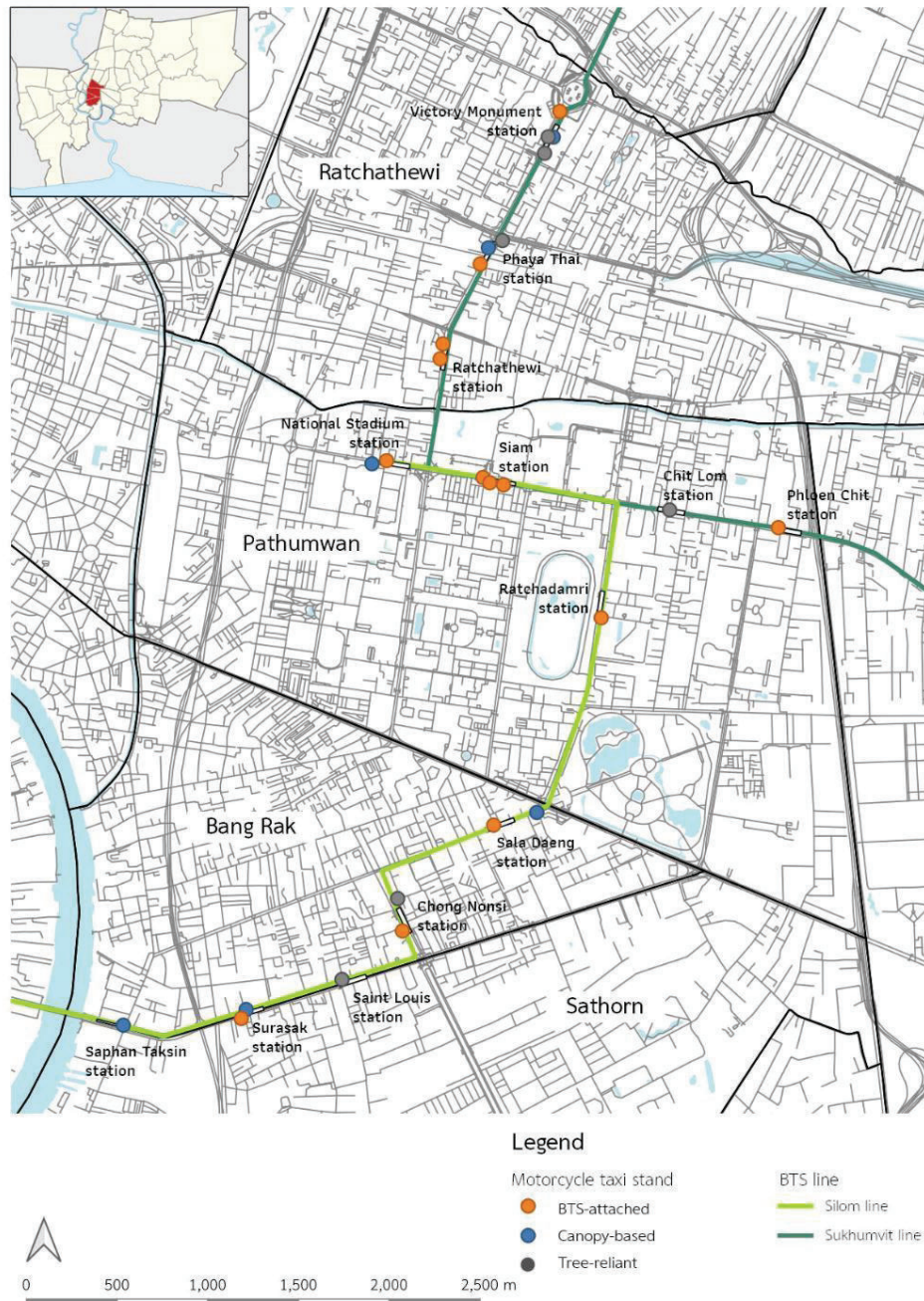


Fig. 2 Distribution of motorcycle taxi stands near BTS stations in the CBD of Bangkok by typology

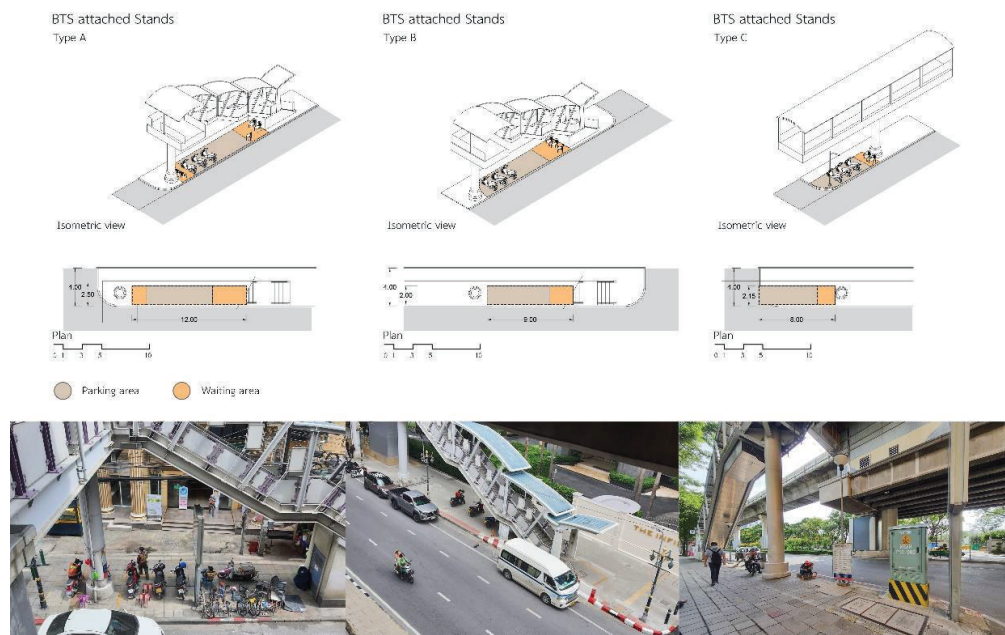


Fig. 3 BTS-attached stands

### 1) BTS-attached Stands

These stands rely on the elements of BTS structures, such as staircases, support pillars, and skywalks, to determine their location and form (see Fig. 3). They are typically found in areas with sidewalks wide enough to accommodate BTS structures. The stands have a linear layout parallel to the road, approximately 2 meters wide and 6 to 12 meters long. The space includes parking and waiting areas within the buffer zone. The drivers typically park their vehicles perpendicular to the road and enter or exit at the sidewalk corner. The waiting area is usually situated at one end of the space. The boundaries of the stand are defined by the structure's profile and the curbside edge. Some stands have yellow lines marked on the pavement by the BMA to delineate the permitted parking area. The BTS stairs provide shade and shape the overhead plane of the stand. Observations reveal various activities occurring under the stairs and around support pillars during extended waiting periods, with additional furniture and equipment serving as amenities.

The stand type can be categorized into three sub-groups: A, B, and C. Type A features convenient parking near the sidewalk corner, Type B requires motorcycles to pass through the pedestrian zone to access the road, and Type C is preferred due to unobstructed sight lines, minimizing accident risks when accessing the road.

### 2) Tree-reliant Stands

This stand typology relies on street plantings like trees or creeper pergolas for shade and stand location (see Fig. 4). These stands are positioned away from BTS structures, typically 4 m or more from the nearest tree. They are found on wider sidewalks lined with street trees. The layout follows a linear pattern parallel to the road in the buffer zone of the sidewalk, with a width of about 2 meters and a length of 6 to 12 meters.

Motorcycles are parked perpendicular to the road, sometimes in roadside or bus bay areas. Waiting areas are clustered under trees or within the shade of vegetation. Stand boundaries are defined by trees, curbs, and other street elements such as post boxes, lighting poles, and electrical cabinets.

This typology can be further categorized into three sub-groups: Type A, B, and C. Type A stands have a defined boundary, with the sidewalk's corner and a tree marking the space. Type B stands are located near the BTS stairway, expanding from the tree towards the structure. Type C stands feature a station-like waiting area with self-made benches and patio umbrellas for shade.

### 3) Canopy-based Stands

This typology of stands is characterized by their reliance on building canopies for shade and their utilization of various building components (see Fig. 5). They are typically located on sidewalks with a minimum width of 2 m and have parking spaces either in the buffer zone or on the roadside. The waiting area is in the frontage zone, where drivers often use steps, edges, or low walls as seating options. In cases where the waiting area is adjacent to a fence, drivers may move their seats closer and use it as a leaning position or for hanging belongings. However, the use of the area in front of the building for waiting depends on the owner's permission, resulting in a more flexible and ambiguous boundary compared to other stand typologies.

This group is divided into three categories: Type A has parking on the sidewalk within designated yellow lines, Type B parks on the roadside or in bus bays, and Types A and B wait under building canopies. Type C stands face restrictions from building owners, resulting in a scattered waiting area. Drivers in Type C may occasionally sit on building steps or stay on their motorcycles.



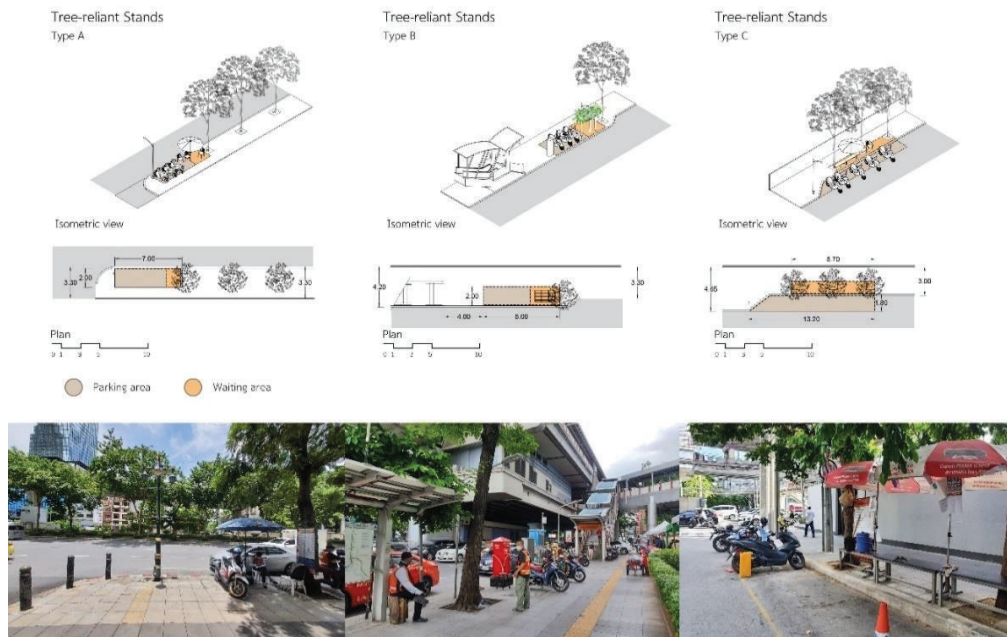


Fig. 4 Tree-reliant stands

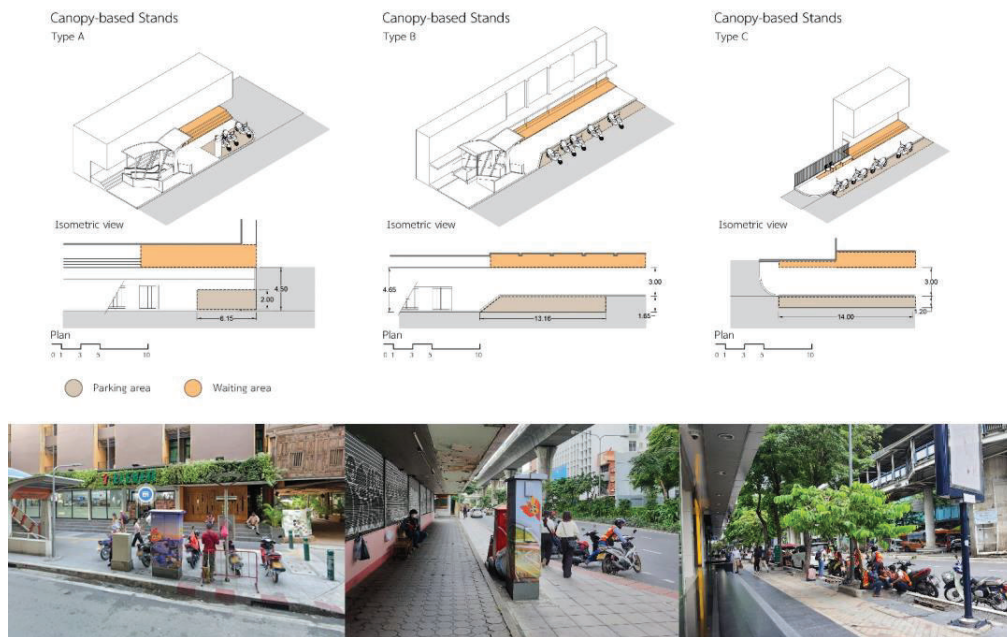


Fig. 5 Canopy-based stands

#### D.Features and Element

The majority of physical amenities and items found within the motorcycle taxi stands were supplied by the members themselves, with only a limited number of objects being obtained through donations from private companies. Various factors that influence the presence of features and elements in the stands included agreement among the group, site conditions, surrounding land use, and the permission of the BMA and the property owner. The surveyed motorcycle taxi stands exhibited the following common features and elements.

##### 1) Fare Rate Sign

All motorcycle taxi Wins displayed fare rate signs in compliance with BMA and DLT regulations. These signs followed standardized formatting guidelines specified by the DLT and were large vinyl signs measuring 1 m × 1.5 m. They included the Win name, fare rates, location, operational advice, and contact number of related agencies. Driver members printed and installed the signs themselves, often attaching them to nearby physical features like BTS pillars, fences, walls, or trees. Some groups created frames and foundations using accessible materials. While most signs were in good condition, a few showed signs of wear with faded or missing text.

### 2) Seating

Most surveyed stands had seating arrangements provided or made by driver members themselves. Plastic chairs measuring 46 cm × 51 cm × 81 cm and handmade wooden benches were commonly found. Some stands even had unique seats such as office chairs, deck chairs, foldable chairs, or sofas. The distribution of chairs varied among stand types, with BTS-attached and Tree-reliant stands having more chairs, while canopy-based stands had few or none. In some cases, drivers used public benches as alternative seating.

### 3) Lighting

The findings indicated that most stands had insufficient lighting infrastructure, relying mainly on streetlights for illumination. However, stands situated beneath BTS structures benefited from the lights installed beneath the stations, which effectively illuminate their stands. Additionally, several motorcycle taxi stands depended on lighting provided by nearby shops, buildings, and prominent landmarks.

### 4) Trash Receptacle

Most Wins had a garbage bag present in their stand areas, typically in the form of a large plastic bag. However, driver members claimed that these bags were intended solely for the shared use of their group members. In cases where stands did not have designated trash bags, drivers gathered their waste for proper disposal in nearby public trash bins or handed it over to the cleaning staff of the BTS SkyTrain or nearby shops.

### 5) Integrated Advertisement

Notably, motorcycle taxi stands exhibited a unique means to incorporate advertisements and help promote neighboring services. Various features within the stands served as a platform for print media advertising, such as the premium umbrellas with a brand logo derived from a camera company. This advertising practice was also witnessed in stands featuring fare rate signs that display beverage ads, shop flyers, or stickers with phone numbers for various services, creating a public relations area-like atmosphere. Furthermore, drivers were found to be a target group for direct product promotion, as evidenced by the provision of product samples and the presence of lucky draw boxes sponsored by beverage companies at the stands.

### 6) Other amenities and elements

The stands featured a mix of shared items and personal belongings, displaying varying quantities and types. Shared items included water cooler boxes, radio, brooms, mats, and back cushions, while personal belongings consisted of food delivery bags, water bottles, and products brought by members for selling during extended waiting periods. BTS-attached stands generally had a higher number of objects compared to other types of stands, with drivers utilizing the space under the BTS stairs for secure storage.

#### E. Comparison of Stands and Transit Stop Standards

Based on the survey results, it was evident that motorcycle taxi stands possessed unique physical characteristics and placement that deviate from the standards and design guidelines for on-street transit stops in several respects.

Table 2 summarizes the evaluation outcomes for the physical conditions of motorcycle taxi stands in comparison to the standards and guidelines for on-street transit stops.

TABLE 2  
COMPARISON OF PHYSICAL CHARACTERISTICS OF MOTORCYCLE TAXI STANDS  
AND DESIGN STANDARDS

Component	Design standards	Motorcycle taxi stand
<b>Location</b>		
Location factor	Site-specific conditions Stop spacing Passenger accessibility	Market conditions Spatial availability Passenger accessibility
Position	Varied Away from sidewalk corners	Mid-block Near sidewalk corners
Parking area	Roadside	Buffer zone/roadside
Waiting area	Buffer zone/frontage zone	Buffer zone/frontage zone
<b>Physical form</b>		
Main structure	Shelter Standardized figures	- -
Materials	Vandalism and scratch resistance Climatic durable	- -
Layout and form	Fixed Permanent Clear and noticeable	Flexible Temporary Unclear and imperceptible
Boundary determination	By shelter form Clear boundary	By surrounding physical elements Vague boundary
Primary source of shade	Shelter canopy	Surrounding physical elements
<b>Features</b>		
Signage	Durable materials Universally intelligible Standard graphic symbol	Non-durable materials Locally intelligible -
Service information	Fare information Schedule of service frequency Real-time arrival information The first and last service time Route map	Fare rates - - - -
	Contact of transit agency	Service areas and destinations Contact of related agencies
Seating	Commuter-oriented Standardized Durable materials User-friendly and comfortable	Service providers-oriented Varied Readily available materials Uncomfortable
Lighting	Sufficient lighting at stops	Neighboring streetlight
Trash receptacle	Anchored to the ground Durable materials With lids	Attached to street features Non-durable materials Without lids
Integrated advertisement	Integrated with shelter components	Integrated with various features and elements
Other amenities	Commuter-oriented Standardized amenities	Service providers-oriented Self-provided facilities

## VIII.COMFORT CONDITIONS OF THE DRIVERS

### A. Demographic and Career Information of Drivers

A total of 75 motorcycle taxi drivers from 25 surveyed stands participated in the study. All participants were male, and the majority fell within the age range of 35 to 50 years, with the oldest participant being 70 years old. Most drivers had over 10 years of experience, with some exceeding 20 years.

They worked an average of 8 to 12 hours daily, depending on individual preference, with a few working more than 12 hours. The peak hours for motorcycle taxi service were 8:00-10:00 and 16:00-19:00, with minimal waiting times of under 5 minutes (see Fig. 6). During off-peak hours, 50% of drivers waited 15-30 minutes, while 38.1% experienced waiting times exceeding 30 minutes (see Fig. 7). These findings highlight the significant time motorcycle taxi drivers dedicate to their work, both on the road and at the stands, which serve as their primary workplaces.

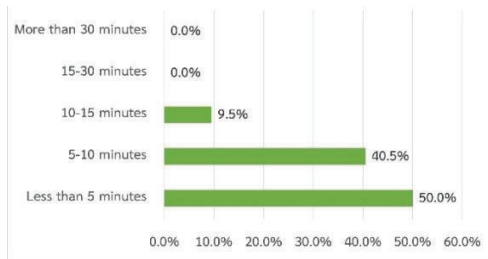


Fig. 6 Waiting periods of the drivers during peak hours

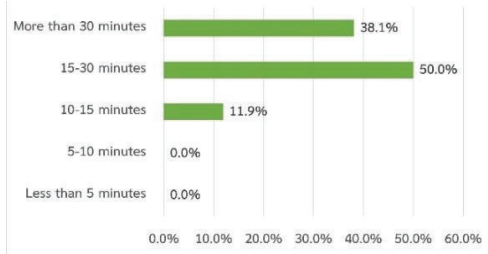


Fig. 7 Waiting periods of the drivers during off-peak hours

### B. Physical Comfort

#### 1) Safety concerns

most motorcycle taxi drivers reported rare encounters with road accidents or criminal incidents during their waiting time at the stands. While they expressed occasional feelings of unsafety due to roadside accidents and speeding vehicles, they generally felt secure from criminal acts. The presence of fellow drivers and well-lit surroundings contributed to their sense of security.

#### 2) Exposure to extreme weather conditions

Approximately 40% of the respondents faced occasional challenges with extreme weather conditions at their stands (see Fig. 8). For example, drivers at tree-reliant stands encountered difficulties during heavy rainfall, leading them to acquire parasols for additional coverage. Canopy-based stand drivers sought refuge in nearby convenience stores during rainy weather. In contrast, drivers at BTS-attached stands had fewer

climatic challenges and appreciated the protection from the sun provided by the BTS stairs. However, they recognized the inadequacy of these structures during rainstorms.

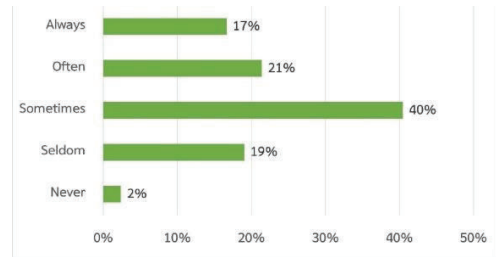


Fig. 8 Frequency of exposure to extreme weather conditions during waiting at the stands

#### 3) Hygiene practices and maintenance of stands

Most respondents reported cleaning and organizing their stands more than 5 times a month, with only a few doing so 1-2 times a month. Cleaning activities mainly involved tasks like sweeping, arranging items, and garbage disposal. The stand floors were regularly cleaned by BMA street sweepers in the mornings. However, due to constant exposure to pollution and weather, there was visible dust accumulation, stains, and signs of wear on various features and elements within the stands.

### C. Functional Comfort

#### 1) Parking issues and conflicts

Most respondents parked their motorcycles on the sidewalk perpendicular to the road, with a few opting for parallel parking on the road or perpendicular parking to the sidewalk. Many drivers faced occasional parking difficulties, primarily due to the lack of shade (30.4%), insufficient parking space (23.9%), and inconvenient parking (21.7%). Sidewalk parking presented challenges in maneuvering due to factors like the absence of ramps, obstructions from street bollards, and the distance from the stand to the sidewalk corner (see Fig. 9)

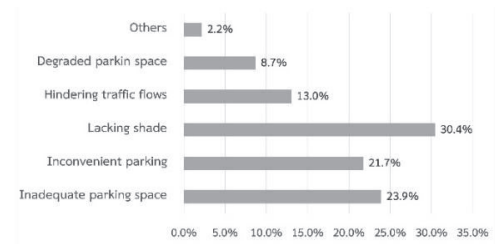


Fig. 9 The types of parking issues reported by participants

These issues occasionally led to various conflicts. One participant recounted an incident where he engaged in a dispute with staffs from a well-known Facebook page after they posted a photo of him using sandbags as ramps for designated sidewalk parking. This led to negative public reactions and subsequent reporting of the incident to the BMA. Likewise, drivers stationed at Siam BTS station encountered misunderstandings from tourists who mistakenly perceived their turning maneuvers near the sidewalk entrance as arbitrary parking. Additionally, conflicts emerged when other forms of public transport parked in close proximity to the stand area.



## 2) Activities during long waiting times at stands

During the period from noon to 15:00, motorcycle taxi drivers experienced the longest waiting times at the stands. They engaged in various activities within the limited space available, such as resting, taking short naps, socializing with fellow drivers, and using smartphones for entertainment and online activities. However, the uncomfortable chairs at the stands often caused fatigue and back pain, limiting their ability to engage in these activities for long periods. Restrictions imposed by the BMA or property owners also prevented drivers

from storing items within the stand area, further limiting their activities. As a result, drivers were seen walking around, smoking, stretching, or interacting with street vendors outside the stand area. In some cases, drivers even assisted street vendors in selling their products. Additionally, small businesses had emerged within some stands such as offering shoe repair services and selling miscellaneous items. Fig. 10 depicts the observed work behavior and activities of motorcycle taxi drivers during extended waiting periods.

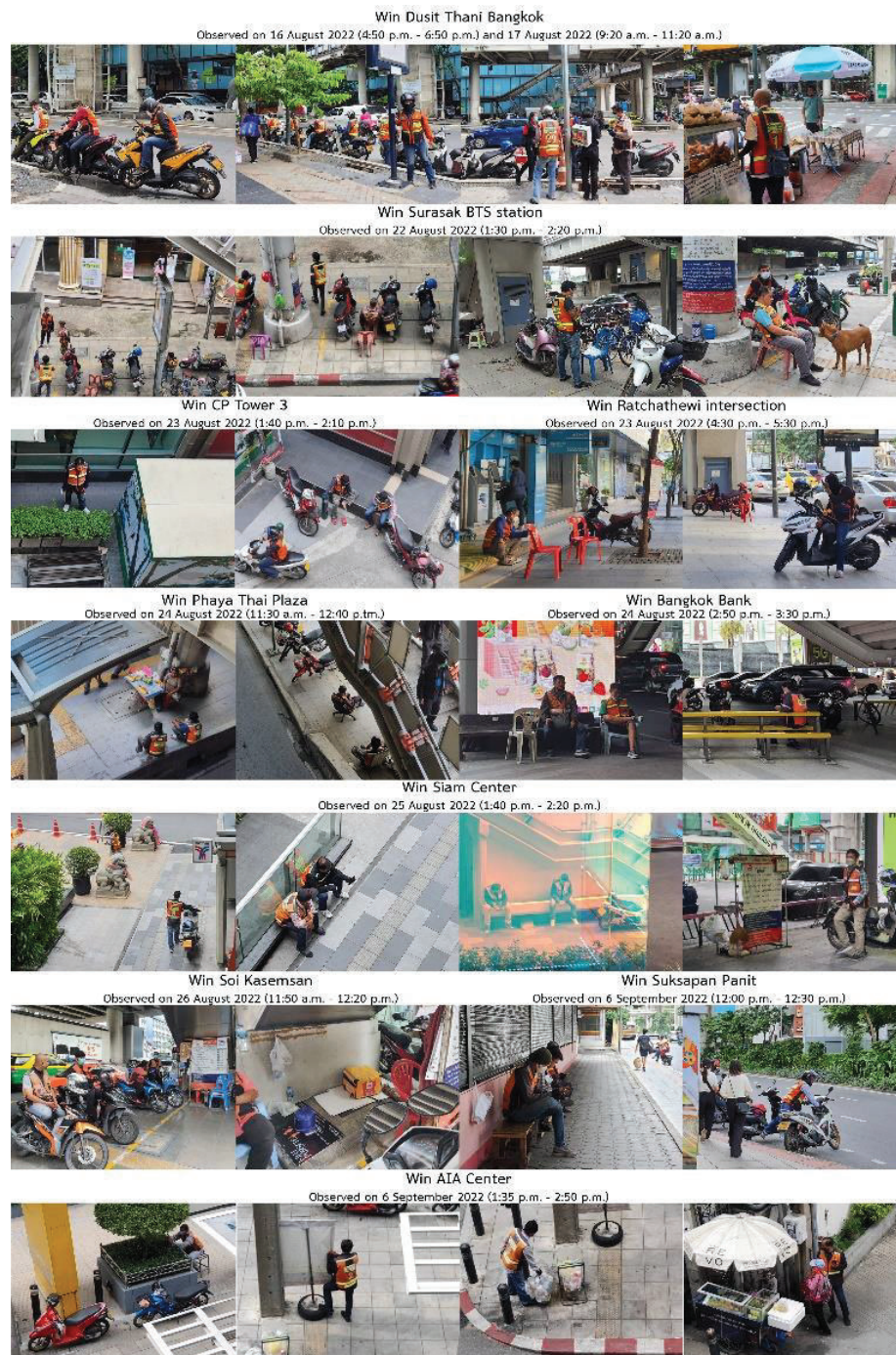


Fig. 10 Observed activities during waiting periods

### 3) Restroom usage patterns and challenges

Based on interviews, motorcycle taxi drivers primarily used gas station restrooms after dropping off passengers on their way back to the stands. Drivers near shopping malls or office buildings accessed the restrooms inside those establishments. However, some drivers faced resistance from property owners when attempting to access restrooms. A similar experience was reported by drivers at Win located in front of commercial buildings. Although one surveyed stand had a nearby public toilet, drivers mentioned the need to pay a fee to use it. As a result, some drivers had to walk or drive to a gas station located 300 meters away, causing potential loss of customers.

### 4) Food consumption patterns

A significant number of respondents reported occasionally consuming food at their motorcycle taxi stands. They typically obtained food and beverages from nearby street food vendors, shops, markets, and plazas that offered affordable options. Drivers accessed these food sources by walking, driving, or with the help of fellow members.

In stands equipped with chairs, drivers at certain locations purchased raw ingredients to prepare meals together on-site. However, for stands without seating, drivers were observed sitting on various surfaces such as BTS support pillars, building steps, or their motorcycle seats while having simple meals.

### 5) Assessment of necessary features and amenities in stands

The survey findings indicated that motorcycle taxi drivers prioritized essential job-related features at the stands, such as a canopy, trash receptacles, seating, signage, fare rate labels, and route/service information. Access to drinking water, a first aid kit, storage for helmets and vests, and food preparation facilities were also valued by some drivers. On the other hand, features like audiovisual equipment, tables and chairs, and board games received lower ratings overall (see Fig. 11).

The assessment of drivers varied based on the characteristics of their stands. Drivers stationed at stands with stable shade and seating showed a higher preference for additional amenities. For example, drivers at stands with seating under planted shade rated food preparation space and clean drinking water as essential. The evaluation of additional features was also influenced by individual preferences, experience, and subjective feelings during the questionnaire participation.

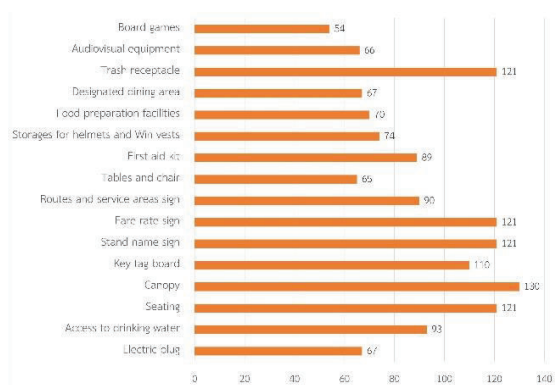


Fig. 11 Assessment of the necessity of motorcycle taxi stand amenities and features

### 6) Opinions on motorcycle taxi stand improvement

The majority of drivers generally adapted to the current state of their stands, resulting in limited feedback or ideas for improvement. However, they emphasized the importance of certain amenities such as durable canopies, ergonomic seating, and standardized stands with quality shelters and signage.

Some drivers recommended the organization and standardization of stands, while others emphasized the need for non-disruptive ramps, separate parking spaces, and dedicated trash receptacles. Additional suggestions encompassed the provision of phone charging outlets, tables and chairs, toilets, hammocks, and televisions.

#### D. Psychological Comfort

##### 1) Collective customization of motorcycle taxi stands

The survey revealed that motorcycle taxi drivers at stands typically stored minimal personal items, primarily a water bottle or flask in the under seat storage. However, stands located near BTS structures had a greater diversity and quantity of belongings compared to those with building canopies. Examples included food delivery boxes stored under the BTS stairway and helmets hung from steel stair beams.

Notably, rather than personalizing their spaces for privacy or individual territory, the drivers engaged in collective practices of space customization. They arranged shared items, decorated stand features to mark boundaries, and gathered together to protect their stand area and express a sense of territoriality.

##### 2) Territorial awareness

During interviews, motorcycle taxi drivers were asked to describe and sketch their stand territory and layout. Their descriptions varied, with many drivers using nearby buildings as reference points. Some drivers gave concise descriptions of specific elements within the stand area. It was observed that stands with unique physical features led to more precise boundary definitions. For example, at the Tree-reliant stand, drivers described their boundary as spanning from the alley corner to the tree, covering about 15 meters, and with parking designated within the BMA's yellow lines. This highlights how the presence of distinct physical elements influenced the drivers' perception of their stand boundaries.

##### 3) Involvement in the stand design and improvement

Most drivers indicated their participation in decision-making processes regarding their motorcycle taxi Wins, including stand design and management. Interviews revealed that the presence of furniture and appliances within the stands was a collective effort, with some drivers contributing financially and others being involved in their creation.

##### 4) Perception of motorcycle taxi stands

The perception of motorcycle taxi stands among drivers varied, with the majority considering them as waiting areas and workspaces. However, other definitions emerged based on individual experiences (see Fig 12). Some drivers (11%) considered the stands as spaces for social interaction with fellow members, vendors, and customers. For 10% of drivers, the stands served as outdoor dining areas. A smaller group (9%) viewed the stands as physical refuges, providing relief from the



day's driving fatigue, while a few drivers (4%) saw the stands as emotional sanctuaries. Additional perspectives included viewing the stands as affinity spaces for collaboration among drivers with shared backgrounds and as supportive spaces for financial and work-related assistance. These diverse perceptions highlight the multifaceted nature of motorcycle taxi stands and the different roles they play in the lives of drivers.

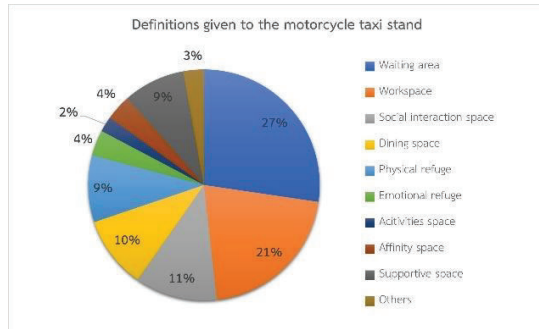


Fig. 12 Definitions of motorcycle taxi stand given by drivers

#### IX. COMPARATIVE ANALYSIS OF ENVIRONMENTAL COMFORT AMONG DIFFERENT TYPES OF STANDS

The physical comfort and psychological comfort of motorcycle taxi stands were assessed using 5-point scale questionnaires. The scores were analyzed to determine the average comfort level for each stand. Then, the average scores were compared across different stand types to identify significant differences and explore relationships between them.

##### A. Analyzing Differences in Physical and Psychological Comfort among Stand Typologies

The average physical comfort scores for each stand type are presented. The dataset includes 13 BTS-attached stands, 6 canopy-based stands, and 6 tree-reliant stands, with average scores of 54.31, 43.17, and 46.50, respectively. T-test analysis was performed with an alpha value of 0.05.

The t-test analysis results, as shown in Tables 3 and 4, indicate significant differences in average physical comfort scores between BTS-attached stands and canopy-based stands, as well as between BTS-attached stands and tree-reliant stands. However, Table 5 demonstrates no significant difference between tree-reliant stands and canopy-based stands.

TABLE 3  
T-TEST ANALYSIS OF PHYSICAL COMFORT DIFFERENCES BETWEEN BTS-ATTACHED AND CANOPY-BASED MOTORCYCLE TAXI STANDS

	BTS-attached	Canopy-based
Mean	54.30769231	43.16666667
Variance	11.56410256	64.56666667
Observations	13	6
Pooled variance	27.15309201	
Hypothesized mean difference	0	
df	17	
t Stat	4.331975872	
P(T<=t) one-tail	0.000226367	
t Critical one-tail	1.739606726	
P(T<=t) two-tail	0.000452734	
t Critical two-tail	2.109815578	

TABLE 4  
T-TEST ANALYSIS OF PHYSICAL COMFORT DIFFERENCES BETWEEN BTS-ATTACHED AND TREE-RELIANT MOTORCYCLE TAXI STANDS

	BTS-attached	Tree-reliant
Mean	54.30769231	46.5
Variance	11.56410256	81.9
Observations	13	6
Pooled variance	32.25113122	
Hypothesized mean difference	0	
df	17	
t Stat	2.785612577	
P(T<=t) one-tail	0.006341732	
t Critical one-tail	1.739606726	
P(T<=t) two-tail	0.012683463	
t Critical two-tail	2.109815578	

TABLE 5  
T-TEST ANALYSIS OF PHYSICAL COMFORT DIFFERENCES BETWEEN CANOPY-BASED AND TREE-RELIANT MOTORCYCLE TAXI STANDS

	Canopy-based	Tree-reliant
Mean	43.16666667	46.5
Variance	64.56666667	81.9
Observations	6	6
Pooled variance	73.23333333	
Hypothesized mean difference	0	
df	10	
t Stat	-0.674660015	
P(T<=t) one-tail	0.257592924	
t Critical one-tail	1.812461123	
P(T<=t) two-tail	0.515185848	
t Critical two-tail	2.228138852	

The average psychological comfort scores for motorcycle taxi stands are 52.23 for BTS-attached type, 48.17 for canopy-based type, and 47.17 for tree-reliant type. T-test analysis was conducted with an alpha value of 0.05.

The t-test analysis results in Tables 6 indicate significant differences in average psychological comfort scores between BTS-attached stands and canopy-based stands. However, Table 7 suggests only slight differences between BTS-attached stands and tree-reliant stands. Additionally, there were no significant differences observed between the canopy-based type and the tree-reliant type (see Table 8).

TABLE 6  
T-TEST ANALYSIS OF PSYCHOLOGICAL COMFORT DIFFERENCES BETWEEN BTS-ATTACHED AND CANOPY-BASED MOTORCYCLE TAXI STANDS

	BTS-attached	Canopy-based
Mean	52.23076923	47.16666667
Variance	11.35897436	89.76666667
Observations	13	6
Pooled variance	34.42006033	
Hypothesized mean difference	0	
df	17	
t Stat	1.748908869	
P(T<=t) one-tail	0.049169004	
t Critical one-tail	1.739606726	
P(T<=t) two-tail	0.098338008	
t Critical two-tail	2.109815578	

TABLE 7

T-TEST ANALYSIS OF PSYCHOLOGICAL COMFORT DIFFERENCES BETWEEN  
BTS-ATTACHED AND TREE-RELIANT MOTORCYCLE TAXI STANDS

	BTS-attached	Tree-reliant
Mean	54.30769231	46.5
Variance	11.56410256	81.9
Observations	13	6
Pooled variance	32.25113122	
Hypothesized mean difference	0	
df	17	
t Stat	2.785612577	
P(T<=t) one-tail	0.006341732	
t Critical one-tail	1.739606726	
P(T<=t) two-tail	0.012683463	
t Critical two-tail	2.109815578	

TABLE 8

T-TEST ANALYSIS OF PSYCHOLOGICAL COMFORT DIFFERENCES BETWEEN  
CANOPY-BASED AND TREE-RELIANT MOTORCYCLE TAXI STANDS

	Canopy-based	Tree-reliant
Mean	48.16666667	47.16666667
Variance	21.36666667	89.76666667
Observations	6	6
Pooled variance	55.56666667	
Hypothesized mean difference	0	
df	10	
t Stat	0.232355766	
P(T<=t) one-tail	0.410473988	
t Critical one-tail	1.812461123	
P(T<=t) two-tail	0.820947975	
t Critical two-tail	2.228138852	

### B. Analyzing the Correlation between Psychological Comfort and the Number of Objects in Stands

The study identified 18 stands with 0-5 objects and 7 stands with more than 6 objects, which included collective items and personal belongings of the drivers. The number of objects was analyzed in relation to score intervals to examine correlation between psychological comfort and the number of items present within the stands. A Chi-square test was performed with an alpha value of 0.10. The results, presented in Table 9, indicate a significant relationship between the number of objects and the level of psychological comfort among the drivers.

TABLE 9

CHI-SQUARE TEST ANALYSIS OF THE RELATIONSHIP BETWEEN  
PSYCHOLOGICAL COMFORT AND OBJECTS QUANTITY IN STANDS

Interval of psychological comfort score	Number of objects		
	0-5	More than 6	Total
30-35	1	-	1
36-40	1	-	1
41-45	3	-	3
46-50	6	-	6
51-55	7	5	12
56-60	-	2	2
Total	18	7	25
Chi-square	10.53240741		
df	5		
Alpha	0.10		
The critical value	9.236		

## X. CONCLUSION AND DISCUSSION

This study investigated the physical conditions of motorcycle taxi stands near BTS stations in the CBD of Bangkok. The stands were evaluated based on location, physical form, and features using integrated standards and design guidelines for on-street transit stops as a criteria. The concept of environment comfort was applied to assess the support these stands provide to work-related activities of motorcycle taxi drivers, including physical, functional, and psychological comfort.

Among the 25 surveyed motorcycle taxi stands, each exhibited unique characteristics but fell short of meeting the standards for public transport stops. Stand locations were primarily determined by operators, considering marketability and high ridership demand. Most stands lacked proper physical infrastructure and relied on surrounding structures and street features instead. These stands were classified into three types based on shared attributes: BTS-attached stands, Tree-reliant stands, and Canopy-based stands. It was observed that all stands lacked standardized amenities and elements, with drivers themselves providing temporary solutions to fulfill their basic needs. Consequently, the absence of standardized amenities resulted in physical and functional discomfort for the drivers.

However, the informal nature of the stands positively influenced the psychological comfort experienced by the drivers. Stands with diverse features were associated with higher psychological comfort and increased territorial awareness compared to stands without such features.

These findings hold significant implications for improving the public transit system and enhancing the work life of motorcycle taxi drivers. Firstly, it is evident that motorcycle taxis have not been adequately integrated into the government public transport planning, despite their importance in Bangkok's transportation network. One proposed solution is to integrate motorcycle taxi stands with mass transit stations and establish standardized designated locations for the stands.

The second issue relates to the lack of a designated responsible agency for stand improvements. Many drivers expressed uncertainty about whom to approach for addressing stand-related issues. One potential solution is to assign this responsibility to the BMA, which already has authority over the area and has been involved in establishing stands. The BMA could serve as the main coordinator, facilitating collaboration with various agencies and obtaining permission to use properties for stand establishment.

Another suggestion is to engage motorcycle taxi drivers in the stand design process. Since each type of stand has unique characteristics and constraints, the heads of Wins can act as representatives, collecting ideas, preferences, and concerns regarding their respective stands and conveying them to the appropriate authorities. Such initiatives have the potential to enhance the public transport system, urban space design, and the overall quality of life for drivers.

## ACKNOWLEDGMENT

The author expresses sincere gratitude to Peamsook Sanit (Ph.D), a distinguished scholar and mentor, for invaluable guidance in structuring the research framework and suggestions on data collection and analysis. Additionally, heartfelt appreciation is extended to the motorcycle taxi drivers who generously dedicated their time and cooperated in participating in the survey and interviews. Their valuable insights into the operations and work life of motorcycle taxis have significantly enriched this study.

## REFERENCES

- [1] A. Ratanawaraha, and S. Chalermpong, "Monopoly rents in motorcycle taxi services in Bangkok, Thailand," *Transportation Research Record: Journal of the Transportation Research Board*, no. 2512, pp. 66–72, Jan. 2015
- [2] N. Kupanich, "Locational and management factors that affect motorcycle taxi fares along BTS lines," Thesis, CUIR, 2013.
- [3] W. Sirijintana, "The relationship between "eyes on the street" performed by motorcycle taxi drivers and crime incidence around in location in Chatuchak district," Thesis, CUIR, 2016.
- [4] N. Punnoi, "The motorcycle taxi driver as a community reporter: guidelines for the promotion of a marginalized group's participation in the improvement of public space by using information and communication technology," *Nakhara: Journal of Environmental Design and Planning*, vol. 4, pp. 145–60, Jun. 2018.
- [5] B. Ibrahim, and A. Bize, "Waiting together: The motorcycle taxi stand as Nairobi infrastructure," *Africa Today*, vol. 65, no. 2, pp. 73-92, 2018.
- [6] J. De Conto, S. Gerges, and C. G. Gonçalves, "Hearing risk in motorcycle taxi drivers of a Southern Brazilian City," *Revista CEFAC* 20, no. 1, pp. 29–36, Feb. 2018
- [7] N. Chuenban, T. Visutsiri, and P. Banhansupawa. Rep. A study of factors relating to health behaviors of the motorcyclists in Bangkok district, Bangkok Metropolitan, 2013.
- [8] S. Arphorn, T. Ishimaru, K. Hara, and S. Mahasandana, "Considering the effects of ambient particulate matter on the lung function of motorcycle taxi drivers in Bangkok, Thailand," *Journal of the Air & Waste Management Association*, vol. 68, no. 2, pp. 139–45, Feb. 2018
- [9] "Multimodal Transportation," Tennessee State Government - TN.gov. Accessed May 25, 2023.
- [10] A. Permana, and A. Petchsathithon, "Assessing the seamlessness of Bangkok Metropolitan public transport by using modified quantitative gap analysis," *International Journal of Built Environment and Sustainability*, vol. 7, no. 1, pp. 81–97, Dec. 2019.
- [11] American Public Transport Association (APTA), *Design of On-street Transit Stops and Access from Surrounding Areas*, APTA SUDS-UD-RP-005-12, Washington, D.C.: APTA Sustainability and Urban Design Program, 2012.
- [12] San Francisco Bay Area Rapid Transit District (BART), *Multimodal Access Design Guidelines (MADG)*, San Francisco: BART, 2017
- [13] Delaware Valley Regional Planning Commission (DVRPC), *SEPTA Bus Stop Design Guidelines*, 18029, Philadelphia: DVRPC, 2019
- [14] Nashville Metropolitan Transit Authority, *Transit Design Guidelines*, WeGo Public Transit (WeGo), Nashville: WeGo, 2019
- [15] R. E. Walton, "Quality of working life: What is it?" *Sloan Management Review*, vol. 15, pp. 11–21, 1973.
- [16] J. C. Vischer, "The concept of environmental comfort in workplace performance," *Ambiente Construido*, vol. 7, no. 1, pp. 21–34, Jan. 2007.
- [17] N. Poapongsakorn, Rep. Why there are motorcycle taxi in Bangkok, TDRI White Paper. Thailand Development Research Institute, 1994.
- [18] Announcement of the Bangkok Board of Directors Regarding Determining the Location of the Motorcycle Taxi Stand and the Criteria for Issuing a Certificate for the Use of Public Motorcycles in Bangkok B.E. 2563 (2020)

# Optical Dressing of N Atoms by a Coherent Em Field

Reuben Shuker

**Abstract**— Theoretical Calculation of the Hamiltonian of N Atoms Interacting with Photons Results in Double Dressing of the Atomic Levels.

An Interesting Staircase States Emerges with Characteristic Quadratic Dependence on the Nuber of the Participating Atoms. This Indicates A Collective Quantum Optic Behavior of the Ensambe..

**Keywords**— Quantum Optics, Entanglement, Atomic States Dressing, Quantum Coherences.

# Understanding the Impact of Climate-Induced Rural-Urban Migration on the Technical Efficiency of Maize Production in Malawi

Innocent Pangapanga-Phiri, Eric Dada Mungatana

**Abstract**— This study estimates the effect of climate-induced rural-urban migrants (RUM) on maize productivity. It uses panel data gathered by the National Statistics Office and the World Bank to understand the effect of RUM on the technical efficiency of maize production in rural Malawi. The study runs the two-stage Tobit regression to isolate the real effect of rural-urban migration on the technical efficiency of maize production. The results show that RUM significantly reduces the technical efficiency of maize production. However, the interaction of RUM and climate-smart agriculture has a positive and significant influence on the technical efficiency of maize production, suggesting the need for re-investing migrants' remittances in agricultural activities.

**Keywords**— climate-smart agriculture, farm productivity, rural-urban migration, panel stochastic frontier models, two-stage Tobit regression.



# The Optimal Production of Long-Beans in the Swamp Land by Application of Rhizobium and Rice Husk Ash

Hasan Basri Jumin

Postgraduate in Agriculture, Islamic University of Riau Indonesia, email. hbjumin@agr.uir.ac.id

**Abstract**— he swamp land contains high iron, aluminum, and low pH. Calcium and magnesium in the rice husk ash can reduce plant poisoning so that plant growth increases in fertility. The first factor was the doze of rice husk, and the second factor was 0.0 g rhizobium inoculant /kg seed, 4.0 g rhizobium inoculant/kg seed, 8 g rhizobium inoculant /kg seed, and 12 g l rhizobium inoculant /kg seed. The plants were maintained under light conditions with a + 11.45 – 12.15 hour photoperiod. The combination between rhizobium inoculant and rice husk ash has been an interacting effect on the production of long bean pod fresh weight. The mean relative growth rate, net assimilation rate, and pod fresh weight are increased by a combination of husk rice ash and rhizobium inoculant. Rice husk ash affected increases the availability of nitrogen in the land, albeit in poor condition of nutrition. Rhizobium is active in creating a fixation of nitrogen in the atmosphere because rhizobium increases the abilities of intercellular and symbiotic nitrogen in the long beans. The combination of rice husk ash and rhizobium could be effected to create a thriving in the land.

**Index Terms**— aluminium, calcium, fixation, iron, nitrogen.

## I. INTRODUCTION

Swamp and marginal land are spread almost throughout the Riau region, especially in the coastal region. The swamp is characterized by soil with excess iron and aluminum, low pH, and poor fertility. Excess iron and aluminum can poison the root hair, thus eliminating the plant and low production. The ashes ash of rice chaff contain SiO<sub>2</sub> (52%), C (31%), K (0.3%), N (0.18%), Fe (0.08%), and potassium (0.14%). It also contains other nutrients such as Fe<sub>2</sub>O<sub>3</sub>, K<sub>2</sub>O, MgO, CaCo, MnO, and Cu in small amounts and some types of organic material. The ashes of rice could be substituted for the calcium or magnesium used in agriculture.

The rice husk ash contains both magnesium and magnesium Calcium and magnesium can reduce plant poisoning so that plant growth increases in fertility.

The rice husk ash in partnership with rhizobium was found to reduce the poisoning caused by an excess of aluminum and iron in the soil, resulting in poor growth and reduced production. Rice husk ash originally from the unshelled paddy separated from the stalk. After burn that waste there became ash with high contents of calcium and magnesium. Calcium and magnesium are materials to be used for increasing the pH and could suppress the iron and aluminum in the swamp land mainly in the coastal area.

Therefore, the rice husk ash is especially useful in improving soil conditions such as increasing absorbent capacity and suppressing the availability of such poisons as aluminum and iron. These favorable conditions allow rhizobium to work more efficiently to fix nitrogen. While rice husk ash increases the number of nutrients in the soil. Rice husk ash originally from the unshelled paddy separated from the stalk. After burn that waste there became ash with highcontents of calcium and magnesium. Calcium and magnesium are materials to be used for increasing the pH and could suppress the iron and aluminum in the swampland mainly in the coastal area

Calcium and magnesium are materials to be used for increasing the pH and could suppress the iron and aluminum in the swamp land mainly the coastal area. Calcium and magnesium are macro essential nutrition for plant growth. Leguminous inoculant is the powder of spore of rhizobium bacterial [7, 8].

Rhizobium has realized an ecological and evolutionary success that has composed our biosphere. Although complex, embrace a dual lifestyle of intracellular infection apart from a free-living phase in cultivated land. Rhizobium symbiosis has distributed and dispersion to hundreds of bacterial species and geographically throughout the globe [2] The dual ability of intracellular residual and symbiotic nitrogen fixation in soybean and other legumes is competent to retain rhizobium in the soil. With less nitrogen fertilizer up to 50%, the legumes are still normally grown and the seed produced is the same if the rhizobium inoculates in seeds. This paper intended to find the relationship between the rice husk ash and rhizobium inoculant on the long beans.to growth and yield.

## II. MATERIALS AND METHODS

### Study area

This research was conducted from august 2019 to december 2019. This experiment was arranged with a randomly simple design with two factors. The first factor was the doze of rice husk ash as follows 0.0 g /plot, 0.6 g/plot, 1.2 g /plot, and 1.8 g/plot. Second factor was 0.0 g rhizobium inoculant /kg seed, 4.0 g rhizobium inoculant / kg seed, 8 rhizobium inoculant /kg seed, and 12 g rhizobium inoculant /kg seed. The plants were maintained under the light condition with + 11.45 – 12.30 hours of photoperiod

### Parameters

#### Mean Relative Growth Rates (MRGR)

The accumulation of dry weight describes as the increase of cell elongation and cell number in the long beans every

day during vegetative growth. The mean relative growth rate (MRGR) can be calculated by sampling plant size for the first time on 7 days after planting ( $t_1$ ) and the second time on 14 days after planting ( $t_2$ ), 21 days after planting for the third time, and 28 days after planting for four times. The equation for calculating the MRGR [12] is as follows;

$$\text{MRGR} =$$

$$\text{MRGR} = \frac{\ln W_2 - \ln W_1}{t_2 - t_1} \quad (1)$$

Where MRGR is the mean relative growth rate;  $W_1$  and  $W_2$  are the biomass dry of long beans at the time measured, beginning ( $t_1$ ) and end ( $t_2$ ) of the sampling until 4 periods of measurement during vegetative growth. and  $\ln$  is the natural logarithm. Equation (1) is the most common formula used when comparing relative differences between rice husk ash and rhizobium inoculant treatments.

#### Net assimilation rates (NAR).

The net assimilation rate is the weight of total dry weight per unit area of leaf in a certain time.

$$E = \frac{1}{L} \frac{dW}{dt} \quad (2)$$

Leaf area was measured on a sub-sample using a leaf area meter and image analysis software. The leaf area ( $L$ ) of long beans was measured four times on days 7, 14, 21, and 28 after long beans planting. The  $W$  and  $L$  means may then be used to accumulate  $E_M$ , an estimate of the mean  $E$  for each time- interval ( $t_2 - t_1$ ), usually as proposed by [14] shown in equation 3 thus;

$$E_M = \frac{(W_2 - W_1) (\log E L_2 - \log E L_1)}{(T_2 - T_1)(L_2 - L_1)} \quad (3)$$

### III. RESULTS AND DISCUSSIONS

Net assimilation rate is meaning the buildup of the plant's dry weight of every centimeter square of any kind leaf area of any time. The treatment without rice husk ash is different from any other treatment where the lowest treatment is averaged. Rice husk ash's release of the right amount would certainly increase vegetation growth, which, in turn, would prompt generic growth in this issue to increase the net assimilation rate.

The growth rate will be comparable to the pattern followed by the net precipitous rate. In addition, the growth rate in plants is likely to indicate a similar pattern. It is just true that the large number of effective leaves carrying out photosynthesis is the dominant factor. In the mean relative growth rate count, the leaf area is not considered. If the increase in net assimilation rate is at the age of 14-21 days, it will also result in increased growth rates in the mean relative growth rate, compare (Figure 1). The trend of expansion in the net assimilation rate directly affects the rate of growth in the mean relative growth rate.

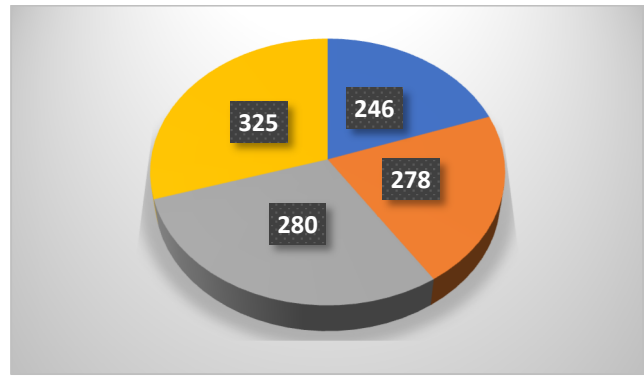


**Figure 1 A.** Net Assimilation Rate 7-14 days ( $246 \times 10^{-4}$  mg/cm<sup>2</sup>/day from treatment of 0 g rhizobium/kg seed,  $278 \times 10^{-4}$  mg/cm<sup>2</sup>/day from treatment of 4 g Rhizobium/kg seed,  $280 \times 10^{-4}$  mg/cm<sup>2</sup>/day from treatment of 8 g Rhizobium/kg seed, and  $325 \times 10^{-4}$  mg/cm<sup>2</sup>/day from treatment of 12 g Rhizobium/kg seed

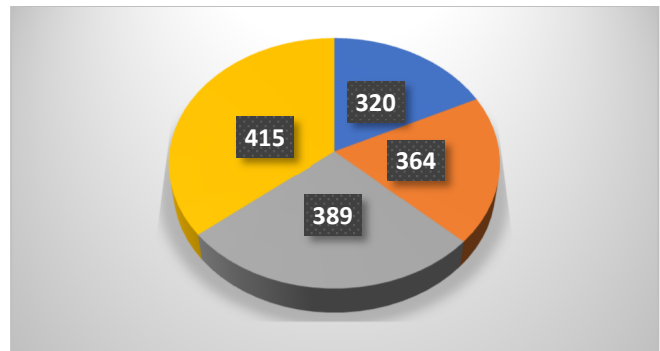
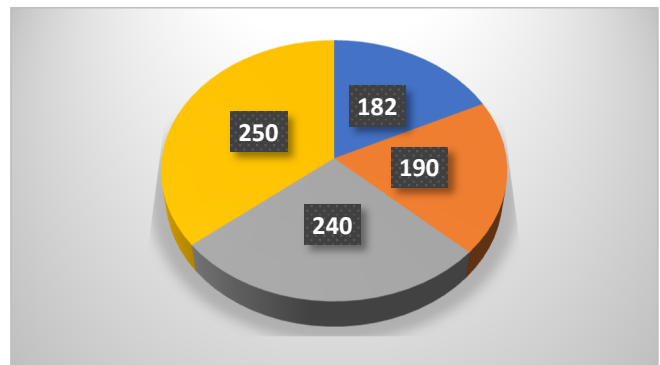


**Figure 1B.** Net assimilation rate 14-21 days ( $320 \times 10^{-4}$  mg/cm<sup>2</sup>/day from treatment of 0 g rhizobium/kg seed,  $364 \times 10^{-4}$  mg/cm<sup>2</sup>/day from treatment of 4 g Rhizobium/kg seed,  $389 \times 10^{-4}$  mg/cm<sup>2</sup>/day from treatment of 8 g Rhizobium/kg seed, and  $415 \times 10^{-4}$  mg/cm<sup>2</sup>/day from treatment of 12 g Rhizobium/kg seed



**Figures 1 C.** Net assimilation rate 21-28 days ( $182 \times 10^{-4}$  mg/cm<sup>2</sup>/day from treatment of 0 g rhizobium/kg seed,  $190 \times 10^{-4}$  mg/cm<sup>2</sup>/day from treatment of 4 g Rhizobium/kg seed,  $240 \times 10^{-4}$  mg/cm<sup>2</sup>/day from treatment of 8 g Rhizobium/kg seed, and  $250 \times 10^{-4}$  mg/cm<sup>2</sup>/day from treatment of 12 g Rhizobium/kg seed

The MRGR is used to calculate the rate of plant growth at a rapid rate in the seedbed. This is also used to make quick decisions on a large study at an equally costly cost. In this study, the above-watered pattern tends to apply completely.

Other parameters such as the number of root nodules and the weight of individual plants would also show a large number on the same treatment of rice husk ash 1.8 kg/plot. This treatment has a positive interaction with rhizobium 12 g/kg seeds. This indication is shown in (Figure 3), long beans are consumed in the young pod, fresh form, and

become the vegetable pods. To apprehend, if a treatment has a positive effect, it can have a noticeable effect on the growth of the plants or negative effects or causes the plant to fail to thrive. The resulting growth will then be seen in the generic growth of the flowers and the seedlings. Rice husk ash and rhizobium dose 1.8 kg/ plant and 12 g/kg seeds are in good condition to increase the production of most root nodules to an average of 51.00. This dose was combined with rhizobium treatment at 1.8 kg/ plant. When the rice husk ash itself the highest was only 48.83 root nodules per plant. The effect of the rhizobium alone is only 46.91 root nodules in each plant (Figure 2).

This means that the rice husk ash is interacting positively with rhizobium, bringing the number of root nodules to 51.00 for each plant. The vegetative growth of long beans was increased by the application of rhizobium under a suitable dose of rice husk ash. Rhizobium could be increased vegetative growth beginning from 4 g/kg seed to 22g/kg seed. If this amount of root nodules is high in the plant's root hair, it means that the ability of the plant to fix nitrogen in the soil's atmosphere is greater. The amount of nitrogen molecules accumulated in the root system increases after the proper doses of treatments of rice husk ash and rhizobium inoculant

Relationship between net assimilation rate and mean relative growth rate was closed and it make an illustration as linear (Figure 2), with equation as  $Y = 0,4544x + 148,75$ ,  $R^2 = 0,2717$ . This equation means that in the case of an increase in net assimilation rate has also led to improvements in mean relative growth rate (Table 1), because the accumulation of assimilation in plant tissues is banked. The building of assimilation in plant organs is due to the leaves taking place more in the photosynthesis activity.

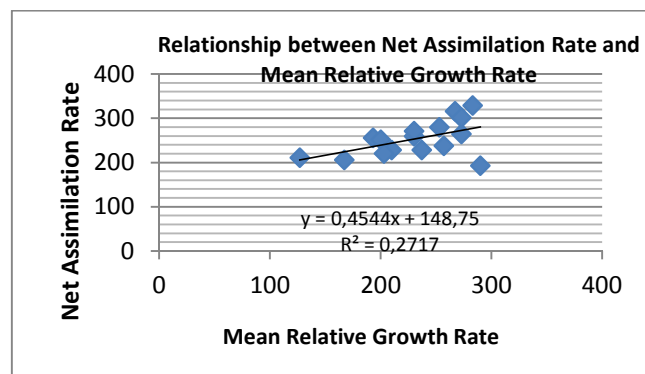


**Figure 2** Relationship between net assimilation rate and mean relative growth rate disclosed as linear pattern

The weight of the long bean pods will be affected by the effectiveness of the treatment of rising husk ash and rhizobium in combination. The combination of two treatments increases the ability of plants to produce heavier pods (Figure 3).

The large leaf area means that the leaf creates more assimilation in the plant's organ. The mean relative growth rate's relationship with the net assimilation rate is very close. Meaning that, if photosynthetic activities in the leaf are rapid, it is also due to the assimilate mound rise in a plant organ, hereafter means relative growth rate is increased.

**Table 1.** Mean relative growth rate of long beans after treated with rice husk ash and rhizobium inoculant (g/day)

Plant Age (day)	Rice husk ash g/plant	Rhizobium g/kg seed			
		4 g/kg seed	8 g/kg seed	12 g/kg seed	Average
7-14	0.299	0.379	0.413	0,476	0.392a
	0.243	0.268	0.303	0.328	0,243b
14-21	0.224	0.241	0.261	0.283	0.231c
21-28	0.254	0.296	0.326	0.362	

Mean value followed by different alphabet/s within column do not differ significantly over one other at  $P < 0.05$  lead by Duncan's Multiple Range Test

A large amount of nitrogen has a good effect on plant growth and can supply nitrogen needs to 75 percent of all plant nitrogen necessities. Thus, only 25 percent of the nitrogen fertilizer addition. Abundant aluminum and iron in the land made a toxicant, eventually, the

land was hazardous to root hair and hereafter killed the plants. This experiment suggests that both treatments have the same effect on the increased weight of the pod. The rice husk ash gives a favorable condition to root hair, while rhizobium with the persistent rooting force, rhizobium will work to improve nitrogen and efficiency.

The long beans as the legumes that grow need bacteria's help to compensate with rhizobium for their necessary for nitrogen. This nitrogen maintains organic compounds such as sucrose and glucose as abundance in the root nodules (Figure 4). , and rhizobium combined with legumes plants became to be as the host [3, 4, 10, 13].

The rhizospheric site hosts a host of organic substrates secreted by such plants' hormones, role models, and enzymes to reproduce organic compounds. The higher the number of organic matter, the microorganism population also grows. With a specific protein compound present, rhizobium infects the host plant of long beans.

This specific protein is secreted by plants as a signal known to bacteria [3, 5, 9, 13]. In turn, the bacteria secrete lipo-oligosakaride compounds or in time be called nod factors [1, 6, 11]. For a command of 147 host cell divisions. Therefore, it is suggested that symbiosis may occur because of the suitability of the respective substrates produced [5, 10, 13].

When compatibility occurs, bacteria then multiply, forming hyphae to penetrate the root. Bacteria, in turn, propagate themselves inside a root cell called a bacteroid. The infected root cell then swells, forming binders, in which the interior structure, between host cells and the bacteroid, is covered by leg-hemoglobin with a reddish-purple vision. The mechanism of plant root infections by microbes. A bacteroid would require a certain amount of energy to form reduction power (for example NADPH2 feredocrine) and ATP for Controlling the reactions. Energy is obtained from the photosynthesis of the host plant. Sucrose, glucose, and organic acids are transmitted into nodules and oxidation of these materials, further generating energy (oxidational phosphorylation) process. this respiration requires a certain amount of oxygen, which is tied by leghaemoglobin in the vicinity of the bacteroid.

The mechanism is the same Leg-haemoglobin in the blood mammals that are as oxygen carriers are needed for a respiratory process. Enzymes Nitrogenase catalyzes the reduction of the N<sub>2</sub> composed (Goodwin and Mercer, 1983). Factors that affect nitrogen mooring are the (i) supply of photosynthesis, (ii) aeration, (iii) temperature, (iv) land pH, and (v) availability of nitrogen. The final result of the nitrogen fixation by rhizobium at hair the root will disperse to a long beans plant. Thus the long beans plant will be more efficient in the use of nitrogen

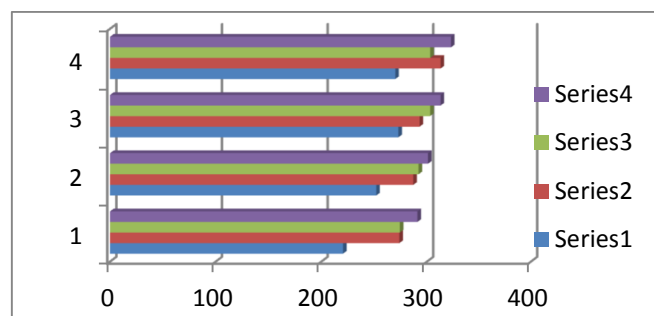


**Figure 3.** Mean dry weight of pod on the long beans after treatment with rice husk ash and rhizobium inoculant (g/plant). **Series 1** (0 g/plant of rice huk), **Series 2** (0.6 g/plant of rice huk ash), **Series 3** (1.2 g/plant of rice huk ash), **Series 4** (1.8 g/plant of rice huk ash), **1** (0 g rhizobium inoculant), **2** (4 g rhizobium inoculant), **3** (8 g rhizobium inoculant), **Series 4** (12 g rhizobium inoculant).

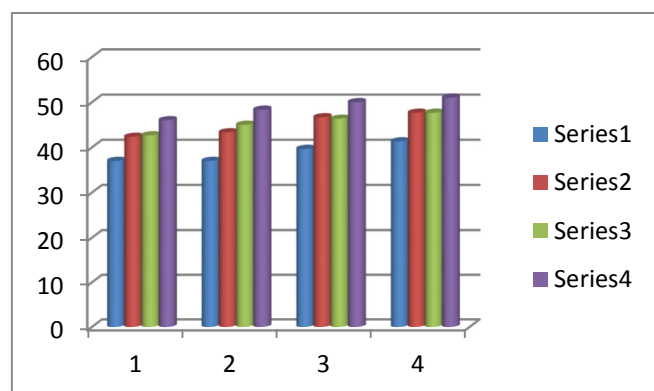


**Figure 4.** The number of root nodules of long beans on the treatment of rice husk ash and rhizobium inoculant (piece/plant). **Series 1** (0 g/plant of rice huk), **Series 2** (0.6 g/plant of rice huk ash), **Series 3** (1.2 g/plant of rice huk ash), **Series 4** (1.8 g/plant of rice huk ash), **1** (0 g rhizobium inoculant), **2** (4 g rhizobium inoculant), **3** (8 g rhizobium inoculant), **Series 4** (12 g rhizobium inoculant)

#### ACKNOWLEDGMENT

We thank to Rector Islamic University of Riau for financial support this research and publish paper. The special thank to Director of Post Graduate in Agronomy programm for assist the administrative affair

#### CONCLUSION

Rice husk ash is an alternative organic fertilizer because it has the full criterion as fertilizer. In addition, rhizobium can always together life and growth as a symbiosis with legumes to increase the nitrogen efficiencies in the long bean. The dose of rice husk ash 1.8 kg/plot and rhizobium 12 g/kg seed is the suitable amount for long beans. Rice husk ash plays not only as nourishing for the long beans but also as a

nutritional balance for the life of rhizobium to add a shortage of nitrogen to the long beans

#### REFERENCES

- [1] L. Battisti, J.C. Lara, and J.A. Leigh., 1992. Specific oligosaccharide form of the *Rhizobium meliloti* exopolysaccharide promotes nodule invasion in alfalfa. Proc. Natl. Acad. Sci. USA 89: 5625-5629.
- [2] B.J Brewin. 2010. Root Nodules (Legume–Rhizobium Symbiosis). Wiley Online Library [https:// doi.org/ 10.1002/9780470015902.a0003720](https://doi.org/10.1002/9780470015902.a0003720).p ub2.
- [3] F.D Dakora, S.B.M Chimpango., A.J. Valentine, A.J. C, Elmerich, and W.E. Newton, W. E. 2008. Biological Nitrogen Fixation: Towards Poverty Alleviation through Sustainable Agriculture. Netherland.
- [4] P. J. Dart. 1977. Host-symbiont relationships in nodule development and nitrogen fixation. In Ayanaba, A. and P.J. Dart (eds). 1977. *Biological Nitrogen Fixation in Farming Systems of the Tropics*. New York: John Wiley and Sons
- [5] C.H. Foyer, and G. Noctor. 2004. Photosynthetic Nitrogen Assimilation and Associated Carbon and Respiratory Metabolism. London. Kluwer Academic Publisher.
- [6] T. W, Goodwin, and E.I. Mercer. 1983. Introduction to Plant Biochemistry. Second Edition. Oxford: Pergamon Press.
- [7] H.B Jumin, A, Sulianto U, Saripah, and T, Rosmawaty, 2019. Rhizobium application to soybean (*Glycine max*. L. Merrill growth on the land polluted by fly ash waste. Pollution Research. 38 (4) : 116-121 (2019)
- [8] H.B, Jumin, Nur Ikhsan. and Maizar 2021. Rhizobium symbiotic mutualism wit rice Beans (*Vigna radiata*) root hair on the land polluted by sodium. Pollution Research. 40:1542-8
- [9] E, Lichtfouse, 2010. Sustainable Agriculture Reviews 3. sociology, Organic Farming, Climate Change, and Soil Science. Netherlands. Springer Long, S.R. 1996. Rhizobium Symbiosis: Nod Factors in Perspective. The Plant Cell. Vol 8: 1895-1898.
- [10] S.R, Long, 1996. Rhizobium Symbiosis: Nod Factors in perspective. The Plant Cell. Vol 8: 1895-1898
- [11] B, Singh, R. Kaur. and Singh, K. 2008. Characterization of Rhizobium Strain Isolated from the Roots of *Trigonella foenumgraecum* (fenugreek). African Journal of Biotechnology. 7 (20): 3671-3676
- [12] D.B South, 1995. Relative Growth Rates: A Critique. South African Forestry Journal, 173:43-48.
- [13] D, Werner, and W.E. Newton. 2005. Nitrogen Fixation in Agriculture, Forestry, Ecology and the Environment. etherlands. Springer
- [14] A.J, Vernon., And J.C.S Allison, 1963. A methods of calculating net assimilation rate, Letter to nature, Nature, 200: 814.

# Tenure Security, Agricultural Diversity and Food Security

Amanuel Hadera Gebreyesus

**Abstract**—In the literature, the study of tenure and food security has largely involved separate lines of inquiry. In effect, the nexus among these has received little attention; and the underinvestment in research related to the relationship between tenure and food security deters generation of tenure-related knowledge and policy guidance for improving food and nutrition security. Drawing from this motivation, we study the relationship among tenure security, agricultural diversity and food security and dietary diversity. We employ IV approaches to examine the effect of tenure security and agricultural diversity on food security and dietary diversity. We find tenure security is inversely related with food insecurity as shown by its negative association with hunger scale, hunger index and hunger category. On the other hand, results suggest that tenure security improves minimum dietary diversity of women while we find no association with child dietary diversity. Moreover, agricultural diversity is positively related with minimum dietary diversity of women, which may point to higher accessibility and consumption of dietary food groups by women. Also, findings suggest that farmers use their human (knowledge and skills) and resource (land) endowments to improve food security and dietary diversity. An implication from this is the importance of not only improving access to land but also long-term tenure security to promote agricultural diversity, food security and dietary diversity.

**Keywords**—tenure security, food security, agricultural diversity, dietary diversity, women.

# Comparative Genomic Scan Reveals Milk Quality Traits in Ethiopian Begait Goat Breeds

Haile Berihulay, Yuehui Ma, Jiang lin, Jianlin Han

**Abstract**—Comparative population genomics analysis offers an opportunity to discover the signals of selection signature in farm animals. Begait is a goat population reared for milk production in Northern Ethiopia, Tigray region. In this study, we systematically re-sequenced using 44 individuals from five Ethiopian goat breeds, which include Aberegalle, Afar, Begait, Central highlands, and Meafure. We used two complementary methods (ZFST and  $\log_2(\theta\pi)$ ) across the whole genome re-sequencing of goat breeds with the aim to identify regions of the genome under selection associated with milk traits. Total genome length of 25.20- 25.40 mb and 65.80- 66.00 mb located on chromosomes 5 and 13 were significantly associated with milk quality traits at  $Z(FST) = 4.36$  and  $\log_2(\theta\pi, ratio) = 1.37$ ; and 65.80- 66.00 mb  $Z(FST) = 2.62$  and  $\log_2(\theta\pi, ratio) = 0.36$ , respectively. Hence, we identified candidate genes associated with milk characteristics (GLYCAM1 and SRC). Moreover, this investigation observed candidate genes related to carcass (ZNF385B, BMP-7, PDE1B, PPP1R1A, FTO, and MYOT) adaptive and immune response genes (MAPK13, MAPK14, SCN7A, IL12A, EST1 DEFB116, and DEFB119). Results from this study will inform larger future studies that will ultimately find use in breed improvement programs.

**Keywords**—adaptation, carcass, genome, goat, trait.

# Autopoiesis: A Case Study in Online Art Therapy

Nárima Alemsan, Francisco Fialho.

**Abstract**—This article approaches the main aspects of therapy for human development and the discussion of creativity and autopoiesis for art therapy in the online context of Maturana's view. Art therapy and creativity are important foundations for the pursuit of human improvement and development. Bringing, thus, new creative perspectives for art therapy in the integral development of the human being as a whole. The methodology is exploratory and descriptive with a case study in the online context. Reflections are pointed out about Maturana's theory. As a result, an infographic of the main benefits found in the literature through the practice of art therapy is presented and the main benefits are listed through an infographic and a word cloud of this practice with a Maturana's view.

**Keywords**—Art, autopoiesis, creativity, art therapy.

## I. INTRODUCTION

IN the last few years, the crisis of the senses has grown due to the excess of technologies and instantaneous facilities. This generates a discharge of dopamine that the brain is not prepared for and there is a certain disconnection with face-to-face reality.

The virtual facilitates a live in many ways; at the same time, it connects people around the world, disconnects too of real emotions of the notion of to be present with all senses. Thinking in this context, online art therapy emerges as a tool for self-knowledge and reconnection with other senses. Art therapy emerges, then, as a new aspect of awareness of the power of the now and reconnection with the emotions of the present. In this context, the general objective of the article is to answer the following research question: what are the benefits of art therapy in the process of autopoiesis in the online context?

The specific objectives are: to determine how the relationship between autopoiesis and art therapy occurs, to deepen the concepts found in the literature and to establish connections and contributions to future works. Thus, this article first aims to identify in the literature the definitions about autopoiesis and creativity. Then, we discuss the relationships and how art therapy benefits people in the process of autopoiesis.

## II. DEVELOPMENT

For discussion, the concepts of this article are presented. In order to better understand how the process and the benefits of art therapy takes place, a table, Table I, with the main concepts identified in the literature is shown.

Approach the concept of autonomy in which "Autonomy concerns one's ability to create, to create, to produce knowledge and implies a lively, active and not passive attitude, dependent on guidance from outside. Because it is autopoietic, the living being is endowed with the capacity for self-creation and self-

construction, hence being autonomous." [1] They [1] argue that it is impossible to analyze knowledge without looking at life and, of course, human development in which everything is connected from the individual to the collective. From the one to the whole, from the molecule to the cosmos, for example. Hence the importance for the perception of this construct to be worked and studied:

"Autonomy concerns your ability to create, to produce knowledge and implies a lively attitude, active and not passive, dependent on external guidance. Because it is autopoietic, the living being is endowed with the capacity for self-creation and self-construction, being, therefore, autonomous". [1]

With Bucho's statement, this capacity for self-creation is inherent to the individual's autonomy. Thus, "The act of human understanding is deeply associated with the deepest roots of life, which biologically speaking, are dynamized throughout the molecular and cellular structure of the human being, which has in itself the phenomenon of cognition as a possibility to create, learn and know. in the interrelation with the surrounding environment." [2]

"The act of knowing is, therefore, the result of the continuous structural changes of the system that produce, in a double effect, the global state in which the cognitive system and the world correlated to it finds itself. Cognition is defined as a function of the living's interaction with the world, or conduct [3].

Based on the concept of autopoiesis, the author Maturana radically breaks with the traditional concept of cognition – as the organism's capture and processing of information from the outside world – and, based on this rupture, offers a new paradigm for understanding the phenomenon of knowing.

"It maintains that this being is creative vital energy - as a universal matrix - quantum cosmic energy - vital generator of the entire structure and organization of the body-creator." [3] This process of self-knowledge is intrinsic and no longer occurs only in the external, being the same as a reflection of this process of self-knowledge and of creating oneself in the continuous action of expressed creativity. Thus, it can be concluded that from this concept it is possible to identify that knowledge also comes from the creative force of the people themselves who build themselves into systems. "It is in this movement of problematic creation of modes of existence that life in its cognitive character must be understood.

"Knowing is the creation of the living itself in the action of the living." [4] Life, therefore, is creation and knowing is an act of poiesis. To better understand self-creation, the following concepts and relationships are presented.

self-creation process

N. Alemsan is a designer and PhD student at the EGC/UFSC graduate Program, Brazil (e-mail: narimalemsan@gmail.com)

F. Fialho, Dr., is a doctor and professor at UFSC; Coordinator of NEDEC and NUCOG at UFSC (e-mail: fapfialho@gmail.com).



Thus, the process of self-creation takes place through the concept of "autopoiesis", that is, one learns by living and one lives to learn in a continuous and infinite process which could be related to the symbol of infinity in which the circles begin in a point and close soon after the cycle starts all over again, in short, in a more cyclical process.

"The cognitive act, for Varela, is much more than simply problem solving." References [5] and [6] state that "[...] a reflexive posture is necessary in the world in which we live; acceptance and respect for oneself and others are necessary without the need for competition."

Treating human beings without competition means breaking teaching paradigms with grades and medals, or rather: If someone loses, someone else wins, is that right? To what extent getting high grades is better compared to someone else, and in Maturana's perspective each one has multiple potentials and talents to be developed. Thinking from this point of view, the improvement of potential is fundamental. More specifically, art therapy develops in the following dimensions: cognitive, psychological, emotional and interrelational. To better understand, the concept of cognition is shown: "cognition is the co-occurrence of a double act of creation (poiesis) that configures, at the same time, the living and the world." [7]

"One of Maturana's most important considerations for education and educating, when seeking to establish the ethological structures of human beings, was the conception that we are constituted in emotion and not in reason." [8] As an example, the art therapy process and its benefits are presented below.

Art Therapy converges with Jung's premise that man is guided by symbols, as it facilitates their contact, understanding and transformation through the creative process [4]. Art therapy is a field that encompasses different types of art, such as dance, painting, sculpture, music, theater, and is based on diverse psychological theories. This arises in an aspect of improvement of the self-knowledge of the being linked to the concept of autopoiesis by Maturana. Expressing feelings and desires through art. Thus, group work in art therapy allows:

- sharing your work and while doing it;
- knowing and recognizing yourself in your relationship with yourself and with other people as well;
- the autonomy of the individual to express himself.

The therapeutic process is, then, a path marked by symbols, which indicates and informs about stages of each person's individuation journey. By individuation we mean the arduous task of becoming an individual who seeks to live fully, integrating his talents, his pains and psychic faults. This is preferably a non-verbal process. This means that the approach and forms of intervention are intended to confront content inherent to primary and pre-verbal psychic processes. This individuation takes place through self-knowledge in the practices of artistic expression of art therapy. In this process of self-knowledge enters the concept of Maturana who defines that this process of autonomy generates self-knowledge and all knowledge is a creation, all creation is a knowledge. According to [9] there is no judgment and no reflections attached to theory for interpretations, in the interaction, precisely for the encounter

to occur in this process, there is an opening to the new, to the unknown, in a process of joint exploration and experience.

Everything is used in some way for individuals to express themselves. To better understand, below is a descriptive table with the main and important definitions found in the literature on the subject.

TABLE I  
DEFINITIONS OF ART THERAPY

Authors	Definition of Art therapy
[6]	"Art therapy is the term that designates the use of artistic resources in therapeutic contexts. [...] it is a broad definition, as it presupposes that the process of artistic making has the potential for healing when the client is accompanied by an experienced art therapist, who builds a relationship with the client that facilitates the expansion of consciousness and self-knowledge, enabling change."
[14]	"Art therapy is emotional healing through unlimited art combined with the therapeutic process. It is the practice that uses the individual's self-expression as a means of revealing oneself to the inner world."
[17]	"There are countless possibilities of conceptualizing art therapy. One of them is to consider it as a therapeutic process resulting from the use of different expressive modalities, which serve the materialization of symbols."
[11]	"Art therapy has been expanding its techniques in several areas of activity with health professionals, using it as a tool in health prevention and promotion. Aiming at the formation of the psychologist and its context, whether in the educational, clinical, community and/or organizational, covering its application in assessments, treatments, prevention and rehabilitation, linked mainly to mental health issues, not being linked only to consultations."
[12]	"The activities carried out involve commands and instructions for specific themes, exploring autonomy in creation, working on the personal representations of the participants, allowing the expression and sharing of their perceptions, thoughts, knowledge and memories."
[10]	"Art Therapy works on visuospatial perception, attention, memory and concentration, providing the individual with the feeling of accomplishment of the artistic work."

Table I, therefore, presented important definitions on the subject. In this way, it can be seen that art therapy has emotional, psychological and self-awareness biases. This article has focused more on the benefits gained through the PROCESS OF INDIVIDUATION AND AWARENESS, BUT DOES NOT ENTIRELY exclude the others as they are interconnected.

#### A. Autopoiesis

Autopoiesis or autopoiesis comes from the Greek (auto = "self" and poiesis = "creation"). Poiesis is therefore a Greek term meaning production. According to Maturana [], the living being is, therefore, a structurally determined autopoietic machine. The structure of each living being specifies four domains (ibid.):

- Domain of state changes, i. e., structural changes without changing the organization, thus maintaining class identity.
- Mastery of destructive changes, i. e., disintegrating changes, losing the organization disappearing as a unit of a certain class.
- Domain of disruptive interactions, that is, interactions that generate changes in state.
- Mastery of destructive interactions, i. e., those that result in

destructive changes.

The living being is, then, a dynamic system (a structurally determined machine) and, as such, its structure is constantly changing, which, in turn, implies constant variation in these structural domains. [16].

Going on the idea that “our experience is inextricably tied to our structure” [15] the authors define that “man is contained only in his own nature, in his human way of operating and self-describe its experiential-perceptive universe, therefore: in its own being”. Thus, to better understand the process of autopoiesis, a table was made with the main definitions:

TABLE II DEFINITIONS OF AUTOPOIESIS	
Authors	Definition of Autopoiesis
[15]	"traditional way of approaching the cognitive act" which, according to him, always has to do with the indication of something external to the subject.
[15]	“The process of identity construction is circular: a network of metabolic productions that, among other things, produce a membrane that makes the very existence of the network possible. This fundamental circularity is therefore a unique self-production of the living unity at the cellular level. The term autopoiesis designates this minimal organization of the living”.
[13]	“meaning, in general, and the limits of meaning, in particular, then guarantee the inextricable interconnection between system and environment [...]” argues that autopoiesis not only characterizes the self-referring system, but also the self-referential system. self-produces, that is, it produces itself as a systemic unit. This means that the system is capable of differentiating itself from its environment, this environment being always the condition of possibility of the system. By differentiating itself from the environment, the system constitutes itself as a discrete unit that reduces complexity.

According to table 2, the discussion of the article will be based on Maturana's definition, in which autopoiesis addressing cognition. The autopoiesis of consciousness is, therefore, the “real basis of individuality” of psychic systems [13] Bringing something external to the subject, it is also necessary to delve into Systems Theory, which is seen in a more integrative way.

With this new conception, (Social Systems) is the book in which the author Luhmann [13] redefines the notions of “system” and “function”, differently from the entire systemic and functionalist tradition, initiating a paradigm shift at three

levels of analysis. in the systems thinking of the social sciences.

### III. METHODOLOGY

#### Methodological procedures

The base theory for the present article is from Maturana, an autopoietic and interpretivist worldview. For the author, in a nutshell, all doing is knowing and all knowing is doing. In the sense that in every action there is a unique experience for each individual with individualities and talents.

The inclusion criteria for the articles were: articles published in Portuguese, English and Spanish, between 2017 and 2021 in order to collect more recent studies; all published articles related to Art Therapy and Autopoiesis.

Strategies to locate the articles were adapted for each database, having as a guideline the question and the inclusion criteria of the integrative review, previously established to maintain coherence in the search for articles and avoid bias.

Then, an online questionnaire was developed and applied in Facebook groups that had art professionals who already work in the area with the objective of collecting relevant information for the discussion of the article. For data collection, it took 4 weeks to collect responses plus the qualitative analysis of the questionnaire responses.

#### A. Discussion

Art therapy presents itself as an important instrument for the development of human beings. To carry out the questionnaire, it extracted the answers of the professionals in relation to the advantages and needs of online art therapy. The questions created for the application of the form were:

*Is art therapy a useful therapy in treating individuals with psychological problems?*

*Is art therapy a tool that can stimulate creativity by promoting individual well-being and improving quality of life in the online context?*

*Is art therapy a tool that contributes to the integral development of the human being?*

*Is art therapy a tool that can stimulate the reconnection of the individual to the collective?*

*Is art therapy a tool that can stimulate the individual's AUTONOMY?*

*Does art therapy allow expanding the patient's general knowledge and providing more integrated care?*

*Does the proposal of creative activities in the treatment favor an improvement in the individual's autonomy of actions?*

*Does the proposal of creative activities in the treatment favor an improvement in expression and dialogue between students?*

*Does art therapy favor the approximation of the human being through dialogues?*

*Is art therapy an instrument that allows the manifestation of individual subjectivity?*

Define in one word the main benefit of art therapy. The questions generally proposed to investigate how art therapy can stimulate creativity and self-knowledge, promoting individual well-being and qualitatively improving quality of life. The last question of the questionnaire aimed to identify in just one word in order to better understand the main benefit.

Analyzing the answers, 28.6% define the main benefit of art therapy as Self-knowledge. Therefore, it has more advantages than disadvantages for people with anxiety disorders. Some of the answers to the last question of the questionnaire were:

*"Art therapy restarts us, gives us autonomy, brings us internal communication to the external."*

*"Mental health."*

*"Self Integration"*

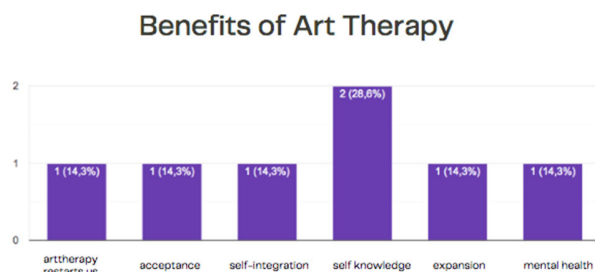
*"Expansion"*

*"Mental health"*

*"Self knowledge"*

*"Acceptance"*

Figure 1 - Graph of the questionnaire responses



Source: Own authorship (2022)

Analyzing the answers in Figure 1, 38.6% define the main benefit of art therapy as Self-knowledge.

#### IV. RESULTS

Knowledge also comes from the creative force of people who build themselves into systems. Therefore, with this article it can be concluded that art therapy seen from Maturana's point of view favors the integral development of the human being in dimensions such as: cognitive, psychological, emotional and interrelational. Taking a new look at the understanding of what we call knowing and acting in the world, thus allowing the

construction of a world and a better future for all.

As a result, it is present the analysis of the questionnaire applied to an online group of art professionals in order to identify benefits of the practice. An infographic is also presented with the main inherent quests of the human being along with the benefits of the practice of art therapy and the relationship with Maturana's theory.

#### A. Recommendations

As a result, an infographic of the main benefits found in the practice of autopoiesis in art therapy is presented, as shown in Figure 2 below:

Figure 2 - Infographic of the benefits of Art Therapy in the practice of autopoiesis



Source: Own authorship (2022)

The benefits are numerous identified according to Figure 3 are: self-knowledge, improvement of sense perception, self-awareness, expansion of knowledge through techniques and observation, improvements in cognition, sense of self-construction, development of creativity and construction.

#### V. CONCLUSIONS

The article, thus, managed to achieve the general objective and brought important contributions on the subject in question, correlating with Maturana's theory on autopoiesis. Art therapy emerges, then, as a new aspect of awareness of the power of the now and reconnection with the emotions of the present.

Life is, therefore, a non-linear construction of cycles of autopoiesis in which self-construction takes place in the potentialities of searches inherent to the human being and one of the searches is to express oneself using what is more human than we have the expression of the creativity that emerges. of the love of feeling full or reaching fullness in self-realization.

Such searches are expressed through the constant practice of artistic expression and in the integral development of the human being with the 3 aspects identified through the analysis: dialogue with oneself and with others, loving oneself (in the construction of self-esteem) and in the construction of autonomy in the action of each practice within art therapy. Some limitations found: few databases, lack of exploring the more behavioral aspect.

Here are some suggestions for future work: apply this study

to more people and companies as well, deepen the study with more databases, set up an observation and establish similarities and differences between face-to-face and online art therapy.

Art therapy thus becomes an important tool for professionals in the field to understand how the integral improvement of the human being takes place. Bringing expression and creativity as foundations for the autopoiesis of the human being in a more integral vision of self-knowledge.

Life, therefore, is creation and knowing oneself is an act of poiesis.

#### ACKNOWLEDGMENT

Thanks the possibility of improving studies and conscience. Honest gratitude to the tutor and university for support, persistent help and encouragement.

#### REFERENCES

- [1] J. L. C. Bucho. THE TREE OF COMPETENCES IN CREATIVITY: TREE OF KNOWLEDGE AND LIFE.
- [2] M.G. Ditrlich. The body-creator: the key to a hermeneutics of the work of art. *Fragments of Culture*, Goiânia: Publisher of the Catholic University of Goiás, 14(5), 2004.
- [3] M. Koefender. Art therapy, an oasis in the condition of human health: art, health and spirituality., 2020.
- [4] G.G.L. Bilbao, V.E. Cury. The artist and his art: a phenomenological study. *Paidéia* (Ribeirão Preto), pp 16(33), 91-100, 2006.
- [5] A.D. Eirado, E. Passos. "The notion of autonomy and the dimension of the virtual. (Psychology under study)", 9, 77-85., 2004.
- [6] S. Ciornai. "Paths in art therapy Gestalt art therapy, art in psychotherapy, supervision in art therapy", (Vol. 62). Editorial Summus., 2004.
- [7] B., Vianna, L.A.B. Andrade, & N.M. Vaz,. Teaching is impossible, and learning inevitable: comments on the epistemology of Humberto Maturana. *Revista Helius*, 3(2, fasc. 2), pp. 1183-1227, 2020.
- [8] M., Naputano, & Justo, J.S. Maturana's biology of knowing and some considerations applied to education. *Science & Education* (Bauru), 24, 729-740, 2018.
- [9] Fiorindo<sup>1</sup>, P. P. (2014). Art Therapy and Analytical Psychology.
- [10] De Souza, H. S.; Pereira, M. S. Rehabilitation through art: A new perspective in the treatment of neuropsychological disorders. [Monograph] Candido Mendes University, Rio de Janeiro, RJ, Brazil. [accessed in 2021 Nov 21] Available at: [http://www.avm.edu.br/docpdf/monografias\\_publicadas/c203998.pdf](http://www.avm.edu.br/docpdf/monografias_publicadas/c203998.pdf), 2009.
- [11] A.C.D. Reis. "Art therapy: art as an instrument in the work of the Psychologist. (Psychology: Science and Profession)", 34, 142-157, 2014.
- [12] T.M. Duarte, R.F.C, Santos. "Art therapy and cognitive aspects: an integrative review", 2021.
- [13] N. Luhmann. "Social systems: outline of a general theory. (Voices Publisher)", 2016.
- [14] Martinie, J.M.T., Filha, M.T.J.C., & Menta, S.A. (2002). Art therapy: occupational therapy resource in the elderly. *Multithemes*.
- [15] H. Maturana, and F. Varela. "The tree of knowledge. (Sao Paulo: Palas Athena), 2.", 2001.
- [16] M.A. Moreira. "Maturana's epistemology. *Science & Education* (Bauru)", 10, pp. 597-606, 2004.
- [17] A. Philippi. But what exactly is Art Therapy? *Images of Transformation Magazine*, 5, 4-9, 1998.

# Creating Inclusive Workplace Practices to Support Individuals with Dyslexia Across the Employment Lifecycle; Perspectives from Employers, Managers and Employees with Dyslexia

Shae Wissell,<sup>1</sup> Leila Karimi<sup>2&4</sup>, Tanya Serry<sup>3</sup>, Lisa Furlong<sup>3&5</sup> and Judith Hudson<sup>6</sup>

<sup>1</sup> School of Psychology and Public Health, University, Bundoora, Australia

<sup>2</sup> School of Health and Biomedical Sciences, Psychology Department, RMIT University, Melbourne, Australia

<sup>3</sup> School of Education, La Trobe University, Bundoora, Australia

<sup>4</sup> School of Medicine and Healthcare Management, Caucasus University, Tbilisi, Georgia

<sup>5</sup> Child Well-being Research Institute, University of Canterbury, New Zealand

<sup>6</sup> School of Education, University Tasmania, Hobart, Australia

## *Abstract—*

**Background:** Employment and job security are key influences on health and wellbeing. Dyslexia affects approximately 1 in 10 individuals and is a lifelong disability. Little is known about the workplace practices through the lens of individuals with dyslexia and those who employ and manage dyslexic employees. **Materials and Methods:** Individual structured interviews were used to seek perspectives from two participant groups. The first study investigated the perspectives of 14 Australian adults with dyslexia in relation to their experiences, progression and performance management in the workplace. This data were analysed within the Job Demands-Resources Model of Burnout (JD-R Model), which explores links between workplace characteristics and employee wellbeing. The second study explored the perspectives of four employers and managers about their experiences and self-efficacy managing dyslexic employees as well as their views on workplace inclusivity. Deductive content analysis was utilised to categorise and analyse the responses of participants. **Results:** Study 1: Of the 14 participants (adults with dyslexia) all reported experiencing challenges at different points throughout their employment, including a lack of awareness of dyslexia as a disability, exhaustion and discrimination. Many felt indecisive about whether to disclose their dyslexia in the workplace. A minority reported receiving positive, useful support from team members following disclosure. Study 2: Responses from employers and managers (n=4) indicated that although they personally had a some awareness of the challenges facing employees with dyslexia, they felt there was a lack of broader awareness and understanding of dyslexia as a disability, which could make it challenging for those with dyslexia, across their workplaces. They felt with the right reasonable adjustments in place those with dyslexia could complete work tasks to a high standard. By merging the results from these two studies, we were able to gain a better understanding of some of the workplace challenges faced by people with dyslexia and ways to improve organisational practices and inclusion. Although this study was conducted in a single state in Australia with a relatively small sample size, we present preliminary evidence demonstrating that employees with dyslexia face unique challenges

related to their disability and this was often amplified by low levels of understanding about dyslexia from their peers. Additionally, employers and managers felt there was a lack of understanding of dyslexia as a disability and that workplaces could be doing more to create an inclusive working environment. At present, dyslexia appears to be a risk factor to career satisfaction and success for many with the condition. To mitigate these difficulties, workplace awareness training and the adoption of inclusive workplace practices could improve outcomes for employees with dyslexia. With an inclusive, supportive, educated workplace environment, we would expect more employees with dyslexia to flourish, however further research particularly in an Australian setting is necessary to build on these findings, so we can gain a deeper and broader understanding of the issues faced by employers, managers and dyslexic employees.

**Keywords:** dyslexia, adults, disability, inclusion and diversity, workplaces, Australia, job demands resource model of burn out, employers, managers.

# The Reception of Caspar David Friedrich: A Case Study in the Contested Cultural Legacy of the German 19th Century

Zhaoyu Cheng

**Abstract**— This essay examines the reception of Caspar David Friedrich in a range of cultural contexts and periods, using myriad writings, exhibitions, and images as supporting evidence. Drawing on theories of reception, it is argued that the history of reception of Friedrich's paintings in its following centuries is forged as much by the artist himself -which can be elucidated through the lenses of paradigmatic shift (or, *Prädisposition*), the gap theory (*Unbestimmtheitsstele*), and the inner communicativeness of the work- as by the audiences of his works. Various social and political forces are partially responsible for constituting the meaning of his paintings. Through the examination of his audiences' reception, two types of narratives are put into investigation: one depicting Friedrich as a romantic art maker and one treating him as a German national symbol. Each narrative is argued to demonstrate the case of essentialization—the process of reducing a complex event to one facet and treating it as an entirety—while in certain radical circumstances, it develops into mythification and 'pseudomorphoses.' But the condition that permits essentialization is rooted in the artistic characteristic constructed by the artist himself. Friedrich's oeuvre communicates with every audience individually, and eradicates the notion of 'intended audience,' even though some of his works are directly commissioned by one individual. Thus, audiences are not intended to be forced to accept a singular interpretation or asked to conceal one's non-German cultural background, which prevents the possibility of having a unanimous narrative and justifies for projecting personal social prejudices onto the reception that leads to essentialization. The obvious setbacks of this method are that some cultures or periods will be excluded from the discussion and some heterogeneous situations where different narratives interwoven are being dichotomized. Notwithstanding, this paper aims to shed some light on the peculiarity of Friedrich's history of reception and thereby to investigate the dynamic interaction between the painter and audiences.

**Keywords**— Caspar David Friedrich, German art, romanticism, reception theory, historiography.



# Antibacterial Evaluation of Zn(II)-Porphyrin-Based Nanostructure: Bactericidal Effect from the Point of View of Nanoparticles Formation

Sajedehtehrani Nejad, Rahmatollah Rahimi, Sadegh Rostamnia, Mahboubeh Rabbani

**Abstract**— In recent decades, Chronic infections lead patients to become increasingly susceptible to multidrug resistant bacteria strains. Metal-based porphyrin complexes are critical pigments that can self-assemble and create geometric nano structures that have antibacterial activity against gram-positive and gram-negative bacteria. In this study Zinc (II) porphyrin-based molecules, ZnTPP (zinc(II)tetrakis(4-phenyl)porphyrin), were synthesized and self-assembled during acid-base neutralization. The product was identified by UV-Vis, PXRD, FT-IR, and FE-SEM analysis. The antibacterial activity of synthesized nanoparticles compared with the molecular form of the porphyrin compound was investigated by determining the average zone of inhibition growth of diameter method. The antibacterial performance of synthesized porphyrinic nanoparticles was also evaluated for two strains of each *E. coli* and *S. aureus* bacteria with the MIC and MBC values determination. The equal achieved values of MIC and MBC of Zinc (II) porphyrin nanoparticles for both *E. coli* (ATCC 25922) and *S. aureus* (ATCC 25923) bacteria make the self-assembled ZnTPP nanoparticles as bactericidal agents.

**Keywords**— Zinc (II) porphyrin, antibacterial, nanoparticles, self-assembly, bacteria strains.

# Conspiracy Theories Affecting Radicalization Trajectories: Anti-Government Conspiracy Theories And Great Replacement Narratives on Telegram

Julius Brejohn Calvert

**Abstract**— The radicalization of violent extremism continues to produce strenuous challenges for private citizens, businesses, and political institutions around the world. Namely, the proliferation of potentially harmful content such as conspiracy theories and disinformation. Previous research has implicated the involvement of various socio-cognitive mechanisms, group processes, and individual personality traits in the facilitation of an individual's pathway to committing non-violent/ violent actions. This research conceptualizes propagandist content as an influencer of an individual's cognitive processes. The current paper compares narratives and conspiracy theories that are being shared in anti-government and white supremacist extremist communities on Telegram. The present research utilized an exploratory observation methodology to collect comments, video clips, photos, and news articles in four open communities (n=200). Comparative analyses performed on the narratives coded (n=247) report that 37% and 40% fit into alleged mass corruption and anti-diversity narrative domains, respectively. A total of 18% pushed false and often fabricated information concerning the COVID-19 pandemic. Meanwhile, 2% focused on LGBT+ issues, and 3% of narratives targeted migrants and Immigration policies.

**Keywords**— Cognitive Science, Social Psychology, Domestic Extremism, Conspiracy Beliefs.

## I. INTRODUCTION

The term *conspiracy theory* has been used in the general population extensively, and many individuals (especially those with access to the internet) may be able to recall at least one that they have heard [7]. However, researchers have previously grappled with defining the term 'conspiracy theory' thus, many varying definitions exist and are used to describe this peculiar phenomenon. For instance, citing Keeley, 1999 and Pigden, 1995, Douglas and colleagues define a conspiracy theory as an attempt by an individual, or groups of individuals to explain any causal factors for a significant social or political event, and often these contain claims of a secret plot being orchestrated by two or more powerful entities [5], [21]. The present research defines a conspiracy theory as multiple networks of misinformation or disinformation which can be utilized to explain any ultimate causes of social, political, or significant events. Furthermore, although varying definitions are ascribed to the term, certain characteristics of conspiracy theories exhibited are universal. For instance, redundancy among various conspiratorial claims can be found in some anti-vaccination disinformation. Adherence to rumors surrounding the Polio vaccine has led to new upticks in the number of cases in some developing countries and has historically featured tales of infertility as an

alleged result of receiving inoculation [5], [7], [9]. The recirculation of claims of adverse effects from receiving vaccinations may morph over time, and 'adapt' to the social environment in which it is to be propagated. In a recent study, 3,000 participants in the United States responded to an online survey that was employed to assess their belief in conspiracy theories regarding the Covid-19 pandemic. The participant's political partisanship, tendency to observe events as being explained by a conspiracy and the extent to which they experience feelings of uncertainty were measured using several multi-item psychological scales. Of the participants, nearly 30% of them agreed that "*Former CEO Bill Gates is creating a tracking device to be injected with the coronavirus vaccine*" was probably true, while 16% agreed that the statement was true [15]. In an American societal context, some conspiracy theories sown into varying aspects of popular culture pertain to the alleged containment of highly intelligent extraterrestrial creatures by the United States Military at a compound in New Mexico, Arizona. This conspiracy theory recycles claims that the United States government is run by a few powerful people who harbor malicious intentions, in this case with the goal of deceiving the public in mass. However, despite the popularity of the Area 51 conspiracy theory few, if any, violent events have resulted from the widespread propagation of these claims. By contrast, anti-vaccination conspiracy theories have been used by an array of actors to encourage demonstrations, some of them violent, in countries including Canada, the United States, Australia, and Germany [19]. Furthermore, rising trends of ideologically motivated crime linked to the *Qanon super-conspiracy theory* (or *Qanon conspiracy theory*) have been reported by several investigative entities including The National Consortium for the Study of Terrorism and Responses to Terrorism (START) which published the *Qanon Offenders in the United States* brief detailing data collected on Qanon followers who have been arrested and accused of committing a crime. In the United States alone a little over one-hundred individuals have been arrested and accused of engaging in criminal activity. Several characteristics of the criminal charges stick out across the wide collection of criminal behaviors, notably violent behavior was not always the outcome, as in an unsolved 2019 case involving a woman throwing objects at a church in Massachusetts. Video evidence shows this woman allegedly proceeding to 'tag' the building with references to "JFK Jr.," and "David de Rothschild", an allusion to several antisemitic conspiracy theories frequently cited in Qanon mythology. Initially, the data were collected in the United States however this was expanded to include the rising international cases [10]. At first glance, the premise of some claims espoused by Qanon adherents may appear outlandish as there ceases to be demonstrable evidence of a large human/child-trafficking ring being run by large networks of political leaders and celebrities. Sentiments of paranoid distrust in authority figures (e.g., law enforcement), perceptions that abuse against children is not receiving adequate media or government attention or fearing perceived attacks on

spirituality appear to give the Qanon mythology its allure. Indeed, an Arizona resident was arrested in 2019 after they allegedly live streamed themselves tampering with the water tanks owned by an organization, they previously accused of trafficking children. Moreover, early psychological research into conspiracism emphasized psychological dysfunction as one significant predictor of the likelihood of an individual adopting a conspiracy theory. In their 2018 meta-analysis of the psychological literature on conspiracy theories, Goreis & Voracek identify several individuals correlates of conspiracy belief that revealed pathological tenants of paranoia, schizotypy, narcissism, and anomia [7]. Research into the potential psychopathology of a 'conspiracist mindset' has shifted to understanding non-clinical and sub-clinical traits which more accurately assess the widespread phenomena of belief in varying conspiracy theories given recent evidence demonstrating that in general, belief in conspiracy theories is a popular occurrence [5], [22]. Furthermore, prior investigations have revealed compelling evidence which suggests belief between individual conspiracy theories are strongly correlated thus if someone believes in one conspiracy theory, they are more likely to adhere to an additional conspiracy theory [16]. Consequently, some psychologists and social science researchers have hypothesized conspiracy theories might form a mutually supportive network of beliefs that cyclically reinforce themselves, though conceptualization of the 'monological belief system' has failed to explain how contradicting conspiracy theories are able to be held by an individual simultaneously [4], [24]. Wood, Douglas, and Sutton analyzed these findings to explain the peculiarity of an individual's capability to hold contradictory conspiratorial beliefs. Their study demonstrated that adherence to contradictory conspiracy theories is driven by more subliminal 'agreements' among varying conspiratorial beliefs. These 'agreements' refer to 'higher-order beliefs' which indirectly construct the individual's perceptions of their world [24]. Accompanying 'higher-order beliefs', such as the need for certainty (e.g., can be expressed as obtaining information from unreliable sources after a major event), are complex cognitive processes that have been thought to underlie the process of several social phenomena such as the use of conspiracy theories in ideologically extreme content.

#### *Narratives can act as 'affective agonists'*

General political attitudes are considered by many researchers to be the product of normal psychosocial processes. Thus, affective radicalization generally refers to the process of an individual or their ingroup adhering to an ideology, cause, or movement to the extent of great extremity, beyond these normative psychological processes. A popular representation of radicalization centers on extreme social-political ideologies such as Anarchism or Nazism. However, in several studies, radicalization has been recorded in other domains such as religion. This paper's objective seeks to examine how conspiracy theories influence an individual's radicalization trajectory. As radicalization is both a cognitive and an affective process, the messaging within the narrative can prove to be reasonably effective depending on the target, and the narrative domain. A notable event in the United States, the Jan 6th attack, which took place in early 2021, consisted of many adherents who gathered under the pretense of protesting an allegedly illegal federal election. The crowd was composed of an amalgamation of different types of right-wing 'conspiracy theorists, political extremists, and general citizens who may have not engaged in these prolonged intergroup interactions under normative circumstances. Some recent studies present a clearer understanding of how election fraud conspiracy theories were spread

months prior to this display of violent antisocial behavior, which initially spurred vicious rows in online discourse [20]. Epidemic factors—characteristics modulating the spread and transmission of a conspiracy theory— may have included increased anxieties over a change of governing administrations, salience of political polarization, social prejudice discussed in popular media, or fear over public health regulations [9]. Endemic factors—a baseline of societal discourse which is mostly present in a variety of contexts— could have included access to information via the internet or actors propagating constant disinformation online years prior to the attack to name a few [15], [20], [25]. A culmination of both epidemic and endemic factors might enable a particular conspiracy theory, election fraud in this case, to transmit an 'affective- agonist' termed a narrative. This paper's conceptualization of a narrative parallels a trojan horse design in which conspiracy theories are used by malicious actors to implicitly transmit a specific narrative— through exposure—to vulnerable individuals. Narratives can infer larger themes of evil or harm in society should be dealt with by a range of means (e.g., being manipulated by a totalitarian political system requires armed action to bring an end to the evil acts) based on one or multiple networks of conspiracy theories (e.g., claims of tampered voting machines favoring a particular political candidate in an election). Narratives are often used in the radicalization process to change the affective state and goals of the target to align with the message being disseminated. In recent years an emerging focus on the neural correlates of the cognitive processes involved in radical thinking has taken way. Amodio and colleagues examined political attitudes using functional neuroimaging methods and found significant underactivity in regions associated with monitoring conflicting situations were prevalent in conservative participants [1]. Their study is in line with some cognitive antecedents of radicalization. For instance, Gerber and colleagues in their study on the cognitive flexibility of partisans demonstrated that 'left-leaning participants were more tolerant of uncertain situations and complex circumstances. Conservative participants showed less cognitive flexibility [3]. Furthermore, Zmigrod [26] argues for a neurocognitive model of political behavior in which neurocognitive dispositions- biologically based differences in information processing, evaluations, and making decisions- are stable and implicit processes within the 'political brain'. The present research then seeks to evaluate the implicit messaging within content that is ultimately aimed at persuading people to change or reinforce their political convictions in an extreme manner.

#### *Communities*

Usage of the private-messaging social media platform, Telegram, to disseminate extreme content and conspiracy theories has captivated researchers in recent years. Thus, four communities operating on the private-messaging social media platform (version 8.1.4) made up the sources for all samples collected in the present study. The War on Whites revised the name of the community and migrated from the original channel in March of 2022. Prior to migrating to the new channel, the community hosted 1,806 subscribers and increased its audience to 4,758 subscribers in May of 2022. The Western Chauvinist channel hosts 41,473 subscribers, Expose the 'Pedos' End the Cabal hosts 26,272 subscribers and Dismantling the Cabal hosts 55,219 subscribers.

#### *Narrative Inclusion*

A set of descriptive criteria were designed to categorize the content collected during each observational period. Media expressing unreasonable skepticism and mistrust in vaccines, public health institutions/ figures, public health procedures, or regulations was

coded as anti- vaccination. Figure A provides an example of such a post. Media included as mass corruption usually contained claims alleging illegal or severely unethical actions were being committed by government entities such as the federal government, or persons perceived as “elite”. In communities where Qanon mythology was prevalent, some popular figures received constant allegations of committing several crimes against children. Anti- “wokeness” is a term often used in far-right communities referring to a stereotyped political platform associated with left-leaning political parties and communities. Media that unreasonably criticized efforts to remedy racial tensions and perceived social inequalities were included. Most media coded in this category featured distasteful representations of other ethnic identities, and frequently expressed fears over being replaced and shunned in society based on white identity. Another narrative category, anti-LGBTQ, included media signaling extreme aversion to actions, remarks, and popular culture that promotes socially progressive ideals regarding the LGBTQ+ community. Anti-immigration coded media generally had extreme political positions regarding refugee and migration policies, and distasteful characterizations of migrants. During the initial observation stage, the content was analyzed using the inclusion criterion detailed in the previous. Following the initial assessment, the content meeting at least one criterion was then coded in Microsoft Excel (Figure B).

### Results

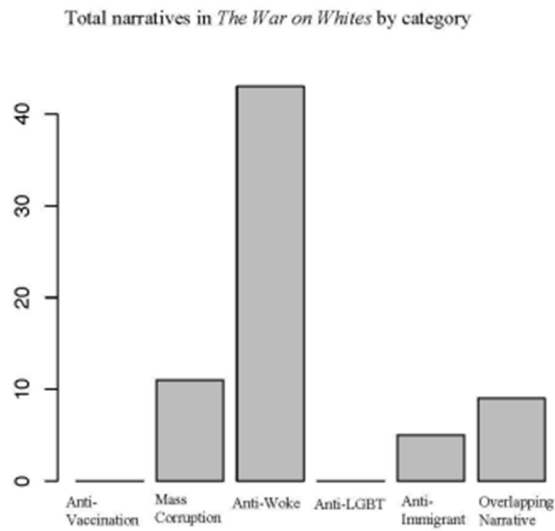
Narratives extracted from the content collected across four communities (n=247) were transferred into R (ISwR package). A total of five narrative visualizations were generated. Four graphs detail aggregates of narrative domains by the community (figure C-F). A basic measure for overlapping narratives was designed to assess the salience of the chosen narrative domains in this paper (Figure G). Finally, a comparative analysis was performed on the data to further assess the content and narratives. The War on whites contributed a total of 23% (n= 68) narratives across all four criteria, excluding anti-vaccination narratives (Figure C). The Western Chauvinist channel contributed slightly more narratives totaling about 24% (n= 72) of the entire sample. Expose the Pedos’ end The Cabal contributed the largest amount of content (n= 94) to the current sample collected in this paper. Lastly, Dismantling the Cabal shared 22% (n= 67) of the total sample. A total of 37% (n= 88) of narratives focused on allegations of mass corruption being committed by government authorities and various celebrities. The highest narrative domain concerned narratives that expressed overt racial prejudice (40%). Of the total narratives collected in this domain, many featured calls for “white unity”, references to Adolf Hitler, the Democratic Socialist Party (DSP), and often the content was of news stories relating to criminal activities in one’s area. There were 17% overlapping narrative domains, most of which were coded across two anti- government channels (DTC and WC).



Figure A. This snapshot of a video features anti-vaccination narratives.

	A	B	C	D	E	F	G	H	I	J	K	L	M	N	O	P
1	Index	Anti_vax	Mass_corrupt	Anti_race	Anti_LGBT	Anti_imm	Overlap_race	Conspiracy	Conspiracy	Media_type	Notes	Interpretation				
2	1									News	Antisocialist	Antisocialist				
3	2									Article	Antisocialist	Antisocialist				
4	3									Article	Antisocialist	Antisocialist				
5	4									Article	Antisocialist	Antisocialist				
6	5									Article	Antisocialist	Antisocialist				
7	6									Article	Antisocialist	Antisocialist				
8	7									Article	Antisocialist	Antisocialist				
9	8									Article	Antisocialist	Antisocialist				
10	9									Article	Antisocialist	Antisocialist				
11	10									Article	Antisocialist	Antisocialist				
12	11									Article	Antisocialist	Antisocialist				
13	12									Article	Antisocialist	Antisocialist				
14	13									Article	Antisocialist	Antisocialist				
15	14									Article	Antisocialist	Antisocialist				
16	15									Article	Antisocialist	Antisocialist				
17	16									Article	Antisocialist	Antisocialist				
18	17									Article	Antisocialist	Antisocialist				
19	18									Article	Antisocialist	Antisocialist				
20	19									Article	Antisocialist	Antisocialist				
21	20									Article	Antisocialist	Antisocialist				
22	21									Article	Antisocialist	Antisocialist				
23	22									Article	Antisocialist	Antisocialist				
24	23									Article	Antisocialist	Antisocialist				
25	24									Article	Antisocialist	Antisocialist				
26	25									Article	Antisocialist	Antisocialist				
27	26									Article	Antisocialist	Antisocialist				
28	27									Article	Antisocialist	Antisocialist				
29	28									Article	Antisocialist	Antisocialist				
30	29									Article	Antisocialist	Antisocialist				
31	30									Article	Antisocialist	Antisocialist				
32	31									Article	Antisocialist	Antisocialist				
33	32									Article	Antisocialist	Antisocialist				
34	33									Article	Antisocialist	Antisocialist				
35	34									Article	Antisocialist	Antisocialist				
36	35									Article	Antisocialist	Antisocialist				
37	36									Article	Antisocialist	Antisocialist				
38	37									Article	Antisocialist	Antisocialist				
39	38									Article	Antisocialist	Antisocialist				
40	39									Article	Antisocialist	Antisocialist				
41	40									Article	Antisocialist	Antisocialist				
42	41									Article	Antisocialist	Antisocialist				
43	42									Article	Antisocialist	Antisocialist				
44	43									Article	Antisocialist	Antisocialist				
45	44									Article	Antisocialist	Antisocialist				

Figure B. Data were coded into Microsoft Excel prior to their transfer to RStudio.



**Figure C.** The total amount of narratives coded from *The War on Whites*. *The War on whites* contributed a total of 23% (n= 68) narratives across all four criteria, excluding anti-vaccination and anti-lgbt narratives.

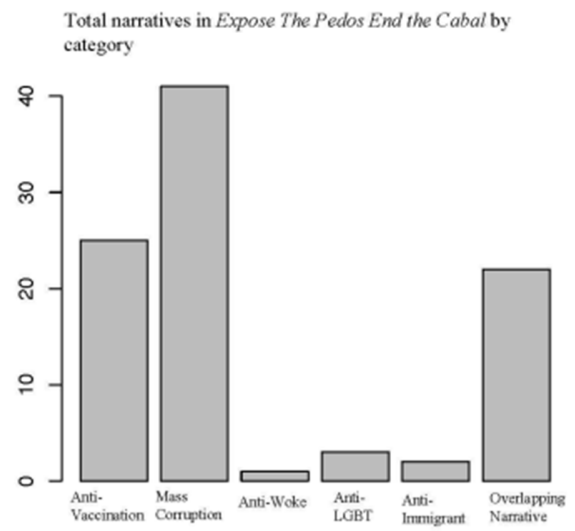


**Figure E.** The total amount of narratives coded from *Expose the Pedos End the Cabal*.

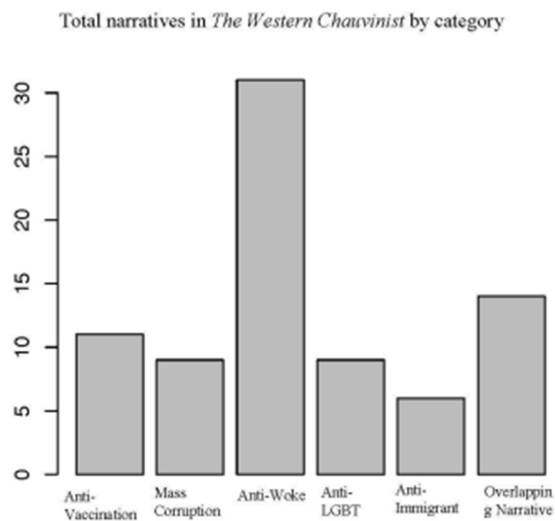


**Figure D.** The total number of narratives coded from *The Western Chauvinist*.

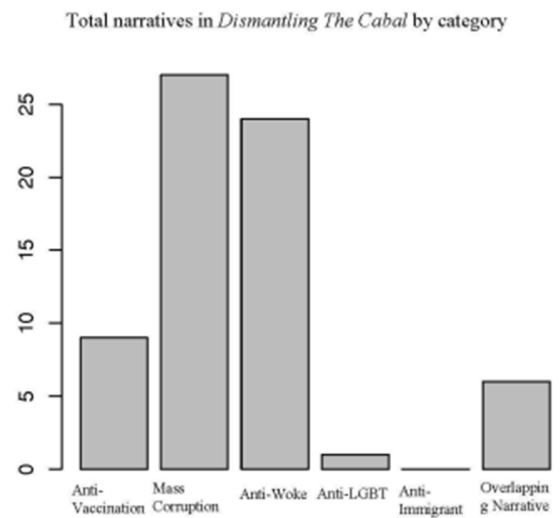


**Figure F.** The total amount of narratives coded from *Dismantling the Cabal*.

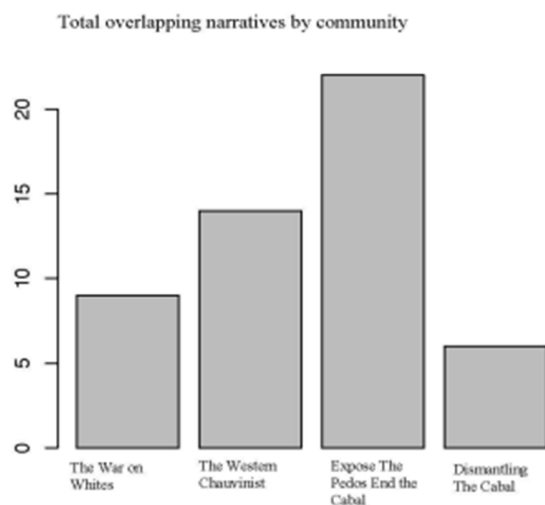


**Figure G.** Total amount of overlapping narrative domains in each community.

## II. DISCUSSION

Individuals who regularly engage with disinformation have been shown to harbor more prejudice views and be cognitively inflexible. The present research report is in line with previous analyses demonstrating that far-right disinformation and propaganda often targets minority communities, political figures and institutions. However, very little can be inferred about the broader ecological nature of extremism on social media websites given the limitations of the current data utilized by the present study.

## ACKNOWLEDGMENT

J. Calvert thanks Sheehan Kane for supervising original data collection at the National Consortium for the Study of Terrorism and Responses to Terrorism.

## REFERENCES

- [1] Amodio, D. M., & Cikara, M. (2021). The Social Neuroscience of Prejudice. *Annual Review of Psychology*, 72(1), 439–469. <https://doi.org/10.1146/annurev-psych-010419-050928>
- [2] Bélanger, J. J., Moyano, M., Muhammad, H., Richardson, L., Lafrenière, M.-A. K., McCaffery, P., Framand, K., & Nociti, N. (2019). Radicalization leading to violence: A test of the 3N model. *Frontiers in Psychiatry*, 10. <https://doi.org/10.3389/fpsy.2019.00042>
- [3] Decety, J., Pape, R., & Workman, C. I. (2017). A multilevel social neuroscience perspective on radicalization and terrorism. *Social Neuroscience*, 13(5), 511–529. <https://doi.org/10.1080/17470919.2017.1400462>
- [4] Douglas, K. M., & Sutton, R. M. (2008). The hidden impact of conspiracy theories: Perceived and actual influence of theories surrounding the death of princess diana. *The Journal of Social Psychology*, 148(2), 210–222. <https://doi.org/10.3200/socp.148.2.210-222>
- [5] Douglas, K. M., Uscinski, J. E., Sutton, R. M., Cichocka, A., Nefes, T., Ang, C. S., & Deravi, F. (2019). Understanding conspiracy theories. *Political Psychology*, 40(S1), 3–35. <https://doi.org/10.1111/pops.12568>
- [6] Goldenberg, A. (n.d.). Destroying families, dividing communities, undermining democracy. Network Contagion Research Institute CONTAGION AND IDEOLOGY REPORT. Retrieved June 3, 2022, from <https://eagleton.rutgers.edu/wp-content/uploads/2021/01/NCRI-The-QAnon-Conspiracy-FINAL.pdf>
- [7] Goreis, A., & Voracek, M. (2019). A systematic review and meta-analysis of psychological research on conspiracy beliefs: Field characteristics, measurement instruments, and associations with personality traits. *Frontiers in Psychology*, 10. <https://doi.org/10.3389/fpsyg.2019.00205>
- [8] Göttsche-Astrup, O., van den Bos, K., & Hogg, M. A. (2020). Radicalization and violent extremism: Perspectives from research on group processes and intergroup relations. *Group Processes & Intergroup Relations*, 23(8), 1127–1136. <https://doi.org/10.1177/1368430220970319>
- [9] Heltzel, G., & Laurin, K. (2020). Polarization in America: Two possible futures. *Current Opinion in Behavioral Sciences*, 34, 179–184. <https://doi.org/10.1016/j.cobeha.2020.03.008>
- [10] Islam, M. S., Kamal, A.-H. M., Kabir, A., Southern, D. L., Khan, S. H., Hasan, S. M., Sarkar, T., Sharmin, S., Das, S., Roy, T., Harun, M. G., Chughtai, A. A., Homaira, N., & Seale, H. (2021). Covid-19 vaccine rumors and conspiracy theories: The need for cognitive inoculation against misinformation to improve vaccine adherence. *PLOS ONE*, 16(5). <https://doi.org/10.1371/journal.pone.0251605>
- [11] Jensen, M. A., & Kane, S. (2021). Qanon-inspired violence in the United States: An empirical assessment of a misunderstood threat. *Behavioral Sciences of Terrorism and Political Aggression*, 1–19. <https://doi.org/10.1080/19434472.2021.2013292>
- [12] Jensen, M. A., Atwell Seate, A., & James, P. A. (2020). Radicalization to violence: A pathway approach to studying extremism. *Terrorism and Political Violence*, 32(5), 1067–1090. <https://doi.org/10.1080/09546553.2018.1442330>
- [13] Jungkunz, S. (2021, January 1). Political polarization during the COVID-19 pandemic. *Frontiers*. Retrieved May 17, 2022, from <https://doi.org/10.3389/fpos.2021.622512>
- [14] Kruglanski, A. W., Fernandez, J. R., Factor, A. R., & Szumowska, E. (2019). Cognitive mechanisms in violent extremism. *Cognition*, 188, 116–123. <https://doi.org/10.1016/j.cognition.2018.11.008>
- [15] Kruglanski, A. W., Gelfand, M. J., Bélanger, J. J., Sheveland, A., Hetiarachchi, M., & Gunaratna, R. (2014). The psychology of radicalization and deradicalization: How significance quest impacts violent extremism. *Political Psychology*, 35, 69–93. <https://doi.org/10.1111/pops.12163>
- [16] Miller, J. M. (2020). Do covid-19 conspiracy theory beliefs form a monological belief system? *Canadian Journal of Political Science*, 53(2), 319–326. <https://doi.org/10.1017/s0008423920000517>
- [17] Narvaes, R., & Martins de Almeida, R. M. (2014). Aggressive behavior and three neurotransmitters: Dopamine, GABA, and serotonin—a review of the last 10 years. *Psychology & Neuroscience*, 7(4), 601–607. <https://doi.org/10.3922/j.psns.2014.4.20>
- [18] Pereira, P. S., Silveira, A. da, & Pereira, A. (2020). Disinformation and conspiracy theories in the age of covid-19. *Frontiers in Sociology*, 5. <https://doi.org/10.3389/fsoc.2020.560681>
- [19] Renström, E. A., Bäck, H., & Knapton, H. M. (2020). Exploring a pathway to radicalization: The effects of social exclusion and rejection sensitivity. *Group Processes & Intergroup Relations*, 23(8), 1204–1229. <https://doi.org/10.1177/1368430220917215>
- [20] Ross, A. R., Modi, M., Paresky, P., Jussim, L., Harrell, B., Goldenberg, A., Goldenberg, P., Finkelstein, D., Farmer, J., Holden, K., Riggelman, D., Shapiro, J., & Finkelstein, J. (2021, October 4). A contagion of institutional distrust: Viral disinformation of the COVID vaccine and the road to reconciliation. Network Contagion Research Institute. Retrieved from <https://networkcontagion.us/reports/a-contagion-of-institutional-distrust/>
- [21] Tusche, A., Kahnt, T., Wisniewski, D., & Haynes, J.-D. (2013). Automatic processing of political preferences in the human brain. *NeuroImage*, 72, 174–182. <https://doi.org/10.1016/j.neuroimage.2013.01.020>
- [22] van Prooijen, J.-W., & van Vugt, M. (2018). Conspiracy theories: Evolved functions and psychological mechanisms. *Perspectives on Psychological Science*, 13(6), 770–788. <https://doi.org/10.1177/1745691618774270>
- [23] Weissflog, M., Choma, B. L., Dywan, J., van Noordt, S. J., & Segalowitz, S. J. (2013). The political (and physiological) divide: Political orientation, performance monitoring, and the anterior cingulate response. *Social Neuroscience*, 8(5), 434–447. <https://doi.org/10.1080/17470919.2013.833549>



- [24] Wood, M. J., Douglas, K. M., & Sutton, R. M. (2012). Dead and alive. *Social Psychological and Personality Science*, 3(6), 767–773. <https://doi.org/10.1177/1948550611434786>
- [25] Youngblood, M. (2020). Extremist ideology as a complex contagion: The spread of far-right radicalization in the United States between 2005 and 2017. *Humanities and Social Sciences Communications*, 7(1). <https://doi.org/10.1057/s41599-020-00546-3>
- [26] Zmigrod, L. (2020). A neurocognitive model of ideological thinking. <https://doi.org/10.31234/osf.io/sq4da> G. O. Young, “Synthetic structure of industrial plastics (Book style with paper title and editor),” in *Plastics*, 2nd ed. vol. 3, J. Peters, Ed. New York: McGraw-Hill, 1964, pp. 15–64.

# The Effectiveness of Congressional Redistricting Commissions: A Comparative Approach Investigating the Ability of Commissions to Reduce Gerrymandering with the Wilcoxon Signed-Rank Test

Arvind Salem

**Abstract**— Voters across the country are transferring the power of redistricting from the state legislatures to commissions to secure “fairer” districts, by curbing the influence of gerrymandering on redistricting. Gerrymandering, intentionally drawing distorted districts to achieve a political advantage, has become extremely prevalent, generating widespread voter dissatisfaction, and resulting in states adopting commissions for redistricting.

However, the efficacy of these commissions is dubious, with some arguing that they constitute a panacea for gerrymandering, while others contend that commissions have relatively little effect on gerrymandering. A result showing that commissions are effective would allay these fears, supplying ammunition for activists across the country to advocate for commissions in their state, reducing the influence of gerrymandering across the nation. However, a result against commissions may reaffirm doubts about commissions and pressure lawmakers to make improvements to commissions or even abandon the commission system entirely. Additionally, these commissions are publicly funded: so, voters have a financial interest and responsibility to know if these commissions are effective. Currently, nine states place commissions in charge of redistricting, Arizona, California, Colorado, Michigan, Idaho, Montana, Washington, and New Jersey (Hawaii also has a commission but will be excluded for reasons mentioned later).

This study compares the degree of gerrymandering in the 2022 election (“after”) to the election in which voters decided to adopt commissions (“before”). The before election provides a valuable benchmark for assessing the efficacy of commissions since voters in those elections clearly found the districts to be unfair, therefore comparing the current election to that one is a good way to determine if commissions have improved the situation. At the time Hawaii adopted commissions, it was merely a single at-large district so its before metrics could not be calculated, and it was excluded.

This study will use three methods to quantify the degree of gerrymandering: the efficiency gap, the percentage of seats and the percentage of votes difference, and the mean-median difference. Each of these metrics has unique advantages and disadvantages, but together, they form a balanced approach to quantifying gerrymandering.

The study uses a Wilcoxon Signed-Rank Test with a null hypothesis that the value of the metrics is greater than or equal to in the after election than before and an alternative hypothesis that the

value of these metrics is greater in the before election than after using a 0.05 significance level and an expected difference of 0. Accepting the alternative hypothesis would constitute evidence that commissions reduce gerrymandering to a statistically significant degree.

However, this study could not conclude that commissions are effective. The p values obtained for all three metrics ( $p=0.42$  for the efficiency gap,  $p=0.94$  for the percentage of seats and percentage of votes difference, and  $p=0.47$  for the mean-median difference) were extremely high and far from the necessary value needed to conclude that commissions are effective. These results halt optimism on commissions and should spur serious discussion about the effectiveness of these commissions and ways to change them moving forward so that they can accomplish their goal of generating fairer districts.

**Keywords**- Commissions, elections, gerrymandering, redistricting.

# An Auxiliary Technique for Coronary Heart Disease Prediction by Analyzing ECG Based on ResNet and Bi-LSTM

Yang Zhang, Jian He

**Abstract**—Heart disease is one of the leading causes for death in the world, and coronary heart disease (CHD) is one of the major heart diseases. Electrocardiogram (ECG) is widely used in the detection of heart diseases, but the traditional manual method for CHD prediction by analyzing ECG requires lots of professional knowledge for doctors. This paper introduces sliding window and continuous wavelet transform (CWT) to transform ECG signals into images, and then ResNet and Bi-LSTM are introduced to build the ECG feature extraction network (namely ECGNet). At last, an auxiliary system for coronary heart disease prediction was developed based on modified ResNet18 and Bi-LSTM, the public ECG dataset of CHD from MIMIC-3 was used to train and test the system. The experimental results show that the accuracy of the method is 83%, and the F1-score is 83%. Compared with the available methods for CHD prediction based on ECG, such as kNN, decision tree, VGGNet, etc., this method not only improves the prediction accuracy, but also could avoid the degradation phenomenon of deep learning network.

**Keywords**—Bi-LSTM, CHD, ECG, ResNet, Sliding window.

## I. INTRODUCTION

HEART disease is the main cause of death nowadays, and CHD is the most common form of cardiovascular disease, accounting for about 13% of deaths in the United States [1]. Timely diagnosis of CHD is crucial to reduce the health risks caused by CHD such as cardiac arrest, so researchers began to study auxiliary diagnostic techniques for CHD.

In medicine, the auxiliary diagnostic techniques of CHD mainly include the auxiliary diagnosis based on physiological indicators, based on cardiac medical imaging and based on ECG. Among them, studies on auxiliary diagnosis based on physiological indicators: Kannel et al. found that major risk factors such as hypertension, high cholesterol and diabetes are related to CHD [2]; Uyar et al.'s study on the general population showed that high levels of creatinine in blood can increase the risk of CHD [3]; In addition, blood cholesterol and glycoprotein levels in patients with CHD have been found to be consistently and significantly increased [4]. However, these measurements and analyses of many physiological indicators of CHD will increase the complexity of auxiliary diagnosis. In contrast, the auxiliary diagnosis of CHD based on medical imaging has the characteristics of accuracy and efficiency. For example, Madani et al. used a deep learning model [5] on echocardiogram images

to judge CHD; Shi et al. applied Coronary arteriography (CAG) technique to the identification and diagnosis of CHD in Chinese medicine and achieved good results [6]. However, imaging test for CHD are expensive and the use of imaging techniques can be physically damaging to patients. ECG monitors patients' real-time ECG signals to assist doctors in disease diagnosis, and is a commonly used auxiliary diagnostic technique for CHD [7]. For example, Jin et al. used ECG signals to predict clinically important parameters related to patients with CHD (such as heart rate and axial migration) [8]; Wang et al. analyzed the nonlinear dynamic characteristics of ECG to diagnose CHD [9].

With the development of IT technology, researchers apply machine learning techniques to the study of CHD auxiliary diagnostic technology. Among them, the techniques using traditional machine learning algorithms are based on statistical analysis, decision tree and artificial neural network. For example, Cross et al. proposed a risk scoring system for clinical risk factors of CHD based on Cox regression model using physiological indicators such as serum protein, etc. to prevent the occurrence of CHD [10]; Meghan et al. studied the relationship between serum ferritin and the risk of CHD by using logistic regression and found that the risk of CHD increased by 5.1% for every 10 units of serum ferritin increase [11]. However, the simple prediction effect of these regression analysis methods is not significant. In terms of relevant research based on decision tree: Maryam et al. established a prediction model of CHD based on 12 physiological indicators by using decision tree algorithm [12]; Karaolis et al. used C4.5 decision tree to predict the occurrence of CHD based on three groups of physiological indicators, with an accuracy of 75% [13]. However, the method based on decision tree ignores the correlation between data and is prone to overfitting. In terms of research based on artificial neural network: Rajeswari et al. proposed to use artificial neural network technology to mine knowledge from medical data to identify the risk level of CHD [14]. However, artificial neural networks are less efficient to train against large architectures. Most of the above machine learning methods for CHD diagnosis are based on numerous physiological indicators. With the success of deep learning technology in natural language processing (NLP), computer vision and other aspects, researchers have tried to apply deep learning technology in the auxiliary diagnosis of CHD in recent years. For example, Han et al. found in a comparative study that VGGNet19 convolutional network could effectively improve the efficiency of left ventricular segmentation of echocardiography and play an important role in the diagnosis of

Yang Zhang is a Master's Student, Faculty of Information Technology, Beijing University of Technology (corresponding author, phone: (+86)18851966351; e-mail: 1271157595@qq.com).

Jian He is An Associate Professor, Faculty of Information Technology, Beijing University of Technology.

CHD [15]; Li et al. proposed a Deep Neural Network (DNN) based model named craftNet, which is used to accurately identify manual features to detect CHD and achieved a good accuracy [16]. Although ECG is an important technology in the auxiliary diagnosis of CHD, there is currently a lack of application of deep learning in the analysis of ECG data. In this paper, ECG scalogram is constructed by sliding window and CWT, and ECG time-frequency feature extraction network is constructed by combining ResNet and Bi-LSTM techniques, an ECG auxiliary diagnosis network with ResNet and Bi-LSTM is implemented named ECGNet. In addition, the ECG datasets exposed by MIMIC-3 was used for network training and testing, and the effectiveness of the proposed method was verified by experiments.

The remainder of this paper is organized as follows. Section II analyzes the ECG differences between CHD patients and normal people, and introduces the technology of Butterworth high-pass filter to denoise the original ECG signals, and the technology of sliding window and CWT to extract the time-frequency features of ECG. Section III introduces the network architecture of ECGNet and the principles of ResNet and Bi-LSTM respectively. Section IV introduces the implementation method of ECGNet. Section V uses MIMIC-3 ECG datasets for network training and verification, and analyzes the experimental results. Section VI presents the conclusion, and the suggestion for future works.

## II. METHODOLOGY

In this section, based on the analysis of ECG features of CHD patients, noise in ECG data is filtered by Butterworth high-pass filter, secondly, sliding window and CWT techniques are introduced to realize time-frequency feature conversion of ECG signals, which provide the basis for the subsequent construction of deep learning-based auxiliary diagnosis of CHD.

### A. ECG Feature analysis for CHD

Since myocardial ischemia caused by CHD can cause specific changes in ECG, ECG is an important tool to monitor heart status and is commonly used in clinical diagnosis of CHD. Compared with the ECG of a normal person, the ECG of patients with CHD has three characteristics: (1) the T-wave is sometimes low, or inverted, bidirectional; (2) Downward or upward movement of the ST segment in the ECG; (3) The decrease or disappearance of R-wave in electrocardiogram. Fig. 1 compares the ECG images of normal person and patients with CHD. I, II and III in the figure are the data sampled from the three lead positions of the ECG, it can be seen that data from CHD patient in all three lead positions may have all three of these characteristics, so it is only necessary to select one of the lead positions to study the characteristics of coronary patients, and in this paper the lead III portion of the ECG is selected.

Generally, ECG data collected by instruments and devices are susceptible to effects such as respiration, which can generate ultra-low frequency signal noise, thus leading to baseline roaming effect [17]. To this end, a 0.5Hz Butterworth high-pass filter is used to remove baseline drift caused by

motion, sensor impedance and respiration. The ideal high-pass filter cannot be realized by electronic components and has ringing phenomenon. Therefore, Butterworth high-pass filter is the most commonly used high-pass filter in practice. The transfer function of the filter is shown refer to (1):

$$H(u, v) = 1 / (1 + (D_0 / D(u, v))^{2n}) \quad (1)$$

$D(u, v)$  Represents the distance from the midpoint of the frequency to the frequency plane and is the cut-off frequency. When  $D(u, v)$  is greater than the  $D_0$ , the corresponding  $H(u, v)$  gradually close to 1, so as to make the high frequency part to pass; When  $D(u, v)$  is less than the  $D_0$ ,  $H(u, v)$  gradually tend to be 0, realize the low frequency part of the filter. In this paper, the low-frequency signal noise in ECG data is filtered by Butterworth high-pass filter.

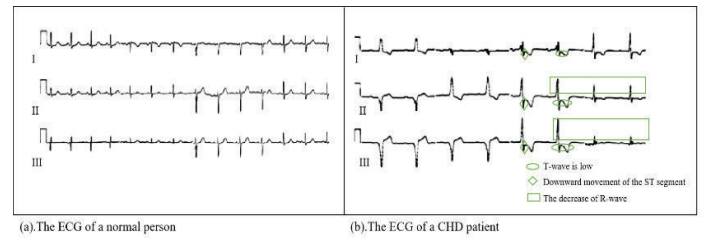


Fig. 1 Comparison of ECG between normal and CHD patients.

### B. Sliding Window for ECG

Since the human ECG data collected by ECG is continuous stream data, it cannot be directly applied to machine learning algorithms. In this regard, the sliding window technique is introduced in this paper to segment the ECG data. In this paper, a timestamp is set for each ECG data, as new ECG data are continuously generated, the system continuously updates the old data in the window according to the first-in-first-out principle based on the timestamp. The sliding window maintains the integrity and temporal order of ECG data, which provides the basis for subsequent feature extraction and analysis based on deep learning models.

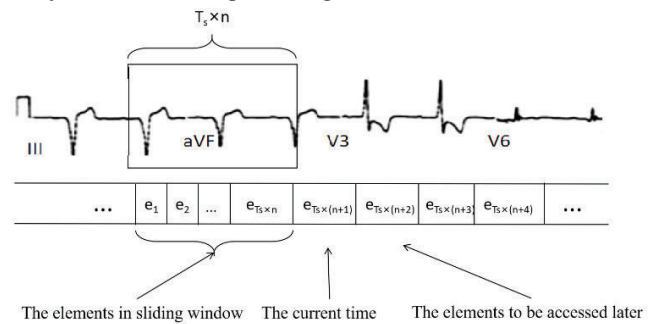


Fig. 2 Sliding window of ECG data.

Fig. 2 shows an example of a sliding window of ECG data. In this case, the newly sensed data elements come from the right side of the window, and the elements on the left side of the window are moved out of the window according to the first-in-first-out principle. The sliding window contains a total of  $T_s \times n$  time periods of sensed data (i.e., the window size).  $T_s$  is the sampling period,  $n$  is the sampling frequency, each element  $e_j$  in the window is the denoised ECG data sampled at moment  $j$ ,

and  $T$  is the total duration of ECG data sampling for a patient. With the sliding window, the continuous ECG data of a patient can be divided into  $N$  segments referring to (2).

$$N = \frac{T - T_s \times n}{s} + 1 \quad (2)$$

### C. Frequency Feature Analysis based on Wavelet

For the ECG data after denoising and sliding window processing, this paper uses the continuous wavelet transform (CWT) to convert the ECG data into a scalogram which contains the time-frequency domain features of the ECG to provide a basis for developing ECG-based deep learning algorithms. The scalogram is defined as the absolute value of the CWT of the signal, which as a function of time and frequency [18] can identify the low-frequency and fast-changing frequency components of the ECG signal. The original ECG data is a one-dimensional vector signal that can be converted into a three-channel RGB image by the CWT. Compared with the short-time Fourier transform, the CWT can provide better temporal localization for short-time, high-frequency events, and better frequency localization for low-frequency, long-time events.

ECG signals have rich information in the time-frequency domain. The wavelet coefficients of the CWT can be used to locate the different frequency components. The CWT is defined referring to (3):

$$\text{CWT}_x^\psi(\tau, s) = \Psi_x^\psi(\tau, s) = \frac{1}{\sqrt{|s|}} \int x(t) \psi\left(\frac{t-\tau}{s}\right) dt \quad (3)$$

$x(t)$  is primary time domain signal,  $\Psi(t)$  is wavelet basis,  $\tau$  and  $s$  are translation and scale transformation of the wavelet basis.

Fig. 3 shows the ECG scalogram generated by CWT of a segment of ECG data, which contains the time-domain and frequency-domain features of the ECG signal of the patient over a period of time, which provides a basis for the study of deep learning-based auxiliary diagnosis techniques for CHD.

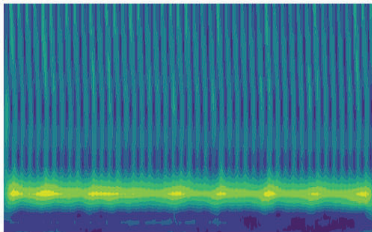


Fig. 3 Scalogram image of an ECG data

## III. CHD PREDICTION NETWORK BASED ON ECG SIGNAL

In this section, ResNet and Bi-LSTM are introduced to construct the network architecture for CHD auxiliary diagnosis, and the principles and important parameters of ResNet and Bi-LSTM are introduced.

### A. Architecture of the ECGNet

The denoised original ECG is converted into ECG scalogram by sliding window and CWT, and the features of these

scalograms can be extracted using convolutional networks. Based on the analysis and comparison of classical convolutional neural networks such as LeNet-5[19], AlexNet[20], VGGNet[21], ResNet, and combining the advantages of RNN recurrent neural networks in processing continuous serialized data, we propose a network architecture oriented to ECG feature extraction, namely ECGNet. As shown in Fig. 4, ECGNet consists of input layer, ResNet layer, Bi-LSTM layer, Fully connected layer, and Softmax layer.

The input layer denoises the patient's original ECG data and generates a multi-segment ECG scalograms through sliding window and CWT processing. The ResNet layer consists of several convolutional and residual blocks and pooling layers, which extracts time-frequency features from multi-segment ECG scalograms. After that, the Bi-LSTM layer extracts the  $N$  segment feature data from the ResNet layer through the bidirectional long and short-term memory network. Finally, the feature data extracted by ResNet layer and Bi-LSTM layer are classified through the Fully connected layer and Softmax layer, and the category with the highest probability is output as the prediction result.

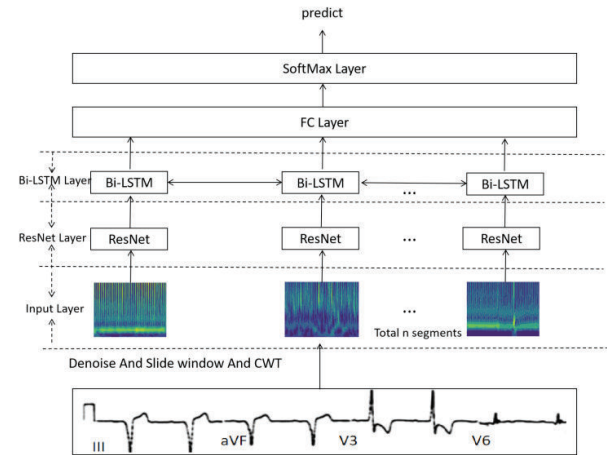


Fig. 4 ECGNet Architecture

### B. ECG Feature Extraction based on ResNet

Residual network is a kind of deep neural network, which is composed of multiple residual units. As shown in Fig. 5, each residual unit is implemented through a forward neural network and a shortcut connection. The core idea is the introduction of residual edge, that is, an edge connected directly from the input to the operation " $\oplus$ ", on which  $h$  transformation is applied to the original input  $X_i$ . The residual unit can realize the fusion of features at different scales, and the residual network formed by it can effectively solve the gradient dispersion and degradation problems due to the increasing depth of deep learning network [22].

The  $i$ -th residual unit is shown in Fig. 5, whose input is  $X_i$ ,  $F$  is network mapping transformation of input  $X_i$ , which can be a multilayer perceptron network, can also be a convolutional neural network and so on.  $X_{i+1}$  is the output of the " $\oplus$ " operation after the  $F$  and  $h$  transformations of the input  $X_i$ , and then the activation function  $f$ . The residual unit can be calculated referring to (4) and (5).



$$\mathbf{x}_{i+1} = f(h(\mathbf{x}_i) + F(\mathbf{x}_i, \mathbf{W}_i)) \quad (4)$$

If the equation  $h$  is the identity function, i.e.  $h(\mathbf{x}_i) = \mathbf{x}_i$ ; According to the equation (4), The features learned from shallow layer 1 to deep layer L can be calculated referring to (5)

$$\mathbf{x}_L = \mathbf{x}_1 + \sum_{i=1}^{L-1} F(\mathbf{x}_i, \mathbf{W}_i) \quad (5)$$

Experimental analysis proves that when  $h$  is the identity function,  $F$  is the convolutional network, and the activation function  $f$  is Relu, the residual network effect is optimal [22]. At the same time, based on the residual unit can form a deep network containing hundreds or thousands of layers, The network can effectively solve the gradient dispersion and degradation problems caused by the increasing number of layers in the deep learning network and can extract multi-scale feature fusion. Therefore, this paper adopts the fusion of convolutional network and constant shortcut connection of residual units to construct the feature extraction network of ECG scalogram.

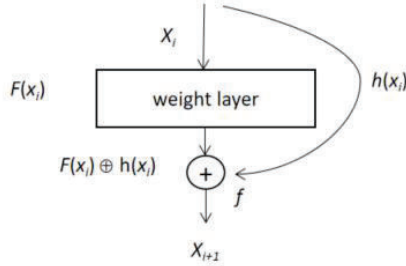


Fig. 5 residual block

### C. ECG Feature Extraction based on Bi-LSTM

ResNet can generate  $n$  ECG feature vectors based on the sliding window, and there are temporal dependencies between these neighboring feature vectors. In this paper, Bi-LSTM is introduced to extract these temporal dependencies. As an improved cyclic neural network (RNN), Bi-LSTM can solve the problem of long distant dependence between data that RNN cannot process.

As shown in Fig. 6, the Bi-LSTM structural model can be divided into two independent LSTMS.  $X_1, X_2 \dots X_n$  is the input,  $\vec{h}_t$  and  $\overleftarrow{h}_t$  represents the output of forward LSTM and reverse LSTM, that is, the output of Bi-LSTM network  $H_i$  is the stack of forward LSTM and reverse LSTM. The input sequences were respectively input into two LSTM neural networks in forward and reverse directions for feature extraction, whose expressions are shown referring to (6) and (7).

$$\vec{h}_t = f(\vec{b} + [\mathbf{x}_t, \mathbf{h}_{t-1}] \times \vec{w}) \quad (6)$$

$$\overleftarrow{h}_t = f(\overleftarrow{b} + [\mathbf{x}_t, \mathbf{h}_{t+1}] \times \overleftarrow{w}) \quad (7)$$

$f$  is the activation function; The output of forward LSTM is  $\vec{h}_t$ ; Forward bias and weight are the  $\vec{b}$  and  $\vec{w}$ ; The output of the reverse LSTM neural network is  $\overleftarrow{h}_t$ ; and the reverse bias and weight are  $\overleftarrow{b}$  and  $\overleftarrow{w}$ . By splicing forward LSTM neural network and reverse LSTM neural network together, the output  $H_i$  of Bi-LSTM neural network can be obtained referring to (8).

$$H_i = c + g([\vec{h}_t, \overleftarrow{h}_t] \times U) \quad (8)$$

$g$  is the activation function;  $H_i$  is the output of Bi-LSTM; The biases and weights are  $c$  and  $U$ . The idea of Bi-LSTM model design is to make the characteristic data obtained at time  $t$  contain the information between the past and the future. Experimental results show that this neural network model is superior to a single LSTM model in feature extraction efficiency and performance.

In this paper, ECGNet adopts a single layer Bi-LSTM network architecture to extract the ECG feature vectors fused with ECG temporal correlations. These ECG feature vectors pass through the subsequent FC layer and Softmax layer to classify.

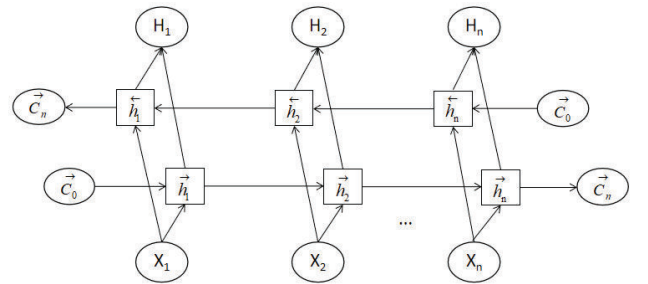


Fig. 6 structure of Bi-LSTM

## IV. IMPLEMENTATION

In this section, based on the above ECGNet architecture, we optimize the ResNet18 residual network and combines Bi-LSTM to design and implement ECGNet.

### A. Implementation of ResNet

This paper optimizes the network model of ResNet18 and generates the residual network model shown in Fig. 7. This model includes 8 residual units, which are composed of 17 convolution layers and two pooling layers. For the 640x480x3 ECG scalogram generated by CWT, it was first uniformly reduced to 320x240x3 size images as the input of the residual network.

C1 is the first convolution block, the block contains only one layer, the kernel size is 7 x7, stride is 2, padding is 3, output channel is 64, after the layer feature vector into 64x160 x120.

S1 is the Max pooling layer, the kernel size is 3x3, stride is 2, padding is 1, after the layer feature vector into 64x80x60.

C2 to C5 are convolution blocks with residual structure. Every convolution block contains four convolution layers and two residual units, every two convolution layers have one shortcut links, each convolution layer's kernel size is 3x3, and the padding is 1. C2 convolution block's stride is 1, output channel is 64, after the C2 layer feature vector is still 64x80x60. C3 convolution in addition to the first layer's stride is 2, the rest of the stride is 1, the output of the channel is 128, after the C3 layer feature vector into 128x40x30. C4 convolution block layer in addition to the first layer's stride is 2, the rest of the stride is 1, the output of the channel is 256, after the C4 layer feature vector into 256x20x15. C5 in addition to the first layer's

stride is 2, the rest of the stride is 1, the output channel number is 512, after the C5 layer feature vector into  $512 \times 10 \times 7$ .

S2 is an Average pooling layer, after the layer feature vector into  $512 \times 1 \times 1$ .

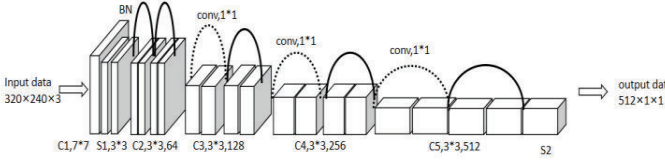


Fig. 7 Implementation of ResNet

Through the above residual network, the input ECG scalogram with the size of  $320 \times 240 \times 3$  is converted into  $512 \times 1 \times 1$  feature vectors for subsequent Bi-LSTM network processing.

### B. Implementation of Bi-LSTM

The above vector generated by ResNet is the feature vector generated by convolution of an ECG scalogram, since the sliding window divides the ECG data into  $N$  segments,  $N$ -segment  $512 \times 1 \times 1$  vectors are generated. These vectors are arranged in the order  $X_1 \sim X_N$ . After a single layer of Bi-LSTM, a feature vector  $v$  containing the entire ECG data of a patient is generated. The hidden layer of Bi-LSTM is set to 256, and other parameters are default values. After that, classification results are output through the Fully connected layer and Softmax layer. As in Fig. 8.

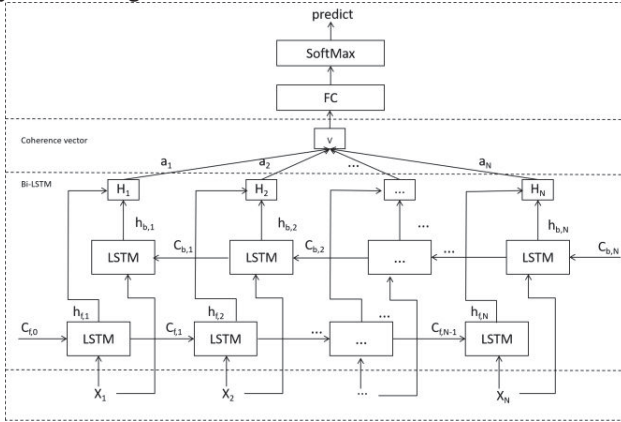


Fig. 8 Implementation of Bi-LSTM

### C. Loss Function

The loss function adopted by ECGNet is cross-entropy loss function, which is often used in the loss calculation of classification problems. It can capture the difference of the relative size of prediction probability and further measure the performance of different classifiers in a more detailed way. Its expression is referring to (9):

$$\text{Loss} = \frac{1}{N} \sum_{i=1}^N y_{ij} \log(p_{ij}), j = 1, 2, \dots, C \quad (9)$$

$N$  is the sample number;  $C$  is classification number;  $y_{ij}$  expresses the case of a sample  $i$  belong to the sample  $j$ , which only has two values, 0 or 1; And  $p_{ij}$  expresses the probability of a sample  $i$  forecast for the sample  $j$ , which values range of  $[0, 1]$ .

## V. EXPERIMENT AND ITS ANALYSIS

In this section, we use MIMIC-3 ECG datasets for network training and testing, and analyzes the experimental results.

### A. Data set preparation

In this paper, we use PhysioNet's MIMIC-3 (Marketplace for Medical Information in Intensive Care) database [23], which is a publicly available multiparametric intensive care database provided by the Massachusetts Institute of Technology. The dataset contains physiological data such as ECG, photovolumetric pulse wave signals (PPG), arterial blood pressure signals (ABP) and respiratory signals (RESP) collected from patients in ICU wards, which has been successfully used in several research areas after more than 10 years of multidisciplinary construction.

This paper uses ECG data from the matched subset of the MIMIC-3 waveform database [24] to predict CHD. This dataset uses ICD-9 codes to code for CHD and assigns ICD-9 codes to each CHD patient in the MIMIC-3 database. This paper randomly selected 1230 patients from the large MIMIC-3 dataset for the study, of which 406 patients were diagnosed with coronary heart disease. Data from 904 of the 1230 patients were randomly selected for training (which contained 302 patients with CHD), 100 patients were used for validating (which contained 35 patients with CHD) and 226 patients were used for testing (which contained 69 patients with coronary heart disease).

For the ECG data of 1230 patients, we sequentially performed denoising, sliding window, and CWT to generate multi-segment ECG scalograms.

### B. Model evaluation criteria and Systematic experiment

In this paper, accuracy rate, recall rate and F1-score which take both accuracy rate and recall rate are used as evaluation indexes of the model, F1-score is shown referring to (10).

$$F_1 = \frac{2 \times \text{Precision} \times \text{Recall}}{\text{Precision} + \text{Recall}} \quad (10)$$

Precision describes how many of the positive cases predicted by the bi-classifier are accurate, which defined referring to (11), recall represents the recall of the results defined referring to (12), which describes how many of the true positive cases in the test set are selected by the bi-classifier, i.e., how many true positive examples were recalled by that bi-classifier.  $TP$  in (11)(12) indicates that the real and predicted results are positive examples;  $FP$  indicates that the true result is a negative case and the predicted result is a positive case; and  $FN$  indicates that the true result is a positive case and the predicted result is a negative case.

$$\text{Precision} = \frac{TP}{TP + FP} \quad (11)$$

$$\text{Recall} = \frac{TP}{TP + FN} \quad (12)$$

This paper selected a server equipped with Ubuntu operating system, which was specifically configured with E5-2620 CPU, 125 GB memory and TESLA M40 graphics acceleration



card. This paper used Pytorch and Python to implement ECGNet.

The training parameters of ECGNet network are as follows: 60 batches are used, batch size is 16, 70 epoches are run, learning rate is 0.001, Adam optimizer is used, cross entropy loss function is adopted. The above parameter sets are used as inputs to train the model.

### C. Experimental Analysis

First of all, in order to verify the effect of Butterworth high-pass filter on denoising, this paper compares the results of the ECGNet with and without denoising in the early stage, as shown in Table I. The results show that it is necessary to introduce Butterworth high-pass filter to filter low frequency waveforms.

TABLE I  
COMPARISON RESULTS OF DENOISING OR NOT

Denoise or not	Accuracy	Recall	F1-score
Denoise	0.83	0.85	0.83
Not Denoise	0.72	0.73	0.72

In order to verify the validity of the ECGNet network model proposed in this paper, the research group compared the model with two traditional machine learning algorithms, K-NN [25] (k takes 3) and decision tree, as well as the popular deep learning algorithm for medical image classification: VGGNet (9 convolutional layers, 3 pooling layers and 1 global average pooling layer, all of the kernel size is 3x3) and ResNet18, ResNet34 and ResNet50, as shown in Table II. The results of table show that ECGNet model is significantly superior to these models. This may be due to the limited ability of traditional machine learning methods such as K-NN and decision tree to extract time-frequency features, while deep learning models such as VGGNet only rely on convolution, so they cannot extract and remember sequential features in ECG data. Therefore, the effectiveness of the proposed model combining sliding window and Bi-LSTM is proved.

TABLE II  
COMPARISON RESULTS OF DIFFERENT MODELS

Model	Accuracy	Recall	F1-score
VGGNet	0.63	0.66	0.65
ResNet18	0.7	0.71	0.7
ResNet34	0.7	0.68	0.69
ResNet50	0.66	0.65	0.66
ECGNet	0.83	0.85	0.83
K-NN	0.61	0.59	0.6
Decision Tree	0.58	0.6	0.59

This paper also conducted experimental analysis on the sliding window length and step size used for data segmentation, and the results are shown in Fig. 9. It can be seen that as the

window length increases from 20s to 45s, the F1-score predicted by CHD generally increases first and then decreases, among which, the window length reaches the maximum peak at 30s. This indicates that the F1-score of CHD prediction is not higher with the longer sliding window length, but has an optimal state is at 30s. Too small or too large window length is not conducive to feature extraction. After determining the size of the sliding window length, this paper analyzed the influence of the window step size. The window step size is usually smaller than the window length, which causes a partial overlap of active data between two adjacent windows. As can be seen from the Fig. 9, with the window step size increasing from 1s to 25s, F1-score of CHD prediction generally increased first and then decreased, reaching the peak value at 15s. Through experiment, this paper found that the prediction accuracy of CHD is the highest when the window step is half of the window length.

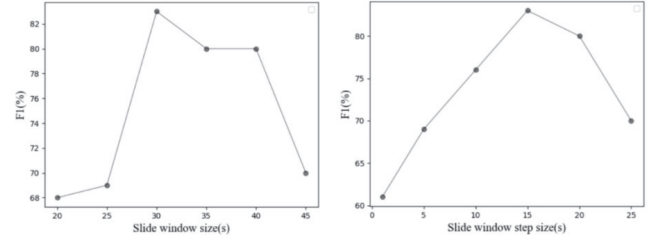


Fig. 9 Comparison of different sliding window size and step size

At the same time, this paper also compared the performance of increasing the number of Bi-LSTM layers with the same parameter settings as above, as shown in Table III. This comparison test is based on the ECGNet, just simply increasing the number of Bi-LSTM layers to compare and observe the effect of the model with different layers of Bi-LSTM. The table shows that the Bi-LSTM model with single layer has better results than that with two or three layers. Perhaps because single-layer Bi-LSTM is sufficient to memorize ECG data temporal dependencies. Therefore, a single-layer Bi-LSTM is used in this paper.

TABLE III  
COMPARISON RESULTS OF DIFFERENT BI-LSTM LAYERS

Layer number	Accuracy	Recall	F1-score
1	0.83	0.85	0.83
2	0.79	0.80	0.79
3	0.75	0.72	0.73

## VI. CONCLUSION

In this paper, we use sliding window, CWT technique to extract the ECG time-frequency domain features of CHD patients, and propose a CHD auxiliary diagnosis model ECGNet that fuses ResNet and Bi-LSTM network, with this model, the ECG signals of patients can be used for CHD auxiliary diagnosis, and this paper conducts experimental comparison based on the publicly available MIMIC-3 ECG database, the experimental results show that the method is

better than some traditional image classification methods K-NN, decision tree, VGGNet, ResNet18, ResNet34 and ResNet50. By comparing different sliding window length and step size, it is found that setting the sliding window length as 30s and step size as 15s is optimal. And after the comparison of increasing the number of Bi-LSTM layers, it was found that ECGNet is a better model for CHD auxiliary diagnosis.

The deep learning CHD auxiliary diagnosis network designed in this paper based on ECG data analysis can be further improved and refined in subsequent studies. For example, although ECG data is an effective mean to CHD, in practice, doctors often combine physiological indicators such as blood pressure, cholesterol and blood glucose to auxiliary diagnosis. Therefore, in the future, the group will study the auxiliary diagnostic technique of CHD by integrating ECG with other physiological indicators.

#### REFERENCES

- [1] Benjamin, E. J. et al. (2019). Heart Disease and Stroke Statistics—2019 Update: A Report from the American Heart Association. American Heart Association, 139, 56–528.
- [2] Kannel, W. B., Castelli, W. P., Gordon, T. & McNamara, P. M. (1971). Serum cholesterol, lipoproteins, and the risk of coronary heart disease. The Framingham study. *Ann Intern Med*, 74(1), 1-12.
- [3] Irie, F., Iso, H., Sairenchi, T., Fukasawa, N., Yamagishi, K., Ikehara, S., Kanashiki, M. (2006). The relationships of proteinuria, serum creatinine, glomerular filtration rate with cardiovascular disease mortality in Japanese general population. *Kidney Int.*, 69(7), 1264-71.
- [4] Burchfiel, C. M., Tracy, R. E., Chyou, P. & Strong, J. P. (1997). Cardiovascular Risk Factors and Hyalinization of Renal Arterioles at Autopsy. *Arteriosclerosis, Thrombosis, and Vascular Biology*, 17(4), 760–768.
- [5] Madani, A., Arnaout, R., Mofrad, M., Arnaout, R. (2018) Fast and accurate view classification of echocardiograms using deep learning. *npj Digital Medicine*, 1, 6.
- [6] Shi Z X , Gu W L . [Exploration of TCM syndrome differentiation of coronary heart disease and coronary arteriography][J]. *Chinese Journal of Integrated Traditional & Western Medicine*, 2007, 27(1):76.
- [7] Yan Z , Jiang S , Jiao N , et al. The clinical diagnosis effect analysis of electrocardiogram(ECG)and ultrasonic cardiogram(UCG) for coronary atherosclerotic heart disease(CHD)[J]. *China Modern Doctor*, 2015.
- [8] Jin, Z., Sun, Y., Cheng, A. C. (2009) Predicting cardiovascular disease from real-time electrocardiographic monitoring: An adaptive machine learning approach on a cell phone. *Conf Proc IEEE Eng Med Biol Soc.*, 6889-92.
- [9] Wang Z , Ning X , Du G , et al. Nonlinear Dynamical Characteristics of ECG Signals of CHD Patients[J]. *Journal of Nanjing University (Natural Sciences)*, 2001.
- [10] Cross D S , McCarty C A , Hytopoulos E , et al. Coronary risk assessment among intermediate risk patients using a clinical and biomarker based algorithm developed and validated in two population cohorts[J]. *Current Medical Research & Opinion*, 2012, 28(11):1819.
- [11] Meghan, E., Olesnevech, et al. Serum ferritin levels associated with increased risk for developing CHD in a low-income urban population.[J]. *Public Health Nutrition*, 2012.
- [12] Maryam, Tayefi, Mohammad, et al. hs-CRP is strongly associated with coronary heart disease (CHD): A data mining approach using decision tree algorithm[J]. *Computer Methods & Programs in Biomedicine*, 2017.
- [13] Karaolis M A , Moutiris J A , Hadjipanayi D , et al. Assessment of the Risk Factors of Coronary Heart Events Based on Data Mining With Decision Trees[J]. *IEEE Trans Inf Technol Biomed*, 2010, 14(3):559-566.
- [14] Rajeswari K , Vaithyanathan D V , Amirtharaj D P . A Novel Risk Level Classification of Ischemic Heart Disease using Artificial Neural Network Technique - An Indian Case Study[J]. 2011.
- [15] Han X , Liang G . Echocardiographic Features of Patients with Coronary Heart Disease and Angina Pectoris under Deep Learning Algorithms[J]. Hindawi Limited, 2021.
- [16] Li Yong, He Zihang, Wang Heng, Li Bohan, Li Fengnan, Gao Ying, Ye Xiang. Craftnet: a deep learning ensemble to diagnose cardiovascular diseases. *Biomed Signal Process Control* 2020;62:102091.
- [17] A. E. Awodeyi, S. R. Alty, and M. Ghavami, "Median based method for baseline wander removal in photoplethysmogram signals," in 2014 IEEE International Conference on Bioinformatics and Bioengineering.IEEE, 2014, pp. 311–314.
- [18] Y.-H. Byeon, S.-B. Pan, and K.-C. Kwak, "Intelligent deep models based on scalograms of electrocardiogram signals for biometrics," *Sensors*, vol. 19, no. 4, p. 935, 2019.
- [19] Wang, Changhong, Low-Power Fall Detector Using Triaxial Accelerometry and Barometric Pressure Sensing [C]. *IEEE Transactions on Industrial Informatics* (2016):1-1. DOI:10.1109/TII.2016.2587761.
- [20] Gjoreski, Hristijan, RAREFall — Real-time activity recognition and fall detection system [C]. *IEEE International Conference on Pervasive Computing & Communications Workshops IEEE*, 2014. 7395664, pp.139-145 DOI:10.1109/PerComW.2014.6815182.
- [21] Koniusz P, Cherian A, Porikli F. Tensor Representations via Kernel Linearization for Action Recognition from 3D Skeletons (Extended Version) [C]. 14th European Conference, ECCV 2016. Vol.9908, pp.37-53 DOI:10.1007/978-3-319-46493-0\_3.
- [22] He K , Zhang X , Ren S , et al. Deep Residual Learning for Image Recognition[C]// 2016 IEEE Conference on Computer Vision and Pattern Recognition (CVPR). IEEE, 2016.
- [23] A. E. Johnson, T. J. Pollard, L. Shen, L.-W. H. Lehman, M. Feng, M. Ghassemi et al., "Mimic-iii, a freely accessible critical care database," *Scientific data*, vol. 3, no. 1, pp. 1–9, 2016.
- [24] B. Moody, G. Moody, M. Villarreal, G. Clifford, I. Silva, "Mimic-iii waveform database matched subset (version 1.0)," 2020. [Online]. Available:<https://physionet.org/content/mimic3wdb-matched/1.0/>
- [25] Simonyan K , Zisserman A. Very Deep Convolutional Networks for Large-Scale Image Recognition[J]. *Computer ence*, 2014.

# Assisted Prediction of Hypertension Based on Heart Rate Variability and Improved Residual Networks

Yong Zhao<sup>1</sup>, Jian He<sup>1</sup>, Cheng Zhang<sup>1</sup>

<sup>1</sup> Beijing University of Technology, Beijing 100124, China

**Abstract**—Cardiovascular diseases caused by hypertension are extremely threatening to human health, and early diagnosis of hypertension can save a large number of lives. Traditional hypertension detection methods require special equipment and are difficult to detect continuous blood pressure changes. In this regard, this paper firstly analyzes the principle of heart rate variability(HRV) and introduces sliding window and power spectral density(PSD) to analyze the time domain features and frequency domain features of HRV, and secondly, designs an HRV-based hypertension prediction network by combining Resnet, attention mechanism and multilayer perceptron, which extracts the frequency domain through the improved ResNet18 features through a modified ResNet18, its fusion with time-domain features through an attention mechanism, and the auxiliary prediction of hypertension through a multilayer perceptron. Finally, the network was trained and tested using the publicly available SHAREE dataset on PhysioNet, and the test results showed that this network achieved 92.06% prediction accuracy for hypertension and outperformed K Near Neighbor(KNN), Bayes, Logistic, and traditional Convolutional Neural Network(CNN) models in prediction performance.

**Keywords**—feature extraction, heart rate variability, hypertension, residual networks;

## I. INTRODUCTION

With the continuous improvement of people's living conditions and quality of life, many chronic diseases are emerging and becoming invisible killers of health. Although the risks associated with these chronic diseases are generally manageable with proper management [1]. However, the complications associated with these chronic diseases can pose a greater risk to people's health. With the changes in the lifestyle of our people, some bad habits (such as staying up late, drinking, smoking, etc.) have led to an increasing number of people suffering from chronic non-communicable diseases such as hypertension, which have become an important public health problem in China. According to the China Cardiovascular Health and Disease Report 2020 released in July 2021, hypertension leads the list of cardiovascular disease deaths among the total causes of death among urban and rural residents in China, higher than other diseases.

In medicine, there are two main methods of adjunctive monitoring of hypertension. The first is direct manometry, which is an invasive approach. It involves a catheter delivered through a skin puncture into a peripheral artery (e.g., within the radial artery), and a monitor measurement device is attached to the

end of the catheter to display blood pressure values. The second type of measurement is indirect, of which the most common and reliable is the Koch sound method [2]. The cuff is inflated and deflated by an air pump, and the popping and vanishing sounds produced by the compressed arterial vessel wall are captured by a pickup, which in turn outputs the corresponding cardiac systolic and diastolic pressures. Both the manual and electronic Koch sound methods are susceptible to interference from external sounds, and differences in pulse strength from person to person affect the measurement results. In addition, blood pressure testing devices based on the Koch sound method require the wearing of special equipment, which makes it difficult to measure blood pressure for a long time and continuously, and cannot accurately reflect the trend of blood pressure changes in patients over a period of time.

The human heart produces a series of electrophysiological changes during the beating process, which are transmitted to the body surface and picked up by electrodes. These signals are presented continuously on the time axis to form the electrocardiogram(ECG) [3]. Researchers have found that the human heart beats rhythmically and with small variations over time due to the interaction between sympathetic and parasympathetic nerves in the human AutonomicNervousSystem (ANS) [4], [5]. HRV is one of the more popular non-invasive ECG monitoring indicators in recent years. Analysis of HRV can indirectly quantify the tension and balance of myocardial sympathetic and vagal nerves, as well as analyze the activity of the autonomic nervous system [6], [7], [8]. For example, HRV can be used as an independent predictor of the risk of sudden cardiac death [9]. Abrishami et al. [10] proposed an expert system for assisted detection of hypertension based on a multilayer neural network. The system used the patient's systolic blood pressure, smoking status, age, weight, and body mass index as inputs and predicted the patient's hypertension diagnosis through a multilayer neural network with good experimental results. Ren et al. [11] used LSTM to classify text sequences in electronic medical records and combined with auto-encoder to classify numerical data in electronic medical, then the output of the two classifiers with merged into a fully connected layer and predicted kidney disease in hypertensive patients by Softmax classification, and finally the effectiveness of the model was verified by experiments and comparison with other algorithms. Some researchers have carried out hypertension assisted prediction by extracting feature parameters such as time domain and frequency domain of heart rate variability and combining them with machine learning algorithms. For example, Wang et al. [12] 2015 constructed a prediction model

Yong Zhao,Beijing University of Technology(corresponding author, phone:(+86)18735724319;e-mail:1030678904@qq.com).

Jian He is a professor at the Department of Information Science at Beijing University of Technology.

Cheng Zhang is a PhD student at the Department of Information Science, Beijing University of Technology.

based on logistic regression and artificial neural network based on no measurement to predict hypertension, and used binary logistic regression to predict important risk factors leading to hypertension, and the experimental results showed that the accuracy of the model reached more than 72%; Pavithran et al. analyzed 35 male subjects' HRV and other conventional indicators (including Pavithran et al. analyzed the HRV during deep breathing, the ascending response during static standing and isometric grip strength in 35 male subjects, and the experimental results showed that parasympathetic function is impaired in hypertensive patients, leading to a decrease in their HRV compared to the normal population [13], [14]. Overall, there is a lack of hypertension prediction techniques based on deep learning algorithms for HRV. Lan et al. collected PPG signals from 24 hypertensive patients and 19 healthy individuals for 6 consecutive hours using a smart wearable device, extracted 6 HRV features and achieved 85.47% accuracy in hypertension classification [15]. Since the PPG waveform does not carry important high-frequency components and is highly sensitive to motion artifacts [16], the accuracy of its hypertension prediction is affected. In this paper, we analyze the HRV characteristics of hypertensive patients by ECG signal and combine with deep learning algorithm to investigate the HRV-based hypertension assisted prediction technique.

The following contents of this paper are organized as follows: Chapter 2 introduces the sliding window and PSD to analyze the time-domain and frequency-domain characteristics of HRV on the basis of the comparative analysis of HRV differences between normal and hypertensive patients; In the third chapter, we introduce the hypertension prediction network based on HRV, which combines ResNet18, attention mechanism and multi-layer perceptron. The frequency domain features are extracted from the PSD map, and the attention mechanism is combined with the time-domain features, and the hypertension classification prediction is realized by the multi-layer perceptron. In Chapter 4, network training and experiments were carried out on the publicly available SHA-REE [17] data set, and the prediction results of hypertension were compared with those of traditional machine learning algorithms. Finally, this paper summarizes.

## II. RELATED WORK

Heart rate variability analysis methods are mainly time-domain analysis and frequency-domain analysis [18], [19], [20]. In this section, based on the analysis of HRV characteristics of hypertensive patients, introduces the sliding window and PSD techniques to realize the conversion of time-frequency domain characteristics of ECG data, which provides the basis for the subsequent construction of an improved residual network-based hypertension-assisted prediction.

### A. Analysis of HRV in hypertensive patients

Due to the elevated blood pressure, changes in vasodilation and accelerated heartbeat may be induced. Therefore, extracting the heartbeat interval sequence on the basis of ECG and analyzing its HRV characteristics is a necessary step

for the auxiliary prediction of hypertension. Fig. 1 compares the heartbeat interval images of a normal person and a hypertensive patient, where the horizontal axis indicates the heartbeat interval sequence in one minute and the vertical axis indicates the time difference between this heartbeat and the previous one. The upper figure shows the heartbeat interval sequence of a normal person with a mean time difference of 886.12 and 68 heartbeats per minute; the lower figure shows the heartbeat interval sequence of a hypertensive patient with a mean time difference of 793.54 and 77 heartbeats per minute. The HRV values of hypertensive patients are low compared to normal subjects. Based on the above differences in HRV between healthy people and hypertensive patients, the HRV time-frequency domain characteristics were analyzed to provide a basis for subsequent studies.

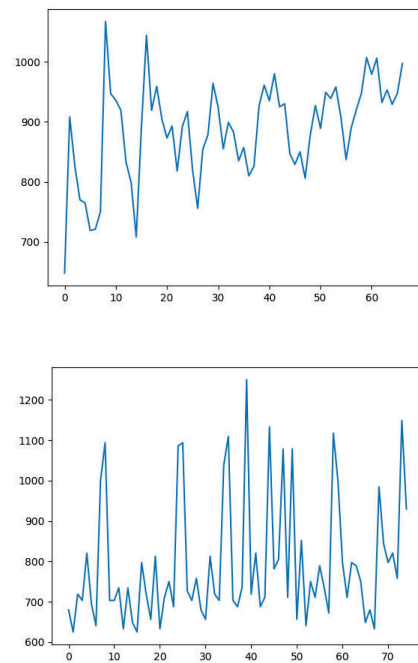


Fig. 1: Heartbeat interval diagram

### B. HRV time-frequency domain characterization

Usually, ECG data collected by instrumentation are susceptible to respiration and exercise, thus causing missing data points and data noise, which in turn have an impact on subsequent analysis. In this regard, when extracting the features of heart rate variability, in order to accurately extract the feature vector of heart rate variability as an auxiliary prediction criterion; firstly, the raw ECG data are sampled using cubic spline interpolation to improve the temporal accuracy of peak detection. Second, to reduce potential long-term drift in the signal, a high-pass Butterworth filter is applied to the raw data, and finally, a Savitzky-Golay filter is applied to smooth the data, thereby reducing spikes while maintaining temporal accuracy.



After pre-processing the raw data, the processed data needs to be extracted with time-frequency domain features. Since ECG data has characteristics such as continuity and long-term, and the traditional analysis methods for static data cannot meet this scenario. In this regard, sliding window technique is used in this paper. As shown in Fig. 2: a window of 20s ECG data is used to cache the ECG data through the sliding window, and wave detection and feature analysis are performed on the ECG data within each window, and the corresponding time stamp is set to save its time-frequency domain feature results. In this way, as new data are continuously generated, the data within the window is continuously updated and its analysis results are continuously saved according to the first-in-first-out rule of the sliding window.

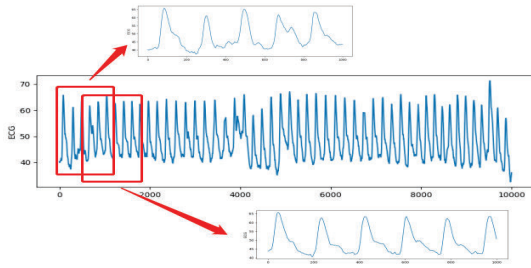


Fig. 2: Sliding window to extract features

For ECG data, peak detection is susceptible to uncorrelated prominent P- and T-waves. Specifically, traditional amplitude-based analysis may occasionally detect non-R-wave peaks with similar or greater amplitudes than R waves. Therefore, K-means clustering is used for ECG data to distinguish R waves from the P and T waves prevalent in the signal and then extract RR interval sequences. For the extracted RR interval sequence, the time domain signal level analysis is first performed to extract its time domain feature parameters, the main parameters are R-R Interval Mean (RR), Standard Deviation of Normal-to-Normal intervals (SDNN), Root Mean Square of Successive Differences (RMSSD), and Percentage of RR intervals greater than 50ms in total RR intervals (PNN50), which are described as shown in Table I.

TABLE I: Time domain characteristics.

Features	Feature Description
RR(Mean)	RR interval mean
SDNN	RR Standard deviation of continuous normal RR interval
RMSSD	The root mean square of the difference between adjacent R-R intervals
PNN50	RR The number of adjacent normal R-R intervals with a difference greater than 50ms as a percentage of the total number of heartbeats

Next, the PSD estimation is used to extract the frequency domain characteristic parameters of heart rate variability from the PSD. The conversion of the signal from the time domain to the frequency domain requires the Fourier transform, whose formula is shown in equation (1):  $f$  is the frequency component of  $x$ ,  $t$  denotes time, and the formula can be interpreted as the time domain signal  $x(t)$  multiplied by an exponential term consisting of a specified frequency ( $e^{-2\pi ift}$ ),

and then integrated over the entire time axis to obtain the frequency domain signal, which serves to identify the spectral component of the signal. PSD is the square of the fast Fourier transform taking the mode. Its formula is shown in equation (2): power spectrum is to reflect the variation of signal power with frequency in unit frequency band, that is, the distribution of signal power in the frequency domain.

$$S(f) = \int_{-\infty}^{+\infty} x(t) * e^{-2\pi ift} dt \quad (1)$$

$$P = \lim_{T \rightarrow \infty} \frac{1}{T} \int |S(f)|^2 df \quad (2)$$

The raw ECG data is a one-dimensional signal, and the PSD is used to convert the ECG data into a three-channel RGB image containing the frequency domain features of the heartbeat interval, which contains the frequency domain features of the heartbeat interval within a sliding window, providing a basis for studying the improved residual network-based hypertension-assisted prediction technique.

### III. METHOD

This section firstly introduces the network architecture fusing Resnet [21], attention mechanism and multilayer perceptron, secondly, the principle of Resnet and the extraction of frequency domain features based on the improved Resnet18, and finally, the fusion of time-frequency domain feature vectors based on the attention mechanism is introduced.

#### A. Network Architecture

The pre-processed ECG data is converted into one RGB image by sliding window and PSD, and the convolutional network can be used to extract the features of these images. In this paper, based on the analysis and comparison of traditional convolutional networks such as KNN [22], Bayes [23], Logistic [24], and CNN [25], we propose a network architecture that fuses Resnet, attention mechanism and multilayer perceptron, as shown in Fig. 3, which consists of input layer, Resnet layer, fusion layer, fully connected layer and softmax layer.

The input layer passes the RGB images into the Resnet layer, which consists of multiple convolution blocks and residual blocks, and it extracts the frequency domain features of multiple images, after which the fusion layer uses the attention mechanism to fuse the frequency domain feature vectors with the time domain feature vectors; finally, the feature vectors are classified by the fully connected layer (which is essentially a multilayer perceptron) and the softmax layer, and the category with the highest probability is used as the prediction result and output.

#### B. Resnet-based frequency domain feature extraction

To address the problem of decreasing accuracy as the network training deepens, ResNet proposes a residual learning method to alleviate the difficulty of training deeper networks. This is shown in Fig. 4. Each residual module contains two paths, one of which is a direct connection path of the input feature, and the other path does two to three convolution

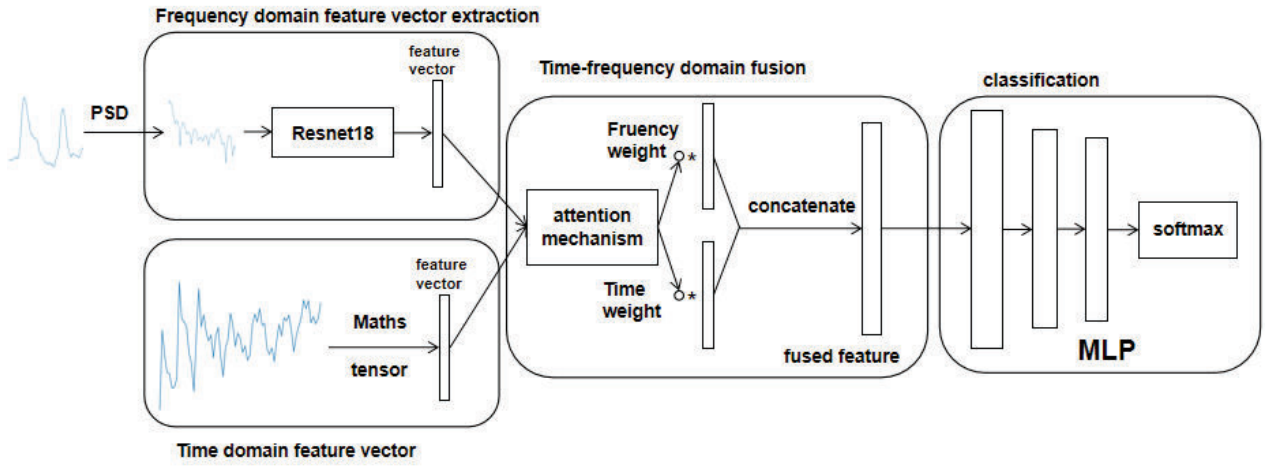


Fig. 3: Network architecture diagram

operations on that feature to obtain that residual feature  $F(x)$ , and the two paths have their own weights. Finally, the two results are added up as the input of the next layer. If the result after convolution is not good, then the weight of this path of convolution is set to 0, the final result is  $x$ . The constant mapping of the input ensures that the effect is no worse than the original one. The addition of the residual module can avoid the problem of gradient disappearance, further improve the fitting ability of the model, and mitigate the impact of increasing the number of layers of the network.

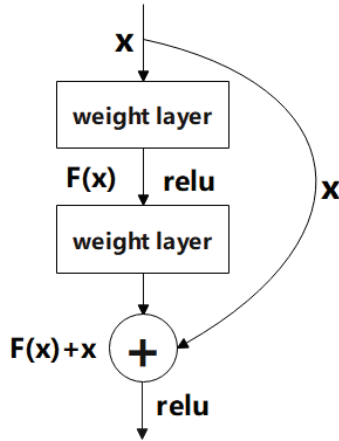


Fig. 4: Residual unit

The improved Resnet18 mainly consists of an input layer, an intermediate layer, and an average pooling layer, as shown in Fig. 5. The input layer mainly includes a convolutional layer and a maximum pooling layer; the intermediate layer, shown as the dashed line in the figure, has four convolutional blocks containing residual modules, and finally passes through an average pooling layer for the output of feature values.

This input contains a  $7*7$  convolution kernel with a step size of 2 and a  $3*3$  maximization pool with a step size of 2. By this step, the image becomes a  $56*56$  feature map, which greatly reduces the required storage size. The middle layer, with a total

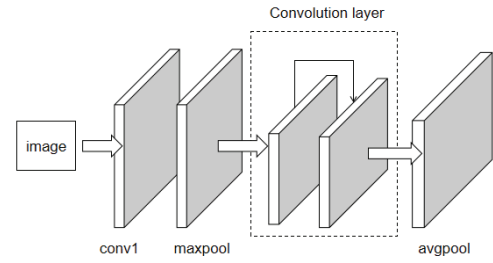


Fig. 5: Resnet18 architecture

of four convolutional blocks, the convolutional layer is the core component of CNN, responsible for extracting the features of the original data, and can maintain the spatial continuity of the image, extracting the local features of the data, and the convolutional kernel has parameter sharing capability, which can effectively reduce the number of parameters in the convolutional layer. Firstly, a convolutional layer with a convolutional kernel size of  $3*3$ , a step size of 2, a padding of 1, and an output channel of 64, the output of this layer is  $64*112*112$ . Secondly, a convolutional layer with a convolutional kernel size of  $3*3$ , a step size of 1, and a padding of 1, the output of this layer is  $128*56*56$ . Finally, a convolutional layer with two  $1*1$  and one downsampling. Each layer has a step size of 2 and a padding of 1. Each layer doubles the output channels and halves the output vector size. The final output vector size is  $512*7*7$ . After an average pooling layer, the output vector size is  $512*1*1$ .

### C. Attention-based mechanism for time-frequency domain feature fusion

Firstly, the frequency domain feature vector generated by the Resnet layer above and the computed time domain feature vector are jointly used as the input of the attention mechanism, secondly, the correlation between vector  $q$  and each input vector is calculated by the scoring function to derive a score, the higher the score, the higher the weight, and then the feature



vector is weighted and stitched using the concat function; finally, the fully connected layer and softmax layer to output the classification results. Among them, the scoring function is shown in equation (3); where  $x$  is the query, the  $x_i$  is the key, and  $y_i$  is the value corresponding to the key, and the attention weight between query  $x$  and  $x_i$ . The attention weight between  $\propto (x, x_i)$ , if a key  $x_i$  is closer to the given query  $x$ , then the attention weight assigned to the value corresponding to this key  $y_i$  the greater the attention weight assigned to the value corresponding to this key.

$$f(x) = \sum_{i=1}^n \propto (x, x_i) y_i \quad (3)$$

After the residual network the input is 224\*224\*3 images are converted into 512\*1\*1 feature vectors for the subsequent fusion of attention mechanisms.

#### IV. EXPERIMENTAL DESIGN AND ANALYSIS OF RESULTS

##### A. Experimental data set

The dataset used in this paper was derived from the publicly available dataset of SHAREE, which was developed to investigate the possibility of identifying subjects with cardiovascular and cerebrovascular events based on heart rate variability analysis. The data information contains ECG data, basic patient information, etc. A total of 1260 cases, including 139 hypertensive patients, and the rest are healthy people. Hypertension is commonly found in the middle-aged and elderly population, and the age of hypertensive patients in this dataset is concentrated in [60-70] years, with an average age of 71.76 years. In machine learning, to reflect the generalization performance of the algorithm, the experiment randomly selected three-quarters of the dataset as training samples, and the remaining as test samples. The presence or absence of hypertension symptoms was used as the labeling outcome to build a binary classification model.

In order to verify the validity of the auxiliary prediction model for hypertensive patients, it is necessary to evaluate its predictive effect, and this paper looks at The model is evaluated in three dimensions: accuracy, recall, and AUC.

(1) Accuracy: the degree of prediction accuracy of the presence of hypertension versus the absence of hypertension, as shown in equation (4). Where  $TP$  indicates the number of patients with hypertension correctly predicted,  $TN$  indicates the number of patients with not hypertension correctly predicted,  $FN$  indicates the number of patients with hypertension incorrectly predicted, and  $FP$  indicates the number of patients with not hypertension incorrectly predicted.

$$accuracy = \frac{TP + TN}{TP + FN + FP + TN} \quad (4)$$

(2) Recall: the number of correctly predicted hypertensive patients as a proportion of all hypertensive patients in the sample set, as shown in the equation (5).

$$recall = \frac{TP}{TP + FN} \quad (5)$$

(3) F1 value: It is an evaluation indicator that combines the two indicators of Precise and Recall, and is used to reflect the

overall indicator in a comprehensive manner. Its formula is shown in equation (6).

$$F1 = \frac{2 * accuracy * recall}{accuracy + recall} \quad (6)$$

##### B. Analysis of results

First, in order to verify the usefulness of data preprocessing, two comparison experiments based on the improved residual network were conducted in the preliminary stage of this paper, one using the preprocessed data and one using the unprocessed data, and the results are shown in Table II. The results show that it is necessary for the raw data to be preprocessed. Next, the processed data were put into the model

TABLE II: Comparison of data pre-processing

Testing	Pre-processing	Not pre-processed
Accuracy	91.03	82.7
Recall Rate	93.46	84.28
F1	0.91	0.83

for testing, and the results of 10 tests were averaged, and the results are shown in Table III. The average accuracy of the ten classification predictions was 92.06%, the average recall was 93.55%, and the average F1 value was 0.92.

TABLE III: Classification prediction results based on Resnet18

Testing	Accuracy/%	Recall/%	F1
TEST1	90.03	99.87	0.95
TEST2	93.46	98.28	0.96
TEST3	94.10	97.90	0.95
TEST4	91.30	83.25	0.87
TEST5	90.57	83.76	0.87
TEST6	89.73	96.85	0.93
TEST7	91.52	94.63	0.93
TEST8	95.81	97.82	0.96
TEST9	91.57	92.67	0.92
TEST10	92.51	90.44	0.91
Average	92.06	93.55	0.92

In order to verify the effectiveness of the network model proposed in this paper, the model is compared with KNN, Bayes, Logistic and CNN algorithms. The  $k$  value of the K-NN algorithm is taken as 2; the principle of Bayes implementation is: how to get the probability of an event after exchange if a conditional probability is known; Logistic classification is supervised learning and must require manual labeling; CNN is a traditional convolutional neural network. the performance evaluation results obtained from the mean value of the four classification algorithms after 10 runs using the same data, the same training and test length As shown in Table IV. It can be seen that the mean value of Bayes algorithm is significantly lower than the other 4 algorithms, probably due to the strong independence of Bayes' law on the features of the model, which does not take into account the connection between the features. the average accuracy of KNN, Logistic, and CNN algorithms are all around 80%. And the average accuracy of the residual network proposed in this paper is the highest, around 92%, and the F1 value is also the highest, at 0.92.

TABLE IV: Prediction results of different algorithms

Classification Algorithm	Accuracy/%	Recall/%	F1
KNN	79.84	77.21	0.79
Bayes	49.44	39.28	0.44
Logistic	76.92	80.42	0.77
CNN	88.64	82.38	0.85
Resnet18	92.06	93.55	0.92

Finally, this paper also compares the effect of the number of layers of the multilayer perceptron on the accuracy with the same parameters and training data as above, simply by increasing or decreasing the number of layers of the multilayer perceptron and observing the classification effect of the multilayer perceptron with different number of layers. The results are shown in Table V.

TABLE V: Accuracy rate of different layers

Number of layers	Accuracy/%	Recall/%	F1
2	89.48	90.25	0.89
3	92.06	93.55	0.92
4	88.26	87.35	0.87

When the number of layers is 2, it may not be able to extract its features comprehensively and finely, resulting in low accuracy, while when the number of layers is 4, it may have low accuracy due to overfitting of features because of the high number of layers. Therefore, the number of layers of the multilayer perceptron selected in this paper is 3.

## V. CONCLUSION

Since the early symptoms of hypertension are not obvious, it is difficult for patients themselves to detect it. This paper seeks to provide accurate early warning and prediction of people's risk of developing hypertension with minimal loss of economy and effort. This paper focuses on a hypertension-assisted prediction model based on HRV time-frequency domain features incorporating residual networks, attention mechanisms and multilayer perceptrons, and experimental comparisons based on the publicly available SHAREE dataset, and the results show that this model achieves good results in aiding the prediction of hypertension compared with the other four classification algorithms, and can provide medical personnel with clearer and more accurate guidance and support for further examinations. In the future, this paper will continue to adjust the network structure, including the number of layers of convolutional layers, the size of convolutional kernel, etc. In addition, we will continue to optimize the model parameters and try to use more models for fusion.

## REFERENCES

- [1] C. Troeger, M. Forouzanfar, P. C. Rao, I. Khalil, A. Brown, R. C. Reiner, N. Fullman, R. L. Thompson, A. Abajobir, M. Ahmed *et al.*, "Estimates of global, regional, and national morbidity, mortality, and aetiologies of diarrhoeal diseases: a systematic analysis for the global burden of disease study 2015," *The Lancet infectious diseases*, vol. 17, no. 9, pp. 909–948, 2017.
- [2] A. Meidert, J. Briegel, and B. Saugel, "Principles and pitfalls of arterial blood pressure measurement," *Der Anaesthesist*, vol. 68, pp. 637–650, 2019.
- [3] P. Lamba and K. Rawal, "A survey of algorithms for feature extraction and feature classification methods," in *2019 International Conference on Automation, Computational and Technology Management (ICACTM)*. IEEE, 2019, pp. 338–341.
- [4] C. M. van Ravenswaaij-Arts, L. A. Kollee, J. C. Hopman, G. B. Stoeltinga, and H. P. van Geijn, "Heart rate variability," *Annals of internal medicine*, vol. 118, no. 6, pp. 436–447, 1993.
- [5] J. P. ZBILUT and L. LAWSON, "Decreased heart rate variability in significant cardiac events," *Critical care medicine*, vol. 16, no. 1, pp. 64–66, 1988.
- [6] G. Wilson, "A review of "the polyvagal theory: Neurophysiological foundations of emotions, attachment, communication, and self regulation" stephen w. porges.(2011). new york: Ww norton, 272 pp., \$45.00 (hardback)." 2012.
- [7] B. Folkow, "Physiological aspects of primary hypertension," *Physiological reviews*, vol. 62, no. 2, pp. 347–504, 1982.
- [8] S. Oparil, "The sympathetic nervous system in clinical and experimental hypertension," *Kidney international*, vol. 30, no. 3, pp. 437–452, 1986.
- [9] B. Xhyheri, O. Manfrini, M. Mazzolini, C. Pizzi, and R. Bugiardini, "Heart rate variability today," *Progress in cardiovascular diseases*, vol. 55, no. 3, pp. 321–331, 2012.
- [10] Z. Abrishami and H. Tabatabaee, "Design of a fuzzy expert system and a multi-layer neural network system for diagnosis of hypertension," *Bull Environ Pharmacol Life Sci*, vol. 4, no. 11, pp. 138–145, 2015.
- [11] Y. Ren, H. Fei, X. Liang, D. Ji, and M. Cheng, "A hybrid neural network model for predicting kidney disease in hypertension patients based on electronic health records," *BMC medical informatics and decision making*, vol. 19, pp. 131–138, 2019.
- [12] A. Wang, N. An, G. Chen, L. Li, and G. Alterovitz, "Predicting hypertension without measurement: A non-invasive, questionnaire-based approach," *Expert Systems with Applications*, vol. 42, no. 21, pp. 7601–7609, 2015.
- [13] P. Pavithran, M. Madanmohan, R. Mithun, M. Jomal, and H. Nandeesha, "Heart rate variability in middle-aged men with new-onset hypertension," *Annals of Noninvasive Electrocardiology*, vol. 13, no. 3, pp. 242–248, 2008.
- [14] A. Gunther, I. Salzmänn, S. Nowack, M. Schwab, R. Surber, H. Hoyer, O. Witte, and D. Hoyer, "Heart rate variability—a potential early marker of sub-acute post-stroke infections," *Acta neurologica Scandinavica*, vol. 126, no. 3, pp. 189–196, 2012.
- [15] K.-c. Lan, P. Raknim, W.-F. Kao, and J.-H. Huang, "Toward hypertension prediction based on ppg-derived hrv signals: A feasibility study," *Journal of medical systems*, vol. 42, pp. 1–7, 2018.
- [16] K. M. Warren, J. R. Harvey, K. H. Chon, and Y. Mendelson, "Improving pulse rate measurements during random motion using a wearable multichannel reflectance photoplethysmograph," *Sensors*, vol. 16, no. 3, p. 342, 2016.
- [17] PhysioNet, <https://www.physionet.org/content/shareedb>.
- [18] H. Kawano, R. Okada, and K. Yano, "Histological study on the distribution of autonomic nerves in the human heart," *Heart and vessels*, vol. 18, no. 1, p. 32, 2003.
- [19] J. L. Hamilton and L. B. Alloy, "Atypical reactivity of heart rate variability to stress and depression across development: Systematic review of the literature and directions for future research," *Clinical psychology review*, vol. 50, pp. 67–79, 2016.
- [20] C. Schiweck, D. Piette, D. Berckmans, S. Claes, and E. Vrieze, "Heart rate and high frequency heart rate variability during stress as biomarker for clinical depression. a systematic review," *Psychological medicine*, vol. 49, no. 2, pp. 200–211, 2019.
- [21] K. He, X. Zhang, S. Ren, and J. Sun, "Deep residual learning for image recognition," in *Proceedings of the IEEE conference on computer vision and pattern recognition*, 2016, pp. 770–778.
- [22] A. M. Alsayat, "Efficient genetic k-means clustering algorithm and its application to data mining on different domains," Ph.D. dissertation, Bowie State University, 2016.
- [23] D. Niedermayer, "An introduction to bayesian networks and their contemporary applications," *Innovations in Bayesian networks: Theory and applications*, pp. 117–130, 2008.
- [24] C.-c. Chen, K. Mondal, P. Vervliet, A. Covaci, E. P. O'Brien, K. J. Rockne, J. L. Drummond, and L. Hanley, "Logistic regression analysis of lc-ms/ms data of monomers eluted from aged dental composites: A supervised machine-learning approach," *Analytical Chemistry*, 2023.
- [25] A. Roslin, M. Lebedev, T. Mitchell, I. Onederra, and C. Leonardi, "Processing of micro-ct images of granodiorite rock samples using convolutional neural networks (cnn). part iii: Enhancement of scanco micro-ct images of granodiorite rocks using a 3d convolutional neural network super-resolution algorithm," *Minerals Engineering*, vol. 195, p. 108028, 2023.

# Twitter Ego Networks and the Capital Markets: A Social Network Analysis Perspective of Market Reactions to Earnings Announcement Events

Gregory D. Saxton

**Abstract**—Networks are everywhere: lunch ties among co-workers, golfing partnerships among employees, inter-locking board-of-director connections, Facebook friendship ties, etc. Each network varies in terms of its *structure* – its size, how inter-connected network members are, and the prevalence of sub-groups and cliques. At the same time, within any given network, some network members will have a more important, more central *position* on account of their greater number of connections or their capacity as “bridges” connecting members of different network cliques. The logic of network structure and position is at the heart of what is known as *social network analysis*, and this paper applies this logic to the study of the stock market. Using an array of data analytics and machine learning tools, this study will examine 17 million Twitter messages discussing the stocks of the firms in the S&P 1,500 index in 2018. The study’s core proposition is that the ultimate effect of any market-relevant information is contingent on the characteristics – including the size, activity level, density, influence, norms, and embedded resources – of the network through which it flows. To test this proposition, this study operationalizes each of the core network characteristics and examine their influence on market reactions to 2018 quarterly earnings announcement events.

**Keywords**—Data analytics, investor-to-investor communication, social network analysis, Twitter

## I. INTRODUCTION

**S**Ocial media has transformed how we see financial information. The new financial information environment is characterized by the broader range of actors who are involved in producing, transforming, and disseminating stock market-relevant information – no longer is this solely the domain of financial analysts, corporate annual reports, and proprietary newsletter writers. While social media does appear to convey market-relevant information [3], [5], [8], [26], side-by-side with any dispassionate market analysis comes “clickbait,” “firestorms,” “information silos,” and “alternative facts” [2], [4], [31], [34]. As seen in recent events, we are in a new era where a tweet from a celebrity can temporarily wipe out \$1.3 billion of Snapchat’s value [40], where a single short-seller’s tweet can cause NVIDIA’s stock to drop 6.9% [30], or where a misguided tweet by Tesla founder Elon Musk in 2018 (“funding secured”) can seriously rattle investor confidence.

The driving force of these diverse phenomena is the heavily network-dependent nature of social media [22].<sup>1</sup> Yet existing

literature has thus far essentially ignored the network view of financial communication, instead choosing to examine social media through the lens of mainstream financial accounting theory, which, with its focus on one-way disclosure of information, is ill-equipped for understanding such decentralized, network-driven communicative contexts. While financial accounting scholars may understand that information flows through networks, they have tended to posit such networks as unimportant “black boxes.” In order to develop a better understanding of how information flows through, or is processed by, the social media environment, this study contends it is critical to utilize an approach specifically designed to conceptualize and measure network effects. This project therefore delves into the black box by employing an approach, *social network analysis* (SNA), specifically designed for network-level analyses and widely used within sociology, communication, economics, and other fields to examine network effects.

Leveraging conceptual and methodological tools from social network analysis, this study will examine the roughly 17 million Twitter messages in 2018 that discuss stocks of the 1,500 firms in the S&P 1,500 list. Each of these 1,500 stocks has a distinct Twitter discussion network – what is known as an *ego network* – that varies in terms of core network characteristics such as size, density, values, influence, and embedded resources. The study’s general argument is that the speed, nature, and influence of the information that flows through a network is contingent on such network characteristics. This argument is tested in examining whether network characteristics influence the market effects of tweeting around quarterly company earnings announcement events. Around each earnings announcement window, the study will employ network analysis tools and machine learning algorithms in Python to first map the 1,500 “cashtag” ego networks and then measure each of the core ego network characteristics (size, density, cohesion influence, values, maximum flow, and embedded resources). A series of OLS regressions will then be used to test whether these network characteristics influence market reactions to quarterly company earnings announcements.

This study seeks not only to deliver insights into the effects of social media on the financial markets, but also whether information has a variable market effect depending on the characteristics of the network through which it flows. Overall, social network analysis has received scant attention from financial accounting scholars; this study will add to the literature in bringing a network perspective to analyses of the production,

Gregory D. Saxton is Professor of Accounting at the Schulich School of Business, York University, 4700 Keele St. West, Toronto, ON, Canada (phone: 416-736-2100, x44218, e-mail: gsaxton@yorku.ca)

<sup>1</sup>The essentially networked nature of social media is one where communicative outcomes such as attention, firestorms, outrage culture, doxing attacks, and information cascades are heavily influenced by the array of formal and informal relationships among users [22].



dissemination, and impact of market-relevant information. At a practical level, this project also aims to inform the investor community, regulators, and the media about how social media networks influence the markets. In an age where social media is playing an increasingly important role in (mis)information dissemination, it is worthwhile to understand whether and how these media may be manipulating or unduly influencing the capital markets. The SNA perspective may hold the key to helping us understand social media's complex role in firms' information environment.

This paper is organized as follows. The next section summarizes the state of knowledge of existing research in the area of social media and accounting information and outlines the theoretical framework. The third section presents the methods and design for the proposed study. The final section briefly summarizes the goals, limits, and advantages of the proposed study.

## II. BACKGROUND AND HYPOTHESES DEVELOPMENT

### A. The Social Media Context

The proliferation of social media platforms such as Twitter, Facebook, Instagram and LinkedIn has changed the information environment in which contemporary organizations operate. On the one hand, social media has fundamentally increased the scale of market-relevant information that is produced. It has opened up the environment to a range of new actors and information sources [37]. It has accelerated the pace at which information is disseminated [5]. And it has led to the rise of new informational phenomena. As noted earlier, social media is not solely conveying disinterested information by traditional financial information gatekeepers; "fake news" and "clickbait" are just as likely to be found, while social media also serve to fuel online "firestorms" and to shelter closely-held views through "echo chambers" and "information silos" [2], [4], [31], [34]. As is argued in more detail later on, the role of this new information environment cannot be disentangled without understanding its fundamentally network-dependent nature [22].

### B. The Efficient Markets Hypothesis and Accounting Research on Social Media

That accounting information has an impact on the capital markets is well established. In the capital markets context, the predominant efficient markets hypothesis presupposes that relevant new information will be incorporated into stock price more or less instantaneously as it spreads to key market actors [15]. Implicitly, there is a rapid dissemination process that occurs as relevant information is spread from actor to actor in the market network. However, the theory does not posit any powerful role for precisely how the information is spread, nor does it consider important the topology or landscape of the network. In line with this information perspective, the focus on social media in mainstream accounting-based capital markets research has thus been in identifying new sources of market-relevant information. Working within this perspective, recent accounting literature has indeed found that the information

communicated on social media platforms is market relevant [3], [5], [8], [26].<sup>2</sup>

While such research provides evidence of a link between information and market outcomes, mainstream accounting theory provides little understanding of precisely how information spreads or is changed – or comes to have a different effect – as it flows through networks of investors, analysts, journalists, academics, and other interested players. Nor still can existing studies tell us how the effects of a piece of information may be impacted by variation in the size, density, centrality, or structure of a firm's online discussion network. In effect, while accounting scholars may acknowledge that information flows through networks, they have tended to posit such networks as unimportant "black boxes." Leveraging the conceptual and methodological tools of social network analysis, this study seeks to delve into the black box and investigate what takes place between the production or disclosure of information and market outcomes. The major theoretical contribution will be in how it incorporates an explicitly network-centric perspective into a financial accounting study.

### C. The Social Network Analysis Perspective

The capital markets have experienced a burgeoning number of actors – including investors, spammers, firms, regulators, information intermediaries, ratings agencies, the media, and professional and amateur analysts – interacting on social media to share information related to company performance [37]. It is posited that the influence of such communication is contingent on the structure of social (network) resources found within the social media networks. Existing literature provides solid implicit support for this privileging of social resources. A key reason lies in the primacy of the formalized *social network* in social media platforms [22], [23]. Few activities – from making connections to reading, liking, sharing, and commenting on messages – occur on social media without being mediated by a formal friend/follower relationship [12], [41]. On social media, the social network is key. Moreover, the extremely tight relationship between the social network and organizational outcomes is distinct from what occurs off-line. Off-line, a TV ad could reach millions without a firm having any substantial social resources or pre-existing social network; at the very least, the size of the audience is divorced from the organization's social capital. This would be highly improbable on social media: without a pre-existing network, a message would simply not reach a large enough number of followers to be successful. In short, offline, the relationship between social/network resources and audience outcomes is tenuous; on social media, it is paramount.

In effect, social media are highly network-dependent [22]. In order to develop a better understanding of how information

<sup>2</sup>Prior research has been absorbed by the type and quantity, and to a lesser extent the quality, of the information that has been disclosed. What has not been studied explicitly is the structure of the networks through which the disclosed information flows. Such research would run counter to the typical strong- and semi-strong forms of the efficient markets hypothesis, which posits the key element of information is its disclosure; whether and how this information is aggregated, disseminated, or flows through a network, is an "automatic," almost immediate process that is not important for understanding market efficiency.

flows through, or is processed by, the social media environment, it is therefore contended it is critical to utilize an approach specifically designed to conceptualize and measure network effects.<sup>3</sup> For this very reason, this study employs *social network analysis* (SNA), a sociological approach that examines social and organizational phenomena through the lens of the networks of social relationships among sets of actors (Freeman, 1979; Lin, 1999; Worrell et al., 2013). Using the analytical tools provided by SNA, this paper proposes to study the market effects of information flowing from different types of investor-to-investor communities that vary in terms of core network-level characteristics. This approach dovetails with the importance accorded to social network analyses in related fields such as information systems, communication, sociology, and organizational behavior, which have developed an array of sophisticated tools and methodologies for analyzing the structure of virtual networks and communities [16]. SNA has also been used by accounting scholars in non-financial markets contexts [36], [42]. Yet save for a study on earlier Web 1.0 technology by Das and Sisk [11], a theoretical piece by Hirshleifer and Teoh [21], and a study of what *leads to* greater network centrality [13], finance and financial accounting scholars have, to the best that is known, yet to leverage SNA to study the flow of accounting information through digital media.<sup>4</sup> By employing social network analysis tools to examine the importance of social media networks in determining stock market outcomes, the current project seeks to push financial markets scholars in this direction.<sup>5</sup>

#### D. Social Media-Based Cashtag Networks

The most relevant communities on Twitter are the *cashtag networks* focused on communication related to specific company stocks. These networks constitute ephemeral and changing networks of actors linked by their use of stock-ticker symbols called “cashtags” in their tweets. The cashtag innovation, announced by Twitter in the following tweet from July 30, 2012, is one of the key reasons Twitter has become a central social media platform for the production and dissemination of stock-related information:

*Now you can click on ticker symbols like \$GE on twitter.com to see search results about stocks and companies*

Cashtag networks are investor-to-investor communities focused on individual company stocks. Contributors represent a mix of professional and amateur investors, executives, analysts, journalists, and academics who share information

on share price, their latest trades, and micro-analyses of company- and stock-related information along with commentaries, opinions, and rumors.<sup>6</sup> For example, Citron Research (@CitronResearch) sent this tweet about NVIDIA:

*Citron readers know we have long been fans of NVDA, but now the mkt is disregarding headwinds. In 2017 we will see \$NVDA head back to \$90.*

Each publicly-traded firm has its own decentralized, user-generated cashtag network, with messages – and, by extension, users – connected by the inclusion of the same cashtag in a tweet. For instance, the community of investors interested in Apple stock (ticker: AAPL) would include the \$AAPL cashtag in each tweet related to Apple stock. The collection of \$AAPL tweets – and the users who send them – constitute the AAPL-focused cashtag network.

#### E. Key Ego Network Characteristics of Twitter Cashtag Networks

This study concentrates on the 1,500 firms in the *S&P 1,500* index. Each of the 1,500 stocks in the *S&P 1,500* has a distinct Twitter discussion network with a single actor or node – the cashtag – at its core. This is what is known in the SNA literature as an *ego network* [14].<sup>7</sup> Each of the 1,500 ego networks varies in terms of core network characteristics such as size, density, influence, norms and values, level of activity, and embedded resources. This study’s general argument is that the speed, nature, and influence of the information that flows through a network is contingent on such network characteristics. This research will thus examine whether these network characteristics influence market reactions around quarterly company earnings announcement events.

*Volume/Level of Activity.* The SNA literature has conceptualized a number of relevant characteristics of ego networks. A first feature is the level of activity. On Twitter, this characteristic is reflected in *volume*, or the number of relevant cashtag tweets sent, and is the basic characteristic examined in previous accounting literature documenting the market relevance of social media [5]. In line with previous research [3], [5], [8], [26], it is expected that stronger market reactions will come from more active networks.<sup>8</sup>

*Size.* A second core characteristic of ego networks is *size*, or the number of actors connected to the cashtag [1], [24]. In a cashtag ego network, the cashtag (e.g., \$AAPL) is the “ego” – the core – and size is reflected in the number of users connected to the cashtag. *Ceteris paribus*, a larger network should amplify any market reaction. At any given level of activity, more users should strengthen the market effect.

*Density, Compactness, Clustering, and Cohesion.* The SNA literature has also been interested in conceptualizing the extent of interconnectedness of users in a given ego network [19].

<sup>6</sup>Cashtag tweets thus contain a mix of information, news, commentaries, opinions, company analyses, and stock recommendations.

<sup>7</sup>Networks can be generally be analyzed at three different levels: the network level, the sub-network level, or the actor (“ego-centric”) level [36]. This study focuses on the ego-centric, or ego network, level.

<sup>8</sup>Note that this relates heavily to *degree centrality*: “Clearly, since degree centrality is a local property and the ego degree centrality of ego is the same as the degree of the actor in the whole network there is no issue” (p. 32) [14]

<sup>3</sup>With its focus on one-way disclosure of information, existing financial accounting theory is ill-equipped for understanding this heavily network-dependent context; it is mostly silent, notably, regarding how network structure amplifies, filters, and changes financial information.

<sup>4</sup>Hentschel and Alonso [20] also studied cashtag networks in a communication context.

<sup>5</sup>Such insights invite scholars to combine theories from psychology and sociology with the methods from social network analysis to bring fresh evidence to bear on important accounting and capital markets phenomena. The goal should be to employ social network analysis tools, which have been successfully used in other accounting contexts [36], to examine the importance of virtual networks in determining market efficiency, the information asymmetry between insiders and outsiders, and other important outcomes.

The most common dimension is *network density* [7].<sup>9</sup> At the network level, the density or, conversely, the sparseness of a community of ties can be considered the aggregation manifestation of strong/weak ties [18]. SNA scholars have also explored distance-based extensions to density that convey the compactness and/or cohesion of the network members. Ego networks are also often analyzed in terms of how “clustered” the network is; that is, how prevalent *cliques* are in the network. Overall, it is expected that denser networks will magnify market reactions. At the same time, there is evidence that less compact, more diverse networks may foster creative thinking and innovation [33], which could moderate the scope of the market reaction.

*Tie Strength.* Networks further vary in terms of how tightly connected network members are. Because the “digital footprints” of social media relationships are public and visible, at the dyadic level we can observe *tie strength* in the length and/or number of interactions [18] as well as multiplexity, or the number of different types (e.g., friend/follower relationship, @USER mentions, direct messages, retweets) of interactions (e.g., [38], [43]). Such indicators of tie strength can be aggregated to generate measures of the average strength of ties within each ego network. In general, networks with stronger ties among users can be expected to experience amplified market reactions to new information.

*Network Norms and Values.* Social media are effectively public, transparent communication systems, which offers the possibilities to observe cognitive facets of social capital such as the strength of a network’s *norms and values* (e.g., [9], [25], [35]) or the presence of shared codes, narratives, and systems of meaning (see [32]). For instance, norms of reciprocity are indicated by reciprocal favoriting/archiving, retweeting, and friending behaviors, while Big Data analytic techniques such as machine learning can be used to capture core cognitive features – such as commitment, identity, solidarity, expectations and obligations, and trust – that are reflected in the language used in tweets [6], [17]. Stronger communities are more likely to have similar opinions, which could strengthen market reactions to new information.

*Embedded Resources and Influence.* Network scholars have also focused on the notion of *embedded resources* (Lin, 1999). On social media sites such as Twitter, we can directly observe embedded resources, such as authority, wealth, power, status, and occupation, through data embedded in users’ profiles as well as in their publicly visible friend and follower contacts. The openness of the Twitter API combined with cheap computing power hence renders it possible to determine not only the size of each follower’s network – the number of followers the follower has – but also its *influence* within that network.<sup>10</sup> The point is, some followers, as well as some networks, are simply more valuable. It is expected that networks with more influential message senders will see amplified market reactions.

<sup>9</sup>An extension of size and density is the *diameter* of the network.

<sup>10</sup>There are some who are similarly interested. For instance, Hirshleifer and Teoh [21] argue that scholars should pay more attention to investors’ degree of *social influence* as a determinant of thought and behavior contagion in investment communities.

*Maximum Flow.* When considering the speed and likelihood of any given piece of information spreading, the connectedness of all actors in the network is also important. Maximum flow reflects the potential flow of information by taking into account the number of different pathways information can reach any given actor. Aggregated to the network level, this represents a solid measure of the potential impact of a piece of information. All other things equal, the greater the maximum flow, the more quickly information will reach key market actors.

## F. Core Proposition

In short, networks vary along a number of structural and cognitive dimensions, including network size, level of activity, density, cohesion, tie strength, network norms and values, embedded resources and influence, and maximum flow. It is argued that these network characteristics can influence the scope and nature of the market reaction to any information that flows through the network. The core proposition is as follows:

**Core Proposition:** *The network characteristics of a company’s cashtag network will influence the market reaction to earnings announcement events.*

## III. METHOD

### A. Information Events: Earnings Announcements of S&P 1,500 Firms

The project will use a large sample of publicly traded corporations: The 1,500 constituent firms on the S&P 1,500 list in 2018. In line with previous research [5], the events this study will examine are all quarterly earnings announcements dates for the 1,500 sample firms in 2018.<sup>11</sup> All of the analyses mentioned below are based on 3-day event windows surrounding earnings announcements in 2018.

### B. Twitter Cashtag Data

The heart of the data used are the *cashtag* tweets – tweets containing stock-ticker symbols such as \$AAPL for Apple or \$MSFT for Microsoft. Each of the 1,500 firms in the sample has its own decentralized, user-generated cashtag network, with messages – and, by extension, users – connected by the inclusion of the same cashtag in a tweet. There are thus 1,500 distinct ego networks.

A dataset was purchased from Twitter comprising all tweets that contain the cashtags for any of the stock tickers for the S&P 1,500 firms during the last two months of 2017 and all of 2018. The dataset contains approximately 17 million tweets. The data are provided in JSON format and will be incorporated into a MongoDB database. After initial cleaning it will be then exported from MongoDB into a Python *PANDAS* (Python Data Analysis Library) dataframe. It is in *PANDAS* that the majority of the data manipulations will take place.

<sup>11</sup>[5] argue that earnings announcements are “one of the most common and arguably the most important news event to investors” (p. 6).



### C. Independent Variables: Event-Specific SNA Measures of Cashtag Networks

A core tenet of this project is that applying the conceptual and methodological tools of social network analysis (SNA) will help build understanding of the social media context. The SNA perspective would look to map cashtag networks and then recognize that each network varies in terms of core network characteristics such as size, centrality, density, influence, values, embedded resources, and community/cliue structure. In line with extant SNA research, these measures will be operationalized for each company-specific ego network.

The project will thus employ network analysis to map cashtag networks and then operationalize network variation in terms of core network characteristics including size, centrality, density, influence, values, and embedded resources. To generate the network measures, first, an event-date dataset created using *Compustat* and *Eventus* will be imported into *PANDAS*. With the event-date dataset, it is then possible to generate the social network analysis measures on the Twitter data. For this the study will use the Python SNA package *Networkx*. For each of the 1,500 firms' quarterly event dates, *Networkx* and *PANDAS* will be used to calculate the following social network analysis measures for the 7-day period immediately preceding each earnings announcement event date:

- 1) *Level of Activity*, measured as the total number of tweets sent;<sup>12</sup> 2) *Size*, which capture the total number of ties as measured by the number of unique message senders [1], [24]; 3) *Influence*, measured as the total number of retweets garnered by all ego network tweets; 4) *Density*, measured via *Networkx* as the density of the company's cashtag discussion network as indicated by connections among the users sending company-specific cashtag tweets; 5) *Compactness*, measured as the *Networkx* distance-based cohesion score generated from the user co-mention network in each cashtag community;<sup>13</sup> 6) *Clustering*, operationalized as the ego network's *clustering coefficient*; 7) *Embedded Resources* [29], measured as the total number of followers for all users sending company-specific cashtag tweets; 8) *Network Norms and Values* [9], [24], [35], [32], which will be measured via Big Data machine learning algorithms found in the Python package *scikit-learn* to capture norms of reciprocity as reflected in reciprocal retweeting and shared values as reflected in the language used in tweets [6], [17]; and 9) *Maximum Flow*, a measure in *Networkx* that takes into account the number of different pathways information can reach any given actor and, which, aggregated to the network level, represents a measure of the potential reach of a piece of information.

In short, for each company earnings announcement, this study will use *PANDAS* combined with *Networkx* and *scikit-learn* to generate a date-specific cashtag network that will then

<sup>12</sup>In addition to the raw counts (e.g., *Firm Tweet*), this study will also measure activity in terms of "abnormal" levels, where, as in Blankespoor et al. [5], "abnormal is defined using the firm as its own control. This allows [me] to remove any firm fixed effects (p. 12) that may be correlated with the measure of information asymmetry. *Abnormal Firm Tweets* will thus measured as the number of tweets in the 3-day event period (-1, +1) divided by the number of tweets in the 30-day period before the earnings announcement.

<sup>13</sup>Compactness is related to the cohesion or, flipping the concept around, the *diversity* [33] of the network.

be used to generate a series of 7-day network measures. With 1,500 firms making four quarterly earnings announcements each per year, a total of 6,000 date-specific networks will be generated in 2018 to create the above network measures. This dynamic, computationally intensive approach to network measurement has only recently become possible given cheaper computing power and the data analytic tools offered by Python and similar platforms. It represents a significant expansion compared to previous network studies, which have tended to limit themselves to a single network [36] or, in more recent studies, a single cross-sectional snapshot [13].

### D. Dependent Variables

It would be expected that firms' online information networks to have an effect on volume, price, volatility, information asymmetry, and the speed at which new information is incorporated into market prices. To examine the market effects of Twitter-based network characteristics, the initial analyses will focus on cumulative abnormal returns around the quarterly earnings announcement events. The dependent variable, *CAR*, is cumulative abnormal returns over the event window. In line with previous literature [10], the event period is the two-day window around the event from trading day  $t$  to  $t + 1$ . With expected returns based on a market model calculated over the [-252, -21] pre-event period,

and the abnormal return computed for each day  $t$  in the event window, the cumulative abnormal return for each security/event is calculated as the cumulative daily abnormal return over the  $t_0$  through  $t_{+1}$  window:

$$CAR_{i,(t_0,t_{+1})} = \sum_{t=t_0}^{t_{+1}} AR_{i,t}$$

Additional dependent variables that could be examined include cumulative abnormal volume, information asymmetry [5],<sup>14</sup> and post-earnings announcement drift [27].<sup>15</sup>

### E. Control Variables

In line with predominant financial accounting research, this study will also include a suite of information environment, market reaction, and financial and stock return control variables, including *WSJ* data from Factiva; financial data from Compustat; analyst information from I/B/E/S; institutional ownership data from *Thomson Reuters Institutional (13f) Holdings data*; and stock return data from CRSP.

<sup>14</sup>In line with existing literature [28] information asymmetry is measured as the change in the bid-ask spread. Predicated on an argument made by Leuz and Verrecchia [28], Blankespoor et al. [5] argue that "information asymmetry plays a critical role in the liquidity of capital markets...[and thus] use the bid-ask spread as [their] main proxy for information asymmetry, as it captures market makers' and other liquidity suppliers' ... willingness to trade..." (pp. 12-13). This study proposes to employ a similar variable, which measures the difference in the average daily spread in the period after the earnings announcement and the average daily spread in the period preceding the earnings announcement.

<sup>15</sup>As in [27], this study could measure post-earnings announcement drift as the "buy and hold returns of the stock from two days after the earnings announcement through one day after the subsequent earnings announcement minus the buy and hold return of the appropriate portfolio matched by size and book to market of the Fama-French six portfolios" (p. 52) [27].

## IV. CONCLUSION

Implicitly, scholars have long recognized that information flows through networks. However, capital markets researchers have tended to posit such networks as relatively unimportant “black boxes.” This study has argued that we need to better understand the processes of how information flows through and is affected by networks of market-oriented actors. The recent widespread adoption of social media tools by firms and investors alike presents a unique opportunity to study network-based informational dynamics. Consequently, this study has presented a design for this study that strives to help develop network-level theories of the effects of information flows on the capital markets.

The study thus takes an explicitly network-based view and employs tools from social network analysis to help capture the stock market effects of social media-based discussion networks. Overall, network analysis has received scant attention from financial scholars. It is believed this study will make a unique contribution by advancing understanding of the relationship between network characteristics and market outcomes and by developing novel methodological approaches to the dynamic measurement of core network features in Big Data [39].

By merging the latest social network analysis tools from the social sciences with the economic concepts of the financial accounting literature, this project tests how important the ever-growing online networks of professional and amateur investors, analysts, and journalists are in determining market efficiency, information asymmetry, and other topics central to capital markets research. Beyond the theoretical contributions noted above, this project aims to inform the investor community, regulators, and the media about how social media networks influence the markets. In an age of social media-driven “clickbait,” “instant celebrity,” “information silos,” “truthiness,” “alternative facts” and “fake news,” it is worthwhile to understand whether and how these media may be manipulating or unduly influencing the capital markets.

## ACKNOWLEDGMENT

The author would like to thank Dean Neu, Jeff Everett, Giri Kanagaretman, and Veljko Fotak for helpful comments and suggestions.

## REFERENCES

- [1] Manju K Ahuja, Dennis F Galletta, and Kathleen M Carley. Individual centrality and performance in virtual R&D groups: An empirical study. *Management Science*, 49(1):21–38, 2003.
- [2] Hunt Allcott and Matthew Gentzkow. Social media and fake news in the 2016 election. *Journal of Economic Perspectives*, 31(2):211–236, 2017.
- [3] Eli Bartov, Lucile Faurel, and Partha S Mohanram. Can Twitter help predict firm-level earnings and stock returns? *The Accounting Review*, 93(3):25–57, 2018.
- [4] Pierre R Berthon and Leyland F Pitt. Brands, truthiness and post-fact: Managing brands in a post-rational world. *Journal of Macromarketing*, 38(2):218–227, 2018.
- [5] Elizabeth Blankespoor, Gregory S Miller, and Hal D White. The role of dissemination in market liquidity: Evidence from firms’ use of Twitter. *The Accounting Review*, 89(1):79–112, 2014.
- [6] Johan Bollen, Huina Mao, and Alberto Pepe. Modeling public mood and emotion: Twitter sentiment and socio-economic phenomena. In *ICWSM*, 2011.
- [7] Stephen P Borgatti and P C Foster. The network paradigm in organizational research: A review and typology. *Journal of Management*, 29(6):991–1013, 2003.
- [8] Hailiang Chen, Prabuddha De, Yu Jeffrey Hu, and Byoung-Hyoun Hwang. Wisdom of crowds: The value of stock opinions transmitted through social media. *The Review of Financial Studies*, 27(5):1367–1403, 2014.
- [9] J S Coleman. Social capital in the creation of human capital. *American Journal of Sociology*, 94:95–120, 1988.
- [10] Asher Curtis, J. Vernon Richardson, and Roy Schmardebeck. Investor attention and the pricing of earnings news. In Gautum Mitra and Xiang Yu, editors, *Handbook of Sentiment Analysis in Finance*, pages 212–232. OptiRisk Systems, Uxbridge, UK, aug 2016.
- [11] S R Das and Jacob Sisk. Financial communities. *Journal of Portfolio Management*, 31(4):112–123, 2005.
- [12] Lisette de Vries, Sonja Gensler, and Peter S.H. Leeftang. Popularity of brand posts on brand fan pages: An investigation of the effects of social media marketing. *Journal of Interactive Marketing*, 26(2):83–91, may 2012.
- [13] Roger S. Debreceny, Asheq Rahman, and Tawei Wang. Corporate network centrality score: Methodologies and informativeness. *Journal of Information Systems*, 31(3):23–43, may 2017.
- [14] Martin Everett and Stephen P Borgatti. Ego network betweenness. *Social Networks*, 27(1):31–38, 2005.
- [15] Eugene F Fama. The behavior of stock-market prices. *The Journal of Business*, 38(1):34–105, 1965.
- [16] Christian Fieseler, Matthes Fleck, and Miriam Meckel. Corporate social responsibility in the blogosphere. *Journal of Business Ethics*, 91(4):599–614, 2010.
- [17] Alec Go, Richa Bhayani, and Lei Huang. Twitter sentiment classification using distant supervision. *CS224N Project Report, Stanford*, pages 1–12, 2009.
- [18] Mark S Granovetter. The strength of weak ties. *American Journal of Sociology*, 78(6):1360–1380, 1973.
- [19] Robert A Hanneman and Mark Riddle. Introduction to social network methods, 2005.
- [20] Martin Hentschel and Omar Alonso. Follow the money: A study of cashtags on Twitter. *First Monday: Volume 19, Number 8 - 4 August 2014*, 2014.
- [21] DAVID HIRSLEIFER, SONYA SEONGYEON LIM, and SIEW HONG TEOH. Driven to Distraction: Extraneous Events and Underreaction to Earnings News. *The Journal of finance (New York)*, 64(5):2289–2325, 2009.
- [22] Gerald C Kane, Maryam Alavi, Giuseppe Joe Labianca, and Stephen P Borgatti. What’s different about social media networks? A framework and research agenda. *MIS Quarterly*, 38(1):274–304, 2014.
- [23] Andreas M Kaplan and Michael Haenlein. Users of the world, unite! The challenges and opportunities of social media. *Business Horizons*, 53(1):59–68, 2010.
- [24] Mami Kikuchi and Cynthia-Lou Coleman. Explicating and measuring social relationships in social capital research. *Communication Theory*, 22(2):187–203, 2012.
- [25] Mami Kikuchi and Cynthia-Lou Coleman. Explicating and measuring social relationships in social capital research. *Communication Theory*, 22(2):187–203, 2012.
- [26] Lian Fen Lee, Amy P. Hutton, and Susan Shu. The role of social media in the capital market: Evidence from consumer product recalls. *Journal of Accounting Research*, 53(2):367–404, may 2015.
- [27] Alina Lerman. Individual investors’ attention to accounting information: Evidence from online financial communities. *Contemporary Accounting Research*, 37(4):2020–2057, dec 2020.
- [28] C Leuz and B E Verrecchia. The economic consequences of increased disclosure. *Journal of Accounting Research*, page 38, 2000.
- [29] Nan Lin. Building a network theory of social capital. *Connections*, 22(1):28–51, 1999.
- [30] Kevin McCoy. NVIDIA shares fall 7% on short-seller’s warnin, 2016.
- [31] Amalia R Miller and Catherine Tucker. Health information exchange, system size and information silos. *Journal of Health Economics*, 33:28–42, 2014.
- [32] Janine Nahapiet and Sumantra Ghoshal. Social capital, intellectual capital, and the organizational advantage. *Academy of Management Review*, 23(2):242–266, 1998.

- [33] Salvatore Parise, Eoin Whelan, and Steve Todd. How Twitter users can generate better ideas. *MIT Sloan Management Review*, pages <http://sloanreview.mit.edu/article/how-twitter-use>, 2015.
- [34] J Pfeffer, T Zorbach, and K M Carley. Understanding online firestorms: Negative word-of-mouth dynamics in social media networks. *Journal of Marketing Communications*, 20(1-2):117–128, mar 2014.
- [35] Robert D Putnam. *Bowling alone: The collapse and revival of American community*. Simon and Schuster, New York, NY, 2000.
- [36] Alan J Richardson. Regulatory networks for accounting and auditing standards: A social network analysis of Canadian and international standard-setting. *Accounting, Organizations and Society*, 34(5):571–588, 2009.
- [37] Gregory D Saxton. New media and external accounting information: A critical review. *Australian Accounting Review*, 22(3):286–302, 2012.
- [38] Michael Szell, Renaud Lambiotte, and Stefan Thurner. Multirelational organization of large-scale social networks in an online world. *Proceedings of the National Academy of Sciences*, 107(31):13636–13641, 2010.
- [39] Miklos A Vasarhelyi, Alexander Kogan, and Brad M Tuttle. Big Data in accounting: An overview. *Accounting Horizons*, 29(2):381–396, feb 2015.
- [40] Justina Vasquez. Kylie Jenner Tweeted About Snapchat. Then Its Stock Lost \$1.3 Billion in Value. *Time*, feb 2018.
- [41] Richard D Waters and Jia Y Jamal. Tweet, tweet, tweet: A content analysis of nonprofit organizations' Twitter updates. *Public Relations Review*, 37(3):321–324, 2011.
- [42] James Worrell, Molly Wasko, and Allen Johnston. Social network analysis in accounting information systems research. *International Journal of Accounting Information Systems*, 14(2):127–137, jun 2013.
- [43] Anna Wu, Joan M DiMicco, and David R Millen. Detecting professional versus personal closeness using an enterprise social network site. In *Proceedings of the SIGCHI Conference on Human Factors in Computing Systems*, pages 1955–1964. ACM, 2010.

**Gregory D. Saxton** is an Associate Professor of accounting at the Schulich School of Business. Previously Dr. Saxton was an associate professor of communication at the University at Buffalo. Saxton studies the role and effects of technology – especially Big Data and social media – on the flow of information to and from organizations. He focuses on nonprofit organizations but also has an interest in financial markets and for-profit contexts. #BigData #analytics #nonprofits #accounting #information #communication #CSR #socialmedia

# Circular Economy Maturity Models: A Systematic Literature Review

D. Kreutzer, S. Müller-Abdelrazeq, I. Isenhardt

**Abstract**— Resource scarcity, energy transition and the planned climate neutrality pose enormous challenges for manufacturing companies. In order to achieve these goals and a holistic sustainable development, the European Union has listed the circular economy as part of the Circular economy Action Plan. In addition to a reduction in resource consumption, reduced emissions of greenhouse gases and a reduced volume of waste, the principles of the circular economy also offer enormous economic potential for companies, such as the generation of new circular business models.

However, many manufacturing companies, especially small and medium-sized enterprises, do not have the necessary capacity to plan their transformation. They need support and strategies on the path to circular transformation because this change affects not only production but also the entire company. Maturity models offer an approach to determine the current status of companies' transformation processes. In addition, companies can use the models to identify transformation strategies and thus promote the transformation process. While maturity models are established in other areas, e.g. IT or project management, only a few circular economy maturity models can be found in the scientific literature.

The aim of this paper is to analyze the identified maturity models of the circular economy through a systematic literature review (SLR) and, besides other aspects, to check their completeness as well as their quality. For this purpose, circular economy maturity models at the company's (micro) level were identified from the literature, compared, and analyzed with regard to their theoretical and methodological structure. A specific focus was placed, on the one hand, on the analysis of the business units considered in the respective models and, on the other hand, on the underlying metrics and indicators in order to determine the individual maturity level of the entire company.

The results of the literature review show, for instance, a significant difference in the number and types of indicators as well as their metrics. For example, most models use subjective indicators and very few objective indicators in their surveys. It was also found that there are rarely well-founded thresholds between the levels. Based on the generated results, concrete ideas and proposals for a research agenda in the field of circular economy maturity models are made.

**Keywords**—assessment, circular economy, maturity model, transformation, systematic literature review.

## I. INTRODUCTION

**P**OLITICAL goals such as the European Union's climate targets for 2030 and societal changes such as the growing sustainability awareness of entire generations have a major influence on manufacturing companies [1]. On the one hand, they have the goal of maximizing profits and operating cost-efficiently, and on the other hand, they must and want to consider social, ecological and political factors. Manufacturing

companies cannot ignore these factors, also due to political framework conditions such as the goals of the European Union (EU) or also media interest, such as in the Fridays for Future movement, as this can have a direct or indirect influence on their customer segments [2]. In order to remain viable for the future, companies are increasingly focusing on sustainable business practices [2].

Due to increasing resource scarcity worldwide, the need to reshape the "metabolism of humanity" in relation to finite raw materials has been recognized in the recent past [3]. Since the early 21st century, therefore, the notion of the circular economy has increasingly become the focus of industry, governments and economic alliances. The idea of the circular economy has been around for more than 50 years. However, it has only recently gained widespread attention due to increasing threats such as climate change [4]. Acute problems such as the shortage of raw materials or climate change are becoming difficult to solve due to the established linear economy with end-to-end chains for raw materials, from extraction, use to disposal [5]. The principle of circular economy, where material flows consist of e.g. materials designed for circulation in socio-economic systems with recycling as a key strategy, has generated more and more attention in recent years in the wake of the increasingly urgent need for a more sustainable "industrial metabolism" [3].

On a political level, the circular economy is listed as a measure of the European Green Deal for sustainable development and has many potentials to achieve the planned climate neutrality of the EU. Between 45% and 70% of global CO<sub>2</sub> emissions can be reduced through a circular economy [6]. Frans Timmermans, Executive Vice-President for the European Green Deal, also sees the shift from linear value creation to the circular economy as necessary not only to strengthen but also to maintain the economic competitiveness of businesses [7]. The circular economy has the essential difference to linear value creation that products gain "value" along the value chain (purchase to disposal), as they flow into the value chains of other products and do not lose "value" [5].

In order to achieve a far-reaching establishment of the principle of the circular economy, manufacturing companies must be shown ways and strategies of how to implement a change in their structures and processes to this end. It is important not to remain in a general and theoretical framework, but to provide concrete and clearly defined methods for practice. Particular attention should be paid to small and

D. Kreutzer\*, S. Müller-Abdelrazeq and I. Isenhardt are with RWTH Aachen University, Chair of Production Metrology and Quality Management & Institute for Information Management in Mechanical Engineering, Germany,

52068 Aachen, Dennewartstr. 27 (\* corresponding author, phone: +49 2418091174, e-mail: dennis.kreutzer@ima.rwth-aachen.de).



medium-sized enterprises (SMEs), as they represent 99% of European enterprises [8]. As the transition to circular company structures is very complex, a broad base of know-how is needed, which is not available to many companies [9]. The concept of the circular economy is largely based on new technologies and business models [9]. It also requires structural changes in all areas of business, from product development, resource sourcing and supply chains to the structure of use and end-of-life design [9], [10].

Maturity models (MM) are helpful tools to support these business challenges [11]. A maturity model comprises a sequence of maturity levels for a class of objects and thereby describes a desired or typical development path of these objects in successive, discrete ranks, starting at an initial stage up to full maturity [12]. Progressing along this development path means a steady increase in the performance or quality of the object under consideration, with the maturity model serving as a scale for assessment [12].

Evaluation systems are used to calculate and present maturity. According to *Bensiek*, two approaches can be distinguished here [13]. Scoring and level-based maturity levels. In scoring, points are awarded for different characteristics. These points are added up and represent the developmental stage depending on the total number of points. In the case of stage-based maturity levels, it is defined that a maturity level can only be reached if all the requirements set for the maturity level are met, whereby skipping a stage is basically not possible. In this context, maturity levels can be assigned organization-wide or specific to a field of action. [13] The aim of this paper is to explore the development of MM in the area of circular economy for manufacturing companies. *Bensiek* [13] and *Becker et al.* [12] emphasize that before developing a new model, it is preferable to examine existing models and their possible adaptability. Therefore, this paper identifies existing circular economy maturity models for manufacturing companies through a systematic literature review (SLR) and evaluates them according to defined analysis criteria.

## II. METHOD

SLRs collect answers from the literature on specific questions or hypotheses, consolidate the results and identify the need for further research on a particular research topic [14]. In the context of this paper, an SLR was chosen to identify and contrast circular economy maturity models for manufacturing companies and to highlight the respective focus of the model, as well as the research gaps. These results are useful for academia to get a time-saving overview of the research field of MM in the Circular economy and to drive further research based on the synthesized results. For traceability, therefore, objectivity and replicability must always be present when conducting an SLR [15]. For this reason, SLRs follow a fixed procedure, but the number of steps varies from author to author. *Kitchenham and Charters* [16] for example, propose a three-stage procedure consisting of the main phases (1) planning, (2) implementation and (3) reporting, which is further subdivided into several sub-phases. *Denyer and Tranfield* [17] on the other

hand, recommend a similar procedure according to the phases (1) formulation of the research question, (2) finding studies, (3) study selection and (4) analysis and synthesis as well as (5) reporting and use of the results. Another scientifically recognized approach is based on the *Preferred Reporting Items for Systematic reviews and Meta-Analyses (PRISMA)* method. [15]. This divides the SLR into the four phases of identification, screening, eligibility and inclusion.

Building on these approaches, our SLR is divided into the five phases of (1) problem formulation and question identification; (2) literature search; (3) eligibility criteria & screening/ evaluation of research; (4) research analysis and interpretation; and (5) presentation of results. This approach is also inspired by *Correia et al.* [18], who conducted an SLR on MMs in supply chain sustainability. Figure 1 presents a diagram of the methodology that depicts the five phases of the SLR. In this chapter, the first four phases are discussed in more detail, whereas the results are consolidated in chapter *Results*.

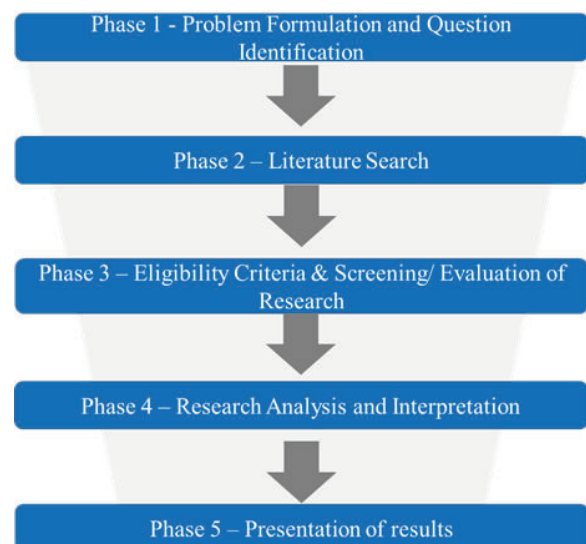


Fig. 1 Procedure for the systematic literature review

### *Phase 1 - Problem Formulation and Question Identification*

Maturity models are intended to represent changes in an entity's competencies in a stage or stadium-like manner and along a desired or logical pathway [19]. These stages are represented by levels or stages, which represent a path from a baseline state to full maturity. Each level/stage contains criteria and characteristics that must be met in order to reach it, as well as concrete approaches for advancing to higher levels [20]. The application of the models is mainly limited to the analysis of actual states in order to determine the maturity level of a company in the predetermined characteristics. Through the maturity approach, companies can also use the models to identify transformation strategies and thus continuously drive the transformation process forward [21]. Concrete improvement approaches can then be formulated from the descriptions of the levels and incorporated into the company's strategic planning [12].

Due to this relevance, it is of high importance for

manufacturing companies to obtain an overview of existing maturity models from the scientific literature, which can support them in their model selection and thus promote their circular business transformation. In the research area of maturity models in the Circular economy, some literature analyses have already been carried out, but these were related to other sectors, such as IT, project management or supply chain management (e.g. [22]). *Correiera et al.* identified 11 maturity models to assess and promote sustainability in the supply chain [18]. *Montag et al.* identified 35 models and frameworks to develop a Circular Supply Chain Maturity Model based on them [23]. However, structural changes are needed in all areas of the company, from product development, resource procurement and supply chains to the structure of use and the conception of the product's end of life [9]. Accordingly, there is currently a lack of a review of the literature on holistic maturity models for manufacturing companies, which leads to the first research question as follows:

**RQ1: Which circular economy maturity models already exist for manufacturing companies at micro level in the literature?**

The selected characteristics of the model on the basis of which maturity is determined is a critical point, as these form the basis of the model. According to *Akkasoglu*, the maturity-relevant characteristics are subject to the five requirements of goal conformity, independence, completeness, interpretability and influenceability [24]. Considering previous literature from other research areas, the selected criteria may vary depending on the maturity model. *Correiera et al.* identified variations in their SLR maturity models from missing to 24 characteristics, for example [18]. Considering the maturity measurement for manufacturing companies, it is of great importance by which characteristics maturity is captured, which leads to the following research question:

**RQ2: What characteristics influence the circular maturity of a manufacturing company?**

In addition to the definition and number of maturity-relevant characteristics, the measurement method is also crucial for determining the maturity level. The measurement method includes the type of questions used to gather information for the respective characteristic. According to *Bensiek*, three measurement methods occur in maturity models [13]: open-ended questions, closed-ended questions and Likert scale questions. The commonly used Likert scale allows users to indicate their level of agreement ("strongly agree" to "strongly disagree") with a statement [25]. In a survey with closed questions, several concrete expressions of the characteristic are given for answering. In contrast, open-ended questions do not give any answer options [11], [26]. Thus, questionnaire-based models insist on self-assessments and thus involve a certain subjectivity or fuzziness compared to the use of exact values with units of measurement [27]. This leads to the third research question:

**RQ3: Which measurement methods are used to record the characteristics relevant to maturity?**

*Phase 2 - Literature Search*

In the second phase of the SLR, the search strategy for the literature search is determined and databases are searched using keywords. Due to the increasing publication on the internet, we concentrated exclusively on scientific electronic literature databases. According to *Gusenbauer and Haddaway*, the four well-known academic literature databases SCOPUS, Web of Science, EBESCOhost and Emerald Insights are suitable for an SLR [28]. In view of the selected research area, the titles and abstracts were examined by means of a keyword search of the four databases in the fixed period from 2000 to 2023. The results were continuously narrowed down using a three-stage keyword entry procedure linked with AND operators ("Circular Economy" AND "Maturity"; "Circular economy" AND "Maturity" AND "Model"; "Circular economy" AND "Maturity" AND "Model" AND "Manufacturing"). This three-step process allows Circular economy Maturity models for manufacturing companies to be identified without losing any models in the last search function if one were to start with this one. Through this process, a total of 533 publications were identified across all four databases. The keyword searches of the SCOPUS and Web of Science databases yielded more than twice as many publications as ScienceDirect and EBESCOhost. The overview of the number of identified models per search term and database is shown in Table I.

TABLE I  
KEYWORD SEARCH USED IN THE DATABASES

Keyword Search	SCOPUS	Web of Science	ScienceDirect	EBESCOhost	Total
Circular economy AND Maturity	121	122	50	44	337
Circular economy AND Maturity AND Model	55	60	22	21	158
Circular economy AND Maturity AND model AND manufacturing	13	14	6	5	38
Total	189	196	78	70	533

*Phase 3 - Eligibility Criteria & Screening/ Evaluation of Research*

In the third phase, the scientific literature identified is narrowed down using eligibility criteria to identify only the most relevant literature [29]. Since the literature search was conducted separately for each database, all duplicates were excluded in a first step.



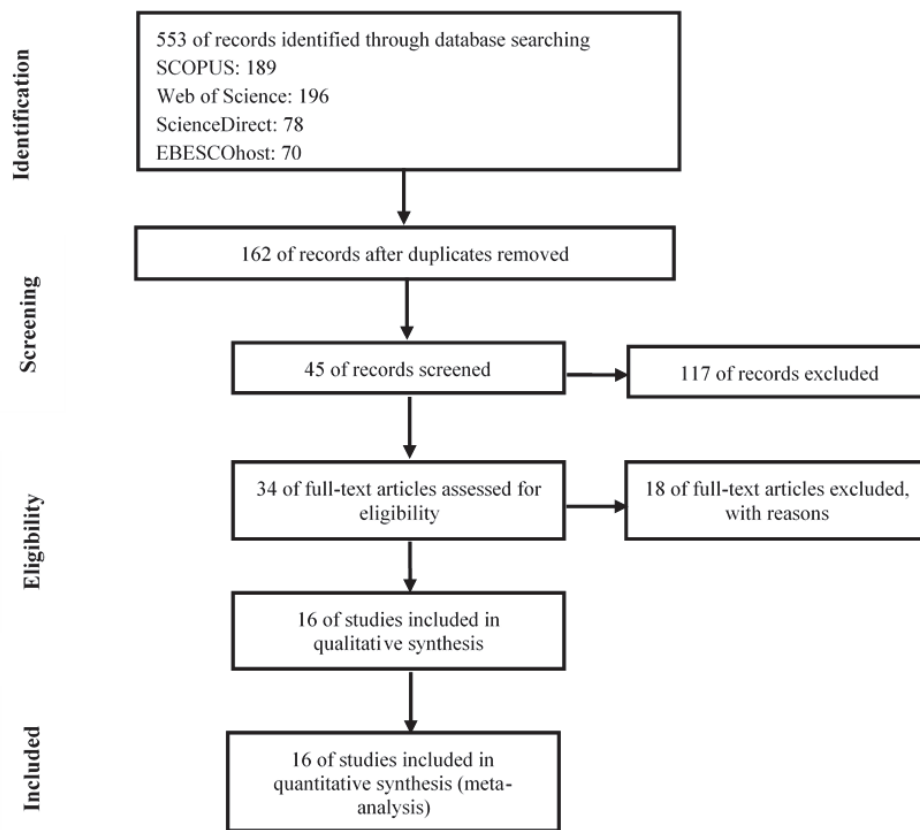


Fig. 2 PRISMA diagram

This resulted in 162 publications from the original 533 publications. During the subsequent screening process, the titles and summaries of all results were read in order to exclude the publications that did not fall within the scope of the circular economy maturity models for manufacturing companies. This resulted in the exclusion of 117 publications. This included some readiness models that will not be considered in this SLR. Although the term "readiness" is understood in a very similar way to "maturity" and both terms refer to an evolutionary process, the term "readiness" refers to the readiness of an organization to start the development process and the term "maturity" refers to the level of maturity the organization is already at [30].

Subsequently, all remaining publications were checked for additional criteria:

- *Written in English:* The publication must be written in English so that it is accessible to a broad scientific community.
- *Published in scientific journals or conferences:* The literature must have been published in a scientific journal or presented at a scientific conference. This excludes unpublished literature and guarantees scientific quality.
- *Presentation of a maturity model as output:* This excludes publications without a clear model. This exclusion criterion was defined in order to be able to derive clear phases and maturity-relevant characteristics or their measurement methods.

- *Focus on micro-level:* This excludes publications whose Circular economy maturity models focus on meso-level (e.g. networks) and macro-level (e.g. nations).

Based on these criteria and the number of models identified, 16 models were identified for further analysis. The entire search process is illustrated by the PRISMA flowchart in Fig. 2.

#### Phase 4 - Research Analysis and Interpretation

The fourth phase describes the analysis of the identified publications for specific analysis criteria in order to obtain statements about the research questions. Seven analysis categories with different numbers of subcategories were defined. We followed the analysis categories of *Correia et al.*, but added "maturity-relevant characteristics" for RQ 2 and "measurement method" for RQ 3 (see Table II) [18]. If no sufficient information could be identified in a subcategory, this was marked as "not identifiable".

TABLE II  
CATEGORIES FOR THE LITERATURE REVIEW ANALYSIS PARTLY BASED ON *CORREIRA ET AL.* [18]

Category	Subcategories	Description
Paper identification	Authors	List of authors
	Publication date	Year of publication
	Publication type	Journal article, conference proceedings, etc.
Scope	Maturity Scope	Process, whole company
Typology [31]	Structured models	A formal and complex structure, similar to the CMMI
	Maturity grids	A set of maturity levels that address different aspects of a research field
	Likert scale questionnaires	A series of questions where survey participants rank the company on a scale of 1 to n
	Hybrid models	A combination of characteristics of maturity grids and Likert scale model structure
	Others	Other information not included in the previous subcategories
Architecture [32]	Staged	A cumulative set of areas that define each level. All areas of a level must be successfully achieved before the next level can be entered.
	Continuous	A set of areas that can be addressed separately. Instead of addressing all areas of a given level, the focus of optimisation can be on a specific area
	Others	Other information not included in the previous subcategories
Components [31,32]	Number of maturity levels	Count of the number of maturity levels
	Descriptors	The name for every level of maturity
	Level description	The value is "Yes" if it contains the description or summary of the characteristics of the individual levels, otherwise "No".
	Maturity-relevant characteristics	Various approaches to analysing or assessing the level of maturity, taking into account one or more common characteristics. Alternatively, it may be a set of activities that contribute to achieving a number of objectives that contribute to attaining a higher level of maturity.
Measuring method	Metrics	Subjective/fuzzy or objective/distinct measuring method
Validation	Validation	Information about the validation and number of validation phases
Model development	Development basis	Building on a model or own developed concept

### III. RESULTS

In this chapter, the 16 identified refection models are analyzed using the criteria from Table II and the results are described in detail. Fig. 3 shows the number of publications and the type of publication over time. It is noticeable that 14 of the 16 maturity models were published in journals and only two as conference proceedings. In addition, the number of models increases with the years, whereby the year 2023 is still excluded due to its incompleteness.

#### Scope, Typology and Architecture of the maturity models

According to *Bensiek*, the scope of a maturity model can be action-specific or organization-wide [13]. To answer RQ 1, it can be stated that all 16 models have a holistic approach to organizational maturity assessment, but differ in the specific task focus. *Brendzel-Skowera* [33] e.g. focuses on the implementation of business models for SME, whereas *Heazendonck & van den Bergh* [34] examine Belgian ports on their circular maturity. This focus on the holistic approach is also reflected in the maturity-relevant characteristics for answering RQ 2, which are explained in more detail in the subchapter components.

Although all models focus on the Circular economy maturity assessment for companies or organizations, the model of *Kayikci et al.* [35] provides a broader framework for

consideration. In addition to circular maturity, it also measures circular readiness as well as maturity and readiness for Industry 4.0 transformation.

The maturity model typology can differ from model to model. Of the 16 models, nine models can be assigned to a structural typology (e.g. [36]). Despite this predominant typology among the models, other models can be assigned to a different typology, such as the maturity model by *Uztürk & Büyükožkan* [37] which applies to a maturity level grid representation. Other authors also use a grid representation, but combine this with a Likert scale questionnaire to form a hybrid model, such as by *Sacco et al.* [38]. The models of *Górecki* [39] and *Vegter et al.* [40] could not be assigned to any of the other typologies and were therefore labelled "Others".

The most commonly used form of maturity model architecture is the stage-by-stage representation of Circular economy maturity. Eleven out of 16 models, such as *Acerbi et al.* [36] prefer this representation. The continuous representation is taken up by four models, such as e.g. *Golinska-Dawson et al.* [41]. Only one model, that of *Górecki*. [39] uses neither a stepwise nor a continuous representation, but tabulates the maturity of each component separately. The detailed analysis and comparison of the identified maturity models is shown in Table III.

TABLE III  
COMPARISON OF THE MATU

Paper identification	Scope	Typology	Architecture	Validation	Model development	Components	Level description	Maturity-relevant characteristics	Measuring Method
Author, Publication date, Publication type	Scope	Typology	Architecture	Validation	Development basis	Number of maturity levels	Descriptors		Metrics
Acerbi et al, 2021, Journal Article [36]	Manufacturing companies, whole company focus	Structured model	Staged	Two complementary workshops evaluating its applicability and value.	New model	5	1 - Linearity, 2 - Industrial CE Piloting, 3 - Systematic Materials Management, 4 - CE Thinking, 5 - Full Circularity	no fixed set, exemplarily mentioned: <ul style="list-style-type: none"> <li>1 (legal responsibilities, company performance)</li> <li>2 (company interested in changing, pilot experimentation, process parameter material and energy consumption, the strategic level)</li> <li>3 (reuse, refurbish, recycle, and remanufacture materials; controlling; stakeholder management)</li> <li>4 ( stakeholder management, controlling)</li> <li>5 (strategic, process, stakeholder management)</li> </ul>	Not identifiable
Brendzel-Skowera, 2021, Journal Article [33]	Business models for SMEs; whole company	Hybrid (structured model and Likert scale)	Staged	Model was tested at 99 SMS	Combination of Business Model Canvas, the CMMI and R2Pi classification of CE Business models	6	L1. Initial, L2. Managed, L3. Defined, L4 Quantitatively managed, L5. Optimising	- L1: lack of knowledge about the assumptions of circular economy and business models dedicated to it, low environmental awareness; failure to limit the negative impact on the environment; environmental activities undertaken for pragmatic reasons; - L2: low level of knowledge about circular economy and business models dedicated to it; most of the processes regarding the area of environmental activities are identified and defined; environmental impact awareness; pragmatism in activities limiting negative impact on the environment; monitoring environmental indicators - L3: awareness of the impact on the environment and awareness of the existence of circular economy; environmental management system (formal or not) defined processes for the area of environmental activities; pragmatic and altruistic reasons for limiting negative impact on the environment; qualified employees for environmental protection - L4: familiarity with the rules of circular economy; work on redesigning the business model towards circular economy formalized environmental management system; process quality measures are built into the enterprise's decision-making system; the causes of process deviations are eliminated -L5: circular business model implemented; improvement of the organisation through process monitoring in terms of possible improvements; formalised environmental management system; raising awareness of the company's stakeholders when it comes to ecology	

TABLE III  
COMPARISON OF THE MATURITY MODELS (CONT.)

Paper identification	Scope	Typology	Architecture	Validation	Model development	Components	Level description	Maturity-relevant characteristics	Measuring Method
Author, Publication date, Publication type	Scope	Typology	Architecture	Validation	Development basis	Number of maturity levels	Descriptors		Metrics
Gólska-Dawson et al., 2021, Journal Article [41]	Responsible Resource Management in Remanufacturing for SMEs; remanufacturing as an CE transition practice	Hybrid (maturity grid and Likert scale)	Continuous, based on score (0-100%)	Tested at 4 SMEs	New model	5	ML1 (very low); ML2 (low); ML3 (medium); ML4 (high); ML5 (very high)	All based on the characterization of the responsible resource management practices: 4 Resource groups: Water, Emissions, Energy, Material	Not identifiable
Górecki, 2019, Journal Article [39]	Companies in the construction industry	Other (no Levels, staged etc.) not mentioned	Others	Not identifiable	New model	Not identifiable	No	Human resources; technical infrastructure; organizational culture; Organizational structure; management of construction projects; organization management	Not identifiable
Haezendonck & van den Berghe, 2020, Journal Article [34]	Belgian Ports	Structured Model	Staged	Tested through 5 Belgian ports	New model, maturity level based on R-strategies from Potting et al.	3	Energy Recovery; Recycling; Orchestrating new cargo streams	Not identifiable	Not identifiable
Howard et al., 2018, Conference proceedings [45]	Whole company level	Structured Model	Staged	Tested with 8 cases from dairy and baking sector in UK	Based on CMM	5	1 - Initiate; 2 - Manage; 3 - Improve; 4 - Inspire; 5 - Govern	Not separated into clear dimensions: <ul style="list-style-type: none"> <li>1 (within firm) - Efficiency focus; Waste reduction</li> <li>2 (within firm) - Effective measures: materials, energy, water; Linear connections, CE awareness</li> <li>3 (supply chain) - Cont. improvement; Supplier improvement; some closed loops; Known nutrients; Optimised SKUs ( Stock Keeping Unit); Skills focus;</li> <li>4 (sector) - Leads the sector; Drivers best practice; Regenerative and restorative; Regional capability; Investment plans; People focus</li> <li>5 (whole system) - System governance; policymaker links; Informs 6 informed by civic society; Includes wider stakeholders; NGOs; CE vision connects local, regional and national interests</li> </ul>	Not identifiable

TABLE III  
COMPARISON OF THE MATURITY MODELS (CONT.)

Paper identification	Scope	Typology	Architecture	Validation	Model development	Components	Level description	Maturity-relevant characteristics	Measuring Method
Author, Publication date, Publication type	Scope	Typology	Architecture	Validation	Development basis	Number of maturity levels	Descriptors		Metrics
Julkovski et al., 2022, Journal Article [46]	Whole company, example on craft breweries	Structured Model	Staged	Tested with 22 craft breweries from Portugal and Brazil	Adapted from Grant and Penypacker ; Ellen MacArthur Foundation (2015); Schmem et al. (2019a, 2019b); Salo et al. (2020); and Kardian	6	Non-existent (0); Executed (1); Managed (2); Established (3); Predictable (4); Optimised (5)	Yes Based on technical and biological cycles: collect, retain/ extend, share, reuse/redistribute, remanufacture/renew	Not identifiable
Kayikci et al., 2022, Journal Article [35]	Whole company; focus on SMEs	Hybrid: Maturity grid & Questionnaire	Continuous	Different rounds through DELPHI method; tested with Turkish fashion industry	New model, level based on Grant and Penypacker (2006)	6	Non-existent (0); Executed (1); Managed (2); Established (3); Predictable (4); Optimised (5)	No Economic, Environmental, Social, Policy, Process, Product, Strategy, Technology	Not identifiable
Romero & Molina, 2014, Conference proceedings [43]	Whole company, Green Virtual Enterprise Breeding Environments	Structured Model	Staged	Not identifiable	New model	4	L1: performed L2: managed L3: Standardised L4: Innovating	Yes Material; Energy; Transportation; Marketing; Human resources; Information and communication system; Environment, health and safety; Production processes; Quality of life and community connections; Waste management	Not identifiable

TABLE III  
COMPARISON OF THE MATURITY MODELS (CONT.)

Paper identification	Scope	Typology	Architecture	Validation	Model development	Components	Level description	Maturity-relevant characteristics	Measuring Method
Author, Publication date, Publication type	Scope	Typology	Architecture	Validation	Development basis	Number of maturity levels	Descriptors		Metrics
Sacco et al., 2021, Journal Article [38]	Whole company	Hybrid Maturity grid & Questionnaire	Continuous	3 validation rounds	New model, Categories based on Porters Value Chain	0-100%	No	No	Subjective: 23; Objective: 3  Firm Infrastructure: Strategy & Vision; Environmental management; Cooperation & industrial symbiosis HR Management: Training; Employee satisfaction & participation Technology development: Eco-design Procurement: Supplier selection & auditing Inbound& outbound logistics: Direct logistic, Reverse logistic, Operations: Resource consumption, Waste management, Marketing& sales: Marketing & communication
Schnem et al., 2019, Journal Article, [47]	Whole company; Business model in production chain	Structured Model	Staged	Applied to 105 Business models in Brazil	Adaptation: Level Based on Grant and Pennypacker (2006) Characteristics based on EMF-CE-Model	6	Non-existent (0); Executed (1); Managed (2); Established (3); Predictable (4); Optimised (5)	Yes	Technical Cycle: Collect; Keep/Extend; Share; Reuse/Redistribute; Remanufacture/refurbish  Biological Cycle: Collect; Cascade Exploitation; Extraction of biochemical raw materials; Anaerobic digestion; Biogas; Biosphere regeneration; Biochemical raw materials; Agriculture/collection
Schnem et al., 2020, Journal Article [48]	Whole company; wine chain production	Structured Model	Staged	Applied to 105 Business models in Brazil	Adaptation: Level Based on Grant and Pennypacker (2006) Characteristics based on EMF-CE-Model	6	Non-existent (0); Executed (1); Managed (2); Established (3); Predictable (4); Optimised (5)	Yes	Technical Cycle: Collect; Keep/Extend; Share; Reuse/Redistribute; Remanufacture/refurbish  Biological Cycle: Collect; Cascade Exploitation; Extraction of biochemical raw materials; Anaerobic digestion; Biogas; Biosphere regeneration; Biochemical raw materials; Agriculture/collection
Uhrenholt et al., 2022, Journal Article [44]	Whole company	Structured Model	Staged	Not identifiable	New conceptual model based on literature	6	None; Basic; explorative, systematic, integration, regenerative	Yes	Value creation; Governance; People and skills; Supply chain and partnership; Operations and technology; Product and material  Not identifiable



TABLE III  
COMPARISON OF THE MATURITY MODELS (CONT.)

Paper identification	Scope	Typology	Architecture	Validation	Model development	Components			Measuring Method		
						Development basis	Number of maturity levels	Descriptors	Level description	Maturity-relevant characteristics	Metrics
Author, Publication date, Publication type	Scope	Typology	Architecture	Validation							
Ünal & Sinha, 2023, Journal Article [42]	Whole company sustainability	Structured Model	Staged	Validated through 17 interviews with CEOs from firms	New model development based on C2C practices		5	1 - Basic; 2 - Bronze; 3 - Silver; 4 - Gold; 5 - Platinum	No	Material Health; Material reutilization; Renewable energy; Water stewardship; Social fairness	Not identifiable
Uztürk & Büyükoçkan, 2022, Journal Article [37]	Whole company, agriculture as an example	Maturity grid	Continuous	Tested with an example agriculture farm in Turkey	New model development, dimensions form the literature		4	Emerging, established, leading, ultimate	No	Product; Process; Business Model; Technology; Stakeholder	Not identifiable
Vegter et al., 2023, Journal Article [40]	Maturity model is focused on material flow though a CE supply chain	Not identifiable	Staged	Only the dynamic flow diagram is tested	Not identifiable		4	1 - virgin materials only; 2 - combination (virgin and recovered materials); 3 - recovered materials only; 4 – deterioration	Yes	Not identifiable	Not identifiable

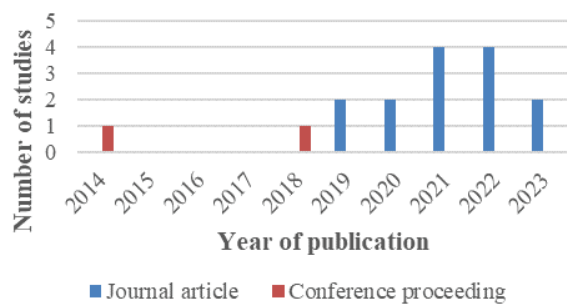


Fig. 3 Number of identified maturity models per year

#### Validation and Model development

According to *Bruin et al.* it is of particular importance to test the maturity models after their development and to validate them for validity, reliability as well as generalizability [11]. 13 of the 16 identified models name a validation process, although this varies widely: Some models apply their model to a different number of companies, e.g. *Brendzel-Skowera* [33] which tests its model on 99 SMEs. Another form of validation consists of interviewing experts, as done by *Ünal & Sinha* [42] who interviewed 17 CEOs from different companies. However, not only through interviews, also through workshop concepts, as by *Acerbi et al.* [36] can also be used to validate the maturity models. A comprehensive validation approach was used by *Sacco et al.* [38] who tested their model for completeness and reliability in three validation iteration steps (1. self-validation, 2. expert validation, 3. company validation). Only the models of *Górecki* [39], *Romero & Molina* [43] and *Uhrenholt et al.* [44] do not mention any validation steps.

In terms of model development, the models of *Brendzel-Skowera* adapt [33] and *Howard et al.* [45] adapt the Capability Maturity Model Integration (CMMI) to classify maturity levels into 1 - Initial, 2 - Managed, 3 - Defined, 4 - Quantitatively managed and 5 - Optimising. Four other models ([46], [35], [47], [48]) use the designation of maturity levels according to *Grant and Pennypacker* with the levels (0) meaning non-existent, one (1) executed, two (2) managed, three (3) established, four (4) predictable, and five (5) optimised. [49]. Another aspect of model development concerns the combination of different model components, such as *Brendzel-Skowera*, who combines the Business Model Canvas with the CMMI and the R2Pi to create a new aggrandized model [33].

#### Components

This subchapter answers RQ 2. An important component of a maturity model are the maturity levels, which represent to the user how advanced the transformation to a specific area is [12]. Table III shows that the number of maturity levels, but also the way they are presented, varies in terms of scale. While 14 of the 16 models use fixed levels in the form of an ordinal scalar, such as *Romero & Molina* [43] (L1: performed; L2: managed; L3:

Standardised; L4: Innovating), the model according to *Sacco et al.* [38] uses an interval scale from 0 to 100%. [50]. All 16 models use an upstream literature review for the maturity-related characteristics, such as *Sacco et al.* which is oriented towards the eight enterprise domains of the Porter Value Chain to be able to map a holistic enterprise maturity [38].

The model by *Górecki* [39] does not specify a number of levels. Regarding the naming of the individual levels, six models use the names of other known maturity models, as described in the subchapter *Validation and Model development*. Regarding the description of the individual levels, the SLR shows that half of the models give a description of the levels and the other half only mention the levels but do not go into more detail about the particular classification of the respective maturity level.

Table III shows that the definitions and also the number of elements used to capture the respective maturity vary depending on the model and are not uniform. Some models, such as *Uhrenholt et al.* [44] use the same six maturity-relevant characteristics, such as "value creation", which have different characteristics depending on the level of the six maturity levels, consistently throughout the entire model. Other models, such as *Howard et al.* [45] cite a different number and also definitions of maturity-relevant characteristics per maturity level that is significant for the respective level. In addition, there are also models that use a combination of both variants. *Brendzel-Skowera*, for example, uses individual characteristics such as "Knowledge about circular economy and business models dedicated to it." [33] consistently, but also adds additional characteristics per level. This insight also includes the thresholds between the levels, which in some cases (e.g. *Brendzel-Skowera* [33]) or the delimitation of the maturity levels is described by characteristics such as "absent" to "low level". None of the models uses numerical threshold values that can be used to identify the assignment to a specific maturity level.

This wide variation of the models in terms of definition also relates to the number of characteristics used. Fig. 4 shows the number of maturity levels used (Y-axis) in relation to the number of characteristics used (X-axis) in 15 of the 16 models. Due to the interval scale of the model according to *Sacco et al.* [38] it is therefore not shown in the figure. It is clear that the number of maturity levels lies between three and six levels, with four models each having five levels (e.g. *Acerbi et al.* [36]) and six models six levels (e.g. *Kayikci et al.* [35]). Only for the model of *Górecki* [39] no maturity levels are given.

The variance in the number of levels is also evident in the number of characteristics. Here the number ranges from none mentioned characteristics (*Haезendonck & van den Berghe* [34] and *Vegter et al.* [40]) to 26 maturity-relevant characteristics (*Howard et al.* [45]). The mean value across all models is about eight characteristics.

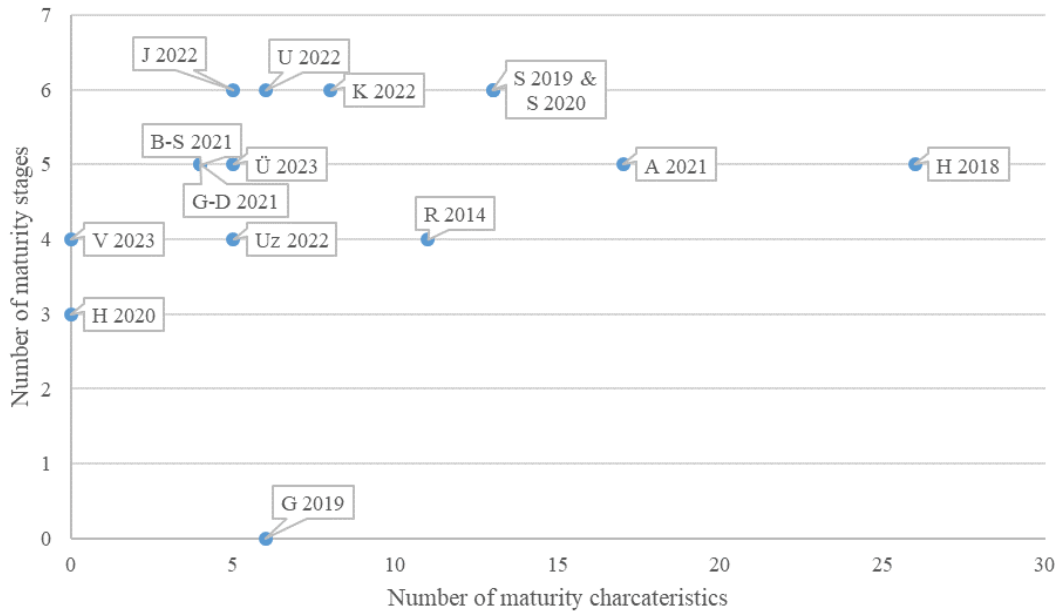


Fig. 4 Number of stages depending on the characteristics. Legend: A 2021 - Acerbi *et al.* [36]; B-S 2021 - Brendzel-Skowera [33]; G-D 2021 - Golinska-Dawson *et al.* [41]; G 2019 - Górecki [39]; H 2020 - Haezendonck & van den Berghe [34]; H 2018 - Howard *et al.* [45]; J 2022 - Julkovski *et al.* [46]; K 2022 - Kayikci *et al.* [35]; R 2014 - Romero & Molina [43]; S 2019 - Sehnem *et al.* [47]; S 2020 - Sehnem *et al.* [48]; U 2022 - Uhrenholt *et al.* [44]; Ü 2023 - Ünal & Sinha [42]; Uz 2022 - Uztürk & Büyükoğkan [37]; V 2023 - Veger *et al.* [40]

#### Measuring method

To answer RQ 3, the measurement methods of the maturity-relevant characteristics were analyzed. In questionnaire-based maturity models, in this study mostly hybrid models, the availability and transparency of the underlying questionnaire have a great influence on the answering of the research question. With structured models, such as the maturity model according to Uhrenhold *et al.* [44] it is necessary to provide information about the measurability of the individual (sub-) characteristics. After analyzing all maturity models, it can be concluded that very few models provide sufficient information about the underlying metrics or questionnaires used. Only the model according to Sacco *et al.* [38] allows a division into subjective or "fuzzy" and objective or "distinct" measurement methods. Here, self-assessments using e.g. Likert scales are classified as subjective or "fuzzy" measurement methods and values with clear units (e.g. kg, etc.) as objective measurement methods. In the Sacco *et al.* model, circularity is also assessed in addition to the question about the maturity of the company [38]. Due to the focus of this study on maturity, only the questions related to maturity were considered. It was possible to index 23 subjective and three objective measurement methods of the individual questions, whereby the objective questions referred to relative numbers in % (e.g. question item 17 "Which percentage of your suppliers are audited with regard to their circular economy practices?" [38]).

#### IV. DISCUSSION

The results of this SLR show the great variety and high diversity in the individual circular economy maturity models

for manufacturing companies in terms of typology, architecture, number and definition of maturity-relevant characteristics as well as the number of maturity levels. With regard to the design of the maturity models, the SLR shows that 11 of 16 models use a tiered representation. This representation is based on the assumption that specific criteria must be met in order to reach a maturity level [20]. To reach a higher level, all criteria of the lower level must be fulfilled. In contrast, four models use a continuous representation. This representation addresses the evolutionary nature of change and is based on the assumption that development is dependent on situational factors, which means that not all criteria need to be met to reach a higher level of maturity [51].

As a rule, the number of maturity levels varies among the models, whereby the higher the number of maturity levels, the greater the precision of the assessment, but also the complexity of the characteristics relevant to the maturity level [52]. The SLR confirms the variations in the number of maturity levels, which ranges from three to six. The variations can also be seen in the type and number of maturity-relevant characteristics, which form the basis of any maturity model. According to Correia *et al.* there is no ideal number of characteristics for determining maturity in maturity models, as the trade-off between perceived complexity and independence of the characteristics should be taken into account when creating the model [18]. In the identified models, the number of characteristics used varies from zero to 26, with an average of eight characteristics, and thus most models include less than ten characteristics for assessment. This can be justified by the fact that these models are more general in design and are not fixed

to a specific industry to be applied by many organizations.

Another variation is evident in the definition or meaning of the maturity-relevant characteristics of the models. Although all models use a holistic approach to determine maturity, the definition of the model-dependent characteristics is different. In Table IV, the characteristics are assigned to the ranges of Porter's Value Chain [53] which represents the value creation of interrelated company activities and divides the company units involved into eight areas. It is noticeable that all models (e.g. *Firm infrastructure* or *Operations*) and other categories, such as *Inbound & outbound logistics*, represent some

categories according to Porter only by individual models. The category *Service* cannot be assigned to any model and is therefore completely missing. This distribution may be due to the fact that the characteristics are named differently and therefore there may be overlaps between the categories. In addition, the characteristics are named in varying degrees of detail, so that the characteristics of individual models possibly address the Services category, but do not mention them by name or do not distinguish them.

TABLE IV  
CLASSIFICATION OF THE MATURITY-RELEVANT CHARACTERISTICS TO PORTER'S VALUE CHAIN

Porter's Value Chain Categories	Maturity-relevant characteristics	Reference
<b>Firm infrastructure</b>	Stakeholder management; Strategic management	Acerbi et al. [36]
	Circular business model / Environmental management / Awareness of the company's stakeholders	Brendzel-Skowera [33]
	Organizational culture/ Organizational structure/ Organization management	Górecki [39]
	Circular economy Vision	Howard et al. [45]
	Policy /Strategy	Kayikci et al. [35]
	Quality of life and community connections/ Environment,	Romero & Molina [43]
	Strategy & Vision/ Environmental management/ Cooperation & industrial symbiosis	Sacco et al. [38]
	Value creation/ governance/ partnership	Uhrenholt et al. [44]
<b>HR management</b>	Business Model/ Stakeholders	Uztürk & Büyüközkan [37]
	Knowledge about circular economy	Brendzel-Skowera [33]
	Human resources	Górecki [39]
	Social	Kayikci et al. [35]
	Human resources/ health and safety	Romero & Molina [43]
	Training; Employee satisfaction & participation	Sacco et al. [38]
	People & skills	Uhrenholt et al. [44]
<b>Technology development</b>	Social fairness	Ünal & Sinha [42]
	Technical infrastructure	Górecki [39]
	Technology	Kayikci et al. [35]
	Information and communication system	Romero & Molina [43]
	Eco-design	Sacco et al. [38]
	Technology	Uhrenholt et al. [44]
<b>Procurement</b>	Technology	Uztürk & Büyüközkan [37]
	Supplier improvement / Regional capability	Howard et al. [45]
	Supplier selection & auditing	Sacco et al. [38]
	Supply chain	Uhrenholt et al. [44]
<b>Inbound &amp; outbound logistics</b>	Transportation	Romero & Molina [43]
	Direct logistic / Reverse logistic,	Sacco et al. [38]
<b>Operations</b>	reuse, refurbish, recycle and remanufacture materials / Process management	Acerbi et al. [36]
	Project management	Górecki [39]
	Water, Emissions, Energy, Material	Golinska-Dawson et al. [41]
	Efficiency measurements: materials, energy, water	Howard et al. [45]
	collect, retain/ extend, share, reuse/redistribute, and remanufacture/renew	Julkovski et al. [46]
	Product / Process/	Kayikci et al. [35]
	Material/ Energy/ Waste management	Romero & Molina [43]
	Resource consumption/ Waste management,	Sacco et al. [38]
	Technical Cycle: Collect; Keep/Extend; Share; Reuse/Redistribute; Remanufacture/refurbish	Sehnm et al. 2019 [47] & 2020 [48]
	Biological Cycle: Collect; Cascade Exploitation; Extraction of biochemical raw materials; Anaerobic digestion; Biogas; Biosphere regeneration; Biochemical raw materials; Agriculture/collection	
	Operations/ Product and material	Uhrenholt et al. [44]

TABLE IV  
CLASSIFICATION OF THE MATURITY-RELEVANT CHARACTERISTICS TO PORTER'S VALUE CHAIN (CONT.)

<b>Operations</b>	Material Health; Material reutilization; Renewable energy; Water stewardship	Ünal & Sinha [42]
	Product/ Process	Uztürk & Büyüközkan [37]
<b>Marketing &amp; sales</b>	Economic	Kayikci et al. [35]
	Marketing	Romero & Molina [43]
	Marketing & communication	Sacco et al. [38]
<b>Service</b>	-	-

Every maturity model has the goal of assessing performance, which should primarily be done objectively [21], [13]. However, the models studied do not provide much detailed information about their underlying assessment method based on metrics. On the one hand, this lack of information is reflected in the absence of threshold values between two maturity levels, since in all models it is not comprehensible at which level of a characteristic relevant to the maturity level the change to a higher maturity level takes place. On the other hand, the lack of information is also reflected in the transparency of the questionnaire, which is a preferred method for assessing the performance of the identified models. Although it is mentioned that a questionnaire is used and the answer options are Likert-based, there is a lack of information about the concrete questions in most maturity models. Only the model according to *Sacco et al.* [38] is transparent in this respect, so that all questions were accessible for analysis. For this reason, an analysis of the measurement method can only be carried out for this model. The distinction between subjective (or fuzzy) and objective (or “distinct”) measurement methods gives an indication of the objectivity of the performance evaluation. In the model, the method of subjective self-assessment predominates over the objective one, illustrated by the use of units or relative references in %.

Maturity models are used to determine the current situation, to derive and prioritize improvement measures on this basis and then to monitor the success of their implementation [12]. However, the analyzed maturity models only represent rough steps to improve the maturity level. This lack of information was also noted by *Correrira et al.* in their analysis of maturity levels [18]. Although the maturity models with a stage representation represent a more detailed information base for transformation than the continuous representation method, they also lack concrete guidelines.

## V. CONCLUSION, LIMITATIONS AND FUTURE RESEARCH

The SLR aimed to provide a systematic overview of existing circular economy maturity models for manufacturing companies. By applying keyword combinations in the four electronic databases EBESCOhost, SCOPUS, Web of Science and Emerald Insights, 16 maturity models were selected. The results show that the number of published models is steadily increasing over time, but is at a low level compared to the absolute number of models identified. This confirms the need for research in this area.

The identified maturity models were examined for various analysis criteria, including the considered frame of reference of the maturity models. This allowed the first research question

(RQ1) to be answered. All models focus on the entire company with a holistic approach to maturity assessment, but differ in their concrete use case (e.g. Heazendonck & van den Berghe [34]). Differences also show in the different structure and architecture of the models. With regard to the model typology, a structural approach predominates, followed by the grid representation. The preferred variant of the architecture is the stepwise representation, which 11 of 16 models use.

With regard to the maturity-relevant characteristics (RQ2), the SLR shows that these vary in number and definition and are model-dependent. Some models consider the same characteristics across all maturity levels, while other models apply a different number and definition of characteristics depending on their level. This variation is also reflected in the number and definition of maturity levels, which are adopted or redefined from known maturity models, depending on the model analyzed.

To answer the third research question (RQ3), the measurement methods of the models were analyzed, which are often questionnaire-based. The results of the SLR show that the models provide little information about the underlying metrics and their questionnaires and lack transparency. Only the maturity model according to *Sacco et al.* [38] allowed a clear conclusion about subjective and objective measurement methods. Here, subjective self-assessments by Likert clearly outweigh objective measurement methods through the reference to measurement units.

### *Research Implications for research and practice*

The SLR contributes to a comprehensive overview, analysis and synthesis of the literature in the field of circular economy maturity models. By consolidating the different models, their focus, measurement methods and characteristics, academia as well as business organizations such as manufacturing companies can compare the individual models. The paper also provides the basis to engage more with the emerging research field of circular economy maturity models and can serve as a basis for model selection for manufacturing companies that want to assess their circular maturity.

### *Limitations and future research*

It should be noted when using the SLR that authors were limited in some areas. By conducting a literature search, there is very often a risk that not all relevant literature can be identified through the use of electronic databases. On the one hand, this concerns the four databases used, but also the choice of keywords, which, although applied in a three-stage search procedure, cannot give any indication of completeness. In addition, one criterion for the selection of literature was scientific publications at conferences or in scientific journals.



Some consulting firms develop their own models, but these were not included during the research because insufficient information was available on the structure.

The SLR provides the basis for further research in the area of circular economy maturity models. In the following, indications for further research activities are given:

#### A: Maturity-relevant characteristics

The SLR identified a large variance in the maturity-based characteristics used across the models. In addition, Porter's service category was not addressed by any of the models [53]. This evidence should be addressed in further research activities. Through a detailed analysis of the identified characteristics and the interdependencies between them, interdependencies can be identified and a basic set of indicators can be established that allows the maturity of manufacturing companies to be assessed. When creating the indicator set, however, care should be taken to ensure that it can be adapted depending on the industry, etc. The first basis could be the overview of characteristics and interdependencies. A first basis could be the overview of the characteristics in Table IV and the inclusion of circular economy readiness models. In addition to maturity models, readiness models indicate the readiness of an organization for a transformation. These are often also questionnaire-based and it could be examined to what extent indicators are suitable for adaptation in the area of maturity models.

#### B: Thresholds between levels & measurement methods

Due to the identified lack of description of the maturity models in the models, it is necessary that the individual maturity levels are described in more detail. In addition, the threshold values between the levels should also be addressed in the future creation of the models. Due to the lack of detailed description and the lack of quantitative data, the focus of future work should be placed on the integration of data-based thresholds in order to be able to represent the distinction between maturity levels numerically. This also applies to the chosen measurement methods of the characteristics. Here it should be clear which measurement method is used in the questionnaire. In addition, the future focus should also be on the integration of objective measurement methods, e.g. through indicators with measurement units. Through this, different methods for aggregating subjective and objective measurement methods should be tested.

#### REFERENCES

- [1] European Commission, Communication from the Commission to the European Parliament, the European Council, the Council, the European Economic and Social Committee and the Committee of the Regions. The European Green Deal, 2019.
- [2] M. Geissdoerfer, D. Vladimirova, S. Evans, Sustainable business model innovation: A review, *Journal of Cleaner Production* 198 (2018) 401–416. <https://doi.org/10.1016/j.jclepro.2018.06.240>.
- [3] W. Haas, F. Krausmann, D. Wiedenhofer, M. Heinz, How Circular is the Global Economy?: An Assessment of Material Flows, Waste Production, and Recycling in the European Union and the World in 2005, *J of Industrial Ecology* 19 (2015) 765–777. <https://doi.org/10.1111/jiec.12244>.
- [4] A. Chizaryfar, P. Trucco, C. Nuur, The transformation to a circular economy: framing an evolutionary view, *J Evol Econ* 31 (2021) 475–504. <https://doi.org/10.1007/s00191-020-00709-0>.
- [5] Ellen MacArthur Foundation, Towards the circular economy Vol. 1: an economic and business rationale for an accelerated transition, 2013.
- [6] L. Haigh, M. de Wit, C. von Daniels, A. Collorichini, J. Hoogzaad, The Circular Gap report 2021., 2021.
- [7] European Union, Executive Vice-President Frans Timmermans' opening remarks at the Circular Economy Stakeholder Conference: Speech from 03.11.2020, 2020.
- [8] European Union, Small and medium-sized enterprises. Brief description of the European Union, 2021.
- [9] M. Ferasso, T. Beliaeva, S. Kraus, T. Clauss, D. Ribeiro-Soriano, Circular economy business models: The state of research and avenues ahead, *Bus Strat Env* 29 (2020) 3006–3024. <https://doi.org/10.1002/bse.2554>.
- [10] D.C. Pigosso, T.C. McAloone, Making the transition to a Circular Economy within manufacturing companies: the development and implementation of a self-assessment readiness tool, *Sustainable Production and Consumption* 28 (2021) 346–358. <https://doi.org/10.1016/j.spc.2021.05.011>.
- [11] T. de Bruin, R. Freeze, U. Kulkarni, M. Rosemann (Eds.), Understanding the Main Phases of Developing a Maturity Assessment Model, 2005.
- [12] J. Becker, R. Knackstedt, J. Pöppelbuß, *English: Development of maturity models for IT management, original: Entwicklung von Reifegradmodellen für das IT-Management*, *Wirtsch. Inform.* 51 (2009) 249–260. <https://doi.org/10.1007/s11576-009-0167-9>.
- [13] T. Bensiak, *English: Systematics for maturity-based performance evaluation and improvement of business processes in SMEs, original: Systematik zur reifegradbasierten Leistungsbewertung und -steigerung von Geschäftsprozessen im Mittelstand*. Dissertation, 2013.
- [14] Y. Xiao, M. Watson, Guidance on Conducting a Systematic Literature Review, *Journal of Planning Education and Research* 39 (2019) 93–112. <https://doi.org/10.1177/0739456X17723971>.
- [15] D. Moher, A. Liberati, J. Tetzlaff, D.G. Altman, The PRISMA Group, Preferred Reporting Items for Systematic Reviews and Meta-Analyses: The PRISMA Statement., *PLoS Med*: 6 (2009) 1–6. <https://doi.org/10.1371/journal.pmed.1000097.g001>.
- [16] B. Kitchenham, S. Charters, Guidelines for performing systematic literature reviews in software engineering, 2007.
- [17] D. Denyer, D. Tranfield, Producing a systematic review, in: D. A. Buchanan, A. Bryman (Eds.), *The SAGE Handbook of Organizational Research Methods*, Sage Publications Inc, pp. 671–689.
- [18] E. Correia, H. Carvalho, S. Azevedo, K. Govindan, Maturity Models in Supply Chain Sustainability: A Systematic Literature Review, *Sustainability* 9 (2017) 64. <https://doi.org/10.3390/su9010064>.
- [19] J. Poepelbuss, M. Roegliger, What makes a useful maturity model? A framework of general design principles for maturity models and its demonstration in business process management, 2011.
- [20] T. Mettler, *English: Supply management in hospitals: Construction and evaluation of a configurable maturity model for targeted design, original: Supply-Management im Krankenhaus: Konstruktion und Evaluation eines konfigurierbaren Reifegradmodells zur zielgerichteten Gestaltung*. Zugl.: Sankt Gallen, Univ., Diss., 2010, first. Aufl., Sierke, Göttingen, 2010.
- [21] T. de Bruin, R. Freeze, U. Kulkarni, M. Rosemann (Eds.), Understanding the Main Phases of Developing a Maturity Assessment Model, 2005.
- [22] R. Wendler, The maturity of maturity model research: A systematic mapping study, *Information and Software Technology* 54 (2012) 1317–1339. <https://doi.org/10.1016/j.infsof.2012.07.007>.
- [23] L. Montag, T. Klünder, M. Steven, Paving the Way for Circular Supply Chains: Conceptualization of a Circular Supply Chain Maturity Framework, *Front. Sustain.* 2 (2021) 101. <https://doi.org/10.3389/frsus.2021.781978>.
- [24] G. Akkasoglu, *English: Methodology for the design and application of application-specific maturity models taking into account information insecurity, original: Methodik zur Konzeption und Applikation anwendungsspezifischer Reifegradmodelle unter Berücksichtigung der Informationsunsicherheit*. Dissertation, Nürnberg-Erlangen, 2013.
- [25] R. Likert, The Method of Constructing an Attitude Scale, in: G.M. Maranell (Ed.), *Scaling: A sourcebook for behavioral scientists.*, Routledge, 2017, pp. 233–242.
- [26] C. Knoblinger, J. Oehmen, E. Rebentisch, W. Seering, K. Helten, Requirements for Product Development Self-Assessment Tools (2011).
- [27] P. Fraser, J. Moultrie, M. Gregory, IEEE, The Use of Maturity Models/Grids as a Tool in Assessing Product Development Capability, in: *Managing technology for the new economy*: Cambridge, UK, 18 - 20 August 2002, IEEE Operations Center, Piscataway, NJ, 2002, pp. 244–249.



- [28] M. Gusenbauer, N.R. Haddaway, Which academic search systems are suitable for systematic reviews or meta-analyses? Evaluating retrieval qualities of Google Scholar, PubMed, and 26 other resources, *Research Synthesis Methods* 11 (2020) 181–217. <https://doi.org/10.1002/jrsm.1378>.
- [29] A. Liberati, D.G. Altman, J. Tetzlaff, C. Mulrow, P.C. Gøtzsche, J.P.A. Ioannidis, M. Clarke, P.J. Devereaux, J. Kleijnen, D. Moher, The PRISMA statement for reporting systematic reviews and meta-analyses of studies that evaluate health care interventions: explanation and elaboration, *PLoS Med.* 6 (2009) e1000100. <https://doi.org/10.1371/journal.pmed.1000100>.
- [30] Z.M. Çınar, Q. Zeeshan, O. Korhan, A Framework for Industry 4.0 Readiness and Maturity of Smart Manufacturing Enterprises: A Case Study, *Sustainability* 13 (2021) 6659. <https://doi.org/10.3390/su13126659>.
- [31] Roberto Santana Tapia, Maya Daneva, Pascal van Eck, Roel Wieringa, Towards a business-IT aligned maturity model for collaborative networked organizations, 2008 12th Enterprise Distributed Object Computing Conference Workshops (2008).
- [32] P. Fraser, J. Moultrie, M. Gregory, The use of maturity models/grids as a tool in assessing product development capability, *IEEE International Engineering Management Conference* (2002).
- [33] K. Brendzel-Skowera, Circular Economy Business Models in the SME Sector, *Sustainability* 13 (2021) 1–21. <https://doi.org/10.3390/su13137059>.
- [34] E. Haezendonck, K. van den Berghe, Patterns of Circular Transition: What Is the Circular Economy Maturity of Belgian Ports?, *Sustainability* 12 (2020) 1–15. <https://doi.org/10.3390/su12219269>.
- [35] Y. Kayikci, Y. Kazancoglu, N. Gozacan-Chase, C. Lafci, L. Batista, Assessing smart circular supply chain readiness and maturity level of small and medium-sized enterprises, *Journal of Business Research* 149 (2022) 375–392. <https://doi.org/10.1016/j.jbusres.2022.05.042>.
- [36] F. Acerbi, V. Järnefelt, J.T. Martins, L. Saari, K. Valkokari, M. Taisch, Developing a Qualitative Maturity Scale for Circularity in Manufacturing, in: A. Dolgui, A. Bernard, D. Lemoine, G. von Cieminski, D. Romero (Eds.), *Advances in Production Management Systems: Artificial Intelligence for Sustainable and Resilient Production Systems*. IFIP WG 5.7 International Conference, APMS 2021 Nantes, France, September 5–9, 2021 Proceedings, Part III, Springer International Publishing, Cham, 2021, 377–385.
- [37] D. Uztürk, G. Büyüközkan, 2-Tuple Linguistic Model-based Circular Maturity Assessment Methodology: A Case for Agriculture, *IFAC-PapersOnLine* 55 (2022) 2036–2041. <https://doi.org/10.1016/j.ifacol.2022.10.007>.
- [38] P. Sacco, C. Vinante, Y. Borgianni, G. Orzes, Circular Economy at the Firm Level: A New Tool for Assessing Maturity and Circularity, *Sustainability* 13 (2021) 1–17. <https://doi.org/10.3390/su13095288>.
- [39] J. Gorecki, Circular Economy Maturity in Construction Companies, *IOP Conf. Ser.: Mater. Sci. Eng.* 471 (2019) 1–8. <https://doi.org/10.1088/1757-899X/471/1/112090>.
- [40] D. Vegter, J. van Hillegersberg, M. Olthaar, Performance measurement system for circular supply chain management, *Sustainable Production and Consumption* 36 (2023) 171–183. <https://doi.org/10.1016/j.spc.2023.01.003>.
- [41] P. Golinska-Dawson, K. Werner-Lewandowska, M. Kosacka-Olejnik, Responsible Resource Management in Remanufacturing—Framework for Qualitative Assessment in Small and Medium-Sized Enterprises, *Resources* 10 (2021) 1–17. <https://doi.org/10.3390/resources10020019>.
- [42] E. Ünal, V.K. Sinha, Sustainability trade-offs in the circular economy: A maturity-based framework, *Business Strategy and the Environment* (2023) 1–21. <https://doi.org/10.1002/bse.3386>.
- [43] D. Romero, A. Molina, Towards a Sustainable Development Maturity Model for Green Virtual Enterprise Breeding Environments, in: 19th IFAC World Congress IFAC 2014, Kapstadt, 2014, pp. 4272–4279.
- [44] J.N. Uhrenholt, J.H. Kristensen, M.C. Rincón, S. Adamsen., S.F. Jensen, B.V. Waehrens, Maturity Model as a Driver for Circular Economy Transformation, *Sustainability* 14 (2022) 1–17. <https://doi.org/10.3390/su14127483>.
- [45] M. Howard, S. Boehm, D. Eatherly, M. Loble, N. Mustafee, L.S. Vamvakieridou-Lyroudia, A Capability Maturity Model for the Circular Economy: An Agri-food Perspective, in: *Academic Symposium: Circular Economy Disruptions – Past, Present and Future*, Exeter, UK, 2018, pp. 1–3.
- [46] D.J. Julkovski, S. Sehnem, M. Da Conceição Pereira Ramos, C.J.C. Jabbour, Circular business models and the environment: Maturity levels of the circular economy and innovation in greener craft breweries, *Business Strategy and the Environment* (2022) 1–24. <https://doi.org/10.1002/bse.3311>.
- [47] S. Sehnem, L.M. Campos, D.J. Julkovski, C.F. Cazella, Circular business models: level of maturity, *MD* 57 (2019) 1043–1066. <https://doi.org/10.1108/MD-07-2018-0844>.
- [48] S. Sehnem, N.O. Ndubisi, D. Preschlak, R.J. Bernardy, S. Santos Junior, Circular economy in the wine chain production: maturity, challenges, and lessons from an emerging economy perspective, *Production Planning & Control* 31 (2020) 1014–1034. <https://doi.org/10.1080/09537287.2019.1695914>.
- [49] K. P. Grant, James S. Pennypacker, Project management maturity: an assessment of project management capabilities among and between selected industries, *IEEE Transactions on Engineering Management* (2006).
- [50] A. Smith-Gillespie, R2Pi - The route to circular economy: Defining the Concept of Circular Economy Business Model. A Part of Deliverable 2.1, 2017.
- [51] J.L. King, K.L. Kraemer, Evolution and organizational information systems, *Commun. ACM* 27 (1984) 466–475. <https://doi.org/10.1145/358189.358074>.
- [52] M. Schröder, *English: Structured improvement of supply chain risk management, original: Strukturierte Verbesserung des Supply Chain Risikomanagements*, Springer Gabler, Wiesbaden, Heidelberg.
- [53] M. Porter, *Competitive Advantage: Creating and Sustaining Superior Performance* (1985).

# Design a Circular Business Framework for the Construction Companies in the Developing Economies

Shreya Kanther

**Abstract—** This research will design a toolkit for the construction companies in India to bring confidence and achieve the acceptance of Circular Business Models (CBMs) within the construction sector. It will develop a business framework by looking into cases of large scale construction companies including Bechtel Corporation, SKANSKA, Turner Construction, AECOM and EMCOR that are applying a circular economy model in their construction practices. These are some of the largest construction companies in the US and have been around since generations. They all have been embracing new technologies and setting benchmarks with a deep commitment to excellence and contribution to creating a regenerative built environment. The selected companies deliver projects with the purpose of growing economies, improving the resiliency of the world's infrastructure, tackling critical environmental challenges and getting closer to net zero to build a cleaner, greener and safer space. Through this research, these companies' business models will be analyzed and the learnings from their practices will be used in generating a model for the Indian construction companies. The framework will be developed by exhaustively analyzing the existing construction trends, methods and needs in both industrialized and developing economies.

**Keywords—** circular economy, developing economies, industrialized economies, architecture and design.

# Circular Economy: An Overview of Principles, Strategies, and Case Studies

Dr. Dina M. Bakr

**Abstract**— The concept of a circular economy is gaining increasing attention as a way to promote sustainable economic growth and reduce the environmental impact of human activities. The circular economy is a systemic approach that aims to keep materials and resources in use for as long as possible, minimize waste and pollution, and regenerate natural systems. The purpose of this article is to present a summary of the principles and tactics employed in the circular economy, along with examples of prosperous circular economy projects implemented in different sectors across Japan, Austria, the Netherlands, South Africa, Germany, and the United States. The paper concludes with a discussion of the challenges and opportunities associated with the transition to a circular economy and the policy interventions that can support this transition.

**Keywords**— Circular Economy, Waste Reduction, Sustainable Development and Recycling.

Dina M. Bakr is with Arab Academy for science, Technology and Maritime Transport, College of Management and technology (AAST-CMT) (phone: +201093221855; e-mail: dinabakr@aast.edu).

# See No Evil: Corporate Environmental, Social and Governance Profile and EPS-Motivated Repurchases

Feng Zhao

**Abstract**—Convention wisdom suggests that firms with high environmental, social, and governance (ESG) ratings would curb short-term oriented activities, such as stock repurchases conducted just to meet the EPS targets. However, we present puzzling evidence that EPS-motivated repurchases are positively associated with the ESG ratings, mainly coming from its environmental and governance components. We provide an explanation to this puzzle that the long-run stock out-performance following EPS-motivated repurchases is around 6% per year, which could make firms favor such repurchases in the cost of their ESG ratings. Furthermore, we show that financial reporting opacity following EPS-motivated repurchases is equally severe for firms with high ESG ratings, hence implying the presence of “greenwashing”.

**Keywords**—ESG, earnings-per-share targets, stock repurchases, long-run stock returns, opacity.

# Circular Tool and Dynamic Approach to Grow the Entrepreneurship of Macroeconomic Metabolism

M. Areias, D. Simões, A. Figueiredo, A. Rahman, F. Figueiredo, J. Nunes

**Abstract**— It is expected that close to 7 billion people will live in urban areas by 2050. In order to improve the sustainability of the territories and its transition towards circular economy, it's necessary to understand its metabolism and promote and guide the entrepreneurship answer. The study of a macroeconomic metabolism involves the quantification of the inputs, outputs and storage of energy, water, materials and wastes for an urban region. This quantification and analysis representing one opportunity for the promotion of green entrepreneurship. There are several methods to assess the environmental impacts of an urban territory, such as human and environmental risk assessment (HERA), life cycle assessment (LCA), ecological footprint assessment (EF), material flow analysis (MFA), physical input-output table (PIOT), ecological network analysis (ENA), multicriteria decision analysis (MCDA) among others. However, no consensus exists about which of those assessment methods are best to analyze the sustainability of these complex systems.

Taking into account the weaknesses and needs identified, the CiiM - Circular Innovation Inter-Municipality project, aims to define an uniform and globally accepted methodology, through the integration of various methodologies and dynamic approaches to increase the efficiency of macroeconomic metabolisms and promoting entrepreneurship in a circular economy.

The pilot territory considered in CiiM project has a total area of 969,428 ha, comprising a total of 897,256 inhabitants (about 41% of the population of the Center Region). The main economic activities in the pilot territory, which contribute to a gross domestic product of 14.4 billion euros, are: social support activities for the elderly; construction of buildings; road transport of goods, retailing in supermarkets and hypermarkets; mass production of other garments; inpatient health facilities; and the manufacture of other components and accessories for motor vehicles. The region's business network is mostly constituted of micro and small companies (similar to the Central Region of Portugal), with a total of 53,708 companies identified in the CIM Region of Coimbra (39 large companies), 28,146 in the CIM Viseu Dão Lafões (22 large companies) and 24,953 in CIM Beiras and Serra da Estrela (13 large companies).

For the construction of the database, was taking into account data available at the National Institute of Statistics (INE), General

Directorate of Energy and Geology (DGEG), Eurostat, Pordata, Strategy and Planning Office (GEP), Portuguese Environment Agency (APA), Commission for Coordination and Regional Development (CCDR) and Inter-municipal Community (CIM), as well as dedicated databases.

In addition to the collection of statistical data, it was necessary to identify and characterize the different stakeholder groups in the pilot territory that are relevant to the different metabolism components under analysis. The CiiM project also adds the potential of a Geographic Information System (GIS), so that it is possible to obtain geospatial results of the territorial metabolisms (rural and urban) of the pilot region.

This platform will be a powerful visualization tool of flows of products/services that occur within the region and will support the stakeholders, improving their circular performance and identifying new business ideas and symbiotic partnerships.

**Keywords**— Circular Economy Tools, Life Cycle Assessment Macroeconomic Metabolism, Multicriteria Decision Analysis, Decision Support Tools, Circular Entrepreneurship, Industrial and Regional Symbiosis.

**Acknowledgements** - This work was supported by CiiM Project and Maria Areias and Ana Figueiredo thanks their research contracts funded by CiiM Project - CENTRO-04-3560-FSE-072501 - Centro Portugal Regional Operational Program (Centro2020), under the PORTUGAL 2020 Partnership Agreement, through the European Regional Development Fund (ERDF). Filipa Figueiredo and Anishur Rahman also thanks their research contracts funded by Interface Mission under the PRR - Recovery and Resilience Plan – Re-C05-i02 – Interface Mission – nº 01/C05-i02/2022, Collaborative Laboratories Base Fund. Centre Bio R&D unit | BLC3 thanks their support funded by Fundação para a Ciência e Tecnologia (FCT) UIDP/05083/2020.

M. Areias is with Associação CECOLAB - Collaborative Laboratory Towards Circular Economy, Oliveira do Hospital, Portugal (phone: +351 238 011 400; e-mail: maria.areias@cecolab.pt).

D. Simões is with Associação CECOLAB - Collaborative Laboratory Towards Circular Economy, Oliveira do Hospital, Portugal (phone: +351 238 011 400; e-mail: diogo.simoess@cecolab.pt).

A. Rahman is with Associação CECOLAB - Collaborative Laboratory Towards Circular Economy, Oliveira do Hospital, Portugal (phone: +351 238 011 400; e-mail: anishur.rahman@cecolab.pt).

A. Figueiredo is with Associação CECOLAB - Collaborative Laboratory Towards Circular Economy, Oliveira do Hospital, Portugal (phone: +351 238 011 400; e-mail: ana.figueiredo@cecolab.pt).

F. Figueiredo is with Associação CECOLAB - Collaborative Laboratory Towards Circular Economy, Oliveira do Hospital, Portugal (phone: +351 238

011 400; e-mail: filipa.figueiredo@cecolab.pt), Centre Bio R&D Unit, Association BLC3 – Technological and Innovation Campus, Rua Nossa Senhora da Conceição, nº. 2. Lagares da Beira 3405-155 Oliveira do Hospital, Portugal and Centre for Environmental and Marine Studies (CESAM), Department of Environment and Planning, University of Aveiro, 3810-193 Aveiro, Portugal.

J. Nunes is with Centre Bio R&D Unit, Association BLC3 – Technological and Innovation Campus, Rua Nossa Senhora da Conceição, nº. 2. Lagares da Beira 3405-155 Oliveira do Hospital (phone: +351 238 641 059; e-mail: joao.nunes@blc3.pt, Portugal and Associação CECOLAB - Collaborative Laboratory Towards Circular Economy, Oliveira do Hospital, Portugal.

# Business Intelligent to a Decision Support Tool for Green Entrepreneurship: Meso and Macro Regions

A. Rahman, M. Areias, D. Simões, A. Figueiredo, F. Figueiredo, J. Nunes

**Abstract**— The circular economy (CE) has gained increased awareness among academics, businesses, and decision-makers as it stimulates resource circularity in the production and consumption systems. A large epistemological study has explored the principles of CE but scant attention eagerly focused on analysing how CE is evaluated, consented to, and enforced using economic metabolism data and business intelligent framework. Economic metabolism involves the ongoing exchange of materials and energy, within and across socio-economic systems, and requires the assessment of vast amounts of data to provide quantitative analysis related to effective resource management. Limited concern, the present work has focused on the regional flows pilot region from Portugal. By addressing this gap, this study aims to promote eco-innovation and sustainability in the regions of Intermunicipal Communities Região de Coimbra, Viseu Dão Lafões and Beiras e Serra da Estrela, using this data to find precise synergies in terms of material flows and give companies a competitive advantage in form of valuable waste destinations, access to new resources and new markets, cost reduction and risk sharing benefits. In our work, emphasis on applying artificial intelligence (AI) and more specifically on implementing state-of-the-art deep learning algorithms is placed, contributing to construction a business intelligent approach. With the emergence of new approaches generally highlighted under the sub-heading of AI and machine learning (ML), the methods for statistical analysis of complex and uncertain production systems are facing significant changes. Therefore, various definitions of AI and its differences from traditional statistics are presented, and furthermore, ML is introduced to identify its place in data science and the differences in topics such as big data analytics and in production problems that using AI and ML are identified. A lifecycle-based approach is then taken to analyse the use of different methods in each phase to identify the most useful technologies and unifying attributes of AI in manufacturing.

Most of macroeconomic metabolisms models are mainly direct to contexts of large metropolis, neglecting rural territories, so within this project, a dynamic decision support model coupled with artificial intelligence tools and information platforms will be developed, focused on the reality of these transition zones between the rural and urban. Thus, a real decision support tool is under development, which will surpass the scientific developments carried out to date and will

allow to overcome imitations related to the availability and reliability of data.

**Keywords**— Circular Economy, Artificial Intelligence, Economic Metabolisms, Machine Learning.

**Acknowledgements** - This work was supported by CiiM Project and Maria Areias and Ana Figueiredo thanks their research contracts funded by CiiM Project - CENTRO-04-3560-FSE-072501 - Centro Portugal Regional Operational Program (Centro2020), under the PORTUGAL 2020 Partnership Agreement, through the European Regional Development Fund (ERDF). Filipa Figueiredo and Anishur Rahman also thanks their research contracts funded by Interface Mission under the PRR - Recovery and Resilience Plan – Re-C05-i02 – Interface Mission – nº 01/ C05-i02/2022, Collaborative Laboratories Base Fund. Centre Bio R&D unit | BLC3 thanks their support funded by Fundação para a Ciência e Tecnologia (FCT) UIDP/05083/2020.

M. Areias is with Associação CECOLAB - Collaborative Laboratory Towards Circular Economy, Oliveira do Hospital, Portugal (phone: +351 238 011 400; e-mail: maria.areias@cecolab.pt).

D. Simões is with Associação CECOLAB - Collaborative Laboratory Towards Circular Economy, Oliveira do Hospital, Portugal (phone: +351 238 011 400; e-mail: diogo.simoese@cecolab.pt).

A. Rahman is with Associação CECOLAB - Collaborative Laboratory Towards Circular Economy, Oliveira do Hospital, Portugal (phone: +351 238 011 400; e-mail: anishur.rahman@cecolab.pt).

A. Figueiredo is with Associação CECOLAB - Collaborative Laboratory Towards Circular Economy, Oliveira do Hospital, Portugal (phone: +351 238 011 400; e-mail: ana.figueiredo@cecolab.pt).

F. Figueiredo is with Associação CECOLAB - Collaborative Laboratory Towards Circular Economy, Oliveira do Hospital, Portugal (phone: +351 238

011 400; e-mail: filipa.figueiredo@cecolab.pt), Centre Bio R&D Unit, Association BLC3 – Technological and Innovation Campus, Rua Nossa Senhora da Conceição, nº. 2. Lagares da Beira 3405-155 Oliveira do Hospital, Portugal and Centre for Environmental and Marine Studies (CESAM), Department of Environment and Planning, University of Aveiro, 3810-193 Aveiro, Portugal.

J. Nunes is with Centre Bio R&D Unit, Association BLC3 – Technological and Innovation Campus, Rua Nossa Senhora da Conceição, nº. 2. Lagares da Beira 3405-155 Oliveira do Hospital (phone: +351 238 641 059; e-mail: joao.nunes@blc3.pt, Portugal and Associação CECOLAB - Collaborative Laboratory Towards Circular Economy, Oliveira do Hospital, Portugal.



# PLA Production from Multi Supply Lignocellulosic Biomass Residues: A Pathway for Agrifood Sector

S. Ribeiro, D. Farinha, H. Sales, R. Pontes, J. Nunes\*

**Abstract**— The demand and commitment to sustainability in the agrifood sector introduce new opportunities for new composite materials. Composite materials are emerging as a vital entity for the sustainable development. Polylactic acid (PLA) has been recognized as a potential polymer with attractive characteristics for agrifood sector applications. PLA that can be beneficial for the development of composites, biocomposites, films, porous gels, and so on. The production of PLA from lignocellulosic biomass residues matrix is a key option towards a sustainable and circular bioeconomy and a non-competitive application with feed and food sector. The Flui and BeirInov projects presents new developments in the production of PLA composites to value the Portuguese forest ecosystem, with high amount of lignocellulosic biomass residues and available. A performance production of lactic acid from lignocellulosic biomass undergoes a process of autohydrolysis, saccharification and fermentation, originating a lactic acid fermentation medium with a 72.27g.L<sup>-1</sup> was obtained and a final purification of 72%. The high purification PLA from multi lignocellulosic residues representing one economic expensive process, and a new materials and application for the polymers and a combination with others types of composites matrix characteristic is the drive-up for this green market.

**Keywords**— Polylactic acid; Lignocellulosic Biomass; Agrifood; Composite materials.p

**Acknowledgements** - This work was supported by BeirInov Project (CENTRO-01-0247-FEDER-113492), FLUI project (CENTRO-01-0247-FEDER-113565) funded by European Regional Development Fund (ERDF) and Interface Mission under the PRR - Recovery and Resilience Plan – Re-C05-i02 – Interface Mission – nº 03/C05-i02/2022. Centre Bio R&D unit | BLC3 and Rita Pontes thanks their support funded by Fundação para a Ciência e Tecnologia (FCT) UIDP/05083/2020 and UIDB/05083/2020.

S. Ribeiro with Centre Bio R&D Unit, Association BLC3 – Technological and Innovation Campus, Rua Nossa Senhora da Conceição, nº. 2. Lagares da Beira 3405-155 Oliveira do Hospital (phone: +351 238 641 059; e-mail: sonia.ribeiro@blc3.pt

D. Farinha is with Centre Bio R&D Unit, Association BLC3 – Technological and Innovation Campus, Rua Nossa Senhora da Conceição, nº. 2. Lagares da Beira 3405-155 Oliveira do Hospital (phone: +351 238 641 059; e-mail: diana.farinha@blc3.pt

H. Sales is with Centre Bio R&D Unit, Association BLC3 – Technological and Innovation Campus, Rua Nossa Senhora da Conceição, nº. 2. Lagares da Beira 3405-155 Oliveira do Hospital (phone: +351 238 641 059; e-mail: helia.sales@blc3.pt

R. Pontes is with Centre Bio R&D Unit, Association BLC3 – Technological and Innovation Campus, Rua Nossa Senhora da Conceição, nº. 2. Lagares da Beira 3405-155 Oliveira do Hospital (phone: +351 238 641 059; e-mail: rita.pontes@blc3.pt

J. Nunes is with Centre Bio R&D Unit, Association BLC3 – Technological and Innovation Campus, Rua Nossa Senhora da Conceição, nº. 2. Lagares da Beira 3405-155 Oliveira do Hospital (phone: +351 238 641 059; e-mail: joao.nunes@blc3.pt

# Portuguese Pine Resin: The Economic and Activity Decline to a New Forestry and Biotechnology Approach

C. Nunes, S. Ribeiro, H. Faustino, H. Sales, R. Pontes, J. Nunes

**Abstract**— Pine resin activity in Portugal was one of the most important and major non-wood forestry, representing a strategic natural resource for Portuguese Bioeconomy and an important social activity for rural regions. Pine forests representing a stock of atmospheric carbon, contributing to greenhouse effect mitigation and social and environmental important services returns. They are important sources of numerous useful products, including not only wood and cellulose but also nonwood products used by the chemical, food, and pharmaceutical industries, as well as for biorefineries. Portuguese pine forest area decreases from 1 million hectares to 400 mil hectares in the last 20 years. Portugal in 80's decade was one of the world's TOP 3 producers, with a middle annual production of 140 mil tones.year<sup>-1</sup>. With the pressure of the social desertification, forest fires, phytosanitary problems (e.g. nematode of the pine wood) and the decrease of economic value and competitiveness of the Portuguese forest, the actual middle annual production is less than 10 mil tones.year<sup>-1</sup> (lesser 92%). This significant decrease representing an annual economic loss of approximately 130-140 million Euros. year<sup>-1</sup> for forest primary sector in Portugal. The Biopinus project design new forestry approach and strategic biotechnologies knowledge to increase the economic value of Pine resin in Portugal, with an impact on the growth of the economic value of Pine resin from 1,1 to 1,5 Euros/kg.

**Keywords**— Pine Resin; Bioeconomy; Economic value; Biotechnology.

**Acknowledgements** - This work was supported by Biopinus Project - CENTRO-01-0247-FEDER-072630 Centro Portugal Regional Operational Program (Centro2020), under the PORTUGAL 2020 Partnership Agreement, through the European Regional Development Fund (ERDF) and Interface Mission under the PRR - Recovery and Resilience Plan - Re-C05-i02 - Interface Mission - n° 03/C05-i02/2022.Centre Bio R&D unit | BLC3 and Rita Pontes thanks their support funded by Fundação para a Ciência e Tecnologia (FCT) UIDP/05083/2020 and UIDB/05083/2020.

C. Nunes is with Centre Bio R&D Unit, Association BLC3 – Technological and Innovation Campus, Rua Nossa Senhora da Conceição, n°. 2. Lagares da Beira 3405-155 Oliveira do Hospital (phone: +351 238 641 059; e-mail: carolina.nunes@blc3.pt

S. Ribeiro with Centre Bio R&D Unit, Association BLC3 – Technological and Innovation Campus, Rua Nossa Senhora da Conceição, n°. 2. Lagares da Beira 3405-155 Oliveira do Hospital (phone: +351 238 641 059; e-mail: sonia.ribeiro@blc3.pt

H. Faustino is with Centre Bio R&D Unit, Association BLC3 – Technological and Innovation Campus, Rua Nossa Senhora da Conceição, n°. 2. Lagares da Beira 3405-155 Oliveira do Hospital (phone: +351 238 641 059; e-mail: helio.faustino@blc3.pt

H. Sales is with Centre Bio R&D Unit, Association BLC3 – Technological and Innovation Campus, Rua Nossa Senhora da Conceição, n°. 2. Lagares da Beira 3405-155 Oliveira do Hospital (phone: +351 238 641 059; e-mail: helia.sales@blc3.pt

R. Pontes is with Centre Bio R&D Unit, Association BLC3 – Technological and Innovation Campus, Rua Nossa Senhora da Conceição, n°. 2. Lagares da Beira 3405-155 Oliveira do Hospital (phone: +351 238 641 059; e-mail: rita.pontes@blc3.pt

J. Nunes is with Centre Bio R&D Unit, Association BLC3 – Technological and Innovation Campus, Rua Nossa Senhora da Conceição, n°. 2. Lagares da Beira 3405-155 Oliveira do Hospital (phone: +351 238 641 059; e-mail: joao.nunes@blc3.pt) and BLC3 Evolution Rua Nossa Senhora da Conceição, n°. 2. Lagares da Beira 3405-155 Oliveira do Hospital.

# Ecodesign of Bioplastic Films for Food Packaging and Shelf-Life Extension

S. Ribeiro, D. Farinha, E. Pereira, H. Sales, F. Figueiredo, R. Pontes, J. Nunes\*

**Abstract**— Conventional plastic impacts in Planet, natural resources contamination, human health as well as animals, are the most attraction environmental and health attention. The lack of treatment in the end-of-life (EoL) phase and uncontrolled discard, allows plastic to be found everywhere in the world. Food waste are increase significantly with a final destination to landfills. To face these difficulties, new packaging solutions are needed with the objective of prolonging the shelf-life of products as well as equipment solutions for the development of the mentioned packaging. FLUI project thus presents relevance and innovation to reach a new level of knowledge and industrial development, focused in Ecodesign. Industrial equipment field for the manufacture of new packaging solutions based on biodegradable plastics films to apply in the food sector. With lesser environmental impacts and new solutions that make it possible to prevent food waste, reduce the production e consequent poor disposal of plastic of fossil origin. It will be a paradigm shift at different levels, from industry to waste treatment stations, passing through commercial agents and consumers. It can be achieved through the life cycle assessment (LCA) and ecodesign of the products, which integrates the environmental concerns in the design of the product as well as through the entire life cycle. The FLUI project aims to build a new bio-PLA extrusion equipment with the incorporation of bioactive extracts, through the production of flexible mono- and multi- layer functional films (FLUI systems). The new biofunctional and biodegradable films will prompt the extension of packaged products' shelf-life, reduce food waste and contribute to reducing consumption of non-degradable fossil plastics, as well as the use of raw material from renewable sources.

**Keywords**— Food packing; Bioplastics; Ecodesign; Circular Economy.

**Acknowledgements** - This work was supported by FLUI project (CENTRO-01-0247-FEDER-113565) funded by European Regional Development Fund (ERDF), Interface Mission under the PRR - Recovery and Resilience Plan – Re-C05-i02 – Interface Mission – nº 03/C05-i02/2022. Filipa Figueiredo thanks their research contract in Interface funded by Mission under the PRR - Recovery and Resilience Plan – Re-C05-i02 – Interface Mission – nº 01/ C05-i02/2022, Collaborative Laboratories Base Fund.. Centre Bio R&D

S. Ribeiro with Centre Bio R&D Unit, Association BLC3 – Technological and Innovation Campus, Rua Nossa Senhora da Conceição, nº. 2. Lagares da Beira 3405-155 Oliveira do Hospital (phone: +351 238 641 059; e-mail: sonia.ribeiro@blc3.pt

D. Farinha is with Centre Bio R&D Unit, Association BLC3 – Technological and Innovation Campus, Rua Nossa Senhora da Conceição, nº. 2. Lagares da Beira 3405-155 Oliveira do Hospital (phone: +351 238 641 059; e-mail: diana.farinha@blc3.pt

E. Pereira is with Associação CECOLAB - Collaborative Laboratory Towards Circular Economy, Oliveira do Hospital, Portugal (phone: +351 238 011 400; e-mail: elsa.pereira@cecolab.pt).

H. Sales is with Centre Bio R&D Unit, Association BLC3 – Technological and Innovation Campus, Rua Nossa Senhora da Conceição, nº. 2. Lagares da Beira 3405-155 Oliveira do Hospital (phone: +351 238 641 059; e-mail: helia.sales@blc3.pt

F. Figueiredo is with Associação CECOLAB - Collaborative Laboratory Towards Circular Economy, Oliveira do Hospital, Portugal (phone: +351 238

unit | BLC3 and Rita Pontes thanks their support funded by Fundação para a Ciência e Tecnologia (FCT) UIDP/05083/2020 and UIDB/05083/2020.

011 400; e-mail: filipa.figueiredo@cecolab.pt), Centre Bio R&D Unit, Association BLC3 – Technological and Innovation Campus, Rua Nossa Senhora da Conceição, nº. 2. Lagares da Beira 3405-155 Oliveira do Hospital, Portugal.

R. Pontes is with Centre Bio R&D Unit, Association BLC3 – Technological and Innovation Campus, Rua Nossa Senhora da Conceição, nº. 2. Lagares da Beira 3405-155 Oliveira do Hospital (phone: +351 238 641 059; e-mail: rita.pontes@blc3.pt

J. Nunes is with Centre Bio R&D Unit, Association BLC3 – Technological and Innovation Campus, Rua Nossa Senhora da Conceição, nº. 2. Lagares da Beira 3405-155 Oliveira do Hospital (phone: +351 238 641 059; e-mail: joao.nunes@blc3.pt

# Policies for Circular Bioeconomy in Portugal: Barriers and Constraints

A. Fonseca, A. Gouveia, E. Ramalho, R. Henriques, F. Figueiredo, J. Nunes

**Abstract**— Due to persistent climate pressures, there is a need to find a resilient economic system that is regenerative in nature. Bioeconomy offers the possibility of replacing non-renewable and non-biodegradable materials derived from fossil fuels with ones that are renewable and biodegradable, while a Circular Economy aims at sustainable and resource-efficient operations. The term "Circular Bioeconomy", which can be summarized as all activities that transform biomass for its use in various product streams, expresses the interaction between these two ideas. Portugal has a very favourable context to promote a Circular Bioeconomy due to its variety of climates and ecosystems, availability of biologically based resources, location, and geomorphology. Recently, there have been political and legislative efforts to develop the Portuguese Circular Bioeconomy. The Action Plan for a Sustainable Bioeconomy approved in 2021, is composed of five axes of intervention, ranging from sustainable production and the use of regionally based biological resources to the development of a circular and sustainable bioindustry, through research and innovation. However, as some statistics show, Portugal is still far from achieving circularity. According to Eurostat, Portugal has circularity rates of 2.8%, which is the second lowest among the member states of the European Union. Some challenges contribute to this scenario, including sectorial heterogeneity and fragmentation, prevalence of small producers, lack of attractiveness for younger generations, and absence of implementation of collaborative solutions amongst producers and along value chains.

Regarding the Portuguese industrial sector, there is a tendency towards complex bureaucratic processes, which leads to economic and financial obstacles and an unclear national strategy. Together with the limited number of incentives the country has to offer to those that pretend to abandon the linear economic model, many entrepreneurs are hesitant to invest the capital needed to make their companies more circular. Absence of disaggregated, georeferenced, and reliable information regarding the actual availability of biological resources is also a major issue. Low literacy on bioeconomy among many of the sectoral agents and in society in general, directly impacts the decisions of production and final consumption. The WinBio project seeks to outline a strategic approach for the management of weaknesses/opportunities in the technology transfer process given the reality of the territory, through road mapping and national and international benchmarking. The developed work included the identification and analysis of agents in the interior region of Portugal, natural endogenous resources, products, and processes associated with potential development. Specific flow of biological wastes, possible

value chains, and the potential for replacing critical raw materials with bio-based products was accessed, taking into consideration other countries with a matured bioeconomy.

The study found food industry, agriculture, forestry, and fisheries generate huge amounts of waste streams, which in turn provide an opportunity for the establishment of local bio-industries powered by this biomass. The project identified biological resources with potential for replication and applicability in the Portuguese context. The richness of natural resources and potentials known in the interior region of Portugal is a major key to developing the Circular Economy and sustainability of the country.

**Keywords**—Circular Bioeconomy; Interior Region of Portugal; Public Policy; Regional Development.

**Acknowledgements** - This work was supported by WinBio Project and Ana Fonseca, Edgar Ramalho and Ana Gouveia thanks their research contracts funded by WinBio "Waste & Interior & Bioeconomy": da Ciência às Empresas para o Desenvolvimento da Bioeconomia Circular e Sustentável no Interior, POCI-01-0246-FEDER-181335, under Programa Operacional Temático Competitividade e Internacionalização—COMPETE 2020, through the European Regional Development Fund (ERDF). Filipa Figueiredo and Rita Henriques also thanks their research contracts funded by Interface Mission under the PRR - Recovery and Resilience Plan – Re-C05-i02 – Interface Mission – nº 01/ C05-i02/2022, Collaborative Laboratories Base Fund. Centre Bio R&D unit | BLC3 thanks their support funded by Fundação para a Ciência e Tecnologia (FCT) UIDP/05083/2020.

A. Fonseca is with CECOLAB - Collaborative Laboratory Towards Circular Economy, Oliveira do Hospital, Portugal (phone: +351 238 011 400; e-mail: ana.fonseca@cecolab.pt).

A. Gouveia is with CECOLAB - Collaborative Laboratory Towards Circular Economy, Oliveira do Hospital, Portugal (e-mail: ana.gouveia@cecolab.pt).

E. Ramalho is with CECOLAB - Collaborative Laboratory Towards Circular Economy, Oliveira do Hospital, Portugal (edgar.ramalho@cecolab.pt).

R. Henriques is with CECOLAB - Collaborative Laboratory Towards Circular Economy, Oliveira do Hospital, Portugal (rita.henriques@cecolab.pt).

F. Figueiredo is with Associação CECOLAB - Collaborative Laboratory Towards Circular Economy, Oliveira do Hospital, Portugal (phone: +351 238 011 400; e-mail: filipa.figueiredo@cecolab.pt), Centre Bio R&D Unit,

Association BLC3 – Technological and Innovation Campus, Rua Nossa Senhora da Conceição, nº. 2. Lagares da Beira 3405-155 Oliveira do Hospital, Portugal and Centre for Environmental and Marine Studies (CESAM), Department of Environment and Planning, University of Aveiro, 3810-193 Aveiro, Portugal.

J. Nunes is with Centre Bio R&D Unit, Association BLC3 – Technological and Innovation Campus, Rua Nossa Senhora da Conceição, nº. 2. Lagares da Beira 3405-155 Oliveira do Hospital (phone: +351 238 641 059; e-mail: joao.nunes@blc3.pt, Portugal and Associação CECOLAB - Collaborative Laboratory Towards Circular Economy, Oliveira do Hospital, Portugal.

# Agricultural Organized Areas Approach for Resilience to Droughts, Nutrient Cycle and Rural and Wild Fires

D. Pereira, M. Moura, J. Campos, J. Nunes\*

**Abstract**—As the Ukraine war highlights the European Economic Area's vulnerability and external dependence on feed and food, agriculture gains significant importance. Transformative change is necessary to reach a sustainable and resilient agricultural sector. Agriculture is an important drive for bioeconomy and the equilibrium and survival of society and rural fires resilience. The pressure of (1) water stress, (2) nutrient cycle, and (3) social demographic evolution towards 70% of the population in Urban systems and the aging of the rural population, combined with climate change, exacerbates the problem and paradigm of rural and wildfires, especially in Portugal. The Portuguese territory is characterized by (1) 28% of marginal land, (2) the soil quality of 70% of the territory not being appropriate for agricultural activity, (3) a micro smallholding, with less than 1 ha per proprietor, with mainly familiar and traditional agriculture in the North and Centre regions, and (4) having the most vulnerable areas for rural fires in these same regions. The most important difference between the South, North and Centre of Portugal, referring to rural and wildfires, is the agricultural activity, which has a higher level in the South. In Portugal, rural and wildfires represent an average annual economic loss of around 800 to 1000 million euros. The WinBio model is an agri-environmental metabolism design, with the capacity to create a new agri-food metabolism through Agricultural Organized Areas, a private-public partnership. This partnership seeks to grow agricultural activity in regions with (1) abandoned territory, (2) micro smallholding, (3) water and nutrient management necessities, and (4) low agri-food literacy. It also aims to support planning and monitoring of resource use efficiency and sustainability of territories, using agriculture as a barrier for rural and wildfires in order to protect rural population.

**Keywords**—Agricultural Organized Areas; Residues; Climate Change, Drought; Nutrients; Rural and Wild Fires.

**Acknowledgements** - This work was supported by WinBio Project "Waste & Interior & Bioeconomy": da Ciência às Empresas para o Desenvolvimento da Bioeconomia Circular e Sustentável no Interior, POCI-01-0246-FEDER-181335, under Programa Operacional Temático Competitividade e Internacionalização—COMPETE 2020, through the European Regional Development Fund (ERDF) and Interface Mission under the PRR - Recovery and Resilience Plan – Re-C05-i02 – Interface Mission – nº 03/C05-i02/2022. Centre Bio R&D unit | BLC3 thanks their support funded by Fundação para a Ciência e Tecnologia (FCT) UIDP/05083/2020.

D. Pereira is with Centre Bio R&D Unit, Association BLC3 – Technological and Innovation Campus, Rua Nossa Senhora da Conceição, nº. 2. Lagares da Beira 3405-155 Oliveira do Hospital (phone: +351 238 641 059; e-mail: diogo.pereira@blc3.pt).

M. Moura is with Centre Bio R&D Unit, Association BLC3 – Technological and Innovation Campus, Rua Nossa Senhora da Conceição, nº. 2. Lagares da Beira 3405-155 Oliveira do Hospital (phone: +351 238 641 059; e-mail: maria.moura@blc3.pt).

J. Campos is with Centre Bio R&D Unit, Association BLC3 – Technological and Innovation Campus, Rua Nossa Senhora da Conceição, nº. 2. Lagares da Beira 3405-155 Oliveira do Hospital (phone: +351 238 641 059; e-mail: joana.campos@blc3.pt).

J. Nunes is with Centre Bio R&D Unit, Association BLC3 – Technological and Innovation Campus, Rua Nossa Senhora da Conceição, nº. 2. Lagares da Beira 3405-155 Oliveira do Hospital (phone: +351 238 641 059; e-mail: joao.nunes@blc3.pt).

# Designing a Model to Increase the Flow of Circular Economy Startups using a Systemic and Multi-Generational Approach

L. Marques, J. Rocha, A. Fernandes, M. Moura, C. Caseiro, F. Figueiredo, J. Nunes

i02/2022. Centre Bio R&D unit | BLC3 thanks their support funded by Fundação para a Ciência e Tecnologia (FCT) UIDP/05083/2020.

**Abstract**— The implementation of circularity strategies other than recycling, such as reducing the amount of raw material, as well as reusing or sharing existing products, remains marginal. The European Commission announced that the transition towards a more circular economy could lead to the net creation of about 700,000 jobs in Europe by 2030, through additional labour demand from recycling plants, repair services and other circular activities. Efforts to create new circular business models in accordance with completely circular processes, as opposed to linear ones, have increased considerably in recent years. In order to create a societal Circular Economy transition model, it is necessary to include innovative solutions, where startups play a key role. Early-stage startups based on new business models according to circular processes often face difficulties in creating enough impact. The StartUp Zero Program designs a model and approach to increase the flow of startups in the Circular Economy field, focusing on a systemic decision analysis and multi-generational approach, considering Multi-Criteria Decision Analysis to support a decision-making tool, which is also supported by the use of a combination of an Analytical Hierarchy Process and Multi-Attribute Value Theory methods. We define principles, criteria and indicators for evaluating startup prerogatives, quantifying the evaluation process in a unique result. Additionally, this entrepreneurship program spanning 16 months involved more than 2400 young people, from ages 14 to 23, in more than 200 interaction activities.

**Keywords**—Circular Economy; Entrepreneurship Startups; Multi-Criteria Decision Analysis.

**Acknowledgements** - This work was supported by StartUp Zero project, POCI-03-33B5-FSE-072556 under the Programa Operacional Temático Competitividade e Internacionalização—COMPETE 2020, through the European Regional Development Fund (ERDF), by i-CERES project - Innovation and advanced production systems applied to strategic “Trás-os-Montes” plants and fungi based on biotechnology and digitalization, NORTE-01-0145-FEDER-000082, by the Interface Mission under the PRR - Recovery and Resilience Plan – Re-C05-i02 – Interface Mission – n° 01/C05-i02/2022, Collaborative Laboratories Base Fund and by Interface Mission under the PRR - Recovery and Resilience Plan – Re-C05-i02 – Interface Mission – n° 03/C05-

L. Marques is with Centre Bio R&D Unit, Association BLC3 – Technological and Innovation Campus, Rua Nossa Senhora da Conceição, n°. 2. Lagares da Beira 3405-155 Oliveira do Hospital (phone: +351 238 641 059; e-mail: luis.marques@blc3.pt)

J. Rocha is with CECOLAB - Collaborative Laboratory Towards Circular Economy, Oliveira do Hospital, Portugal (phone: +351 238 011 400; e-mail: joao.bernardo@blc3.pt).

A. Fernandes is with CECOLAB - Collaborative Laboratory Towards Circular Economy, Oliveira do Hospital, Portugal (e-mail: andreia.fernandes@cecolab.pt).

C. Claudia is with CECOLAB - Collaborative Laboratory Towards Circular Economy, Oliveira do Hospital, Portugal (claudia.caseiro@cecolab.pt).

F. Figueiredo is with Associação CECOLAB - Collaborative Laboratory Towards Circular Economy, Oliveira do Hospital, Portugal (phone: +351 238 011 400; e-mail: filipa.figueiredo@cecolab.pt), Centre Bio R&D Unit, Association BLC3 – Technological and Innovation Campus, Rua Nossa Senhora da Conceição, n°. 2. Lagares da Beira 3405-155 Oliveira do Hospital, Portugal.

J. Nunes is with Centre Bio R&D Unit, Association BLC3 – Technological and Innovation Campus, Rua Nossa Senhora da Conceição, n°. 2. Lagares da Beira 3405-155 Oliveira do Hospital (phone: +351 238 641 059; e-mail: joao.nunes@blc3.pt, Portugal and Associação CECOLAB - Collaborative Laboratory Towards Circular Economy, Oliveira do Hospital, Portugal.



# Teacher-Child Interactions within Learning Contexts in Prekindergarten

Laurent, A., Letarte, M.-J., Lemelin, J.-P., & Morin, M.-F.

**Abstract**—This study aims at exploring teacher-child interactions within learning contexts in public prekindergartens of the province of Québec (Canada). It is based on previous research showing that teacher-child interactions in preschools have direct and determining effects on the quality of early childhood education and could directly or indirectly influence child development. However, throughout a typical preschool day, children experience different learning contexts to promote their learning opportunities. Depending on these specific contexts, teacher-child interactions could vary, for example, between free play and shared book reading. Indeed, some studies have found that teacher-directed or child-directed contexts might lead to significant variations in teacher-child interactions. This study drew upon both the bioecological and the Teaching Through Interactions frameworks. It was conducted through a descriptive and correlational design. Fifteen teachers were recruited to participate in the study. At Time 1 in October, they completed a diary to report the learning contexts they proposed in their classroom during a typical week. At Time 2, seven months later (May), they were videotaped three times in the morning (two weeks' time between each recording) during a typical morning class. The quality of teacher-child interactions was then coded with the Classroom Assessment Scoring System (CLASS) through the contexts identified. This tool measures three main domains of interactions: emotional support, classroom organization, and instruction support, and 10 dimensions scored on a scale from 1 (low quality) to 7 (high quality). Based on the teachers' reports, five learning contexts were identified: 1) shared book reading, 2) free play, 3) morning meeting, 4) teacher-directed activity (such as craft), and 5) snack. Based on preliminary statistical analyses, little variation was observed within the learning contexts for each domain of the CLASS. However, the instructional support domain showed lower scores during specific learning contexts, specifically free play and teacher-directed activity. Practical implications for how preschool teachers could foster specific domains of interactions depending on learning contexts to enhance children's social and academic development will be discussed.

**Keywords**—Teacher practices, teacher-child interactions, preschool education, learning contexts, child development.

Angélique Laurent is with the University of Sherbrooke, Canada (e-mail: [angelique.laurent@usherbrooke.ca](mailto:angelique.laurent@usherbrooke.ca)).

# Creating an Enabling Learning Environment for Learners with Visual Impairments in Lesotho Rural Schools by Using Asset-Based Approaches

*Mamochana, A. Ramatea, Fumane, P. Khanare*

**Abstract**— Enabling the learning environment is a significant and adaptive technique necessary to navigate learners' educational challenges. However, research has indicated that quality provision of education in the environments that are enabling, especially to learners with visual impairments (LVIs, hereafter) in rural schools remain an ongoing challenge globally. Hence, LVIs often have a lower level of academic performance as compared to their peers. To balance this gap and fulfill learners' fundamental human rights of receiving an equal quality education, appropriate measures, and structures that make enabling learning environment a better place to learn must be better understood. This paper, therefore, intends to find possible means that rural schools of Lesotho can employ to make the learning environment for LVIs enabling.

The present study aims to determine suitable assets that can be drawn to make the learning environment for LVIs enabling. The study is also informed by the transformative paradigm and situated within a qualitative research approach. Data were generated through focus group discussions with twelve teachers who were purposefully selected from two rural primary schools in Lesotho. The generated data were then analyzed thematically using Braun and Clarke's six-phase framework. The findings of the study indicated that participating teachers do have an understanding that rural schools boast of assets (existing and hidden) that have a positive influence in responding to the special educational needs of LVIs. However, the participants also admitted that although their schools boast of assets, they still experience limited knowledge about the use of the existing assets and thus, realized a need for improved collaboration, involvement of the existing assets, and enhancement of academic resources to make LVIs' learning environment enabling. The findings of this study highlight the significance of the effective use of assets. Additionally, coincides with literature that shows recognizing and tapping into the existing assets enable learning for LVIs.

In conclusion, the participants in the current study indicated that for LVIs' learning environment to be enabling, there has to be sufficient use of the existing assets. The researchers, therefore, recommend that the appropriate use of assets is good, but may not be sufficient if the existing assets are not adequately managed. Hence, LVIs experience a vicious cycle of vulnerability. It was thus, recommended that adequate use of assets and teachers' engagement as active assets should always be considered to make the learning environment a better place for LVIs to learn in the future.

**Keywords**— Assets-based approaches, enabling learning environment, rural schools, learners with visual impairments.

Mamochana, A. Ramatea is a Ph.D. student in the School of Education Studies at the University of the Free State, Bloemfontein, South Africa, mamochanaramatea@gmail.com <https://orcid.org/0000-002-6424-2143>

Fumane P. Khanare is a Senior Lecturer in the Department of Psychology of Education at the University of the Johannesburg, Gauteng, South Africa, Fumanek@uj.ac.za <https://orcid.org/0000-0002-1707-9179>

# Exploring The Use of Universal Design for Learning to Support Deaf Learners in Lesotho Secondary Schools: English Teachers' Voice

Ntloyalefu J.Palime, Fumane P. Khanare

**Abstract**— English learning has been found as one of the prevalent areas of difficulty for Deaf learners. However, studies conducted indicated that this challenge experienced by Deaf learners is an upsetting concern globally as is blamed and hampered by various reasons such as the way English is taught at schools, lack of teachers' skills and knowledge, therefore, impact negatively on their academic performance. Despite any difficulty in English learning, this language is considered nowadays as the key tool to an educational and occupational career especially in Lesotho. This paper, therefore, intends to contribute to the existing literature by providing the views of Lesotho English teachers, which focuses on how effectively Universal Design for Learning can be implemented to enhance the academic performance of Deaf learners in the context of the English language classroom.

The purpose of this study sought to explore the use of Universal Design for Learning (UDL) to support Deaf learners in Lesotho secondary schools. The present study is informed by an interpretative paradigm and situated within a qualitative research approach. Ten participating English teachers from two inclusive schools were purposefully selected and telephonically interviewed to generate data for this study. The data were thematically analyzed. The findings indicated that even though UDL is identified as highly proficient and promotes flexibility in teaching methods teachers reflect limited knowledge of the UDL approach. The findings further showed that UDL ensures education for all learners, including marginalized groups, such as learners with disabilities through different teaching strategies. This means that the findings signify the effective use of UDL for the better performance of the English language by DLs. This aligns with literature that shows mobilizing English teachers as assets help the DLs to be engaged and have control in their community by defining and solving problems using their resources and connections to other networks for assets and exchange.

The study, therefore, concludes that teachers acknowledged that even though they assume to be knowledgeable about the definition of UDL, they have a limited practice of the approach, thus they need to be equipped with some techniques and skills to apply for supporting the performance of Deaf learners by using UDL approach in their English teaching. The researchers recommends the awareness of UDL principles by the Ministry of Education and Training and teachers training Universities, as well as teachers' training colleges, for them to include it in their curricula so that teachers could be properly trained on how to apply it in their teachings effectively.

**Keywords**— Deaf learners, Lesotho, support learning, universal learning design.

N. J. Palime is a Ph.D. Student in the University of the Free State, In South Africa Bloemfontein (+266 57785913; e-mail: justinahpalime@gmail.com ).

F. P. Khanare is a Senior Lecturer at the Department of Educational Psychology in the University of the Johannesburg, Gauteng, South Africa. (E-mail: Fumanek@uj.ac.za ).

# Teaching and Learning with Picturebooks: Developing Multimodal Literacy with a Community of Primary School Teachers in China

Fuling Deng

**Abstract—** Today's children are frequently exposed to multimodal texts that adopt diverse modes to communicate myriad meanings within different cultural contexts. To respond to the new textual landscape, scholars have considered new literacy theories which propose picturebooks as important educational resources. Picturebooks are multimodal, with their meaning conveyed through the synchronisation of multiple modes, including linguistic, visual, spatial, and gestural acting as access to multimodal literacy. Picturebooks have been popular reading materials in primary educational settings in China. However, often viewed as “easy” texts directed at the youngest readers, picturebooks remain on the margins of Chinese upper primary classrooms, where they are predominantly used for linguistic tasks, with little value placed on their multimodal affordances. Practices with picturebooks in the upper grades in Chinese primary schools also encounter many challenges associated with the curation of texts for use, designing curriculum, and assessment. To respond to these issues, a qualitative study was conducted with a community of Chinese primary teachers using multi-methods such as interviews, focus groups, and documents. The findings showed the impact of the teachers' increased awareness of picturebooks' multimodal affordances on their pedagogical decisions in using picturebooks as educational resources in upper primary classrooms.

**Keywords—** picturebook education, multimodal literacy, teachers' response to contemporary picturebooks, community of practice.

# The New World Kirkpatrick Model as an Evaluation Tool for a Publication Writing Programme

Eleanor Nel

**Abstract**— Research output is an indicator of institutional performance (and quality), resulting in increased pressure on academic institutions to perform in the research arena. Research output is further utilised to obtain research funding. Resultantly, academic institutions face significant pressure from governing bodies to provide evidence on the return for research investments. Research output has thus become a substantial discourse within institutions, mainly due to the processes linked to evaluating research output and the associated allocation of research funding. This focus on research outputs often surpasses the development of robust, widely accepted tools to additionally measure research impact at institutions. A publication writing programme, for enhancing research output, was launched at a South African university in 2011. Significant amounts of time, money, and energy have since been invested in the programme. Although participants provided feedback after each session, no formal review was conducted to evaluate the research output directly associated with the programme. Concerns in higher education about training costs, learning results, and the effect on society have increased the focus on value for money and the need to improve training, research performance, and productivity. Furthermore, universities rely on efficient and reliable monitoring and evaluation systems, in addition to the need to demonstrate accountability. While publishing does not occur immediately, achieving a return on investment from the intervention is critical. A multi-method study, guided by the New World Kirkpatrick Model (NWKM), was conducted to determine the impact of the publication writing programme for the period of 2011 to 2018. Quantitative results indicated a total of 314 academics participating in 72 workshops over the study period. To better understand the quantitative results, an open-ended questionnaire and semi-structured interviews were conducted with nine participants from a particular faculty as a convenience sample. The purpose of the research was to collect information to develop a comprehensive framework for impact evaluation that could be used to enhance the current design and delivery of the programme. The qualitative findings highlighted the critical role of a multi-stakeholder strategy in strengthening support before, during, and after a publication writing programme to improve the impact and research outputs. Furthermore, monitoring on-the-job learning is critical to ingrain the new skills academics have learned during the writing workshops and to encourage them to be accountable and empowered. The NWKM additionally provided essential pointers on how to link the results more effectively from publication writing programmes to institutional strategic objectives to improve research performance and quality, as well as what should be included in a comprehensive evaluation framework.

**Keywords**— evaluation, framework, impact, research output.

# Threat Analysis: A Technical Review on Risk Assessment and Management of National Testing Service (NTS)

1<sup>st</sup> Beenish Urooj

Department of Computer Science and  
Engineering  
Ghulam Ishaq Khan Institute of  
Engineering Sciences and Technology  
Topi, Pakistan  
beenish.urooj@giki.edu.pk

2<sup>nd</sup> Ubaid Ullah

Department of Project Management  
Northeastern University  
Toronto, Canada  
ubaidullah.dhillon@gmail.com

3<sup>rd</sup> Sidra Riasat

Department of Computer Science  
COMSATS University Islamabad  
Islamabad, Pakistan  
sidrariasat4@gmail.com

**Abstract**— National Testing Service-Pakistan (NTS) is an agency in Pakistan that conducts student success appraisal examinations. In this research paper, we must present a security model for the NTS organization. The security model will depict certain security countermeasures for a better defense against certain types of breaches and system malware. We will provide a security roadmap, which will help the company to execute its further goals to maintain security standards and policies. We also covered multiple aspects in securing the environment of the organization. We introduced the processes, architecture, data classification, auditing approaches, survey responses, data handling, and also training and awareness of risk for the company. The primary contribution is the Risk Survey, based on the maturity model meant to assess and examine employee training and knowledge of risks in the company's activities.

**Keywords**— NTS, risk assessment, threat factors, security, services

## I. INTRODUCTION

National Testing Service-Pakistan (NTS) is a student achievement assessment agency based in Pakistan. It's the same as the Educational Testing Service in the United States (ETS). Two key tests of the NTS are the National Aptitude Test (NAT) and the Graduate Assessment Test (GAT) (GAT). NAT is meant for college and university students. GAT is aimed at graduates who are seeking postgraduate education. NTS exams are often used to evaluate the credentials of students who study abroad [1]. We must propose a safety model for this company in this report. The security model shows certain countermeasures for enhanced protection against types of infringements and malware systems. To maintain safety regulations and policies, we shall develop a plan to help the organization fulfil its future objectives. The security objective of this organization is because it is owned by thousands of candidates throughout Pakistan. They safeguard their identity, their papers, and their application to supply a suitable testing program, which might lead to several infringements. A few of the factors that explain why the firm requires security are (Information violation, credibility assurance, data modification, and deletion, Content distribution and fair selection, prompt access to resources) [2].

NTS is divided into five main functional departments and is very dependent or inter-connected on their flow of work. The departments are Quality Management, Secretariat, Office Division, Operation & Co-ordination, and Academics. Each department has its unique role in the organization [3]. NTS manages paper-based reviews. To increase transparency,

integrity, consistency, and more significantly, the reputation of the whole system in stringent security circumstances, Standard operating procedures (SOPs) are created for every test operation. To boost the safety and convenience of the whole institute to realize its better ambitions, the Testing Services and Corporate Affairs Division is the support services arm of the National Testing Service. In October of 2014, NTS established the International Collaboration and Accreditation Division. The division's overarching goal is to establish links, network, communicate, and interact with international agencies and educational institutions responsible for the development of testing and assessment commodities, teaching, training, infrastructure development, research and development, and quality assurance [4]. Since NTS is a multi-activity company, it follows well-thought-out Standard Operating Procedures (SOPs) to ensure professionalism and improve the likelihood of each event's success. Contents oversee gathering information about the topics being tested. The databank receives the collection, which will be used for testing purposes. [5] The content is contributed by an academic committee made up of university professors who oversee designing curricula, regulating testing, and fostering consistency.

Section II presents the background and provides the framework and analysis work. Section III and IV elaborates risk analysis and planning which shows the parameters used in the paper. Section V shows the Assessment based on the chosen maturity model, describing the comparison view of the research papers implemented in this report. VI elaborated the results and analysis based on the survey we provided and lastly, section VII concludes the discussion and conclusion.

## II. LITERATURE REVIEW

In this section, we will describe a little overview of the standards, purpose of the security for this organization. Another strategy is to outlook the threat rate, NTS vision, and further organization background strategies and policies for the organization. We covered the company's architecture and security layout in the introduction and the purpose of our report in detail.

The first thing that is to be concerned about is whether NTS is using the ISO standard 9001 (2015). The standard ISO 9001 highlights the importance of quality management [6]. A quality management program at the most basic level is a set of rules or guidelines for regular operating processes that allow you to assess the "quality" of different aspects of your company. In essence, NTS follows ISO 9001 (2015) standard



and is an ISO 9001-2008 certified company under our engagement with the Organization. They claim that they maintain their operations' quality management. They have a comprehensive Quality Management department for the execution of standards and regulations accordingly. M&E and R&A data upkeep is the emphasis of the department. To follow up on the standard, the treat rate is notified based on quality management of the organization and that is why there is a need for security in this organization. The purpose of security is to provide reliability for the organization and to ensure integrity and confidentiality. [7] The security objective of this agency is to ensure that the intellectual property of thousands of applications in Pakistan is maintained by this agency. They operate a competent testing regime and so can target numerous violations of their identification, personal papers, and applications. A few of the factors in [8] that explain why the company requires security are (Breach of information, to ensure credibility, modification, and destruction of data, fair selection and content distribution, timely access of resources).

The organization is majorly vulnerable to internal threats as compared to external threats. The most common threat this organization faces is an Insider's Job [9], which is the biggest loophole in a company because they are familiar with the infrastructure of the organization, and more importantly, they happen to never leave any clues because of their awareness of the departments. For example, a clerk is manipulated or compromised by powerful influence, and they leak the testing material. Another internal threat is Privilege Escalation [10]. Former employees can access the previous systems because of the negligence of not having a proper retiring protocol. They still have logins and provisions just like the currently employed. Additionally, Employee awareness is getting to a point of potential threats in this organization. For example, an employee leaving a system or a document unnoticed in front of an unaccounted visitor or even an employee. NTS is not majorly exposed to external threats [11], but it is still prone to attacks from outside the organization. System or website hijack is an external threat to the organization which also nullifies the websites' non-responsiveness. Timely access to the company websites resources is a critical factor of an organization and ensures quality management and maintenance. [12] The attack can include DOS attacks etc. Social Engineering is also an external threat that this organization faces, which reduces the credibility of the company and disrupts the integrity and respect of the organization. In case of an accident or an incident, the NTS reports it to the departmental heads and forms a committee of experts from each of the departments, and investigates the matter privately. We can imply the system's security, authentication services, mitigate privilege escalation, awareness of employees, provisional audits, and physical security, etc.

The future 10-year plan of NTS focuses on past and future business experiences of the firm. By 2020, a total of 10 million stakeholders were agreed upon for NTS Vision-20 20. The NTS effort was focused on during the 10-year plan:

- Testing and Assessment (T&A)
- Human Resource Development (HRD)
- Network and Partnership Building (NPB)
- Institutional Capacity Building (ICB)
- Regional and International Cooperation (RIC)
- Research and Development (R&D)
- Information and Knowledge Management (IKM)

The primary focus of NTS Vision-2020 [13] will be on facilities for public institutions, government, corporations, private businesses, and careers, as well as human resource organizations. International standard test and evaluation products and services will be provided on the TOEFL, TOEIC, SAT (I and II), ACT, GRE (Generic and Subject), GMAT, MCAT, LSAT, Workforce Evaluation for Job Fit, and other models, while considering local security criteria's, conditions/environment, and education framework. NTS intends to manage CBT throughout the country through a LAN/WAN network of academic institutions using central developed/controlled software while maintaining strict security. NTS's mission is to develop, maintain, encourage, and provide secure educational and technical testing and evaluation standards. Their core objectives include effective, transparent, secure, and international quality assessments to determine candidates' level of competence for entry, scholarship, and recruiting purposes. Also research educational, professional, and testing processes to recognize the systems' current instructional and organizational differences. Professional evaluation by training and appraisal is used to develop the capabilities of educational and vocational individuals and organizations and to generate and distribute educational and professional learning standards knowledge and analysis.

We also performed a SWOT analysis on NTS to measure out the threat rate and the positive properties of the company. As we have already discussed NTS has five departments which further exceeds to divisional sections Every department has a key role that they have to carry out to maintain the process flow of the organization and to conduct each examination securely. [14] Up next we are defining major weaknesses that his organization possesses and the risk relying on against those weaknesses and followed by that a SWOT analysis which gives you a predefined flow of your organization's functions. Table 1 dictates the NTS SWOT analysis and explains each section with its appropriate qualities of weakness according to the organization. The four sections each have NTS calculates factors for the categories and the SWOT analysis helps users or viewers to accumulate the frequency of how a company is efficiently working or where it lacks security. Strength defines the optimistic features of the organization. Weaknesses are there to carry out the values where there flaws in the systems. Opportunities offer futuristic approaches for the company and lastly, the threats, equal up to the certain acts that endanger the company's reputation or confidentiality.

TABLE I. NTS SWOT ANALYSIS

Helpful		Harmful	
Internal origin	<i>Strengths</i>	<i>Weaknesses</i>	
	<ul style="list-style-type: none"><li>• Interlinked optimistic culture.</li><li>• Preserve content integrity.</li><li>• Operational efficiency maintained (Cost-effective examination conduction).</li><li>• Expanding testing services and centers.</li><li>• Expertise in the content making.</li><li>• Divisional departments with collaborative roles&amp; SOP.</li></ul>	<ul style="list-style-type: none"><li>• Reputation decline (Paper breach).</li><li>• Printing Press (Missing prints).</li><li>• Brand marketing (NO social media).</li><li>• No financial resources.</li></ul>	
External origin	<i>Opportunities</i>	<i>Threats</i>	
	<ul style="list-style-type: none"><li>• An increase in testing services gathers more customers/applicants.</li><li>• Opportunity to go against competitors, growth of operational capabilities.</li><li>• Partners help expand the services.</li><li>• Leading testing service promotes market trends.</li></ul>	<ul style="list-style-type: none"><li>• No backup for online testing in case of societal change.</li><li>• Suppliers can be a threat during of provisional distribution of the paper.</li></ul>	

### III. PLANNING AND RISK ANALYSIS

Before analysing risks, we deeply understand different processes of NTS organization and after that, we categorize weak processes as it is also a risk and suggest some additional

processes to lower the risk rate of the organization. Here is an overview of these processes in table III.

TABLE III. WEAK/ADDITIONAL PROCESSES OF NTS ORGANIZATION

Categorization	Processes
Weak Processes	<b>Testing Integrity</b> <ul style="list-style-type: none"> <li>This process needs to be made strong as many breaches are occurring and tests are getting leaked.</li> </ul>
	<b>Result Merits</b> <ul style="list-style-type: none"> <li>Most of the students are not transferred their result cards and they have no other option other than to print them out from the website. Genuine result cards should be addressed to every applicant for preventing any duplication risks.</li> </ul>
	<b>Divisional Test Conduction</b> <ul style="list-style-type: none"> <li>Divisional tests should be given the same attention by sending out supervisors and security officials for reducing any inefficiency.</li> </ul>
Additional Processes/ Departments	<b>Forensics Team</b> <ul style="list-style-type: none"> <li>There is a need for a forensics department in this organization as they only can control and have a proactive approach towards the root of the breaches.</li> </ul>
	<b>Employee Training</b> <ul style="list-style-type: none"> <li>Employee training needs to be the top SOP requirement for this organization as most of the attacks can be prevented by spreading awareness of what is right and what is wrong.</li> </ul>
	<b>Content Evaluation</b> <ul style="list-style-type: none"> <li>Another sub-department should be made for handling the content-making processes. The content should be made by different professors for each test, or the test categories and tasks should be shuffled between content makers to reduce any test leaking threats.</li> </ul>
	<b>Increase in Physical Security</b> <ul style="list-style-type: none"> <li>Physical security must be considered a prominent security policy for every data center where a test is being taken.</li> </ul>

After highlighting different processes which need improvement, we also suggest SOPs for those Processes. Integrity should be maintained by giving minimal access to each of the departments or the respective authorities. Access should be logged and audited and maintained by the data custodian so it can achieve efficiency and non-modification of the data. Previous employees should be properly logged off the systems and their access should be terminated after leaving the job. The addition of the forensics team will be of prime value because they have the experience to apply proactive approaches to mitigate breaches and how to control them. They have the right measures on how to properly investigate and prosecute the attackers or threat actors in court. Employee training can conduct through a monthly schedule of training sessions set by the head of each department according to the SOP of maintaining work relations a secret. Another SOP of work punishment should be introduced as well so the employee has the information of gaining a penalty if someone approaches a wrong turn. An SOP of content evaluation should be advised which is to change content makers every time a new test curriculum needs to be generated. SOP of two-

factor authentications [16] should be developed which proves that the result has been addressed and not just posted on the website and the applicant should also authenticate the result and check his credentials and right merits. This weak process should be improved by implementing a stronger SOP policy of maintaining authentication a top priority in divisional test centers. The addition of more physical security should be the new SOP for each centre. Testing should be sealed off with the right security parameters. Guards, cameras, checking procedures, and detectors should be introduced.

#### A. Business Risk Assessment/Categorization

Organizations are exposed to a variety of threats, which can sometimes result in a significant loss. However, whereas many major organizations have comprehensive "risk management" divisions, smaller enterprises are less likely to do so. A threat to a company's power to fulfil its goals is referred to as a business risk. The threat in business refers to the possibility that a company's or company's objectives will not come out as anticipated, that it will miss its target, or that it will fail to reach its objectives. Our business objectives

related to risk management [17], can be categorized as strategic, financial, operational, or compliance-related. We will discuss each risk one by one and after that, we will categorize each process in an organization on basis of these business risks.

TABLE IV. PROCESS CATEGORIZATION BASED ON BUSINESS RISKS

Categorization based on Risks and their Processes			
Strategic		Operational	
<ul style="list-style-type: none"><li>• Testing affiliation with different organizations</li><li>• Testing services links with other agencies and corporate sectors</li><li>• Categorized Testing</li><li>• Marketing</li></ul>		<ul style="list-style-type: none"><li>• Paper distribution while test</li><li>• Paper monitoring</li><li>• Testing merit/ marketing</li><li>• Authentication</li><li>• Testing submission</li><li>• Test monitoring hiring</li><li>• Data centers organization</li><li>• Test auditing</li><li>• Employee’s training</li><li>• Paper generation</li><li>• Data maintenance</li><li>• Customer’s Coordination Operations</li><li>• Roll no slips distribution</li><li>• IT maintenance</li><li>• Student Applications</li><li>• Categorized Testing</li><li>• Paper Distribution to Centers</li><li>• Test Dates Scheduling</li><li>• Testing Irregularities/ Paper Cancellation</li><li>• Administration Record Keeping Process</li><li>• Result Validity</li></ul>	
Financial		Compliance	
<ul style="list-style-type: none"><li>• Finance handling</li><li>• Student Applications</li></ul>		<ul style="list-style-type: none"><li>• Monitoring test centers</li><li>• Testing integrity</li><li>• Test auditing</li><li>• Paper generation</li><li>• Data maintenance</li><li>• Content making</li><li>• Review Panel for Risk Assessment</li><li>• Test Dates Scheduling</li><li>• Up-to-date Announcement for Applicants through E-mails and SMS</li><li>• Result Validity</li></ul>	

Based on these five maturity dimensions, we created a survey for employees to get their knowledge about different risks and threats for the organization and get responses from them. We add different questions related to security and Risk assessment. And after getting results and feedback which will be discussed in the results section, we came to know that they have even no basic knowledge about the basic risks and threats to their organization and they have no idea how to respond to them. We came up with the consensus that the general crowd knows the policies of what to do if there is a breach and they have the knowledge about the strong passwords and security controls, but the employees are clueless about types of malware they can face. Another factor we noticed is the employee's lack of knowledge about internal threats as well.

## V. RESULT AND ANALYSIS

### A. Maturity Model

The survey is conducted based on the servitization maturity model (SeMM). Survey 1 was circulated in NTS employees and some of them were filled by social workers. After analysing the feedback, we came up with the consensus that the general crowd knows the policies of what to do if there is a breach and they have the knowledge about the strong passwords and security controls, but the employees are clueless about types of malware there are. Another factor we noticed is the employee's lack of knowledge about internal threats as well. About 50 % plus employees think it is ok to bring your work laptop to your homes and also to let a close friend/employee have the access to testing material which is wrong on every level and poses a great threat to the organization's confidentiality and integrity.

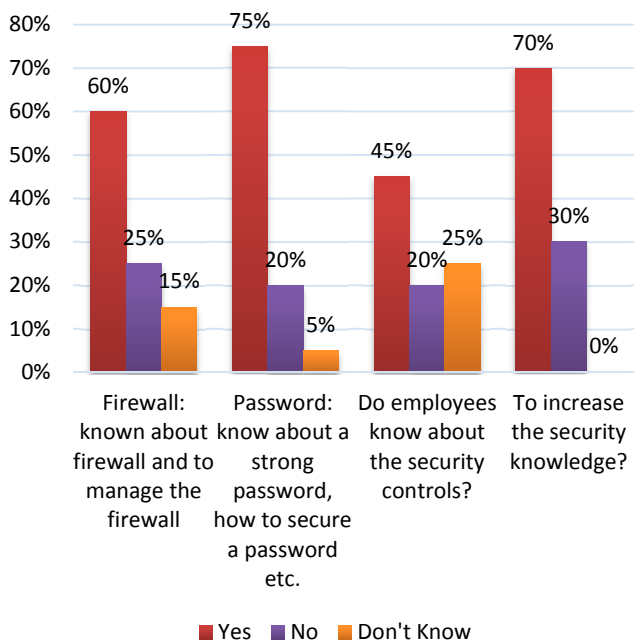


Fig. 1. Results of Employee Security Training

The result shows the employees do not need strict training. But as the systems are becoming intelligent and the rapid growth of the technology; therefore, employees need to aware of the current situation. The result of the Monitor testing awareness is shown in Figure 2.

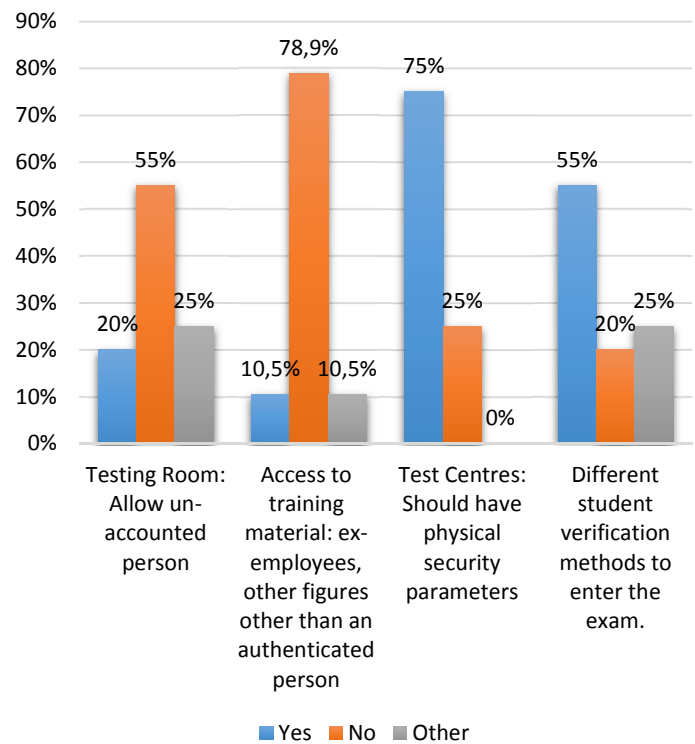


Fig. 2. Result of Monitoring/ Applicant Testing Awareness

We came up with the conclusion at the end of the survey responses and constructed a security awareness training program, which we thought was needed for these employees after analyzing these responses. Aware the employees about computer malware and about the organization's internal attacks, which are the main backdoors currently present inside NTS, and it holds still. There should be two different types of training sessions for the employees after analyzing the survey results. Firstly, employees' security training sessions regarding computer threats, malware, cyber-attacks, and how to find out the malware. Secondly, training for internal threats and risk factors. Figure 3 shows the recommendation based on the selection process after reviewing the result concluded by the maturity model survey.

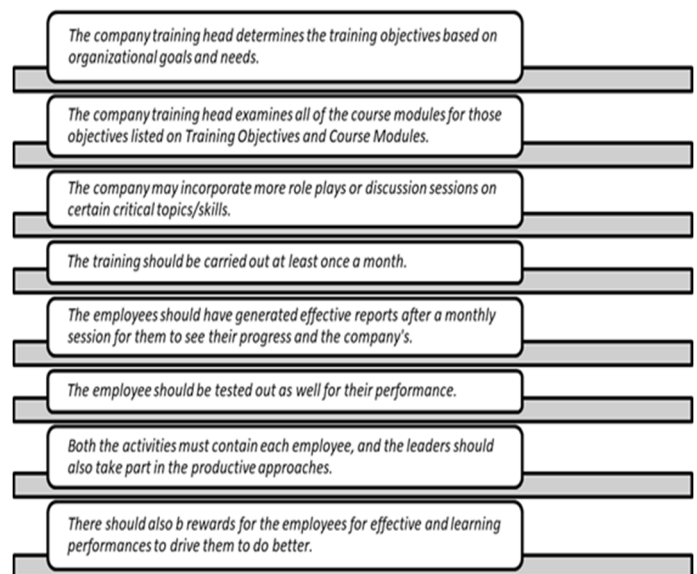


Fig. 3. Recommendation Based on Survey

### B. Risk Assessment based on defined processes

A risk assessment is a formal document that identifies potential dangers and suggests ways to deal with them. It lays out a strategy to follow if something goes wrong. A risk

assessment is usually part of a larger risk management strategy and is part of health and safety compliance. Figure 4 shows the responses based on the authentication and data maintenance and handling we asked from the employees.

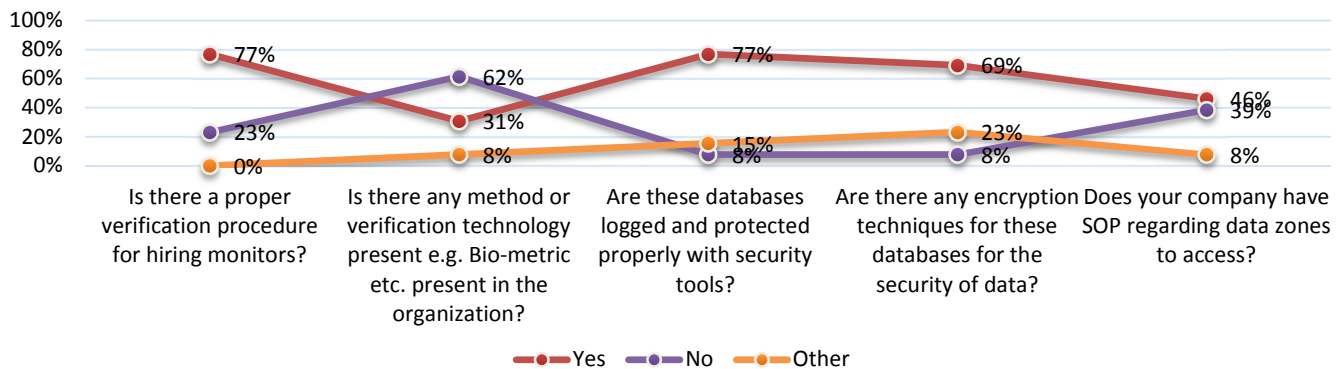


Fig. 4. Result based on Authentication and Data Handling

Figure 5 focuses on the responses that how well an organization handles the security processes and how it maintains company auditing.

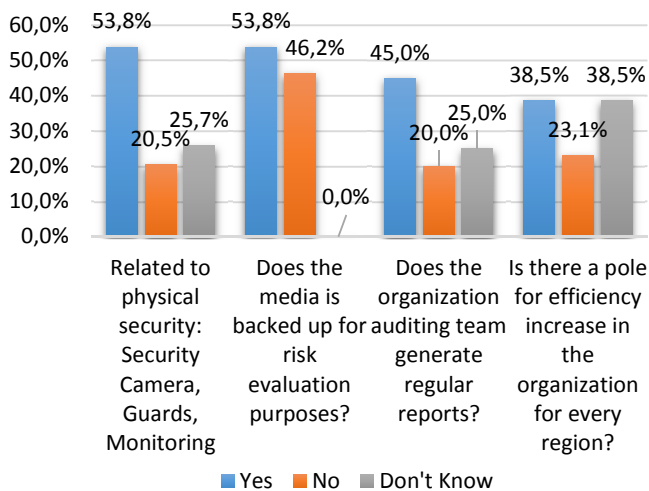


Fig. 5. Result based on Security and Audit Processes

Results show that the organization achieves half of the security related to this still more precautions should be taken to improve the physical security during tests.

### VI. CONCLUSION

This research paper is based on the overall security analysis of the National Testing Service (NTS). The purpose is to provide the necessary measures and inspect the values that are needed to maintain the quality of the organization. The paper discusses organization architecture, processes, and standards it follows. We also elaborated on risk factors, processes for risk analysis. The major contribution stands with the conducted survey in terms of risk involved in the company's processes and another one based on a maturity model designed to analyze and examine the employee.

### REFERENCES

[1] W. M. AFRIDI, "What is the purpose of NTS?," 13 March 2014. [Online]. Available: <https://www.dawn.com/news/861032/what-is-the-purpose-of-nts>.

[2] "Audit Report on the Accounts of District Education Authorities of 19 Districts of Punjab," gov.pk, 2018.

[3] "Nts.org.pk," NTS, [Online]. Available: <https://www.nts.org.pk/departments.php>. [Accessed 20 June 2021].

[4] T. Beteille, N. Tognatta, M. Riboud, S. Nomura and Y. Ghorpade, Ready to Learn: Before School, In School, and Beyond School in South Asia, 2020.

[5] nts.org, "We Offer Data Processing Services," [Online]. Available: <https://www.nts.org.pk/new/services.php#dvd>. [Accessed 20 June 2021].

[6] R. Tricker, "Quality Management System – requirements," in MDD Compliance Using Quality Management Techniques, 2020.

[7] A. AlKalbani, H. Deng, B. Kam and X. Zhang, "Information Security Compliance in Organizations: An Institutional Perspective," Data and Information Management, 2017.

[8] S. Lesia, S. Pochtovyuk, L. Shevchuk and O. Bilyk, "Introduction of Innovative Educational Methods in the Organization of the Education Process of Electrical Engineers," in 2020 IEEE Problems of Automated Electrodive. Theory and Practice (PAEP), Kremenchuk, Ukraine, IEEE, 2020, pp. 1-4.

[9] N. Saxena, E. Hayes, E. Bertino, P. Ojo, K. K. Choo and P. Burnap, "Imoact and Key Challenges of Insider Threats on Organization and Critical Businesses," Electronics, vol. 9, p. 1460, 2020.

[10] S. Efthimia, "Cybersecurity Education Status and Curriculum Analysis," 2021.

[11] N. Y. Conteh, "Ethical Hacking, Threats, and Vulnerabilities in Cybersecurity," in Ethical Hacking Techniques and Countermeasures for Cybercrime Prevention, New Orleans, IGI Global, 2021, p. 18.

[12] J. B. Ulven and G. Wangen, "A systematic review of cybersecurity risks in higher education," Future Internet, 2021.

[13] "NTS™ - Pakistan," 2021. [Online]. Available: <https://www.nts.org.pk/new/vision-2020.php>. [Accessed 20 June 2021].

[14] E. GÜREL, "SWOT ANALYSIS: A THEORETICAL REVIEW," Journal of International Social Research, 2017.

[15] B. P. Woolf, V. Shute, K. VanLehn, W. Burleson, J. L. King, D. Suthers, B. Bredeweg, R. Luckin, R. S. J. D. Baker and E. Tonkin, "A Roadmap of Education Technology," Technology, 2020.

[16] J. Stewart, "Two-Factor Authentication," educause, 2019.

[17] M. Thakur, "WallStreetMojo," 2021. [Online]. Available: <https://www.wallstreetmojo.com/risk-categories/>. [Accessed 20 June 2021].

[18] A. Samimi, "Risk Management in Information Technology," Progress in Chemical and Biochemical Research, vol. 3, no. 2, pp. 30-134, 2020.

[19] B. Cole, "Risk Management," TechTarget, 2020.

[20] F. Adrodegari and N. Saccani, "A maturity model for the servitization of product-centric companies," Journal of Manufacturing Technology Management, vol. 31, no. 4, pp. 775-797, 2020. J. Stewart, "Two-Factor Authentication," educause, 2019.

# Open Access in the Economic Sphere: A Framework Interpreting the Rise of the UK, US and China at Different Historical Times

Guanghua Yu

**Abstract—** This article has examined the rise of the UK, US, and China at different historical times to explain the argument that it is open access in the economic sphere, as well as institutional building related to the protection of property rights, contract enforcement, financial market, the rule of law, and human resource accumulation that determine economic and human development. Both the UK, after the Glorious Revolution in the seventeenth century, and China, after its adoption of the open door policy at the end of the 1970s, follow such a path of development. The difference between the UK and China in moving toward that path is the different coordination of elites. While the coordination of elites in the UK through parliament played important roles in forcing the government to consider the wider encompassing interest in society after the Glorious Revolution, the coordination of elites in China has mainly been achieved by the Communist Party of China such that the Chinese Government has started to pay greater deal of attention to the wider encompassing interest in the country from 1978. The article has also examined the rise of the US following colonial settlement to independence and institutional building thereafter. The US case is similarly consistent with the argument that open access in the economic sphere and institutional building matter the most to economic development. More decentralized methods of the coordination of elites in the US among colonies (states), the federal governments, and other political groups similarly shaped the path towards open access in the economic sphere and institutional building. As such, open access in the political sphere plays an indirect role in development at best. If that is correct, there are possibilities that different political systems are able to achieve coordination of elites so that governments will turn their attention to development.

**Keywords—** open access, interconnected institutions, democracy, development.



# Place Attachment and Human Ethos: A Narrative-Integrative Review and an Attempt to Apply It to the Case of Residents of Jardim Pantanal

Adriano Francisco de Oliveira, Sandra Maria Patricio Ribeiro

**Abstract**— We understand ethos as a natural, continuous and reciprocal molding relationship (as what) existing between place, subjectivity and behavior”. Based on this concept, this study aims to understand the relationship built over time and through everyday interactions between the residents of Jardim Pantanal and the place where they live, which form the concrete ethical reality of these residents. Objective: The work (which is under development) is divided into two parts: it aims at a narrative-integrative review about the concepts of "Place Attachment" and "Human Ethos" together with a verification of the possibility of applying this form of understanding in a concrete situation, as is the case of neighborhood residents. Method: 10 residents of the region will be selected who were removed from their homes by the government and who returned to live in the place after 6 months. Data collection will be carried out through a socioeconomic analysis of the participants, a semi-structured interview and application of an adult attachment scale.

Preliminary results: Throughout the review, it was possible to return to some basic concepts related to attachment to place; the term place appears as equivalent to house, street, neighborhood, city; attachment reveals aspects related to connection, also enabling understanding through connection with the neighborhood. All of this contributes to the existence of a framework of meanings for Place Attachment, which makes methodological possibilities that glimpse the understanding of the subject difficult. What is common in all this reflection is, in my view, the departure from the term attachment as postulated by Bowlby, in addition to the imprecision related to the term place; consequently, if attachment begins at birth and accompanies the human being throughout life, it is not difficult to conclude that he is also susceptible to places. That said, it seems to me useful and necessary, for the understanding of attachment to place, to resume (or take) the sense of attachment as elaborated by Attachment Theory. it is noted that the sense of attachment used today approaches theoretical matrices and moves away from what was originally thought about attachment; mainly from John Bowlby. At the same time, thinking about the contemporary ethos in this study means being aware of the different contributions, transdisciplinary, and seeking, as much as possible, to investigate the possibility of applying this way of understanding the ethos in a concrete situation, consequently offering contributions to the study regarding the Place attachment.

**Keywords**— Psychology, Attachment, Place, Place Attachment.

# Evaluating Language Loss Effect on Autobiographical Memory by Examining Memory Phenomenology in Bilingual Speakers

Anastasia Sorokina

**Abstract**— Graduate language loss or attrition has been well documented in individuals who migrate and become emersed in a different language environment. This phenomenon of first language (L1) attrition is an example of non-pathological (not due to trauma) and can manifest itself in frequent pauses, search for words, or grammatical errors. While the widely experienced loss of one's first language might seem harmless, there is convincing evidence from the disciplines of Developmental Psychology, Bilingual Studies, and even Psychotherapy that language plays a crucial role in the memory of self. In fact, we remember, store, and share personal memories with the help of language. Dual-Coding Theory suggests that language memory code deterioration could lead to forgetting. Yet, no one has investigated a possible connection between language loss and memory. The present study aims to address this research gap by examining a corpus of 1,495 memories of Russian-English bilinguals who are on a continuum of L1 (first language) attrition. Since phenomenological properties capture how well a memory is remembered, the following descriptors were selected - vividness, ease of recall, emotional valence, personal significance, and confidence in the event. A series of linear regression statistical analyses were run to examine the possible negative effects of L1 attrition on autobiographical memory. The results revealed that L1 attrition might compromise perceived vividness and confidence in the event, which is indicative of memory deterioration. These findings suggest the importance of heritage language maintenance in immigrant communities who might be forced to assimilate as language loss might negatively affect the memory of self.

**Keywords**— L1 attrition, autobiographical memory, language loss, memory phenomenology, dual coding.

# Expanding Behavioral Crisis Care: Expansion of Psychiatric and Addiction-Care Services through a 23/7 Behavioral Crisis Center

Garima Singh

## **Abstract—**

**Objectives:** Behavioral Crisis Center (BCC) is a community solution to a community problem. There has been an exponential increase in the incidence and prevalence of mental health crises around the world. The effects of the crisis negatively impact our patients and their families and strain the law enforcement and emergency room. The goal of the multi-disciplinary care model is to break the crisis cycle and provide 24-7 rapid access to an acute and crisis stabilization. We initiated our first BCC care center in 2020 in the midst of the COVID pandemic and have seen a remarkable improvement in patient care and positive financial outcome.

**Background:** Mental illnesses are common in the United States. Nearly one in five U.S. adults live with a mental illness (52.9 million in 2020). This number represented 21.0% of all U.S. adults. To address some of these challenges and help our community, In May 2020, we opened our first Behavioral crisis center (BCC). Since then, we have served more than 2500 patients and is the first southwest Missouri's first 24/7 facility for crisis-level behavioral health and substance use needs. It has been proven to be a more effective place than emergency departments, jails, or local law enforcement.

**Methods:** BCC was started in 2020 to serve the unmet need of the community and provide access to behavioral health and substance use services identified in the community. Funding was possible with significant investment from the county and Missouri Foundation for Health, with contributions from medical partners. It is a multi-disciplinary care center consisting of Physicians, nurse practitioners, nurses, behavioral technicians, peer support specialists, clinical intake specialists, and clinical coordinators and hospitality specialists. The center provides services including psychiatry care, outpatient therapy, community support services, primary care, peer support and engagement. It is connected to a residential treatment facility for substance use treatment for continuity of care and bridging the gap, which has resulted in the completion of treatment and better outcomes.

**Results:** BCC has proven to be a great resource to the community and the Missouri Health Coalition is providing funding to replicate the model in other regions and work on a similar model for children and adolescents. Overall, 29% of the patients seen at BCC are stabilized and discharged with outpatient care. 50% needed acute stabilization in a hospital setting and 21% required long-term admission, mostly for substance use treatment. The local emergency room had a 42% reduction in behavioral health encounters compared to the previous 3 years. Also, by a quick transfer to BCC, the average stay in ER was reduced by 10 hours and time to follow up behavioral health assessment decreased by an average of 4 hours. Uninsured patients are also provided Medicaid application assistance which has benefited 55% of individuals receiving care at BCC.

**Conclusions:** BCC is impacting community health and improving access to quality care and substance use treatment. It is a great investment for our patients and families.

**Keywords—** BCC, behavioral health, community health care, addiction treatment.

Garima Singh is with the Burrell Behavioral Health, United States (e-mail: garima.singh@burrellcenter.com).

# Role of Tele-health in Expansion of Medical Care

Garima Singh, Kunal Malhotra

## **Abstract—**

**Objective:** The expansion of telehealth has been instrumental in increasing access to medical services, especially for underserved and rural communities. In 2020, 14 million patients received virtual care through telemedicine and the global telemedicine market is expected to reach up to \$185 million by 2023. It provides a platform and allows a patient to receive primary care as well as specialized care using technology and the comfort of their homes. Telemedicine was particularly useful during COVID-pandemic and the number of telehealth visits increased by 5000% during that time. It continues to serve as a significant resource for patients seeking care and to bridge the gap between the disease and the treatment.

**Method:** As per APA (American Psychiatric Association), Telemedicine is the process of providing health care from a distance through technology. It is a subset of telemedicine, and can involve providing a range of services, including evaluations, therapy, patient education and medication management. It can involve direct interaction between a physician and the patient. It also encompasses supporting primary care providers with specialist consultation and expertise. It can also involve recording medical information (images, videos, etc.) and sending this to a distant site for later review.

**Results:** In our organization, we are using telepsychiatry and serving 25 counties and approximately 1.4 million people. We provide multiple services, including inpatient, outpatient, crisis intervention, Rehab facility, autism services, case management, community treatment and multiple other modalities. With project ECHO (Extension for Community Healthcare Outcomes) it has been used to advise and assist primary care providers in treating mental health. It empowers primary care providers to treat patients in their own community by sharing knowledge.

**Conclusion:** Telemedicine has shown to be a great medium in meeting patients' needs and accessible mental health. It has been shown to improve access to care in both urban and rural settings by bringing care to a patient and reducing barriers like transportation, financial stress and resources. Telemedicine is also helping with reducing ER visits, integrating primary care and improving the continuity of care and follow-up. There has been substantial evidence and research about its effectiveness and its usage.

**Keywords—** telehealth, telemedicine, access to care, medical technology.

# Monitoring Public Attitudes Towards Tourism Valorisation of the Dinara Nature Park's Dry Grasslands

Sven Ratković

**Abstract**— The survey of public attitudes and knowledge was conducted as part of the Dinara back to LIFE project during June and July 2020. The aim of the research was to collect public opinions and knowledge on the topics of the biodiversity of Dinara, perception of tourist potential, sustainable development, and acceptance of the project. The research was conducted using the survey method in the cities of Sinj, Knin, Vrlika, and Trilj, and the municipalities of Hrvace, Otok, Kijevo, and Civljane, where a total of 404 people were surveyed. The respondents perceive the cultural and recreational potential of Dinara and recognize it as a potential for agriculture and tourism. According to respondents, the biological diversity of Dinara is most affected by fires and human activity. When it comes to nature protection, the majority of respondents don't trust local self-government units and relevant ministries. The obtained results indicate the need for informing and educating the community, and they serve to adjust the project activities and better guide the touristic development of the project area. The examination will be repeated in the last project year (2023).

**Keywords**— protected area tourism, Dinara Nature Park, dry grasslands, touristic infrastructure.

# Enhancing Archaeological Sites: Interconnecting Physically and Digitally

Eleni Maistrou, D. Kosmopoulos, Carolina Moretti, Amalia Konidi, Katerina Boulougoura

**Abstract**— InterArch is an ongoing research project that has been running since September 2020. It aims to propose the design of a site-based digital application for archaeological sites and outdoor guided tours, supporting virtual and augmented reality technology. The research project is co-financed by the European Union and Greek national funds, through the Operational Program Competitiveness, Entrepreneurship, and Innovation, under the call RESEARCH - CREATE – INNOVATE (project code: T2EΔK-01659). It involves mutual collaboration between academic and cultural institutions and the contribution of an IT applications development company. The research will be completed by July 2023 and will run as a pilot project for the city of Ancient Messene, a place of outstanding natural beauty in the west of Peloponnese, which is considered one of the most important archaeological sites in Greece. The applied research project integrates an interactive approach to the natural environment, aiming at a manifold sensory experience. It combines the physical space of the archaeological site with the digital space of archaeological and cultural data while at the same time, it embraces storytelling processes by engaging an interdisciplinary approach that familiarizes the user with multiple semantic interpretations. The mingling of the real-world environment with its digital and cultural components by using augmented reality techniques could potentially transform the visit on-site into an immersive multimodal sensory experience. To this purpose, an extensive spatial analysis along with a detailed evaluation of the existing digital and non-digital archives is proposed in our project, intending to correlate natural landscape morphology (including archaeological material remains and environmental characteristics) with the extensive historical records and cultural digital data. On-site research was carried out, during which visitors' itineraries were monitored and tracked throughout the archaeological visit using GPS locators. The results provide our project with useful insight concerning the way visitors engage and interact with their surroundings, depending on the sequence of their itineraries and the duration of stay at each location. InterArch aims to propose the design of a site-based digital application for archaeological sites and outdoor guided tours, supporting virtual and augmented reality technology. Extensive spatial analysis, along with a detailed evaluation of the existing digital and non-digital archives, is used in our project, intending to correlate natural landscape morphology with the extensive historical records and cultural digital data. The results of the on-site research provide our project with useful insight concerning the way visitors engage and interact with their surroundings, depending on the sequence of their itineraries and the duration of stay at each location.

**Keywords**— archaeological site, digital space, semantic interpretations, cultural heritage.



# Experimental Investigation of Air-Water Two-Phase Flow Pattern in T-Junction Microchannel

N. Ibrahim-Rassoul <sup>1,\*</sup>, Ek. Si-Ahmed <sup>1,2</sup> and L.Tadrist<sup>3</sup>

<sup>1</sup>USTHB-Faculty of Physics Laboratory of Theoretical and Applied Fluid Mechanics, B.P. 32, El-Alia, 16111 Alger, Algeria

<sup>2</sup> University of Nantes, GEPEA, UMR-6144 CNRS, 37, Bd de l'Université, BP 406, Saint-Nazaire 44602, France

<sup>3</sup>Aix-Marseille Université, Laboratoire IUSTI, CNRS UMR 7343, 13453 Marseille Cedex 13, France

## Abstract:

Water management plays a crucial role in the performance and durability of PEM fuel cells. Whereas the membrane must be hydrated enough, liquid droplets formed by water in excess can block the flow in the gas distribution channels and hinder the fuel cell performance. The main purpose of this work is to increase the understanding of liquid transport and mixing through mini- or micro-channels for various engineering or medical process applications including cooling of equipment according to the operations considered. For that purpose and as a first step, a technique was developed to automatically detect and characterize two-phase flow patterns that may appear in such. The investigation, mainly experimental, was conducted on transparent channel with a 1mm x 1mm square cross section and a 0.3mm x 0.3 mm water injection normal to the gas channel.

Three main flow patterns were identified liquid slug, bubble flow and annular flow. A flow map has been built according to the flow rate of both phases. As a sample the following figures show representative images of the flow structures observed. An analysis and discussion of the flow pattern, in mini-channel, will be provided and compared to the case old micro-channel.

**Keywords:** Two phase flow, Clean Energy, Minichannels, Fuel Cells. Flow patterns, Maps.

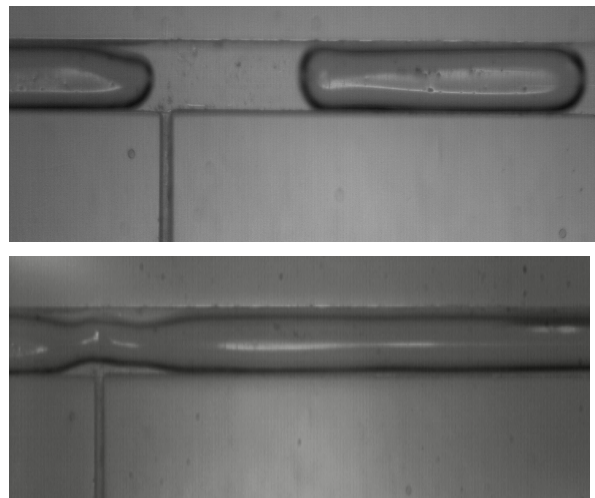
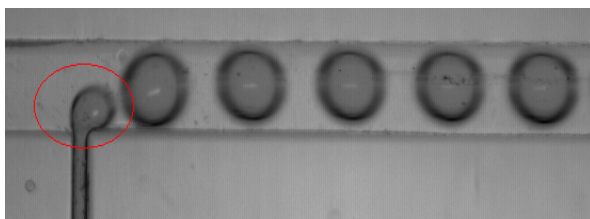
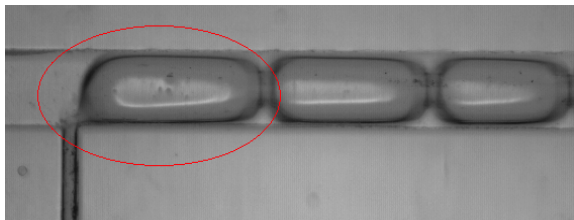


**Figure 1:** Figure illustrating Four flow patterns in the T-Junction.

1. Ben A. Eaton, Charles R. Knowles and I.H. Silberbrg : The Prediction of Flow Patterns, Liquid Holdup and Pressure Losses Occurring During Continuous Two-Phase Flow In Horizontal Pipelin, Reprinted from June, 1967, Iwme of Journal of Petroleum Technology.
2. Hong-Cheol Sin, Sung-Min Kim :Experimental investigation of two phase flow regimes in rectangular micro-channel with two mixer types, Chemical engineering Journal , 2022

# A Case Report on the Multidisciplinary Approach on Rectal Adenocarcinoma in Pregnancy

Maria Cristina B. Cabanag, MD

Author

Elijinese Marie S. Culangen, MD, FPOGS, FPSUOG

Co-author

Department of Obstetrics and Gynecology  
Dr. Paulino J. Garcia Memorial Research and Medical Center  
Philippines

## Abstract:

Pregnancy is a period in a woman's life wherein the body may undergo different physiological changes. These changes can be attributed to the interplay of hormones in the body but in rare occasions can mask a more sinister-type of disease such as malignancy. Colorectal cancer (CRC) in pregnancy is an epidemiologically rare disease worldwide. In the Philippines, no available studies had been reported yet posing a dilemma for its appropriate diagnosis and management. Signs and symptoms of colorectal malignancy may camouflage a normal pregnancy, and when overlooked, impedes appropriate approach. This case of a 38-year-old, elderly primigravid, presented with hematochezia on her 25<sup>th</sup> week age of gestation, diagnosed with rectal adenocarcinoma warranting a predicament on its appropriate care and management. This paper explores on the repertoire of the different diagnostic and treatment approaches of colorectal cancer (CRC) in the second trimester of pregnancy, with the least possible maternal and fetal hazard.

**Keyword:** cancer in pregnancy, chemotherapy in pregnancy, colorectal cancer, hematochezia in pregnancy.

## INTRODUCTION:

Among Filipina non-pregnant women, there are six organs which are commonly associated with cancer such as the breast, lungs, cervix, colon/rectum, ovary and liver<sup>1</sup>. In the Philippines, colorectal cancer ranks third as the most common cause of cancer deaths in the non-pregnant women<sup>2</sup> but not much is known to Filipina pregnant women.

Globally, the incidence of colorectal cancer and pregnancy is rare with one in every 13,000 pregnancies<sup>3</sup>. As of this writing, there are still insufficient studies correlating pregnancy and colorectal cancer in the country thus posing a dilemma in its early diagnosis and treatment.

The diagnosis of colorectal cancer in pregnant women is usually delayed, because there is a significant overlap in signs and symptoms between a colorectal malignancy and normal pregnancy, impeding its proper diagnosis<sup>3</sup>. Once diagnosed, it would be a challenge to give necessary

treatment as there will be only few options available. Hence, the primary objective of this report is to highlight the importance of history and physical examination together with an appropriate diagnostic approach as a crucial step in its early detection and management.

### **CASE REPORT:**

This is a case of a 38-year-old, elderly primigravid, married, Filipino, Roman Catholic, who worked as a primary school teacher in Cabanatuan City, Nueva Ecija. She consulted at a tertiary hospital for hematochezia and was admitted under General Surgery service for her bleeding anorectal mass. She was referred to Obstetrics and Gynecology service and was co-managed for her pregnancy.

History of present condition started four weeks prior to admission, on her 25<sup>th</sup> week age of gestation, when she suddenly noticed a blood-tinged stool and a palpable, reducible anorectal mass upon defecation. No other medications were taken aside from her regular prenatal medications. Two days prior to admission, she noticed her undergarments to be mildly soaked with blood. Fetal kicks were perceived but no lumbosacral pain nor watery vaginal discharge were noted. She immediately consulted her obstetrician and was immediately referred to a tertiary hospital for further evaluation and management. At the emergency room, she was noted to be pale with rectal bleeding approximately 10cc of blood associated with body weakness hence admitted.

Antepartum prenatal care began at twenty weeks gestation of her last menstrual period with unremarkable baseline laboratories. First trimester symptoms were nausea, vomiting and decreased appetite. She was started on multivitamins once a day, ferrous sulfate twice a day and calcium tablet twice a day. On 22<sup>nd</sup> weeks age of gestation, she began to experience frequent morning sickness, weight loss and constipation, which she dismissed, and thought to be common signs and symptoms of pregnancy.

Past medical history showed usual childhood diseases such as Rubella, Parotitis, and Varicella. She is a non-hypertensive, non-diabetic, non-asthmatic and has no allergies to food and medications. She denies any history of major illness, trauma, previous hospitalizations nor other major operations.

She denies any heredo-familial diseases nor congenital anomalies. She was a daughter of a farmer and the youngest of five siblings. A dedicated primary school teacher for ten years with a low level income. She denies any vices, has a sedentary lifestyle and consumes a balanced-diet. Her menarche was at the age of twelve with subsequent menses occurring every 28-35 days lasting for four days consuming three moderately soaked pads per day not associated with dysmenorrhea. She had her coitarche at thirty-three years old with only one sexual partner which later became her husband. Review of systems were deemed to be unremarkable.

On physical examination, she was awake, alert, ambulatory, conscious, coherent, and not in cardio-respiratory distress. Her blood pressure was 110/70mmHg, tachycardic at 110 beats per minute, respiratory rate of 20 cycles per minute and was afebrile. She had pale palpebral conjunctivae, anicteric sclerae, with symmetrical chest expansion and clear breath sounds on both lung fields. Precordium was adynamic, tachycardic, without murmurs appreciated. Clinical examination of the breast revealed unexceptional and no palpable lymph nodes in the neck, groin and axilla. The abdomen was globular with fundic height of 26cm, with fetal heart tone best appreciated on the left upper quadrant with 145-150 beats per minute, normoactive bowel sounds, and non-tender upon palpation on all quadrants. Speculum examination showed a smooth, bluish vaginal wall and a smooth cervix deflected anteriorly with no lesions and ulcerations and with whitish mucoid discharge. On internal examination, the vaginal introitus admitted 2 fingers with

ease. The cervix was soft, closed, with no cervical motion tenderness, uterus was enlarged to 6 months size, with no adnexal mass nor tenderness and no evident bleeding. On anal inspection, there was a thrombosed irregular, fungating mass protruding out of the anus measuring approximately 1.5 x 1.0 centimeters. Digital rectal examination showed good sphincteric tone, with irregular, soft, fungating anorectal mass measuring 5x4cm on the left rectal wall. Rectal vault not collapsed with minimal bleeding per examining finger.

Initial impression was Gravida 1 Para 0, Pregnancy Uterine 28 weeks 6 days age of gestation, elderly primigravid, to consider Rectal Cancer. The preliminary plan was anemia correction with fetal surveillance by performing a Biophysical Profile Scoring (BPS) with a Nonstress test (NST) and complete the diagnostic work-up for rectal malignancy which include a colonoscopy and biopsy of the rectal mass. Nonstress test was reactive. Her severe anemia (hemoglobin of 70) was corrected with blood transfusion of 2 units of packed RBC and increased dosage of Iron tablet to twice a day. BPS showed pregnancy uterine of 29 weeks and 4 days age of gestation, live, single, breech, estimated fetal weight of 1385 grams (+/- 202 grams), fetal heart rate of 155 beats per minute, with deepest vertical pocket of 12.2 centimeters, polyhydramnios, anterior placenta grade II, no previa, BPS score of 8/8. Colonoscopy showed a rectal mass of 1cm from the anal verge extending to the perianal area with a colonic polyp (Figure 1). Followed by a biopsy revealing rectum adenocarcinoma and tubulovillous adenoma of colonic polyp respectively (Figure 2). Carcinoembryonic Antigen (CEA) was also requested and was noted to be elevated to 270.7 ng/ml. Dexamethasone 6mg was completed intramuscularly for fetal lung maturity. To prevent preterm delivery, vaginal Progesterone was inserted before bedtime. As the diagnosis of CRC was confirmed, patient underwent Magnetic Resonance Imaging (MRI) of the abdomen to establish the stage of malignancy. MRI showed a single intrauterine fetus; lobulated soft tissue signals along the mid to distal rectum with associated narrowing of the lumen measuring 2.3cm in maximum thickness and approximately 8.5cm in length; mild pelvocaliectasia, bilateral and prominent left inguinal lymph node (Figure 3). An incidental finding of small nodular signals on lower lobe of both lungs were noted thus a Chest MRI was recommended showing pulmonary parenchymal nodules which appear intermediate on T1 and hyperintense on T2 in both middle to lower lung fields, the largest of which is at the medial segment of the right middle lobe measuring 0.7cm probably metastatic (Figure 4).

On her 30<sup>th</sup> week of pregnancy, patient was diagnosed with Rectal Adenocarcinoma Stage IV. She still presented with same symptoms but is now associated with tenesmus. Because of the clinical picture, patient was subjected into a multidisciplinary discussion with a team of obstetrician, perinatologist, neonatologist, oncologist, onco-surgeon, radiologist, palliative doctor and nutritionist. A family conference was also held together with an in-house Psychiatrist to counsel the family on the patient's medical condition and also to cater to the emotional stress of dealing with such burden. Psychosocial counseling was also rendered to the patient all throughout pregnancy. With the patient's consent, she underwent neoadjuvant chemotherapy with modified FOLFOX-6 (Oxaliplatin, fluorouracil and leucovorin calcium). Weight loss was apparent and nutritional build-up was started. Continuous fetomaternal surveillance with NST and serial BPS (Figure 5) were performed every 2 weeks. Her last BPS showed a pregnancy uterine of 31 weeks and 2 days age of gestation, live, single, breech by fetal biometry, estimated fetal weight of 1905 grams (+/- 253 grams), fetal heart rate of 140 beats per minute, with deepest vertical pocket 6.4 centimeters, normohydramnios, anterior placenta grade II, no previa, BPS score of 8/8. Subsequent medical examinations showed a regular evolution of pregnancy.

On her 33<sup>rd</sup> week of pregnancy, after 2 cycles of chemotherapy, patient underwent Primary Low Transverse Cesarean Section under Combined Spinal - Epidural Anesthesia for Non-Reassuring Fetal Heart Rate Pattern (persistent variable decelerations with mild variability) and delivered to a preterm, 33 weeks by Ballard score, cephalic, live baby boy, single cord coil, thickly meconium stained, Birthweight of 2,000g, Apgar score of 8,9, appropriate for gestational age. Patient tolerated the procedure well with an estimated blood loss of 700ml. Baby was admitted at Neonatal Intensive Care Unit for prematurity but expired on the 3<sup>rd</sup> hospital day due to Respiratory Distress Syndrome. The patient was discharged on post-operative day 4. Subsequent chemotherapy was scheduled on her follow-up. 3 months after delivery, patient was noted to have jaundice and a palpable firm, non-movable, non-tender abdominal mass measuring 10x12cm. During the interim, patient had completed 4 cycles of neoadjuvant chemotherapy but was continuously losing weight and showed signs of deterioration. Eight months from the time of diagnosis of Rectal Adenocarcinoma Stage IV, patient refused further treatments and lost her battle to cancer.

### **CASE DISCUSSION:**

Cancers of the reproductive-aged women, such as colorectal cancer, maybe encountered in pregnancy. In women less than 50 years old, common risk factors that could predispose to colorectal malignancy include smoking, alcohol consumption, physical inactivity and obesity<sup>4</sup> but never pregnancy<sup>5</sup>. Colorectal cancer is an uncommon malignancy to encounter during pregnancy, and its diagnosis is often delayed because some symptoms may be similar to pregnancy such as morning sickness, decreased appetite, constipation and body weakness<sup>6</sup>. Hematochezia is also common in pregnancy and can be mistaken as hemorrhoids rather than a malignancy<sup>7</sup>. The patient is a 38-year-old, elderly primigravid, who had presented with above symptoms. Hematochezia and constipation were thought to be attributed to bleeding hemorrhoids, and her gradual weight loss was assumed from her morning sickness and loss of appetite. These symptoms that were often seen in pregnancy can be habitually overlooked and may be given a wrong impression, therefore, should prompt immediate investigation.

Malignancy during pregnancy is a diagnostic challenge. Physiologic changes in pregnancy can modify the most commonly used laboratory test and disguised the malignancy. Hemoglobin and hematocrit can have lower values in women who commonly suffer anemia during pregnancy<sup>8</sup>. Some serum tumor markers may be physiologically elevated in pregnancy and its sensitivity and specificity may be lower<sup>9</sup>. But CEA, the serum tumor marker used for colorectal cancer, is not influenced by pregnancy in all three trimesters<sup>10</sup>. The patient had severe anemia and elevated CEA upon admission leaning more to the diagnosis of colorectal cancer.

Certain imaging modalities may pose more of fetal harm rather than maternal benefit. Colonoscopy and biopsy are the golden standard tests used to diagnose colorectal cancer. However, these have relative contraindications and may complicate pregnancy<sup>11</sup> but may be relatively safe during the second trimester<sup>12</sup>. In this case, colonoscopy revealed a 1cm rectal carcinoma from the anal verge and a biopsy result of rectal adenocarcinoma and tubilovillous adenoma. The precariousness on fetal safety of some imaging modalities may result in underutilization of the necessary imaging tools resulting on its suboptimal staging. Ultrasound and MRI are the only preferred imaging modalities during pregnancy for its detailed locoregional disease assessment and lack of radiation exposure making it safe for the unborn fetus<sup>10</sup>. Magnetic resonance imaging (MRI) can be safe in all trimesters and be useful in staging the disease<sup>14,16</sup>. Her whole abdominal MRI revealed a single intrauterine fetus with narrowing of the middle to distal

rectum and lobulated lesions of both hepatic lobes probably metastasis with an incidental finding of small nodular signals on the lower lobe of both lungs. Hence, a chest MRI was also requested revealing pulmonary parenchymal nodules on middle to lower lung fields, probably metastatic. Based on her clinical presentation<sup>15</sup>, she was diagnosed to have Rectal Adenocarcinoma Stage IVB.

As the incidence of CRC in young adults is expected to rise, primary care providers have the ability to make the diagnosis early to expedite treatment and hopefully improve outcomes. Therefore, it is imperative that primary care providers take a careful history, perform a thorough physical exam, and have a high index of suspicion for CRC when young patients present with persistent or worrisome symptoms. This case demonstrates the importance of intimately involving the patient in the decision making process.

The malignancy in Rectal cancer Stage IVB had already metastasize to distant organs and tissues like the liver or lungs. The treatment options for non-pregnant women of this stage of cancer varies on how extensive the malignancy is. Surgery is one treatment option that will remove the rectal cancer and metastasis, followed by chemotherapy or chemoradiation<sup>17</sup>. However, in a pregnant women with colorectal cancer after 20 weeks of gestation, chemoradiation is contraindicated and surgical intervention may be delayed to increase fetal survival and lung maturation<sup>18</sup>. As the malignancy had metastasized to the lungs and liver, neoadjuvant chemotherapy was advised to reduce the size of distant metastasis<sup>19</sup>. In general, chemotherapy is safer during the second and third trimesters but is associated with increased incidence of preterm birth and intrauterine growth restriction<sup>20</sup>. Chemotherapy was delayed at the discretion of the patient for fear of fetal harm, and the awareness of its unpleasant side effects.

Ultimately, it is the patient's autonomy to decide between the treatment risk of her unborn fetus or the benefit of her well-being. As physicians, they must be willing to adapt to the treatment plans in accordance to the patient's wishes and be understanding to the complexity and ethical issues surrounding pregnant patients with a possible life-threatening terminal illness.

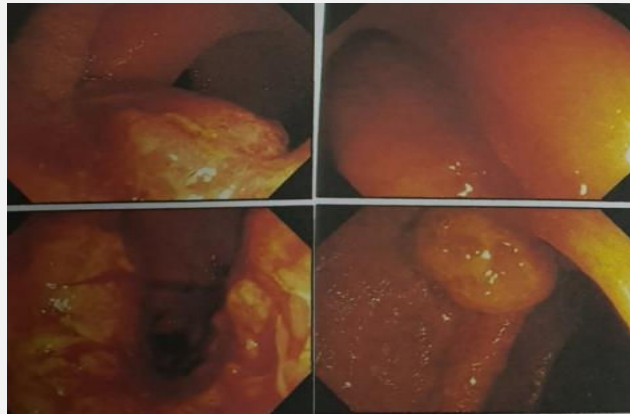
## CONCLUSION:

Colorectal cancer in pregnancy is associated with diagnostic and therapeutic challenges. It is difficult to diagnose as the signs and symptoms such as hematochezia, morning sickness, and loss of appetite can be easily attributed to normal pregnancy leading to late diagnosis in advanced stages. Moreover, pregnancy requires alternative use of diagnostic tools, further hampering rapid and appropriate diagnosis. This paper would like to highlight the importance of using appropriate diagnostic imaging promptly upon suspicion of pathology. In conclusion, attention to unspecific symptoms, early diagnosis, and active treatment might be fundamental to change the clinical course of Colorectal cancer.



**APPENDIX:**

**FIGURE 1**

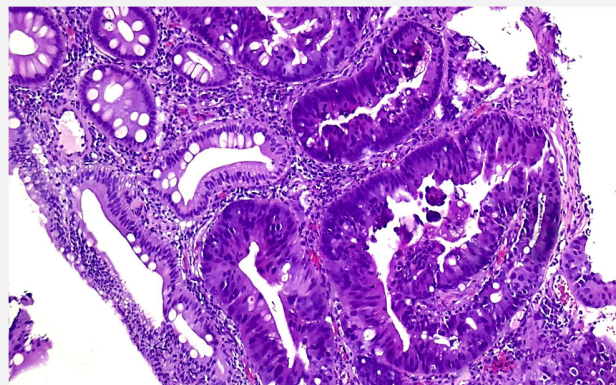


**Colonoscopy**

Rectal carcinoma 1cm from the anal verge (left)

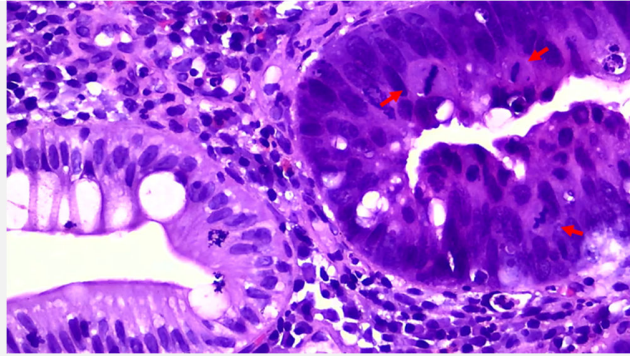
Colonic polyp (right)

**FIGURE 2**



**a. Rectum Adenocarcinoma (LPO)**

Low power – malignant glands (right ) seen beside normal colonic glands (left)



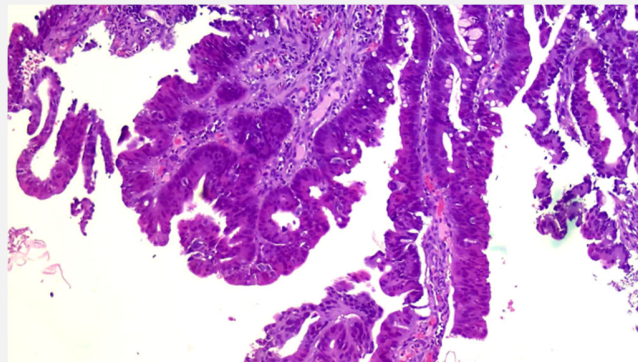
**b. Rectum Adenocarcinoma (HPO)**

The malignant glands:

- ovoid, hyperchromatic nuclei, and moderate amounts of eosinophilic cytoplasm.
- loss of polarity

Invasion of smooth muscle tissue is noted

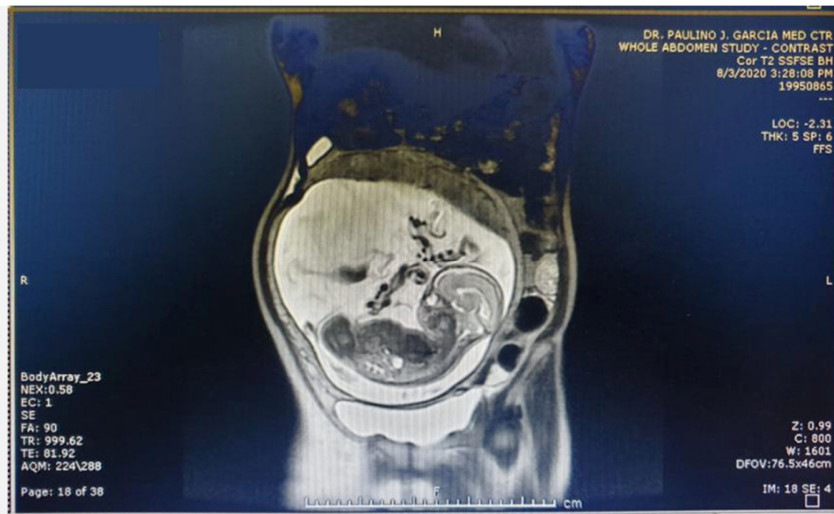
normal colonic type epithelium / gland (left)



**c. Tubilovillous adenoma (LPO)**

Pedunculated polypoid lesions with macroscopic finger-like projections

**FIGURE 3**



### Abdominal MRI

MRI showed single intrauterine fetus; lobulated soft tissue signals along the mid to distal rectum with associated narrowing of the lumen measuring 2.3cm in maximum thickness and approximately 8.5cm in length. Associated high signal on perirectal fat stranding signals. Portion of the lesion approximates the mesorectal fascia anteriorly in the distal rectum, no other abnormal wall thickening along the rest of the gastrointestinal tract. Liver not enlarged and shows smooth marginal outline, with lobulated lesions on both hepatic lobes which are worrisome for metastasis. Mild pelvocaliectasia, bilateral prominent left inguinal lymph node. Incidental note of small nodular signals in the lower lobe of both lungs.

FIGURE 4

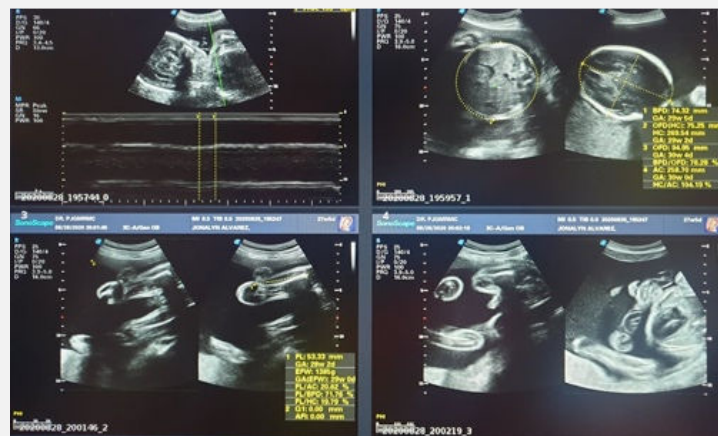


### Chest MRI

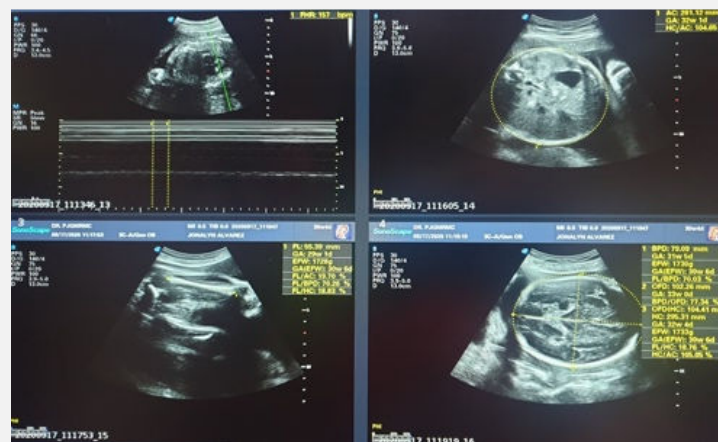
Pulmonary parenchymal nodules which appear intermediate on T1 and hyperintense on T2 in both middle to lower lung fields, the largest of which is at the medial segment of the right middle lobe measuring 0.7cm

probably metastatic. Incidentally, several hepatic nodules and masses in both lobes of the liver, these appears hypointense on T1, hyperintense on T2 and exhibits significant fluid restriction, the largest lesion appears trilobed, occupies segments VIII/V of the right lower lobe measuring approximately 8.1 x 5.3cm, probably metastatic.

**Figure 5**



August 27, 2020



September 17, 2020

Serial BPS showed a live, intrauterine pregnancy, in cephalic presentation, with an estimated fetal weight of 1850g +/- 241g, with good cardiac activity, adequate amniotic fluid volume, and a posterior placenta Grade II.

## REVIEW OF RELATED LITERATURE:

1. University of the Philippines' Institute of Human Genetics, National Institutes of Health.

2. Sung, Hyuna PhD, Ferlay, Jacques MSc, et. Al., Global Cancer Statistics 2020: GLOBOCAN Estimates of Incidence and Mortality Worldwide for 36 Cancers in 185 Countries. ACS Journal. 2020
3. Gens, Helena C and Barbosa, Laura R, Colorectal cancer in pregnant women. JCOL. 2017; 256
4. GBD 2019 Colorectal Cancer Collaborators. "Global, regional, and national burden of colorectal cancer and its risk factors, 1990–2019: a systematic analysis for the Global Burden of Disease Study 2019." *The Lancet. Gastroenterology & Hepatology* 7.7 (2022): 627.
5. Frédéric Amant, Sileny N. Han, Mina Mhallem Gziri, Tineke Vandenbroucke, Magali Verheecke, Kristel Van Calsteren; Management of cancer in pregnancy; Best Practice & Research Clinical Obstetrics & Gynaecology; Volume 29, Issue 5; 2015; Pages 741-753.
6. Vitoratos N, Salamalekis E, Makrakis E, Creatsas G. Sigmoid colon cancer during pregnancy. *Eur J Obstet Gynecol Reprod Biol.* 2002;104(1):70–2. [PubMed] [Google Scholar] [Ref list]
7. Woods JB, Martin JN, Jr, Ingram FH, Odom CD, Scott-Conner CE, Rhodes RS. Pregnancy complicated by carcinoma of the colon above the rectum. *Am J Perinatol.* 1992;9(2):102–10. [PubMed] [Google Scholar] [Ref list]
8. Philippine Obstetrical and Gynecological Society. Clinical Practice Guidelines on Iron Defeiciency Anemia. Nov 2015. Page 10
9. Han SN, Lotgerink A, Gziri MM, Van Calsteren K, Hanssens M, Amant F. Physiologic variations of serum tumor markers in gynecological malignancies during pregnancy: A systematic review. *BMC Med.*; 2012;10:86.
10. Sarandakou A, Protonotariou E, Rizos D. Tumor markers in biological fluids associated with pregnancy. *Crit Rev Clin Lab Sci.*; 2007;44:151–178.
11. Monireh Toosi, Leila Moaddabshoar, Seyed Ali Malek-Hosseini, Mohammad Reza Sasani, Maral Mokhtari, Mohammad Mohammadianpanah; Rectal cancer in pregnancy: A diagnostic and therapeutic challenge; *Journal of the Egyptian National Cancer Institute*; Volume 26, Issue 3; 2014; Pages 175-179.
12. Cappell MS, Fox SR, Gorrepati N. Safety and efficacy of colonoscopy during pregnancy: an analysis of pregnancy outcome in 20 patients. *J Reprod Med.* 2010 Mar-Apr;55(3-4):115-23. PMID: 20506671.
13. Vandecaveye V, Amant F, Lecouvet F, et al; Imaging modalities in pregnant cancer patients; *International Journal of Gynecologic Cancer* 2021;**31**:423-431.
14. Michielsen K, Vergote I, Op de Beeck K, et al. Whole-body MRI with diffusion-weighted sequence for staging of patients with suspected ovarian cancer: A clinical feasibility study in comparison to CT and FDG-PET/CT. *Eur Radiol.* 2014;24:889–901.
15. American Joint Committee on Cancer. Chapter 20 - Colon and Rectum. In: *AJCC Cancer Staging Manual*. 8th ed. New York, NY: Springer; 2017.
16. Alorainy, Ibrahim A et al. "Attitude towards MRI safety during pregnancy." *Annals of Saudi medicine* vol. 26,4 (2006): 306-9. doi:10.5144/0256-4947.2006.306
17. Kelly SR and Nelson H. Chapter 75 – Cancer of the Rectum. In: Niederhuber JE, Armitage JO, Dorshow JH, Kastan MB, Tepper JE, eds. *Abeloff's Clinical Oncology*. 6th ed. Philadelphia, Pa. Elsevier: 2020.
18. Yang H, Han X. Colorectal cancer in pregnancy: a case report and literature review. *J Gastrointest Oncol* 2021;12(2):885-891. doi: 10.21037/jgo-21-31

19. Leonard GD, Brenner B, Kemeny NE: Neoadjuvant chemotherapy before liver resection for patients with unresectable liver metastases from colorectal carcinoma. *J Clin Oncol* 23 (9): 2038-48, 2005.
20. Cao S, Okekpe CC, Dombrovsky I, Valenzuela GJ, Roloff K. Colorectal Cancer Diagnosed During Pregnancy With Delayed Treatment. *Cureus*. 2020 May 24;12(5):e8261. doi: 10.7759/cureus.8261. PMID: 32596079; PMCID: PMC7313435.



# Microbiological Analysis of Polluted Water with Pesticides in Ben Mhidi (Northeastern of Algeria)

Aimeurnadjette, Hammoudi Abd Erahmen, Bordjibaouahiba

**Abstract**— For many years, the pesticides used in agriculture have been responsible for environmental degradation, particularly noticeable in the areas of intensive agriculture, particularly through contamination of surface and groundwater. Our study was conducted to isolate and identify the microflora of water polluted by pesticides in an area with an agricultural vocation (Ben M'Hidi) subject to the pesticide effect for several years. Isolated fungal strains were identified based on the morphology of their vegetative and reproductive apparatus. The micromycètes were obtained; they belong mainly to the genera *Aspergillus*, *Penicillium* and *Trichoderma*. Furthermore, most bacterial strains characterized in this work, are that of the genus *Aeromonas*, *Pseudomonas* that are widely represented in the study of the biodegradation of pesticides.

**Keywords**— isolated, strains, polluted, pesticides.

# Collision Tumor of Plasmacytoma with Hematological and Non-Hematological Malignancies

Arati Inamdar, Siddharth Bhattacharyya., Kester Haye

**Abstract**—Collision tumors are rare entities characterized by neoplasms of two different cell population with distinct separating boundaries. Such tumors could be benign, malignant or a combination of both. The exact mechanism of origin for collision tumors is predicted to be tumor heterogeneity or concurrent occurrence of neoplasm in the same organ. We present two cases of plasmacytoma presenting as a collision tumor one with tumor of hematological origin and another with non-hematological origin namely Chronic Lymphocytic Leukemia and Adenocarcinoma of colon, respectively. The immunohistochemical stains and flowcytometry analysis performed on the specimens aided in correct diagnosis. Interestingly, neoplastic cells of plasmacytoma in the first case demonstrated strong cytokeratin along with weak Epithelial Specific Antigen/ Epithelial cell adhesion molecule Monoclonal Antibody (MOC31) positivity indicating that tumor may influence the microenvironment of the tumor in the vicinity. Furthermore, the next-generation sequencing studies performed on the specimen with plasmacytoma and chronic lymphocytic lymphoma demonstrated BReast CAncer gene (*BRCA2*) and Tumor Necrosis Factor Alpha Induced Protein 3 (*TNFAIP3*) as a disease associated variants suggestive of risk for multiple tumors including collision tumors. Our reports highlight the unique collision tumors involving plasmacytoma which have never been reported previously as well as provide necessary insights about the underline genetic aberrations and tumor heterogeneity through sequencing studies and allows clonality assessment for subsequent tumors.

**Keywords**—*BRCA2*, Collision tumor, Chronic lymphocytic leukemia, Plasmacytoma.

A. I. Author is a Pathologist with the Hospital of University of Pennsylvania, PA, USA (phone: 215-662-6550; fax: 215-615-3931; e-mail: Arati.inamdar@pennmedicine.upenn.edu).

S. B. Author is a Hematopathologist and Program Director of Hematopathology Fellowship program at Hospital of University of

Pennsylvania, PA, USA. (e-mail: Siddharth.bhattacharyya@pennmedicine.upenn.edu).

K. H. Author is a Gastro Intestinal special Pathologist with the Hospital of University of Pennsylvania, PA, USA, (e-mail: Kester.haye@pennmedicine.upenn.edu).

# Size and Content of the Doped Silver Affected the Pulmonary Toxicity of Silver-Doped Nano-Titanium Dioxide Photocatalysts and the Optimization of These Two Parameters

Xiaoquan Huang, Congcong Li, Tingting Wei, Changcun Bai, Na Liu, Meng Tang

**Abstract—** Silver is often doped on nano-titanium dioxide photocatalysts (Ag-TiO<sub>2</sub>) by photodeposition method to improve their utilization of visible-light while increasing the toxicity of TiO<sub>2</sub>. However, it is not known what factors influence this toxicity and how to reduce toxicity while maintaining the maximum catalytic activity. In this study, Ag-TiO<sub>2</sub> photocatalysts were synthesized by the photodeposition method with different silver content (AgC) and photodeposition time (PDT). Characterization and catalytic experiments demonstrated that silver was well assembled on TiO<sub>2</sub> with excellent visible-light catalytic activity, and the size of silver increased with PDT. In vitro, the cell viability of lung epithelial cells A549 and BEAS-2B showed that the higher content and smaller size of silver doping caused higher toxicity. In vivo, Ag-TiO<sub>2</sub> catalysts with lower AgC or larger silver particle size obviously caused less pulmonary pro-inflammatory and pro-fibrosis responses. However, the visible light catalytic activity decreased with the increase in silver size. Therefore, in order to optimize the Ag-TiO<sub>2</sub> photocatalyst with the lowest pulmonary toxicity and highest catalytic performance, response surface methodology (RSM) was further performed to optimize the two independent variables of AgC and PDT. Visible-light catalytic activity was evaluated by the degradation rate of Rhodamine B, the antibacterial property was evaluated by killing log value for *Escherichia coli*, and cytotoxicity was evaluated by IC<sub>50</sub> to BEAS-2B cells. As a result, the RSM model showed that AgC and PDT exhibited an interaction effect on catalytic activity in the quadratic model. AgC was positively correlated with antibacterial activity. Cytotoxicity was proportional to AgC while inversely proportional to PDT. Finally, the optimization values were AgC 3.08 w/w% and PDT 28 min. Under this optimal condition, the relatively high silver proportion ensured the visible-light catalytic and antibacterial activity, while the longer PDT effectively reduced the cytotoxicity. This study is of significance for the safe and efficient application of silver-doped TiO<sub>2</sub> photocatalysts.

**Keywords—** Ag-doped TiO<sub>2</sub>, cytotoxicity, inflammation, fibrosis, response surface methodology.

# Using FETPs to Support nOPV Campaigns in Uganda

Nicholas Ayebazibwe

## **Abstract—**

### **Introduction**

A polio outbreak due to cVDPV2 was declared in Uganda on 25 August 2021. The outbreak was declared after Polio Virus was detected from a sample collected from the Lubigi National Water and Sewerage Corporation environmental surveillance (ES) site. In addition, neighboring countries such as the Democratic Republic of Congo (DRC) and South Sudan have also reported outbreaks of cVDPV2 in the recent past. The porous Uganda borders, pockets of unimmunized children and weak Acute Flaccid Paralysis (AFP) surveillance indicators were among factors that provided a rationale for implementing two rounds of a nation-wide house-to-house Polio campaign. In response to these threats, the Ministry of Health secured 10,997,500 doses of the Novel Oral Polio Vaccine type 2 (nOPV2) that were administered in round 1, in January 2022 and 12 million doses for Round 2 vaccination campaign that was conducted between 4th to 11th November 2022. The purpose of this supplementary immunization activity (SIA) was to address the gaps in population immunity and to interrupt the transmission of the poliovirus throughout the country while targeting the population at risk, children under five years comprising 20.5% of the Ugandan population. A house-to-house implementation strategy was deployed in order to achieve a high vaccination coverage. This approach was used in efforts to reach every single child including those in villages, refugee settlements and hard to reach areas. The African Field Epidemiology Network (AFENET) with support from the US CDC deployed FETP residents to support the Uganda MOH during the scheduled Polio campaign. The team worked in 2 districts, Wakiso and Mukono, located in the central region of Uganda.

### **Methodology**

Below is a summary of key activities conducted:

**District planning meetings and vaccinator trainings:** A number of meetings were held at district level to review microplans, identify gaps ahead of the campaign, and take measures to address gaps in microplanning. This was conducted with DHT (district health team members). Key thematic areas reviewed included vaccines, cold chain and logistics, social mobilization and advocacy, data management, and finance.

These trainings were cascaded from district to subcounty level. Team members facilitated trainings using MoH issued field guides, and trained district supervisors, health workers, vaccine accountability monitors (VAMs), village health team (VHT) members, and local council (LC) chairpersons.

**Field supervision:** Intra-campaign supportive supervision was conducted. Supervisors worked with District supervisors to supervise vaccination teams. Missed pockets of households were reached, finger and house marking assessed, and teams guided on correct practices during the campaign.

### **Achievements**

Overall, the Polio campaign was successfully implemented in the two districts supported. The administrative coverage for the supported districts is summarized below. Overall Round 2 coverage was 109.7%. There were a total of 18 sub counties supported in round 2, and 17/18 (94%) achieved the minimum set target of 95% coverage.

### **Challenges**

These were some of the challenges;

- Incomplete micro plan
- Inadequate teams than the required especially for the municipal areas
- Inadequate budget for social mobilization. All social mobilization activities started in the week for the campaigns
- Wrong fingers marked for some children in some villages
- Houses without eligible children not marked and wrong labeling of some houses.
- Some of the facilities were not achieving their required target population coverage and hence there were many zero doses during the campaign.

**Keywords—** Polio, Campaigns, Uganda, Vaccine, Support.

# The Effects of Whitening Toothpastes Containing Blue Covarine on the Discoloration of Resin Composites and Teeth

Elham Zajkani<sup>1</sup>, Paria Faraji Dizaji<sup>2</sup>, Saeideh Asdag<sup>3</sup>

Department of Operative and Restorative Dentistry, Zanjan University of Medical Sciences

## Abstract

**Objective:** The objective of the present study was to investigate the effects of whitening toothpaste containing blue covarine and hydrogen peroxide on the discoloration of resin composites and teeth. **Materials and Methods:** This experimental-laboratory study was conducted on 72 samples of Omnicroma resin composite (One-Shade, Tokuyama) and extracted human anterior teeth. The samples (teeth and composites) were divided into three groups; Colgate Max White Ultimate Catalyst toothpaste, Close Up Diamond Attraction toothpaste, and the control group. Then, the samples were placed in tea solution for seven days, and the control group was placed in water. Next, the samples were brushed with toothpaste twice a day for 30 days. The colorimetric of the samples was done by spectrophotometer at three stages, including before staining, after staining, and after brushing. One-way analysis of variance and Tukey's test were used for data analysis.  $P < 0.05$  was considered as the significant level. **Results:** The results showed that the tea solution significantly discolored the composite and tooth samples ( $E\Delta > 3.3$ ), while the  $E\Delta$  of the control group was less than 3.3. The use of whitening toothpastes led to significant discoloration of the composite and tooth samples, although the color of the samples did not reach the baseline level. Intra-group comparison of resin composite samples showed that  $E\Delta$  after brushing the teeth with the Colgate toothpaste was significantly higher than that of the Close Up toothpaste group ( $P < 0.05$ ), but no significant difference was observed between the two groups in the tooth samples ( $P > 0.05$ ). **Conclusion:** Using both Colgate Max White and Close Up Diamond Attraction toothpaste, especially Colgate Max White toothpaste, had an effect on the whiteness of resin composites and teeth in case of discoloration.

**Keywords:** Tooth paste, bleaching, resin composite, discoloration.

## INTRODUCTION

In recent years, resin composites have become very popular, so that they are now the first choice for direct restoration of anterior and posterior teeth. Aesthetic features in accordance with the natural color, the ability to connect to dental tissues, reducing the need to remove too much dental tissue and lower cost compared to indirect materials are the reasons for the popularity of resin composites.<sup>[1]</sup>

One of the problems related to the use of resin composites is their discoloration. Any discoloration may affect the beauty. The discoloration of composites depends on factors such as the type of organic matrix, the type of filler and the types of colors, which are aggravated by some foods and drinks.<sup>[2]</sup>

Discoloration may be due to many reasons. Common reasons for discoloration include poor oral hygiene, dental plaques, or tobacco. Drinks such as coffee, tea, and soft drinks, which are common drinks of humans, play an important role in the discoloration of resins.<sup>[3,4]</sup>

Bleaching (whitening by chemical method) is one of the methods of removing external and internal pigments,

which is accepted to improve the beauty of the appearance. Bleaching is commonly done on teeth. The result of bleaching on resin composites depends on the bleaching material and composition of the composite, as well as the duration of bleaching.<sup>[5]</sup>

There are various methods for bleaching, including whitening toothpastes, over the counter (OTC) whitening gels and strips, whitening mouthwashes, in-office bleaching, and at-home bleaching using a tray.<sup>[6]</sup>

In-office bleaching treatments are performed by a dentist using high doses of bleaching agents in a shorter period of time, while at-home bleaching treatments at lower concentrations of bleaching compounds are performed by the patient himself under the supervision of a dentist in a longer period of time.<sup>[7]</sup>

Teeth bleaching at high concentrations of peroxide has many side effects and biological risks. Studies have shown that chemicals in bleaching products increase the surface degradation of adhesive materials in composite restorations, which finally reduces the compliance and life of composite restoration.<sup>[8]</sup>

One of the methods to improve the color of teeth at a low cost is to use whitening toothpastes. These toothpastes, in

addition to the therapeutic properties (anti-caries and reducing gingivitis) in common with ordinary toothpastes, have abrasive materials or absorbent particles, peroxide, enzymes, or elements with a whitening effect. A study found that blue covarine whitening toothpaste had the greatest whitening effect on tooth enamel.<sup>[8]</sup>

In contrast, another study found that blue covarine whitening toothpaste had no significant effect on the discoloration of composites.<sup>[9]</sup>

Colgate Max White Ultimate Catalyst whitening toothpaste is the newest product of Colgate Co. and the first enzyme-enhanced toothpaste<sup>[10]</sup>, the effect of which on the discoloration of composites and teeth has not yet been studied. Given few studies conducted on the effect of whitening toothpastes from different brands on the discoloration of composites and teeth, we attempted to investigate the effect of Colgate and Close Up whitening toothpastes on the discoloration of tooth enamel and resin composite.

- The discoloration of Omnicroma composite and teeth samples after being placed in black tea concentrate solution is different.
- The discoloration of Omnicroma composite and teeth samples after using whitening toothpaste (Close Up and Colgate) is different.
- The discoloration of Omnicroma composite and teeth samples before staining, after exposure to black tea concentrate solution and brushing by whitening toothpastes is different.

## MATERIALS AND METHODS

The present study is an experimental-laboratory study. This study was approved by the Ethics Committee of Zanzan University of Medical Sciences with the code of ethics A-11-365-13. In this study, 36 samples of extracted human anterior teeth and 36 samples of resin composite were examined. For the sample size of  $n = 12$ , a study by Reinhardt et al. (11) was used, taking into account the average composite discoloration score (EΔ), 95% confidence level, and 80% test power. Finally, the samples were divided into 3 groups including Colgate Max White toothpaste, Close Up Diamond Attraction toothpaste, and control of resin composite and tooth samples.

Tooth samples that were free of any caries, fractures and restorations were selected. After cleaning the teeth from debris, they were cleaned with pumice powder, placed in chloramine T solution (10%) for a week for disinfection, and then they were kept in water solution at room temperature until the study was conducted (Figure 1). For composite samples, Omnicroma resin composite (One-Shade, Tokuyama) was used (Figure 1). First, disk-shaped samples with a diameter of 8 mm and a thickness of 2 mm were prepared from the resin composite. A plastic washer device with a central hole of 2 mm thickness and 8 mm diameter was placed on a celluloid strip on a glass plate. The resin composite was placed inside the central cavity and covered with a celluloid strip and a glass plate. A constant pressure of 5 kg weight was applied to the

samples for 3 min to obtain a sample with a smooth surface. Then, the samples were cured with Woodpecker LED (China) for 20 seconds with an intensity of 850 mw/cm<sup>2</sup> according to the instructions of the manufacturer. A digital caliper was used to measure the thickness of the samples, and the samples with a difference of more than 0.5 mm in thickness were discarded. Then, the lower and upper surfaces of the samples were polished by a diamond disc (TOR VM, Russia) in coarse, medium, fine and superfine sizes and with a hand-piece at low rate and medium pressure to achieve the maximum surface smoothness for 10 seconds. At each stage of polishing, the samples were washed with water and dried with a tissue. Finally, the samples were washed and dried, and to complete the polymerization process, they were placed in an incubator for 24 hours in distilled water at a temperature of 37°C.



**Figure 1:** Tooth and resin composite samples

Next, the staining process (artificial aging) was performed. The samples (24 teeth and 24 composites) were immersed in black tea (Jahan, Iran) concentrate solution for one week (7 days) to get color. To prepare the coloring solution (tea), 16 g of tea powder was dissolved in 500 ml of boiling water. Each sample was completely immersed in the solutions by means of a piece of thread in a vertical position. It should be noted that the samples of the control group ( $n = 12$ ) were immersed in distilled water solution. The colorimetric of all samples after staining was done using a spectrophotometer (SpectroShade, Handy Dental Type 713000, Verona, Italy) (Figure 2).





**Figure 2:** Colorimetric by a spectrophotometer

After the staining process, the samples (composites and teeth) were divided into 2 groups including Colgate Max White Ultimate Catalyst toothpaste and Close Up Diamond Attraction toothpaste. In the Colgate and Close Up groups, 0.25 g of each toothpaste was mixed with water at a ratio of 1: 3 and brushed by an operator twice a day for 30 seconds, each time for 30 seconds, with an electric toothbrush (Pro-Expert, Oral-B, USA). The samples were brushed with circular movements and washed under running water. Colorimetric was done at three stages, including before staining, after staining, and after brushing. After brushing, the samples were placed in a dark container containing artificial saliva at room temperature. In the control subgroups, the samples were immersed in distilled water (12). At each stage, after colorimetric by spectrophotometer, the samples were washed and dried using sterile gas.

The colorimetric of the samples was done using  $L^*$ ,  $a^*$  and  $b^*$  where  $L^*$  represents lightness\*,  $a^*$  represents the green-red parameter, and  $b^*$  represents the yellow-blue parameter. The discoloration of the samples at three different stages was measured by  $\Delta E$  and based on the following formula:

$$\Delta E = [(\Delta L^*)^2 + (\Delta a^*)^2 + (\Delta b^*)^2]^{1/2} \quad (2)$$

Where  $\Delta a^*$ ,  $\Delta L^*$  and  $\Delta b^*$  were changes in  $a^*$ ,  $L^*$  and  $b^*$  at different time intervals (1). The validity and reliability of this method has already been confirmed (13).

Finally, the data were collected in the study checklist, which contained the following parts:

- The studied groups included Colgate toothpaste (composite), Close Up toothpaste (composite), control (composite), Colgate toothpaste (teeth), Close Up toothpaste (teeth), and control (teeth).
- $a^*$ ,  $L^*$  and  $b^*$  values before staining, after staining, and after brushing
- Discoloration ( $\Delta E$ ) at the stages of before and after staining
- Discoloration ( $\Delta E$ ) at the stages of before staining and after brushing
- Discoloration ( $\Delta E$ ) at the stages of after staining and after brushing

The normal distribution of the data was checked using Kolmogorov-Smirnov test by SPSS version 26. Qualitative data were reported as frequency (percentage), and quantitative data were reported as mean  $\pm$  standard deviation. One-way analysis of variance test was used to compare the average variables between the study groups. Tukey's range test was also used to compare the mean variables in the studied groups. Independent t-test was used to compare composite and tooth samples. In all cases, differences and changes with P less than 0.5 were considered statistically significant.

## RESULTS

According to the study results, in Colgate toothpaste group, the average values of  $\Delta L$ ,  $\Delta a$ ,  $\Delta b$  and  $\Delta E$  of resin composite samples at three colorimetric stages are shown in Table 1. According to the results, the values of  $\Delta E$  after brushing by Colgate toothpaste were equal to 3.01 compared to before staining. The discoloration of resin composite samples in Colgate toothpaste group at three colorimetric stages are shown in Figure 3.

**Table 1:** Discoloration at three stages of colorimetric in the Colgate-composite group

	before staining - after staining	before staining - after brushing	after staining - after brushing
$\Delta L$	$-6.70 \pm 1.02$	$-1.52 \pm 0.63$	$5.18 \pm 1.32$
$\Delta a$	$3.42 \pm 0.52$	$0.22 \pm 0.17$	$-3.21 \pm 0.61$
$\Delta b$	$6.17 \pm 1.14$	$-2.52 \pm 0.39$	$-8.70 \pm 1.11$
$\Delta E$	$9.75 \pm 1.52$	$3.01 \pm 0.45$	$10.65 \pm 1.65$
Data are shown as mean $\pm$ standard deviation.			

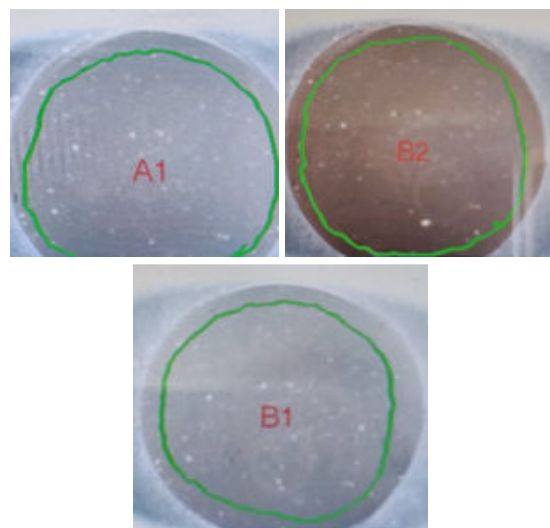


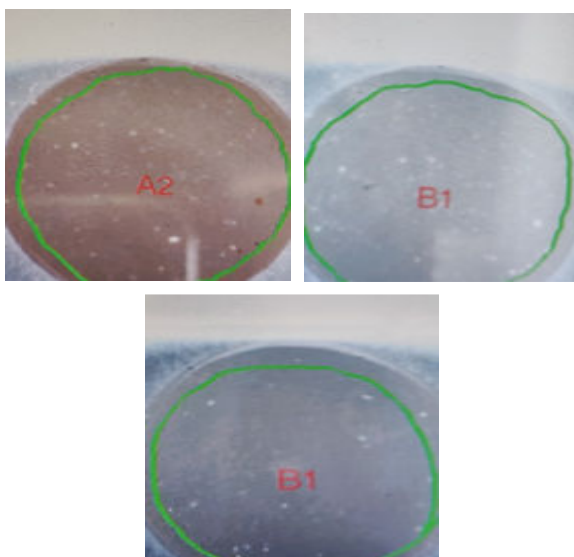
**Figure 3:** Discoloration of composite samples in Colgate toothpaste group at three colorimetric stages

The average values of  $\Delta L$ ,  $\Delta a$ ,  $\Delta b$  and  $\Delta E$  of resin composite samples in Close Up toothpaste group at three colorimetric stages are shown in Table 2. According to the results, the values of  $\Delta E$  after brushing by Close Up toothpaste compared to before staining were 5.62.

**Table 2:** Discoloration of composite samples at three colorimetric stages in Close Up toothpaste group

	before staining - after staining	before staining - after brushing	after staining - after brushing
$\Delta L$	$-7.30 \pm 1.26$	$-5.32 \pm 1.03$	$1.98 \pm 1.06$
$\Delta a$	$3.47 \pm 0.56$	$1.13 \pm 0.38$	$-2.34 \pm 2.46$
$\Delta b$	$6.02 \pm 0.77$	$-1.32 \pm 0.35$	$-7.35 \pm 0.93$
$\Delta E$	$10.09 \pm 1.51$	$5.62 \pm 1.02$	$8.02 \pm 1.12$
Data are shown as mean $\pm$ standard deviation.			

Discoloration of resin composite samples in Close Up toothpaste group at three colorimetric stages are shown in Figure 4.

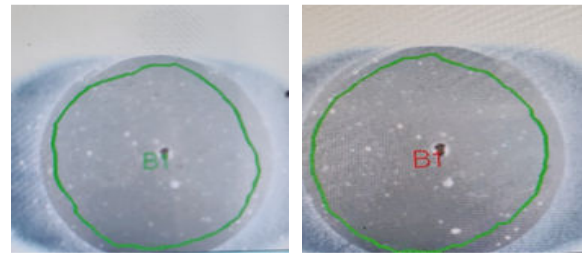
**Figure 4:** Discoloration of composite samples at three stages in Close Up toothpaste group

The average values of  $\Delta L$ ,  $\Delta a$ ,  $\Delta b$  and  $\Delta E$  of resin composite samples the control group at two colorimetric stages are shown in Table 3. According to the results, the values of  $\Delta E$  after immersion in distilled water compared to before staining were equal to 3.08.

**Table 3:** Discoloration at two stages of colorimetric in the composite-control group

	immersion in distilled water – before staining
$\Delta L$	$-2.42 \pm 0.55$
$\Delta a$	$0.42 \pm 0.15$
$\Delta b$	$-1.82 \pm 0.47$
$\Delta E$	$3.08 \pm 0.58$
Data are shown as mean $\pm$ standard deviation.	

The discoloration of the resin composite samples in the control group measured at two stages are shown in Figure 5.

**Figure 5:** Discoloration of composite samples at two colorimetric stages in the control group

According to the study results, a significant difference was observed in the values of  $\Delta L$ ,  $\Delta a$ ,  $\Delta b$  and  $\Delta E$  of composite samples in the control group after immersion in tea solution ( $P=0.000$ ).

The highest  $\Delta E$  after brushing compared to after staining was in Colgate toothpaste group (10.65), followed by Close Up toothpaste group (8.02).  $\Delta E$  of the control group compared to before staining was equal to 3.08 (Fig 4). Comparison of  $\Delta E$  after brushing compared to after staining between three groups of resin composite samples by one-way analysis of variance test showed a significant difference between these groups ( $P=0.000$ ). According to the results of Tukey's post hoc test,  $\Delta E$  of Colgate and Close Up toothpaste groups were significantly higher than the control group ( $P=0.000$ ).  $\Delta E$  of Colgate toothpaste group was significantly higher than that of Close Up toothpaste group ( $P=0.000$ ).

#### Color correction in tooth samples

The average values of  $\Delta L$ ,  $\Delta a$ ,  $\Delta b$  and  $\Delta E$  of tooth samples in Colgate toothpaste group at three colorimetric stages are shown in Table 4. According to the results, the values of  $\Delta E$  after brushing using Colgate toothpaste compared to before staining were 6.75.

**Table 4:** Discoloration of tooth samples at three colorimetric stages in Colgate toothpaste group

	before staining - after staining	before staining - after brushing	after staining - after brushing
$\Delta L$	$-8.82 \pm 3.35$	$4.44 \pm 0.56$	$9.38 \pm 2.83$
$\Delta a$	$4.54 \pm 0.93$	$0.89 \pm 0.83$	$-3.71 \pm 0.59$
$\Delta b$	$2.99 \pm 2.08$	$-4.91 \pm 2.98$	$-7.90 \pm 3.47$
$\Delta E$	$10.57 \pm 3.44$	$6.75 \pm 2.66$	$13.28 \pm 2.66$
Data are shown as mean $\pm$ standard deviation.			

The discoloration of tooth samples in Colgate toothpaste group at three colorimetric stages are shown in Figure 6.

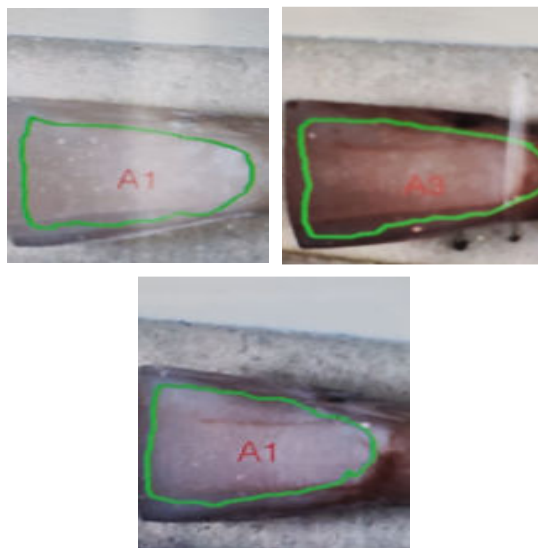


**Figure 6:** Discoloration of tooth samples at three colorimetric stages in Colgate toothpaste group

The average values of  $\Delta L$ ,  $\Delta a$ ,  $\Delta b$  and  $\Delta E$  of tooth samples in Close Up toothpaste group at three colorimetric stages are shown in Table 5. According to the results, the values of  $\Delta E$  after brushing using Close Up toothpaste were equal to 10.69 compared to before staining.

**Table 5:** Discoloration of tooth samples at three colorimetric stages in Close Up toothpaste group

	before staining - after staining	before staining - after brushing	after staining - after brushing
$\Delta L$	$-13.52 \pm 12.91$	$-6.98 \pm 16.10$	$6.54 \pm 6.33$
$\Delta a$	$5.98 \pm 4.54$	$3.71 \pm 2.16$	$-3.82 \pm 2.14$
$\Delta b$	$4.89 \pm 4.76$	$-1.84 \pm 6.66$	$-6.61 \pm 5.06$
$\Delta E$	$15.71 \pm 14.32$	$15.95 \pm 10.69$	$11.47 \pm 6.05$
Data are shown as mean $\pm$ standard deviation.			

The discoloration of tooth samples in Close Up toothpaste group at three colorimetric stages are shown in Figure 7.

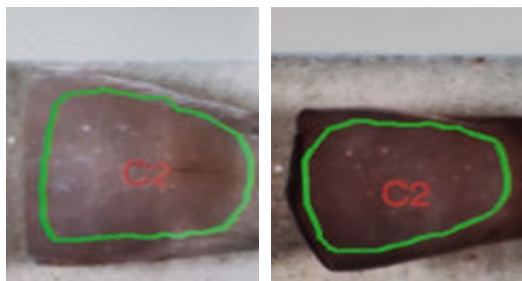


**Figure 7:** Discoloration of tooth samples at three colorimetric stages in Close Up toothpaste group

The average values of  $\Delta L$ ,  $\Delta a$ ,  $\Delta b$  and  $\Delta E$  of tooth samples in the control group at two colorimetric stages are shown in Table 6. According to the results, the values of  $\Delta E$  after immersion in distilled water were equal to 2.89 compared to before staining.

**Table 6:** Discoloration tooth samples at two colorimetric stages in the control group

	immersion in distilled water – before staining
$\Delta L$	$2.05 \pm 1.21$
$\Delta a$	$0.49 \pm 0.13$
$\Delta b$	$1.66 \pm 1.39$
$\Delta E$	$2.89 \pm 1.45$
Data are shown as mean $\pm$ standard deviation.	

The discoloration of tooth samples in the control group at two colorimetric stages are shown in Figure 8.



**Figure 8:** Discoloration of tooth samples at two colorimetric stages in the control group

According to the study results, the highest  $\Delta E$  after brushing compared to after staining was in Colgate toothpaste group was 13.28, followed by Close Up toothpaste group (11.47).  $\Delta E$  of the control group compared to before staining was equal to 2.89.  $\Delta E$  after brushing compared to after staining in the three groups of tooth samples by one-way analysis of variance showed a

significant difference in these groups ( $P=0.000$ ). According to the results of Tukey's post hoc test,  $\Delta E$  of Colgate and Close Up toothpaste groups were significantly higher than the control group ( $P=0.000$ ). However, no significant difference was in  $\Delta E$  between Colgate and Close Up toothpaste groups ( $P=0.524$ ).

Comparison of discoloration of tooth and composite samples in Colgate toothpaste group

The averages of  $\Delta L$ ,  $\Delta a$ ,  $\Delta b$  and  $\Delta E$  of tooth and composite samples after staining - before staining were compared in Colgate toothpaste group by independent t-test (Table 7).

**Table 7:** Discoloration of tooth and composite samples after staining – before staining in Colgate toothpaste group

	Composite samples in Colgate group	Tooth samples in Colgate group	P-value
$\Delta L$	$6.70 \pm 1.02$	$-8.82 \pm 3.35$	0.047
$\Delta a$	$3.42 \pm 0.52$	$-4.54 \pm 0.93$	0.001
$\Delta b$	$6.17 \pm 1.14$	$2.99 \pm 2.08$	0.000
$\Delta E$	$9.75 \pm 1.52$	$10.57 \pm 3.44$	0.459
Data are shown as mean $\pm$ standard deviation.			

The averages of  $\Delta L$ ,  $\Delta a$ ,  $\Delta b$  and  $\Delta E$  of tooth and composite samples after brushing - after staining were compared in Colgate toothpaste group by independent t-test (Table 8).

**Table 8:** Discoloration of tooth and composite samples after brushing - after staining in Colgate toothpaste group

	Composite samples in Colgate group	Tooth samples in Colgate group	P-value
$\Delta L$	$5.18 \pm 1.32$	$9.38 \pm 2.83$	0.000
$\Delta a$	$-3.21 \pm 0.61$	$-3.71 \pm 0.59$	0.054
$\Delta b$	$-8.70 \pm 1.11$	$-7.90 \pm 3.47$	0.455
$\Delta E$	$10.65 \pm 1.65$	$13.28 \pm 2.66$	0.008
Data are shown as mean $\pm$ standard deviation.			

Comparison of discoloration of tooth and composite samples in Close Up toothpaste group

The averages of  $\Delta L$ ,  $\Delta a$ ,  $\Delta b$  and  $\Delta E$  of tooth and composite samples after staining - before staining were compared in Close Up toothpaste group by independent t-test (Table 9).

**Table 9:** Discoloration of tooth and composite samples after staining - before staining in Close Up toothpaste group

	Composite samples in Close Up group	Tooth samples in Close Up group	P-value
$\Delta L$	$-7.30 \pm 1.26$	$-13.25 \pm 12.91$	0.111
$\Delta a$	$3.47 \pm 0.56$	$5.98 \pm 4.54$	0.071
$\Delta b$	$6.02 \pm 0.77$	$4.89 \pm 4.76$	0.388

$\Delta E$	$10.09 \pm 1.51$	$15.71 \pm 14.32$	0.190
Data are shown as mean $\pm$ standard deviation.			

The averages of  $\Delta L$ ,  $\Delta a$ ,  $\Delta b$  and  $\Delta E$  of tooth and composite samples after brushing - after staining were compared in Close Up toothpaste group by independent t-test (Table 10).

**Table 10:** Discoloration of tooth and composite after brushing - after staining in Close Up toothpaste group

	Composite samples in Close Up group	Tooth samples in Close Up group	P-value
$\Delta L$	$1.98 \pm 1.06$	$6.54 \pm 6.33$	0.023
$\Delta a$	$-2.34 \pm 0.46$	$-3.82 \pm 2.14$	0.029
$\Delta b$	$-7.35 \pm 0.93$	$-6.61 \pm 5.06$	0.623
$\Delta E$	$8.02 \pm 1.12$	$11.47 \pm 6.05$	0.066
Data are shown as mean $\pm$ standard deviation.			

## DISCUSSION

The success of restorative materials of resin composites depends on color stability and non-discoloration over time.<sup>[9]</sup> Although composite restorations discolor in the mouth, the important issue is the range of such discoloration, which should be at a level that cannot be seen by the eye.<sup>[10,11]</sup> The objective of this study was to investigate the effect of Colgate Max White and Close Up whitening toothpastes on tooth and Omnicroma resin composite discoloration.

In the present study, tea solution was used for coloring. Our results showed that the tea solution caused significant discoloration in the composite and tooth samples ( $\Delta E < 3.3$ ), while  $\Delta E$  of the control group was less than 3.3. Also, no significant difference was in the discoloration of tooth and composite.  $\Delta E$  less than 1 cannot be seen by humans,  $\Delta E$  between 1 and 3.3 can be seen by specialists, and  $\Delta E$  more than 3.3 can be seen by ordinary people.<sup>[14,15]</sup> Tea is a common drink among the Iranians that contains yellow pigments and can be effective in changing the color of composites. The discoloration due to color absorption is probably due to the absorption of foreign colored substances.<sup>[16]</sup> Also, during immersion, due to the lower polarity and faster diffusion of pigments, tea caused more discoloration than other solutions such as coffee, juice and soft drinks. Of course, the coloration of tea depends on the amount of tea consumed daily and the duration of drinking it, between different people to some extent is variable.<sup>[17]</sup> In the present study, the duration of immersion in the tea solution for all samples was the same and equal to 7 days, which simulated approximately 7 months of tea consumption.<sup>[11]</sup> Also, in this study, to simulate with the mouth while drinking tea, according to previous studies, the samples were placed in the desired solution in the incubator with a temperature of 37° C,



which is almost equivalent to the temperature of tea when drinking.<sup>[18]</sup>

The results of our study were consistent with the study results of Dinç Ata et al.<sup>[19]</sup>, Farah et al.<sup>[20]</sup>, and Duc et al.<sup>[21]</sup> In a study by Zajkani et al., the discoloration of the samples was less than in our study. The reasons for the difference can be attributed to the method of the colorimetric of the samples, the type of resin composite, and the type of tea solution used.<sup>[22]</sup> According to the results of the present study, the use of whitening toothpastes led to significant discoloration of the composite and tooth samples, although the color of the samples did not reach the baseline level. Also, according to the results, Colgate Max White toothpaste was more effective than Close Up toothpaste in composite samples. In this study, Colgate enzyme toothpaste and Close Up toothpaste containing blue covarine were used. Colgate toothpaste contains hydrogen peroxide, triacetin and carboxylesterase, and the synergistic effect of these three compounds led to significant whitening in the studied samples. According to the manufacturer's claim, Colgate Max White is the first enzyme-enhanced whitening toothpaste that increases its effect along with the whitening compounds in the toothpaste, which was observed in our study samples.<sup>[3]</sup> Close Up Diamond Attraction toothpaste contains blue covarine particles, which based on Blue Foam Technology, together with the ingredients in the toothpaste, leads to the improvement of discoloration of teeth and composites. Schwarzbald et al. investigated the effect of whitening toothpastes with enzymatic effect on tooth enamel whitening and its surface roughness and observed that these toothpastes significantly whiten teeth and the advantage of their use over abrasive and carbon toothpastes is that the change in tooth color is done without distorting the surface.<sup>[23]</sup> Tao et al. in a study showed that the use of toothpaste containing blue covarine significantly discolored teeth immediately after brushing, both in the laboratory and in the clinical settings.<sup>[24]</sup> Also, the study results were consistent with the study of Vaz et al., who observed that using only toothpaste containing blue covarine and microbead abrasives had a visible result.<sup>[8]</sup>

In a study on the effect and function of whitening toothpastes on the external discoloration of tooth enamel, Alshara et al. concluded that whitening toothpastes chemically and mechanically discolored tooth enamel.<sup>[25]</sup> One of the strengths of our study was that the toothpastes used in addition to the mechanical method also lead to chemical whitening of the teeth. One of the weaknesses of our study was its laboratory nature, the use of a type of composite, and the lack of comparison with other abrasive toothpastes.

In a study by Collins et al., which compared the tooth color in the baseline state and immediately after brushing with silica whitening toothpaste containing blue covarine and gel toothpaste as a control group, it was shown that toothpaste containing blue covarine was significantly more effective than the toothpaste used in the control group and made the teeth significantly whiter (immediately after brushing).<sup>[26]</sup> However, the study

results of Hashemi et al. were inconsistent with the present study, so that the  $\Delta E$  values in our study were higher than those reported by Hashemi et al. for common whitening toothpaste and that containing blue covarine applied 90 days twice a day for 30 seconds each time with a toothbrush on three types of composite Filtez 250, Filtez 350 and Anterior Gradia. They concluded that the discoloration of none of the composite samples was significant ( $\Delta E > 3.3$ ) and the toothpastes used had no significant effect on the discoloration of the composites.<sup>[9]</sup> The difference in our results with this study can be attributed to the difference in the type of resin used, the duration of immersion and the use of coloring solution. Resin composite is composed of mineral fillers in an organic matrix, which can be degraded in different media and discolored due to the penetration of the material into the composite. The polymerization and cross-linking of the composite is an important factor of the effect of solutions on it. In addition, the chemical composition of the matrix, filler, and silane play a role in the degradation of the composite in different media.<sup>[10,17,24]</sup> In a study by Al-Shalan, the significant discoloration of all three types of restorative materials (resin composite Filtek Z250, glass ionomer modified resin GC Fuji II LC and glass ionomer Ketac Molar Quick) was observed when brushing with whitening toothpastes for 2 min twice in day for 15 days. The most discoloration was related to the restorative material Ketac Molar Quick using Colgate Optic White toothpaste.<sup>[27]</sup>

## CONCLUSION

The study results showed that the tea solution significantly discolored the composite and tooth samples ( $\Delta E > 3.3$ ), while the  $\Delta E$  of the control group was less than 3.3. The use of whitening toothpastes led to significant color changes in the composite and tooth samples, although the color of the samples did not reach the baseline level. Intra-group comparison of resin composite samples showed that  $\Delta E$  of Colgate toothpaste group was significantly higher than that of Close Up toothpaste group, but for tooth samples, no significant difference was between the two groups. Finally, according to the results of the present study, it is recommended to use both Colgate Max White and Close Up toothpastes, especially Colgate Max White toothpaste, to whiten resin composites and teeth in case of discoloration.

## REFERENCES

1. Vaz VTP, Jubilato DP, Oliveira MRMd, Bortolatto JF, Floros MC, Dantas AAR, et al. Whitening toothpaste containing activated charcoal, blue covarine, hydrogen peroxide or microbeads: which one is the most effective? *Journal of Applied Oral Science*. 2019;2:1-8.
2. Hashemi kamangar SS, Hoseinpour F, Kiomarsi N, Dehaki MG, Kharazifard MJ. Effect of an optical whitening toothpaste on color stability of tooth-colored

- restorative materials. *European journal of dentistry*. 2020;14(01):085-91.
3. Al-Shalan T. Effect of whitening toothpastes on color stability of different restorative materials. *Int J Medical Science Clinical Invention*. 2017;4(3):2790-6.
  4. Tao D, Smith RN, Zhang Q, Sun JN, Philpotts CJ, Ricketts SR, et al. Tooth whitening evaluation of blue covarine containing toothpastes. *Journal of dentistry*. 2017;67:S20-S4.
  5. Collins LZ, Naeeni M, Platten SM. Instant tooth whitening from a silica toothpaste containing blue covarine. *Journal of dentistry*. 2008;36:21-5.
  6. Reinhardt JW, Balbierz MM, Schultz CM, Smetich B, Beatty MW. Effect of tooth-whitening procedures on stained composite resins. *Operative dentistry*. 2019;44(1):65-75.
  7. Kapse BS, Nagmode PS, Vishwas JR, Karpe HB, Basatwar HV, Godge SP. Cone-beam Computed Tomographic Analysis of Canal Transportation and Centering Ability of Three Different Nickel-Titanium Rotary File Systems. *Open Access Macedonian Journal of Medical Sciences*. 2021;9(D):30-6.
  8. Demarco FF, Collares K, Correa MB, Cenci MS, Moraes RRd, Opdam NJ. Should my composite restorations last forever? Why are they failing? *Brazilian oral research*. 2017;31(56):92-9.
  9. Ardu S, Duc O, Di Bella E, Krejci I. Color stability of recent composite resins. *Odontology*. 2017;105(1):29-35.
  10. Mahdisiar F, Nasoohi N, Safi M, Sahraee Y, Zavareian S. Evaluating the effect of tea solution on color stability of three dental composite (In Vitro). *Res Dent Sci*. 2014;11(1):21-6.
  11. Ghavam M, Poorhaghighi M, Mohammadi M. color stability of IDM Composite Resin. *Power*. 2000;2:4-8.
  12. Sakaguchi RL, Powers JM. *Craig's restorative dental materials-e-book*: Elsevier Health Sciences; 2019:184-225.
  13. Ahmad I. *Protocols for predictable aesthetic dental restorations*: John Wiley & Sons; 2008:213-284.
  14. Hasani-Tabatabaei M, Yassini E, Moradian S, Elmamooz N. Color stability of dental composite materials after exposure to staining solutions: A spectrophotometer analysis. *Journal of Islamic dental association of iran*. 2009;21(1):69-78.
  15. Zajkani E, Abdoh Tabrizi M, Ghasemi A, Torabzade H, Kharazifard M. Effect of staining solutions and repolishing on composite resin color change. *Journal of Islamic Dental Association of Iran*. 2013;25(3):139-46.
  16. Darabi F, Seyed-Monir A, Mihandoust S, Maleki D. The effect of preheating of composite resin on its color stability after immersion in tea and coffee solutions: An in-vitro study. *Journal of clinical and experimental dentistry*. 2019;11(12):e1151.
  17. Lee S, Huang H, Lin C, Shih Y. Leached components from dental composites in oral simulating fluids and the resultant composite strengths. *Journal of Oral Rehabilitation*. 1998;25(8):575-88.
  18. Barutçigil Ç, Yıldız M. Intrinsic and extrinsic discoloration of dimethacrylate and silorane based composites. *Journal of Dentistry*. 2012;40:e57-e63.
  19. Dinç Ata G, Gokay O, Müjdeci A, Kivrak TC, Mokhtari Tavana A. Effect of various teas on color stability of resin composites. *Am J Dent*. 2017;30(6):323-8.
  20. Farah RI, Elwi H. Spectrophotometric evaluation of color changes of bleach-shade resinbased composites after staining and bleaching. *The journal of contemporary dental practice*. 2014;15(5):587-94.
  21. Duc O, Di Bella E, Krejci I, Betrisey E, Abdelaziz M, Ardu S. Staining susceptibility of resin composite materials. *Am J Dent*. 2019;32(1):39-42.
  22. Schwarzbald CG, Cuevas-Suárez CE, Pacheco RR, Ribeiro JS, Carreño NLV, Lund RG, et al. In vitro efficacy of commercial and experimental proteolytic enzyme-based whitening dentifrices on enamel whitening and superficial roughness. *Journal of Esthetic and Restorative Dentistry*. 2021;33(6):849-55.
  23. Alshara S, Lippert F, Eckert GJ, Hara AT. Effectiveness and mode of action of whitening dentifrices on enamel extrinsic stains. *Clinical oral investigations*. 2014;18(2):563-9.
  24. Miranda DdA, Bertoldo CEdS, Aguiar FHB, Lima DANL, Lovadino JR. Effects of mouthwashes on Knoop hardness and surface roughness of dental composites after different immersion times. *Brazilian oral research*. 2011;25(2):168-73.



# Tracking of Intramuscular Stem Cells by Magnetic Resonance Diffusion Weighted Imaging

Balakrishna Shetty

## **Abstract—**

**Introduction:** Stem Cell Imaging is a challenging field since the advent of Stem Cell treatment in humans. Series of research on tagging and tracking the stem cells has not been very effective. The present study is an effort by the authors to track the stem cells injected into calf muscles by Magnetic Resonance Diffusion Weighted Imaging.

**Materials and methods:** Stem Cell injection deep into the calf muscles of patients with peripheral vascular disease is one of the recent treatment modalities followed in our institution. 5 patients who underwent deep intramuscular injection of stem cells as treatment were included for this study. Pre and two hours Post injection MRI of bilateral calf regions was done using 1.5 T Philips Achieva, 16 channel system using 16 channel torso coils. Axial STIR, Axial Diffusion weighted images with  $b=0$  and  $b=1000$  values with back ground suppression (DWIBS sequence of Philips MR Imaging Systems) were obtained at 5 mm interval covering the entire calf. The invert images were obtained for better visualization. 120ml of autologous bone marrow derived stem cells were processed and enriched under c-GMP conditions and reduced to 40ml solution containing mixture of above stem cells. Approximately 40 to 50 injections, each containing 0.75ml of processed stem cells, was injected with marked grids over the calf region. Around 40 injections, each of 1ml normal saline, is injected into contralateral leg as control.

**Results:** Significant Diffusion hyper intensity is noted at the site of injected stem cells. No hyper intensity noted before the injection and also in the control side where saline was injected conclusion: This is one of the earliest studies in literature showing diffusion hyper intensity in intramuscularly injected stem cells. The advantages and deficiencies in this study will be discussed during the presentation.

**Keywords—**stem cells, imaging, DWI, peripheral vascular disease.

# Burnout Prevalence and Contributing Factors among Healthcare Workers during the COVID19 Pandemic: Across-Sectional Survey Study in an Urban Community in Thailand

Jadsada Kunno, Busaba Supawattanabodee, Chavanant Sumanasrethakul, Budsaba Wiriyasirivaj, Pataraporn Yubonpant

## **Abstract—**

**Background:** Burnout is associated with an increased risk for severe COVID-19. Few studies have examined burnout prevalence related to healthcare workers during the pandemic. This study investigated the burnout prevalence and contributing factors among HCWs, including medical staff and support staff, during the COVID-19 pandemic in an urban community in Thailand.

**Methods:** A cross-sectional online survey was distributed among HCWs in Bangkok, Thailand, from July–August 2021. The independent t-test and one-way analysis of variance (ANOVA) were used to compare the contributing factors and burnout items. Variable factors associated with burnout among HCWs were used in multiple linear regression models.

**Results:** A total of 517 HCWs' survey responses were received. Most participants were medical staff (55.3%), female (83.4%), and over the age of 35 (59.4%); most participants (65.6%) did not have any diseases but had family members that did (63.6%). The prevalence of overall burnout was presented among medical staff (25.9%). The results of the multiple linear regression models found that female (vs. male,  $\beta$  0.088; 95% CI 0.033, 6.614) was higher associated with overall burnout score. In addition, hours of sleep as  $> 6$  hr./day (vs.  $\leq 6$  hr./day,  $\beta$ -0.120; 95% CI-6.012,-0.969) was lower associated with overall burnout score.

**Conclusion:** This study highlights the importance of addressing burnout among HCWs, in which female medical staff who slept less than six hours per day were associated with burnout. Our study further suggested that both intervention and identification are needed of frontline HCWs to prevent and reduce the risk of burnout, as the proportion of females compared to males is high. Thus, the government should provide support in these areas to prevent a humanitarian crisis.

**Keywords—** COVID-19, coronavirus disease, HCWs, health care workers, CBI, Copenhagen burnout inventory, CI, confidence interval.

# Comparison The Effectiveness of Pain Cognitive- Behavioral Therapy and Its Computerized Version on Reduction of Pain Intensity, Depression, Anger and Anxiety in Children with Cancer: A Randomized Controlled Trial

Najmeh Hamid<sup>1</sup>, Vajiheh Hamedy<sup>2</sup>, Zahra Rostamianasl<sup>3</sup>

<sup>1</sup> . Professor of clinical psychology, Shahid Chamran University of Ahvaz, Ahvaz, Iran

\*Correspondence Author. E-mail: n.hamid@scu.ac.ir

<sup>2</sup> . Ph.D. Student in clinical Psychology, Shahid Chamran University of Ahvaz, Ahvaz, Iran

<sup>3</sup> . B. A. Student in Psychology, Azad University of Tehran, Tehran, Iran

## Abstract

**Background:** Cancer is one of the medical problems that have been associated with pain. Moreover, the pain combined by negative emotions such as anxiety, depression and anger. poor pain management causes negative effects on the quality of life which results in negative effects that continue a long time after the painful experiences.

**Objectives:** The aim of this research was comparison the effectiveness of Common Cognitive Behavioral Therapy for Pain and its computerized version on reduction of pain intensity, depression, anger and anxiety in children with cancer.

**Methods:** The research method of this “Randomized Controlled Clinical Trial” was a pre, post-test and follow up with a control group. In this research, we have examined the effectiveness of Common Cognitive Behavioral Therapy for Pain and its computerized version on reduction of pain intensity, anxiety, depression and anger in children with cancer in Ahvaz. Two psychological interventions (cognitive behavioral therapy for pain and the computerized version) were compared with the control group. The sample consisted of 60 children aged 8 to 12 years old with different types of cancer of Shafa hospital in Ahvaz. According to the including and excluding criteria such as age, socioeconomic status, clinical diagnostic interview and other criteria, 60 subjects were selected. Then, randomly, 45 subjects were selected. The subjects randomly divided into three groups of 15 (two experimental and one control groups). The research instruments included Spielberger Anxiety Inventory (STAY-2) and International Pain Measurement Scale. The first experimental group received 6 sessions of cognitive-behavioral therapy for 6 weeks, and the second group was subjected to a computerized version of cognitive-behavioral therapy for 6 weeks, but the control group did not receive any interventions. For ethical considerations, a version of computerized cognitive-behavioral therapy was provided to them. After 6 weeks, all three groups were evaluated as post-test and eventually after one-month follow-up.

**Results:** The findings of this study indicated that both interventions could reduce the negative emotions (pain, anger, anxiety, depression) associated with cancer in children in compare with control group ( $p < 0.0001$ ). In addition, there were no significant differences between the two interventions ( $p < 0.01$ ). It means both interventions are useful to reduce the negative effects of pain and enhance the adjustment.

**conclusion:** we can use cCBT in situations in which there is no access to psychologist and psychological services. In addition, can be a useful alternative for conventional psychological interventions.

**Keywords:** pain, children, psychological intervention, cancer, anger, anxiety, depression.

# The Impact of Diseases and Epidemics in the Field of Medicine and Health in General

Bousseka Asma

**Abstract—** The pharmaceutical industry is one of the most important structures and foundations for the management and development of the modern world, especially the advanced part of it, meaning that there are some exceptions for third world countries. As the world today has witnessed radical transformations and changes, some of which made it better and some of which affected the path of its growth. At the beginning of my research, there was a detailed presentation overview of the current situation of the world in terms of growth and development, and it was a proceeded through that overview as the introduction to my research. In the first chapter, had divided it into three sections, each topic was unique to one of the new methods of manufacturing, deducing and developing medicines. Several examples of various recently developed medicines were used. In the second chapter, dealt with the defects and shortcomings that pioneers and drug makers at various levels, as well as various regions and major companies, suffer from, on the basis that they are international, especially those specialized in the manufacture of medicines related to viruses and chronic diseases, as well as incurable. As for the third chapter, it was devoted to marketing methods, methods of achieving sales, as well as the basics of spreading medicines and preparing the minds of consumers. Through my research, the one concluded that the current world has become completely different from the world we used to know, and it mean by saying the field of manufacturing, selling and marketing medicines. It was noted that one of the biggest factors that affected the change in the field of medicine was the corona disaster. At the end of my research, it was left with nothing but to show the importance and necessity of the pharmaceutical industry and its effective role, not only in the development of mankind, but its main role is in the survival of mankind.

**Keywords—** diseases, medicine, health, epidemics.

# Improving Functionality of Radiotherapy Department Through: Systemic Periodic Clinical Audits

Kamal Kaushik, Trisha, Dandapni, Sambit Nanda, A. Mukherjee, S. Pradhan

## **Abstract—**

**Introduction:** As complexity in radiotherapy practice and processes are increasing, there is a need to assure quality control to a greater extent. At present, no international literature available with regards to the optimal quality control indicators for radiotherapy; moreover, few clinical audits have been conducted in the field of radiotherapy. The primary aim is to improve the processes that directly impact clinical outcomes for patients in terms of patient safety and quality of care.

**Procedure:** A team of an Oncologist, a Medical Physicist and a Radiation Therapist was formed for weekly clinical audits of patient's undergoing radiotherapy audits. The stages for audits include Pre planning audits, Simulation, Planning, Daily QA, Implementation and Execution (with image guidance). Errors in all the parts of the chain were evaluated and recorded for the development of further departmental protocols for radiotherapy.

**Evaluation:** The errors at various stages of radiotherapy chain were evaluated and recorded for comparison before starting the clinical audits in the department of radiotherapy and after starting the audits. It was also evaluated to find the stage in which maximum errors were recorded. The clinical audits were used to structure standard protocols (in the form of checklist) in department of Radiotherapy, which may lead to further reduce the occurrences of clinical errors in the chain of radiotherapy.

**Results:** The aim of this study is to perform a comparison between number of errors in different part of RT chain in two groups (A- Before Audit and B-After Audit). Group A: 94 pts. (48 males, 46 female), Total no. of errors in RT chain: 19 (9 needed Resimulation). Group B: 94 pts. (61 males, 33 females), Total no. of errors in RT chain: 8 (4 needed Resimulation).

**Conclusion:** After systematic periodic clinical audits percentage of error in radiotherapy process reduced more than 50% within 2 months. There is a great need in improving quality control in radiotherapy, and the role of clinical audits can only grow. Although clinical audits are time-consuming and complex undertakings, the potential benefits in terms of identifying and rectifying errors in quality control procedures are potentially enormous. Radiotherapy being a chain of various process. There is always a probability of occurrence of error in any part of the chain which may further propagate in the chain till execution of treatment. Structuring departmental protocols and policies helps in reducing, if not completely eradicating occurrence of such incidents.

**Keywords—**audit, clinical, radiotherapy, improving functionality.



# Bacterial Interactions of Upper Respiratory Tract Microbiota

Sarah Almuhayya, Andrew Mcbain, Gavin Humphreys

## **Abstract—**

**Background:** The microbiome of the upper respiratory tract (URT) has received less research attention than other body sites. This study aims to investigate the microbial ecology of the human URT with a focus on the antagonism between the corynebacteria and staphylococci.

**Methods:** Mucosal swabs were collected from the anterior nares and nasal turbinates of 20 healthy adult subjects. Genomic DNA amplification targeting the (V4) of the 16S rRNA gene was conducted and analyzed using QIIME. Nasal swab isolates were cultured and identified using near full-length sequencing of the 16S rRNA gene. Isolates identified as corynebacteria or staphylococci were typed using (rep-PCR). Antagonism was determined using an agar-based inhibition assay.

**Results:** Four major bacterial phyla (Actinobacteria, Bacteroidetes, Firmicutes, and Proteobacteria) were identified from all volunteers. The typing of cultured staphylococci and corynebacteria suggested that intra-individual strain diversity was limited. Analysis of generated nasal microbiota profiles suggested an inverse correlation in terms of relative abundance between staphylococci and corynebacteria. Despite the apparent antagonism between these genera, it was limited when investigated on agar. Of 1000 pairwise interactions, observable zones of inhibition were only reported between a single strain of *C.pseudodiphtheriticum* and *S.aureus*. Imaging under EM revealed this effect to be bactericidal with clear lytic effects on staphylococcal cell morphology.

**Conclusion:** Nasal microbiota is complex, but culturable staphylococci and corynebacteria were limited in terms of clone type. Analysis of generated nasal microbiota profiles suggested an inverse correlation in terms of relative abundance between these genera suggesting an antagonism or competition between these taxonomic groups.

**Keywords—** nasal, microbiota, *S.aureus*, microbial interaction.

# Characterization of Soil Microbial Communities from Vineyard under a Spectrum of Drought Pressures in Sensitive Area of Mediterranean Region

Gianmaria Califano, Júlio Augusto Lucena Maciel, Olfa Zarrouk, Miguel Damasio, Jose Silvestre, Ana Margarida Fortes

**Abstract**— Global warming, with rapid and sudden changes in meteorological conditions, is one of the major constraints to ensuring agricultural and crop resilience in the Mediterranean regions. Several strategies are being adopted to reduce the pressure of drought stress on grapevines at regional and local scales: improvements in the irrigation systems, adoption of interline cover crops, and adaptation of pruning techniques. However, still, more can be achieved if also microbial compartments associated with plants are considered in crop management. It is known that the microbial community change according to several factors such as latitude, plant variety, age, rootstock, soil composition and agricultural management system. Considering the increasing pressure of the biotic and abiotic stresses, it is of utmost necessity to also evaluate the effects of drought on the microbiome associated with the grapevine, which is a commercially important crop worldwide. In this study, we characterize the diversity and the structure of the microbial community under three long-term irrigation levels (100% ET<sub>c</sub>, 50% ET<sub>c</sub> and rain-fed) in a drought-tolerant grapevine cultivar present worldwide, Syrah. To avoid the limitations of culture-dependent methods, amplicon sequencing with target primers for bacteria and fungi was applied to the same soil samples. The use of the DNeasy PowerSoil (Qiagen) extraction kit required further optimization with the use of lytic enzymes and heating steps to improve DNA yield and quality systematically across biological treatments. Target regions (16S rRNA and ITS genes) of our samples are being sequenced with Illumina technology. With bioinformatic pipelines, it will be possible to obtain a characterization of the bacterial and fungal diversity, structure and composition. Further, the microbial communities will be assessed for their functional activity, which remains an important metric considering the strong inter-kingdom interactions existing between plants and their associated microbiome. The results of this study will lay the basis for biotechnological applications: in combination with the establishment of a bacterial library, it will be possible to explore the possibility of testing synthetic microbial communities to support plant resistance to water scarcity.

**Keywords**— microbiome, metabarcoding, soil, vinegrape, syrah, global warming, crop sustainability.

# The Effect of Aerobic Training and Taxol Consumption on IL 8 and PAI-1 in Cervical Cancer

Alireza Barari, Maryam Firoozi, Maryam Ebrahimzadeh, Romina Roohani Ardeshiri, Maryam Kamarloeei

**Abstract**—Background: The purpose of this study was to analyze the effect of six-week aerobic training and taxol consumption on interleukin-8 and Plasminogen Activator Inhibitor-1 (PAI-1) in mice with cervical cancer. Materials and Methods: In this experimental study, 40 female C57 mice with cervical cancer, eight weeks old, were randomly divided into 4 groups including: control, taxol supplement, training, and training-taxol supplement. The implantation of cancerous tumors was performed under the skin at the upper of the pelvis. The program training was included: endurance training for six weeks, 3 sessions per week and 50 minutes per session, at the speed of 14-18 m/s. Taxol supplement at a dose of 60 mg/kg per day was injected intraperitoneally. Data analysis was performed using t-test and one-way ANOVA and if statistically significant, Bonferroni post hoc was used at the significance level  $p < .05$ . Results: The results showed that there was a significant difference between the levels of interleukin 8 ( $P < 0.05$ ,  $F = 12.25$ ) and the PAI-1 ( $P < 0.05$ ,  $P = 0.10737$  between the 4 groups. The results of this study showed a significant difference between the control group and the training - complementary group. Six weeks of aerobic training and taxol consumption have a significant effect on the level of PAI-1 and interleukin-8 mice with cervical cancer. Conclusion: Considering the effect of training on these variables, this type of exercise can be used as a complementary therapeutic approach with other therapies for cervical cancer.

**Keywords**—Cervical cancer, taxol, endurance training, interleukin 8, plasminogen activator inhibitor-1.

## I. INTRODUCTION

CERVICAL cancer is one of the most common cancers among women in developing countries which is caused by human papillomavirus infections. Infection with this virus can lead to the cervical squamous cell carcinoma that is very fatal [1]. Various types of cytokines play different roles in developing and expanding of cancer [2]. On the one hand, they can cause developing and metastases of cancer and, on the other hand, they can inhibit the cancer progression by anti-inflammation and anti-tumor effects [2], [3]. Interleukin-8 is one of the pre-inflammation cytokines that is known as a chemokine. It specifically plays a role in chemotaxis of WBCs especially neutrophils and lymphocytes and it is a trigger and enhancer of angiogenesis. This cytokine is secreted by natural cells such as fibroblasts and monocytes [4]. Researches show that interleukin-8 can increase the growth and angiogenesis of cancer tumors and this way it can impact on the growth of tumor [5]. Also, according to several studies, PAI-1 is related to an enhanced risk of many malignancies. PAI-1 is a key element in inhibition of fibrinolysis by inactivation of tissue-type and urokinase-type plasminogen activator [6], [7]. There are several

experimental evidences that show that the plasminogen activator system plays a role in the demolition of the base membrane and extracellular matrix and leads to the attack of tumor cells and metastases [8], [9]. Expression of PAI-1 gene is highly associated with deterioration, existence and also other effective parameters such as metastasis to lymphatic nodes, depth of tumor penetration and size of tumor [10].

An increase is observed in circulating concentrations of pre-inflammation cytokines such as interleukine 8 after endurance training [11]. Another research demonstrated that contraction activities and exercising play a role in the expression of interleukin-8 [12], [13]. Findings of another research show the effects of six weeks of endurance training on a meaningful decrease in interleukin-8 levels of tumor tissue and volume of tumor [3]. It also has been shown that aerobic exercises lead to a decrease of PAI-1 gene expression [14]. In contrast, another study demonstrated that regular exercise with medium intensity does not lead to a decrease in PAI-1 gene expression but may control it [15]. Thus, the impact of aerobic exercises on increase or decrease in expression of this gene which has a crucial role in the progression of tumors in cervical cancer is not completely clear and requires more expanded studies in this field. On the other hand, using plants as a drug for preventing and treatment of diseases has been considered by traditional medicine specialists since ancient times. By the beginning of the 16th century, it has been the most esteemed way to cure diseases. Among these, the yew tree has a great medicinal value because of Paclitaxel material with the trade name of Taxol [16]. Taxol is a diterpene with a complex structure. Today, it is effectively used worldwide as a most important natural anti-tumor composition with a different mechanism in comparison with other similar drugs in this field to cure all types of cancers such as skin, lung, urinary tracts, esophagus and lymph nodes [16], [17].

According to the significance of curing cancer, implementing studies around the role of cytokines in improving patients with cancer becomes important. Considering that today most of the attempts are about preventing and treatment of diseases without using drugs, an active lifestyle is important in preventing and treatment of diseases and the use of therapeutic exercises becomes more and more significant [12], [15], [18].

Research has shown that aerobic exercise affects plasminogenesis and thus reduces inflammation, but existing results especially about cancer, is not firm. Also, there are plenty of studies about mechanisms of effects of physical activities on the health of cancer patients, but the interaction

Alireza Barari is with the Islamic Azad University, Ayatollah Amoli Branch, Iran, Islamic Republic Of (e-mail: alireza54.barari@gmail.com).

between exercise and some cytokines is not completely clear. Therefore, by considering the effect of Taxol on the treatment of cancer and importance of mentioned cytokines in increasing the function of body's immune, performing studies that represent the impact of exercising specifically aerobic exercising on levels of interleukin-8 and PAI are substantial. Considering the physical activity as an intervener along with taking Taxol extract in order to improve the health condition of patients with cervical carcinoma and change in intensity and duration of exercise and nutrition status of subjects are among matters that can make this study different from other researches. In this study, the parallel effects of six weeks of aerobic exercising and consumption of Taxol on levels of interleukin and PAI in mice with cervical cancer have been studied.

## II. MATERIALS AND METHODS

This research was an experimental study in which it was possible to control factors influencing results. In this study, ethics on working with laboratory animals such as food and water availability, proper maintenance condition, and, killing the mice were noticed. In this study, 40 rats were transferred from the Iranian Pasteur Institute at Karaj to the research center. After entering and two weeks of adaptation with new environment, animals were randomly divided into four groups of cancer-Taxol supplement (S), cancer-training (T), training (C), and cancer-Taxol supplement-training (ST). For the homogenization of subjects in terms of weight, they were first weighed and then categorized in cages with weighted differences of  $20 \pm 2$ .

During familiarizing with new environment and treadmill and also protocol implementation period animals were kept in five-member groups in transparent polycarbonate  $15 \times 15 \times 30$  cages produced by Razi Rad company. Ambient temperature with  $22 \pm 4.1$  °C and lighting cycle with 12:12 darkness hours and  $55 \pm 4$  humidity. Rats are fed with pellets from livestock feed producing centers. Subjects of this study were fed with products of Behparvar livestock feed company. The mentioned amount of feed was put in the cages according to their weekly weighing.

At the end of 6th week of running the research, in completely equal situations, 48 hours after the last training and injection (to eliminate the acute effects of exercise and supplementation) and after 10 to 12 hours of fasting, all animals were anointed and sacrificed with intraperitoneal injection of ketamine (60 mg/kg weight) and xylosin (5 mg/kg weight) with a ratio of 5 to 2. After splitting of the abdominal cavity, the liver tissue was carefully separated. After washing with distilled water and weighing, it was frozen at 70 °C. Liver factors levels were determined by ELISA with special kits. In this study, levels of interleukin-8 were measured in milligrams with gene kit produced by China Stabiofarm Company. Levels of PAI were measured in nanogram per milliliter by ELISA with China Stabiofarm Company kit. Taxol supplement taken from Blue pure extract of Yew tree skin was injected to peritonea about 60 milligrams per 1 kilogram of mice body weight. The endurance training program was performed in 6 weeks and 5 sessions per

week. In the first two weeks, training time was about 25 minutes at a speed of 14 meters per minute. In the second two weeks, the training was enhanced to 30 minutes at a speed of 16 meters per minute. Then, in the last two weeks (week 4 and 5) training was accomplished at a speed of 18 meters per minute in 30 minutes. Considered training intensity was about 50-65% of the maximum consumed oxygen by mice.

## III. RESULTS

Results of the ANOVA test showed that there is a significant difference between the mean values of the interleukin-8 variable in the four groups ( $p \leq 0.05$ ). It also has been demonstrated with Tukey's follow-up test that meaningful level lower than 0.05 to compare "control" and "training-supplement" groups represents significant differences between the two groups. That is, 6 weeks of aerobic training along with consuming Taxol has a significant effect on interleukin-8 levels in mice with cervical cancer. According to Fig. 1, using supplement plus performing the training led to a decrease in the levels of this variable. According to results, there is a significant difference between "control" and "training" groups because of a meaningful level lower than 0.05. That is, training without supplementation led to a decrease in the level of interleukin-8 and a significant difference with the control group. There was not a significant difference between "training" and "supplement" groups. That is, taking supplemental Taxol alone or practicing alone has had a similar effect on a decrease in the level of interleukin 8. Difference between "training" and "training-supplement" was also not significant but there was a significant difference between "supplement" and "training-supplement" groups. That is, supplementation of the Taxol plus training is more effective than supplementation alone, and the effect of the training alone in reducing the level of interleukin-8 is similar to the effects of exercises with Taxol in reducing the level of this variable. But the most impact is still related to "training-supplement" group (Fig. 1).

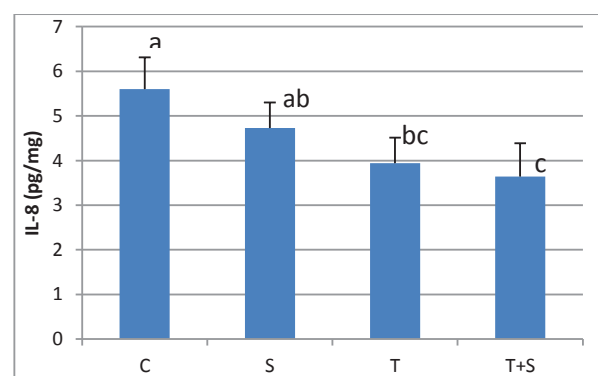


Fig. 1 Mean values of interleukine-8 in each subject groups (similar letters demonstrate lack of significant difference and different letters indicate significant difference)

Results of the ANOVA test showed that there is a significant difference between the mean values of the PAI variable in the four groups ( $P < 0.05$ ). Also, Tukey's follow-up test showed that a meaningful level lower than 0.05 for comparison of "control"

group with all other groups indicates a significant difference. That is, six weeks of aerobic training plus consuming Taxol has a significant effect on the level of PAI in mice with cervical cancer. According to Fig. 2, consuming supplementation plus training reduces the level of this variable. Comparison of other groups did not show any significant difference, i.e., the effect of using supplementation alone or training alone was almost the same with the effect of training along with the use of the extract on the decrease in the levels of PAI in mice with cervical cancer. But the most relevant effect was still related to the "training-supplementation" group (Fig. 2).

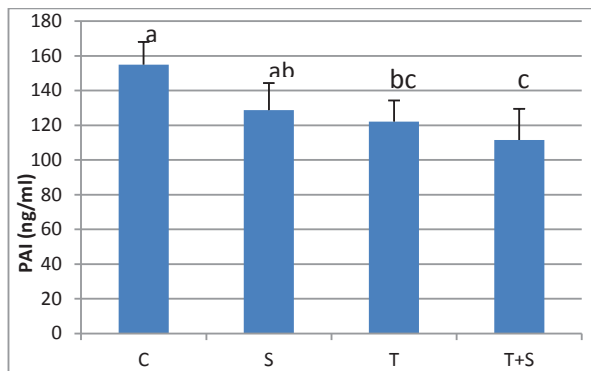


Fig. 2 Mean values of PAI in each subject groups (similar letters demonstrate lack of significant difference and different letters indicate significant difference)

#### IV. DISCUSSION

Results of this study showed that using Taxol and endurance training significantly decreased interleukin-8 levels in mice with cervical cancer. So, "training-supplement" group showed the lowest level of interleukin-8 compared to other groups. The results of this study about the decrease of interleukin-8 after endurance training are consistent with the findings of some other studies [3], [12], [13], [18]. Kazemi et al. [3] showed that six weeks of endurance training reduced interleukin-8 levels in mice with breast cancer. Finding of his study, similar to findings of [12] and [13], showed that exercising plays a role in the expression of interleukin-8. Results of Murphy et al. also showed a reduction in interleukin-8 in mice with cancer, after 20 weeks of aerobic training [19]. Indeed, it is possible that a decrease in some of the cytokines (especially IL-8) has an important consequence for cancer. Research has shown that chronic inflammation plays an important role in the growth, progression and survival of cancer [20]-[22]. It is believed that interleukin-8 is not only a factor in the activation of replication pathways in cancer cells, but also controls apoptotic pathways through interaction with nuclear factor kappa light-chain of activated B cells (NF-kB). That is because the reduction in expression of interleukin-8 in tumor cells can be a way for a decrease in growth and metastasis of these cells [23]. It seems that exercising can have a major role in decrease of tumor growth and in improving the cancer disease through enhancing regulation of anti-tumor factors and apoptotic pathway stimulating factors such as IFN- $\gamma$ , IL-2, and reduction in factors that are effective in angiogenesis and inflammation factors. In

this study, results from the Taxol consuming group indicates a reduction in the interleukin-8 levels compared to cervical cancer group. Increase in usage of Taxol for basic researches and cancer chemotherapy requires an improvement in existing methods to produce this herbal product [24]. Results of this study demonstrated that six weeks of using Taxol reduced the interleukin-8 levels in experimental groups. Taxol is an anti-tumor complex biochemical composition which is mainly extracted from Yew herbs. This anti-tumor drug has a different mechanism compared to other common anti-tumor drugs. Various studies showed that Taxol polymerizes Tubulin and prevents its depolymerization, therefore, mitosis replication cycle is stopped [25]. Taxol causes transcription to stop in the G2/M phase of mitosis with abnormal division duct formation and thereby, it causes the death of replicating cells [24]. However, the results of this study are not consistent with [26] after the treadmill training of submaximal and [27] after aerobic power combinations. Possible reasons for this discrepancy can include the differences in the exercise protocol, type of subjects, and duration of exercise, activity intensity, and stage of cancer progression. Also, the results of this study showed that six weeks of aerobic exercise along with Taxol consumption had a significant effect on the level of plasminogen-1 activator inhibitor in mice with cervical cancer. "Training-supplement" group showed the lowest level of PAI but there were not a significant difference between "training-supplement", "training" and "supplement" groups. The results of this study are consistent with [28] which showed that physical activity reduces the PAI in the male body. The results of [14] and [29] on the effect of aerobic exercise on reducing the level of PAI are consistent with the present study. PAI-1 develops tumor growth, invasion, metastasis, and angiogenesis, and it seems that these processes take place in interaction with vitronectin, integrin, and other components of the plasminogen activation system and by affecting the extracellular matrix [30]. The incremental regulation of PAI-1 expression extends breast cancer to more aggressive stages, and this process is partially affected by angiogenesis [31]. Laboratory studies have shown that PAI-1 acts as a positive initiator for angiogenesis by promoting the migration of endothelial cells to fibronectin-rich tumor tissue and PAI-1 inhibitors prevent angiogenesis [32]. Study about PAI-1 deficient mice showed that angiogenesis was approximately 60% reduced compared to wild-type mice, while in mice with high expression of PAI-1, angiogenesis increased approximately threefold [33]. The results of studies have shown that Taxol in the presence of low picomolar concentrations inhibits angiogenesis by inhibiting the production of angiogenesis factors and preventing the protein expression of hypoxia-induced alpha-factor. The results of this study, consistent with previous studies [3], [11], [14], showed that Taxol reduces PAI-1 levels. Therefore, given the anti-angiogenic properties that Taxol has shown, its anti-tumor properties are over pre-reinforced. In addition, high expression of PAI-1 has been found in many types of cancers. High levels of PAI-1 are also associated with poor prognosis in breast and other cancers [34]. Some quantitative studies have investigated the effect of sports activities on PAI-1 in non-cancer subjects.



Similarly, higher levels of PAI-1 have been observed in inactive women compared to active women [35]. However, the results of this study are in contradiction with [36], which showed that eight weeks of exhaustive activity in the training group caused a significant increase in this gene compared to the control group. This study also contradicts the results of [15], which showed that moderate-intensity regular exercises did not reduce the activity of this gene. Probably the reduction of the levels of the studied genes is related to regular muscle contraction and activation of fibrinolysis through exercising. Decreased inflammatory factors and decreased inflammation are probably due to a reduction in the release of cytokines in response to regular muscle contraction.

**Conclusion:** results of this study demonstrated that consumption of Taxol and endurance exercises significantly reduced levels of interleukin-8 and PAIs in mice with cervical cancer. According to the downturned effect of exercises on these variables, this type of exercise can be used as a complementary therapeutic approach along with other treatments for cervical cancer.

#### REFERENCES

- [1] Dannenberg AJ, Altork: NK, Boyle Jo, Dang C, Howe LR, weksler BB, et al. Cyclooxygenase 2: a pharmacological target for the prevention of cancer. *Lancet oncol*; 2001; 2:544-51.
- [2] Kim JH, Banton SA, Awad M, Yadalam A, Sher S, et al Training-Related Metabolic Adaptations in American-Style Football Participants. *Ann Sports Med Res*; 2015; 2(8): 1048.
- [3] Kazemi A, Agha Alinejad H, Eslami R, Ehsan P, Baghaei R, Dabaghzadeh R et al. Investigating the Effect of Endurance Training on Tumor Level of IL-8 and Serum Level of IL-17 in Female Mice with Breast Cancer. *J Fasa Univ Med Sci*. 2015; 5 (3) :347-355
- [4] Snoussi, K., Mahfoudh, W., Bouaouina, N., Ahmed, S.B., Helal, A. N., Chouchane, L. (2008). Genetic variation in IL-8 associated with increased risk and poor prognosis of breast carcinoma. *Hum Immunol*, 67(1-2), 13-21.
- [5] Shao, N., Lu, Z., Zhang, Y., Wang, M., Li, W., Hu, Z. (2015). Interleukin 8 Upregulates integrin B3 Expression and Promotes estrogen receptor-negative breast cancer cell invasion by activating the PI3k/Akt/ NF- KB Pathway. *Cancer Let*, 364(2), 165- 172.
- [6] Shaghghi Z, Bonyadi M, Somi MH, Khoshbaten M. Association of plasminogen activator inhibitor-1 gene polymorphism with inflammatory bowel disease in Iranian Azari Turkish patients. *Saudi J Gastroenterol* 2014; 20(1): 54-8.
- [7] YasarYildiz S, Kuru P, ToksoyOner E, Agirbasli M. Functional stability of plasminogen activator inhibitor-1. *SciWorld J* 2014; 2014: 858293.
- [8] Horvaticherceg G, Herceg D, Kralik M, Kulic A, Bencezigan Z, TomicbBrzac H, et al. Urokinase plasminogen activator and its inhibitor type-1 as prognostic factors in differentiated thyroid carcinoma patients. *Otolaryngol Head Neck Surg* 2013; 149:533-40.
- [9] Horvaticherceg G, Herceg D, Kralik M, Bencezigan Z, TomicbBrzac H, Kulic A. Urokinasetype plasminogen activator and its inhibitor in thyroid neoplasms a cytosol study. *Wien KlinWochenschr* 2006; 118:601-9.
- [10] Hazelbag, S., Kenter, G. G., Gorter, A., Fleuren, G. J. (2004). Prognostic relevance of TGF-beta1 and PAI-1 in cervical cancer, *Int J Cancer*, 112(6), 1020-8.
- [11] Capelli, K., Felicetti, M., Capomaccio, S., Pieramati, C., Silvestrelli, M., Verini-Supplizi, A. (2009), Exercise-induced up-regulation of MMP-1 and IL-8 genes in endurance horses. *BMC Physiol*, 24, 9-12.
- [12] Addison, C.L., Daniel, T.O., Burdick, M.D., Liu, H., Ehlert, J. E., Xue, Y. Y. (2000). The CXC chemokine receptor 2, CXCR2, is the putative receptor for ELR+CXC chemokine-induced angiogenic activity. *J Immunol*, 165, 5269-5277.
- [13] Nieman, D. C., Davis, J. M., Henson, D. A., Walberg- Rankin, J., Shute, M., Dumke, C. L. (2003). Carbohydrate ingestion influences skeletal muscle cytokine mRNA and plasma cytokine levels after a 3-h run. *J ApplPhysiol*, 94, 1917- 25.
- [14] Cooper, J. A., Nagelkirk, P. R., Coughlin, A. M., Pivarnik, J. M., Womack, C. J. (2004). Temporal changes in tPA and PAI-1 after maximal exercise. *Med Sci Sports Exerc*, 36(11), 1884-1887.
- [15] Väisänen, S. B., Humphries, S. E., Luong, L. A., Penttilä, I., Bouchard, C., Rauramaa, R. (2000). Regular exercise, plasminogen activator inhibitor-1 (PAI-1) activity and the 4G/5G promoter polymorphism in the PAI-1 gene. *ThrombHaemost*, 82(3), 1117-20.
- [16] Hla T, Bailey DB, Liu CH, Schaefer HJ, Trifan OC. Cyclooxygenase-1 and-2 isoenzymes. *IYBCB* 1999; 31:551-57.
- [17] Kim JH, Banton SA, Awad M, Yadalam A, Sher S, et al Training-Related Metabolic Adaptations in American-Style Football Participants. *Ann Sports Med Res*; 2015; 2(8): 1048.
- [18] Barari A, Mojhd M, Farzanegi P and Ghasemi M. Effect of Six Weeks of Endurance Training and Aloe Vera on COX-2 and MMP-9 Levels in Mice with Breast Cancer. *Journal of ShahidSadoughi University of Medical Science*. Apr 2016; 24 (1):65-73
- [19] Murphy, E. A., Davis, J. M., Barrilleaux, T., McClellan, J., Steiner, J., Carmichael, M. (2011). Benefits of exercise training on breast cancer progression and inflammation in C3 (1)SV40Tag mice. *Cytokine*, 55(2), 274-9.
- [20] Korkaya H, Liu S, Wicha MS. Breast cancer stem cells, cytokine networks, and the tumor microenvironment. *J Clin Invest* 2011;121: 3804-9.
- [21] Vendramini-Costa DB, Carvalho JE. Molecular link mechanisms between inflammation and cancer. *Curr Pharm Des* 2012;18:3831-52.
- [22] Pierce BL, Ballard-Barbash R, Bernstein L, Baumgartner RN, Neuhauser ML, Wener MH, et al. Elevated biomarkers of inflammation are associated with reduced survival among breast cancer patients. *J Clin Oncol* 2009;27:3437-44.S
- [23] Shao N, Chen LH, Ye RY, Lin Y, Wang SM. The depletion of interleukin-8 cause's cell cycle arrest and increases the efficacy of docetaxel in breast cancer cells. *BiochemBiophys Res Commun*. 2013; 431(3):535-41.
- [24] Mohammadi-Motlagh Hamid-Reza, Mansouri Kamran, Mostafae Ali. Plants as useful agents for angiogenesis and tumor growth prevention. *Physiology and Pharmacology*, 2010; 14 (3), 297-312.
- [25] Oaknin A, Díaz de Corcuera I, Rodríguez-Freixinós V, Rivera F, del Campo JM. SEOM guidelines for cervical cancer. *ClinTranslOncol*. 2012;14(7):516-9.
- [26] Rogers LQ. , Amanda Fogleman, Rita Trammell, Patricia Hopkins-Price, Sandy Vicari, Krishna Rao, Billie Edson, Steven Verhulst, Kerry S. Courneya, and Karen Hoelzer. Effects of a physical activity behavior change intervention on inflammation and related health outcomes in breast cancer survivors: pilot randomized trial. *Integr Cancer Ther*. 2013 Jul; 12(4): 323-335.
- [27] Gómez AM1, Martínez C, Fiuza-Luces C, Herrero F, Pérez M, Madero L, Ruiz JR, Lucia A, Ramírez M. Exercise training and cytokines in breast cancer survivors. *Int J Sports Med*. 2011 Jun;32(6):461-7.
- [28] Hilberg, T., Gläser, D., Reckhart, C., Prasa, D., Stürzebecher, J., Gabriel, H. H. (2003). Blood coagulation and fibrinolysis after longdurationtreadmill exercise controlled by individual anaerobic threshold. *Eur J ApplPhysiol*, 90, 639-642.
- [29] Kulaputana, O., Richard, F. M., Ioana, G., Dana, A. Ph., Andrew, P. G., James, M. H. (2005). Human gender differences infibrinolytic responses to exercise training and their determinants, *Exp Physio*, 90, 881-887.
- [30] Rakic JM, Maillard C, Jost M, Bajou K, Masson V, Devy L, et al. Role of plasminogen activatorplasmin system in tumor angiogenesis. *Cell Mol Life Sci*. 2003; 60:463-473.
- [31] Beaulieu LM, Whitley BR, Wiesner TF, Rehault SM, Palmieri D, Elkhouloun AG, et al. Breast cancer and metabolic syndrome linked through the plasminogen activator inhibitor-1 cycle. *Bioessays*. 2007; 29:1029-1038.
- [32] Isogai C, Laug WE, Shimada H, Declercq PJ, Stins MF, Durden DL, et al. Plasminogen activatorinhibitor-1 promotes angiogenesis by stimulating endothelial cell migration toward fibronectin. *Cancer Res*. 2001; 61:5587-5594.
- [33] McMahon GA, Petittclerc E, Stefansson S, Smith E, Wong MK, Westrick RJ, et al. Plasminogenactivator inhibitor-1 regulates tumor growth and angiogenesis. *J Biol Chem*. 2001; 276:33964-33968.
- [34] Steiner E, Pollow K, Hasenclever D, Schormann W, Hermes M, Schmidt M, et al. Role ofurokinase-type plasminogen activator (uPA) and plasminogen activator inhibitor type 1 (PAI-1)for prognosis in endometrial cancer. *GynecolOncol*. 2008; 108:569-576.
- [35] DeSouza CA, Jones PP, Seals DR. Physical activity status and adverse age-related differences incoagulation and fibrinolytic factors in women.

ArteriosclerThrombVasc Biol. 1998; 18:362–368.

- [36] Maleki, Fatemeh, Debiidi Roshan, Wali Allah. (2011). The Effect of Regular Physical Exercises and Exitant Activities Before and After on the Complex of Activating Histogenic and Regulatory Plasminogenins in the Wistar Mice, Sport Sciences, Vol. 5, 109-95.